CONTROL ALGORITHMS FOR THE LEACHING PROCESS IN THE HYDROMETALLURGY SHOP AT THE ACHINSK ALUMINA COMBINE

UDC669.712.1

V. M. Polyanskii, A. F. Karfidov, and V. V. Petrovskii

The leaching of sinter cake is one of the basic processes in the production of alumina from nephelite raw material, so that the control of the process is a matter of vital importance.

To solve this problem, a control subject with a settled raw material processing technology (see Figure) was selected in the leaching department of the Achinsk Alumina Combine hydrometallurgy shop.

The purpose of control is to produce stable concentrations in terms of Al_2O_3 and a stable caustic ratio α ($\alpha = \frac{102}{62}\frac{K}{A}$, where A and K are the concentrations of Al_2O_3 and K_2O_{ct}, g/liter) in the overflow from the tubular leacher. A mathematical model for the statics of the process was created, embodying the principal of a materials balance in terms of the control subject flow constituents.

The sinter is leached with a circulating solution which is a mixture of soda-alkali solution and concentrated wash water from the thickener filters. The circulating solution is prepared in a separate circulating solution unit and is distributed to the tubular leachers. The separate materials balances for the tubular leacher and the circulating solution unit were reduced to a single materials balance for the whole control subject.

The tubular leacher materials balance per ton of sinter is represented by the following equations.

Aluminum oxide balance:

$$1000\frac{a_1}{100}\cdot\frac{\eta_3}{100} + (V_T - V_3)A_5 = (V_T - V_3)A. \quad (1)$$

Total alkali balance:

$$1000\frac{n_1}{100}\frac{\eta_3}{100} + (V_T - V_3)N_5 = (V_T - V_3)N. \quad (2)$$

Alkaline carbonate balance:

$$(V_T - V_3)Y_5 - \beta(V_T - V_3)Y_5 = (V_T - V_3)Y. \quad (3)$$

Symbols:

η_3 and η_3 are the percentage extraction of Al_2O_3 and K_2O_{total} respectively into the tubular apparatus overflow;

β is the degree of causticization; the proportion of total alkaline carbonate converted to caustic alkali;

V_T is the flow of circulating solution into the tubular leacher, m^3/ton of sinter;

V_3 is the amount of circulating solution (m^3/ton of sinter) going into the rod mill with the slime from the tubular leacher;

a_1 and n_1 are the respective percentages of Al_2O_3 and K_2O_{total} in the sinter;

A_i, N_i, and Y_i are the respective concentrations (g/liter) of Al_2O_3, K_2O_{total}, and alkaline carbonate at point i, i = 1, 2, 3, and 5;

A, N, and Y are the concentrations of Al_2O_3, K_2O_{total}, and alkaline carbonate at point 4.

The amount of circulating solution going into the rod mill with the slime is calculated as follows:

$$V_3 = 0.74R_4 - V_m$$

where R_4 is the liquid-to-solid ratio of the mill pulp and V_m is the flow of circulating solution into the mill, m^3/ton of sinter.

The following relationship exists between the concentrations of Al_2O_3, K_2O_{total}, K_2O_{ct} and alkaline carbonate:

$$Y = N - K, \quad (3a)$$

where K is the concentration of K_2O_{ct}.

The materials balance is represented by three equations, because three basic indices characterize the properties of the sinter (extraction in terms of Al_2O_3 and K_2O and the degree of alkaline carbonate causticization) and the stripping properties of solutions also have three indices (the concentration of Al_2O_3, K_2O_{ct}, and K_2O_{total}).

The materials balance for the circulating solution unit is described by the following equations:

For Al_2O_3:

$$V_1A_1+V_2A_2=(V_1+V_2)A_5. \quad (4)$$

For K_2O_{total}:

$$V_1N_1+V_2N_2=(V_1+V_2)N_5. \quad (5)$$

For alkaline carbonate:

$$V_1 + Y_1 + V_2Y_2 = (V_1 + V_2)Y_5 \quad (6)$$

In (4) - (6) V_1 and V_2 are the flow rates of soda-alkali solution and wash water respectively, m^3/hr.

Since the relationship $V_1 : V_2 = q$ mainly affects the caustic ratio in the overflow from the tubular apparatus and V_T (the circulating solution flow rate per ton of sinter) mainly affects the Al_2O_3 concentration in the overflow from the tubular apparatus, q and V_T were chosen as the controlling influences to produce stable Al_2O_3 concentrations and a stable caustic ratio α in the overflow from the tubular leacher. Since $V_T = V_1 + V_2$,

$$V_1 = \frac{V_Tq}{q+1}, \qquad V_2 = \frac{V_T}{q+1}.$$

After substituting V_T, V_1, and V_2 into equations (4), (5), and (6) we obtain:

$$A_5 = \frac{A_1q + A_2}{q+1},$$

$$N_5 = \frac{N_1q + N_2}{q+1}, \quad (5a)$$

$$V_5 = \frac{Y_1q + Y_2}{q+1}, \quad (6a)$$

After designating the yield of Al_2O_3 and K_2O_{total} (kg) from 1 ton of sinter into the discharge from the tubular leacher $p_a = 0.1\, a_1\varepsilon_3$ and $p_n = 0.1n_1\varepsilon_3$ and substituting equations (4a) - (6a) into equations (1) - (3) we obtain the following after mathematical conversions:

$$(A - A_1)\frac{q(V_T - V_2)}{q+1} + (A - A_2)\frac{V_T - V_2}{q+1} = p_a. \quad (7)$$

$$(N - N_1)\frac{q(V_T - V_2)}{q+1} + (N - N_2)\frac{V_T - V_2}{q+1} = p_n. \quad (8)$$

$$1 - \frac{Y(q+1)}{Y_1q + Y_2} = \beta. \quad (9)$$

Thus, p_a, p_n, and β were obtained with the controlling influences q and V_T. To obtain the necessary values of A_0 and α_0 it is assumed that the extractions from the sinter into the overflow will remain as before, p_a, p_n, and β, with new values for the controlling parameters q_0 and V_{T0}. This means that the same disturbances which operated in the preceding control session will operate in the control subject in the next control session.

However, p_a, p_n, and β are adjusted on receiving the chemical analysis of the tubular apparatus overflow after each control session in terms of those chemical analyses and flow rates which resulted in an overflow of the specified quality. Hence one may write the following on the assumption of previous p_a, p_n, and β values for the next session:

$$(A_0 - A_1)\frac{q_0(V_{T0} - V_2)}{q_0 + 1} + (A_0 - A_2)\frac{V_{T0} - V_2}{q_0 + 1} = P_a. \quad (10)$$

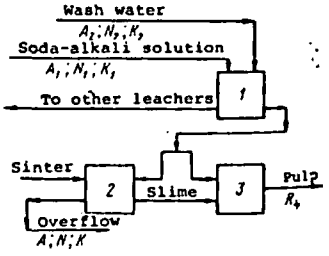

Diagram showing the control exercised over the composition of the overflow from the tubular leacher: 1 - unit for the circulating solution; 2 - tubular leacher; 3 - rod mill.

$$(N_0 - N_1)\frac{q_0(V_{T0} - V_2)}{q_0 + 1} + (N_0 - N_2)\frac{V_{T0} - V_2}{q_0 + 1} = \rho_n. \quad (11)$$

$$1 - \frac{Y_0(q_0 + 1)}{Y_1 q_0 + Y_2} = \beta. \quad (12)$$

We obtain the following mathematical model for control of the leaching process after equating the left-hand parts of equations (7) - (9) and (10) - (12) and taking account of (3a) and (3b), after making certain conversions:

$$\left.\begin{aligned}[(A_0 - A_1)q_0 + A_0 - A_2]\frac{V_{T0} - V_2}{q_0 + 1} &= [(A - A_1)q + A - A_2]\frac{V_T - V_2}{q + 1},\\ [(N_0 - N_1)q_0 + N_0 - N_2]\frac{V_{T0} - V_2}{q_0 + 1} &= [(N - N_1)q + N - N_2]\frac{V_T - V_2}{q + 1},\end{aligned}\right\} \quad (13)$$

where

$$N_0 = \frac{(N - K)(q + 1)[(N_1 - K_1)q + N_2 - K_2]}{[(N_1 - K_1)q + N_2 - K_2](q_0 + 1)} + K_0, \quad K_0 = \frac{62}{102}A_0\alpha_0.$$

The mathematical model is represented by a nonlinear system of equationswhich is solved by the heuristic method and by Newton's method. A program was created according to the algorithm described below using the mathematical model, in which the heuristic method of solving this sytem of equations was programmed. The program was written in mnemonic code for the M-2000 computer.

The control algorithm is as follows. The controlling effects are adjusted once in 2 hr. The results of the latest chemical analyses and those values of controlling effects q and V_T for which the latest tubular leacher overflow analyses were obtained, as well as A_0 and α_0, are fed into the computer. Equation system (13) is solved, i.e., our mathematical model is solved relative to the new unknown controlling effects q_0 and V_{T0}. The controlling effects are adjusted by means of the new q_0 and V_{T0} values.

In the course of the next 2 hr the flow rates which occurred in the operation of the control subject during the 2 hr are collected and the procedure for finding q_0 and V_{T0} is repeated. The leaching process is controlled in this way.

A series of statistical data on the operation of the control subject and the process workers, as well as a series of chemical analyses for the subject, were collected to check the mathematical model. The reverse problem was solved from these data: the values of A_0 and α_0 in thetubular apparatus overflow were calculated according to the chemical analyses and to the relationships which the process workers maintained on the basis of their personal experience. A series of A_0 and α_0 values was worked through in this way, and then these calculated A_0 and α_0 values were compared with those actually occurring in the tubular apparatus overflow. It was calculated by the Student criterion that the calculated values of A_0 and α_0 did not differ significantly from the actual values in the tubular apparatus overflow.

In 1974 the proposed control algorithm was put into pilot operation in the shop direct, and the effectiveness of the system which had been developed was confirmed.

PNE-522
FINAL REPORT

Plowshare civil, industrial and scientific uses for nuclear explosives

PROJECT SCHOONER

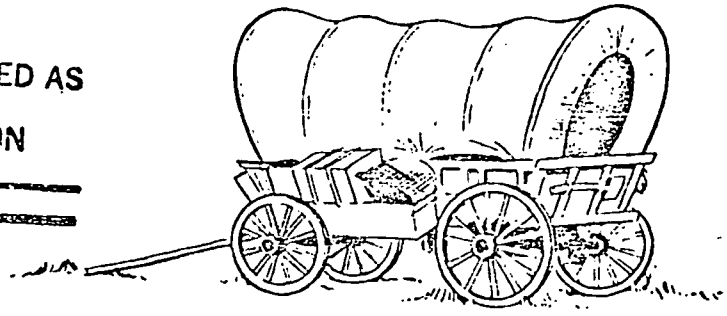

A Contribution to the Analysis of Seismic Data from Cratering and Contained Events

P5881

Environmental Research Corporation
Alexandria, Virginia

ISSUED: JUNE 30, 1970

BLANK PAGE

LEGAL NOTICE

[illegible] Division of Technical Information Extension, Oak Ridge, Tennessee

BLANK PAGE

PNE-522
NUCLEAR EXPLOSIONS — PEACEFUL APPLICATIONS (TID-4500)

SCHOONER EVENT

A CONTRIBUTION TO THE ANALYSIS OF SEISMIC DATA FROM CRATERING AND CONTAINED EVENTS

July 18, 1969

W.W. Hays, R.A. Mueller, C.T. Spiker, Jr.

Environmental Research Corporation
813 N. Royal Street
Alexandria, Virginia

Prepared under
Contract AT(29-2)-1163
for the
Nevada Operations Office
U. S. Atomic Energy Commission

BLANK PAGE

TABLE OF CONTENTS

LIST OF ILLUSTRATIONS

LIST OF ILLUSTRATIONS
(Continued)

LIST OF ILLUSTRATIONS
(Continued)

LIST OF ILLUSTRATIONS
(Continued)

LIST OF TABLES

LIST OF TABLES
(Continued)

ABSTRACT

Schooner, a nuclear cratering detonation, provides experimental verification of scaling theory which shows that so far as generation of seismic motions is concerned, a cratering detonation can be considered as a contained detonation buried at a relatively shallow depth.

Comparison of the seismic data observed from Schooner and other cratering and contained detonations at Nevada Test Site shows several basic differences in the characteristics of the ground motion. The shallow depth of burial of the cratering detonation causes the seismic energy efficiency to be significantly diminished relative to that of an equivalent yield contained detonation. The spectral composition of the ground motion generated by a cratering detonation is characterized by a lower amplitude level and a shift to the low frequency end of the spectrum. The general deficiency of high frequencies causes the peak vector particle velocities and accelerations to be lower than mean values predicted on the basis of experience with equivalent yield contained detonations. The peak vector particle velocity correlates almost exclusively with the surface wave mode time window for cratering detonations. The level of peak vector particle acceleration and velocity recorded from a cratering detonation at instrument

sites located on alluvium is significantly reduced, relative to that of equivalent yield contained detonations, as a consequence of the lower seismic energy efficiency and the reduced high frequency spectral composition.

The Schooner detonation provides data which will be useful in the prediction and analysis of future nuclear cratering detonations.

CHAPTER 1

INTRODUCTION

1.1 GENERAL BACKGROUND

As part of the continuing Plowshare Program, Project Schooner was a nuclear cratering experiment conducted by the Atomic Energy Commission to develop excavation technology through peaceful uses of nuclear explosives. Extension of this technology is essential to the planning of such proposed nuclear excavation as a sea level canal across the American Isthmus. Five previous cratering events at the Nevada Test Site (see Figure 1-1) are listed in chronological order below, along with a brief description of their respective environments.

- Danny Boy took place in the basalt caprock forming Buckboard Mesa, Area 18, NTS
- Sedan was a relatively large-yield event in the thick alluvium of Yucca Flat, Area 10, NTS
- Palanquin was detonated in a rhyolitic flow on Pahute Mesa, Area 20, NTS
- Cabriolet was about 3,000 feet from Palanquin and shared the same environment
- Buggy I was a row-charge event featuring 5 simultaneous and equally spaced detonations in the basalt caprock of Chukar Mesa, Area 30, NTS

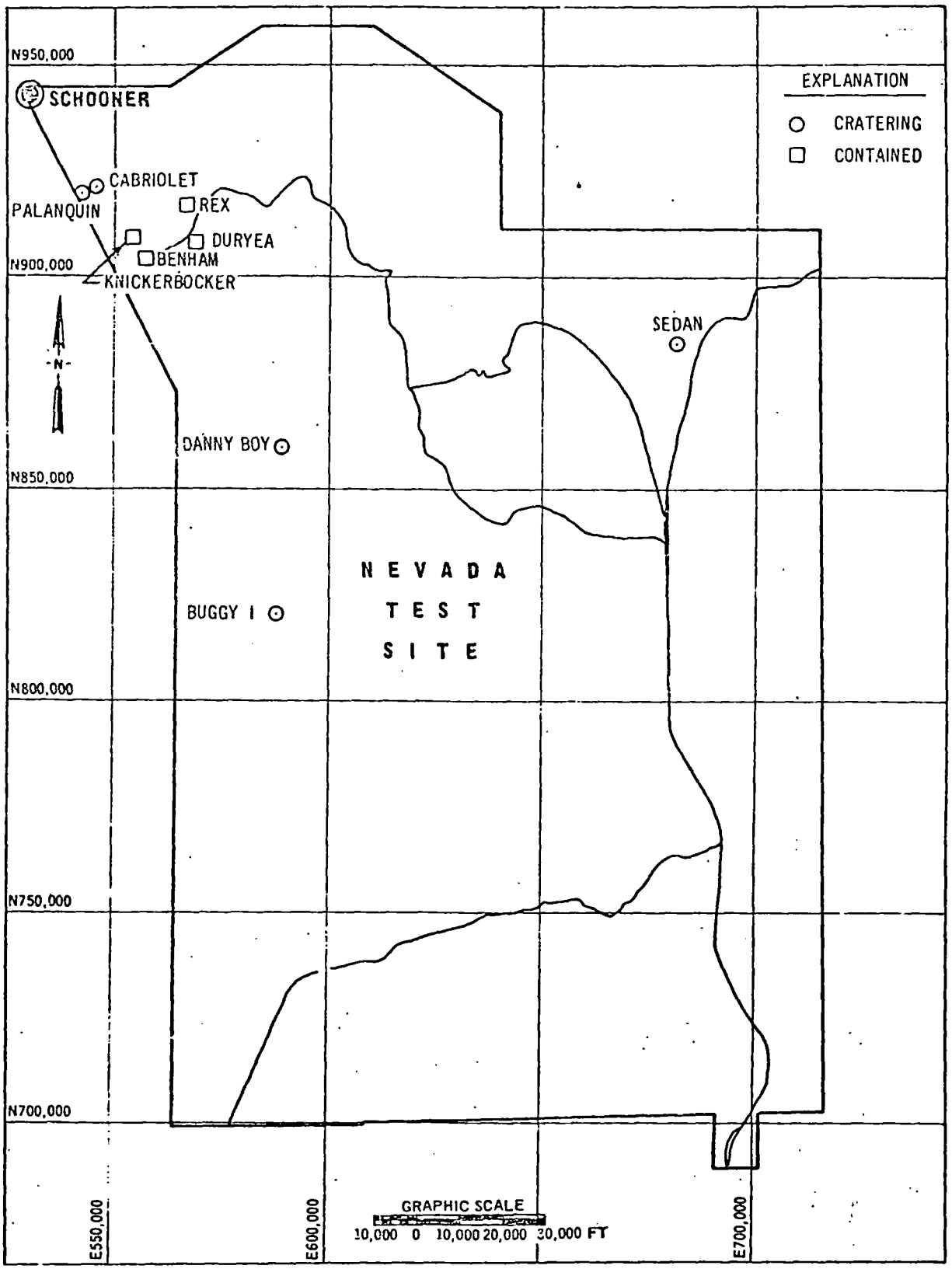

Figure 1-1. Area Map of Nevada Test Site Showing the Location of Schooner Relative to Five Other Nuclear Cratering Detonations and Four Nuclear Contained Detonations

Other nuclear and high explosive cratering experiments have been conducted, but because of their specialized nature, they are not incorporated in this study.

1.2 SCHOONER EVENT-ENVIRONMENT AND TECHNICAL DATA

The Schooner experiment consisted of the detonation of a minimum-fission nuclear device with a yield of 31±4 kilotons. The explosion took place at a depth of 355 feet in a layered tuffaceous medium of Area 20, Nevada Test Site, on December 8, 1968, at 0800:00.149.6 (PST), 1600:00.149.6 (GMT). The emplacement hole was U20u at geodetic coordinates:

Longitude W 116°33' 57.1419"
Latitude N 37°20' 36.3187"

and Nevada State Coordinates (Central Zone):

N 944,010.09
E 529,300.50

In this area of Pahute Mesa, relatively flat-lying ash-flow tuffs of Tertiary age crop out at the surface and display a thickness greater than 450 feet at the Schooner site. The surface topography is relatively flat with surface ground zero at an elevation of 5562.4 feet MSL. The nearest fault occurs about 2,000 feet from the crater. The water table is at a depth of approximately 1,300 feet in Pahute Mesa drill hole No. 2 (Figure 1-2) which is located some 860 feet northwest of the Schooner site.

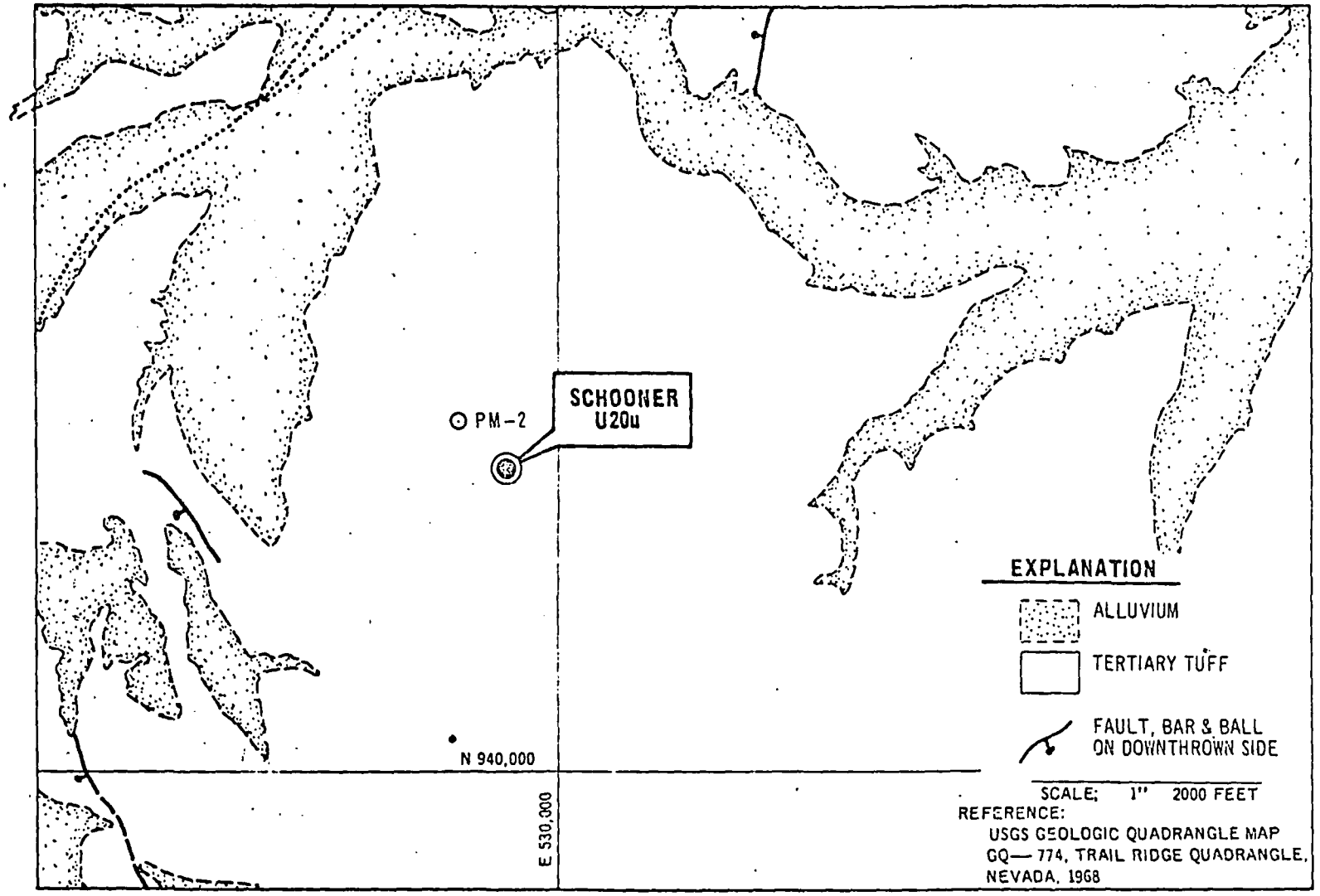

Figure 1-2. Generalized Geologic Map of the Schooner Crater Site, Pahute Mesa, Nevada

The crater resulting from the Schooner experiment was characterized by the following dimensions and volumes (Tewes, 1969):

1) Radius of apparent crater (R_a)... 129.8 meters 426 ft.

2) Maximum depth of apparent crater (D_a)..... 63.4 meters 208 ft.

3) Average apparent crater lip crest height (H_{al})..... 13.4 meters 44 ft.

4) Radius of apparent lip crest (R_{al})..... 147.2 meters 483 ft.

5) Radius of outer boundary of continuous ejecta (R_{eb})..... 539 meters 1768 ft.

6) Lip volume, apparent (V_{al})..... 2,099,000 cubic meters

..... 2,745,330 cubic yards

7) Crater volume, apparent (V_a)..... 1,745,000 cubic meters

..... 2,282,870 cubic yards

1.3 RESPONSIBILITY OF ERC IN PROJECT SCHOONER

Environmental Research Corporation, under contract to the Nevada Operations Office of the U. S. Atomic Energy Commission, is responsible to the Office of Effects Evaluation for providing ground motion evaluations of selected nuclear events. Our responsibility in Project Schooner was to provide the Office of Effects Evaluation with the following:

1. An instrumentation plan designed to document ground motions, utilizing available instruments.

2. Predictions of ground motion at each proposed instrument station for instrument calibration.

3. Processed seismic data (corrected seismograms, Band-Pass Filter (BPF) spectra, etc.).

4. Post-shot analysis of Schooner seismic data to determine relationship to predictions and data from other cratering experiments.

1.4 OBJECTIVES OF THIS REPORT

The objectives of this report are summarized as follows:

- To determine the amplitude and frequency characteristics of ground motion from the cratering event Schooner.
- To relate these results to the development of reliable techniques for predicting the ground motions from cratering events, utilizing theoretical and empirical scaling concepts.

Analyses related to these objectives are presented in detail in the chapters which follow. Chapter 2 contains descriptions of the instrumentation employed for the Schooner experiment and a discussion of the processed data utilized in the analysis. Peak ground motions are discussed in Chapter 3, and are compared with predicted values and data from past cratering events. The frequency content of seismic waves from Schooner is investigated and compared with seismic data from the Cabriolet cratering event at common stations. Theoretical scaling of amplitude spectra to simulate the effect of depth of burial for cratering and contained nuclear detonations is applied and analyzed.

In Chapter 4 the amplitude and frequency characteristics of elastic wave types generated by Schooner are determined and compared with similar data from other events.

Reasonable estimates of the radiated seismic energies from cratering and contained events are determined by procedures set forth in Chapter 5. Also the seismic efficiency of the Schooner event is analyzed and compared with the efficiency determined from contained events.

The basic conclusions of the various analyses are summarized in Chapter 6.

CHAPTER 2

DATA ACQUISITION AND PROCESSING

2.1 INSTRUMENTATION

The instrumentation plan for Schooner was designed with the following objectives in mind:

1. To obtain seismic data at points of interest to document the ground motion characteristics of Schooner.
2. To provide data for direct comparison of Schooner ground motions with ground motions from other cratering and contained events.
3. To generate a representative seismic data sample to use for predicting the ground motion characteristics of future cratering events.

The U.S. Coast and Geodetic Special Projects Party (USC&GS) deployed the 17 velocity instruments which recorded the Schooner event (see Figure 2-1). Of these 17 velocity meters, 14 were L-7's and 3 were NC-21's (King, 1969). These instruments recorded three orthogonal components of particle velocity on magnetic tape.

Seismic data recorded with the NC-21 velocity meters were processed and corrected for frequency response by ERC. Only the data recorded with the NC-21 velocity meters required a correction for frequency response (Table 2-1 shows the frequency range of

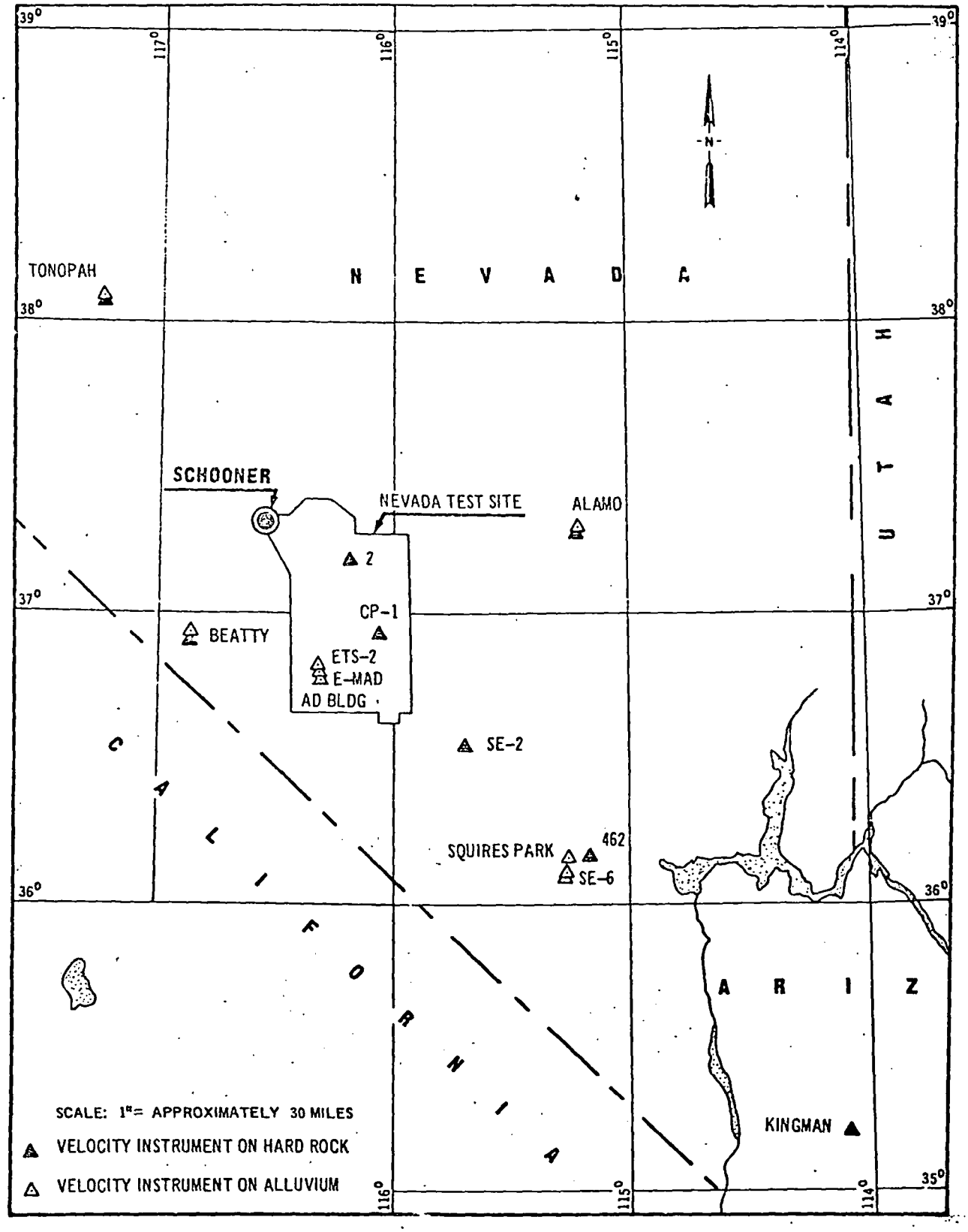

Figure 2-1. Map of Southeastern Nevada Showing Nevada Test Site and Schooner Instrument Stations

Table 2-1. FREQUENCY RANGE OF RECORDED GROUND MOTION DATA

Instrument Type	Frequency Range (Hz) of Instrument Response		Frequency Range (Hz) of Ground Motion after Instrument Correction	
	Low	High	Low	High
NC-21	1.0	45*	0.4	45*
L-7**	0.1	34***	0.1	34***

*Varies with filter setting

**No instrumentation correction applied; filtering applied to eliminate noise outside frequency range of interest

***Limited to 34 Hertz by tape speed

ground motion data recorded by each instrument). Also, particle acceleration and displacement seismograms were derived from the velocity data by differentiation and integration with respect to time.

Locations of the Schooner instrument stations are shown on Figure 2-1 and a summary of station environments, instrument type, and distances is listed in Table 2-2.

2.2 PEAK VECTOR GROUND MOTIONS

Peak values of particle acceleration, velocity and displacement were determined for each component. In addition, the peak value of the resultant vector was obtained to determine the absolute value of particle motion recorded at each station. The resultant vector magnitude is calculated by analyzing simultaneously the three components of motion as a function of time. The peak resultant vector is the largest instantaneous value of the square root of the sum of the squares of the amplitudes of the three components.

$$PM(t) = \sqrt{Z_p(t)^2 + R_p(t)^2 + T_p(t)^2}$$

where

PM = peak résultant vector

$Z_p(t)$ = value of vertical component

$R_p(t)$ = value of radial component

$T_p(t)$ = value of transverse component

TABLE 2-2. SUMMARY OF SCHOONER INSTRUMENT STATIONS YIELDING RECORDS PROCESSED BY ERC

Station	Station Abbreviation	Station Environment	Instrument Type	Slant Distance (km)
Area 12 Camp	2	Hard Rock	L-7	39.3
Beatty	BHR	Hard Rock	L-7	51.2
Beatty #2	BAL	Alluvium	L-7	51.7
ETS-2	ET2	Alluvium	L-7	61.1
E-MAD	E-MAD	Alluvium	L-7	63.9
CP-1	CP-1	Hard Rock	L-7	64.4
NRDS Admin. Bldg.	NRD	Alluvium	L-7	67.6
Tonopah Church	TCH	Hard Rock	NC-21	99.4
Tonopah Motel	TMT	Alluvium	NC-21	99.2
Indian Springs	SE-2	Thin Alluvium	L-7	119.3
Alamo	ALA	Alluvium	L-7	124.0
Alamo	AHR	Hard Rock	L-7	124.0
Squires Park	SQP	Alluvium	L-7	181.8
SE-6	SE-6	Alluvium	L-7, NC-21	187.3
Frenchman Mountain	462	Hard Rock	L-7	189.7
Kingman, Arizona	KAR	Hard Rock	L-7	340.0

The recorded peak values of each of the three components of velocity and the peak particle velocity vector are tabulated in Tables 2-3 and 2-4 for alluvium and hard rock stations respectively. Arrival times and the period of the peak particle velocity are also given in these tables. Values of the derived peak vector particle accelerations and displacements are given in Tables 2-5 and 2-6. The symbol notation used in the tables is as follows:

Instruments

L-7 = Mark Products Velocity Meter

NC-21 = National Geophysical Company Velocity Meter

Components

Z = vertical

R = radial

T = transverse

V = resultant vector

Peak Arrival Times

Arrival times are from shot time except when given in parentheses which indicates time after first motion.

TABLE 2-3. PEAK SURFACE VELOCITY RECORDED AT STATIONS ON ALLUVIUM

STATION/ INSTRUMENT	COMPONENT	DISTANCE (km)	FIRST ARRIVAL TIME (sec)	PEAK VELOCITY (cm/sec)	TIME OF PEAK (sec)	PERIOD (sec)
Beatty	Z	51.7	9.95	4.06×10^{-2}	33.95	1.10
(L-7)	R		9.95	6.03×10^{-2}	48.27	1.56
	T		9.95	3.58×10^{-2}	29.98	1.45
	V			6.84×10^{-2}	48.33	--
ETS-2	Z	61.1	11.55	4.96×10^{-2}	26.23	1.55
(L-7)	R		11.55	5.32×10^{-2}	25.08	0.66
	T		11.55	7.61×10^{-2}	42.12	1.70
	V			8.14×10^{-2}	42.13	--
E-MAD	Z	63.9	12.65	4.55×10^{-2}	49.48	1.45
(L-7)	R		12.65	4.76×10^{-2}	29.20	1.28
	T		12.65	6.97×10^{-2}	50.17	1.92
	V			8.37×10^{-2}	45.35	--
NRDS	Z	67.5	13.35	5.88×10^{-2}	53.88	1.45
Adm. Bldg.	R		13.35	1.01×10^{-1}	29.23	0.82
(L-7)	T		13.35	6.85×10^{-2}	29.00	0.73
	V			1.05×10^{-1}	29.28	--
Tonopah	Z	99.2	--	9.68×10^{-3}	(47.22)	1.77
Motel	R		--	1.47×10^{-2}	(15.24)	0.53
(NC-21)	T		--	2.14×10^{-2}	(19.79)	0.53
	V			2.30×10^{-2}	(19.86)	--
Alamo	Z	124.0	22.65	1.22×10^{-2}	23.85	0.70
(L-7)	R		22.65	2.26×10^{-2}	58.13	0.82
	T		22.65	2.57×10^{-2}	43.43	0.65
	V			3.28×10^{-2}	41.20	--
Squires	Z	181.8	33.05	1.64×10^{-2}	77.25	1.12
Park	R		33.05	3.00×10^{-2}	63.95	2.42
(L-7)	T		33.05	4.32×10^{-2}	64.99	1.74
	V			4.34×10^{-2}	65.07	--
SE-6	Z	187.3	--	2.64×10^{-2}	(92.58)	1.42
(L-7)	N/S		--	5.59×10^{-2}	(64.08)	2.15
	E/W		--	5.10×10^{-2}	(34.08)	1.15
	V			7.02×10^{-2}	(40.90)	--
SE-6	Z	187.3	--	1.16×10^{-2}	(39.12)	1.73
(NC-21)	N/S		--	--	--	--
	E/W		--	2.05×10^{-2}	(33.90)	1.33
	V			2.16×10^{-2}	(33.95)	--

TABLE 2-4. PEAK SURFACE VELOCITY RECORDED AT STATIONS ON HARD ROCK

STATION/ INSTRUMENT	COMPONENT	DISTANCE (km)	FIRST ARRIVAL TIME (sec)	PEAK VELOCITY (cm/sec)	TIME OF PEAK (sec)	PERIOD (sec)
2	Z	39.3	10.35	3.33×10^{-2}	51.12	1.48
(L-7)	R		10.35	4.54×10^{-2}	33.81	1.75
	T		10.35	3.80×10^{-2}	26.02	1.48
	V			5.06×10^{-2}	32.80	--
Beatty	Z	51.2	--	3.19×10^{-2}	(38.02)	1.63
(L-7)	R		--	4.30×10^{-2}	(37.48)	1.60
	T		--	2.95×10^{-2}	(34.57)	1.43
	V			4.72×10^{-2}	(37.47)	--
CP-1	Z	64.4	14.31	2.57×10^{-2}	36.94	1.30
(L-7)	R		14.31	3.61×10^{-2}	43.96	1.53
	T		14.31	3.81×10^{-2}	46.05	2.47
	V			4.51×10^{-2}	46.06	--
Tonopah	Z	99.4	--	1.10×10^{-2}	(48.15)	2.15
Church	R		--	1.38×10^{-2}	(15.23)	0.75
(NC-21)	T		--	2.04×10^{-2}	(19.80)	0.58
	V			2.13×10^{-2}	(19.83)	--
SE-2	Z	119.3	20.75	8.17×10^{-3}	22.29	0.56
(L-7)	R		20.75	1.07×10^{-2}	75.27	1.70
	T		20.75	9.03×10^{-3}	46.02	0.87
	V			1.14×10^{-2}	75.29	--
Alamo	Z	124.0	22.95	1.50×10^{-2}	23.78	0.76
(L-7)	R		22.95	2.03×10^{-2}	41.20	1.22
	T		22.95	2.35×10^{-2}	56.35	1.18
	V			2.49×10^{-2}	55.66	--
462	Z	189.7	31.85	5.25×10^{-3}	66.26	1.44
(L-7)	R		31.85	3.50×10^{-3}	66.46	1.33
	T		31.85	6.00×10^{-3}	63.46	1.08
	V			6.88×10^{-3}	63.55	--
Kingman	Z	340.0	57.65	1.93×10^{-3}	137.52	3.07
(Arizona)	R		57.65	1.39×10^{-3}	128.88	1.95
(L-7)	T		57.65	1.26×10^{-3}	110.72	1.27
	V			2.02×10^{-3}	137.53	--

TABLE 2-5. DERIVED PEAK ACCELERATION AND DISPLACEMENT AT STATIONS ON HARD ROCK

STATION/ INSTRUMENT	COMPONENT	DISTANCE (km)	PEAK ACCELERATION (g)	PEAK DISPLACEMENT (cm)
2	Z	39.3	--	8.88×10^{-3}
(L-7)	R		--	1.48×10^{-2}
	T		--	7.92×10^{-3}
	V			1.83×10^{-2}
Beatty	Z	51.2	--	8.21×10^{-3}
(L-7)	R		--	1.11×10^{-2}
	T		--	7.24×10^{-3}
	V		--	1.21×10^{-2}
CP-1	Z	64.4	1.05×10^{-4}	6.86×10^{-3}
(L-7)	R		1.30×10^{-4}	9.62×10^{-3}
	T		1.27×10^{-4}	1.40×10^{-2}
	V		1.47×10^{-4}	1.56×10^{-2}
Tonopah	Z	99.4	9.69×10^{-5}	3.36×10^{-3}
Church	R		1.42×10^{-4}	2.85×10^{-3}
(NC-21)	T		1.78×10^{-4}	3.36×10^{-3}
	V		1.87×10^{-4}	4.14×10^{-3}
SE-2	Z	119.3	1.07×10^{-4}	2.15×10^{-3}
(L-7)	R		1.10×10^{-4}	3.36×10^{-3}
	T		9.31×10^{-5}	3.06×10^{-3}
	V		1.19×10^{-4}	3.61×10^{-3}
Alamo	Z	124.0	1.27×10^{-4}	2.20×10^{-3}
(L-7)	R		1.56×10^{-4}	3.96×10^{-3}
	T		1.81×10^{-4}	5.00×10^{-3}
	V		2.19×10^{-4}	5.97×10^{-3}
462	Z	189.7	2.96×10^{-5}	1.44×10^{-3}
(L-7)	R		2.56×10^{-5}	1.06×10^{-3}
	T		3.28×10^{-5}	1.50×10^{-3}
	V		3.92×10^{-5}	1.62×10^{-3}
Kingman,	Z	340.0	1.24×10^{-5}	4.95×10^{-4}
Arizona	R		9.15×10^{-6}	4.20×10^{-4}
(L-7)	T		9.42×10^{-6}	3.75×10^{-4}
	V		1.51×10^{-5}	7.80×10^{-4}

TABLE 2-6. DERIVED PEAK ACCELERATION AND DISPLACEMENT AT STATIONS ON ALLUVIUM

STATION/ INSTRUMENT	COMPONENT	DISTANCE (km)	PEAK ACCELERATION (g)	PEAK DISPLACEMENT (cm)
Beatty	Z	51.7	--	9.05×10^{-3}
(L-7)	R		--	1.56×10^{-2}
	T		--	8.52×10^{-3}
	V		--	1.72×10^{-2}
ETS-2	Z	61.1	5.30×10^{-4}	1.25×10^{-2}
(L-7)	R		6.91×10^{-4}	1.23×10^{-2}
	T		5.41×10^{-4}	1.93×10^{-2}
	V		7.61×10^{-4}	2.16×10^{-2}
E-MAD	Z	63.9	--	1.08×10^{-2}
(L-7)	R		--	1.13×10^{-2}
	T		--	1.93×10^{-2}
	V		--	2.18×10^{-2}
NRDS	Z	67.5	4.69×10^{-4}	1.47×10^{-2}
Adm. Bldg.	R		6.83×10^{-4}	2.02×10^{-2}
(L-7)	T		4.79×10^{-4}	1.33×10^{-2}
	V		7.21×10^{-4}	2.26×10^{-2}
Tonopah	Z	99.2	1.41×10^{-4}	3.55×10^{-3}
Motel	R		2.60×10^{-4}	2.66×10^{-3}
(NC-21)	T		2.69×10^{-4}	3.60×10^{-3}
	V		2.83×10^{-4}	4.22×10^{-3}
Alamo	Z	124.0	1.18×10^{-4}	2.40×10^{-3}
(L-7)	R		2.33×10^{-4}	5.16×10^{-3}
	T		3.20×10^{-4}	4.80×10^{-3}
	V		3.52×10^{-4}	5.64×10^{-3}
Squires	Z	181.8	1.04×10^{-4}	3.83×10^{-3}
Park	R		1.80×10^{-4}	9.34×10^{-3}
(L-7)	T		2.13×10^{-4}	1.18×10^{-2}
	V		2.20×10^{-4}	1.19×10^{-2}

(Continued on following page)

TABLE 2-6. DERIVED PEAK ACCELERATION AND DISPLACEMENT AT STATIONS ON ALLUVIUM (Continued)

STATION/ INSTRUMENT	COMPONENT	DISTANCE (km)	PEAK ACCELERATION (g)	PEAK DISPLACEMENT (cm)
SE-6	Z	187.3	1.62×10^{-4}	6.67×10^{-3}
(L-7)	N/S		3.90×10^{-4}	1.69×10^{-2}
	E/W		2.89×10^{-4}	1.28×10^{-2}
	V		4.11×10^{-4}	1.72×10^{-2}
SE-6	Z	187.3	5.70×10^{-5}	2.44×10^{-3}
(NC-21)	N/S		--	--
	E/W		1.12×10^{-4}	5.20×10^{-3}
	V		--	--

2.3 BAND-PASS FILTER SPECTRA

Band-pass filtering of a seismogram is a technique developed to analyze the peak particle velocity recorded from nuclear events as a function of frequency. The three components of particle velocity of a seismogram are individually passed through twelve narrow band-pass filters to obtain information relating to the frequency content of the seismic signal. The peak amplitude of the output from each filter is plotted as a function of the center frequency of the filter and the points are connected, giving a continuous curve called the BPF spectrum.

Band-pass filter spectra from the Schooner event are shown on Figures 2-2 through 2-5. Superposed on each graph is the mean BPF spectrum typically measured at that distance from a contained NTS event of the yield of Schooner. The mean BPF spectrum shown is based on frequency, yield and distance dependent regression equations derived from band-pass filter data observed from 20 underground nuclear detonations at Nevada Test Site. The data sample contains approximately 2,400 spectral amplitudes over the frequency range 0.4 - 11.3 Hz. The distance and yield ranges of the data are 40 - 200 km and 16 kt (yield of Rex) - 825 kt (yield of Greeley), respectively. Thus, the BPF spectrum defined by these equations represents a good approximation of the average spectral composition observed from contained Nevada Test Site detonations.

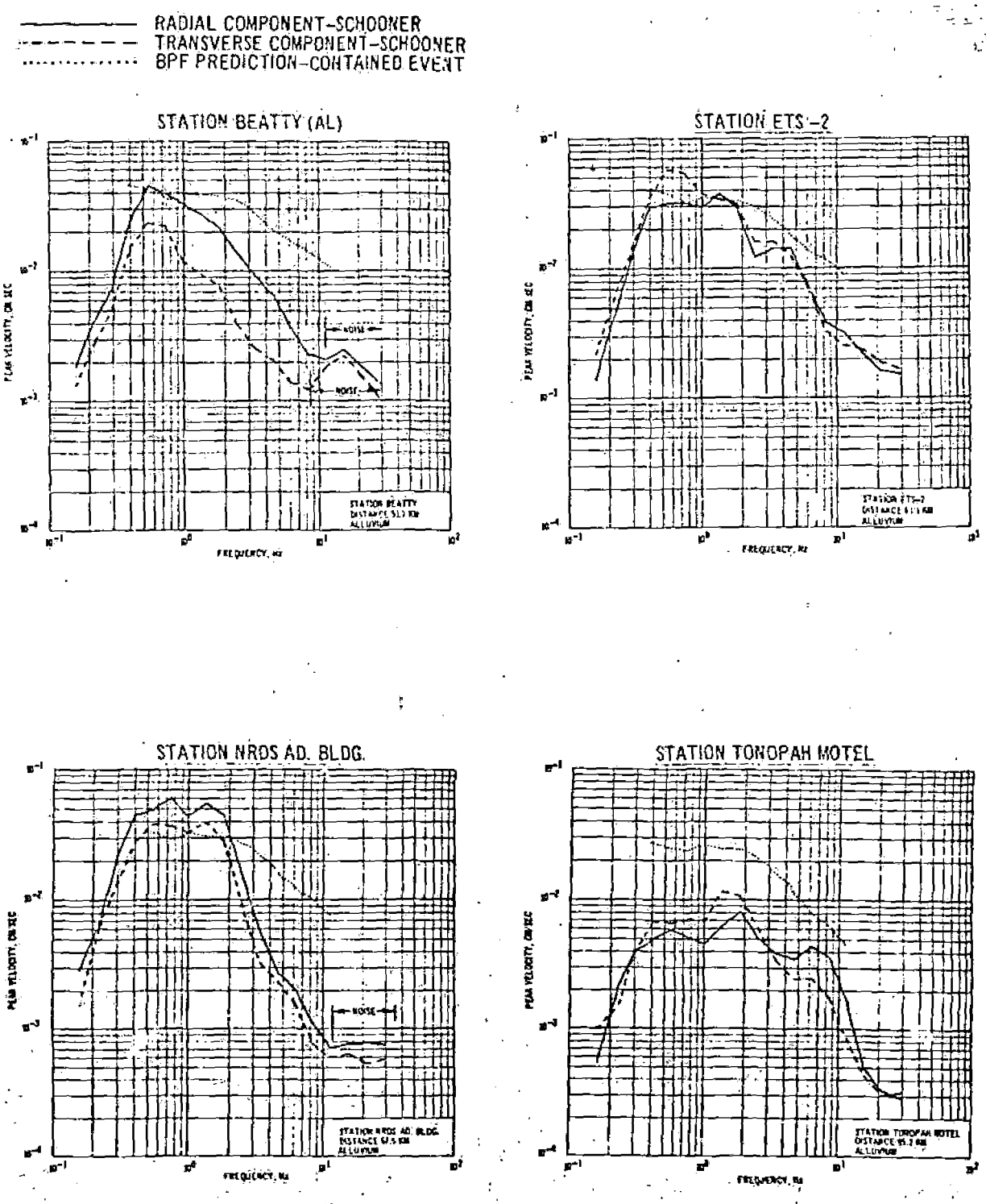

Figure 2-2. Comparison of Observed (Schooner Detonation) and Predicted (equivalent yield contained detonation) BPF Spectra

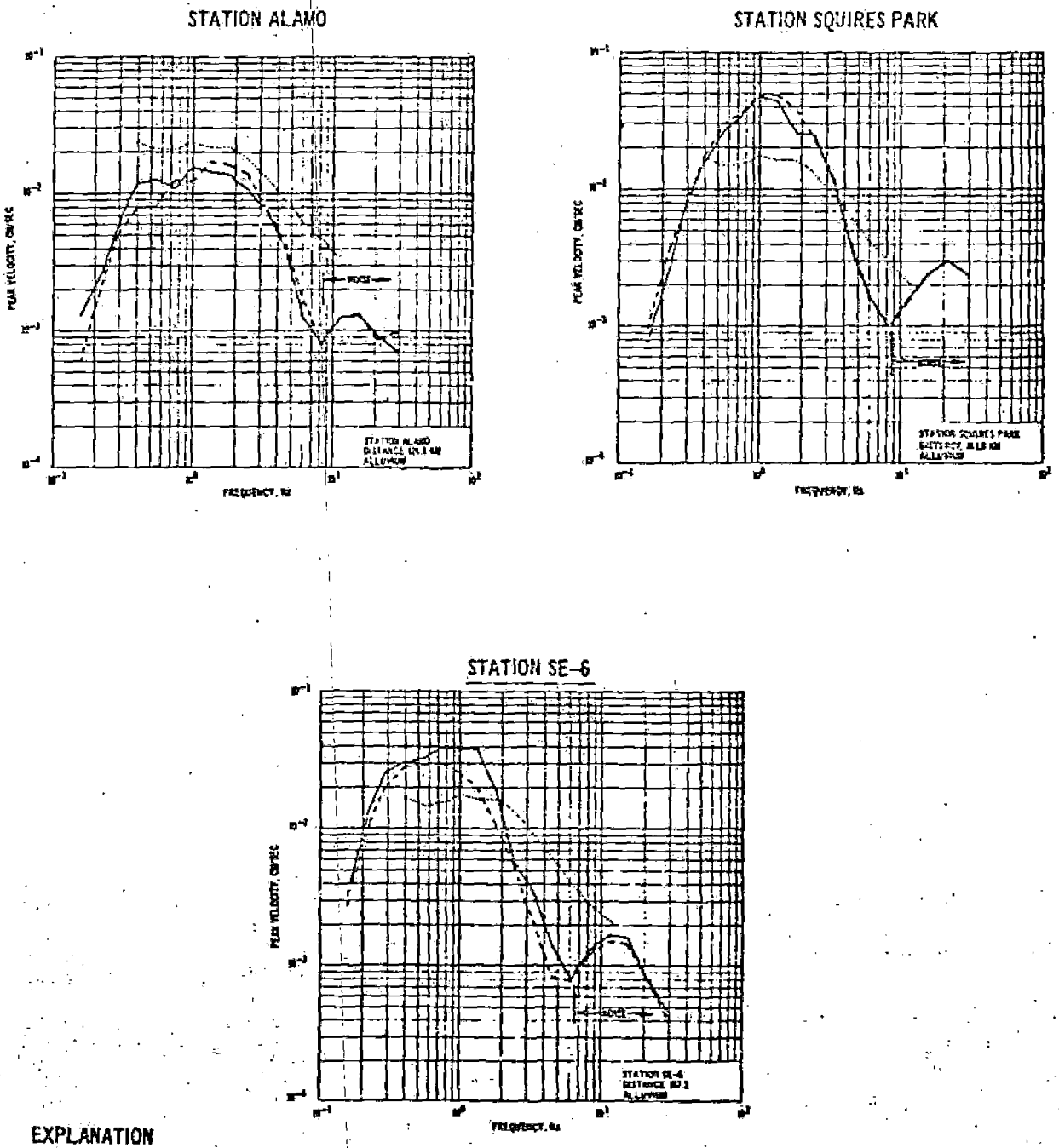

Figure 2-3. Comparison of Observed (Schooner Detonation) and Predicted (equivalent yield contained detonation) BPF Spectra

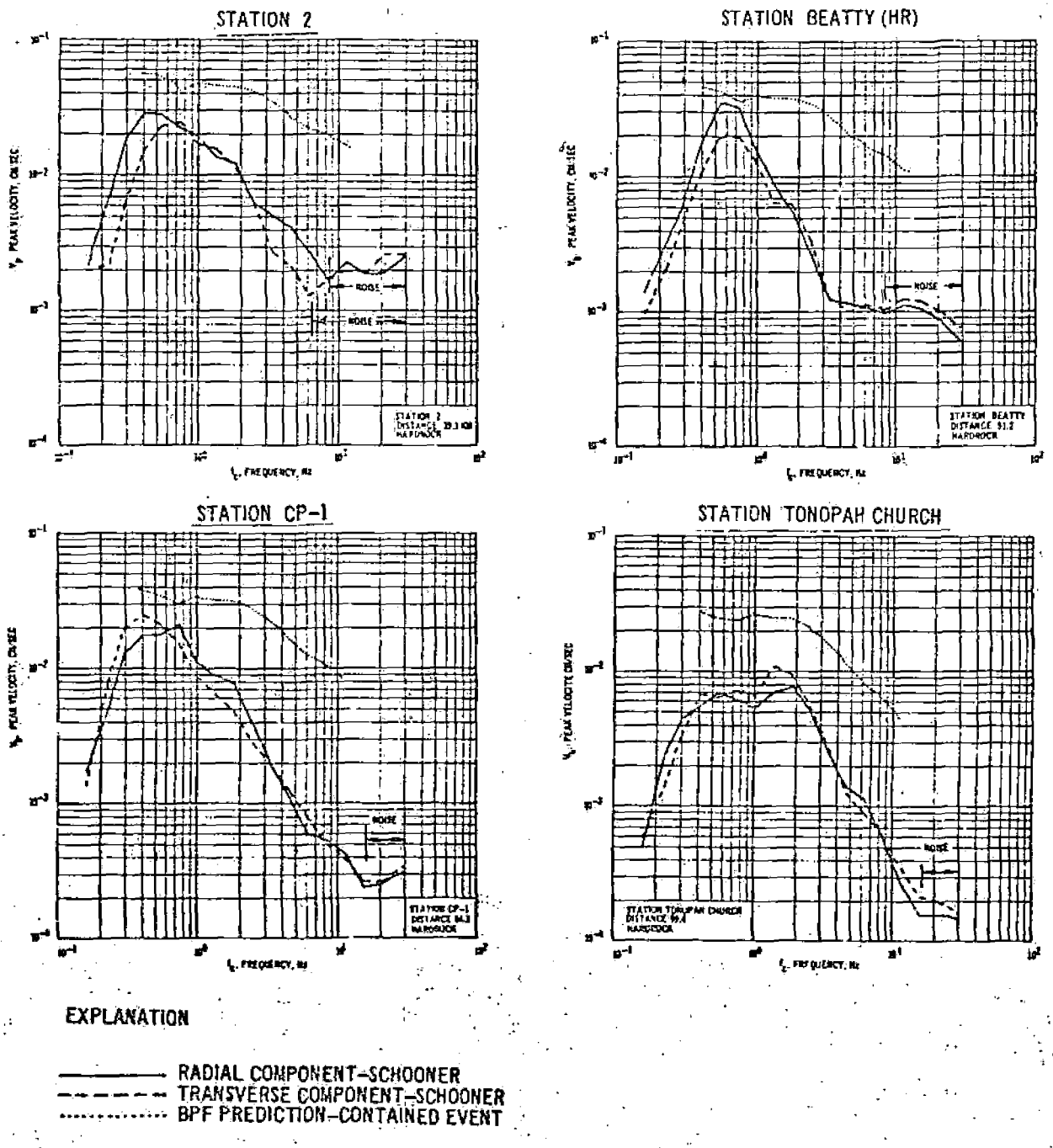

Figure 2-4. Comparison of Observed (Schooner Detonation) and Predicted (equivalent yield contained detonation) BPF Spectra

STATION ALAMO

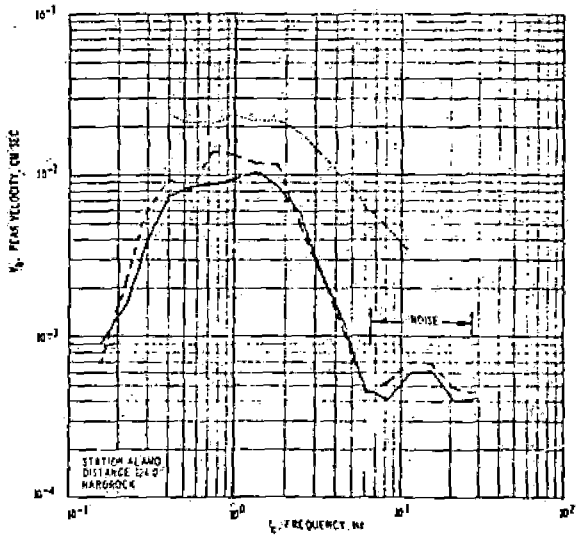

STATION 462

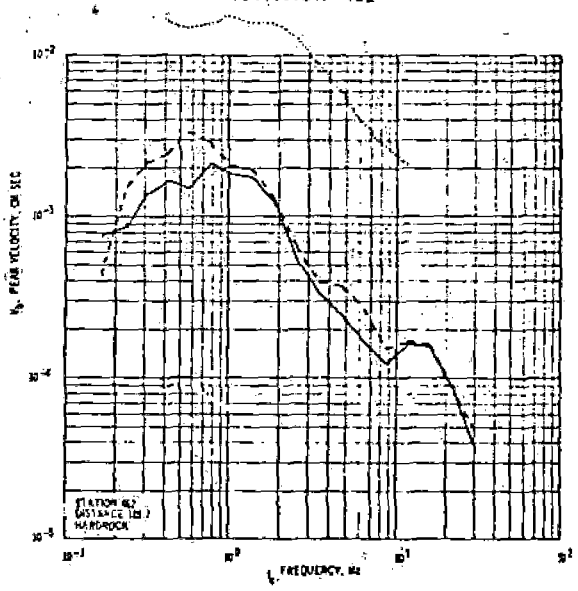

STATION KINGMAN

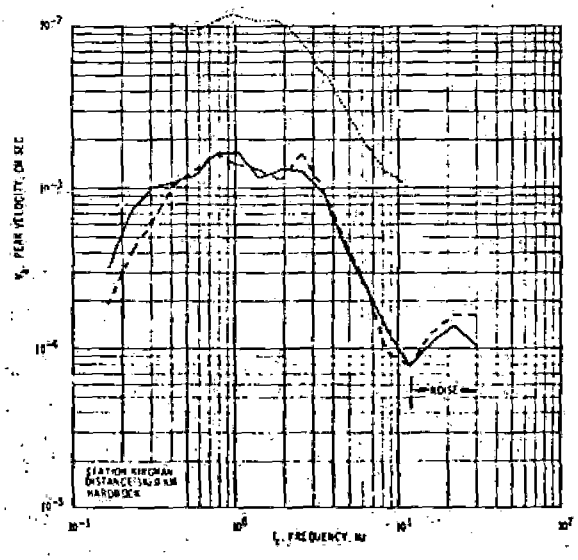

EXPLANATION

——— RADIAL COMPONENT–SCHOONER
– – – – – – TRANSVERSE COMPONENT–SCHOONER
..... BPF PREDICTION–CONTAINED EVENT

Figure 2-5. Comparison of Observed (Schooner Detonation) and Predicted (equivalent yield contained detonation) BPF Spectra

CHAPTER 3

ANALYSIS OF SCHOONER DATA

3.1 PEAK AMPLITUDE DATA

Multiple regression analyses, utilizing a large quantity of peak amplitude data recorded from 99 contained nuclear events detonated on the Nevada Test Site, have resulted in statistically based regression equations (Murphy and Lahoud, 1969). These equations are currently being used to predict the mean peak resultant vector ground motions expected from nuclear tests. A corresponding data sample is not yet available for cratering events. Although only limited cratering data are available, it is now established (Klepinger and Mueller, 1969 and Chapters 4 and 5 of this report) that the amplitude and spectral characteristics of ground motions from cratering events, as well as seismic efficiency, are quite different from that of contained events.

In an effort to define these differences, Klepinger and Mueller (1969) performed a regression analysis on the peak amplitude data sample from the Cabriolet, Palanquin, Sedan, and Danny Boy cratering events. The results of this analysis, and the analysis for contained events discussed above, are compared with Schooner results on Figures 3-1 through 3-6. These figures show

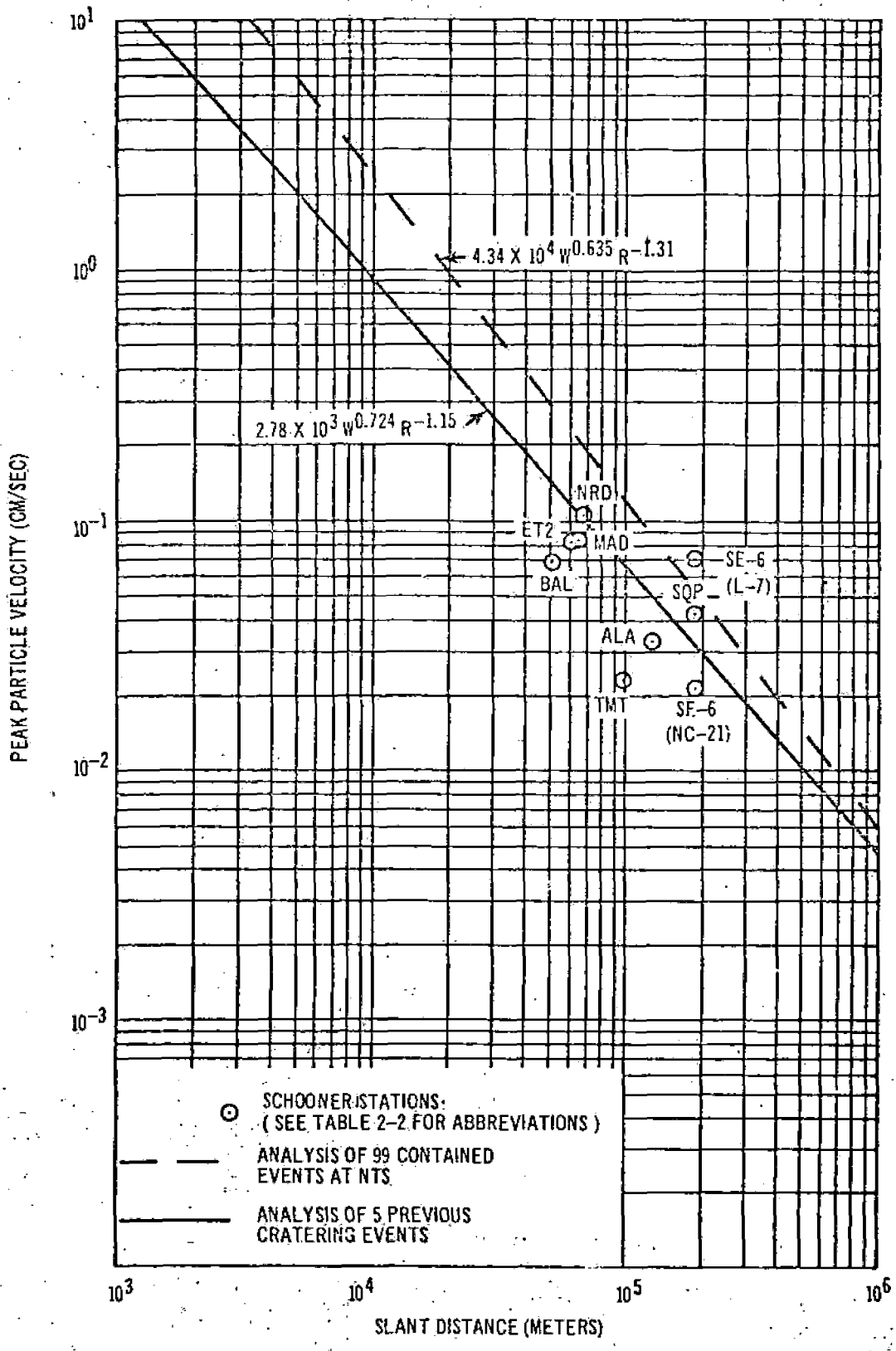

Figure 3-1. Peak Particle Resultant Vector Velocities Recorded for Schooner Compared to Multiple Regression Analyses of Contained and Cratering Event Velocities - Alluvium Sites

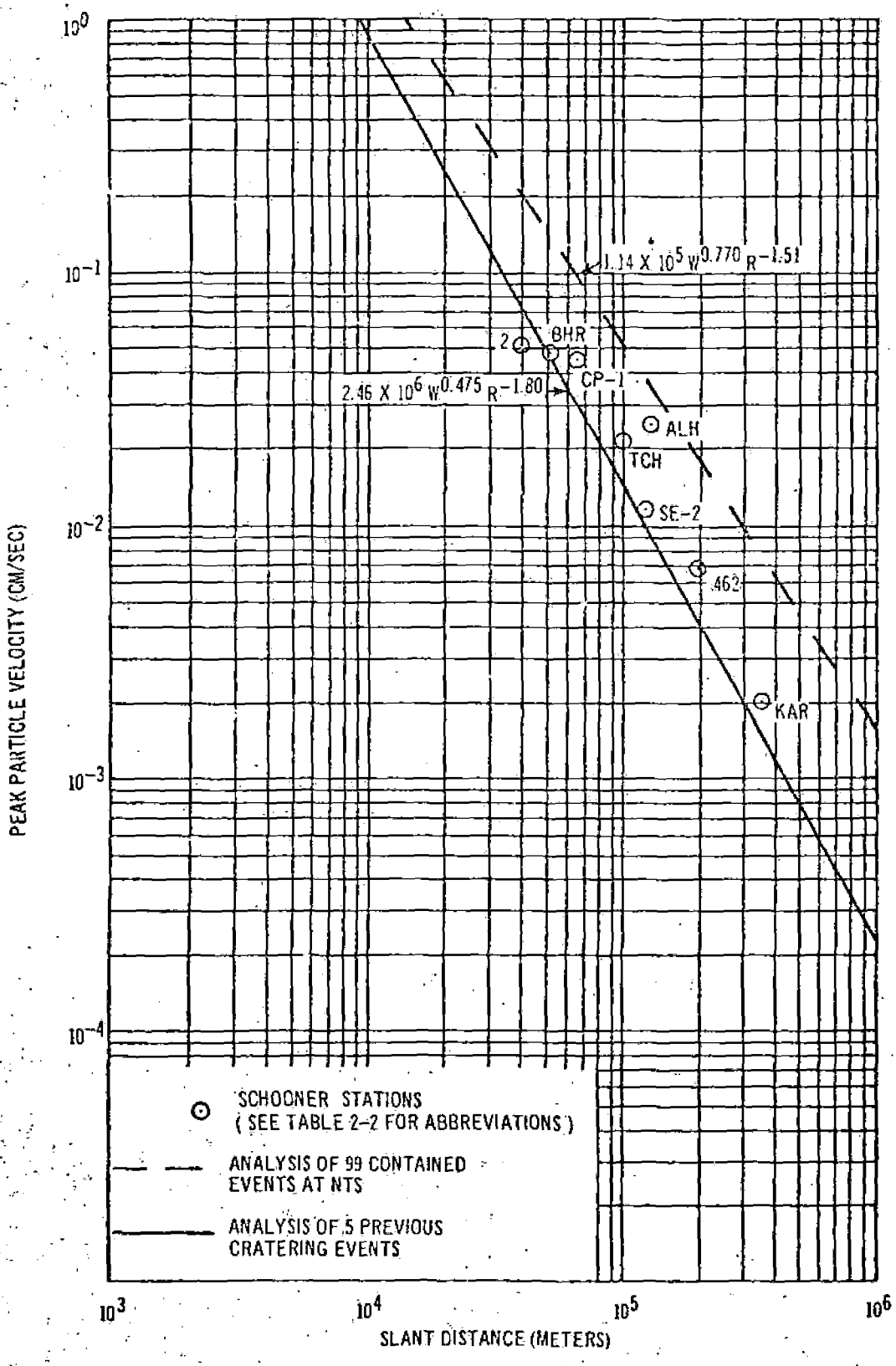

Figure 3-2. Peak Particle Resultant Vector Velocities Recorded for Schooner Compared to Multiple Regression Analyses of Contained and Cratering Event Velocities - Hard Rock Sites

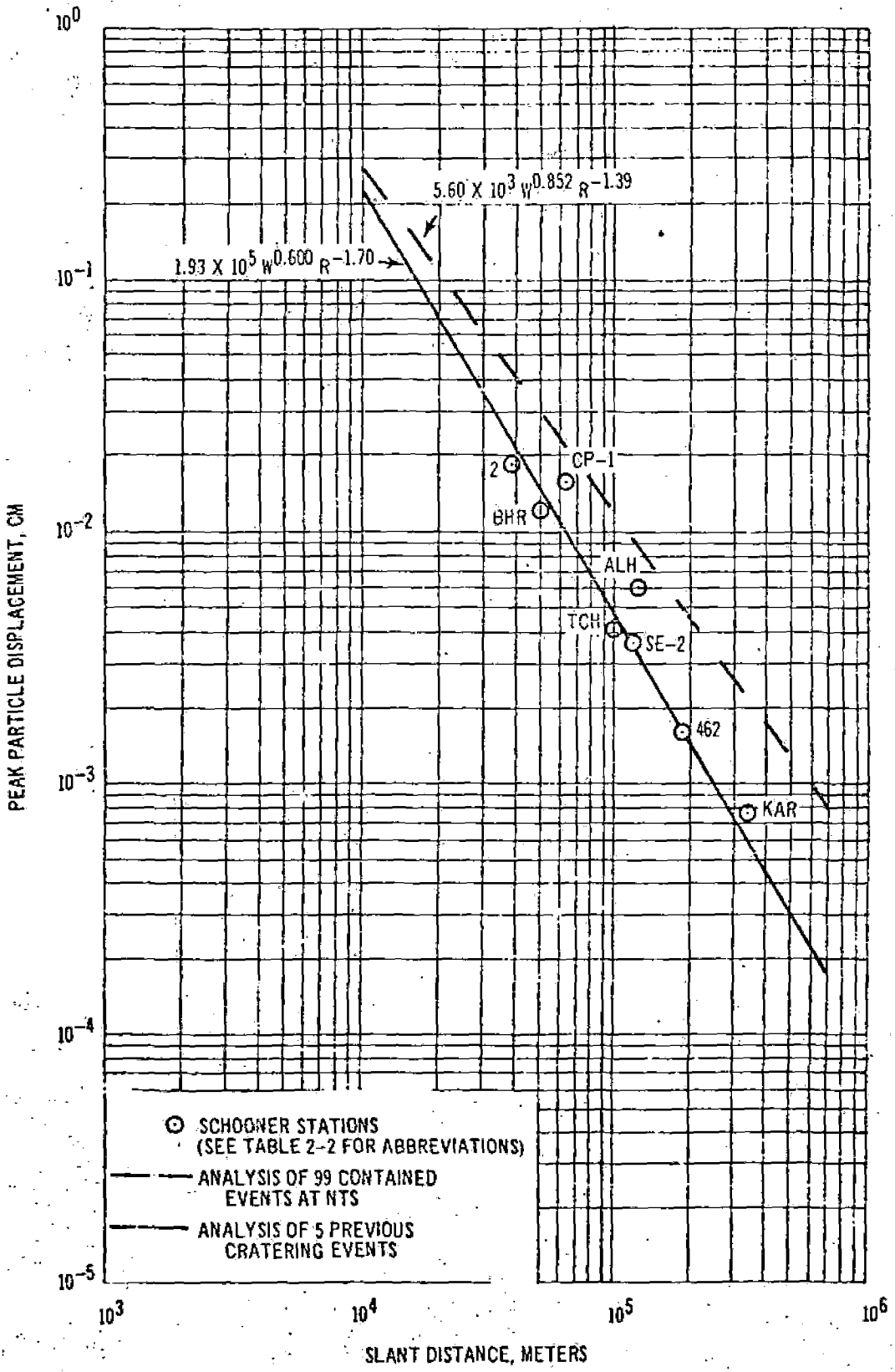

Figure 3-3. Peak Particle Resultant Vector Displacements Derived from Schooner Particle Velocity Seismograms Compared to Multiple Regression Analyses of Contained and Cratering Event Displacements - Hard Rock Sites

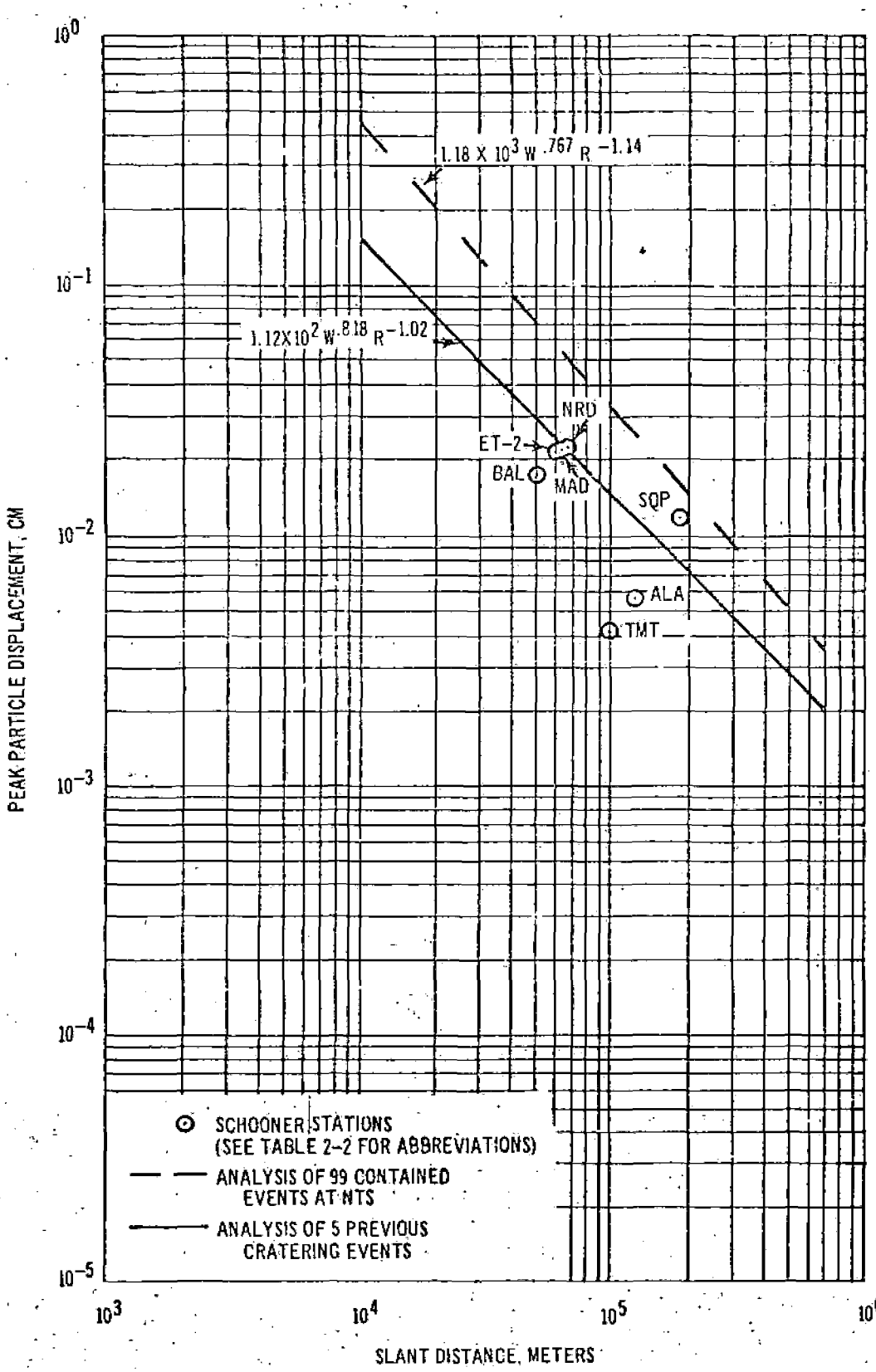

Figure 3-4. Peak Particle Resultant Vector Displacements Derived from Schooner Particle Velocity Seismograms Compared to Multiple Regression Analyses of Contained and Cratering Event Displacements - Alluvium Sites

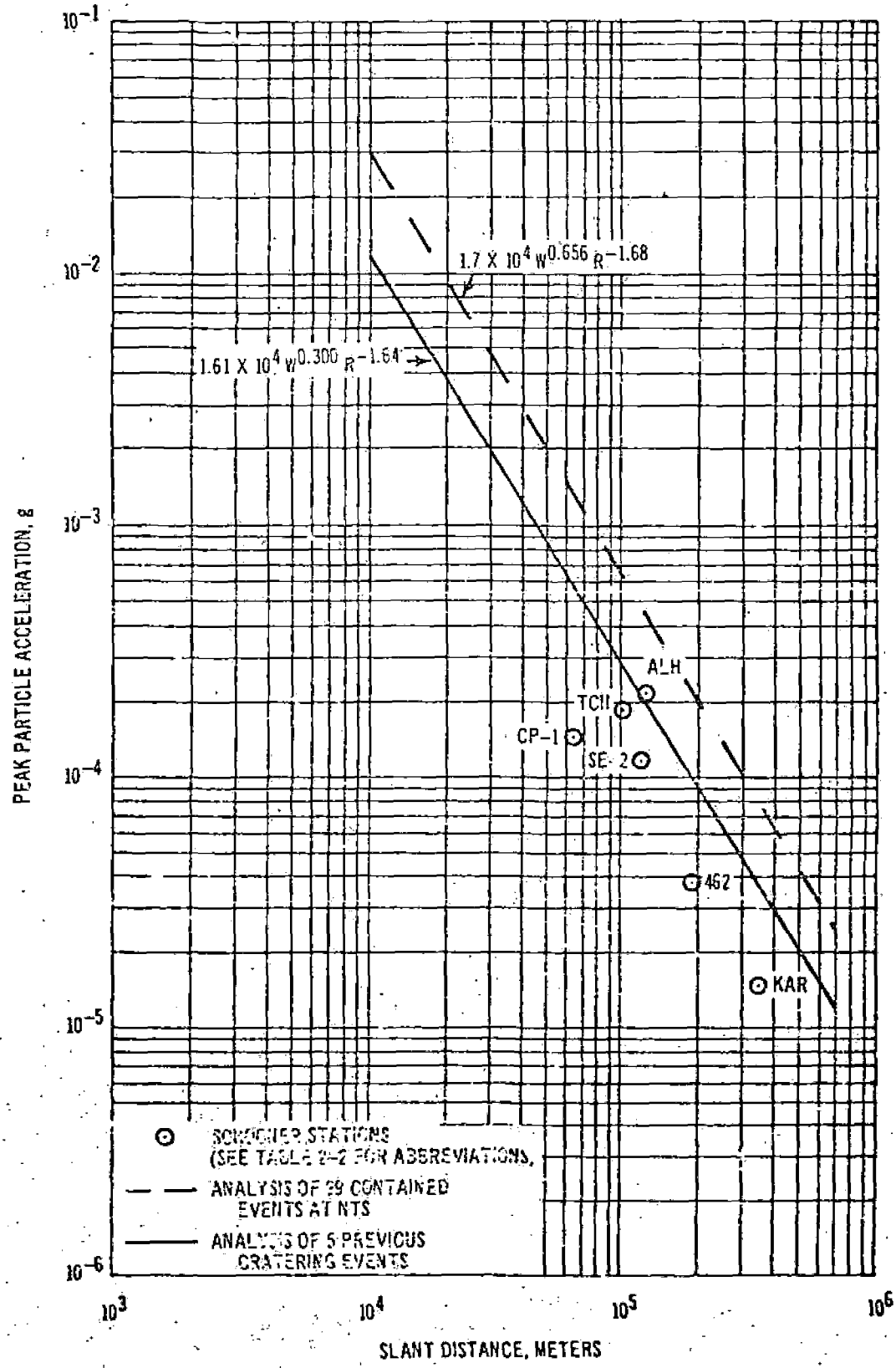

Figure 3-5. Peak Particle Resultant Vector Accelerations Derived from Schooner Particle Velocity Seismograms Compared to Multiple Regression Analyses of Contained and Cratering Event Accelerations - Hard Rock Sites

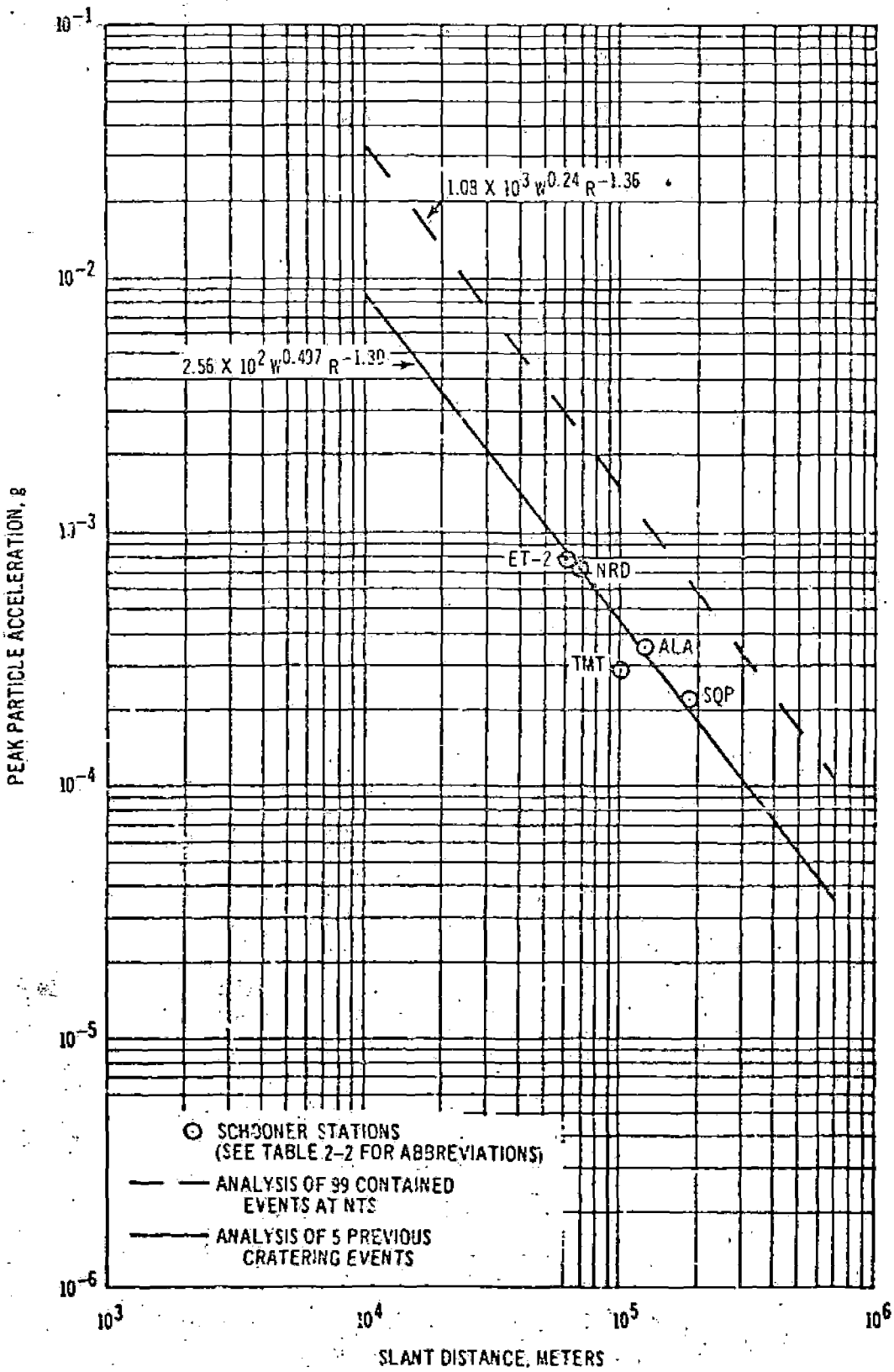

Figure 3-6. Peak Particle Resultant Vector Accelerations Derived from Schooner Particle Velocity Seismograms Compared to Multiple Regression Analyses of Contained and Cratering Event Accelerations - Alluvium Sites

Schooner peak resultant vector particle motions recorded at alluvium and hard rock sites as a function of station distance.

Superposed on these data points are the predicted values of peak particle motions made on the basis of the 99 event data sample and the cratering event data sample. The following observations are made on the basis of these data:

1. Schooner peak vector particle motions recorded at both hard rock and alluvium sites exhibit lower amplitudes than the particle motions predicted on the basis of contained events (with the exception of SE-6). This is consistent with previous experience (Klepinger and Mueller, 1969).

2. Previous experience (Klepinger and Mueller, 1969) indicates a tendency for ground motions generated by cratering events to attenuate faster at hard rock stations than corresponding ground motions from contained events. However, peak vector particle velocities from Schooner (Figure 3-2) appear to decay at about the same rate predicted on the basis of an equivalent yield contained event.

3. Predictions of peak motion based on equivalent yield contained events appear to be conservative estimates of the ground motion levels expected for cratering events. Additional cratering event data are required, however, to establish a sound statistical and physical basis for predicting cratering event peak particle ground motions.

3.2 AMPLITUDE-FREQUENCY DATA

The objectives of this section are twofold: 1) to examine the frequency content of the ground motion resulting from cratering and contained nuclear detonations in order to determine any significant and consistent patterns existing between the two types of

explosions, and 2) to evaluate the observations within a self-consistent theory on the scaling of the amplitude spectra of underground explosions. To accomplish these objectives, parameters influencing the seismic signals must be minimized such that comparisons of the amplitude spectra are effectively comparisons of the sources. Therefore, it is necessary to eliminate, as far as possible, transmission path variables, station site variables, and source media effects.

The contained nuclear detonations Knickerbocker, Duryea and Rex, were detonated within the immediate locality (10 km) of Schooner (Figure 1-1). These contained detonations were executed in rhyolite. Common stations instrumented for these detonations are given in Table 3-1. Comparisons of BPF at these common stations for the various events, scaled to the Cabriolet yield of 2.3 kt, should therefore, indicate any general pattern existing between cratering and contained shots.

Scaling of the Band-Pass Filter (BPF) spectrum, which is an approximation of the Fourier amplitude spectrum, is normally accomplished by applying frequency-dependent yield scaling exponents. These exponents are statistically derived from a large number of underground explosions, the major portion of which are buried at a set scaled depth of 350 to 450 (scaled depth is the ratio, depth

TABLE 3-1. SLANT DISTANCES OF COMMON STATIONS

STATION	EVENT				
	Schooner	Cabriolet	Knickerbocker	Duryea	Rex
SE-6	187.3 km	182.0 km	175.0 km	170.0 km	173.0 km
Alamo	124.0 km	123.0 km	120.0 km		
Tonopah Church	99.4 km	111.0 km	112.0 km	116.0 km	112.0 km
Tonopah Motel	99.2 km	111.0 km	112.0 km	116.0 km	112.0 km
CP-1	64.4 km	57.0 km		48.0 km	

of burial/cube root of yield). Therefore, the empirical scaling may be considered, as a fair approximation, to be scaling at a set scaled depth; although, it has been found theoretically that the yield exponents are also yield and depth dependent (Mueller, 1969) Schooner, Knickerbocker, Duryea and Rex BPF spectra were scaled to 2.3 Kt (Cabriolet yield) by use of the statistical exponents described above. Each spectrum is then appropriately scaled to the Cabriolet depth of burial. Knickerbocker and Duryea are buried at a normal scaled depth while Rex is slightly overburied. The depth of burial for Cabriolet is 171 feet.

Comparisons of the BPF spectra from cratering and contained explosions (Klepinger and Mueller, 1969 and Figures 2-2 through 2-5) indicate that the level and frequency content are different. The spectra from the cratering events are generally somewhat lower in magnitude and the dominant energy content is shifted to lower frequencies. The observation that the spectra are different is not an unexpected result, since cratering and contained events are explicitly different. The fundamental questions are in what respects are they different and how can this be formulated into a quantitative theory. The answers require a consideration of the elastic wave production mechanism and the parameters influencing this mechanism.

A theory using the solution of a spherically symmetric forcing function acting in an infinite homogeneous medium has been developed into a general scaling law of the amplitude spectrum for underground explosions (Mueller, 1969). The analytic development takes into account source parameters such as medium type and device depth of burial. For a particular medium, the elastic radii of two events of arbitrary yield and depth of burial vary as

$$\left(\frac{a_1}{a_2}\right) = \left(\frac{h_2}{h_1}\right)^{1/n} \left(\frac{W_1}{W_2}\right)^{1/3} \qquad (3\text{-}1)$$

where a_1 and a_2 are the elastic radii; i.e., the radii where the material behaves elastically, h_1 and h_2 are the depths of burial, and W_1 and W_2 are the yields of events 1 and 2, respectively. The parameter n is the distance exponent of the shock pressure (or velocity) in the inelastic region. Also, the seismic efficiency defined as the proportion of initial energy (E) reaching the radiation zone of the elastic region ($b = E/W$), for a particular medium, scales as

$$\frac{b_1}{b_2} = \left(\frac{h_1}{h_2}\right)^{2-3/n} \qquad (3\text{-}2)$$

for arbitrary yields and depths of burial. The scaling of the elastic radii, alone, determines the relative shape of the amplitude spectra, whereas the elastic radii in conjunction with the depths of burial determine the level of the spectra. For the rhyolite and tuff (Schooner) media in which these events were detonated, n was taken to be 2.4, the value observed for granite (Perret, 1963).

The BPF amplitude spectra of Schooner, Cabriolet, and the average spectra of the contained detonations, Knickerbocker, Duryea and Rex, (scaled to the Cabriolet yield and depth of burial by the theoretical scaling law) at the distant stations SE-6, Tonopah Church, Tonopah Motel and Alamo are shown in Figures 3-7 to 3-10. Also shown is the average of the empirically scaled spectra for the contained detonations. This average spectrum corresponds to the spectrum of a normal 2.3 kt contained detonation. In all cases the theoretically scaled spectra from the three contained events lie closer to the Schooner and Cabriolet spectra than the empirical curves; in some cases the agreement is excellent.

Two basic conclusions follow. First, as far as the seismic motion is concerned, the nuclear cratering detonations Schooner and Cabriolet may be considered as contained explosions buried

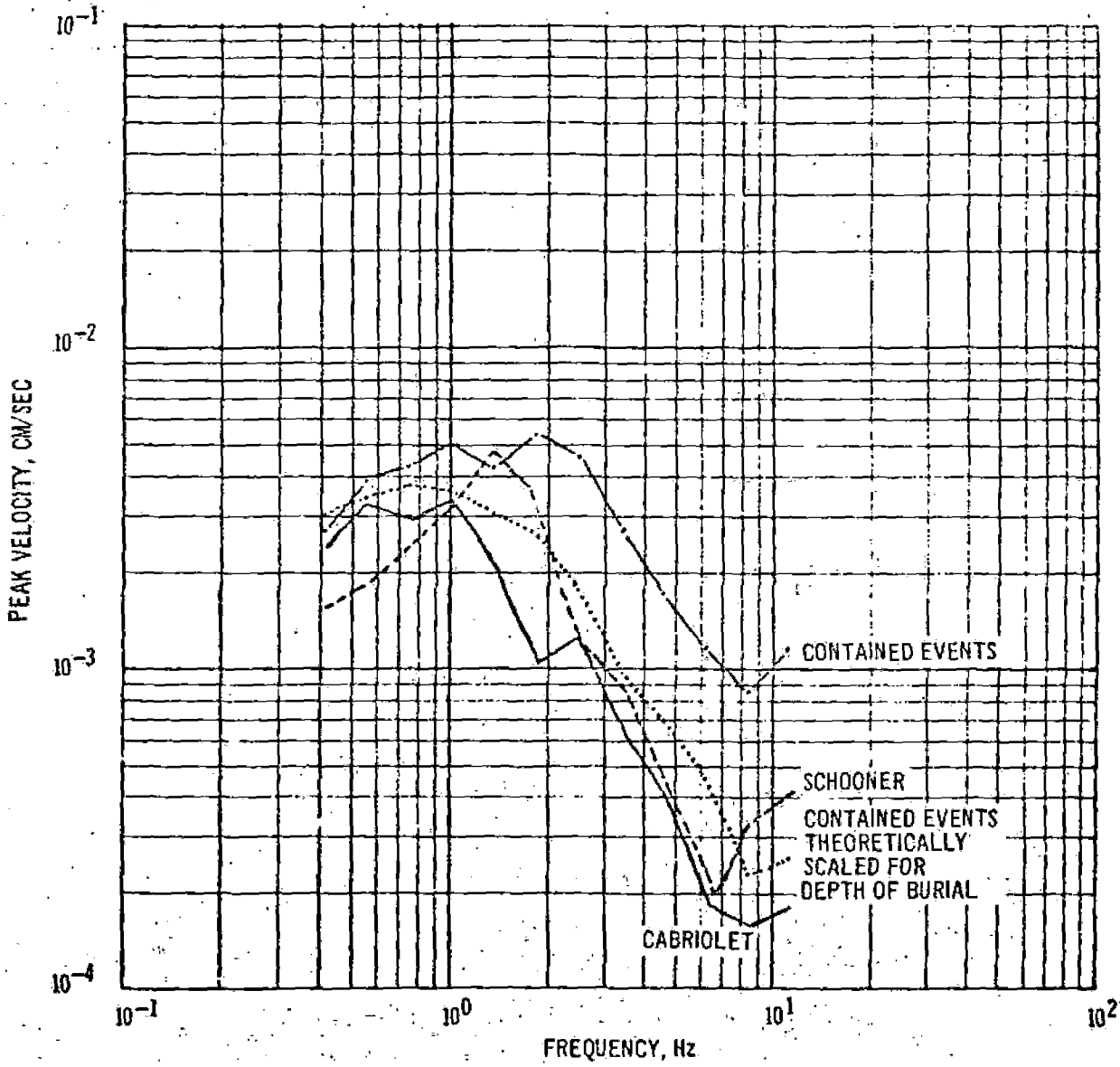

Figure 3-7. Comparison of LPF Data From Schooner, Cabriolet, and Contained Events (Knickerbocker, Duryea and Rex) at 2.3 kt, Radial Component, SE-6

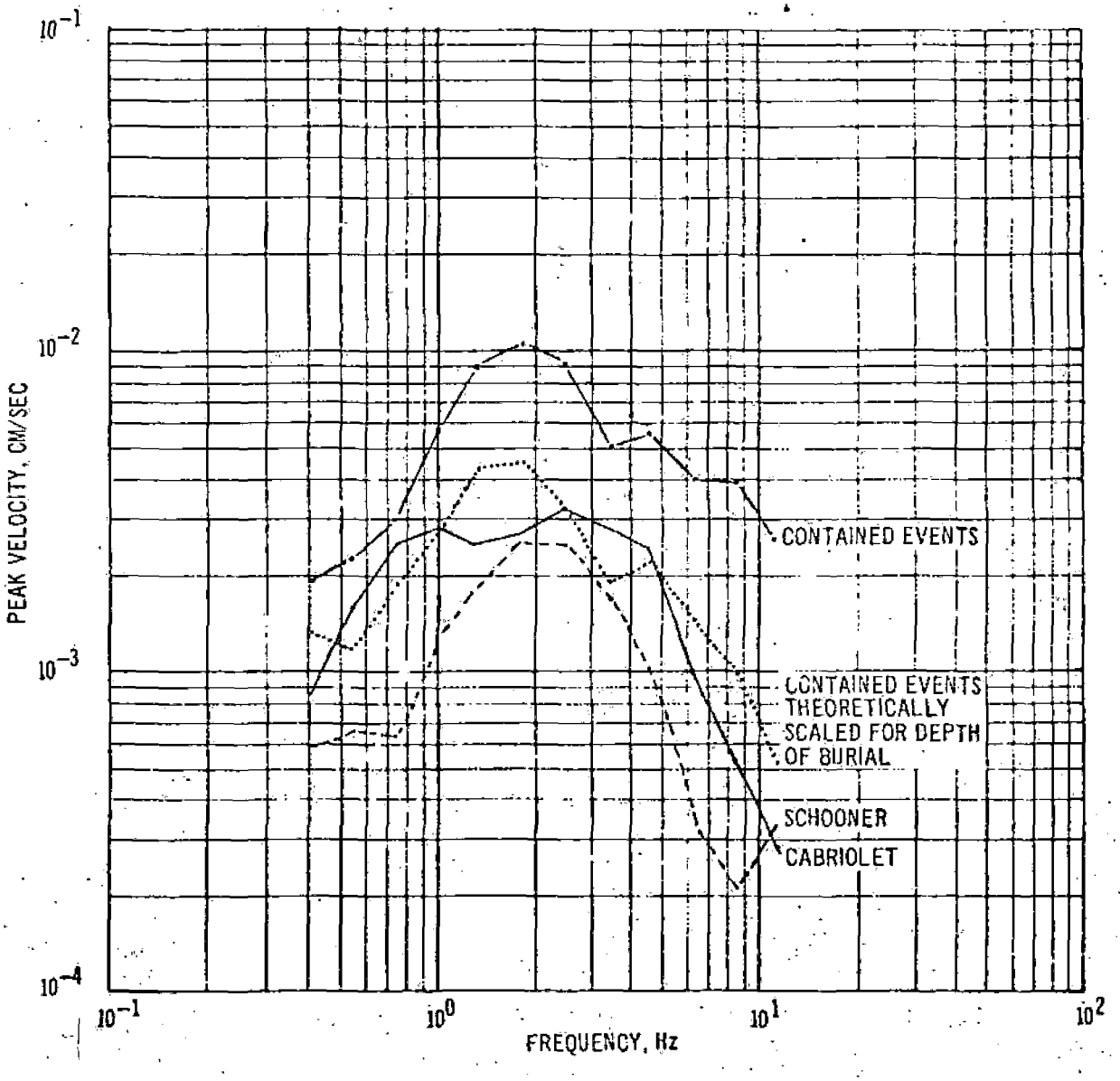

Figure 3-8. Comparison of BPF Data From Schooner, Cabriolet, and Contained Event (Knickerbocker) at 2.3 kt, Radial Component, Alamo

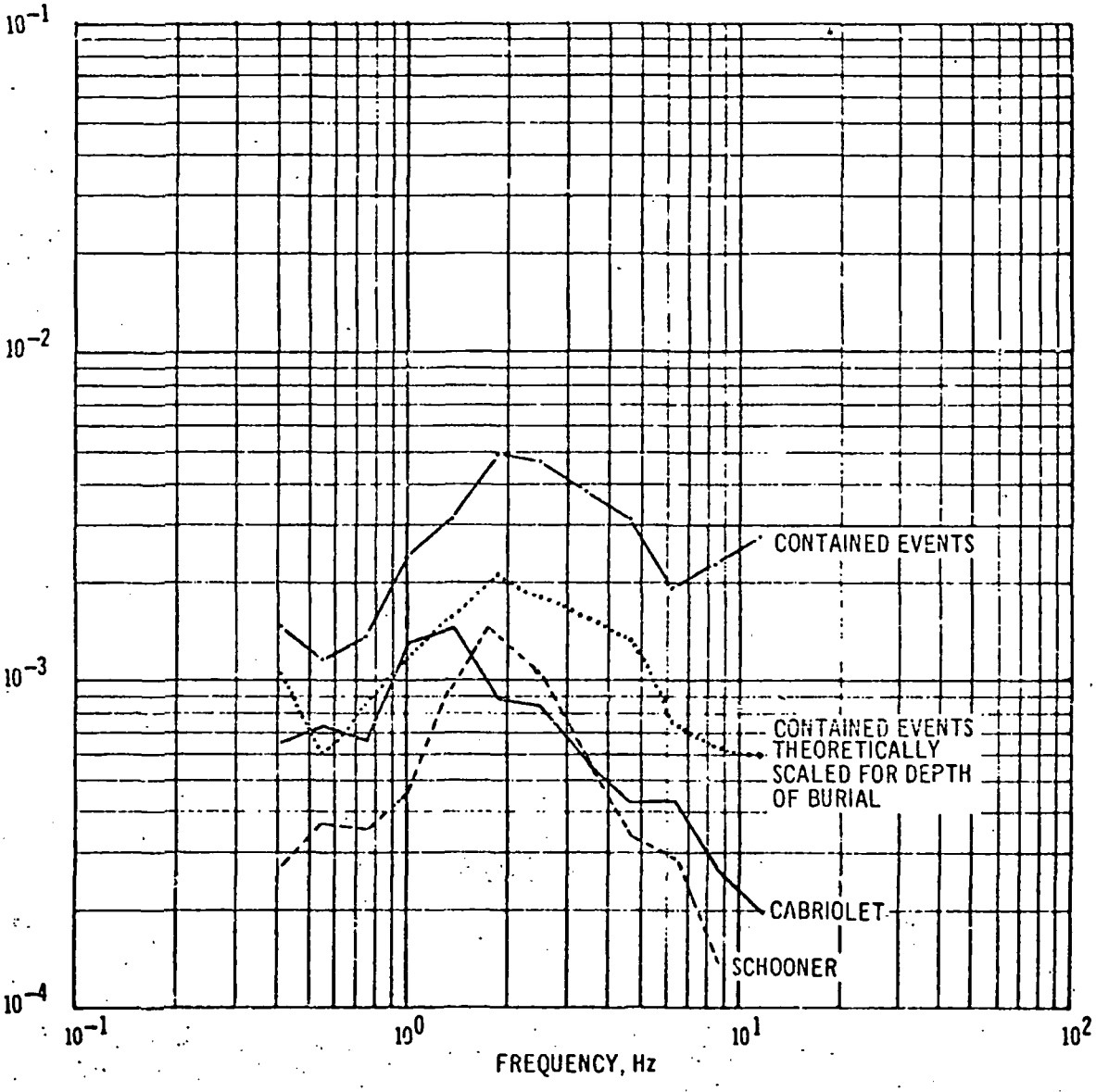

Figure 3-9. Comparison of BPF Data From Schooner, Cabriolet, and Contained Events (Knickerbocker and Duryea) at 2.3 kt, Radial Component, Tonopah Church

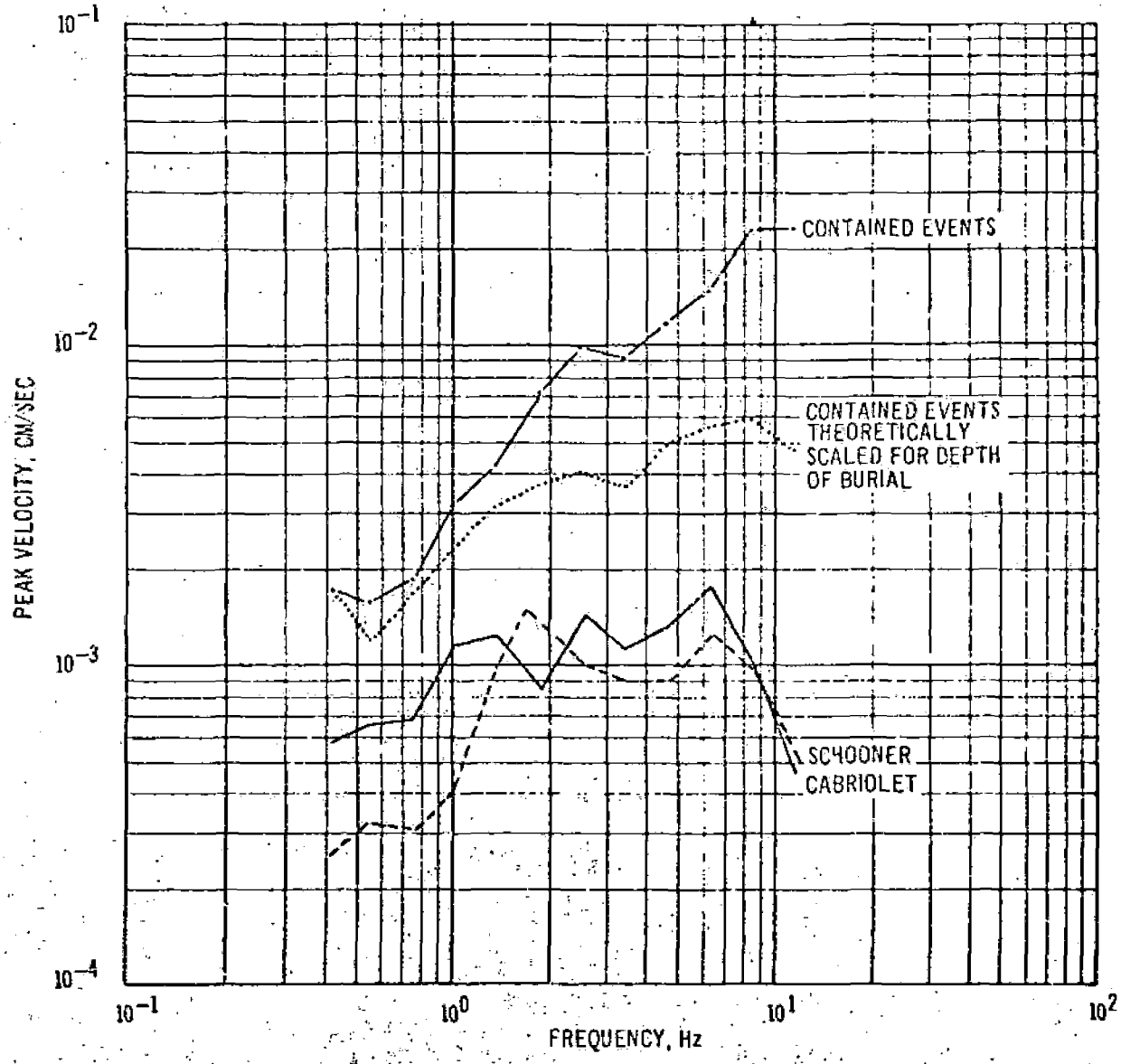

Figure 3-10. Comparison of BPF Data From Schooner, Cabriolet, and Contained Events (Knickerbocker, Duryea, and Rex) at 2.3 kt, Radial Component, Tonopah Motel

at relatively shallow depths of burial using presently available theoretical techniques. The relationships between seismic efficiency, elastic radii and depths of burial (Equations 3-1 and 3-2) adequately account for the differences in amplitude spectra between the contained events and the cratering events. Physically, this suggests that most of the energy that goes into the formation of elastic waves is coupled into the ground before the fireball breaks the surface with a subsequent sudden release of energy to the atmosphere. This description is physically sound, for the shock wave which is the precursor to the elastic waves is liberated into the ground at the end of the vaporization phase. (The vaporization cavity is of the order of a few meters for a one kiloton shot.) Thus, most of the energy going into the elastic region is independent of the cavity expansion after the vaporization phase. Thus, as far as the elastic region is concerned, a cratering event may be considered to be a contained event buried at a relatively shallow depth, with depth of burial controlling the seismic efficiency.

The second conclusion is that for two events of the same yield in the same medium, the dominant spectral amplitude of the event with the shallower depth of burial occurs at lower frequencies. This is evident from Equation (3-1) where the elastic radii scale

inversely to the ratio of depths of burial for equivalent yield and

$$\frac{a_1}{a_2} = \left(\frac{h_2}{h_1}\right)^{1/n} \qquad (3\text{-}3)$$

and the frequency of the dominant energy portion of the amplitude spectrum varies inversly with a. Thus at smaller depths of burial, the amplitude spectrum is shifted to lower frequencies. This characteristic may be noted in the spectra for Schooner and Cabriolet, the two detonations with the shallow depth of burial. The main observation is that the high frequency content of cratering events is considerably reduced relative to that of contained events while the low frequency content is only slightly reduced. This physical result probably has an influence on the characteristics of the peak ground motions observed from cratering detonations. In particular, it appears that the correlation of peak ground motions and elastic wave types might be affected differently for cratering and contained detonations due to the differences in the amplitude spectrum. Also, the resultant amplification of high frequency body waves (Davis and Murphy, 1967) by low velocity surface layers should be affected; although, the basic physical effect of the layered system should be independent of a change from a nuclear cratering detonation input energy source to a nuclear contained detonation input energy source.

Chapter 4 will describe some of the characteristics of the correlation of the peak ground motion and elastic wave types generated by the Schooner detonation.

CHAPTER 4

AMPLITUDE AND FREQUENCY CHARACTERISTICS OF ELASTIC WAVE TYPES

The primary objective of this chapter is to determine the correlation of the amplitude and frequency characteristics of the ground motion generated by Schooner with elastic wave mode windows (P, S, and surface) and to compare the correlation with results obtained from similar analysis of other cratering and contained events.

4.1 IDENTIFICATION OF ELASTIC WAVE TYPE WINDOWS

Figures 4-1 and 4-2 illustrate typical particle velocity seismograms recorded at Beatty (HR), Nevada and Frenchman Mountain, Nevada from the Schooner detonation. The radial-vertical component product waveform is displayed as the bottom trace on each seismogram. Inspection of the seismogram and the component product waveform permits the P, SV, and Rayleigh waves to be identified (Sutton et al., 1967).

Figure 4-3 illustrates the first arrival time as a function of distance from the energy source for three nuclear detonations - Schooner, Cabriolet (cratering detonations), and Benham (contained detonation). These are located on Figure 1-1. Cabriolet and Benham travel time data were added because the three detonation

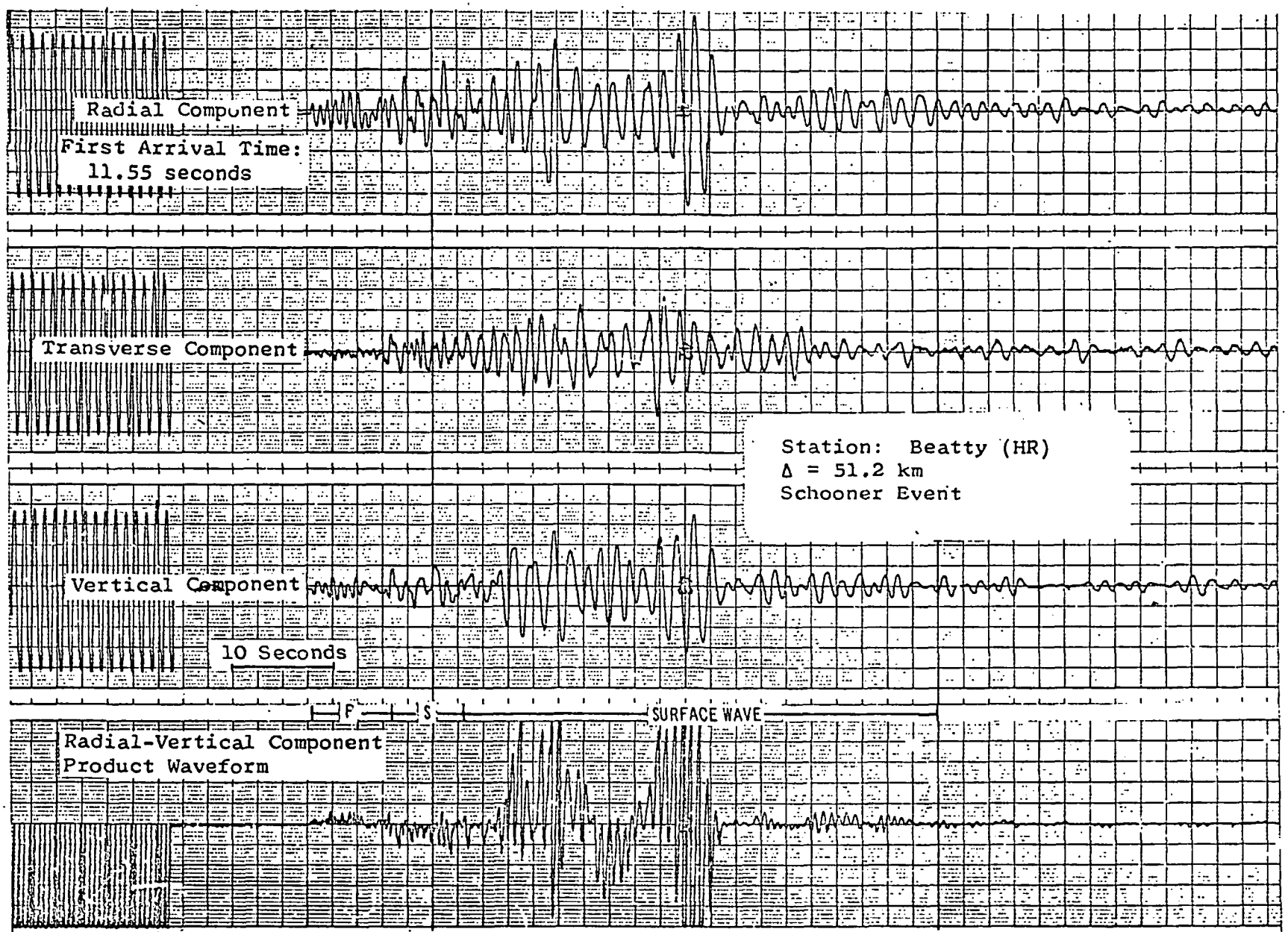

Figure 4-1. Particle Velocity Seismogram Recorded at Beatty (Hard Rock), Nevada - Schooner Event

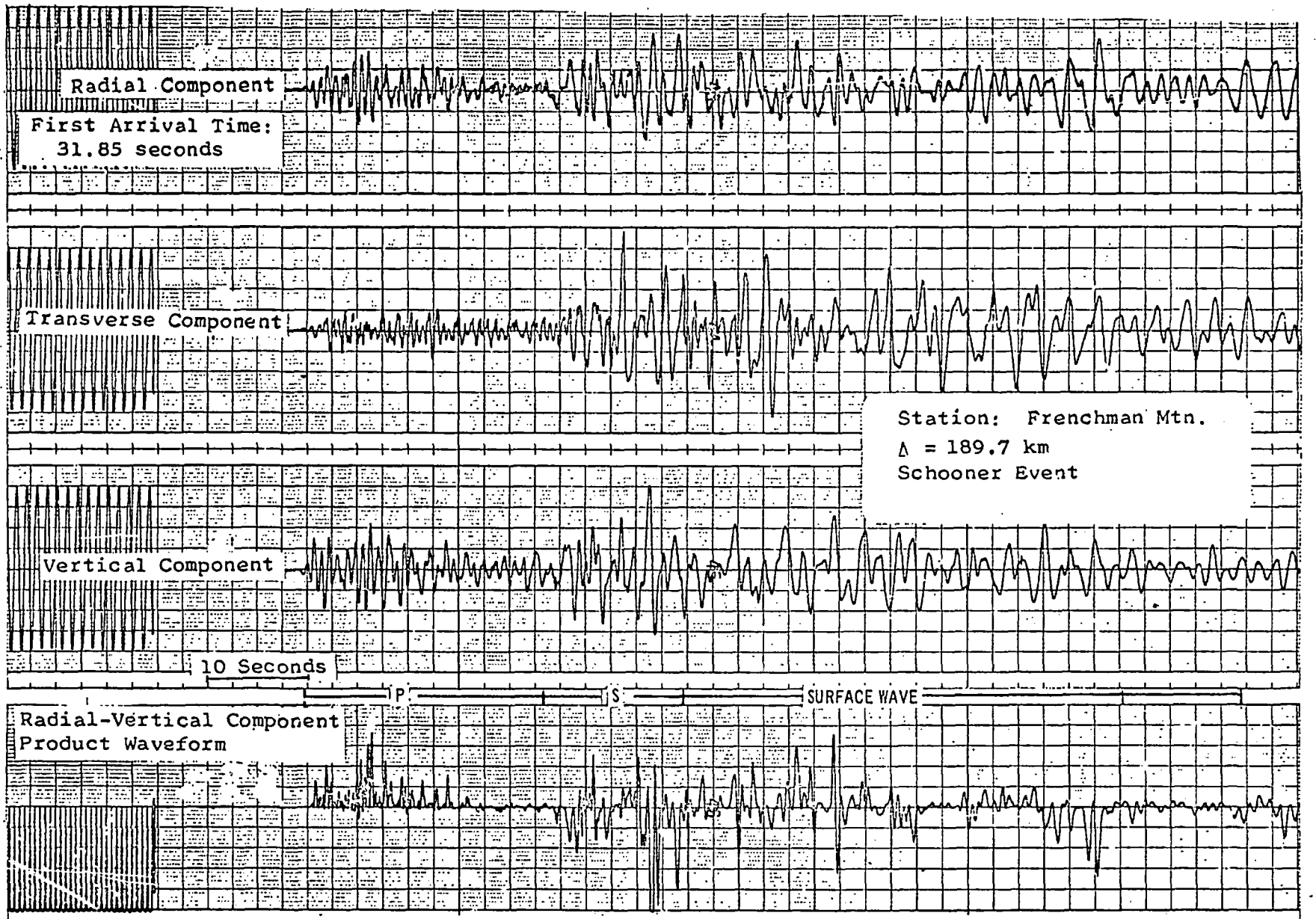

Figure 4-2. Particle Velocity Seismogram Recorded at Frenchman Mountain, Nevada - Schooner Event

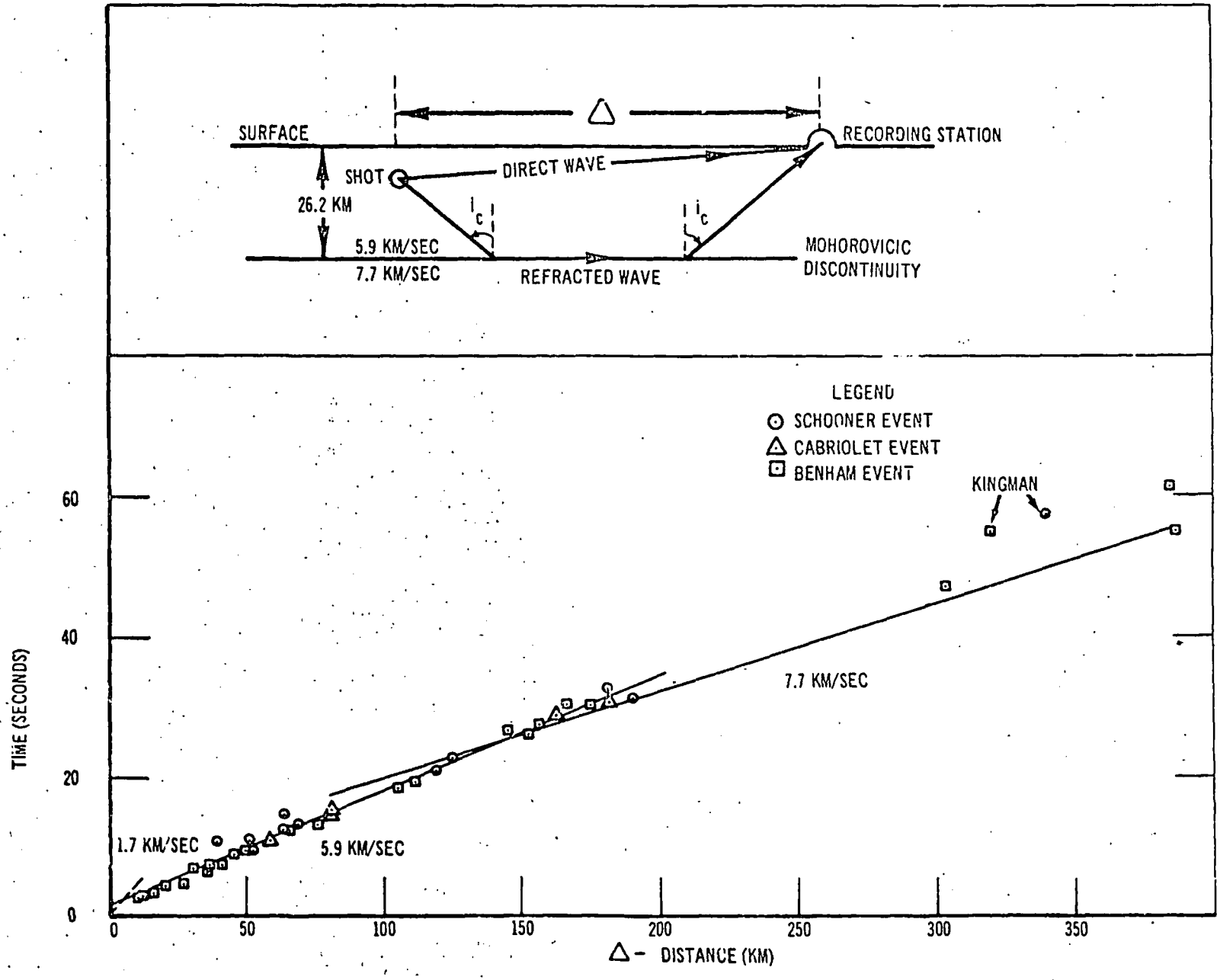

Figure 4-3. First Arrival Time as a Function of Station Distance

points are fairly close together and the Schooner data sample alone is inadequate for analysis.

The first arrival times can be approximated fairly closely by two straight line segments. The first, in the distance interval 0-144 km, indicates a propagation velocity for Pg, the direct wave, of 5.9 km/sec. The second, in the distance interval 144-400 km is based on limited data but suggests a propagation velocity of about 7.7 km/sec for Pn, the P wave critically refracted from the Mohorovicic discontinuity. Data such as this and the two velocity values are typical of the results of other investigators such as Diment, et al. (1961), Stuart, et al. (1964), and Hill, et al. (1967) obtained at the Nevada Test Site (NTS). These values of velocity and the value of 144 km for the critical distance indicate a NTS crustal model with a thickness of 26.2 km.

On the basis of travel time data and the radial-vertical component product waveforms, the time history of a typical seismogram can be divided into three time windows:

1. A P wave window (beginning with the first arrival and extending to the first S wave arrival).
2. A S wave window (beginning at the first S wave arrival; i.e., at a time about 1.7 times the first arrival time, and extending to the onset of the surface wave train).
3. A surface wave window (beginning with the onset of the long period surface wave to the end of significant motion on the seismogram).

These wave mode time windows are necessarily generalized and vary in length and complexity according to factors such as: 1) the distance of the station from the source, 2) the geologic layering at the recording site, and 3) the many complex geological and geophysical parameters of the earth's crust which impress their signature upon the propagating waves. The P wave time window, for example, contains at least the direct wave, the wave critically refracted from the Mohorovicic (M) discontinuity and the reflection from the M discontinuity in an order which depends upon the source-to-station distance relative to the M discontinuity.

4.2 CORRELATION OF PEAK PARTICLE VELOCITY AND ELASTIC WAVE MODE TIME WINDOWS

Each of the particle velocity seismograms recorded from Schooner was analyzed to determine the correlation between the peak vector and the peak horizontal particle velocity with wave mode time window. Table 4-1 lists the results of this analysis. Both the peak vector and the peak horizontal particle velocity correlate with the surface wave mode time window at all Schooner stations except Frenchman Mountain and Alamo. The peak horizontal velocity values occur most often on the transverse component of the seismogram.

The peak vector and the peak horizontal particle velocity observed at seismograph stations which recorded the Cabriolet

RECORDING STATION	DISTANCE (km)	STATION GEOLOGY	WAVE MODE WINDOW WHERE PEAK VECTOR PARTICLE VELOCITY OCCURS			WAVE MODE WINDOW AND COMPONENT WHERE PEAK HORIZONTAL PARTICLE VELOCITY OCCURS		
			P Wave	S Wave	Surface Wave	P Wave	S Wave	Surface Wave
2	39.3	Rock			X			X(R)
Beatty	51.2	Rock			X			X(R)
CP-1	64.4	Rock			X			X(T)
Tonopah Church	99.4	Rock			X			X(T)
SE-2	119.3	Rock			X			X(R)
Frenchman Mountain	189.7	Rock		X			X(T)	
Kingman (Arizona)	340.0	Rock			X			X(R)
Beatty	51.7	Alluvium			X			X(T)
ETS-2	61.1	Alluvium			X			X(T)
E-MAD	63.9	Alluvium			X			X(T)
NRDS (Admin. Bldg.)	67.6	Alluvium			X			X(R)
Tonopah Motel	99.2	Alluvium			X			X(T)
Alamo	124.0	Alluvium		X				X(T)
Squires Park	181.8	Alluvium			X			X(T)
SE-6	187.3	Alluvium			X			X(N/S)

TABLE 4-1. CORRELATION OF PEAK HORIZONTAL AND PEAK VECTOR PARTICLE VELOCITY WITH WAVE MODE TIME WINDOW -- SCHOONER EVENT

detonation, a 2.3 kt nuclear cratering experiment, were identified and correlated with the three wave mode time windows. The results are given in Table 4-2. As observed for Schooner, both the peak vector and the peak horizontal particle velocities correlate primarily with the surface wave mode time window.

Peak vector and horizontal particle velocity values were determined on seismograms recorded from Benham, a 1,100 kt contained nuclear detonation, in order to correlate the peak particle velocity and wave mode time windows for a contained event. The results are shown in Table 4-3. In this case, the peak particle velocities recorded at several stations (Beatty, Tonopah, and NRDS stations) correlate with the P wave time window instead of the surface wave time window. At other stations, the peak particle velocities correlate with the surface wave time window, as noted for Schooner and Cabriolet.

Insufficient data are available at this time to establish a physical basis for the correlation between peak particle velocity and the surface wave mode time window for cratering events. Perhaps the basic difference in the amplitude spectrum of cratering and contained events (i.e., the shift of the dominant energy to the low frequency end of the spectrum for cratering events) enhances the surface wave generation mechanism more for cratering detonations

RECORDING STATION	DISTANCE (km)	STATION GEOLOGY	WAVE MODE WINDOW WHERE PEAK VECTOR PARTICLE VELOCITY OCCURS			WAVE MODE WINDOW AND COMPONENT WHERE PEAK HORIZONTAL PARTICLE VELOCITY OCCURS		
			P Wave	S Wave	Surface Wave	P Wave	S Wave	Surface Wave
CP-1	57.0	Rock			X			X(T)
SE-1	81.0	Rock			X			X(R)
Tonopah Church	111.0	Rock			X			X(T)
Q-25	82.5	Alluvium			X			X(R)
Tonopah Motel	111.0	Alluvium			X			X(T)
Alamo	123.0	Alluvium			X			X(T)
SE-5	163.0	Alluvium			X			X(R)
SE-6	182.0	Alluvium			X			X(N/S)

TABLE 4-2. CORRELATION OF PEAK HORIZONTAL AND PEAK VECTOR PARTICLE VELOCITY WITH WAVE MODE TIME WINDOW -- CABRIOLET EVENT

RECORDING STATION	DISTANCE (km)	STATION GEOLOGY	WAVE MODE WINDOW WHERE PEAK VECTOR PARTICLE VELOCITY OCCURS			WAVE MODE WINDOW AND COMPONENT WHERE PEAK HORIZONTAL PARTICLE VELOCITY OCCURS		
			P Wave	S Wave	Surface Wave	P Wave	S Wave	Surface Wave
2	27.9	Rock	X			X(R)		
Beatty	43.9	Rock	X					X(R)
Tonopah Church	114.1	Rock	X			X(R)		
SE-2	105.0	Rock			X			X(R)
Frenchman Mountain	175.0	Rock			X			X(R)
Kingman (Arizona)	320.0	Rock			X			X(T)
Beatty	44.8	Alluvium	X			X(R)		
ETS (Dewar)	46.7	Alluvium	X			X(R)		
E-MAD	49.4	Alluvium	X			X(R)		
NRDS (Admin. Bldg.)	53.1	Alluvium			X			X(R)
Tonopah Motel	114.1	Alluvium	X			X(R)		
Alamo	116.8	Alluvium			X			X(R)
Squires Park	167.0	Alluvium			X			X(T)
SE-6	172.7	Alluvium			X			X(N/S)

TABLE 4-3. CORRELATION OF PEAK HORIZONTAL AND PEAK VECTOR PARTICLE VELOCITY WITH WAVE MODE TIME WINDOW -- BENHAM EVENT

than for contained detonations. Additional study of data from both cratering and contained detonations is required to establish the basic physical relationship. Also, as more ground motion data from nuclear cratering detonations are obtained, the amplitude of particular wave modes (e.g., the direct P and S waves critically refracted and reflected from the M discontinuity) will be determined as a function of yield and source-recording station distance and compared with similar data from contained nuclear detonations (Hays, 1969).

4.3 DETERMINATION OF FREQUENCY CHARACTERISTICS OF ELASTIC WAVE MODE TIME WINDOWS

Two frequency analysis techniques, Band-Pass filter (BPF) and the Fourier transform, were used to determine the frequency characteristics of elastic wave mode time windows of particle velocity seismograms recorded from Schooner.

Figure 4-4 shows the BPF spectrum of the radial particle velocity observed at two seismograph stations, Beatty (hard rock) and ETS-2 (alluvium.) Superposed on each spectrum are spectra of the three wave mode time windows. Inspection of this figure leads to the following conclusions:

1. The peak radial particle velocity recorded at Beatty correlates with the surface wave mode time window. The peak radial particle velocity recorded at ETS-2 correlates with the S wave mode time window, being slightly greater than the response of the surface wave mode time window.

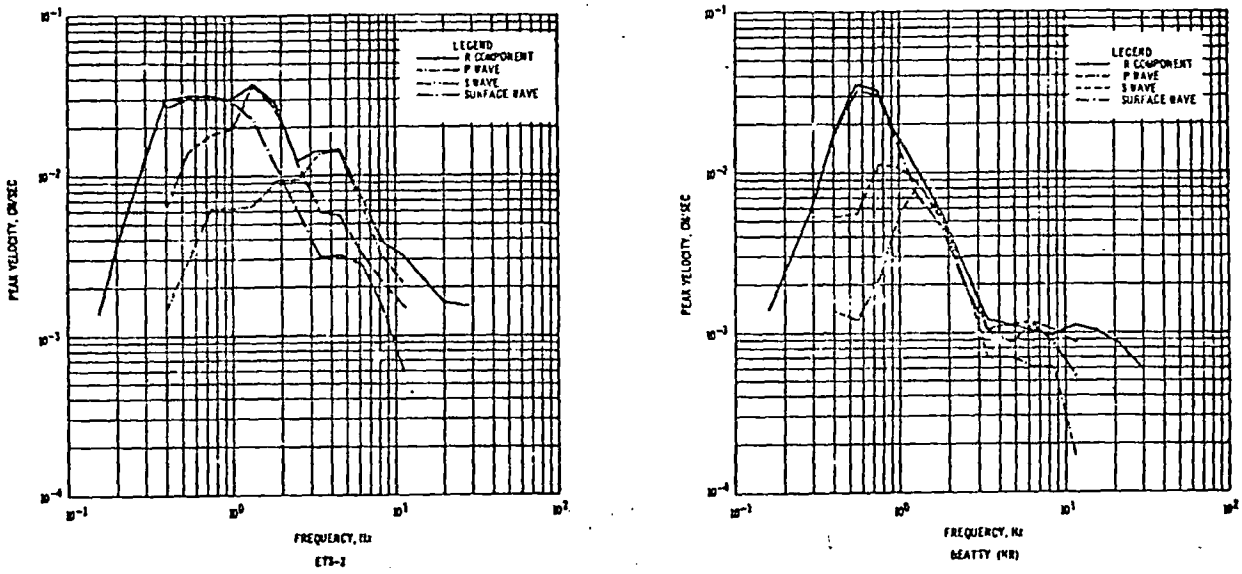

Figure 4-4. Band-Pass Filter Spectra of Wave Mode Windows Measured On the Radial Component of Particle Velocity, Stations Beatty (HR) and ETS-2, Nevada - Schooner Event

2. The individual contribution of the three wave mode windows to the peak radial particle velocity observed on the seismograms is a function of both wave mode window and frequency. That is, the surface wave mode window contribution to the radial particle velocity occurs at a dominant frequency of about 0.8 Hz at Beatty and 1.2 Hz at ETS-2. The P wave mode time window contributes the smallest radial particle velocities at a dominant frequency of about 1.2 Hz and 4.5 Hz respectively for Beatty and ETS-2.

Figure 4-5 illustrates the radial component of particle velocity recorded at five hard rock sites. These stations, with the exception of Beatty, are approximately in-line with the Schooner source, and are distributed over a total distance range of 340 km. The wave mode time windows are identified on each radial component waveform.

The smoothed Fourier amplitude spectra of each of the three wave mode windows illustrated in Figure 4-5 are shown in Figure 4-6. These data support the following conclusions:

1. The surface wave mode time window contributes the peak Fourier amplitude on the five seismograms, as noted earlier.

2. Considering the three amplitude spectra of each individual station, the frequency of the dominant energy varies as a function of the wave mode window. That is, the peak amplitude of the P wave mode window spectrum occurs at a higher relative frequency than the peak amplitude of the other two wave mode spectra. The peak amplitude of the surface wave mode window spectrum occurs at the lowest relative frequency. This phenomenon is related to the well known fact that the three elastic wave types propagate with different wave velocities and, consequently, different characteristic frequencies.

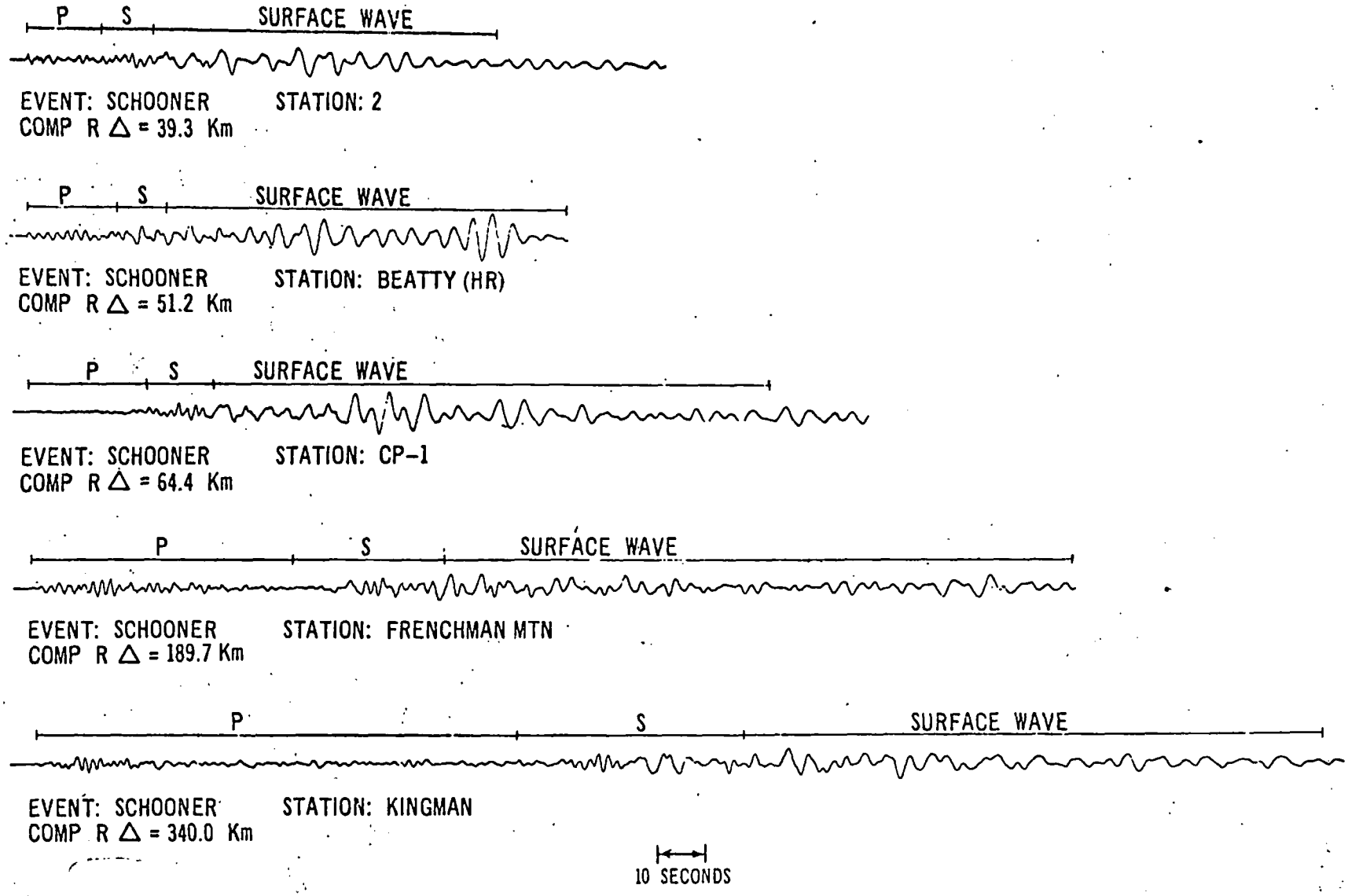

Figure 4-5. Radial Component of Particle Velocity Recorded at Five Stations Located on Hard Rock - Schooner Event

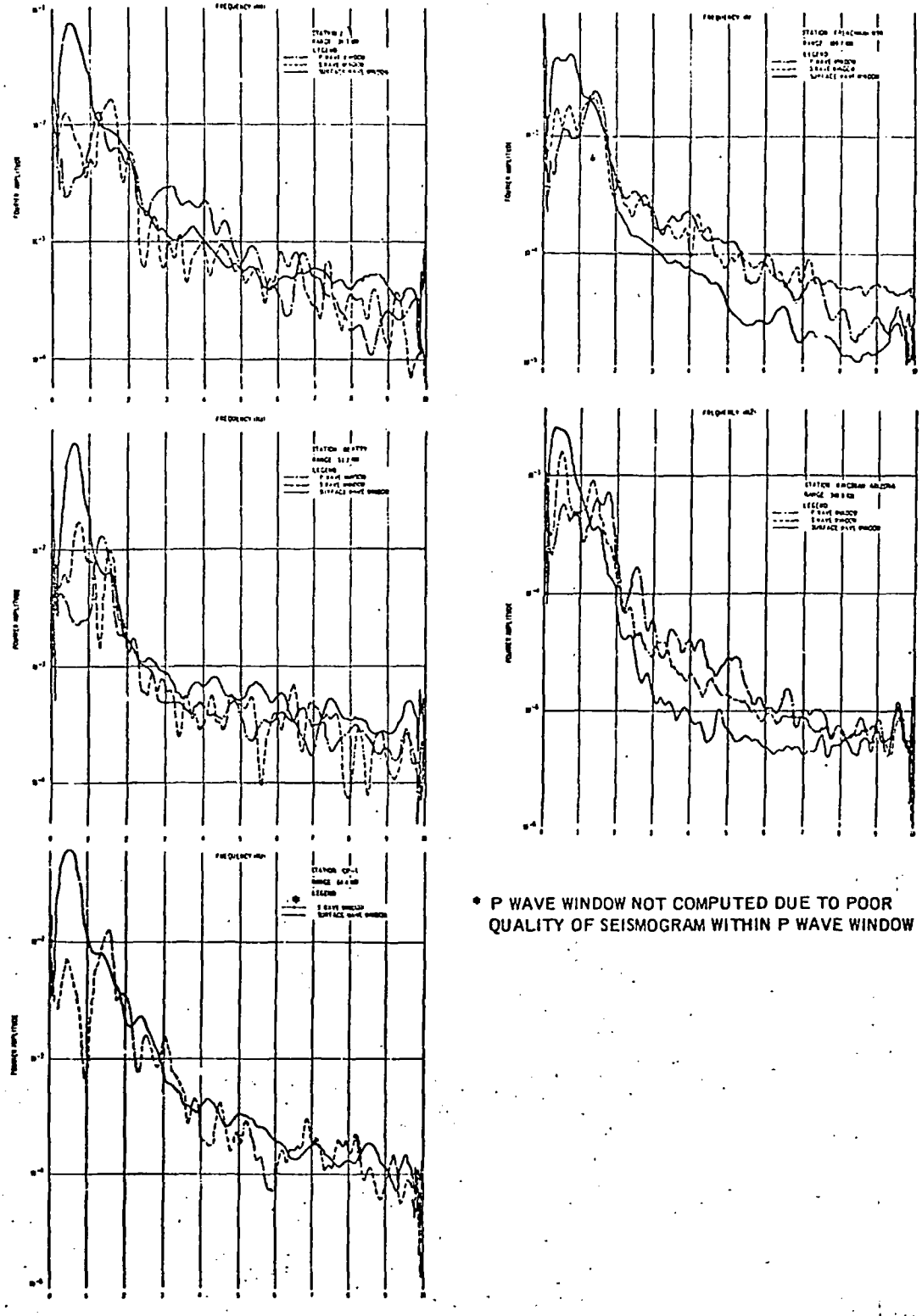

* P WAVE WINDOW NOT COMPUTED DUE TO POOR QUALITY OF SEISMOGRAM WITHIN P WAVE WINDOW

Figure 4-6. Smoothed Fourier Amplitude Spectra of Identified Wave Mode Time Windows - Schooner Event

In summary, the spectral characteristics of the wave mode time windows for Schooner are similar to those observed for contained events (Hays, 1969) with one exception, the apparent dominance of surface wave energy for Schooner. Additional analysis is required to extend this observation to all cratering events.

4.4 FREQUENCY DEPENDENT AMPLIFICATION

Amplification of seismic motion at recording stations located on alluvium has been noted since the early days of seismology. Haskell (1953), Hannon (1964), Davis and Murphy (1967), Murphy and Davis (1969) and a number of others since 1930 have shown that the shallow low velocity layers of the earth's crust act as a filter with respect to the seismic energy arriving at a seismograph station and significantly affect the ground motion.

The transfer function of the layered system is a complex function which has been shown to involve several variables (Davis and Murphy, 1967):

1. The elastic wave type (P, S, Rayleigh, Love)

2. The angle of incidence of the incident wave

3. The physical parameters (thickness, density, rigidity, compressional and shear-wave velocities) of the layered system and the underlying rock.

In actual practice, only the amplitude term of the transfer function is used to calculate a frequency dependent amplification factor for the layered system.

A practical procedure to determine the frequency dependent amplification of a layered system to a seismic input generated by an underground nuclear explosion is to use the seismograms measured at adjacent stations; one located on hard rock and the other on alluvium (or a low velocity surface layer). The basic assumption is made that the input at the base of the alluvium layer is the same as the output measured at the hard rock station; therefore, the amplification factor can be determined by dividing the Fourier amplitude spectrum of the seismic energy measured at the alluvium site by the Fourier amplitude spectrum of the seismic energy measured at the hard rock site. The time history of the seismogram is divided into P, S, and surface wave mode windows, as described in 4.2, and the ratio of the Fourier amplitude spectra of corresponding wave mode windows is taken to determine the amplification factor as a function of a particular incident wave type. Seismic measurements at the pair of stations at Tonopah, Nevada, are well suited for an analysis of this type. The Tonopah Motel station is located on approximately 30 feet of unconsolidated fill overlying dacite. The Tonopah Church station, located about 600 feet away, is on the same material which underlies the Motel station. Thus, it seems reasonable that the output measured at the Church station is identical to the input at the base of the fill at the Motel station.

Figure 4-7 illustrates the radial component of particle velocity recorded at the two Tonopah stations from the Schooner event. The wave mode time windows are identified on the figure.

Fourier amplitude spectra for each of the wave mode windows of Figure 4-7 are shown in Figure 4-8 for the two Tonopah stations. The spectra of both stations exhibit peak amplitudes at approximately 1.3 Hz for the P wave window, 1.4 Hz for the S wave window, and 0.5 Hz for the surface wave window; however, the spectral composition at other frequencies is different. Figure 4-9 shows the amplification factor as a function of frequency for each of the three wave mode windows. The amplification factor is greatest for the P wave window, being a factor of 10 at 7.5 Hz. Amplification factors of 8 at 8.5 Hz and 4 at 6.2 Hz are observed for the S and surface wave windows respectively. The theoretical amplification factor for the P and S wave windows are superposed for reference on the corresponding curves in Figure 4-9. Qualitative agreement between observation and theory is noted showing that the amplification due to the layered system is independent of whether the input energy source is a cratering or a contained nuclear detonation. Lack of agreement between observation and theory is related to the fact that the theoretical model considers a single input pulse at the base of the layered system, whereas the observed P wave (or S wave) window contains several pulses

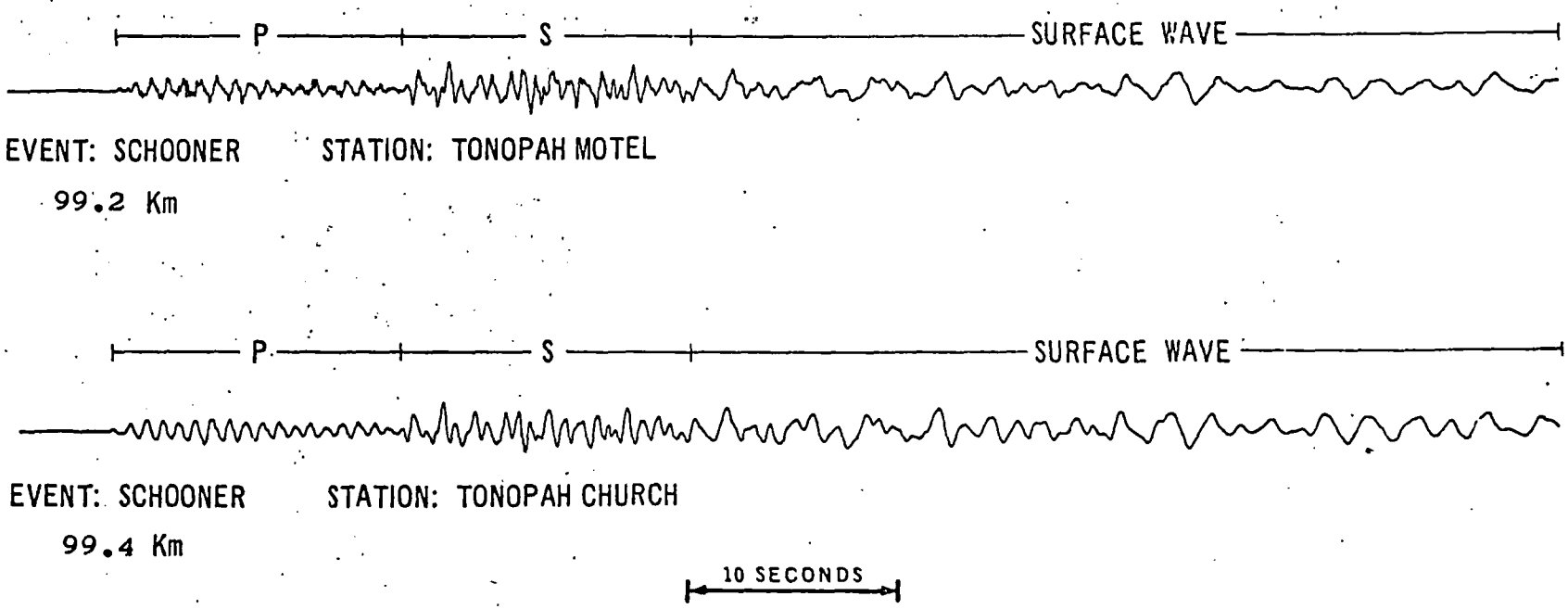

Figure 4-7. Radial Component of Particle ·ocity Recorded at Tonopah Church and Tonopah Motel, ıer Event

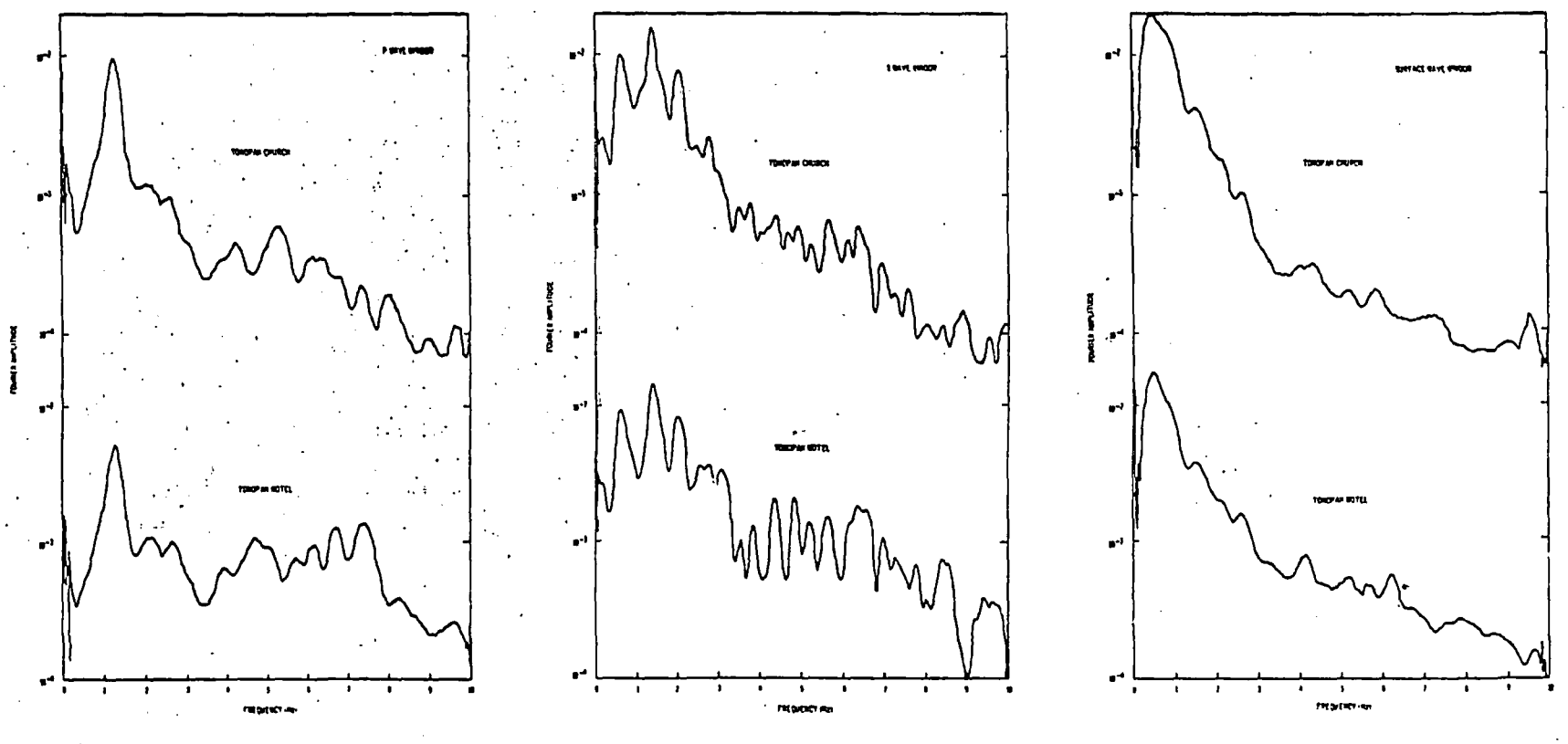

Figure 4-8. Smoothed Fourier Amplitude Spectra of Identified Wave Mode Time Windows, Tonopah Stations - Schooner Event

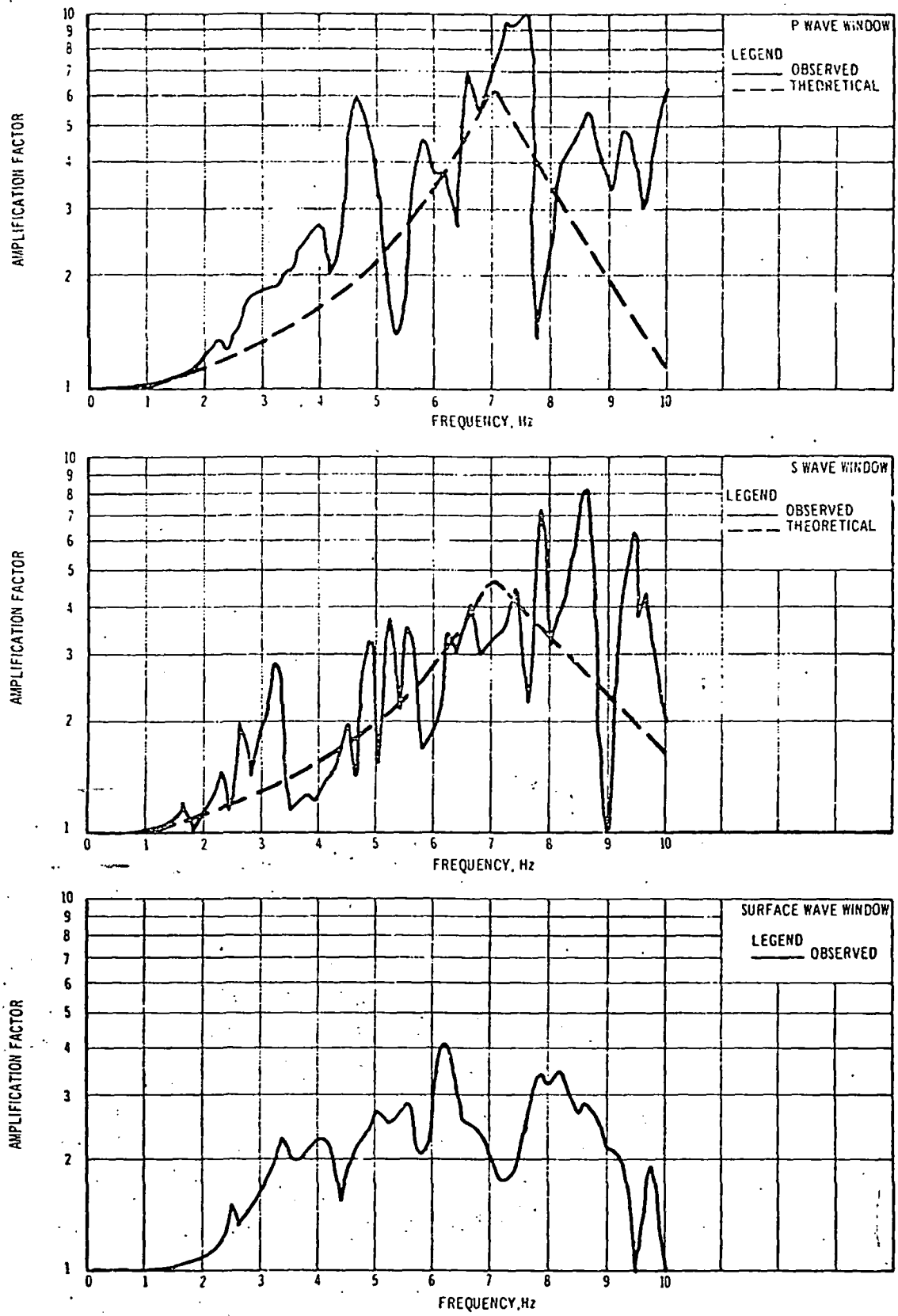

Figure 4-9. Amplification Factor as a Function of Frequency, Tonopah Stations - Schooner Event

(such as the direct wave, the critically refracted wave from the Mohorovicic discontinuity, and the reflected wave from the Mohorovicic discontinuity).

Table 4-4 shows the comparison of the peak vector motions recorded at the Tonopah Church and Tonopah Motel stations from Schooner with the peak motion expected on the basis of the Nevada Test Site prediction equations (Murphy and Lahoud, 1969). Note that the peak particle vector motions recorded at Tonopah from Schooner are lower than the levels of motion expected on the basis of average NTS experience, with the exception of the peak particle velocity recorded at Tonopah Motel which is only slightly higher. This observation is contrary to NTS experience, because the measurements at Tonopah Motel from contained detonations are nearly always higher than the average predicted values.

STATION	MEASURED PEAK VECTOR MOTION			PREDICTED PEAK VECTOR MOTION		
	Acceleration (g)	Velocity (cm/sec)	Displacement (cm)	Acceleration (g)	Velocity (cm/sec)	Displacement (cm)
Tonopah Church	1.87×10^{-4}	2.13×10^{-2}	4.14×10^{-3}	7.0×10^{-4}	5.0×10^{-2}	1.3×10^{-2}
Tonopah Motel	2.83×10^{-4}	2.30×10^{-2}	4.22×10^{-3}	1.6×10^{-3}	1.2×10^{-2}	3.6×10^{-2}

TABLE 4-4. COMPARISON OF MEASURED AND PREDICTED PEAK VECTOR PARTICLE MOTIONS AT TONOPAH CHURCH AND TONOPAH MOTEL, SCHOONER EVENT

An explanation for the lower level of peak vector particle motions recorded at the Tonopah stations from Schooner is related to differences in the seismic spectral composition for equivalent yield cratering and contained events and to the decreased seismic energy efficiency of cratering events as compared to normal contained events. Chapter 5 will compare the seismic energy efficiency of Schooner with other underground nuclear detonations.

CHAPTER 5

SEISMIC ENERGY EFFICIENCY

The objective of this chapter is to determine the amount of energy from underground nuclear explosions which goes to form elastic waves in the far-field radiation zone. This subject has been studied by other investigators for nuclear events, notably by Carder, et. al. (1958 and 1961), Berg , et. al. (1964), Lowrie and Mickey, (1965) and Trembly and Berg, (1966).

The approach taken in this study is to develop the analytic solution of the spherically symmetric Sharpe's problem into an energy equation. The parameters appearing in the equation are evaluated through a self-consistent method within the theory. In principal, once the elastic radius and pressure function acting at the elastic radius are determined, the seismic energy can be calculated with this model.

5.1 THEORY AND ANALYSIS

The displacement potential for wave motion produced by a spherically symmetric exponential pressure function acting in an ideally elastic medium has been derived by Sharpe (1942) and can be stated as

$$\phi = \frac{ap_0}{\rho r \left[(\omega_1/\sqrt{2} - \alpha)^2 + \omega_1^2\right]} \qquad (5\text{-}1)$$

$$\left\{-e^{-\alpha\tau} + e^{-\omega_1\tau/\sqrt{2}} \left[(1/\sqrt{2} - \alpha/\omega_1) \sin \omega_1\tau + \cos \omega_1\tau\right]\right\}$$

$$\text{for } \tau \geq 0$$

$$= 0 \qquad \text{for } \tau < 0$$

where the pressure function acting at the elastic radius (r = a), i.e., the radius at which the medium behaves elastically, is

$$p = p_0 e^{-\alpha\tau} \quad \text{for } \tau \geq 0 \qquad (5\text{-}2)$$

$$= 0 \qquad \text{for } \tau < 0,$$

p_0 is the peak pressure, α is the decay constant = $1/T_0$, T_0 is the time for the pressure to decay to $p_0 e^{-1}$, τ is the retarded time = $t - \frac{(r-a)}{c}$, $\omega_1 = 2\sqrt{2}\ c/3a$, c is the compressional velocity, r is the radial distance from the source, ρ is the density of the medium, and Lame's constants, λ and μ, are assumed equal (Poisson's ratio = 0.25). From the displacement potential ϕ, the displacement in the medium can be determined easily from the relationship $u = \frac{\partial\phi}{\partial r}$, where u is the displacement. The decay time, T_0,

is assumed proportional to the elastic radius, a. The decay constant may then be written as $\alpha = 1/T_0 = k\omega_0$, where $\omega_0 = c/a$. The parameter k, in general, may be a function of the shot point parameters, but, as will be shown later, is not expected to be very sensitive. With the above substitution, the displacement may be calculated to be

$$u = \frac{9ap_0}{4\rho c^2} \left(\frac{a}{r}\right) \left\{\left(\frac{a}{r} - k\right) \frac{e^{-k\omega_0 \tau}}{(3-3k+9k^2/4)} - \frac{e^{-2\omega_0 \tau/3}}{\sqrt{2(3-3k+9k^2/4)}}\right.$$

$$\left.\left[\left(\frac{a}{r}\right) \sin(\omega_1 \tau + \theta_1) - \frac{2\sqrt{3}}{3} \sin(\omega_1 \tau + \theta_1 - \theta_2)\right]\right\} \qquad (5\text{-}3)$$

where

$$\theta_1 = \tan^{-1} \frac{\sqrt{2}}{1-3k/2}$$

$$\theta_2 = \tan^{-1} \sqrt{2}$$

Particle velocity, $v = \partial u/\partial t$, is

$$v = \frac{3p_0}{2\rho c} \left(\frac{a}{r}\right) \left\{-\frac{3}{2} k \left(\frac{a}{r} - k\right) \frac{e^{-k\omega_0 \tau}}{(3-3k+9k^2/4)} + \frac{e^{-2\omega_0 \tau/3}}{\sqrt{2(3-3k+9k^2/4)}}\right.$$

$$\left.\left[\sqrt{3} \left(\frac{a}{r}\right) \sin(\omega_1 \tau + \theta_1 - \theta_2) - 2 \sin(\omega_1 \tau + \theta_1 - 2\theta_2)\right]\right\} \qquad (5\text{-}4)$$

It is to be noted in equation (5-4) that the velocity has a $1/r$ and $1/r^2$ dependence. The far field radiation zone consists of the $1/r$ term only, since the $1/r^2$ term becomes negligibly small at large distances. The far field part of the velocity may thus be written as

$$v_{ff} = \frac{3p_o}{2\rho c}\left(\frac{a}{r}\right)\left\{\frac{3}{2}k^2\frac{e^{-k\omega_o\tau}}{(3-3k+9k^2/4)} - \frac{\sqrt{2}\,e^{-2\omega_o\tau/3}\sin(\omega_1\tau+\theta_1-2\theta_2)}{\sqrt{(3-3k+9k^2/4)}}\right\} \qquad (5\text{-}5)$$

The instantaneous kinetic energy density corresponding to the far field is $1/2\,\rho v_{ff}^2$. Assuming spherical divergence, the total seismic energy (assuming that the total energy is twice the kinetic energy) is

$$E = 4\pi r^2 \rho c \int_o^\infty v_{ff}^2\,dt \qquad (5\text{-}6)$$

where $r \geq a$. For convenience, r is chosen to be a. Thus,

$$E = 4\pi a^2 \rho c \int_0^\infty v_{ff}^2 \Big|_{r=a} dt \qquad (5\text{-}7)$$

Substitution of equation (5-5) in equation (5-7) and integrating gives the seismic energy,

$$E = \frac{\pi p_o^2 a^3}{2\mu} K \qquad (5\text{-}8)$$

where

$$K = \frac{12k^3 - 4k^2 + 16}{9k^4 + 8k^2 + 16}$$

and μ is the modulus of rigidity. This expression determines the seismic energy input at the elastic radius of underground explosions, assuming that most of the motion is radially compressional at that radius, which is a good approximation for tamped nuclear explosions (Perret (1968b)).

For a step function, k = 0, giving a K value of 1, and the radiated energy is simply

$$E_{\text{STEP FN}} = \frac{\pi p_o^2 a^3}{2\mu} \qquad (5\text{-}8a)$$

which is a result that Latter, et.al. (1961a), have obtained for the case of a step function.

In order to evaluate the energy expression (equation 5-8), determinations of p_o, a, k and μ are required. It is assumed that the medium "on the large" has low tensile strength and that the limiting pressure, p_o, is therefore in the neighborhood of the overburden pressure (Latter, et.al., 1961, a and b; and Kisslinger, 1963), in order to keep the medium from going into tension and propagating cracks. Poisson's ratio is taken to be 0.25 and μ is thus equal to $c^2 \rho/3$.

A determination of the elastic radius, a, can be obtained from the amplitude spectra of the particle velocities. The Fourier transform of the displacement for Sharpe's problem at a distance r, has been obtained by Latter, et.al. (1959), as

$$\hat{Z}(\omega) = \frac{\hat{p}a}{4\mu}\left(\frac{1}{r^2} + \frac{i\omega}{rc}\right)\frac{c^2}{\omega_o^2 + i\omega_o\omega - \beta\omega^2} \qquad (5\text{-}9)$$

where ω is the angular frequency, $\beta = (\lambda+2\mu)/4\mu$, $\hat{p}$ is the Fourier transform of the pressure function at a, and the other quantities have been previously defined.

For $r >> c/\omega$, the amplitude spectrum of the displacement is

$$|\hat{Z}| = \frac{a\omega c}{4\mu r} \left| \frac{\hat{p}}{(\omega_o^2 - \beta\omega^2) + i\omega_o\omega} \right| \qquad (5\text{-}10)$$

and the amplitude spectrum of the velocity is simply

$$|\hat{v}| = \omega |\hat{Z}|$$

The Fourier transform of the exponential pressure function is

$$p = \frac{P_o}{\alpha+i\omega}$$

and

$$|\hat{p}| = \frac{P_o}{\sqrt{\alpha^2+\omega^2}}$$

The velocity amplitude spectrum then becomes, with the substitution $a = k\omega_o$,

$$|\hat{v}| = \frac{ap_o}{4\mu r} \cdot \frac{\omega^2}{[\beta^2\omega^6+(\beta^2k^2-2\beta+1)\omega_o^2\omega^4+(k^2-2\beta k^2+1)\omega_o^4\omega^2+k^2\omega_o^6]^{1/2}} \quad (5\text{-}11)$$

Taking the derivative of $|\hat{v}|$ with respect to ω and equating to zero, gives the dimensionless equation

$$\beta^2\left(\frac{\omega_m}{\omega_o}\right)^6 - (k^2-2\beta k^2+1)\left(\frac{\omega_m}{\omega_o}\right)^2 - 2k^2 = 0 \quad (5\text{-}12)$$

$$\omega_o = c/a$$

which specifies the extreme points, ω_m, of the velocity amplitude spectrum. Figure 5-1 shows a plot of ω_m/ω_o versus k, for a Poisson's ratio = 0.25 (β = 0.75). Note that equation (5-12) only applies in the far field. Thus, if the frequency of maximum amplitude lies around 2 Hz and c = 5 km/sec, $r >> c/\omega_m$ or $r >>$ 400 m ensures that the observation distance r, lies in the far field. In practice, to determine an elastic radius from equation (5-12), a value of k and ω_m are needed. If there is significant shear and/or surface wave motion, the frequency of maximum amplitude is determined from the compressional wave window (i.e., the time window on the

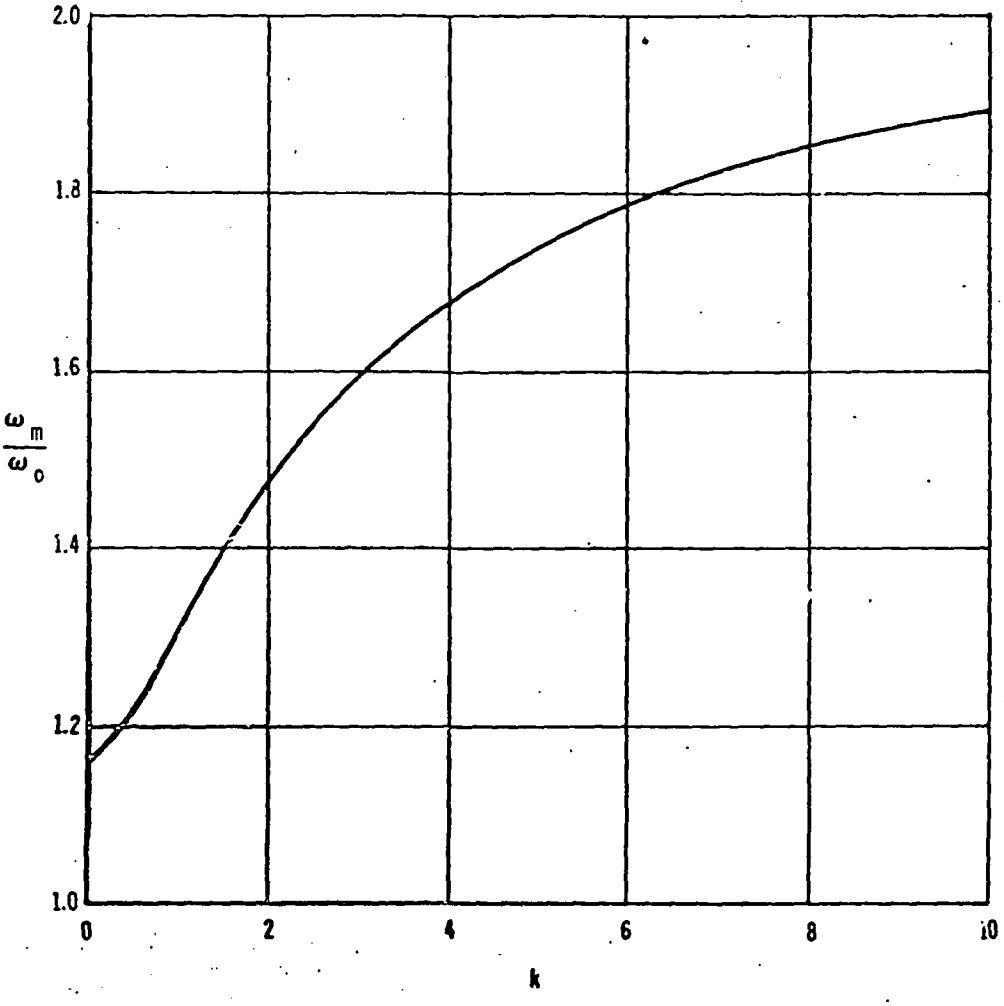

Figure 5-1. Ratio of the Frequency (ω_m) of Peak Spectral Amplitude and Resonant Cavity Frequency (ω_o) Versus the Parameter k

seismogram which is predominantly composed of longitudinal motion) since this model only holds for compressional waves. Although the observation distance must be in the far field, it must be small with respect to the differential attenuation effects of the earth. This would be a function of the dominant frequency content of the compressional waves.

In order to evaluate the constant k, equation (5-12) and the relation $\alpha = k\omega_o$ are used to give the relationship

$$\beta^2 \left(\frac{\omega_m}{\alpha}\right)^6 k^4 + (2\beta-1)\left(\frac{\omega_m}{\alpha}\right)^2 k^2 - \left(\frac{\omega_m}{\alpha}\right)^2 - 2 = 0 \qquad (5\text{-}13)$$

Figure 5-2 shows a plot of k versus (ω_m/α), for a Poisson's ratio of 0.25. It is seen that for a constant ratio of (ω_m/α), k is constant for a particular Poisson's ratio. In general, k is to be considered a function of the shot point parameters. However, k is not expected to vary significantly, since the ratio (ω_m/α) which is proportional to decay time of the pressure pulse at the elastic radius/dominant period of seismic motion should not vary significantly.

The parameter k can be evaluated from a combination of free-field data and far field seismic data. The free-field data give a determination of α, and seismic data determines ω_m.

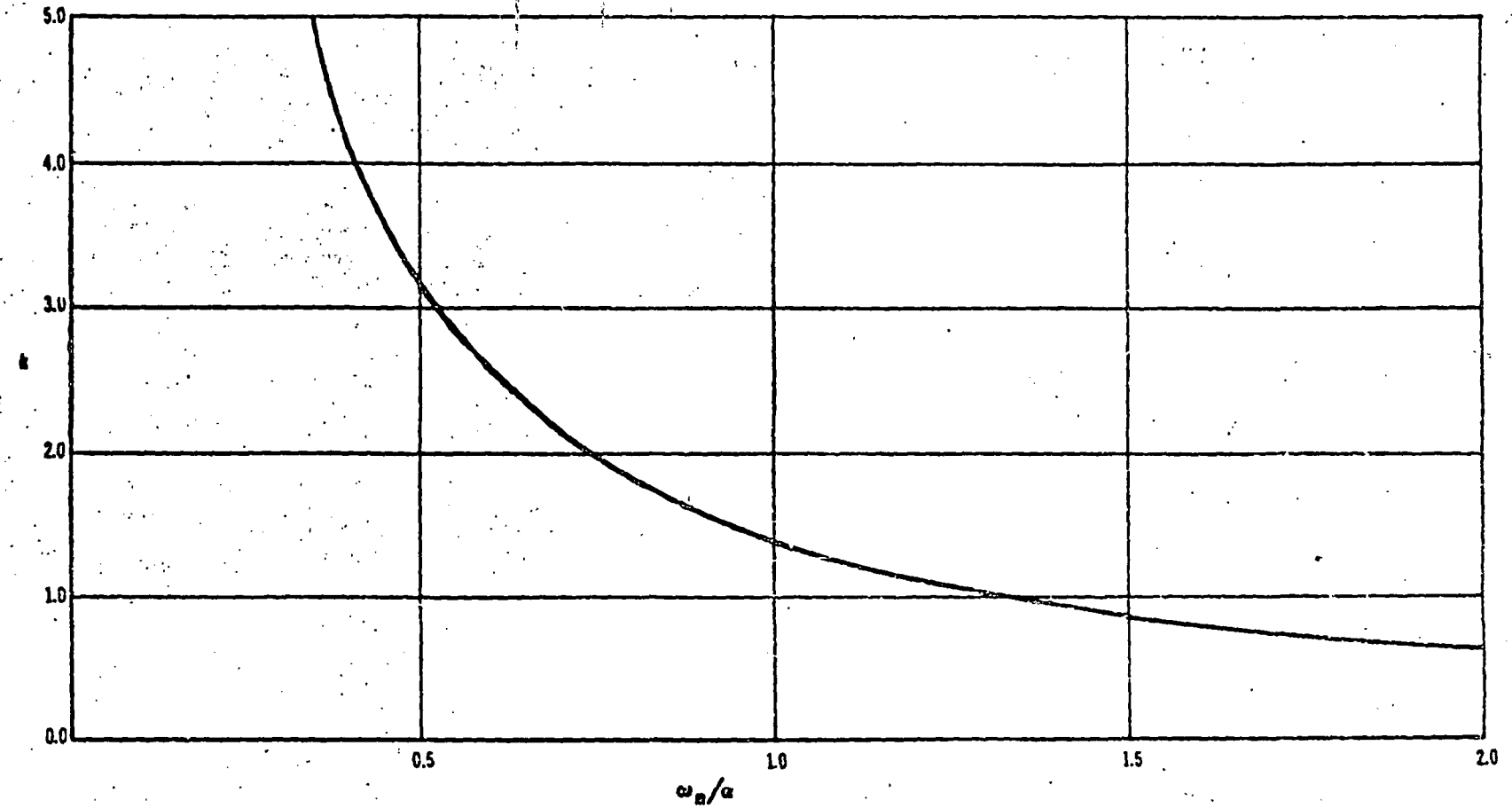

Figure 5-2. The Parameter k Versus the Ratio of the Frequency (ω_m) of Peak Spectral Amplitude and the Decay Constant (α)

5.2 EXAMPLES OF SEISMIC ENERGY EFFICIENCY COMPUTATIONS

The seismic energy efficiency was determined for four contained nuclear detonations (Shoal, Salmon, Boxcar, and Benham), a decoupled nuclear detonation (Sterling), and the nuclear cratering detonation (Schooner). These six events provide an adequate data sample, since they encompass a wide range of yields and physical conditions. Details of the computation performed for each detonation are given below.

Salmon. For the Salmon event (described in Table 5-1), free-field measurements from Perret (1968a) indicate a T_o = 20 msec, which gives α = 50/sec. The band-pass filter spectra which are approximations to Fourier amplitude spectra from the compressional wave windows of stations 10-South (18 km) and 20 South (31 km) are shown in Figures 5-3 and 5-4. Radial horizontal and vertical components of particle motion are shown. The frequency of maximum amplitude, f_m, is estimated to be about 4 Hz. This gives a value of (ω_m/α) of 0.50, and from Figure 5-2, a k value of 3.20. Figure 5-1 gives the relationship $\omega_m = 1.61\ \omega_o$, from which the elastic radius can be evaluated, $a = \frac{1.61c}{\omega_m}$. Using a compressional velocity of 4.67 km/sec gives a_{Salmon} = 299 meters, which corresponds to a peak shock pressure of 370 bars (Perret, 1968). The overburden pressure is 180 bars, which indicates that the limiting pressure p_o = 370 bars is 2.06 times the overburden pressure. Inserting these numbers into equation (5-8) for the seismic energy gives a seismic efficiency (seismic energy/initial energy available) of 5.8%.

TABLE 5-1. RESULTS OF SEISMIC ENERGY CALCULATIONS

Event	Shoal	Salmon	Boxcar	Benham	Schooner	Sterling
Shot Location	Sand Springs Range, Nevada	Tatum Salt Dome, Mississippi	Pahute Mesa, Nevada	Pahute Mesa, Nevada	Pahute Mesa, Nevada	Tatum Salt Dome, Mississippi
Type	Nuclear Contained	Nuclear Contained	Nuclear Contained	Nuclear Contained	Nuclear Cratered	Nuclear Decoupled
Yield (kt)	12.5	5.3	1200	1100	30	0.38
Depth of Burial (ft)	1205	2716	3822	4630	353	2716
Scaled Depth ($ft/kt^{1/3}$)	519	1552	354	447	107	3751
Medium	Granite	Salt	Rhyolite	Tuff	Tuff	Salt
Density(gm/cc)	2.55	2.2	2.1	2.25(av.)	2.23	2.2
Overburden Pressure (bars)	92	180	237	311	236	180
Compressional Velocity (km/sec)	5.55	4.67	3.84	3.66(av.)	3.41	4.67
f_m (Hz)	2.5	4.0	0.75	0.8	1.25	36.0
Seismic Energy Radiated (kt)	2.3×10^{-1}	3.1×10^{-1}	5.5×10^{-1}	6.7×10^{1}	9.5×10^{-2}	3.14×10^{-5} (1.3×10^{15} ergs)
Seismic Energy Efficiency (%)	1.8	5.8	4.6	6.1	0.32	0.008

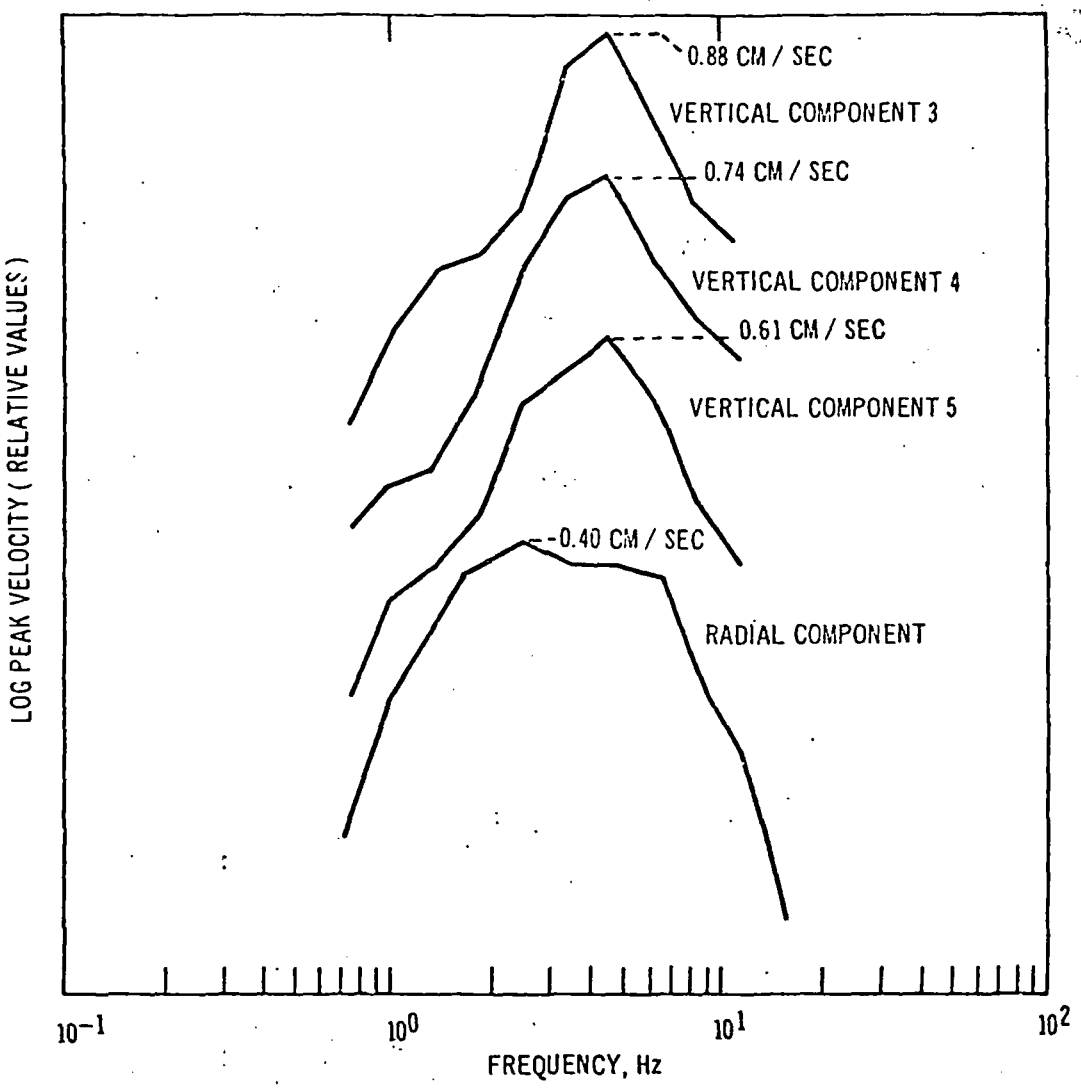

Figure 5-3. Particle Velocity Band-Pass Filter Spectra of the Compressional Wave Window, Salmon Event, Station 10-South (18 km)

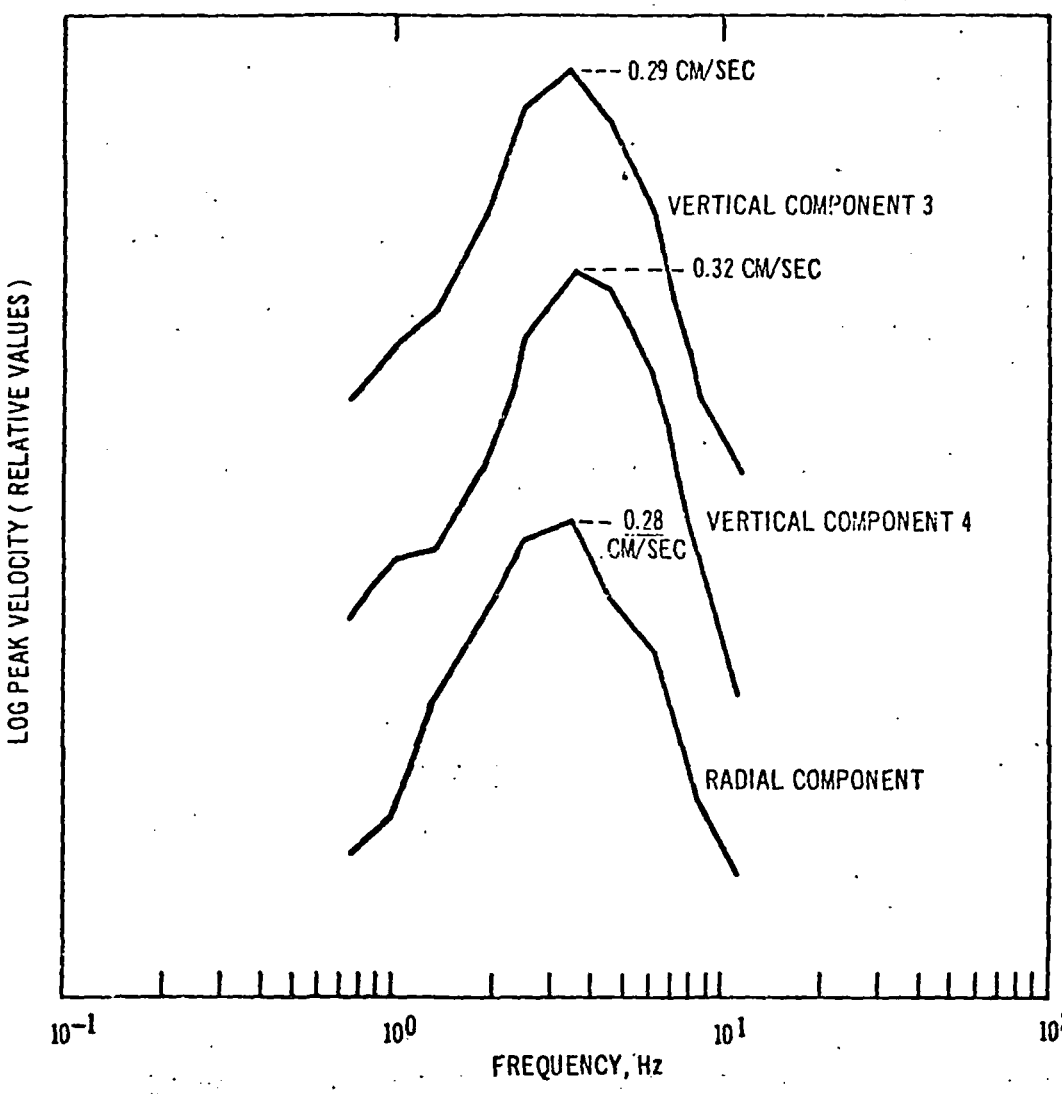

Figure 5-4. Particle Velocity Band-Pass Filter Spectra of Compressional Wave Window, Salmon Event, Station 20-South (31 km)

Shoal. For the Shoal event (described in Table 5-1), free-field measurements from Weart (1965) give an average T_o of 70 msec and α = 14.3/sec. The spectra (Perret, 1967 and Weart, 1965) are not very definitive. They give an estimate of f_m between 2.0 and 3.0 Hz or approximately 2.5 Hz. Thus, ω_m/α is 1.13 and k is 1.22. From Figure 5-1, $\omega_m = 1.35\ \omega_o$, and using a compressional velocity of 5.55 km/sec gives a_{Shoal} = 477 meters which corresponds to a peak shock pressure of about 145 bars (Weart, 1965) Overburden pressure is about 92 bars, and the limiting pressure is 1.58 times as great. Evaluation of the seismic energy gives a seismic efficiency of 1.8%. Trembly and Berg (1966) found a seismic efficiency of 0.7% from experimental observations of the Shoal event. Their theoretical model gave a seismic efficiency of approximately 2% in the southwestern quadrant. Also, they determined an average elastic radius of 510 meters which is comparable with the value of 477 meters determined here.

In general, to determine an elastic radius without free-field measurements, a value of k between 1 and 4 is appropriate. Using an average value of the ratio $\left(\frac{\omega_m}{\omega_o}\right)$ from Figure 5-1, gives the relationship $a = 1.5\ c/\omega_m \pm 13\%$. Although this uncertainty can be tolerated in determining the elastic radius, it would lead to a considerably larger uncertainty in the seismic energy, since the elastic radius appears as a^3. Also there would be uncertainty in the function K appearing in the energy formula. However, this difficulty can be effectively eliminated by rewriting equation (5-8) as

$$E = \frac{\pi p_o^2 c^3}{2\mu\, \omega_m^3} \left[K \left(\frac{\omega_m}{\omega_o} \right)^3 \right] \qquad (5\text{-}14)$$

where the function $K \left(\frac{\omega_m}{\omega_o} \right)^3$, plotted versus k in Figure 5-5, is seen to be relatively insensitive to k for the values of k between 0 and 4. Using an average value of 1.5 for the function gives

$$E = \frac{3\pi\, p_o^2\, c^3}{4\mu\, \omega_m^3} \pm 10\% \qquad (5\text{-}15)$$

and p_o is estimated by the average of Salmon and Shoal results, i.e., 1.8 times the overburden pressure.

Boxcar, Benham and Schooner. As described in Table 5-1, Boxcar and Benham were large yield, contained nuclear events detonated in Pahute Mesa, while Schooner was a nuclear cratering event detonated in the same area. Figures 5-6 through 5-8 show compressional wave amplitude spectra of the radial horizontal components of particle motion at surface stations for the particular events (Boxcar spectra were obtained from Hays (1969)). Equation (5-15) in combination with f_m and the elastic parameters was used to compute the seismic energies. Boxcar and Benham show seismic efficiencies of 4.6% and 6.1%, respectively, while Schooner shows a seismic efficiency of 0.32%. The comparison between contained events and the cratering event in Table 5-1 indicates that cratering events have significantly lower seismic efficiencies than contained events.

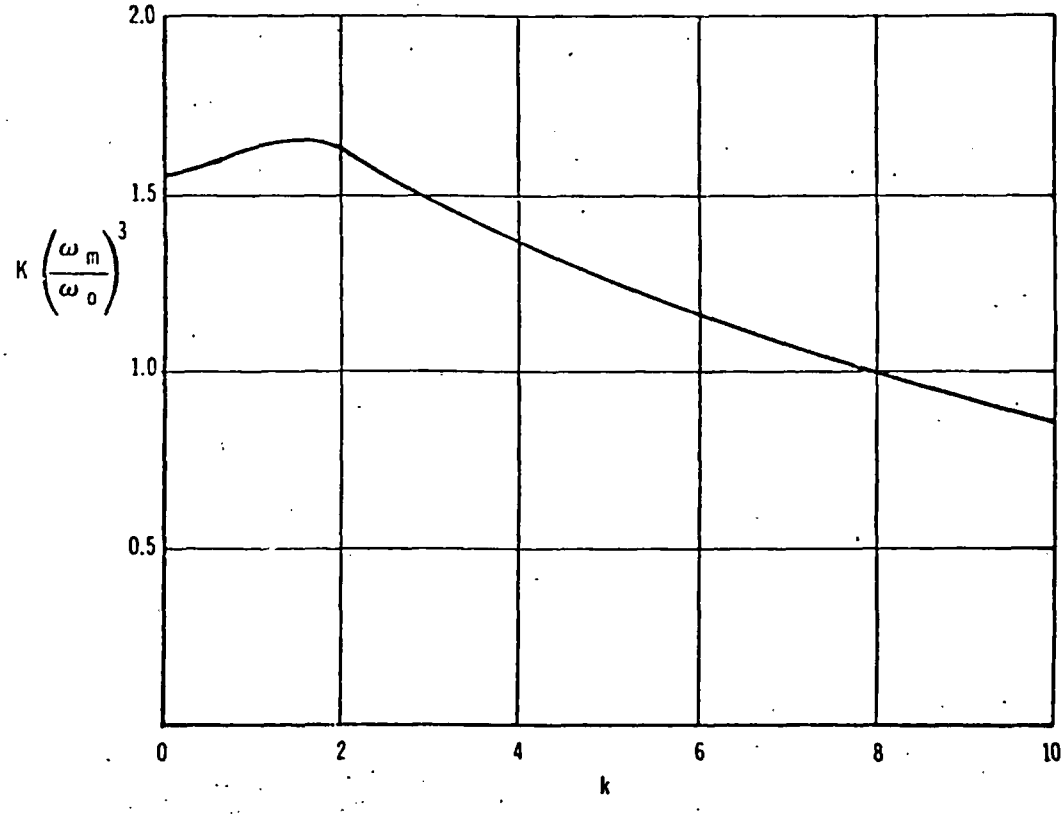

Figure 5-5. The Function K Times the Cube of the Ratio of the Frequency (ω_m) of Peak Spectral Amplitude and Resonant Cavity Frequency (ω_o) Versus the Parameter k

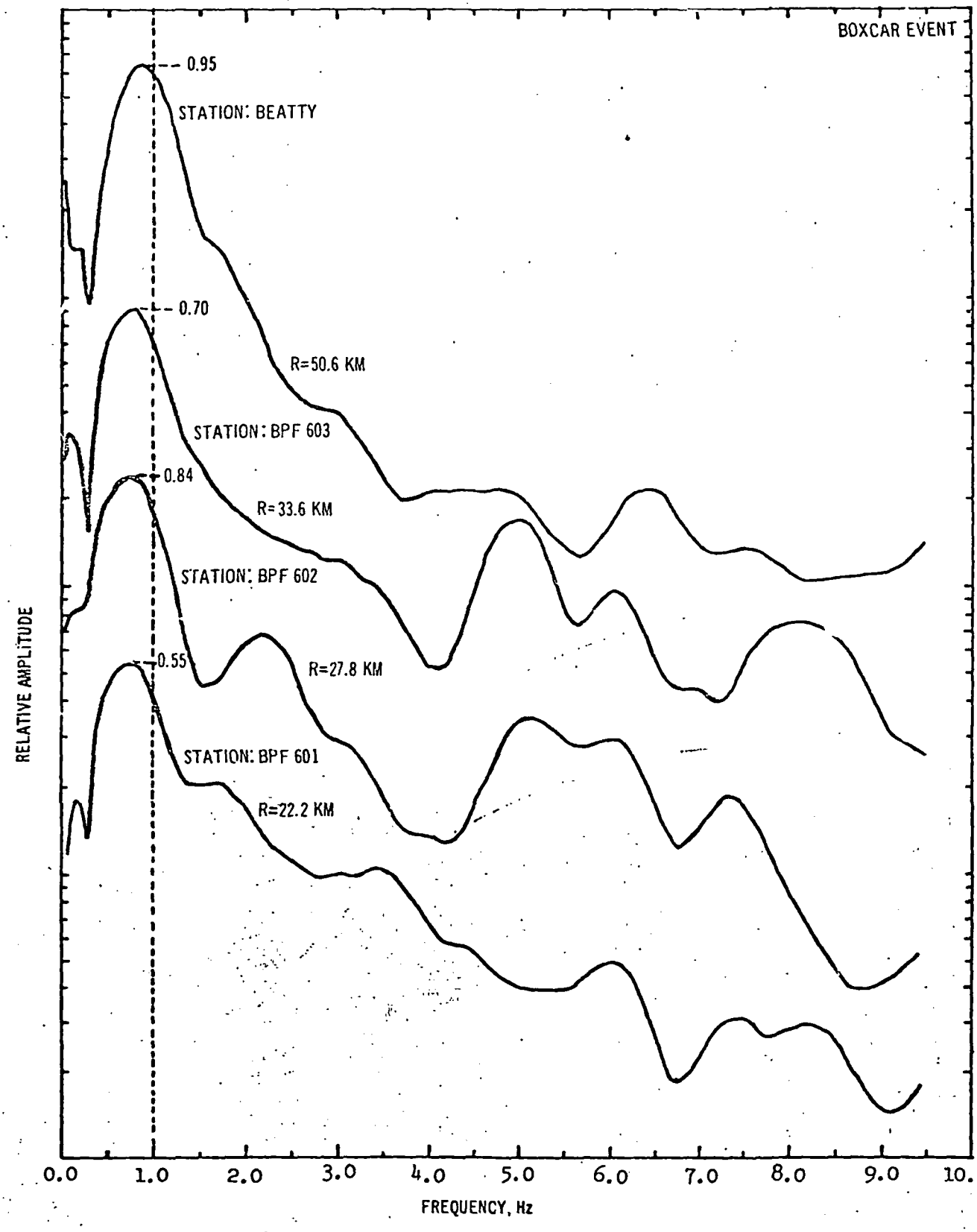

Figure 5-6. Smoothed Fourier Amplitude Spectra of the Compressional Wave Window, Radial Component, Boxcar Event

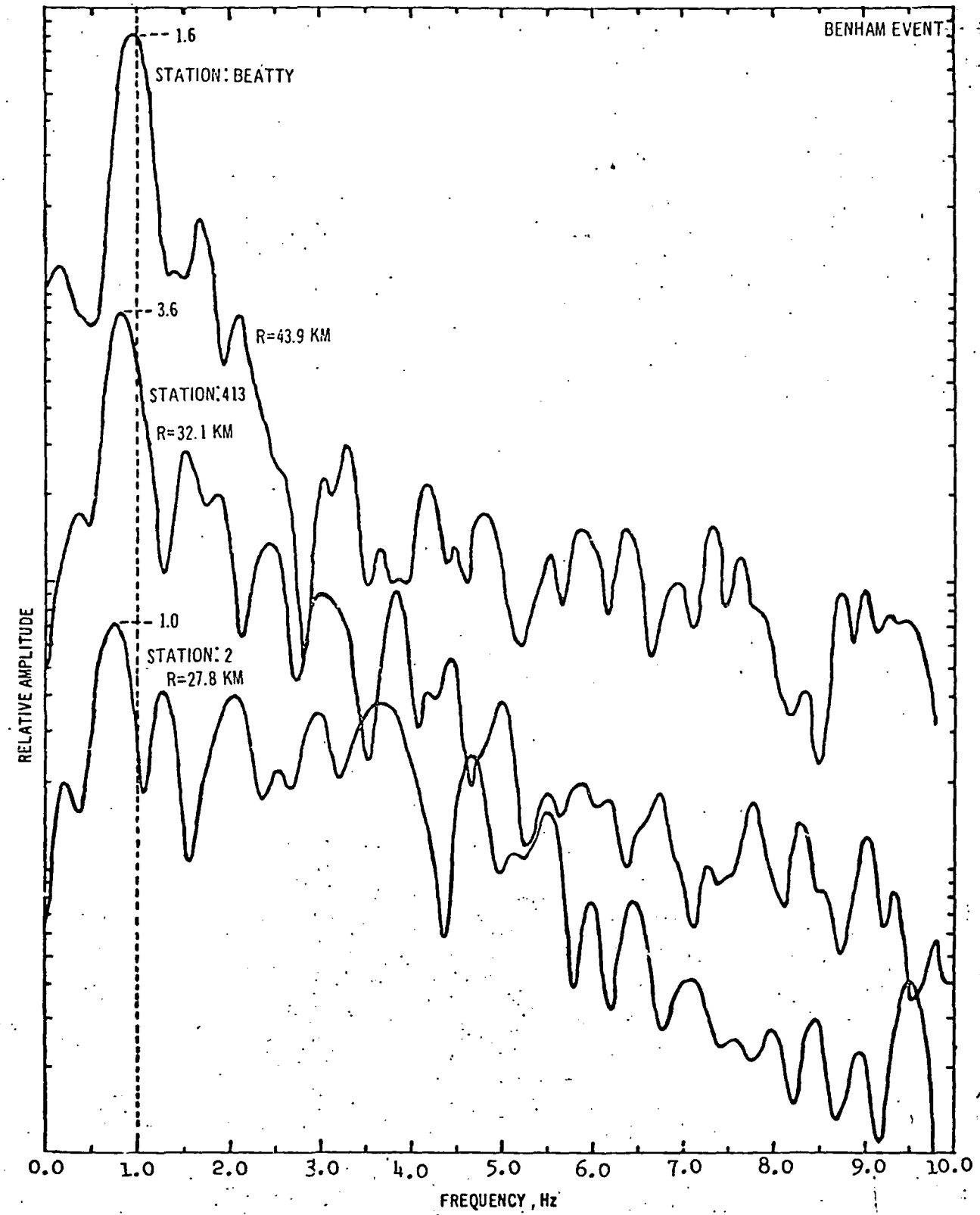

Figure 5-7. Smoothed Fourier Amplitude Spectra of the Compressional Wave Window, Radial Component, Benham Event

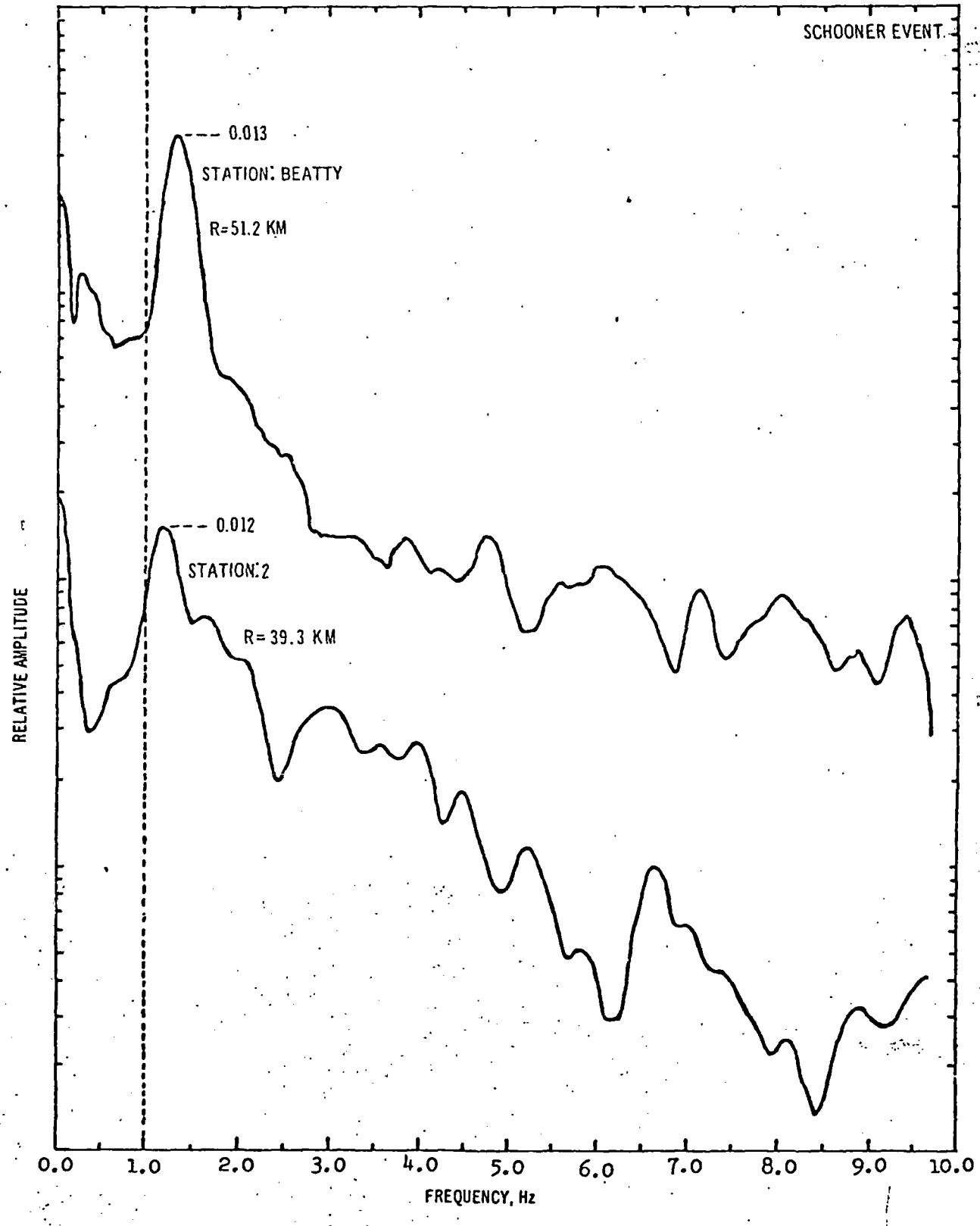

Figure 5-8. Smoothed Fourier Amplitude Spectra of the Compressional Wave Window, Radial Component, Schooner Event

Sterling. The Sterling event was a 380 ton nuclear decoupling shot detonated in the Salmon cavity of 17.4 meters radius. The pressure input at the walls of the cavity consists of a number of spikes oscillating about a mean pressure of about 160 bars. Band-pass spectra at surface stations between 1 and 2 km from the event show a frequency of maximum amplitude around 36 Hz (Davis, 1968). Using the value of (ω_m/ω_o) for a step pressure function (k = 0) from Figure 5-1 gives the relation

$$a = \frac{1.16c}{\omega_m}\Big|_{\text{STEP FN}}$$

which yields an elastic radius of 24 meters. This value of the elastic radius is probably large since the frequencies associated with the ground motion were very high and the differential attenuation effects considerably reduced f_m at 1 and 2 km. This is observed in the spectra obtained at 6 and 7 km where f_m reduces to values between 10 and 20 Hz (Davis, 1968). The free-field data of Perret (1968) obtained at distances between 166 and 660 meters indicate f_m's larger than 40 Hz. This evidence indicates that the medium probably behaved elastically at the cavity wall for the step pressure of 160 bars.

Using equation (5-8a) for the seismic energy liberated by a step pressure function in conjunction with an a of 17.4 meters and p_o of 160 bars gives a radiated energy of 1.3×10^{15} ergs, and

a seismic efficiency of 0.0084%. Perret (1968) experimentally found a mean radiated energy of 3×10^{15} ergs which corresponds to a seismic efficiency of 0.019%. The difference in radiated energies may be due to the significant shear motions associated with the event. The ratio of seismic efficiencies of Salmon/Sterling is 690, or 305 if the higher value is used, which indicates a decoupling factor between 200 and 500 in the radiated energy, assuming that a 380 ton tamped event would have the same seismic efficiency as Salmon.

The conclusions to be drawn are that seismic energies determined by the analytic procedure of this chapter are reasonable estimates, and that, in particular, cratering and decoupled events display significantly lower seismic efficiencies than normal contained events.

CHAPTER 6

SUMMARY AND RECOMMENDATIONS FOR ADDITIONAL WORK

Seismic data were measured at 17 seismic stations for the nuclear cratering detonation, Schooner; and were analyzed and compared with corresponding data observed from other cratering and contained nuclear detonations. Peak vector particle velocities were determined for Schooner and compared with normalized data from other detonations. Measured band-pass filter spectra from Schooner were scaled to account for yield and device depth of burial differences and compared with band-pass filter spectra observed from cratering (Cabriolet) and contained detonations (Knickerbocker, Rex, and Duryea). A preliminary determination of the correlation of the amplitude and frequency characteristics of the ground motion generated by Schooner with specific elastic wave type (P, S, surface) time windows was made and compared with the equivalent correlation for the Cabriolet and Benham detonations. The seismic energy efficiency of Schooner was determined analytically and compared with the seismic energy efficiency of four contained nuclear detonations (Shoal, Salmon, Boxcar, and Benham) and one nuclear decoupled detonation (Sterling). The results of these analyses provide additional insight into the important characteristics of ground motion resulting from nuclear cratering detonations.

6.1 SUMMARY OF CONCLUSIONS

The basic conclusions which resulted from the analyses described above are summarized below:

1. Peak Vector Particle Motion - the peak vector particle velocities recorded at both alluvium and hard rock sites (and the derived peak vector accelerations and displacements) agree qualitatively with results obtained from other cratering events and are low relative to the mean value predicted for equivalent yield contained detonations on the basis of Nevada Test Site experience. The velocities observed from Schooner range from about 0.2 to 1.3 of the mean predicted value for alluvium sites and from 0.4 to 0.7 for hard rock sites. Derived accelerations range from 0.2 to 0.6 of the mean predicted value for alluvium stations and from about 0.1 to 0.5 for hard rock sites. Displacements range from 0.1 to 1.1 and from 0.35 to 0.7 for alluvium and hard rock sites respectively. These results agree qualitatively with spectral results on the basis of depth of burial scaling, as noted below.

2. Band-Pass Filter Spectra - band-pass filter spectra observed from Schooner agree, when scaled for yield and device depth of burial, with the spectra from Cabriolet, (cratering detonation) and Knickerbocker, Duryea and Rex (contained detonations). Before scaling for depth of burial, the band-pass filter spectra from cratering detonations are somewhat lower in magnitude than the mean spectra from equivalent parameter contained detonations and the dominant energy content is shifted to the low-frequency end of the spectrum. Thus, with respect to seismic motions, a cratering event may be considered as a contained event buried at a relatively shallow depth of burial. The relatively shallow depth of burial causes the high frequency spectral composition to be considerably reduced and the low frequency composition slightly reduced relative to that of contained detonations.

3. Amplitude and Frequency Characteristics of Elastic Wave Types - the peak vector and peak horizontal particle velocities observed from Schooner and Cabriolet correlate primarily (with two exceptions) with the surface wave time window. An analogous analysis performed for Benham, a contained detonation, does not lead to the same correlation,

for many of the peak particle velocity measurements occur in the P wave window. Insufficient data are available at this time to explain the apparent correlation of peak particle velocity with the surface wave time window as a physical phenomenon distinctly related to cratering detonations; although, it appears possible that the dominant low frequency spectral composition of cratering detonations may selectively enhance the surface wave generating mechanism. Band-pass filter and Fourier amplitude spectrum analysis of wave mode time windows on the radial component showed that the surface wave mode time window contributes the peak amplitude at the lowest dominant frequency (about 0.5 Hz) in all cases except at ETS-2, the S wave mode time window contributes the intermediate particle velocities (at a dominant frequency of about 0.8 - 1.2 Hz), and the P wave mode time window contributes the smallest particle velocities at the highest dominant frequency (about 1.2 - 4.5 Hz) for Schooner. The transfer function for the shallow layered system at Tonopah, Nevada, derived on the basis of the seismograms recorded at Tonopah Motel and Tonopah Church, verifies that the frequency dependent amplification of the layered system is independent of whether the input energy source is a nuclear cratering or a nuclear contained detonation. However, the peak vector particle motions (particle acceleration, displacement, and velocity) observed at Tonopah are significantly lower than the mean value predicted for equivalent yield contained detonations on the basis of Nevada Test Site experience. The lower level of peak particle motions is related to the diminished high frequency spectral composition and to the decreased seismic energy efficiency of cratering detonations, as is summarized below.

4. Seismic Energy Efficiency - the seismic energy efficiency (radiated energy/initial energy available) is significantly lower (about a factor of 0.1) for nuclear cratering detonations than for equivalent yield nuclear contained detonations. The lower seismic energy efficiency means that cratering detonations are significantly less efficient in forming elastic waves in the radiation field, than contained detonations. The lower seismic energy efficiency is related to the shallower depth of burial for cratering detonations.

On the basis of the results obtained for Cabriolet (Klepinger and Mueller, 1969) and for Schooner, the following guidelines seem

reasonable for making ground motion predictions for NTS cratering detonations:

- Preliminary peak vector motion predictions can be based on NTS experience with equivalent yield contained detonations for planning purposes. These predictions will be conservative for the relatively high frequency ground motions, the peak particle accelerations and velocities, and will need to be reduced by a factor which is related to the shallow depth of burial of cratering detonations relative to the standard scaled depth of detonation. The correction for shallow depth of burial is based on a scaling technique developed by Mueller (1969). The ratio of the scaled depth of detonation of the event under consideration to another event (or set of events) at a standard scaled depth of burial is defined as λ. From theoretical considerations, it can be shown that the peak vector particle acceleration needs to be corrected for depth of burial by the multiplicative factor $\lambda^{0.63}$ and the peak vector particle displacement by $\lambda^{0.48}$. The peak vector particle velocity is corrected on the basis of the characteristics of observed band-pass filter spectra. The multiplicative factor applicable at NTS for peak vector velocities is $0.5+0.5\lambda^{0.63}$.

- Spectral (Pseudo Relative Velocity (PSRV) predictions for planning purposes can also be based on NTS experience with equivalent yield contained detonations. These predictions will be conservative at the short period end of the spectrum, unless a correction for the shallow depth of burial of the cratering detonation is incorporated. This frequency dependent correction (Mueller, 1969) yields a multiplicative constant for each frequency. The magnitude of the constant is related to the ratio of the scaled depth of detonation of the event under consideration to another event (or set of events) at a standard scaled depth of burial. For cratering detonations, the correction for shallow depth of burial reduces the level of PSRV at the short period end of the spectrum while leaving the level at the long period end of the spectrum essentially unchanged.

6.2 RECOMMENDATIONS FOR ADDITIONAL WORK

Useful physical insight into the characteristics of ground motion of a nuclear cratering detonation has been obtained by the analyses contained in this report. However, additional data from cratering detonations are required in order to extend significantly the ability to predict accurately the ground motion characteristics of nuclear cratering detonations. Future Plowshare excavation projects (Yawl, Sturtevant, Phaeton, etc.) will provide the basic data needed to achieve this goal.

Specific recommendations of future work include the following:

1. Determine the similarities and differences of the amplitude and frequency characteristics of ground motion from cratering and equivalent parameter contained detonations.

2. Process and compile a representative ground motion data sample for cratering detonations on which to base statistically derived peak amplitude (acceleration, displacement, and velocity) and PSRV prediction equations.

3. Determine the experimental and theoretical correlation between wave modes, peak ground motion, and frequency dependent amplification for cratering detonations.

4. Determine the experimental and theoretical effect of the physical properties of the source medium on factors such as the amplitude and frequency characteristics, seismic energy efficiency, and wave mode generation of cratering detonations.

These activities will significantly improve the physical basis for making predictions of ground motion for future nuclear cratering detonations.

REFERENCES

Berg, Jr., J. W., L. D. Trembly and P. R. Laun (1964); Primary Ground Displacements and Seismic Energy Near the Gnome Explosions, Bull. Seism. Soc. Am.; 54, 1115-1126.

Carder, D. S., W.K. Cloud, L. M. Murphy and J. Hershberger (1958); Surface Motions for an Underground Explosion, Operation PLUMBOB; WT-1530; U. S. Coast & Geodetic Survey.

Carder, D. S., L. M. Murphy, T. H. Pearch, W. V. Mickey and W. K. Cloud (1961); Surface Motions from Underground Explosions, Operation HARDTACK, Phase II; WT-1741; U. S. Coast & Geodetic Survey.

Davis, A. H. and J. R. Murphy (1967); Amplification of Seismic Body Waves by Low-Velocity Surface Layers; Environmental Research Corporation; NVO-1163-130; AEC.

Davis, L. L. (1968); Analysis of Ground Motion and Containment, Sterling Event; VUF-1035, Environmental Research Corporation.

Diment, W. H., S. W. Stewart and J. C. Roller, (1961); Curstal Structure from the Nevada Test Site to Kingman, Arizona, from Seismic and Gravity Observations; Journal of Geophysical Research; Vol. 66, p. 201.

Hannon, W. J., (1964); An Application of the Haskell-Thomson Matrix Method to the Synthesis of the Surface Motion Due to Dilational Waves; Bulletin of the Seismological Society of America; Vol. 54, p. 2067.

Haskell, N. A., (1953); The Dispersion of Surface Waves on Multilayered Media; Bulletin of the Seismological Society of America, Vol. 43, p. 17.

Hays, W. W., (1969); Amplitude and Frequency Characteristics of Elastic Wave Types Generated by the Underground Nuclear Detonation, Boxcar, Bulletin of the Seismological Society of America, Vol. 59, No. 6 (in press).

Hill, D. P. and L. L. Pakiser, (1967); Seismic Refraction Study of Crustal Structure Between the Nevada Test Site and Boise, Idaho; Geological Society of America Bulletin; Vol. 78, p. 685.

King, K. W., (1969); Ground Motion and Structural Response Instrumentation, Technical Discussions of Off-Site Safety Programs for Underground Nuclear Detonations, U. S. Atomic Energy Commission, Nevada Operations Office, NVO-40, Revision No. 2, Chapter 8.

Klepinger, R. W. and R. A. Mueller, (1969); Analysis of Ground Motion, Cabriolet Event; PNE-958, Environmental Research Corporation.

Latter, A. L., R. E. LeLevier, E. A. Martinelli and W. G. McMillan, (1961a); A Method of Concealing Underground Nuclear Explosions, Journal Geophysical Research, Vol. 66, 943-946.

Latter, A. L., E. A. Martinelli, J. Mathews and W. G. McMillan, (1961b); The effect of Plasticity on Decoupling of Underground Explosions, Journal Geophysical Research; Vol. 66, 2929-2936.

Lowrie, W. R. and W. V. Mickey, (1965); Strong-Motion Seismic Measurements, Project DUGOUT; PNE-605F; U. S. Coast and Geodetic Survey.

Murphy, J. R. and J. A. Lahoud, (1969); "Analysis of Seismic Peak Amplitudes from Underground Nuclear Explosions," Bulletin of the Seismological Society of America, Vol. 59, No. 6 (in press).

Murphy, J. R. and A. H. Davis, (1969); Amplification of Rayleigh Waves in a Surface Layer of Variable Thickness; Environmental Research Corporation; NVO-1163-175; AEC.

Orkild, P. P., (1968); "Report of Exploration Progress, Pahute Mesa-Period July 31, 1966 - January 31, 1968;" U. S. Geological Survey, TID-24290, DTIE.

Perret, W. R., (1963); Free-Field Ground Motion Studies in Granite - Operations Nougat-Shot Hardhat; POR-1803; Sandia Corporation.

Perret, W. R., (1967); Surface Motion Response Spectra, Project Shoal; SC-RR-66-696; Sandia Laboratory.

Perret, W. R., (1968a); Free-Field Particle Motion from a Nuclear Explosion in Salt, Part I, Project Dribble, Salmon Event; VUP-3012; Sandia Laboratory.

Perret, W. R., (1968b); Shear Waves From a Nuclear Explosion in a Salt Cavity; Bull. Seism. Soc. Am. 58; 2043-2051.

Sharpe, J. A., (1942); The Production of Seismic Waves by Explosion Pressures. I; Theory and Empirical Field Observations, Geophysics 18; 144-154.

Stuart, D. J., J. C. Roller, W. H. Jackson, and G. B. Mangan, (1964); Seismic Propagation Paths, Regional Traveltimes, and Crustal Structure in the Western United States; Geophysics; Vol. 29; p. 178.

Sutton, G. H., W. Mitronovas and P. W. Pomeroy, (1967); Short-Period Seismic Energy Radiation Patterns from Underground Nuclear Explosions and Small-Magnitude Earthquakes; Bull. Seism. Soc. Am. 57; 249-267.

Tewes, H. A., (1969); Memorandum-UOPKG 69-18; To: Schooner Distribution; Subject: Schooner Scientific Reports; Lawrence Radiation Laboratory; K-Division, T-105, L-41.

Trembly, L. D. and J. W. Berg, Jr., (1966); Amplitudes and Energies of Primary Seismic Waves Near the Hardhat, Haymaker, and Shoal Nuclear Explosions; Bull. Seism. Soc. Am. 56; 643-653.

Weart, W. D., (1965); Free-Field Earth Motion and Spalling Measurements in Granite, Project Shoal, VUF-2001; Sandia Corporation.

PROJECT SCHOONER REPORTS

Report No.	Agency	Author	Title
PNE-520	LRL	H. A. Tewes	Schooner Summary
PNE-521	Sandia	L. Vortman	Close-In Air Blast
PNE-522	ERC	W. W. Hays R. A. Mueller C. T. Spiker, Jr.	A Contribution to the Analysis of Seismic Data from Cratering and Contained Events
PNE-523	ESSA/ARL		Weather and Radiation Predictions, Schooner Event
PNE-524	USPHS		Off-Site Surveillance, Schooner Event
PNE-525	REECo		On-Site Radiological Safety, Schooner Event
PNE-526	EG&G	H. Nishita W. A. Rhoads	Ecological and Environmental Effects from Local Fallout from Schooner. 1. Soil Thermoluminescence in Relation to Radiation Exposure Under Field Conditions

END

DATE FILMED

8 / 17 / 70

UDC 622.7

Micelle formation and its role in the flotation process

A N Grebnev (Institute of Mineral Resources, MG, Ukrainian SSR)

Summary

The capacity for micelle formation is an undesirable characteristic for a collector, since it leads to a decrease in the concentration of its most flotation-active form (free ions) in the volume of the pulp.

The rate of destruction of the micelles in solutions of collectors of one homologous series is directly proportional to the critical micelle concentration. With dilution of the solution (in the region of flotation concentrations) complete destruction of the micelles of collectors containing C_{16}-C_{18} saturated radicals takes 15-30 min or more. For collectors with unsaturated radicals this time amounts to 2-5 min.

Preliminary dilution of the initial concentrated solutions of the collectors before delivery to the pulp aids destruction of the micelles and leads to increased extraction of the mineral and increased flotation rates. The same effect is achieved by the addition of certain organic oxygen compounds to the concentrated solutions of the collectors.

UDC 622.7.976.8

Concentration of bauxites by means of heterotrophic bacteria

P I Andreev, S I Pol'kin, R A Shavlo, G I Karavaiko and R D Morozova (Institute of Mineral Resources, MG, Ukrainian SSR)

The main raw material for the production of alumina is high grade bauxites, the reserves of which in the USSR are limited. In the meantime considerable reserves of high silicon low-grade bauxites have been proved, and they cannot be processed to alumina by the most effective Bayer process without preliminary concentration. The directives of the 24th Congress of the Communist Party of the Soviet Union provide for a 50-60% increase in alumina production during the ninth five-year Plan.

Analysis of scientific researches into the concentration of low-grade bauxites leads to the conclusion that the existing mechanical methods of concentration have low efficiency. The extraction of alumina in the concentrate rarely exceeds 65-70%, while the quality of the concentrates is as a rule increased by no more than 4-7%. Moreover, there are a series of deposits of kaolinite-boehmite bauxites with a high content of silica, which are not concentrated at all, and their direct treatment to alumina can only be realised by an extremely complex and costly technique, by the sintering method.

The main reasons restricting the possibility of effective concentration of high-silicon bauxites are the extremely fine emulsion-type impregnation of the minerals of the free forms of alumina (boehmite, gibbsite, diaspore) in the cementing mass of the rock and the close mutual intergrowth of the minerals with each other. The main harmful impurity in bauxites is silica, which enters into the composition of various aluminosilicates (kaolinite, halloysite, chlorites, etc). In the concentration process the SiO_2 must be removed with the waste products, but as a result of this operation a considerable part of the Al_2O_3 is lost.

The characteristics of the mechanical concentration of bauxites achieved at the present time can be regarded as the best possible, and no prospect can be foreseen for a substantial improvement in the effectiveness of mechanical methods for the concentration of bauxites. In recent years, in many countries, including the Soviet Union, extensive researches have been carried out in the search for new more effective methods for the extraction of useful components from ores, and the most promising of these is bacterial leaching.

Thiobacilli are mostly used in the bacterial leaching of nonferrous metals, and their action amounts either to direct oxidation of the sulphide minerals or to oxidation of ferrous sulphate to ferric, which is a strong oxidising agent for sulphide minerals. A new direction has begun to develop in bacterial hydrometallurgy. This involves the leaching of nonferrous, rare, and noble metals from rocks and carbonate ores by means of heterotrophic micro-organisms and the products from their activity[1-4]).

The great part played by heterotrophic micro-organisms in the breakdown of silicate minerals has been mentioned by Vernadskii[5]), Vinogradskii[6]), Omelyanskii[7]), Krasil'nikov[8]), Vologdin[9]), and others. Thus, Vernadskii came to the conclusion that the disintegration of the kaolin nucleus (or derivatives of aluminosilicates such as feldspars, etc.) can be related to the development of diatomic algae and, consequently, bacteria. Subsequently, developing these ideas, Vologdin[9]) wrote that "these organisms split the kaolin molecule into alumina and silica". Zajic[10]) gives data which show that heterotrophic micro-organisms are capable of decomposing various silicate minerals. Thus, in the presence of fungi, calcium, magnesium, and zinc silicates were decomposed by 94, 76 and 96% respectively. Bacteria and actinomycetes, isolated from the soil, also dissolved 83-87% of calcium silicate.

Aleksandrov and Ternovskaya[11]) showed that when muscovite and phlogopite are treated with heterotrophic bacteria, more than 22% of the silica present in the minerals can pass into solution. Teshich and Mar'yanovich[12]) give data on the use of heterotrophic bacteria for decomposition of the alumino-silicate core of minerals with release of uranium, beryllium, and manganese into solution. In experiments by Silverman and Munoz[3]) up to 80% of the titanium was leached out from granites, granodiorite, and quartzite in 7 days by means of fungi. The rate of the leaching of uranium from uranium ore and granites increase by 100 and 5 times respectively under the influence of heterotrophic bacteria[3]).

The organic compounds normally formed by microorganisms are also active agents for the decomposition of silicate minerals. Organic acids are capable of destroying the crystal lattices of minerals and transferring the metals into solution in the form of organic-mineral salts or chelates. Thus, according to data of Huang and Keller[13]), 0.5-5 times more silicon dissolves in carbonic acid water and solutions of weakly complexing acids and 50 times more in solutions of strongly complexing acids compared with distilled water. Solutions of weakly and strongly complexing acids dissolve 10 and 100 times more aluminium and iron respectively than distilled water.

The purpose of the present work was to study the possibility of using certain heterotrophic bacteria for the disili-

consisting of high-silica low-grade bauxites of the Smelyanskii and the Vislovskii deposits. The bauxites of the Smelyanskii deposit contain 42 wt.% Al_2O_3, 27.7 wt.% SiO_2, and iron oxides and hydroxides. The main minerals are gibbsite, quartz, and kaolinite. The sample tested of bauxites from the Vislovskii deposit contained (wt.%) 12.6 SiO_2, 48.4 Al_2O_3, 18 FeO, and 4.4 F_2O_3. The main minerals of the bauxites are boehmite, chamosite (chlorite), and kaolinite. To prepare the culture liquid we used a dry preparation of heterotrophic bacteria, obtained by the method of V G Aleksandrov on T-2 medium with the following composition (mg): $6MgSO_4$; 5NaCl; $FeCl_3$ (1% solution) one drop: 400 K_2CO_3, 400 K_2CO_3, phosphate fertiliser with 10% chalk, 6 g: water, 100 ml. In 100 ml of solution we used 20 g of the dry preparation of the heterotrophic bacteria.

In the experiments we used 5-10 g of bauxite. The samples were placed in 200-250 ml conical flasks, 5-7 ml of boiled water was added, and the materials were rubbed against the bottom of the flask to prevent the formation of lumps. A 10-15 ml portion of the culture liquid containing the bacteria was then added, and the flasks were placed in a thermostat at 28-30°C. The flasks were periodically shaken. The results from bacterial concentration of bauxites from the Smelyanskii and the Vislovskii deposits, compared with data on mechanical concentration of the bauxites, are given in the table.

Concentration of bauxites by means of heterotrophic bacteria

Name of product	Yield %	Content %		Extraction %		Experimental conditions
		Al_2O_3	SiO_2	Al_2O_3	SiO_2	
Smelyanskii Deposit						
Concentrate	89.0	41.2	29.1	87.6	93.0	Control
Solution	11.0	47.0	18.2	12.4	7.0	(without bacteria)
Initial bauxite	100	42.0	27.7	100	100	
Concentrate	69.0	53.6	17.6	87.9	44.0	Treatment with
Solution	31.0	16.5	50.0	12.1	56.0	bacteria for 7 days
Initial bauxite	100	42.0	27.7	100	100	
Concentrate	70.0	53.2	18.3	88.2	46.1	Treatment with
Solution	30.0	16.6	49.6	11.8	53.9	bacteria for 7 days
Initial bauxite	100	42.0	27.7	100	100	
Concentrate	63.8	48.4	21.1	74.0	48.3	Flotation
Tailings	36.2	30.1	39.5	26.0	51.7	
Vislovskii Deposit						
Concentrate	92.0	48.1	11.8	91.5	90.5	Control (without
Solution	8.0	51.3	14.2	8.5	9.5	bacteria
Initial bauxite	100	48.4	12.0	100	100	
Concentrate	76.0	53.2	10.3	83.5	65.3	Treatment with bac-
Solution	12.0	24.2	23.1	6.0	23.1	teria for 7 days,
Tailings	12.0	42.6	11.0	10.5	11.6	blown with air with-
Initial bauxite	100	48.4	12.0	100	100	out reagents
Concentrate	71.0	58.7	5.8	87.2	32.7	The same, but washed
Solution	29.0	21.2	29.3	12.8	67.3	twice with hot water
Initial bauxite	100	47.9	12.6	100	100	
Concentrate	57.8	53.2	10.1	65.3	47.0	Magnetic separation
Tailings	42.2	41.0	13.6	31.7	53.0	
Initial bauxite	100	47.1	12.4	100	100	

With the bauxites of the Smelyanskii deposit bacterial concentration secures an increase of the Al_2O_3 content from 42 to 53.2-53.7% with 87.9-88.2% extraction, while the SiO_2 content decreases from 27.7 to 17.6-18.3%. This silica is largely represented by quartz and is not a harmful impurity in the production of alumina by the Bayer method. In the case of the concentration of these bauxites by flotation it was possible to obtain concentrates containing 48.4% of Al_2O_3 with 74% extraction and to reduce the SiO_2 content only from 28 to 21.1%.

Bacterial treatment of samples of the bauxites from the Vislovskii deposit for 7 days followed by washing of the pulp with hot water gave concentrates containing 58.7% of Al_2O_3 with 87.2% extraction and 5.8% SiO_2. The silica ratio (the ratio of Al_2O_3 to SiO_2) was 10.1. According to the state standard GOST 972-50, such a concentrate belongs to bauxite of grade BO and can be treated successfully to alumina by the Bayer method. During concentration of a sample of bauxite by magnetic separation in a strong magnetic field the obtained concentrates in the best case contained 53.2% Al_2O_3 and 10.1 SiO_2 with an extraction of only 65.3% Al_2O_3. Such a concentrate corresponds to bauxite of grade B-3 (the highest sintering grade) and can only be processed to alumina by the Bayer method by sintering.

The alumina released during bacterial decomposition of the aluminosilicates concentrates in the washing waters and can also be extracted. In this case there are practically no losses of alumina in the bacterial concentration of bauxites.

The data presented demonstrate the high effectiveness of the bacterial concentration of bauxites and the good prospects for the use of this method in the production of alumina, since not only bauxites but also other aluminosilicates (nephelines, kaolinites) can be broken down by means of bacteria with subsequent extraction of the alumina.

References

1) I Pare: Eight Congress on the Concentration of Minerals. Leningrad 1969, (2).
2) M T Silverman and E F Munoz: Appl. Microbiol. 1971, (5), 22.
3) R Mague, J Berthelin and Y Dommergues: Compte. Rendues. Acad. Sci. 1973, D.276, (19), 2625.
4) F H Wenberg and F H Erbisch: Transactions. 1971, 250, (9), 207.
5) V I Vernadskii: The problem of decomposing kaolin by organisms. Selected works, Izd. Akad. Nauk SSSR 1960, (5).
6) S N Vinogradskii: Microbiology of the soil. Izd. Akad. Nauk SSSR 1952.
7) V L Omelyanskii: The role of micro-organisms in the weathering of rocks. Selected works. Izd. Akad. Nauk 1953, (1).

IN SITU (3), 209-233 (1977)

CHEMICAL, BIOLOGICAL, AND METALLURGICAL ASPECTS OF LARGE-SCALE COLUMN LEACHING EXPERIMENTS FOR SOLUTION MINING AND IN-SITU LEACHING

L.E. Murr*, L.M. Cathles**, D.A. Reese†, J.B. Hiskey††, C.J. Popp*, J.A. Brierley*, D. Bloss*, V.K. Berry*, W.J. Schlitt***, and P-C. Hsu*

*New Mexico Institute of Mining and Technology, Socorro, New Mexico 87801; **Kennecott Copper Corp. Ledgemont Laboratory, Lexington, Mass.; †Kennecott Copper Corp., Chino Mines Division, Santa Rita, New Mexico; ††New Mexico Tech, now with U.S. Steel Research Center, Pittsburgh, Pa.; ***Kennecott Copper Corp. Research Center, Salt Lake City, Utah.

ABSTRACT

It is well known that the variations in temperature, chemical reactivity, and reaction rates which are presumed to occur and which in some cases have been shown to occur in a leach dump or similar solution mining activity are difficult to duplicate or model on a small laboratory scale, and the degree to which such large-size metallurgical processes can be scaled is not well established. In the present investigations the design criteria and sampling methods for large-scale leach tests on low-grade copper waste are outlined and the results of studies of temperature profiles and associated chemical and biological activity in 185 ton (1.63×10^5 Kg) waste samples (approx. 10.75m in height) are discussed. Various simple scaling features are presented, including drain-down characteristics and waste-body neutralization (of acid consuming minerals) for test samples of 7.0, 4×10^2, and 1.7×10^5 Kg. Simple geometrical scaling laws are shown to closely describe the greater part of these processes. Temperature profiles in a large waste body are shown to be related to or correlated with bacterial activity, which is further shown to be related to available oxygen (and oxygen consumption). Aeration of large waste bodies is shown to be correlated with enhanced bacterial activity and leaching rates, and certain features of bacterial catalysis observed in the large-scale tests are corrob-

orated by detailed laboratory studies of bacterial leaching phenomena utilizing the scanning electron microscope. Long-term data profiles showing a relationship between temperature, bacterial activity, oxygen consumption, and variations in Fe^{2+}, Fe^{3+}, Cu concentration, pH and Eh in the waste body are presented along with the variation of these parameters.

INTRODUCTION

The importance of bacterial activity in the sulfide copper leaching process was first recognized in the recovery of copper in the Rio Tinto (Razzell and Trussel[1]), and since then it has been convincingly demonstrated at least on a laboratory scale that leach solutions inoculated with an appropriate microorganism are much more effective in solubilizing copper from a mineral-bearing waste than those solutions which do not contain any measurable bacterial population or bacterial activity. Although the evidence supporting the effects of bacterial catalysis is overwhelming at the laboratory scale, there has been little direct evidence of the effect of bacterial catalysis in large leach dumps and similar large-scale processes. While Bhappu, et al.[2] have, for example, attempted to determine the extent of bacterial activity within a leach dump, there have been no detailed correlations of leach dump bacterial activity with temperature profile, elemental concentrations (of Fe^{2+}, Fe^{3+}, and Cu) indicative of the efficiency of the copper leaching process; as well as oxygen available within a leach dump. As a result of possible temperature, concentration, and oxygen profiles within a leach dump, and the effect these parameters would be expected to have upon bacterial activity, or the effect bacterial activity may have upon these parameters, it is difficult to characterize such effects in a large leach dump or similar large-scale solution mining operation by studying small-scale, laboratory column tests. There is in general a dearth of information relating to the ability to scale small column leach tests to large leach dump operations or to model such operations, and it is difficult if not impossible to effectively duplicate temperature and biochemical reaction profiles which are expected to occur in a large leach dump,

in small-scale, laboratory column tests of only a few hundred kilograms of waste rock.

Madsen and Groves[3], who recently completed a long-term, large-column (7.9×10^3 Kg) leaching experiment on a low-grade 0.25% copper (chalcopyrite) waste, concluded that enhanced leaching and leaching rates which occurred after aerating the waste body were due primarily to bacterial catalysis. However, there were no direct observations of bacterial population or activity within the waste body, and there was also no attempt to systematically evaluate the changes in solution chemistry, or to determine associated variations in the waste body temperatures with leaching time and aeration. Cathles and Apps[4] have recently developed a dump leaching model which illustrates the importance of air convection and temperature profiles.

The present experiments were devised in an attempt to overcome some of the shortcomings outlined above. In particular, the waste columns tested were considered to be representative of a small leach dump or unit of a large dump or heap because they were able to hold nearly 190 tons (1.7×10^5 Kg) of waste; having a height in the 3.08m-diameter waste column of approximately 10.5m. In addition, the test columns were designed to allow for access to the leach solution as it permeated the waste body, and for periodic sampling of waste particles in order to monitor bacterial population and activity at locations within the waste column; and thermocouples were embedded within the waste body at various locations to allow the temperatures to be measured and corresponding temperature profiles to be determined. The application of simple scaling laws in conducting drain-down experiments and the neutralization of an acid-consuming waste was also tested in the present experimental program. Finally, laboratory studies of bacterial catalysis utilizing the scanning electron microscope were undertaken in an effort to elucidate the detailed nature of the associated microorganisms and their apparent role in the leaching process; particularly pyrite and chalcopyrite surface reactions (corrosion rates).

EXPERIMENTAL METHODS AND DESIGN CRITERIA

The large tanks utilized in these experiments are converted liquid oxygen storage dewars measuring roughly 40 ft (12.3m) in overall height and 10 ft (3.1m) in inside diameter. The inside jacket wall is a 304 stainless steel separated from the outer carbon-steel wall by 1 ft (0.3m) of perlite insulation. Currently two tanks in an array of four have been loaded with low-grade waste and tested for varying periods. Prior to loading, drains were cut into the bottom of each tank and provision for aeration made. An air distribution system consisting of a 5 ft. square 1 in. schedule-80 PVC pipe with 0.125 in. holes spaced 1 in. apart was placed on the flat tank bottom. A 1m high quartzite bed (+2") was placed upon the air distributor and the waste rock loaded by hand (hand placed) to a depth of approximately 0.3m. One tank was loaded with Kennecott Chino Mines Division (CMD) Santa Rita waste rock (~ -4"). The total copper was 0.36% with non-sulfide (acid soluble) copper accounting for 0.14% and the balance disseminated as chalcocite and chalcopyrite; with the chalcopyrite representing < 0.1 wt %. The pyrite/chalcopyrite ratio was determined to be 10.6. The rock matrix was a quartz monzonite which required little detectable neutralization.

Four access ports were cut into the sides of the leach tanks corresponding to irregular depths in the loaded waste body, and alternated at 90° from one another along a diameter. Following the initial hand loading of the waste, the next 3.6m depth was loaded by elevator. Upon reaching the first port level, an array of instruments were installed consisting of a half-section pipe array to collect solution, a lysimeter (porous-cup collector for solution sampling) located in the center of the tank, and at least 2 thermocouples near the center of the waste body; with one acting as a backup. This routine was continued until the waste was fully loaded and all access ports installed. The waste rock was hand loaded to a depth of roughly 0.3m over the instruments installed at each level.

A second tank was loaded in a similar manner with Duval-Sierrita waste (~ -6") with a total copper content of 0.34% of which

0.03% was non-sulfide (acid soluble) copper, and the balance chalcopyrite. The pyrite/chalcopyrite ratio of this rock was determined to be 4, and the matrix, unlike the Kennecott rock, contained a considerable carbonate concentration (~ 2%) to be neutralized. In the loading of the Duval waste, a system of funnels (10 in. diameter) filled with screens and alumina balls were used in place of the pipe half-sections to collect solution at locations within the waste body. In addition, an array of gypsum moisture blocks was placed at various locations (at the gravel bed/waste body interface near the bottom and at each access port level). While in the Kennecott waste body, rock samples were removed periodically by augering through the solution collector opening at the access ports, a separate 2 in. fitting was provided for this purpose in the Duval tank. Each access port was provided with fittings to allow oxygen content to be measured. The top of each tank was vented through a 1 in. opening where oxygen content and air flow could be measured. An air compressor fitted with pressure control valves and a flow meter was used as a source of air (oxygen) through the air distributor at the bottom of the gravel bed.

The solution distributor at the top of each tank consisted of a 1 in. stainless steel shaft through a reservoir connected to the center of an arm extending 9.5 ft. across the inside diameter, with 1/16 in. holes in the upper side at decreasing spacing from the center shaft. The shaft itself was slotted to allow a permanent solution head in the reservoir, and was rotated with a high-torque motor at 1 rpm. The solution circuits normally contained approximately 5000 gal. (22.7×10^3 ℓ) of solution. The circuit itself consisted of a 10,000 gal. stainless steel holding tank (gravity fed from the waste column), a cascade scrap-iron launder, and an array of surge tanks or holding tanks between the launder and the waste column.

Figures 1 and 2 illustrate the principal features of the instrumentation systems at the access ports, the solution circuit, and overall views of the facility described above. Figure 3(a)

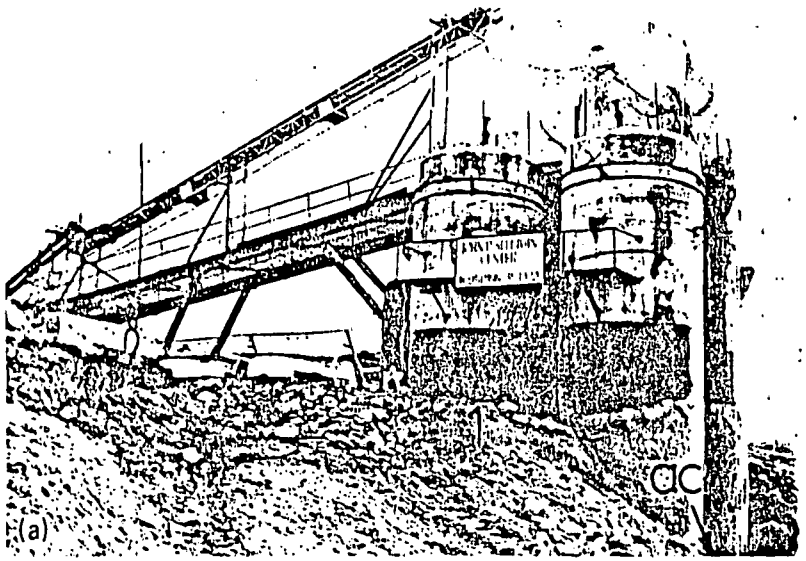

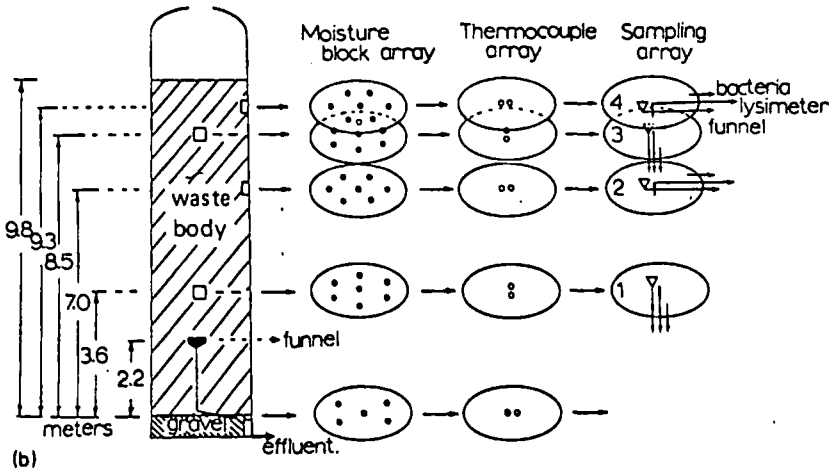

FIG. 1: Large leach tank facility and sampling and instrumentation design. (a) Overall view of leach-tank facility, (b) Duval-Sierrita waste-body sampling and instrumentation design features. Locations and arrays of moisture blocks and thermocouples are shown. The sampling arrays at access ports allow for the extraction of rock particles for determining bacterial population and activity, and solution, extraction either from funnel collectors or a lysimeter. The lysimeter consists of a porous cup through which solution is drawn under vacuum and then expelled under pressure. Access port 1 is shown at (1) in (a) while (ac) denotes the air compressor.

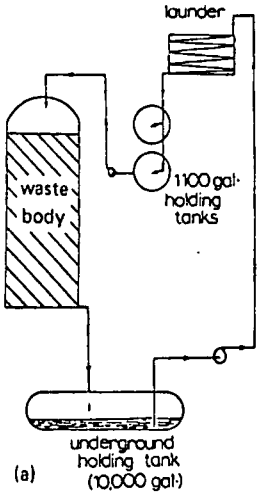

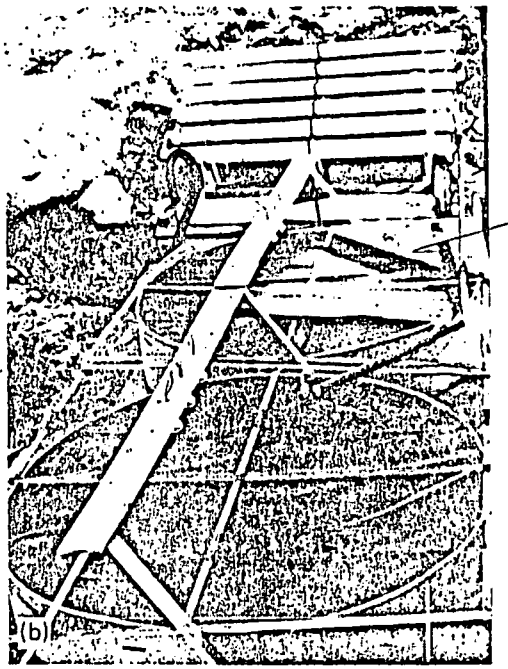

FIG. 2: Solution circuit schematic (a) and full view of launder and holding tanks shown in Fig. 1(a) (b).

illustrates schematically the essential features of the air and solution distributors described above, while Fig. 3(b) compares the drain-down characteristics for the scaled tests. Figure 4(a) and (b) illustrate the waste-body permeabilities throughout the waste column in the dry and solution-saturated states determined by measuring the pressure difference from inlet to outlet at constant flow rate. It is obvious from Fig. 4(a) and (b) that the waste-body permeabilities were considerably different, primarily as a result of differences in particle size distribution and waste body integrity. The variation in permeability is caused by the difference in packing. The waste packed to a greater packing density near the bottom as compared with the top of the waste body as a consequence of the loading technique.

Simultaneous with the loading and initial testing of the Duval-Sierrita waste, smaller column tests were devised to function in a scale test of the large-column leaching experiments. A 0.38m diameter and a 0.10m diameter column were loaded with 405 and 7 Kg of rock sized approximately on a scaled basis by multiplying the large tank maximum rock size (6 in.) by the ratio of the scale column diameter to the large column diameter. It was noted that the ratio column diameter/column height was smaller by a factor 2 for the smaller columns when compared to the large column, and this factor was taken into consideration when scaling the solution and air flow rates. The drain-down characteristics of the smaller columns from a solution-saturated condition were also scaled in terms of initial drain-down flow rate for the large column, and the ratio of retained fluid to saturated fluid volumes determined. These data are listed for comparison in Table 1. Figure 3(b) illustrates the experimentally determined drain-down characteristics for the Duval-Sierrita waste in the large column and the smaller, scaled columns.

Copper and iron analyses were determined by atomic absorption spectroscopy and ferrous iron (Fe^{2+}) by titration methods. Oxygen concentrations were determined at the large waste body access port

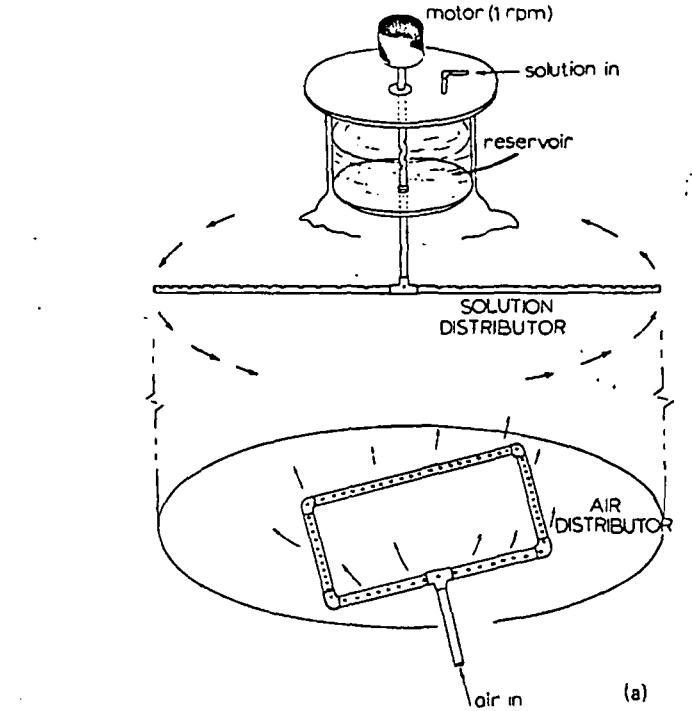

FIG. 3. (a) Schematic view of the solution and air distributors in the large waste columns. (b) Initial drain-down characteristics for the large Duval waste body and the associa' ', smaller scaled columns.

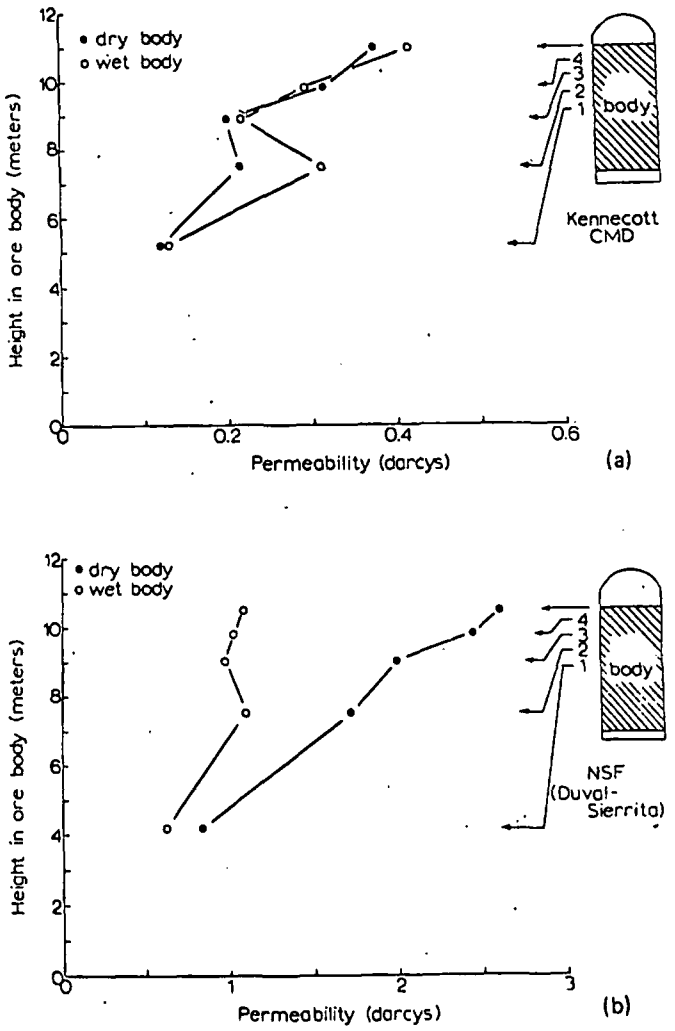

FIG. 4. Waste body permeabilities in the dry and solution-saturated conditions. (a) Kennecott, CMD (Santa Rita) waste body, (b) Duval-Sierrita waste body. The permeability unit, darcy, is equivalent to a fluid flow of 1cc/s-cm^2 (1 centipoise viscosity under a pressure gradient of 1 atmos./cm).

TABLE 1

Duval-Sierrita Waste Scale-Test Data

Test Parameter	Large Column	Medium Column	Small Column
Diameter, d (meters)	3.05	0.38	0.10
Height of Rock, h (meters)	9.75	2.64	0.69
d/h	0.290	0.145	0.145
Maximum Rock Size (in.)	6	0.75	0.20
Initial Drain Rate (ℓ/min.)	4	0.20	0.10
Initial Air Flow Rate (ℓ/min.)	17.5	0.875	0.044
Initial Solution Onfluent (ℓ/min.)	2	0.100	0.005
Retained/Saturated Solution	0.77	0.72	0.68
Waste Body Weight (Kg)	1.7×10^5	4.05×10^2	7

locations using a commercial oxygen meter. Bacterial populations in solution and in the waste body were determined by a most probable number method (MPN) for Thiobacillus ferrooxidans. In addition, laboratory studies involving both Thiobacillus ferrooxidans and a high-temperature microbe (Brierley and Brierley[5]) were conducted to obtain quantitative evidence for bacterial catalysis and to determine more specifically the characteristics of bacterial attachment, the need for attachment, the site of attachment, and the degree of surface corrosion and the effect of bacterial catalysis on surface corrosion and reaction of FeS_2 and $CuFeS_2$ phases. Direct observations of bacterial phenomena and catalytic activity were made by systematic observations in a Hitachi HHS-2R scanning electron microscope operated at 25 kV, and fitted with an Ortec energy-dispersive X-ray analysis facility. Specific sulfide phase regions and other mineral inclusions in the waste particles were in fact determined by X-ray spectroscopy in the scanning electron microscope.

RESULTS AND DISCUSSION

Figures 5 and 6 illustrate some of the preliminary scale data and neutralization characteristics for the Duval-Sierrita waste. The initial inundation for the Sierrita test was made with Socorro

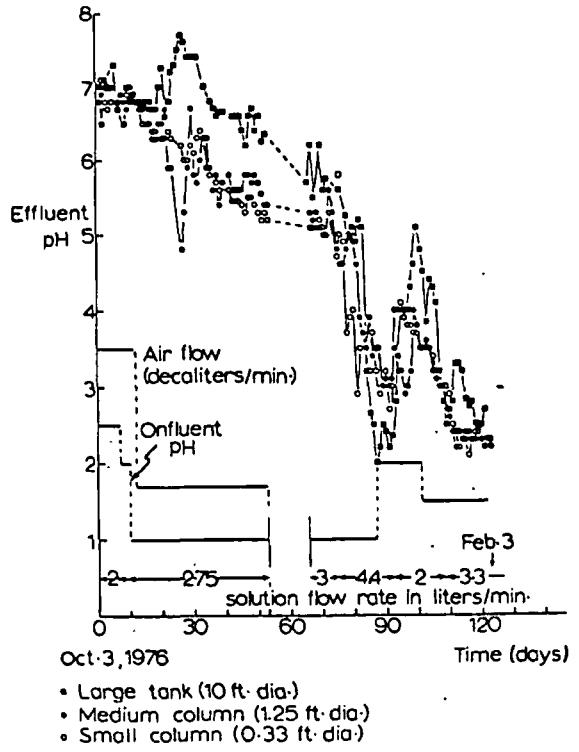

FIG. 5. pH data showing neutralization of the Duval-Sierrita waste rock. The efficiency of the scaling experiments is somewhat apparent.

well water acidified initially to a pH of 2.0. Subsequent solution onfluent pH adjustments and air flow schedules are indicated in Fig. 5. While the initial solution contained no measurable T. ferrooxidans population, the waste body prior to solution inundation was observed to contain evidence of bacteria, which, as demonstrated in the data of Fig. 6(b) increased in the waste body during the neutralization period. However, temperatures even at the end of 120 days were not above 10°C, and the copper in solution averaged only 50 ppm; indicative of no significant bacterial catalysis or leaching.

The Kennecott-Chino Mines waste, by comparison with the Duval-Sierrita waste, was inundated with CMD tail-water which contained

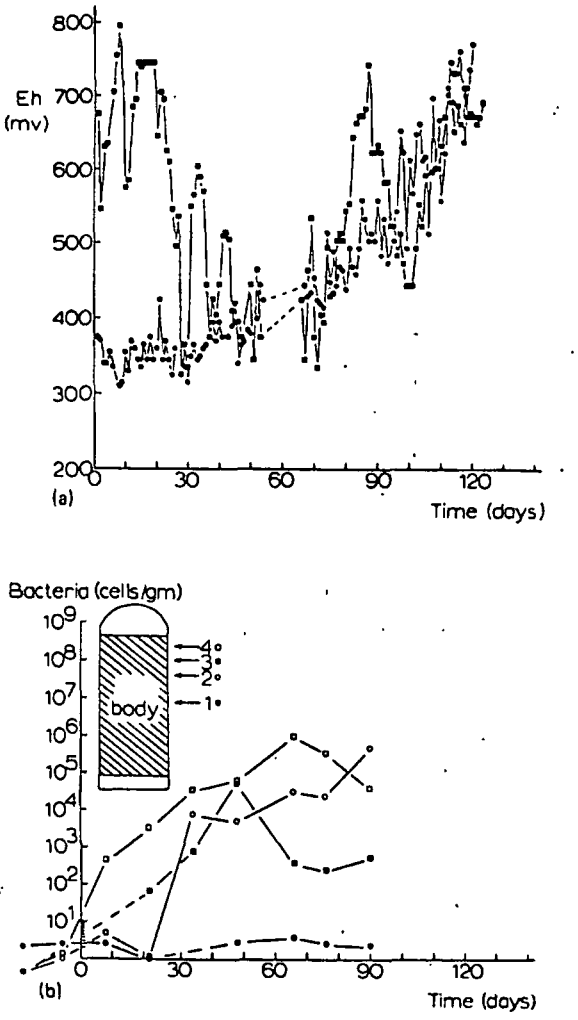

FIG. 6. (a) Eh data for the large and medium-scaled Duval-Sierrita waste bodies corresponding to the neutralization period shown in Fig. 5. (b) Bacterial population profiles (Thiobacillus ferrooxidans) in the large waste body corresponding to the neutralization period shown in Fig. 5.

appreciable numbers (> 10^5 organisms/cc) of bacteria (Thiobacillus ferrooxidans). Unlike the Duval waste, the Kennecott waste required little neutralization, and slightly more than 10% of the total copper (as non-sulfide copper) was extracted during the initial solution inundation. Following the initial inundation, a schedule of solution cycles and aeration rates (including solution rest periods) was followed based in large part on the dump leaching computer model developed by Cathles and Apps[5]. One of the principal reasons for the test was to obtain experimental data to support the model predictions.

Figure 7 illustrates the temperature profiles, oxygen consumption and levels, bacterial count, and copper extracted and solution flow (flush) schedules for roughly the first 300 days of leaching the Kennecott-CMD waste body. It is of particular interest to note that bacterial population, that is the population of Thiobacillus ferrooxidans, began to decline at approximately 45°C, the upper limit for known strains of the microbe (Marchlewitz and Schwartz[6]). While, as shown in Fig. 7, there is some very small decline in oxygen consumption with the decline in the Thiobacillus ferrooxidan population, the oxygen consumption remains high, and the temperature continues to increase. The maximum temperature attained within the waste body was 60°C, and at the final flush [not shown in Fig. 7 (#14)], the temperatures were dramatically quenched, and tended to stabilize thereafter between a maximum (not shown) of 35-40°C; indicative of some equilibrium condition. There was some evidence during bacterial sampling and analysis at the optimum temperatures that a high-temperature microbe was present within the rock, but no detailed evidence was obtained. However, it is well known that the optimum temperature for sulfide leaching catalyzed by Thiobacillus ferrooxidans is 35°C, and that biological oxidation appears to cease around 55°C (Bryner, et al.[7]). It is difficult to believe the acceleration of waste body heating and the associated reactions (particularly with regard to copper solubilization during solution flushes) could be the result of

only chemical oxidation, and a high temperature microorganism would seem to be the only logical alternative.

Figure 8 shows several examples of the flush data following cyclic leaching of primarily non-sulfide copper up to and including flush 6 (Fig. 7). It can be observed in Fig. 8, with reference to Fig. 7, that effluent copper increased with waste-body temperature, pH decreased, and the conversion of Fe^{2+} to Fe^{3+} appeared to increase in the same proportion. The high proportion of Fe^{3+} in the flush effluent, and the increase in the level of Fe^{3+} and the Fe^{3+}/Fe^{2+} ratio with progressive flushes and a corresponding increase in waste-body temperature would seem to be indicative of bacterial oxidation. Furthermore, the large difference between the Fe^{3+}/Fe^{2+} ratio in flushes 10 and 12 might be due in part to the accelerated bacterial catalysis associated with a high-temperature microbe.

Figure 9 shows several samples of the data for solution samples extracted from the various waste-body locations at access ports as shown in Fig. 1(b). It is of interest to compare the waste-body pH and Cu levels and trends with the composite data of Fig. 7. The temperature optimum in Fig. 7 is indeed well correlated with a soluble Cu maximum or increasing Cu concentrations at most waste-body locations.

Duval-Sierrita rock sections having a mesh size of -4 to 6 (~ 3-5mm) were randomly selected from crushed waste material representative of the various column leaching tests and polished flat on one side. The polished samples were washed in distilled water and ultrasonically cleaned. Figure 10 illustrates the dissemination of FeS_2 and $CuFeS_2$ (phase regions) within the matrix. The veinlet structures were generally much more characteristic of the Sierrita material while the separate inclusions of Fig. 10(c) were the overwhelming feature of sulfide dissemination in the Kennecott-CMD waste material. Rock particles containing sections as shown typically in Fig. 10 were placed in sterilized culture media (Berry and Murr[8]) adjusted to a pH of 2.3 in separate flasks; some inoculated with bacteria and others maintained as sterile controls. The high-

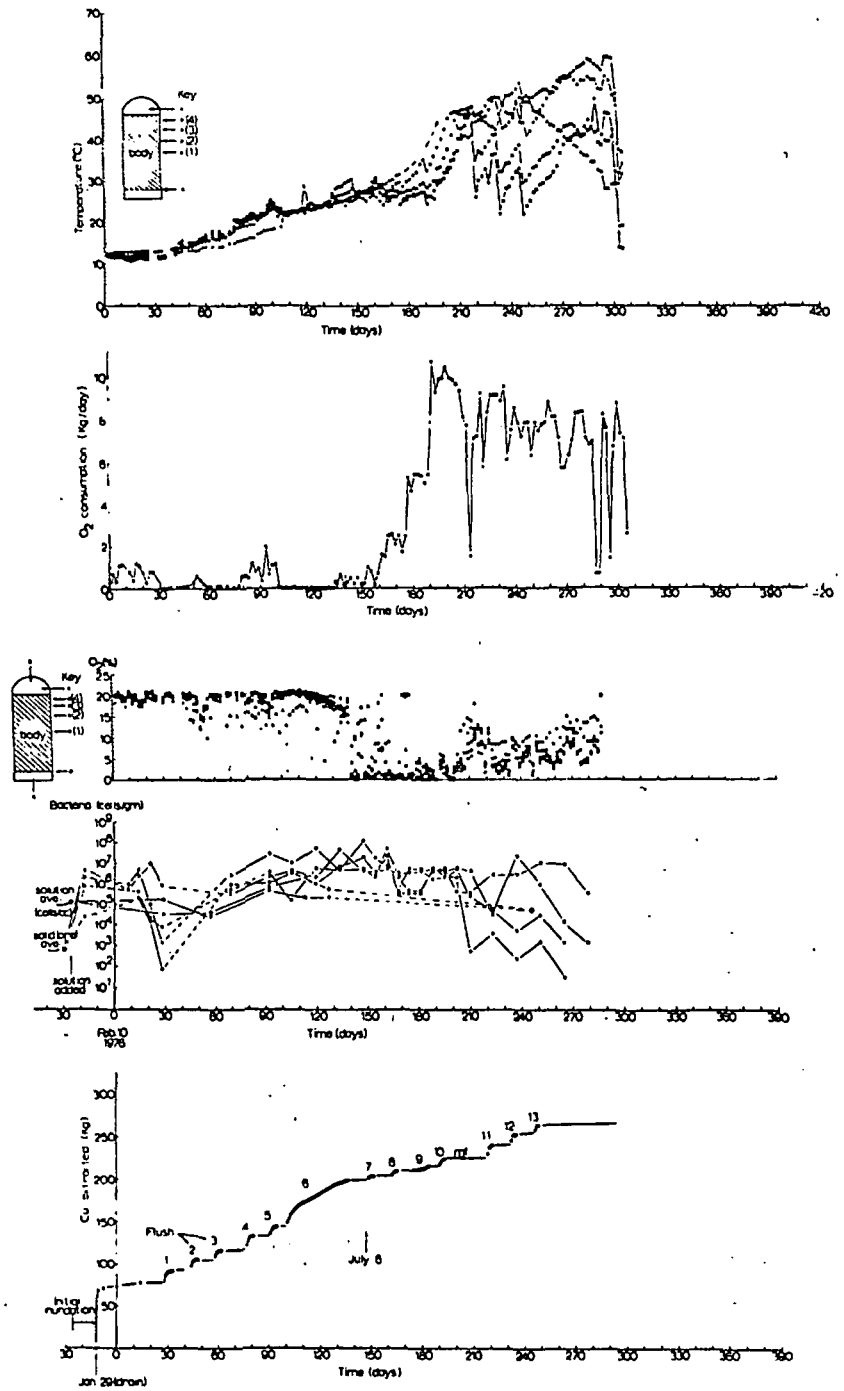

temperature microbe inoculated was a Sulfolobus-like organism; maintained at 55°C during static leaching. Samples were removed periodically for examination in the scanning electron microscope and solution samples were withdrawn at the same time for analysis. Figure 11 illustrates some examples of the results obtained. In Fig. 11(a) and (b), the quantitative difference in Fe^{2+} and Fe^{3+} is observed to be consistent with those observed in the data of Fig. 8 (particularly flush 12). Furthermore, Fig. 12(a-d) clearly illustrate the role of bacteria in catalyzing reactions at the FeS_2 surfaces in the conversion of Fe^{2+} to Fe^{3+} as recently described in detail by Berry and Murr[8]. Figure 13(a) and (b) illustrate the morphologies observed for the high-temperature microbes and the Thiobacillus ferrooxidans.

While Fig. 13(a) and (b) are representative of bacterial attachment for each microorganism, it has been found, in contrast to the conclusions of Duncan and Drummond[9] for example, that Thiobacillus ferrooxidans do not generally attach to the mineral surface but when they do attach, they attach selectively; only on FeS_2, $CuFeS_2$, or other sulfide (e.g. Cu_2S) phase surfaces. This feature has already been demonstrated for the high-temperature microbe by Murr and Berry[10]. Moreover, bacterial attachment, while it does occur, is neither necessary nor sufficient for catalysis.

FIG. 7. Kennecott-Chino Mines waste rock leaching data. Temperature in the waste body, oxygen consumption (and levels) and bacterial population appear to be well correlated and indicative of the role of bacterial catalysis. The numbers in the graph showing cumulative copper extracted indicate periods of solution application or leaching (flushes). The initial solution inundation and draindown occurred at the point denoted "solution added" in the graph showing O_2% and bacterial population. The temperature-quench effects of the solution flushes, particularly at higher waste-body temperatures, are readily observable on comparing the top and bottom graphs. Note that the "body" designated in the keys is the waste rock.

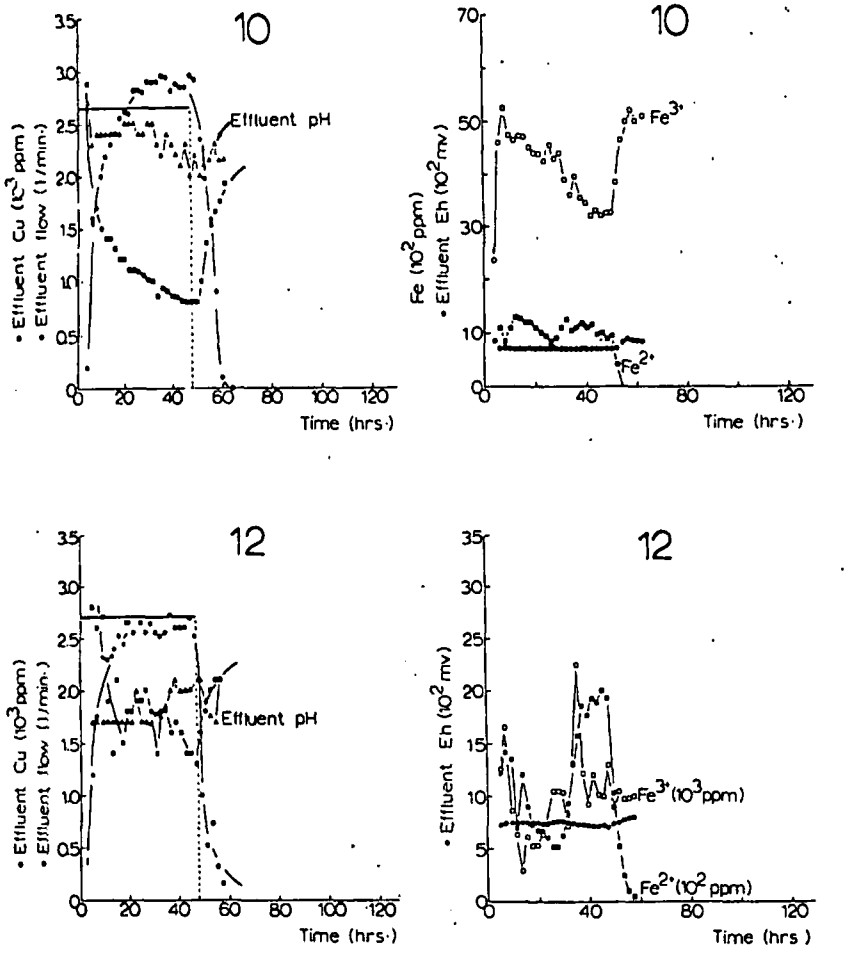

FIG. 8. Examples of solution flush data corresponding to Fig. 7. Each normal flush lasted 48 hrs. as shown. Effluent Cu and Fe^{2+} and Fe^{3+} were analyzed continuously along with Eh and pH at 2 hr. intervals.

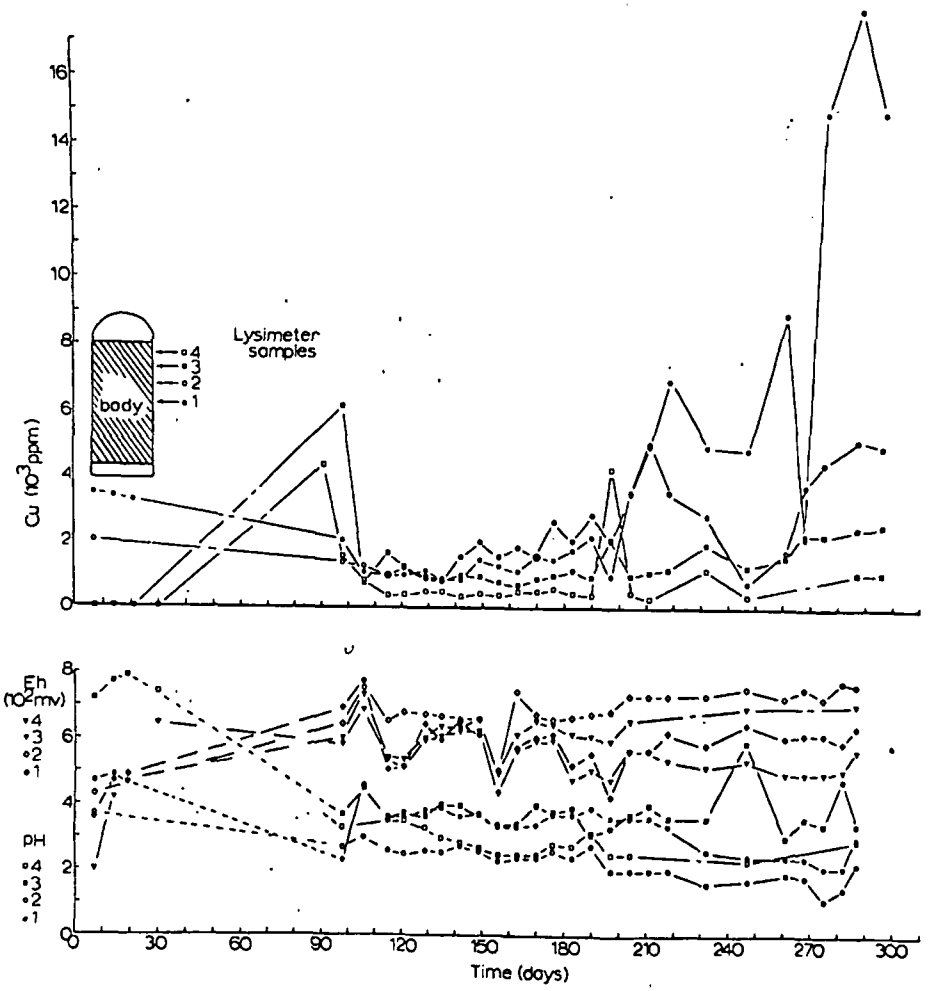

FIG. 9. Cu, Eh, and pH profiles within the Kennecott-CMD monzonite waste column (body). Solution samples were withdrawn from the lysimeters embedded within the waste rock (body) at locations indicated.

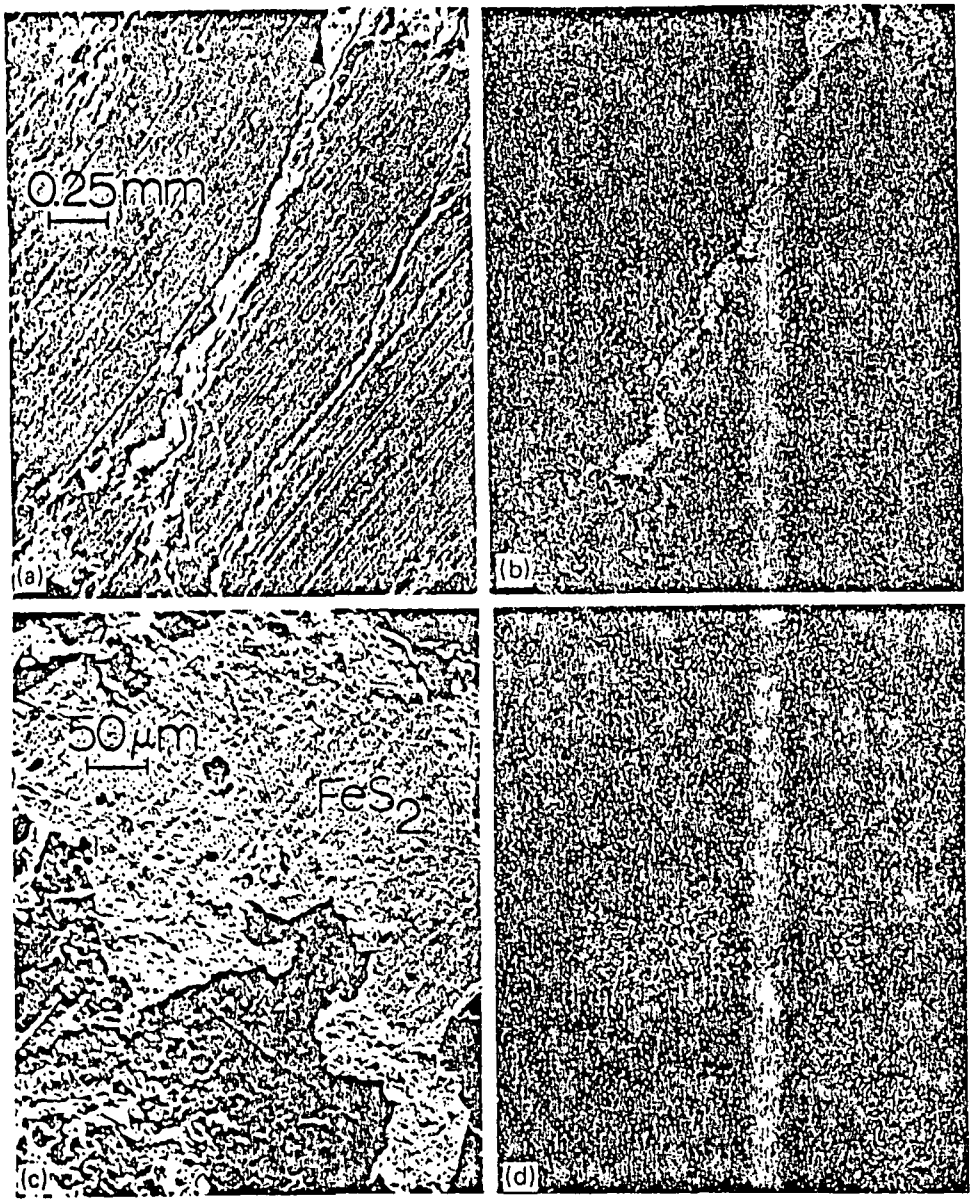

FIG. 10. Examples of sulfide phase dissemination in the Duval-Sierrita waste rock. (a) Veinlet typical of intermixed FeS_2 and $CuFeS_2$, (b) Cu-Fe X-ray map of (a), (c) Intermixed FeS_2 and $CuFeS_2$ phases, (d) Cu X-ray map of (c) showing $CuFeS_2$ regions in relation to FeS_2 regions.

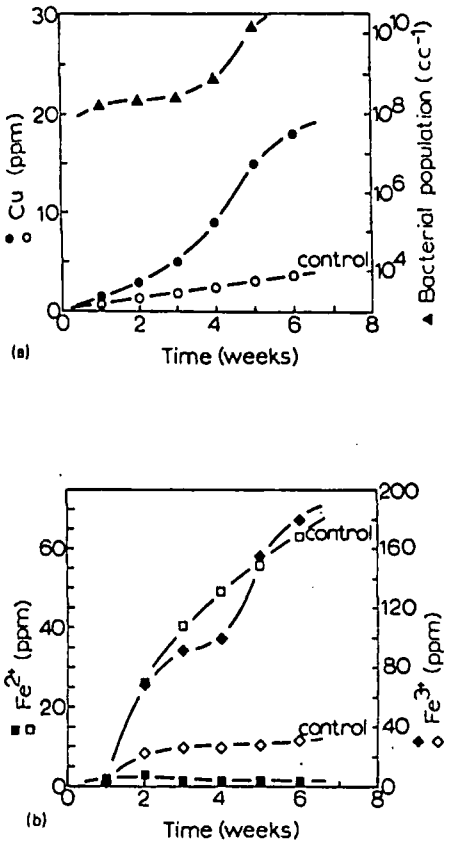

FIG. 11. (a) Quantitative analysis of flask samples of Duval-Sierrita waste showing Cu in solution and a correlation of rate of solubilization with bacterial population; (b) Comparison of Fe^{2+} and Fe^{3+} levels in the same flask samples as (a). The control samples were not inoculated while the test samples were inoculated with a high-temperature, Sulfolobus-like microbe.

SUMMARY AND CONCLUSIONS

The results of this investigation, while incomplete, are encouraging. Certainly the results of Madsen and Groves[3] are illustrated by the present experiments, and the effect of oxygen concentration in the leach dump as it influences bacterial concen-

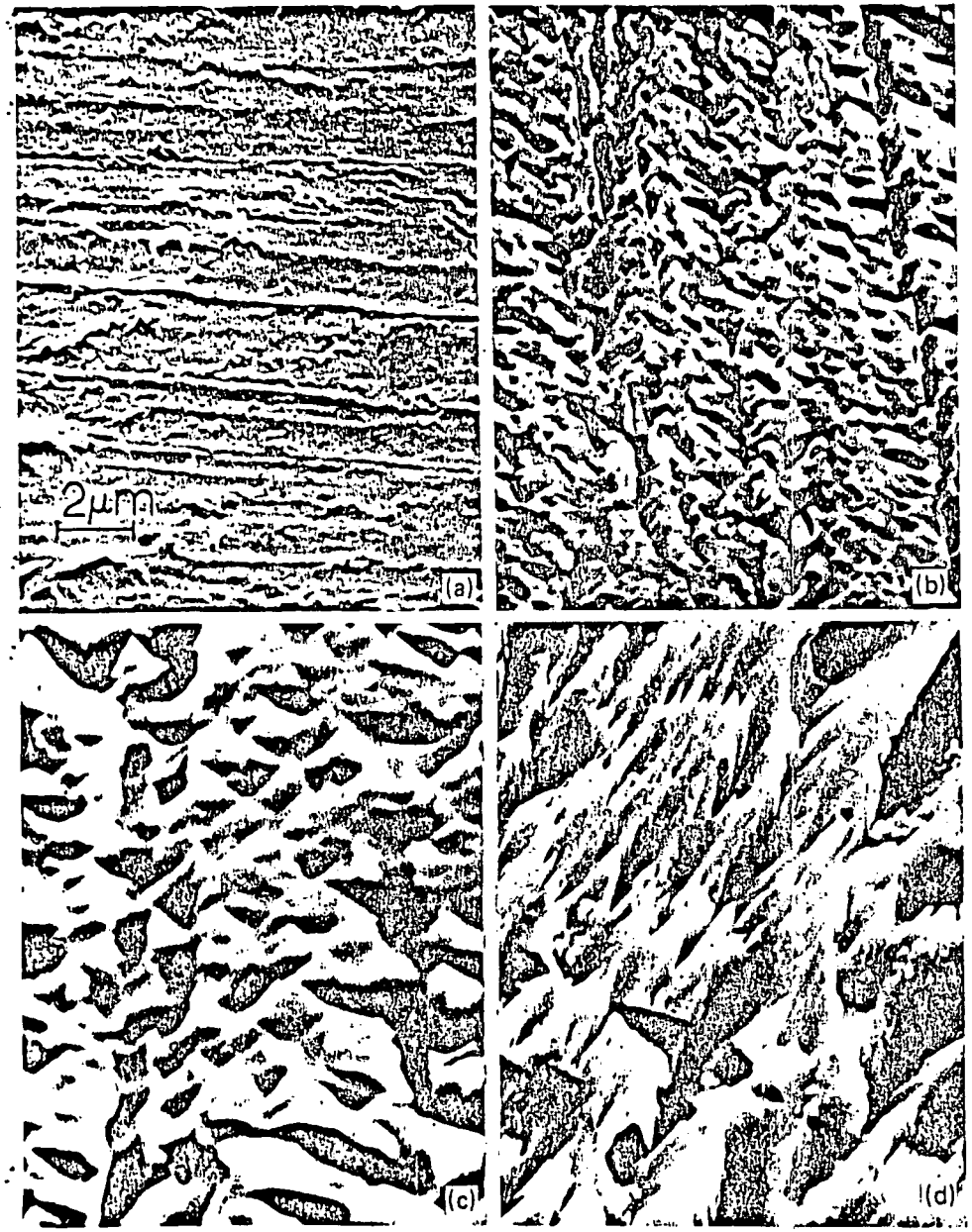

FIG. 12. Surface corrosion of FeS_2 in the high-temperature microbe solution at the same magnification. (a) Surface prior to leaching, (b) after 2 weeks, (c) after 3 weeks, (d) after 6 weeks.

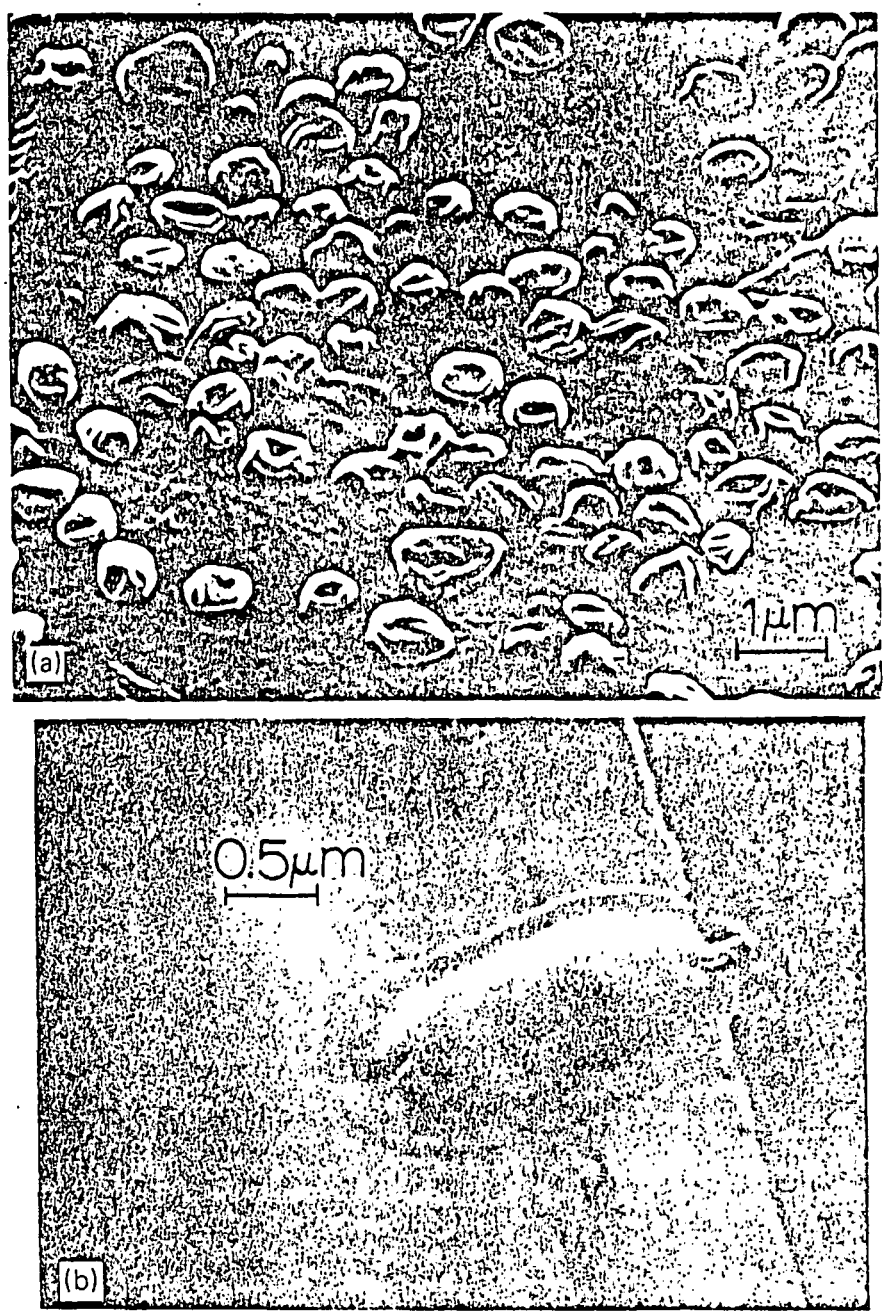

FIG. 13. (a) High-temperature microbes attached selectively to the surface of FeS_2; (b) Thiobacillus ferrooxidan on $CuFeS_2$ surface. Note flagellum and apparent biomatter u which the organism appears to be situated.

tration is shown to be important. The correlation of temperature, bacterial concentration, and oxygen profiles in a large waste body have been demonstrated, and the utility of large waste-body leaching experiments has been overwhelmingly demonstrated. While the scaling data presented is incomplete, and not yet representative of the leaching of copper, a reasonably close correlation and overlap of data has been established in the neutralization of a waste body with regard to solution effluent pH and Eh. There is some hope that this is indicative of the fact that simple scaling laws can be effective in defining certain specific experimental leaching parameters. However, it is doubtful that those features of leaching which are strongly temperature dependent can be scaled adequately unless the temperatures can be controlled. It would seem unreasonable to expect that temperature profiles such as those shown in Fig. 7 could be duplicated in any laboratory column experiment. Finally, although the results, particularly those relating to bacterial concentration, provide additional insight into the role of bacteria in the leaching process, they also are indicative of certain areas which can yield even more meaningful results. In particular, it might be suggested that bacterial activity is temperature limiting (Fig. 7). If this is indeed true, then there are clearly new directions to be followed in enhancing leaching rates and efficiencies, and these must involve more detailed understandings of bacterial phenomena.

ACKNOWLEDGMENTS

This research was supported in part by Kennecott Copper Corporation, Metal Mining Division, and the National Science Foundation (RANN) under Grant AER-76-03758. The help of Phelps-Dodge Corp. and Cities Services Corp. in providing waste rock at the test site is also acknowledged, and a special thanks is extended to Duval Corp. for the provision of the Sierrita (chalcopyrite) waste material.

REFERENCES

1. Razzell, W.E., and Trussell, P.C., Isolation and properties of an iron oxidizing Thiobacillus. J. Bacteriol., 85, 595 (1963).

2. Bhappu, R.B., Johnson, P.H., Brierley, J.A., and Reynolds, D.H., Theoretical and practical studies on dump leaching. Trans. Soc. Min. Engrs. AIME, 244, 307 (1969).

3. Madsen, B.W., and Groves, R.D., Leaching a low-grade copper sulfide ore. Chap. 47 in Extractive Metallurgy of Copper, Vol. II, Y.C. Yannopoulos and J.C. Agarwal (eds.), AIME, New York, 926, 1976.

4. Cathles, L.M., and Apps, J.A., A model of the dump leaching process that incorporates oxygen balance, heat balance, and air convection. Met. Trans., 6B, 617 (1975).

5. Brierley, C.L., and Brierley, J.A., A chemoautotrophic and thermophilic microorganism isolated from an acid hot spring. Can. J. Microbiol., 19, 183 (1973).

6. Marchlewitz, B., and Schwartz, W., Microbe association of acid mine waters, Z. Allg. Mikrobiol., 1, 100 (1961).

7. Bryner, L.C., Walker, R.B., and Palmer, R., Some factors influencing the biological and non-biological oxidation of sulfide minerals. Trans. Soc. Min. Engr. AIME, 238, 56 (1967).

8. Murr, L.E., and Berry, V.K., Direct observations of selective attachment of bacteria on low-grade sulfide ores and other mineral surfaces. Hydromet., 2, 11 (1976).

9. Duncan, D.W., and Drummond, A.D., Microbiological leaching of porphyry copper type mineralization: post leaching observations. Can. J. Earth Sci., 10, 476 (1973).

10. Berry, V.K., and Murr, L.E., An SEM study of bacterial catalysis and its effect on surface reactions at sulfide phases in the leaching of low-grade copper ore. Scanning Electron Microscopy/1977, Vol. I, O. Johari (ed.), IIT Research Institute, Chicago, 137, 1977.

UDC 669.2

Calculation of a cascade of carbonisers for aluminate solutions

R L Dubrovinskii, L I Finkel'shtein and V N Il'inich (All-Union Aluminium and Magnesium Institute, Achinsk Alumina Combine)

In industrial carbonisation of aluminate solutions the excess aluminium oxide passes into the precipitate, but the solution never reaches equilibrium concentrations in the time spent in the stages of the cascade and always remains out of equilibrium when passing from the previous stage to the next stage. As a result of this three lines must be used to describe cascade carbonisation against the R_2O_{carb} - Al_2O_3 coordinates of the R_2O-Al_2O_3-CO_2-H_2O system, i.e.; the equilibrium line (III), the working line (II) of the concentrations of caustic and aluminium oxide leaving the apparatus, and the working line (I) for the state of the system in which neutralisation of the caustic has already occurred but aluminium oxide has not yet separated from the solution (the line of the input concentrations).

Analysis of the operation of the industrial carbonisation cascades of the Achinsk Alumina Combine (AGK) and of the Pikalevo Alumina Combine (PGK) (examples in fig.1a, b) and

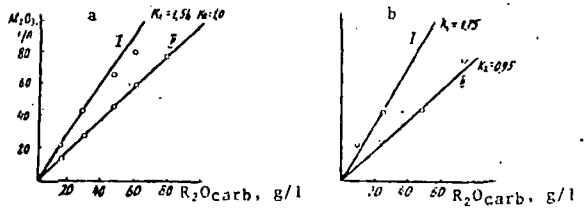

Fig.1 Concentration conditions for industrial cascades for the carbonisation of aluminate solutions. a) Ten-stage cascade of the PGK; b) four-stage cascade of the AGK.

the character of the equilibrium line for solutions with caustic alkali concentrations less than 80 g/l[1]) show that the concentration regimes can be expressed with a practical degree of accuracy by straight lines having gradients $K_1 = \tan\alpha_1$, $K_2 = \tan\alpha_2$, and $K_3 = \tan\alpha_3$. In the general case three principal technologically sound variants are possible (fig.2): $K_1 > K_2 > K_3$ (a); $K_1 < K_2 > K_3$ (b); $K_1 = K_2 > K_3$ (c). The position of the working lines I and II and the equilibrium line III in the coordinates investigated and their gradients determine the kinetic conditions of mass transfer[2])[3]) in the carboniser transfer stages. Graphical solution of the working lines by the methods in the literature[4])[6]) makes it possible, as shown by figs.2a, b, c, to obtain the necessary

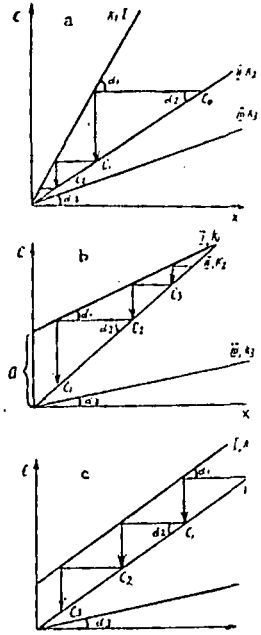

Fig.2 The principal variants of the concentration regimes for cascade carbonisation of aluminate solutions: Decreasing differential regime, $K_1 > K_2 > K_3$; $C = K_1 \cdot X$; $C = K_2 \cdot X$ (a); increasing differential regime, $K_1 < K_2 > K_3$; $C = a + K_1X$; $C = K_2 \cdot X$ (b); uniform differential regime, $K_1 = K_2 > K_3$; $C = a + K_1X$; $C = K_2X$ (c).

working and theoretical equilibrium number of transfer stages, differentials, and concentrations at each stage of the cascade if the initial and final composition of the solution (degree of carbonisation) are known.

Control of the industrial carbonisation process and its regulation cannot be established by graphical methods for the determination of the principal parameters (concentrations, differentials), since the simultaneous given or composite variation in the composition of the initial solution and in the gradients requires a large number of graphical constructions. Solution of the problem in graphical form is even more complicated if it is necessary to optimise the

process or to compare various technological forms taking account of the carbonisation regimes, outputs, flow rates, and number and volume of carbonisation cascade units. An analytic method for determination of the number of units and the concentration regimes in respect of the units of the cascade with regard to their volume, the consumption of solution, and the specified output in the cascade as a whole and in one unit is examined below.

Variant I. $K_1 > K_2 > K_3$, fig.2a. Let us suppose that at the entry to the cascade the solution has an aluminium oxide concentration C_0. In the first stage the caustic concentration X_0 decreases to X_1 on account of carbonisation. For line I it is therefore possible to write:

$$C_0 = K_1 X_1 \tag{1}$$

$$X_1 = C_0 / K_1 \tag{2}$$

At the exit from the first stage of the cascade the caustic concentration has a value X_1 and a state is reached which corresponds to point C_1 on the working line II of the output concentrations. In this case

$$C_1 = K_2 X_1 \tag{3}$$

or

$$C_1 = K_2 (C_0 : K_1) \tag{4}$$

Writing $K_1 / K_2 = m$ for the N-th unit of the cascade, we obtain

$$C_N = C_{N-1} m^{-1} \tag{5}$$

For the various stages of the cascade we obtain the following set of equations

$$\begin{aligned} &C_1 = C_0 m^{-1}, \; C_1 = C_0 m^{-1} \\ &C_2 = C_1 m^{-1}, \; C_2 = C_0 m^{-2} \\ &\underline{C_3 = C_2 m^{-3}, \; C_3 = C_0 m^{-3}} \\ &C_N = C_{N-1} \; m^{-1}, C_N = C_0 m^{-N} \end{aligned} \tag{6}$$

Similarly we obtain expressions for the concentration differentials:

$$\Delta C_N = C_{N-1} \; (1 - m^{-1}) \tag{7}$$

$$\Delta C_N = C_0 m^{-(N-1)} \; (1 - m^{-1}) \tag{8}$$

After transformation of Eq.(6) we obtain the expression

$$N = \frac{\lg C_0 / C_N}{\lg m} \tag{9}$$

In Eq.(9) N is the number of carbonisers in the cascade required for separation of aluminium oxide from a solution with an initial concentration C_0 to a final concentration $C_N (C_f)$ under kinetic conditions characterised by the gradients of the working lines I and II.

Calculations by Eqs. (6) and (9) demonstrate the proximity of the actual and calculated values of the concentrations and the number of units in the cascade as applied to the gradients of the working lines for the carbonisation processes at the AGK and PGK (table).

Cascade	C, g/l Al_2O_3		No. of units	
	Actual	Calc.	Actual	Calc.
4 units, AGK	4.5	-	4	5.5
10 units, PGK	4.5	-	6	6.5
	0.80	0.83	10	-

Variant II. $K_1 < K_2 > K_3$, fig.2b. The solution is simplified if the last unit of the cascade is considered first in the calculation. From the conditions of similarity in the triangles between lines I and II:

$$C_1 = K_2 X_1 \tag{10}$$

$$C_2 = K_1 X_1 + a \tag{11}$$

$$C_2 = K_1 / K_2 C_1 + a = m C_1 + a \tag{12}$$

For the N-th unit we will write

$$C_N = m C_{N-1} + a \tag{13}$$

For a cascade of N stages:

$$\begin{aligned} &C_1 \\ &C_2 = mC_1 + a \\ &C_3 = m^2 C_1 + a \; (1 + m) \\ &\underline{C_4 = m^3 C_1 + a \; (1 + m + m^2)} \\ &C_N = m^{N-1} C_1 + a \; (1 + m + m^2 + \cdots + m^{N-2} \end{aligned} \tag{14}$$

The expression in brackets is a converging series, the sum of which is given by the expression:

$$S_{N-2} = \frac{1 - m^{N-1}}{1 - m} \tag{15}$$

From Eqs.(5), (6), (14), and (15) we obtain:

$$C_N = m^{N-1} C_1 + a \frac{1 - m^{N-1}}{1 - m} \tag{16}$$

After transformation the calculated number of units will amount to

$$N = 1 + \frac{\lg \dfrac{C_N (1 - m) - a}{C_1 (1 - m) - a}}{\lg m} \tag{17}$$

By means of Eq.(7) we obtain the following formula for the concentration differentials:

$$\Delta C_N = C_N - C_{N-1} = m^{N-2} [C_1 (m - 1) + a] \tag{18}$$

By means of Eq.(17) it is possible to calculate the number of units in the cascade for given K_1 and K_2 and initial C_N and final C_1 concentrations of the solution.

Variant III. $K_1 = K_2 > K_3$, fig.2c. The equal gradients of lines I and II lead to equal concentration differentials in the units of the cascade. Consequently, the number of units N in the cascade is determined from the initial C_0 and final C_f concentrations of the solution and the differential ΔC:

$$N = \frac{C_0 - C_f}{\Delta C} \tag{19}$$

Allowing one carboniser in reserve for correction of the conditions:

$$N = \frac{C_0 - C_f}{\Delta C} + 1 \tag{20}$$

IV. Relation between the productivity of the cascade and the carbonisation regime. With a knowledge of the concentration differential in one stage of the cascade ΔC_N and in the whole cascade $(C_0 - C_f)$ and the time τ in which this differential is achieved it is possible to determine the output (the carbonisation rate) Π at each stage of the cascade (Π_N) and in the whole cascade (Π_f):

$$\Pi_N = \Delta C_N / \tau_N \tag{21}$$

$$\Pi_f = C_0 - C_N / \tau_f \tag{22}$$

The average time spent in one stage of the cascade is given by

$$\tau_N = V / Q \tag{23}$$

where Q = the productivity of the cascade in the solution
V = the filled volume of the unit.
Since the volume of the stages in the cascade is the same.

$$\tau_f = N(V/Q) \quad (24)$$

By means of the equations discussed it is possible to obtain a series of new expressions which make it possible to compare various technical variants taking account of the carbonisation regimes, the output, the flow rates, and the number and volume of the units of the cascade for equilibrium and nonequilibrium carbonisation. For example, for the case where $K_1 > K_2$:

$$\Pi_N = \frac{C_0 m^{-(N-1)}(1 - m^{-1})Q}{V} \quad (25)$$

For the case where $K_1 < K_2$:

$$\Pi_N = \frac{m^{N-a}[C_1(m-1)+a]Q}{V} \quad (26)$$

For the case where $K_1 = K_2$:

$$\Pi_N = \frac{(C_0 - C_f)Q}{(N+1)V} \quad (27)$$

The output in the cascade for the three cases can be obtained from the expression:

$$\Pi_f = \frac{C_0 - C_f}{N} \cdot \frac{Q}{V} \quad (28)$$

To calculate the equilibrium carbonisation the K_3 value is used instead of K_2, since the equilibrium line in this case is the line of the output concentrations.

Conclusions

1. By analysis of the cascade carbonisation of aluminate solutions from the standpoint of separation theory it is possible to treat the concepts of the process systematically and to give comparatively simple analytic expressions relating the carbonisation conditions, the number and volume of the cascade units, and the productivity.
2. The equations can be used in the design of carbonisation cascades and in mathematical descriptions of the process as applied to the production control systems and in calculation of the driving forces of the crystallisation process.

References

1) Metallurgists' Handbook of nonferrous metals; Alumina production. Metallurgiya, Moscow 1970, p.31, 91.
2) P Benedek et alia: Scientific principles of chemical technology. Khimiya, Leningrad 1970,
3) V V Kafarov: Principles of mass transfer. Vysshaya shkola, Moscow 1972.
4) W L McCabe et alia: Ind. Eng. Chem., 1925, 17, 606.
5) A N Planovskii et alia: Calculation of plate equipment. Zh. Prikl. Khim., 1955, (2).

UDC 669.70.7+621.357.1

The size of bubbles flowing from horizontal anodes

A I Begunov, V N Kul'kov and I K Skobeev (Irkutsk Polytechnical Institute)

Summary

The dimensions of real gas inclusions emerging from the edge of a horizontal anode were investigated for the electrochemical system: Hg, $Cd/CdCl_2/Cl_2$, C. The statistical equivalent radius of the gas inclusion emerging from the edge of the anode was determined by analysis of a cine film. The effect of the angle of inclination of the surface of the anode to the horizontal was studied. The effect of the angle showed up particularly clearly at an angle equal to or less than 20-30'. With decrease in the angle not only the volume of a single ejection of the gas phase but also the structure of the gas-containing layer varied. The flow mechanism of the gas phase also varies at the same time in film-bubble and film-type regimes. The transition to a pure film-type regime takes place at extremely small angles in the order of 10' or less. The equivalent radius of the ejected gas phase increases with increase in the linear dimensions of the working surface of the electrode to a state corresponding to the formation of a continuous gas film. Further increase in the linear dimension does not alter the equivalent volume of the emerging gas films. The thickness of the film increases at the same time. The results were used to derive an equation for the dependence of the equivalent radius on the anode geometry.

UDC 546.13:621.357.1:542.8

Release of chlorine bubbles in the electrolysis of molten salts

P V Polyakov, V V Burnakin and V N Andreev (Krasnoyarsk Institute of Nonferrous Metals)

Summary

The movement of chlorine bubbles at a vertical anode in an equimolar mixture of sodium and potassium chlorides containing 10 wt.% of lead chloride was investigated by cine photography. The flow at the anode and the thickness of the gas-saturated layer, the diameter of the bubbles leaving the electrode, the frequency of removal of the bubbles, the number of bubbles on the surface of the anode and their distribution in relation to their diameter, the area of the anode surface occupied by the bubbles, their total area, and the vertical component of the velocity of the bubbles were studied.

From the results it was possible to evaluate the mass of chlorine passing into the electrolyte from the surface of the anode. It was found that an increase in the current yield of chlorine (obtained, for example, by selection of appropriate grains of graphite and by variation of the surface relief) reduces the time spent by the bubbles in the electrolyte and reduces the diffusion coefficient with appropriate choice of melt. From the direct observations it follows that with increase in the current density and the height of the anode the thickness of the two-phase flow at the surface of the anode varies little. However, it increases sharply at the electrolyte-atomosphere boundary, and this increases the time spent by the bubbles in the electrolyte and the probability of their contact with the cathode product. By facilitating the passage of the bubbles from the melt into the atmosphere it is possible to reduce the gap between the poles and to increase the height of the anode in the electrolysis cells without reducing the current efficiency.

due to the elevated temperature of the brine. The downhole portion of this pump has since been replaced with carbon steel column pipe and brine-lubricated, butyl shaft bearings. Costwise, this approach will save considerable money over the long pull even though it must be replaced more often. The new components are designed so no special equipment or expertise is needed to pull the pump and the job can be done by our own people.

One other problem which we hope is behind us but is beyond our control was that five inches of rain was recorded in the solar pond area in October, 1972. This is the first time in recorded history there has been heavy precipitation in the area in October. At the time the ponds carried an optimum burden of brine in preparation for the low evaporation season through February and we had no place to discard spent brine so we could replenish the ponds with mine brine. Due to this, we went through almost the entire winter season with essentially no solids production in the ponds and it was necessary to reduce plant production in January, 1973 so pond solids production could catch up. By revising some operating procedures and changing some pipelines and pumping equipment, we feel we have adequately prepared for this situation should it happen again.

Production capability of a solar evaporation operation is a straight-line function with evaporation area available, evaporation rate, and brine concentration. With essentially a fixed evaporation area we have embarked on an extensive test program directed at increasing the evaporation rate of water from brine. The use of brine additives such as radiation-absorbing dyes which also prevent re-radiation hold some promise. Brines of varying depths are being monitored quite closely as this appears to have a decided effect on the evaporation rate. Complete evaluation of this program will perhaps require two or three summer evaporation periods.

Our production is projected at approximately 260,000 tons per year and it now appears that our work force will stabilize at approximately 100 employees, considerably less than the 430 employed when mining conventionally.

As the Texasgulf Inc. publication, The Golden Triangle, stated in the June-July issue of 1972, there are 100 proud parents at the Moab Potash Operations, proud of the fact that they contributed to the rebirth of a mine, proud of their continued contribution to the viability of the operation, and proud of the fact they are contributing to the welfare of mankind by producing one of the essential plant foods, potash.

Chapter 13

CHEMICAL Constraints on In-Situ Leaching and Metal Recovery

R. S. Rickard

AMAX Extractive Metallurgy Laboratory
Golden, Colorado 80401

ABSTRACT

Using a simple model, the necessary chemical conditions for sulfide leaching will be discussed. Also other chemical controlling factors will be reviewed briefly.

INTRODUCTION

For years leaching of mineral dumps for the recovery of metal values has been practiced but recently leaching of ore in heaps or caved material as a primary method of recovery has become more common. This solution mining symposium has been organized to discuss the technology that has made solution mining an accepted extraction method.

The topics that are being discussed in the symposium include fracturing methods, solution control, and other factors all of which govern the success of a leach operation. These papers all will lead to a greater understanding of the operation of large leaching operations.

However, the physical chemistry operating within the dump or in-situ leach system will continue to be a source of speculation for sometime. It has already been stated (1) that there is little understood about the fundamental chemistry of copper dump leaching because of the strong and complex interactions of various parameter within the leach pile. Many studies have been carried out which clearly elucidate some point in leaching mechanisms but when the data is used to model another experiment, it fails completely.

This failure is not due to poor observations in the first study but simply an unrecognized variable confounded the results when the second study was run. It is for these reasons that this paper will not try to deal rigorously with the theoretical aspects of the chemistry but will try to discuss some of the chemical factors which control leaching using the model proposed by Y. Auck and M. E. Wadsworth (Figure 1). (2)

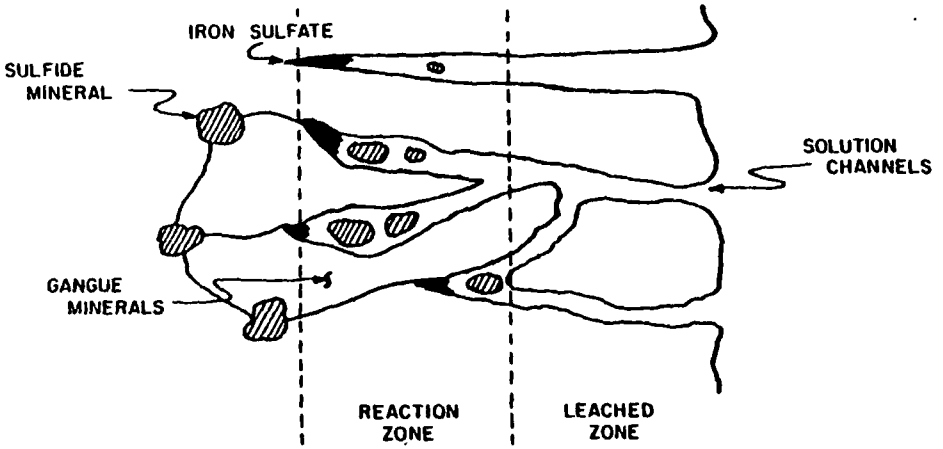

FIG. 1. - Model of A Sulfide Bearing Rock Being Leached

The physical chemical processes of sulfide leaching, in-situ heap or dump, should be considered in two parts. First, thermodynamics which gives a measure of the equilibrium conditions possible. Thermodynamics can be used to determine if leaching is possible and the necessary chemical conditions for leaching. The second physical chemical phenomena to be considered is kinetics. Kinetics, reaction rates, are a measure of the speed at which the system is approaching the thermodynamic equilibrium. To have a good leach system the reaction rates must be sufficiently fast to yield products in reasonable times.

CHEMICAL THERMODYNAMICS

In sulfide leaching the minerals must be oxidized, therefore a chemical system must provide suitable oxidizing power or potential. This oxidizing ability can be calculated using thermodynamics.

In a classic paper Marcel Pourbaix (3) describes thermodynamic calculations and presents a means of graphically displaying the the results of the calculations. Figure 2 shows the iron-water system (Pourbaix Diagram) as a function both of pH (acidity) and

Eh. It is the Eh (volts) which gives an indication of the oxidation (or reduction) potential of a given chemical environment. By using the electrical equivalent it is possible by means of electronic instruments to measure this Eh value. In their book, R. M. Garrels and C. L. Christ (4) give a very readable account of Eh and its measurement and how these measurements can be used in mineral systems.

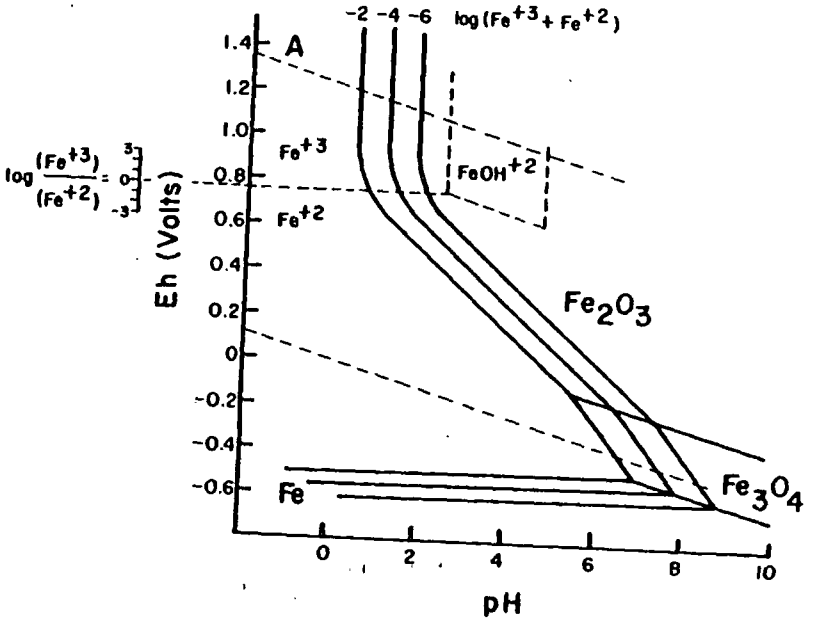

FIG. 2. - Eh-pH Diagram of the Fe-H_2O System (25°C) (3)

To understand the Eh-pH diagrams more clearly a simple discussion of the $Fe^{+3} \rightarrow Fe^{+2}$ reaction might be helpful. The reaction is conventially written as:

$$Fe^{+3} + e^- \rightarrow Fe^{+2}$$

and from the relationships of thermodynamics (4) the expression that relates the measured half cell potential to concentrations of metal ion in solution is:

$$E = E^o - \frac{RT}{nF} \ln \frac{Fe^{+2}}{Fe^{+3}}.$$

After substitution of constants and calculation of the standard potential (E^o) from tabulated data (5) the expression becomes:

$$E = 0.771 + 0.0591 \log \frac{(Fe^{+3})}{(Fe^{+2})}.$$

Now one can measure the Eh or analyze for Fe^{+2} and total iron and determine the Eh of the system. It only has to be determined if a sulfide mineral will oxidize in a solution with a given Fe^{+3} by comparing the mineral oxidation potential with the ferric ions reduction potential.

The oxidation of Cu_2S occurs by: (6)

$$Cu_2S + 4H_2O = 2Cu^{+2} + H_2SO_4 + 6H^+ + 10e^-$$

and the oxidation potential is given by:

$$E = -0.438 + 0.0355\ pH - 0.0059 \log (H_2SO_4)(Cu^{+2})^2$$

The difference in the potential can be calculated and will show that Fe^{+3} ion will oxidize Cu_2S as long as the Fe^{+3}/Fe^{+2} ratio is greater than about 10^{-6}. Many diagrams of the stability regions of minerals in solution have been drawn (4, 6, 7) and inspection of these diagrams will usually indicate quickly the possibility of reaction. Figure 3 shows the Eh-pH stability regions for the important copper minerals and inspection of this diagram (which has been greatly simplified) shows that if the Eh is maintained above 0.5 volts and the below pH4 copper minerals will leach. Comparing Figure 3 with Figure 2 it is obvious that almost any amount of Fe^{+3} ion present will leach these copper minerals.

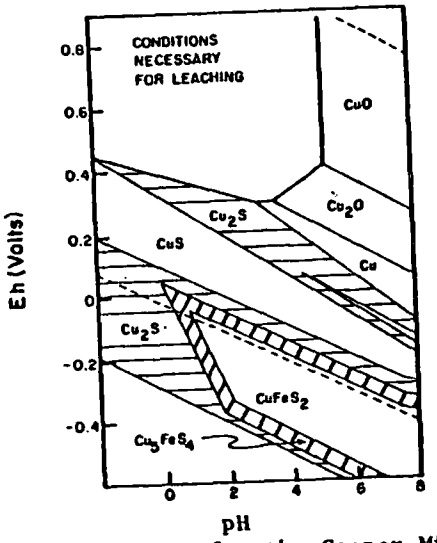

FIG. 3. - Stability Regions for the Copper Minerals in the Cu-Fe-S-H_2O System (0.1M dissolved sulfur species, 0.01M Cu^{+2}, 0.1M Iron Species, 25°C) (6)

These Pourbaix diagrams must be used with some caution. They are based on thermodynamics and some assumptions must be made about the possible reactions that might occur and then the calculations are made and the figures drawn. The first problem is that the assumptions made in calculating a particular diagram may be wrong and second no consideration is given to the rates of reaction. Therefore, many reactions predicted may not be observed because they are a part of a series of reaction and they react so fast that intermediate products are not observed or the reaction doesn't proceed at all. A good review of sulfide mineral leaching reactions has been prepared by R. J. Roman (8).

It now is obvious that to leach sulfide minerals an oxidizing environment must be provided. Many investigators have shown that this oxidant must be at the mineral surface. In the leach model in Figure 1 the oxidant must be present at the sulfide surfaces in the solution channels and must be maintained for continued leaching.

There are any number of oxidants that could be used but ferric ion and oxygen are generally the only two considered. Again referring to Figure 2, line A is the potential when water is in equilibrium with oxygen at one atmosphere pressure. At any reasonable pressures, oxygen will have suitable oxidation power to leach copper sulfide minerals.

Several articles have pointed out the role of bacteria in heap leaching of copper sulfides (9, 10, 11). One of the prime reactions promoted by bacteria is the oxidation of Fe^{+2} to Fe^{+3}. It is obvious that by maintaining a level of bacteria in the heap, in particular in the solution channels, the oxidation potential could be kept at a suitable level because of the continued presence of Fe^{+3} ions.

OTHER CHEMICAL CONSTRAINTS

During the leaching of sulfide ore bodies acid and iron salts are generated by reactions such as (8).

$$4CuFeS_2 + 10H_2SO_4 + 5O_2 \longrightarrow 4CuSO_4 + 2Fe_2(SO_4)_3 + 8S^o + 10H_2O$$

$$4FeS_2 + 6H_2SO_4 + 3O_2 \longrightarrow 2Fe_2(SO_4)_3 + 8S^o + 6H_2O$$

$$2S^o + 3O_2 + 2H_2O \longrightarrow 2H_2SO_4$$

As the relative amounts of the different minerals change so does the leach solution composition. Sulfide minerals will yield sulfur when leached in dilute acid. Here again bacteria are believed to play a major role in sulfide leaching because one type of bacteria is capable of converting sulfur to sulfate. This reaction clears

mineral surfaces of sulfur and help maintain the normal leaching rates.

The acid generated is consumed in part by reacting with the silicates, and other gangue minerals putting alumina, magnesium and silica into solution. In this way, solution channels (Figure 1) are opened for additional leaching.

Iron in solution causes several problems in heap and dump leaching when it builds up in concentration and the pH rises. With in-situ leaching where large volumes of solution are held in the ore body the iron may not be a problem. The iron salts can precipitate as basic sulfates, jarosites, and even hydroxides. As the iron does hydrolyze out of solution additional acid is generated. This system where the iron precipitates because of low acid levels but generates acid during the reaction is buffered. That is the solution will have a reasonably constant pH throughout the system and considerable quantities of reagents is needed to shift the pH. A typical reaction is:

$$Fe_2(SO_4)_3 + 2H_2O = 2Fe(SO_4)(OH) + H_2SO_4.$$

This precipitation occurs around pH 2.4 (10). As solutions are recycled iron salts, and aluminum salts, do build up. If these salts are allowed to precipitate in the heap being leached they can, in combination with slimes (clay type minerals), produce solution barriers. These barriers can be large or they can occur in the small (microscopic) solution channels; both prevent efficient leaching. The precipitation of these salts can be prevented by maintaining sufficient acid in solution. Jarosite type salts can precipitate in the dump at slightly higher acid concentration if suitable conditions are present. A monovalent cation must be present but what appears to be most important is moderate temperatures (above 80°C). The jarosite salts can also be controlled by acid addition.

A positive means of iron removal is needed in heap and dump leaching systems. Generally a bleed stream of solution is treated by raising the pH allowing the iron to precipitate and this settled in a pond.

Aluminum and silica salts can also create problems. Aluminum can generally be controlled by the iron removal system.

CHEMICAL KINETICS

The kinetics of in-situ, heap leaching are not well systemized as yet. Many investigators believe that at temperatures which prevail in a heap diffusion processes control the rate of leaching, (2, 12) while others believe that surface kinetics or chemical kinetics are important (13). To add to the confusion is the

uncertainty of what is the diffusing reactant that is controlling. In the high pressure in-situ model proposed by R. W. Bartlett he believes that oxygen is the diffusing reactant that predominates in the control of the reaction (12).

In dump or heap leaching where the pile is allowed to rest the description of the controlling kinetic features becomes more difficult. In a recent paper (2) the theoretical description of a dump by Harris (14) has been extended into a more comprehensive leaching model. In this model, the water held within the heap and how it drains, is reported to have a profound effect on the kinetics. As the dump drains the water held in solution channels becomes saturated in basic sulfate. The precipitate salt then becomes a diffusion barrier.

SUMMARY

The physical chemistry of leaching of sulfide bearing rock either in place or in piles is a very broad and complex subject. In this field there is a need for a firm understanding of thermodynamics as well as chemical kinetics.

Several points were discussed in a general way. First, that the thermodynamics can be used to aid in developing the necessary chemical conditions that will allow leaching to proceed. Second, there are many unclear points in the chemistry of the system. For example what are the iron salts that precipitate and under what conditions. Last, a very brief review of kinectic considerations in leaching was made. In this area much work has been carried out in the last several years but still the exact mechanism which controls the rate of leaching has not been well established.

All is not bleak, however, great strides have been made and heap leaching has progressed a long way from simply pouring acid on a pile of rocks.

REFERENCES

1. Auck, Y. T. and Wadsworth, M. E., "Laboratory Study in Dump Leaching", Second Tutorial Symposium on Hydrometallurgy, AIME, December 1972, Part 5.

2. Auck, Y. T. and Wadsworth, M. E., "Physical and Chemical Factors in Copper Dump Leaching", International Symposium on Hydrometallurgy, February 1973, p. 645-700.

3. Pourbaix, M. J. N., "Thermodynamics of Dilute Aqueous Solutions" University Microfilms, Inc., Ann Arbor, Michigan, 1963.

4. Garrels, R. M. and Christ, C. L., "Solution, Minerals and Equilibria", Harper and Row, New York, 1965.

5. Pourbaix, M. J. N., "Atlas of Electrochemical Equilibria in Aqueous Solutions," Pergamon Press, New York, 1966.

6. Peters, E., "Thermodynamic and Kinetic Factors in the Leaching of Sulfide Minerals from Ore Deposits and Dumps", SME Short Course - Bio Extractive Mining, February 1970, p 46-75.

7. Peters, E., "Theory of Leaching", First Tutorial Symposium on Hydrometallurgy AIME, May 1972 p II-1 to II-49.

8. Roman, R. J. and Benner, B. R., "The Dissolution of Copper Concentrates", Minerals Science and Engineering, vol. 5, No. 1, January 1973, p 3-24.

9. Malouf, E. E., "Leaching as a Mining Tool", International Symposium on Hydrometallurgy, February 1973, p 615-626.

10. Malouf, E. E., "Bioextractive Mining", SME Short Course - Bio Extractive Mining, February 1970, p 1-45.

11. Malouf, E. E., "Bacterial Leaching", Second Tutorial Symposium on Hydrometallurgy, AIME, December 1972, Part 4.

12. Bartlett, R. W., "A Combined Pore Diffusion and Chalcopyrite Dissolution Kinetics Model for In-Situ Leaching of a Fragmental Copper Porphyry", International Symposium on Hydrometallurgy, February 1973, p 331-374.

13. Peters, E., "The Physical Chemistry of Hydrometallurgy", International Symposium on Hydrometallurgy, February 1972, p 205-228.

14. Harris, J. A., "Development of a Theoretical Approach to the Heap Leaching of Copper Sulfide Ores", Proc. Aust. Inst. Min. Met., 230, 1969, p 81-92.

Chapter 14

ROLE OF MINERALOGY IN HEAP AND IN SITU LEACHING OF COPPER ORES

Laszlo Dudas, Herman Maass and Roshan Bhappu

Mountain States Research and Development
Tucson, Arizona

INTRODUCTION

Chemical and mineralogical constitution play a very important role in the processing of ores because they dictate the method, either physical or chemical, for extracting the mineral or metal. Similarly, the mineralogical nature of the ore, especially the grain size of the valuable minerals, is very important in its processing. The fineness of the grain may be such that physical separation processes may be eliminated in preference to chemical techniques.

In the past, very little attention has been devoted to the geological and mineralogical occurrences which may be potential sources of ores by both the geologist and mineral processing engineer. On the one hand, geologists have devoted less attention to lower grade, complex mineral deposits, and, therefore, may have inadvertently curtailed an exploration program. On the other hand, the metallurgists have neglected to study in detail the geological environments and mineralization of potential ores with the view of determining the critical parameter that could assist in economically processing complex submarginal deposits. In the final analysis, a chemical processing technique converts the valuable metals to a mobile state under conditions similar to those which deposited originally in the host rock. The relationship between ore-genesis and chemical processing is close when the process of mineral or metal deposition in a particular ore deposit is understood--putting the metal in solution by reversing the process of deposition is relatively easy. For this reason, some researchers and educators have been stressing the importance of ore-genesis, geochemistry, mineral equilibria, and ionic equilibria in studying and explaining the

SUBJ
MNG
CDHL

COPPER DUMP AND HEAP LEACHING BIBLIOGRAPHY

COMPILED BY

WILLIAM C. LARSON, GEOLOGIST
TELEPHONE: (612) 725-3464

DENNIS V. DANDREA, GEOPHYSICIST
TELEPHONE: (612) 725-3454

TWIN CITIES MINING RESEARCH CENTER
U.S. BUREAU OF MINES

COPIES OF THIS BIBLIOGRAPHY AND ANY FUTURE UPDATES MAY BE REQUESTED FROM:

TWIN CITIES MINING RESEARCH CENTER
P.O. BOX 1660
TWIN CITIES, MINNESOTA 55111

COPIES OF BUREAU OF MINES INFORMATION CIRCULARS AND REPORTS OF INVESTIGATION MAY BE ORDERED FROM

DIVISION OF PRODUCTION AND DISTRIBUTION
U.S. BUREAU OF MINES
4800 FORBES AVE.
PITTSBURGH, PENNSYLVANIA 15213

~~11 OCTOBER 1979~~

1. ANDERSON, A. E., AND F. K. CAMERON. RECOVERY OF COPPER BY LEACHING, OHIO COPPER CO. OF UTAH. TRANS. AIME, V. 73, 1926, PP. 31-57.

2. ANDERSON, M. L. IMPROVED PRODUCTIVITY FROM IN SITU LEACHING. PROC. ON PRODUCTIVITY IN MINING, UNIV. MISSOURI--ROLLA, ROLLA, MO., MAY 13-15, 1974, ED. BY J. J. SCOTT, PP. 82-83.

3. ANDERSON, M. L. (ASSIGNED TO MOBIL OIL CORPORATION, A CORP. OF NEW YORK). METHODS OF SELECTIVELY IMPROVING THE FLUID COMMUNICATION OF EARTH FORMATIONS. U.S. PAT. 3,565,173, FEB. 23, 1971.

4. ARNOLD, W. D., AND D. J. CROUSE. RADIOACTIVE CONTAMINATION OF COPPER RECOVERED FROM ORE FRACTURED WITH NUCLEAR EXPLOSIONS. OAK RIDGE NATIONAL LABORATORY, REPT. ORNL-4677, SEPTEMBER 1971. 55 PP.

5. AUSTIN, W. L. PROCESS OF EXTRACTING COPPER FROM ORE. U.S. PAT. 975,106, NOV. 8, 1910.

6. BALLARD, J. K. SOLUTION MINING. MIN. ENG., V. 23, NO. 2, FEBRUARY 1971, P. 109.

7. BARTLETT, R. W. A COMBINED PORE DIFFUSION AND CHALCOPYRITE DISSOLUTION KINETICS MODEL FOR IN SITU LEACHING OF A FRAGMENTED COPPER PORPHYRY. PROC. SECOND INTERNAT. SYMP. ON HYDROMETALLURGY, ED. BY D. J. I. EVANS, AND R. S. SHOEMAKER. V. 1, CH. 14, 1973, PP. 331-374.

8. BHAPPU, R. B. ECONOMIC EVALUATION OF IN PLACE LEACHING AND SOLUTION MINING SITUATIONS. PRES. AT A SHORT COURSE IN IN-PLACE LEACHING AND SOLUTION MINING, THE MACKAY SCHOOL OF MINES, UNIV. NEVADA--RENO, RENO, NEV., NOV. 10-14, 1975, 22 PP.

9. BHAPPU, R. B. IN SITU EXTRACTION AND LEACHING TECHNOLOGY. PRES. AT INTER-REGIONAL SEMINAR ON THE ECONOMICS OF MINERAL ENGINEERING, ANKARA, TURKEY, APR. 5-15, 1976, 39 PP.

10. BHAPPU, R. B. IN SITU MINING TECHNOLOGY - PRACTICAL AND ECONOMIC ASPECTS. PRES. AT THE TURKISH MINING INSTITUTE, ANKARA, TURKEY, APR. 5-16, 1976, 29 PP.

11. BHAPPU, R. B., AND F. M. LEWIS. ECONOMIC EVALUATION OF AVAILABLE PROCESSES FOR TREATING OXIDE COPPER ORES. PRES. AT FALL MEETING, SOC. OF MIN. ENG., AIME, ACAPULCO, MEXICO, SEPT. 22-25, 1974, PREPRINT NO. 74-AS-334, 20 PP.

12. BRAITHWAITE, J. W., AND M. E. WADSWORTH. OXIDATION OF CHALCOPYRITE UNDER SIMULATED CONDITIONS OF DEEP SOLUTION MINING. PROC. INTERNAT. SYMP. ON COPPER EXTRACTION AND REFINING, MET. SOC., AIME, LAS VEGAS, NEV., FEB. 22-26, 1976 (PUB. AS EXTRACTIVE METALLURGY OF COPPER--HYDROMETALLURGY AND ELECTROWINNING, ED. BY J. C. YANNOPOULOS AND J. C. AGARWAL). PORT CITY PRESS, BALTIMORE, MD., V. II, 1976, PP. 752-775.

13. BRAUN, R. L., AND A. F. LEWIS. NUCLEAR SOLUTION MINING: PART VIII - OXYGEN DISTRIBUTION. LAWRENCE RADIATION LABORATORY, REPT. UCID-16008, MARCH 1972, 31 PP.

14. BRAUN, R. L., AND R. G. MALLON. COMBINED LEACH-CIRCULATION CALCULATION FOR PREDICTING IN-SITU COPPER LEACHING OF PRIMARY SULFIDE ORE. TRANS. SOC. OF MIN. ENG., AIME, V. 258, NO. 2, JUNE 1975, PP. 103-110.

15. BRIERLEY, C. L. COLUMN LEACHING OF LOW-GRADE CHALCOPYRITE ORE USING THERMOPHILIC BACTERIA. NEW MEXICO BUREAU OF MINES AND MINERAL RESOURCES (SOCORRO, NEW MEXICO). BUMINES GRANT NO. G0177100, JUNE 1978, 44 PP.

16. BRIERLEY, C. L. LEACHING: USE OF A HIGH-TEMPERATURE MICROBE. CH. 31 IN SOLUTION MINING SYMPOSIUM, ED. BY F. F. ALPAN, W. K. MCKINNEY, AND A. D. PERNICHELE. THE AMERICAN INSTITUTE OF MINING, METALLURGICAL, AND PETROLEUM ENGINEERS, INC., NEW YORK, 1974, PP. 461-469.

17. BRINCKERHOFF, C. M. ASSESSMENT OF RESEARCH AND DEVELOPMENT NEEDS AND PRIORITIES FOR IN SITU LEACHING OF COPPER. CONSULTANTS FINAL REPORT, BUMINES CONTRACT J0166036, JULY 26, 1976, 5 PP.

18. BRUYNESTEYN, A., AND D. W. DUNCAN. EFFECT OF PARTICLE SIZE ON THE MICROBIOLOGICAL LEACHING OF CHALCOPYRITE BEARING ORE. PROC. SOLUTION MINING SYMP., AIME ANN. MEETING, DALLAS, TEXAS, FEB. 25-27, 1974, PP. 324-337.

19. CANNON, K. J. SOLVENT EXTRACTION - ELECTROWINNING TECHNOLOGY FOR COPPER. AUSTRALIAN MINING, MARCH 1977, PP. 47-51.

20. CARNAHAN, T. G., AND H. J. HEINEN (ASSIGNED TO THE UNITED STATES OF AMERICA AS REPRESENTED BY THE SECRETARY OF THE INTERIOR, WASHINGTON, D.C.). CHEMICAL MINING OF COPPER PORPHYRY ORES. U.S. PAT. 3,912,330, OCT. 14, 1975.

21. CARNAHAN, T. G., AND H. J. HEINEN. SIMULATED IN SITU LEACHING OF COPPER FROM A PORPHYRY ORE. BUMINES TPR 69, MAY 1973, 11 PP.

22. CARPENTER, F. H., AND R. R. RHAPPU. HYDROMETALLURGY AND LOW GRADE ORE POTENTIAL. PREPS. AT 107TH ANN. MEETING, AIME, ATLANTA, GA., MAR. 6-10, 1977.

23. CATANACH, C. R. DEVELOPMENT AND IN PLACE LEACHING OF MOUNTAIN CITY CHALCOCITE ORE BODY. PROC. INTERNAT. SYMP. ON COPPER EXTRACTION AND REFINING, MET. SOC., AIME, LAS VEGAS, NEV., FEB. 22-26, 1976 (PUB. AS EXTRACTIVE METALLURGY OF COPPER--HYDROMETALLURGY AND ELECTROWINNING, ED. BY J. C. YANNOPOULOS AND J. C. AGARWAL). PORT CITY PRESS, BALTIMORE, MD., V. II, 1976, PP. 849-872.

24. CATANACH, C. R., E. F. MORAN, D. D. PORTER, C. G. RUDERSHAUSEN, AND R. W. SOMMERS. COPPER LEACHING FROM AN OREBODY BLASTED IN PLACE. IN SITU, V. 1, NO. 4, 1977, PP. 283-303.

25. CHAMBERLAIN, C., J. NEWTON, AND D. CLIFTON. HOW CYANIDATION CAN TREAT COPPER ORES. ENG. AND MIN. J., V. 170, NO. 10, OCTOBER 1969, PP. 90-91.

26. CHAMBERLAIN, P. G. IN-PLACE LEACHING RESEARCH AT THE SENECA MINE, MOHAWK, MICH. PRES. AT ANN. SPRING TECHNICAL MEETING OF UPPER PENINSULA SECTION, AIME, MICHIGAN TECHNOLOGICAL UNIV., HOUGHTON, MICH., APR. 21, 1977, 14 PP.; AVAILABLE FROM PETER G. CHAMBERLAIN, U.S. BUREAU OF MINES, P.O. BOX 1660, TWIN CITIES, MINNESOTA 55111.

27. CHILSON, R. F. CONTINUOUSLY LEACHING AN ORE COLUMN. U.S. PAT. 4,071,611, JAN. 31, 1978.

28. COOPER, F. D. COPPER HYDROMETALLURGY: A REVIEW AND OUTLOOK. BUMINES IC 8394, 1968, 14 PP.

29. D'ANDREA, D. V., P. G. CHAMBERLAIN, AND J. K. AHLNESS. A TEST BLAST FOR IN SITU COPPER LEACHING. PRES. AT 1978 AIME ANN. MEETING, DENVER, COLO., FEB. 26 - MAR. 2, 1978, PREPRINT 78-AS-112, 13 PP.

30. D'ANDREA, D. V., P. G. CHAMBERLAIN, AND L. R. FLETCHER. GROUND CHARACTERIZATION FOR IN SITU COPPER LEACHING. PRES. AT 109TH ANNUAL MEETING, SOC. MIN. ENG., AIME, LAS VEGAS, NEVADA, FEB. 24-28, 1980.

31. D'ANDREA, D. V., R. A. DICK, R. C. STECKLEY, AND W. C. LARSON. A FRAGMENTATION EXPERIMENT FOR IN SITU EXTRACTION. PROC. SOLUTION MINING SYMP., AIME ANN. MEETING, DALLAS, TEX., FEB. 25-27, 1974, PP. 143-161.

32. D'ANDREA, D. V., W. C. LARSON, P. G. CHAMBERLAIN, AND J. J. OLSON. SOME CONSIDERATIONS IN THE DESIGN OF BLASTS FOR IN SITU COPPER LEACHING. PRES. AT 17TH U.S. SYMP. ON ROCK MECH., SNOWBIRD, UTAH, AUG. 25-27, 1976, 15 PP.

33. D'ANDREA, D. V., W. C. LARSON, L. R. FLETCHER, P. G. CHAMBERLAIN, AND W. H. ENGELMANN. IN SITU LEACHING RESEARCH IN A COPPER DEPOSIT AT THE EMERALD ISLE MINE. BUMINES RI 8236, 1977, 43 PP.

34. D'ANDREA, D. V., AND S. M. RUNKE. IN SITU COPPER LEACHING RESEARCH AT THE EMERALD ISLE MINE. PROC. JOINT MEETING OF THE MINING AND METALLURGICAL INSTITUTE OF JAPAN AND THE AMERICAN INSTITUTE OF MINING, METALLURGICAL, AND PETROLEUM ENGINEERS, DENVER, COLO., SEPT. 1-3, 1976 (PUB. AS WORLD MINING AND METALS TECHNOLOGY, ED. BY A. WEISS), V. 1, 1976, PP. 409-419.

35. DAVIDSON, D. H. IN-SITU LEACHING OF NON-FERROUS METALS. SCIENCE APPLICATIONS, INC. INTERNAL REPORT 1979, 16 PP.; AVAILABLE FROM SCIENCE APPLICATIONS, INC., 1200 PROSPECT STREET, LA JOLLA, CALIFORNIA.

36. DAVIDSON, D. H. OPTIMIZATION OF IN-SITU LEACHING STRATEGIES. SCIENCE APPLICATIONS, INC. INTERNAL REPORT 1979, 17 PP.; AVAILABLE FROM SCIENCE APPLICATIONS, INC., 1200 PROSPECT STREET, LA JOLLA, CALIFORNIA.

37. DAVIDSON, D. H. IN-SITU LEACHING OF NONFERROUS METALS. MIN. CONG. J., V. 66, NO. 7, JULY 1980, PP. 52-54, 57.

38. DAVIDSON, D. H., AND R. V. HUFF (ASSIGNED TO KENNECOTT COPPER CORP.). WELL STIMULATION FOR SOLUTION MINING. U.S. PAT. 3,917,345, NOV. 4, 1975.

39. DAVIDSON, D. H., R. V. HUFF, AND W. F. SONSTELIE. MEASUREMENT AND CONTROL IN SOLUTION MINING OF DEEP-LYING DEPOSITS OF COPPER OR URANIUM. PRES. AT INSTRUMENT SOC. OF AMERICA MIN. AND MET. IND. DIV. SYMP., DENVER, COLO., NOV. 1-3, 1978, 7 PP.

40. DICK, R. A. IN SITU FRAGMENTATION FOR SOLUTION MINING - A RESEARCH NEED. PRES. AT THE SECOND INTERNAT. SYMP. ON DRILLING AND BLASTING, PHOENIX, ARIZONA, FEB. 12-16, 1973; AVAILABLE FOR CONSULTATION AT BUREAU OF MINES, TWIN CITIES MINING RESEARCH CENTER, MINNEAPOLIS, MINNESOTA.

41. BRAVO CORPORATION. SOLUTION MINING. SECTION 6.6.2 IN ANALYSIS OF LARGE SCALE NON-COAL UNDERGROUND MINING METHODS, BUMINES CONTRACT REPORT S0122058, JANUARY 1974, PP. 455-464.

42. DUDAS, L., H. MAASS, AND P. R. BHAPPU. ROLE OF MINERALOGY IN HEAP AND IN SITU LEACHING OF COPPER ORES. PROC. SOLUTION MINING SYMP., AIME ANN. MEETING, DALLAS, TEXAS, FEB. 25-27, 1974, PP. 193-209.

43. DUNCAN, D. W., AND C. J. TEATHER (ASSIGNED TO BRITISH COLUMBIA RESEARCH COUNCIL). METHOD FOR THE MICROBIOLOGICAL LEACHING OF COPPER, NICKEL, ZINC, MOLYBDENUM. U.S. PAT. 3,266,889, AUG. 16, 1966.

44. DUNCAN, D. W., C. C. WALDEN, AND P. C. TRUSSELL. BIOLOGICAL LEACHING OF MILL PRODUCTS. CAN. MIN. AND MET. BULL., V. 59, NO. 653, SEPTEMBER 1966, PP. 1075-1079.

45. EISENBARTH, W. A. RECONCILATION: ENVIRONMENTAL ISSUES IN IN-SITU MINING VS REGULATORY CONSTRAINTS. PRES. AT URANIUM RESOURCE TECH. SEMINAR II, COLORADO SCHOOL OF MINES, GOLDEN, COLORADO, MAR. 12-14, 1979, 7 PP.

46. ENGINEERING AND MINING JOURNAL. AEC AND KCC WILL JOINTLY STUDY POTENTIAL OF NUCLEAR BLASTING TO MINE COPPER ORE. V. 174, NO. 4, APRIL 1973, PP. 26-30.

47. ENGINEERING AND MINING JOURNAL. ASARCO AND DOW CHEMICAL TO LEACH DEEP COPPER OREBODY IN SITU IN ARIZONA. V. 173, NO. 6, JUNE 1972, P. 19.

48. ENGINEERING AND MINING JOURNAL. COPPER LEACHING WITH CYANIDE - A REVIEW OF FIVE INVENTIONS. V. 168, NO. 9, SEPTEMBER 1967, PP. 123-127.

49. ENGINEERING AND MINING JOURNAL. ECONOMICS PROVIDE MOTIVE FOR GROWTH OF BACTERIA LEACHING. V. 167. NO. 6. JUNE 1966. 543 PP.

50. ENGINEERING AND MINING JOURNAL. THE ESTIMATED COST OF A NUCLEAR LEACHING EXPERIMENT ON COPPER ORE. V. 169, NO. 6. JUNE 1958. P. 186.

51. ENGINEERING AND MINING JOURNAL. INDIA STUDIES POSSIBILITY OF COPPER MINING BY NUCLEAR BLASTS. V. 171. NO. 7, JULY 1970. 33 PP.

52. ENGINEERING AND MINING JOURNAL. KENNECOTT INVESTIGATES SOLUTION MINING POTENTIAL OF DEEP CU DEPOSIT. V. 176. NO. 9. SEPTEMBER 1975. PP. 37, 41.

53. ENGINEERING AND MINING JOURNAL. KENNECOTT SETS SIGHTS ON NUCLEAR TEST FOR IN SITU RECOVERY OF COPPER. V. 168. NO. 11. NOVEMBER 1967. PP. 116-122.

54. ENGINEERING AND MINING JOURNAL. THE OXYMIN PROJECT AT MIAMI, ARIZONA. A SUMMARY OF A PRESENTATION MADE TO MIAMI, ARIZONA TOWN COUNCIL. SEPT. 12, 1977. 9 PP.

55. ENGINEERING AND MINING JOURNAL. RANCHERS BIG BLAST SHATTERS COPPER OREBODY FOR IN-SITU LEACHING. V. 173, NO. 4, APRIL 1972. PP. 98-100.

56. ENGINEERING AND MINING JOURNAL. SOLUTION MINING OPENING NEW RESERVES. V. 175. NO. 7. JULY 1974. PP. 62-71.

57. FEHLNER, F. P. ELECTROCHEMICAL METHOD OF MINING. U.S. PAT. 3,819,231, JUNE 25, 1974.

58. FINLAY, W. L. MOLECULAR MINING OF KEWEENAW COPPER, A PRIME CANDIDATE FOR THE ENLARGEMENT OF NON-RENEWABLE MINERAL RESERVES THROUGH TECHNOLOGY. PANEL DISCUSSION AT THE JOINT NAS-NAE MEETING ON NATIONAL POLICY, WASHINGTON D.C., OCT. 25, 1973. 15 PP.

59. FITCH, J. L., AND R. G. HURD (ASSIGNED TO MOBIL OIL CORPORATION, A CORPORATION OF NEW YORK). IN SITU LEACHING METHOD. U.S. PAT. 3,274,232. OCT. 11, 1966.

60. FLETCHER, D. A. (ASSIGNED TO TALLEY-FRAC CORPORATION, PRYOR, OKLA., A CORP. OF DEL.). WELL FRACTURING METHOD USING EXPLOSIVE SLURRY. U.S. PAT. 3,561,532. FEB. 9, 1971.

61. FLETCHER, J. B. IN PLACE LEACHING. SKILLINGS MINING REVIEW. V. 63, NO. 17, APR. 27, 1974. PP. 7-10.

62. FLETCHER, J. B. IN PLACE LEACHING AT MIAMI MINE, MIAMI, ARIZONA. PPES. AT AIME CENTENNIAL ANN. MEETING, SOC. OF MIN. ENG., AIME, NEW YORK, N.Y., MARCH 1971. AIME PREPRINT 71-AS-40: TRANS. SOC. OF MIN. ENG., AIME, V. 250, NO. 4, DECEMBER 1971. PP. 310-314.

63. FLETCHER, J. B. IN PLACE LEACHING MIAMI MINE. PRES. AT ARIZONA SECTION MEETING, MILLING DIV., AIME, APR. 6, 1962, 9 PP.

64. GERLACH, J. K., AND F. F. PAWLEK. ON THE KINETICS OF PRESSURE LEACHING OF METAL SULFIDES AND ORES. PRES. AT THE TMS-AIME ANN. MEETING, FEB. 25-29, 1968, NEW YORK, 1968, TMS PAPER A68-4, 15 PP.

65. GIRARD, L., AND R. A. HARD. (ASSIGNED TO KENNECOTT COPPER CORPORATION, NEW YORK, N.Y.). STIMULATION OF PRODUCTION WELL FOR IN SITU METAL MINING. U.S. PAT. 3,841,705, OCT. 15, 1974.

66. GRANT, R. F., F. B. RICHARDS, AND H. F. WETHERBEE. LEACHING PROCESS. U.S. PAT. 1,690,446, NOV. 6, 1928.

67. GREENWOOD, C. C. UNDERGROUND LEACHING AT CANANEA. ENG. AND MIN. J., V. 121, NO. 13, MARCH 1926, PP. 518-521.

→ 68. GRISWOLD, G. B. ROCK FRACTURING TECHNIQUES FOR IN PLACE LEACHING. PRES. ANN. MEETING OF THE SOC. OF MIN. ENG., AIME, WASHINGTON D.C., FEB. 16-20, 1969, AIME PREPRINT 69-AS-74, 4 PP.

69. GROVES, P. D., T. H. JEFFERS, AND G. M. POTTER. LEACHING COARSE NATIVE COPPER ORE WITH DILUTE AMMONIUM CARBONATE SOLUTION. PROC. SOLUTION MINING SYMP., AIME ANN. MEETING, DALLAS, TEXAS, FEB. 25-27, 1974, PP. 381-389.

→ 70. HANSEN, S. M. NUCLEAR BLASTING FOR MINING AND LEACHING. WORLD MINING, V. 1, NO. 1, SEPTEMBER 1965, PP. 20-27.

71. HANSEN, S. M., AND A. R. JAGER. HOW TO MAKE ORE FROM MARGINAL DEPOSITS. ENG. AND MIN. J., V. 169, NO. 12, DECEMBER 1968, PP. 75-81.

72. HARD, R. A. (ASSIGNED TO KENNECOTT COPPER CORPORATION, NEW YORK, N.Y.). PROCESS FOR IN-SITU MINING. U.S. PAT. 3,910,635, OCT. 7, 1975.

→ 73. HARDWICK, W. R. FRACTURING A DEPOSIT WITH NUCLEAR EXPLOSIVES AND RECOVERING COPPER BY THE IN-SITU LEACHING METHOD. BUMINES RI 6996, 1967, 48 PP.

74. HEINEN, H. J., T. G. CARNAHAN, AND J. A. FISELE (ASSIGNED TO THE UNITED STATES OF AMERICA, AS REPRESENTED BY THE SECRETARY OF THE INTERIOR, WASHINGTON, D.C.). CHEMICAL MINING OF COPPER PORPHYRY ORES. U.S. PAT. 3,890,007, JUNE 17, 1975.

75. HOCKINGS, W. A., AND W. L. FREYBERGER. LABORATORY STUDIES OF IN SITU AMMONIA LEACHING OF MICHIGAN COPPER ORES. PROC. INTERNAT. SYMP. ON COPPER EXTRACTION AND REFINING, MET. SOC., AIME, LAS VEGAS, NEV., FEB. 22-26, 1976 (PUB. AS EXTRACTIVE METALLURGY OF COPPER--HYDROMETALLURGY AND ELECTROWINNING, ED. BY J. C. YANNOPOULOS AND J. C. AGARWAL). PORT CITY PRESS, BALTIMORE, MD., V. II, 1976, PP. 873-905.

76. HOCKINGS, W. A., AND W. L. FREYBERGER. A PLAN FOR DETERMINING THE FEASIBILITY OF IN SITU LEACHING OF NATIVE COPPER ORES. INSTITUTE OF MINERAL RESEARCH, MICHIGAN TECHNOLOGICAL UNIVERSITY, HOUGHTON, MICHIGAN. PREPARED FOR HOMESTAKE COPPER CO., CALUMET, MICHIGAN, JUNE 14, 1974, 36 PP.

77. HOGAN, D. K. IN-SITU COPPER LEACHING AT THE OLD RELIABLE MINE. MIN. MAG., V. 24, NO. 5, MAY 1974, PP. 353-359.

78. HOLDERREED, F. L. COPPER EXTRACTION BY THE ACID LEACHING OF BROKEN ORE. PINCOCK, ALLEN AND HOLT, INC. REPORT, 1975, 19 PP.

79. HOUGEN, L. P., AND H. ZACHARIASEN. RECOVERY OF NICKEL, COPPER AND PRECIOUS METAL CONCENTRATE FROM HIGH GRADE PRECIOUS METAL MATTES. J. METALS, V. 27, NO. 5, MAY 1975, PP. 6-9.

80. HSUEH, L., P. A. HARD, D. H. DAVIDSON, AND R. V. HUFF (ASSIGNED TO KENNECOTT COPPER CORP.). IN-SITU MINING METHOD AND APPARATUS. U.S. PAT. 4,116,488, SEPT. 26, 1978.

81. HSUEH, L., P. A. HURD, D. H. DAVIDSON, AND R. V. HUFF (ASSIGNED TO KENNECOTT COPPER CORP.). IN-SITU MINING OF COPPER AND NICKEL. U.S. PAT. 4,045,064, AUGUST 30, 1977.

82. HUFF, R. V., AND H. DAVIDSON. IN-SITU LEACHING MATERIALS CONSIDERATIONS. PRES. AT 54TH ANN. FALL TECHNICAL CONFERENCE AND EXHIBITION, SOC. PETROL. ENG., AIME, LAS VEGAS, NEVADA, SEPT. 23-26, 1979, SPE PREPRINT 8320, 6 PP.

83. HUFF, R. V., AND P. A. HUSKA (ASSIGNED TO KENNECOTT COPPER CORP.). WELLBORE OXIDATION OF LIXIVANTS. U.S. PAT. 3,894,770, JULY 15, 1975.

84. HUFF, R. V., AND D. J. MOYNIHAN (ASSIGNED TO KENNECOTT COPPER CORP.). LIXIVIANT RECIRCULATOR FOR IN SITU MINING. U.S. PAT. 4,079,998, MAR. 21, 1978.

85. HUNKIN, G. G. A REVIEW OF IN SITU LEACHING. PRES. AT AIME ANN. MEETING, SOC. OF MIN. ENG., AIME, NEW YORK, N.Y., FEB. 24 - MAR. 4, 1971, AIME PREPRINT 71-AS-89, 23 PP.

86. HURD, B. G., AND J. L. FITCH (ASSIGNED TO MOBIL OIL CORPORATION, A CORPORATION OF NEW YORK). IN SITU LEACHING OF SUBTERRANEAN DEPOSITS. U.S. PAT. 3,278,233, OCT. 11, 1966.

87. ITO, I. PRESENT STATUS OF PRACTICE AND RESEARCH WORKS ON IN-PLACE LEACHING IN JAPAN. PROC. JOINT MEETING OF THE MINING AND METALLURGICAL INSTITUTE OF JAPAN AND THE AMERICAN INSTITUTE OF MINING, METALLURGICAL, AND PETROLEUM ENGINEERS, DENVER, COLO., SEPT. 1-3, 1976 (PUB. AS WORLD MINING AND METALS TECHNOLOGY, ED. BY A. WEISS), V. 1, 1976, PP. 349-364.

88. JACOBY, C. H. (ASSIGNED TO AKZONA INC., ASHEVILLE, N.C.). IN SITU EXTRACTION OF MINERAL VALUES FROM ORE DEPOSITS. U.S. PAT. 3,822,916, JULY 9, 1974.

89. JOHNSON, P. H. (ASSIGNED TO HOWARD E. JOHNSON AND ASSOCIATES). HYDRO-METALLURGICAL METHOD AND APPARATUS. U.S. PAT. 3,264,099. AUG. 2, 1966.

90. JOHNSON, P. H., AND R. R. BHAPPU. CHEMICAL MINING - A STUDY OF LEACHING AGENTS. NEW MEXICO BUREAU OF MINES AND MINERAL RESOURCES, CIRC. 99, 1969, 7 PP.

91. JOHNSON, P. H., AND R. R. BHAPPU. CHEMICAL MINING - THEORETICAL AND PRACTICAL ASPECTS. PRES. AT SME FALL MEETING - ROCKY MOUNTAIN MINERALS CONF., LAS VEGAS, NEVADA, SEPT. 6-8, 1967, 20 PP.

92. KACZYNSKI, D. A., G. W. LOWER, AND W. A. HOCKINGS. KINETICS OF LEACHING METALLIC COPPER IN AQUEOUS CUPRIC AMMONIUM NITRATE SOLUTIONS. PROC. SOLUTION MINING SYMP., AIME ANN. MEETING, DALLAS, TEXAS, FEB. 25-27, 1974, PP. 390-400.

93. KALABIN, A. I. WINNING OF USEFUL ELEMENTS FROM MINERALS BY LEACHING UNDERGROUND. MIN. MAG. (LONDON), V. 118, NO. 2, FEBRUARY 1968, PP. 129-134.

94. KELSEAUX, R. M. (ASSIGNED TO CITIES SERVICE OIL COMPANY, TULSA, OKLA.). STIMULATION OF RECOVERY FROM UNDERGROUND DEPOSITS. U.S. PAT. 3,593,793, JULY 20, 1971.

95. KEYES, H. F. DISCUSSION OF IN PLACE LEACHING AT MIAMI MINE, MIAMI, ARIZONA, BY J. H. FLETCHER, IN TRANS. SOC. OF MIN. ENG., V. 250, NO. 4, DECEMBER 1971, PP. 310-314. TRANS. SOC. OF MIN. ENG., V. 252, NO. 2, JUNE 1972, PP. 186-187.

96. LAMPARD, W. J. (ASSIGNED TO KENNECOTT COPPER CORPORATION, NEW YORK, N.Y.). CONTROLLED IN SITU LEACHING OF ORE DEPOSITS UTILIZING PRE-SPLIT BLASTING. U.S. PAT. 3,863,987, FEB. 4, 1975.

97. LARSON, D. R. A REPORT COMPARING OPEN PIT MINING AND HEAP LEACHING WITH AN IN SITU LEACHING SYSTEM FOR A HYPOTHETICAL OXIDE COPPER DEPOSIT BASED ON THE CHARACTERISTICS OF THE CACTUS DEPOSIT, MIAMI, ARIZONA. M.S. THESIS, UNIV. MINNESOTA, DEPT. OF MINERAL AND METALLURGICAL ENG., JUNE 1973, 254 PP.

98. LASWELL, G. W. CONSIDERATIONS APPLICABLE TO UTILIZATION OF ROTARY DRILLING FOR IN-PLACE RECOVERY OF MINERALS AND HYDROCARBONS. SERVCO DIV. OF SMITH INTERNAT., INC. REPORT, FEBRUARY 1975, 8 PP.

99. LASWELL, G. W. WANTED: ROTARY DRILLING TECHNOLOGY FOR IN SITU MINING SYSTEMS. MIN. ENG., V. 27, NO. 1, JANUARY 1976, PP. 22-26.

100. LEACH, D. L., AND R. L. BRAUN. LEACHING OF PRIMARY SULFIDE ORES IN SULFURIC ACID SOLUTIONS AT ELEVATED TEMPERATURES AND PRESSURES. PRES. AT ANN. MEETING, SOC. MIN. ENG., AIME, NEW YORK, FEB. 16-20, 1975, PREPRINT 75B68, 20 PP.

101. LEWIS, A. E. CHEMICAL MINING OF PRIMARY COPPER ORES BY USE OF NUCLEAR TECHNOLOGY. PROC. SYMP. OF ENGINEERING WITH NUCLEAR EXPLOSIVES, LAS VEGAS, NEV., JAN. 14-16, 1970. CONF. 700101, V. 21, PP. 907-917.

102. LEWIS, A. E. IN SITU PRESSURE LEACHING METHOD. U.S. PAT. 3,640,579. FEB. 8, 1972.

103. LEWIS, A. E. (ASSIGNED TO THE UNITED STATES OF AMERICA AS REPRESENTED BY THE U.S. ATOMIC ENERGY COMMISSION, WASHINGTON, D.C.). SITU LEACHING SOLVENT EXTRACTION-PROCESS. U.S. PAT. 3,823,981, JULY 16, 1974.

104. LEWIS, A. E., AND R. L. BRAUN. NUCLEAR CHEMICAL MINING OF PRIMARY COPPER SULFIDES. PRES. AT THE AIME MEETING, SAN FRANCISCO, CALIF., JAN. 27, 1972, 30 PP.

105. LEWIS, A. E., R. L. BRAUN, C. J. SISEMORE, AND R. G. MALLON. NUCLEAR SOLUTION MINING-BREAKING AND LEACHING CONSIDERATIONS. PROC. SOLUTION MINING SYMP., AIME ANN. MEETING, DALLAS, TEXAS, FEB. 25-27, 1974, PP. 56-75.

106. LEWIS, F. M., AND R. R. RHAPPU. EVALUATING MINING VENTURES VIA FEASIBILITY STUDIES. MIN. ENG., V. 27, NO. 10, OCTOBER 1975, PP. 48-54.

107. LEWIS, F. M., C. K. CHASE, AND R. R. RHAPPU. ECONOMIC EVALUATION OF IN SITU EXTRACTION FOR COPPER, GOLD, AND URANIUM. PROC. JOINT MEETING OF THE MINING AND METALLURGICAL INSTITUTE OF JAPAN AND THE AMERICAN INSTITUTE OF MINING, METALLURGICAL, AND PETROLEUM ENGINEERS, DENVER, COLO., SEPT. 1-3, 1976 (PUB. AS WORLD MINING AND METALS TECHNOLOGY, ED. BY A. WEISS), V. 1, 1976, PP. 333-348.

108. LONGWELL, R. L. IN PLACE LEACHING OF A MIXED COPPER ORE BODY. PROC. SOLUTION MINING SYMP., AIME ANN. MEETING, DALLAS, TEXAS, FEB. 25-27, 1974, PP. 233-242.

109. MALOUF, E. E. COPPER LEACHING PRACTICES. PRES. AT ANN. MEETING, SOC. OF MIN. ENG., AIME, SAN FRANCISCO, CALIF., FEB. 20-24, 1972, AIME PREPRINT 72-AS-84, 7 PP.

110. MALOUF, E. E. INTRODUCTION TO DUMP LEACHING PRACTICE. PART I OF SECOND TUTORIAL SYMP. ON EXTRACTIVE METALLURGY, UNIV. UTAH, DEC. 14-16, 1972, 26 PP.

111. MALOUF, E. E. LEACHING AS A MINING TOOL. INTERNAT. SYMP. ON HYDROMETALLURGY, CHICAGO, ILL., FEB. 25-MAR. 1, 1973, CH. 23, PP. 615-626.

112. MALOUF, E. E. THE ROLE OF MICROORGANISMS IN CHEMICAL MINING. MIN. ENG., V. 23, NO. 11, NOVEMBER 1971, PP. 43-46.

113. MAYLING, A. A. METHOD FOR EXTRACTING COPPER, ZINC, LEAD, NICKEL, COBALT, MOLYBDENUM OR OTHER METAL VALUES FROM LOW-GRADE SULFIDE ORE BODIES. CAN. PAT. 825,473, OCT. 21, 1969.

114. MCKINNEY, W. A. SOLUTION MINING. MIN. ENG., V. 25, NO. 2, FEBRUARY 1973, PP. 56-57.

115. MICHIGAN TECHNOLOGICAL UNIVERSITY. A PLAN FOR DETERMINING THE FEASIBILITY OF AN IN SITU LEACHING OF NATIVE COPPER ORES. PREPARED FOR HOMESTAKE COPPER COMPANY, CALUMET, MICHIGAN. JUNE 14, 1974. 35 PP.

116. MILLER, J. D. PROCESSING OF LEACH LIQUORS PRODUCED BY NUCLEAR SOLUTION MINING. LAWRENCE LIVERMORE LABORATORY, REPT. UCRL-51350, FEB. 15, 1973. 18 PP.

117. MINING CONGRESS JOURNAL. AN EXPERIMENTAL IN-PLACE LEACHING TEST. V. 59, NO. 5, MAY 1973, P. 10.

118. MINING ENGINEERING. KENNECOTT PROPOSES NUCLEAR MINING EXPERIMENTS AT SAFFORD DEPOSIT. V. 19, NO. 11, NOVEMBER 1967, PP. 66-67.

→ 119. MINING ENGINEERING. OXYMIN DETAILS PLANS FOR IN SITU LEACH PROJECT IN ARIZONA. V. 29, NO. 11, NOVEMBER 1977, PP. 13, 16.

→ 120. MINING ENGINEERING. RANCHERS DEVELOPMENT SETS OFF BLAST, WILL LEACH AT BIG MIKE. V. 25, NO. 8, AUGUST 1973, P. 10.

121. MINING MAGAZINE. WINNING OF USEFUL ELEMENTS FROM MINERALS BY LEACHING UNDERGROUND. V. 118, NO. 2, FEBRUARY 1968, PP. 129-134.

→ 122. MINING RECORD (DENVER, COLORADO). RANCHERS BLASTS OLD RELIABLE TO TEST NEW MINING TECHNIQUE. V. 83, NO. 12, MAR. 22, 1972. P. 1.

→ 123. MURPHY, J. NEW RETURNS FROM OLD RELIABLE. SOURCE UNKNOWN. PP. 20-23; COPY AVAILABLE FOR CONSULTATION AT BUREAU OF MINES. TWIN CITIES MINING RESEARCH CENTER, MINNEAPOLIS, MINNESOTA.

124. MYERS, D. L. MINING COPPER IN SITU. THE MINES MAG., V. 31, NO. 6, JUNE 1941, PP. 255-263.

→ 125. OCCIDENTAL MINERALS CORP. THE OXYMIN PROJECT AT MIAMI, ARIZONA. A SUMMARY OF A PRESENTATION MADE TO MIAMI, ARIZONA TOWN COUNCIL, SEPT. 12, 1977. 5 PP.; FOR FURTHER INFORMATION, CONTACT BOB ZACHE, OCCIDENTAL MINERALS CORP., 918 LIVE OAK ST., MIAMI, ARIZONA 85539.

126. OROURKE, J. E., R. J. ESSEX, AND R. K. RANSON. FIELD PERMEABILITY TEST METHODS WITH APPLICATIONS TO SOLUTION MINING. WOODWARD-CLYDE CONSULTANTS (SAN DIEGO, CALIF.), CONTRACT NO. J0265045. BUMINES OPEN FILE REPT. 136-77, JULY 1977, 180 PP.; AVAILABLE FROM NATIONAL TECHNICAL INFORMATION SERVICE, SPRINGFIELD, VA., PB 272 452/AS.

127. ORTLOFF, G. D., C. E. COOKE, JR., AND D. K. ATWOOD (ASSIGNED TO ESSO PRODUCTION RESEARCH COMPANY). MINERAL RECOVERY. U.S. PAT. 3,574,599, APR. 13, 1971.

128. PAY DIRT, ARIZONA EDITION (BISBEE, ARIZONA). OXYMIN PLANS FINAL IN SITU COPPER LEACHING TESTS AT MIAMI, DECEMBER 1979, NO. 486, PP. 1, 4.

129. PETROVIC, L. J., R. A. HARD, AND I. V. KLIMPAR. ECONOMIC CONSIDERATIONS FOR RECOVERING COPPER FROM DEEP SULFIDE DEPOSITS BY NUCLEAR RUBBLIZATION. IN SITU, V. 1, NO. 3, 1977, PP. 235-248.

130. PINGS, W. R. BACTERIAL LEACHING. MINER. IND. BULL., V. 2, NO. 3, MAY 1968, 19 PP.

131. POJAR, M. IN-PLACE LEACHING OF A COPPER SULFIDE DEPOSIT. PRES. AT DULUTH MEETING, SOC. OF MIN. ENG., AIME, DULUTH, MINN., JAN. 16-18, 1974, 9 PP.

132. PORTER, D. D. BLAST DESIGN FOR IN SITU LEACHING. PRES. AT SOUTHWEST MINERAL INDUSTRY CONF., PHOENIX, ARIZ., APR. 27, 1973, 7 PP.; AVAILABLE FROM E. I. DU PONT DE NEMOURS AND CO., INC., WILMINGTON, DEL. 19898.

133. PORTER, D. D., AND H. G. CARLEVATO. IN SITU LEACHING: A NEW BLASTING CHALLENGE. PROC. SOLUTION MINING SYMP., AIME ANN. MEETING, DALLAS, TEXAS, FEB. 25-27, 1974, PP. 33-43.

134. POTTER, G. M. SOLUTION MINING. MIN. ENG., V. 21, NO. 1, FEBRUARY 1969, PP. 68-69.

135. PRESCOTT NEWSPAPER (PRESCOTT, ARIZONA). KIRKLAND BLAST WILL OPEN NEW BODY OF COPPER. APR. 18, 1973, P. 1.

136. RABB, D. D. LEACHING OF COPPER ORES AND THE USE OF BACTERIA. LAWRENCE RADIATION LABORATORY, REPT. UCID-4959, JAN. 22, 1965, 25 PP.

137. RABB, D. D. PENETRATION OF LEACH SOLUTION INTO ROCKS FRACTURED BY A NUCLEAR EXPLOSION. PRES. AT ANN. MEETING OF SOC. OF MIN. ENG., AIME, WASHINGTON, D.C., FEB. 16-20, 1969, V. 1:A, AIME PREPRINT 69-AS-4, 14 PP.

138. RABB, D. D. SOLUTION MINING. MIN. ENG., V. 24, NO. 2, FEBRUARY 1972, PP. 62-64.

139. RAGHAVAN, S. AMMONIACAL LEACHING OF A CHRYSOCOLLA BEARING COPPER ORE. TO BE PRES. AT AIME ANN. MEETING, NEW ORLEANS, LA., FEB. 18-22, 1979.

140. RANCHERS EXPLORATION AND DEVELOPMENT CORP. THE OLD RELIABLE PROJECT - A TEST OF NEW TECHNOLOGY. COMPANY REPORT, 1972, 4 PP.

141. RICKARD, R. S. CHEMICAL CONSTRAINTS ON IN-SITU LEACHING AND METAL RECOVERY. PROC. SOLUTION MINING SYMP., AIME ANN. MEETING, DALLAS, TEXAS, FEB. 25-27, 1974, PP. 185-192.

142. ROMAN, R. J. THE LIMITATIONS OF LABORATORY TESTING AND EVALUATION OF DUMP AND IN SITU LEACHING. IN SITU, V. 1, NO. 4, 1977, PP. 305-324.

143. ROMAN, R. J. SOLUTION MINING. MIN. ENG., V. 26, NO. 2, FEBRUARY 1974, PP. 43-44.

144. ROOT, T. E. LEGAL ASPECTS OF MINING BY THE IN-SITU LEACHING METHOD. PRES. AT 22ND ANN. ROCKY MOUNTAIN MINERAL LAW INST., SUN VALLEY, IDAHO, JULY 22-24, 1976. 18 PP.

145. ROSENBAUM, J. B., AND W. A. MCKINNEY. IN SITU RECOVERY OF COPPER FROM SULFIDE ORE BODIES FOLLOWING NUCLEAR FRACTURING. PROC. SYMP. OF ENGINEERING WITH NUCLEAR EXPLOSIVES, LAS VEGAS, NEV., JAN. 14-16, 1970, CONF. 700101, V. 2, PP. 877-887.

146. ROSENZWEIG, M. D. NEW COPPER TECHNOLOGY IS WINNING THE ORE. CHEM. ENG., V. 74, NO. 25, DEC. 4, 1967, PP. 88-90, 92.

147. ROUSE, J. V. ENVIRONMENTAL ASPECTS OF IN SITU MINING AND DUMP LEACHING. PROC. SOLUTION MINING SYMP., AIME ANN. MEETING, DALLAS, TEXAS, FEB. 25-27, 1974, PP. 3-14.

148. RUDERSHAUSEN, C. G. COPPER SOLUTION MINING AT OLD RELIABLE. PRES. AT NATIONAL MEETING OF AMERICAN INST. OF CHEMICAL ENG., SALT LAKE CITY, NEV., AUG. 18-21, 1974, 11 PP.

149. ST. PETER, A. L. IN SITU LEACHING OF OREBODIES DESIGN AND MANAGEMENT. PINCOCK, ALLEN AND HOLT, INC. REPORT, 1975, 20 PP.

150. ST. PETER, A. L. IN SITU MINING -- A DESIGN FOR POSITIVE RESULTS. PRES. AT 105TH ANN. MEETING, AIME, LAS VEGAS, NEV., FEB. 22-26, 1976, PREPRINT 76-AS-36, 43 PP.

151. SAREEN, S. S., L. GIRARD, III, AND R. A. HARD. STIMULATION OF RECOVERY FROM UNDERGROUND DEPOSITS. U.S. PAT. 3,865,435, FEB. 11, 1975.

152. SCHLITT, W. J., R. P. REAM, L. J. HAUG, AND W. D. SOUTHARD. PRECIPITATING AND DRYING CEMENT COPPER AT KENNECOTTS BINGHAM CANYON FACILITY. MIN. ENG., V. 31, NO. 6, JUNE 1979, PP. 671-678.

153. SCOTT, W. G. (ASSIGNED TO INSPIRATION CONSOLIDATED COPPER COMPANY, A CORPORATION OF MAINE). LEACHING COPPER ORES. U.S. PAT. 2,563,623, AUG. 7, 1951.

154. SELIM, A. A. A DECISION ANALYSIS APPROACH TO IN SITU EXTRACTION OF COPPER. PH.D. THESIS, UNIV. MINNESOTA, MINNEAPOLIS, MINN., MARCH 1976, 659 PP.

155. SELIM, A. A., AND D. H. YARDLEY. THE DESIGN AND COST OF A FRAGMENTATION SYSTEM FOR IN SITU EXTRACTION OF COPPER. PRES. AT 14TH INTERNAT. SYMP. ON THE APPLICATION OF COMPUTER METHODS IN THE MINERAL INDUSTRY, THE PENNSYLVANIA STATE UNIVERSITY, UNIVERSITY PARK, PA., OCT. 14-16, 1976.

156. SELIM, A. A., AND D. H. YARDLEY. IN SITU LEACHING OF COPPER -- AN ECONOMIC SIMULATION APPROACH. PRES. AT 107TH ANN. MEETING, AIME, ATLANTA, GA., MARCH 1977, PREPRINT 77-AS-68, 24 PP.

157. SHEFFER, H. W., AND L. G. EVANS. COPPER LEACHING PRACTICES IN THE WESTERN UNITED STATES. BUMINES IC 8341, 1968, 57 PP.

158. SHOCK, D. A. DEVELOPMENTS IN SOLUTION MINING PORTEND GREATER USE FOR IN SITU LEACHING. MIN. ENG., V. 22, NO. 2, FEBRUARY 1970, P. 73.

159. SHOCK, D. A., AND J. G. DAVIS, II. (ASSIGNED TO CONTINENTAL OIL COMPANY, PONCA CITY, OKLA., A CORP. OF DELAWARE). FRACTURING METHOD IN SOLUTION MINING. U.S. PAT. 3,387,888, JUNE 11, 1968.

160. SHOEMAKER, R. S. AMMONIA REVIVAL FOR THE KEWEENAW. MIN. ENG., V. 24, NO. 5, MAY 1972, PP. 45-47.

161. SKILLINGS MINING REVIEW. EL PASO STUDYING IN SITU LEACHING AT EMERALD ISLE. V. 63, NO. 52, DEC. 28, 1974, P. 8.

162. SKILLINGS MINING REVIEW. OXYMINS IN-SITU COPPER LEACHING PROJECT AT MIAMI, ARIZ. V. 66, NO. 52, DEC. 24, 1977, PP. 1, 10-12.

163. SKILLINGS MINING REVIEW. RANCHERS DETONATES LARGE BLAST AT BIG MIKE MINE IN NEVADA. V. 62, NO. 29, JULY 21, 1973, P. 5.

164. SMITH, P. R., JR., D. W. BAILEY, AND R. E. DOANE. TRENDS IN CHEMICAL PROCESSING AND HYDROMETALLURGY. ENG. AND MIN. J., V. 173, NO. 6, JUNE 1972, PP. 173-177.

165. SPEDDEN, H. R., AND E. E. MALOUF (ASSIGNED TO KENNECOTT COPPER CORPORATION, NEW YORK, N.Y.). CONTROLLED IN-SITU LEACHING OF MINERAL VALUES. U.S. PAT. 3,815,957, JUNE 11, 1974.

166. SPEDDEN, H. R., AND E. E. MALOUF (ASSIGNED TO KENNECOTT COPPER CORPORATION, NEW YORK, N.Y.). IN-SITU GENERATION OF ACID FOR IN-SITU LEACHING OF COPPER. U.S. PAT. 3,834,760, SEPT. 10, 1974.

167. SPEDDEN, H. R., E. E. MALOUF, AND J. D. DAVIS. IN SITU LEACHING OF COPPER--PILOT PLANT TEST. PRES. AT ANN. MEETING, AIME, NEW YORK, FEBRUARY 1971, 21 PP.

168. SPENCE, A. P. (ASSIGNED TO ATLANTIC RICHFIELD CO., NM URANIUM INC., AND U.S. STEEL CORP.). METHOD FOR THE RECOVERY OF A MINERAL. U.S. PAT. 4,082,359, APR. 4, 1978.

169. STAUTER, J. C., AND A. G. FONSECA. LEACHING OF OXIDE COPPER ORE WITH AMMONIUM HYDROGEN SULPHATE: BENCH-SCALE TESTING. CAN. MIN. AND MET. BULL., V. 67, NO. 742, FEBRUARY 1974, PP. 135-136.

170. STECKLEY, R. C., W. C. LARSON, AND D. V. DANDREA. BLASTING TESTS IN A PORPHYRY COPPER DEPOSIT IN PREPARATION FOR IN SITU EXTRACTION. BUMINES RI 8070, 1975. 47 PP.

171. STEWART, R. M., AND K. F. NIERMEYER. NUCLEAR TECHNOLOGY AND MINERAL RECOVERY. PROC. SYMP. ON ENGINEERING WITH NUCLEAR EXPLOSIVES, LAS VEGAS, NEV., JAN. 14-16, 1970. CONF. 700101, V. 2, PP. 864-876.

172. TEWES, H. A., H. B. LEVY, AND L. L. SCHWARTZ. NUCLEAR CHEMICAL COPPER MINING AND REFINING: RADIOLOGICAL CONSIDERATIONS. LAWRENCE LIVERMORE LABORATORY, REPT. UCRL-51345, REV. 1, JUNE 3, 1974, 34 PP.

173. THOMAS, R. W. LEACHING COPPER FROM WORKED-OUT AREAS OF THE RAY MINES, ARIZONA. MIN. AND MET., V. 19, NOVEMBER 1938, PP. 481-485.

174. TRUSSELL, P. C., D. W. DUNCAN, AND C. C. WALDEN. BIOLOGICAL MINING. CAN. MIN. J., V. 85, NO. 3, MARCH 1964, PP. 46-49.

175. U.S. BUREAU OF MINES. PROJECT PROPOSAL: PORPHYRY COPPER - IN SITU RECOVERY BY LEACHING FOLLOWING NON-NUCLEAR FRACTURING. INTERDISCIPLINARY RESEARCH TASK FORCE, COMP. BY L. W. GIBBS, NOV. 23, 1971, (REV. DEC. 6, 1971), 20 PP. AVAILABLE FOR CONSULTATION AT BUREAU OF MINES, TWIN CITIES MINING RESEARCH CENTER, MINNEAPOLIS, MINNESOTA.

176. U.S. ENERGY RESEARCH AND DEVELOPMENT ADMINISTRATION. IN SITU LEACHING OF A NUCLEAR RUBBLIZED COPPER ORE BODY (IN TWO VOLUMES). V. 1, RESULTS OF FEASIBILITY STUDY. U.S. ERDA REPORT NVO-155, JUNE 1975, 30 PP.; V. 2, DETAILED DESIGN, CALCULATIONS, AND PROCEDURES. REPORT NVO-155, JUNE 1975, 318 PP.

177. VAN POOLEN, H. K., AND R. V. HUFF (ASSIGNED TO KENNECOTT COPPER CORP.). OXIDATION OF SULFIDE DEPOSITS CONTAINING COPPER VALUES. U.S. PAT. 3,881,774, MAY 6, 1975.

178. VORTMAN, L. J. AIRBLAST FROM SEQUENTIAL DETONATION OF GROUPS OF CHARGES IN VERTICAL DRILLED HOLES. UNLIMITED RELEASE SAND 75-0194, U.S. ENERGY RESEARCH AND DEVELOPMENT ADMIN. CONTRACT AT(29-1)-789, SEPTEMBER 1975, 48 PP.; AVAILABLE FROM NATIONAL TECHNICAL INFORMATION SERVICE, 5285 PORT ROYAL ROAD, SPRINGFIELD, VIRGINIA 22151, SAND75-0194.

179. WARD, M. H. ENGINEERING FOR IN SITU LEACHING. MIN. CONG. J., V. 59, NO. 1, JANUARY 1973, PP. 21-27.

180. WARD, M. H. SURFACE BLASTING FOLLOWED BY IN SITU LEACHING THE BIG MIKE MINE. PROC. SOLUTION MINING SYMP., AIME ANN. MEETING, DALLAS, TEXAS, FEB. 25-27, 1974, PP. 243-251.

181. WATSON, J. D., SR., W. A. MOD, AND F. N. TEUMAC (ASSIGNED TO DOW CHEMICAL CO.). EXTRACTION OF COPPER, NICKEL, COBALT OR CHROMIUM VALUES FROM SULFIDE, OXIDE OR SILICATE ORES THEREOF. U.S. PAT. 3,475,163, OCT. 28, 1969.

182. WEED, R. C. CANANEAS PROGRAM FOR LEACHING IN PLACE. MIN. ENG., V. 8, NO. 7, JULY 1, 1956, PP. 721-723.

183. WORMSER, F. E. LEACHING A COPPER MINE. ENG. AND MIN. J., V. 116, NO. 16, OCTOBER 1923, PP. 665-670.

184. ZIMMER, P. F., AND M. A. LEKAS. (COMP. AND ED. BY). PROJECT SLOOP (NUCLEAR EXPLOSIVES-PEACEFUL APPLICATIONS). U.S. ATOMIC ENERGY COMMISSION REPORT NO. PNE 1300, JUNE 1, 1967, 44 PP.

there would be no loss in weight.

In this case tungsten would be deposited on the substrate or an alloy would form, however, tungsten itself is unstable in the vapour of its hexachloride (fig.3). X-ray micro-analysis of the surface of tantalum samples obtained at 900 and 1300°C did not reveal tungsten, i.e., the reaction of tantalum with tungsten chloride vapour is realised by reactions leading to the formation of volatile lower chlorides of the two metals.

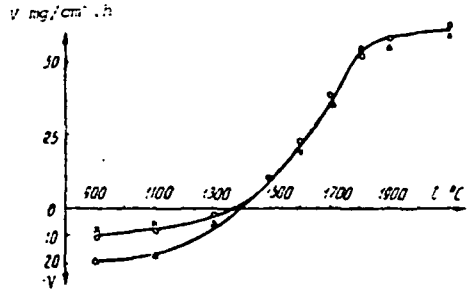

Fig.3 Effect of the substrate temperature on the deposition rate of tungsten during thermal dissociation of the hexachloride. Substrate material: 1 - molybdenum; x - tungsten; 3 - tantalum; P_{WCl_6} = 5.17mm Hg.

Consequently, it is not possible to obtain an alloy of tantalum with tungsten by saturation of the surface of metallic tantalum with tungsten from its chloride under the given conditions. The thermal dissociation of tungsten hexachloride under vacuum is greatly retarded at 1400°C, but "dissolution" of the substrate does not occur[11]).

The deposition rate of tungsten does not depend on the nature of the substrate material at temperatures above 1400°C, increases according to an exponential law up to 1700-1750°C, and passes rapidly into the temperature zone where control of the process is realised by the delivery of the reagents to the reaction surface. Here the obtained maximum deposition rate is much lower than the rate obtained during deposition of tungsten in pure hydrogen with the same P_{WCl_6} value (figs.2 and 3). This can be linked to the suggestion about the difficulty of delivery of tungsten chloride to the reaction surface in an atmosphere of argon. It is evidently possible to extend the kinetic and reduce the diffusion region of the process considerably by replacement of argon by the lighter and more heat-conductive helium.

Investigation of tungsten deposits. Metallographic investigations of the tungsten deposits showed that they have the typical columnar structure of materials deposited from the gas phase. Long thin crystals grow during deposition in hydrogen. With a sharp reduction in temperature (disconnection of the heat supply) cracks form in the deposits The higher the temperature, the more clearly this is expressed. Cracks are not formed with a smooth reduction of temperatures.

SUBJ
MNG
CDR

Coarse-grained deposits are formed on the substrates during thermal dissociation of WCl_6. The thermal stability of these deposits is higher and cracks are not formed in them on rapid cooling. The measured microhardness of the deposits lies within the limits of 406-442 kg/mm² for tungsten obtained by thermal dissociation, i.e , somewhat lower than in the literature[11]).

The lattice constants of tungsten corresponded to 3.166 and 3.155 Å for deposits obtained in hydrogen and argon.

References

1) Deposition from the gas phase. Atomizdat 1970.
2) A I Evstyukhin et alia: Collection: Metallurgy and physical metallurgy of pure metals 1967, (6).
3) I R Karyazin et alia: Collection: Metallurgy of tungsten molybdenum and niobium. Nauka 1967, 124.
4) V P Elyutin et alia: Izv. Vuz. Chernaya Metallurgiya 1964, (3).
5) B S Lysov et alia: Izv. Vuz. Tsvetnaya Metallurgiya 1971, (5).
6) B S Lysov et alia: Izv Vuz Tsvetnaya Metallurgiya 1972, (3).
7) B N Babich et alia: Izv. Akad. Nauk SSSR Metally 1967, (1).
8) Catalysis. Questions of theory and methods of investigation. (Russian translation from English), Moscow IL, 1955.
9) A V Suvorov: Thermodynamic chemistry of the vapour-phase state. Khimiya, Leningrad 1970.
10) B Joyce and R Brodli: Crystallisation from the gas phase. (Russian translation). Mir, Moscow 1965.
11) B P Kreingauz et alia: Metallurgy of nonferrous and rare metals. Nauka, Moscow 1967, 158.

UDC 669.046:699.292

Sov. Non-Fe
1975 v. 3 N 4

Calculation of the degree of reaction along the height of blast furnace for roasting vanadium slag

V P Malyshev and T A Oralov (Chemical-Metallurgical Institute, Academy of Sciences of the Kazakh SSR)

Summary

A method is developed for calculating the degree of reaction along the height of a shaft furnace for the roasting of vanadium slag. The method uses a graph of the distribution of temperatures along the height of the shaft and nonlinear multiple correlation equations obtained in laboratory investigations and having maxima with respect to the temperature and length of the process.

The yield of water soluble and oxidised vanadium in a continuous large-scale laboratory furnace is calculated. It is shown that the accuracy of the calculation lies within the error limits of the macrokinetic equations.

UDC 622.7:541.183.12

Reaction of thiocarbamide with gold cyanide during elution of ion-exchange resin

V M Kuz'minykh, G A Narnov and L A Chursina (Far-Eastern Geological Institute.)

The most effective eluting solution for the desorption of gold cyanide from anion-exchange resins is considered to be an acidic solution of thiocarbamide[13]). Here it is supposed that the following reaction takes place in the elution process:

$$\overline{RAu(CN)_2} + 2HCl + 2Tca = \overline{RCl} + AuTca_2Cl + 2HCN \qquad (1)$$

The dicyanoaurate ion, retained electrostatically, is converted into the cationic complex $AuTca_2^+$, which the ion-exchange resin cannot retain, and it therefore passes into solution[1]). However, reaction (1) only reflects the final result of the elution process, while the intermediate stages comprising the mechanism of desorption of gold from the

resin are unknown.

The present work gives the results from experiments on the processes occurring during elution and some of the problems related to the thermodynamics of the reaction of the gold cyanide complex with thiocarbamide. According to equation (1), the weak hydrocyanic acid is formed together with the gold thiocarbamide complex, and the decomposition of the dicyanoaurate can consequently be controlled by varying the pH of the solution during elution.

The anion-exchange resin AM-2B was used in the experiments. Before the experiments a quantity of the reson (10g) was saturated with gold in a solution of $KAu(CN)_2$. A 100ml portion of a 1M solution of thiocarbamide was then prepared with the addition of hydrochloric acid to pH 1.05. The acidity of the solution was measured by a pH-263 instrument with an accuracy up to a hundredth of a pH unit. The resin, saturated with the dicyanoaurate, was agitated with the eluting solution for 45h, while the pH was measured and samples of the solution were taken for analysis for gold content.

Curve a in fig. 1 shows the variation of the pH of the solution with time. At the end of the experiment the pH of the solution reaches a value of 1.45-1.50 and then decreases extremely slowly, although a considerable amount of gold still remains on the resin. Curve b shows the variation of the pH of the thiocarbamide solution during agitation with the resin without adsorbed gold. Here absorption of a certain amount of oxygen also takes place on account of the weakly basic charactertistics of the resin. Thus, curve a at the same time reflects the absorption of the acid by the resin itself and the neutralisation of HCl through decomposition of the cyanide complex of gold and the formation of hydrocyanic acid.

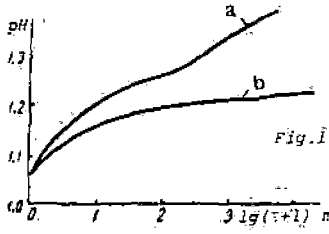

Fig.1 Variation of the pH of the solution during elution.

Fig. 2 shows the variation of the ratio of the amount of gold desorbed into the solution to the amount of neutralised HCl with time. If it is supposed that the desorption process follows reaction (1) strictly, the ratio should be equal to 2.75. However, according to the experimental results (fig. 2), this ratio varies with time and amounts to 4.3. With repeated elution of this sample of resin the Au/HCl ratio amounted to 4.8. This can be explained by the fact that the reaction (1) takes place with an intermediate stage, in which the neutral complex $AuTca_2CN$ is formed. In this compound the cyanide is still firmly attached and is only removed with volatilisation of the hydrocyanic acid from the solution, and the rate of this process depends on the acidity of the solution.

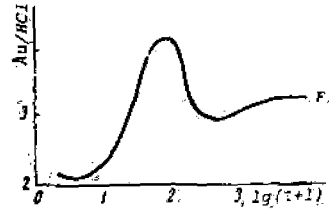

Fig.2 Variation of the Au/HCl ratio during elution.

The strength of the bond between the cyanide and the gold thiocarbamide is demonstrated by the fact that the pH of the solution does not increase when simple gold cyanide is dissolved even in concentrated solutions of thiocarbamide, i.e. the free cyanide is not released:

$$AuCN + 2Tca \rightleftarrows AuTca_2CN \qquad (2)$$

It could be supposed that the following reaction occurs:

$$2AuCN + 2Tca \rightleftarrows AuTca_2^+ + Au(CN)_2^- \qquad (3)$$

However, analysis of the solution after prolonged dissolution of AuCN with a deficiency of thiocarbamide showed that one mole of AuCN passes into solution for two moles of thiocarbamide, and this corresponds to the stoichiometry of reaction (2). Moreover, if the complex $Au(CN)_2^-$ had formed in the strongly acidic medium it would decompose with the formation of a precipitate of AuCN, and this does not in fact occur.

The compound $AuTca_2CN$ was isolated in the pure form from the solution after dissolution of AuCN in a deficiency of thiocarbamide by evaporation and recrystallisation from aqueous and alcohol solutions. The obtained precipitate, which took the form of transparent prismatic crystals, was analysed for gold and silver. The amount of the precipitate used for analysis was 375mg (the amount corresponding to 1 mole of the supposed compound ($AuTca_2CN$). By analysis it was established that the precipitate contained 194mg of gold and 65mg of sulphur, which corresponds to 154mg of thiocarbamide. The residue by difference amounted to 27mg. These data show that the material composition of the precipitate corresponds to the stoichiometry of the supposed formula $AuTca_2CN$.

The compound isolated was submitted to IR spectroscopy. The spectrum was recorded on a UR-20 spectrophotometer. The sample was prepared in the form of a tablet formed under a pressure of 8 ton/cm^2 from a mixture of the investigated compounds and potassium bromide in a ratio of 1:300.

Fig. 3b shows the obtained IR spectrum. For comparison the IR spectrum are given of simple gold cyanide (fig. 3c) obtained under idential conditions, and the spectrum of the thiocarbamide complex of platinum (fig. 3a), given in the literature[1]. In the spectrum of the thiocarbamide complex of platinum there is much in common with the spectrum of the investigated compound. At the same time the spectrum of the gold complex has a perfectly clear absorption peak at 2140cm^{-1}, which is absent in fig. 3a. There is an identical peak in the spectrum of AuCN (2240cm^{-1}).

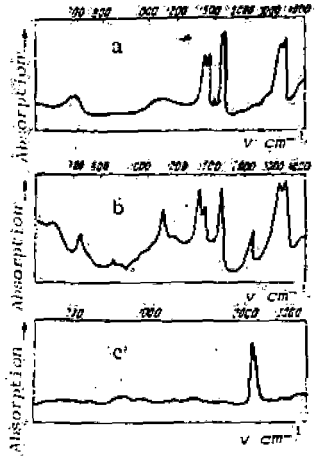

Fig.3 The IR spectra of platinum thiocarbamide (a), $AuTca_2CN$ (b) and AuCN (c).

It is known[2] that cyanide complexes possess characteristic absorption in the region of 2000-2300cm^{-1} (characteristic absorption of the CN group). Thus the isolated compound contains cyanide, which also demonstrates by the existence of the $AuTca_2CN$ complex.

This compound is stable in a weakly acidic medium. With the addition of alkali a yellow precipitate separates, and this becomes brown on drying. The composition of the precipitate is not constant. Its gold content varies between 62 and 77%, and its sulphur content varies between 10 and 15%. In a strongly acidic medium the compound $AuTca_2CN$ eliminates cyanide, which combines into HCN. However, this process only goes to completion in an open vessel, where the HCN can volatilise without hindrance. This is demonstrated by the

following experiment.

Solutions of $AuTca_2CN$, acidified to pH 1.42 and 1.14 with hydrochloric acid, were poured into small flasks, covered with stoppers, and kept at 21°C for a long time. Here the pH in the closed flasks remained constant, which indicated that $AuTca_2CN$ is stable under the given pH values.

To obtain a more detailed idea about the reaction of $Au(CN)_2^-$ with thiocarbamide we studied the process under equilibrium conditions, i.e. in a closed system. For this purpose a solution of $KAu(CN)_2$ was acidified by the addition of a few drops of HCl to pH = 1.06, and a quantity of thiocarbamide was added. The solution was kept for a long time in a closed 20ml glass flask with the surface level under the stopper at 21°C. The final pH value was measured (1.94), and the gold current was determined (0.11g-atom/l).

Since it had been established in the previous experiment that the $AuTca_2CN$ form is stable even in more acidic solutions (pH = 1.14), in the given case the reaction is described as follows:

$$Au(CN)_2^- + 2Tca + H^+ \rightleftarrows AuTca_2CN + HCN \qquad (4)$$

The equilibrium constant of this reaction is given by:

$$K_e = \frac{[AuTca_2CN][HCN]}{[Au(CN)_2^-]\ \gamma\ [H^+]\ \gamma\ [Tca,^2]}$$

Knowing the initial (1.06) and final (1.94) pH values, we can calculate the amount of neutralised HCl (54.4mg). Since it is extremely difficult to determine hydrocyanic acid directly under the given equilibrium conditions, we calculated the HCN concentration from the amount of neutralised HCl ([HCl] = $7.8\cdot10^{-2}$ mole/l). We also calculated the concentration of the formed complex $AuTca_2CN$ ($7.55\cdot10^{-2}$ mole/l), and the remaining $Au(CN)_2^-$ ($3.42\cdot10^{-4}$ mole/l). The thiocarbamide concentration was calculated from the weight of the sample less the thiocarbamide combined into the complex ([Tca] = $5\cdot10^{-1}$ mole/l). On the basis of the foregoing and with regard to the fact that the activity coefficient for monovalent ions in the given solution with an ionic strength of 0.21 is 0.78 we calculated the equilibrium constant:

$$K_e = \frac{7.55\cdot10^{-2}\cdot7.8\cdot10^{-2}}{3.42\cdot10^{-4}\cdot0.78\cdot1.15\cdot10^{-2}\cdot0.78(5\cdot10^{-1})^2} = 98.5$$

With a knowledge of the equilibrium constant of reaction (4) it is possible to estimate the dissociation constant of the complex $AuTca_2CN$. Since:

The $K_{dAu(CN)_2^-}$ value is $5\cdot10^{-39}$ [5]; $K_{dHCN} = 7.9\cdot10^{-10}$ [6]) and consequently:

$$K_{dAuTca_2CN} = \frac{5\cdot10^{-39}}{98.5\cdot7.9\cdot10^{-10}} = 6.42\cdot10^{-32}$$

$$K_e = \frac{K_{dAu(CN)_2^-}}{K_{dAuTca_2CN}\ K_{dHCN}} \quad \text{then}$$

$$K_{dAuTca_2CN} = \frac{K_{dAu(CN)_2^-}}{K_e K_{dHCN}}$$

According to published data[7]), the potential of the thiocarbamide complex of gold (I) $AuTca_2^+$ is 0.38V, i.e. the dissociation constant of $AuTca_2^+$ is $7.9\cdot10^{-26}$. By comparison of these two constants it is possible to conclude that the compound $AuTca_2CN$ is more stable in the closed system, and it is therefore difficult to elute the gold from the resin under equilibrium conditions, as confirmed by the experiments. Since the $AuTca_2CN$ complex is stable in a weakly acidic medium, elution of the resin at a pH greater than 1.2 is very sluggish.

Consequently, to intensify the desorption of the gold from the resin it is necessary to create conditions for rapid removal of hydrocyanic acid from the solution (heating of the solution, increased acidity, large contact surface between the solution and air). The bubbling of air through the solution, which considerably accelerates the volatilisation of HCN, is extremely effective. The formation of the neutral complex $AuTca_2CN$ can be used for adsorption elution by a thiocarbamide solution with low acidity. For this purpose it is necessary to add finely divided activate charcoal to the eluting solution together with the resin and to realise the elution under static conditions. As is known[8]), charcoal has an increased adsorption activity in relation to uncharged complexes. Therefore the $AuTca_2CN$ which forms is readily sorbed by the charcoal. In addition, sorption of HCN occurs, and this also accelerates the elution process.

By experiments it was established that the addition of fine charcoal to the eluting solution in an amount equal to the weight of the resin makes it possible to desorb 99.6% of the gold from the resin at the usual temperature with an initial acidity of pH 1.1-1.15. Here 98.5% of the gold is sorbed on the charcoal, and 1.1% remains in solution. The charcoal is separated from the resin on a 0.5mm sieve. The capacity of the charcoal for gold amounts to 12.5%, i.e. such charcoal can be ignited and the ash melted to gold. The adsorbed hydrocyanic acid can be collected if it is removed from the charcoal by heating to 100-150°C.

References

1) I N Maslenitskii et alia: Metallurgy of noble metals: Metallurgiya, Moscow 1972.
2) I D Fridman et alia: Tsvetnye Metally 1972, (2).
3) E P Zdorova et alia: in Analysis and technology of noble metals: Metallurgiya 1971.
4) A Iamaguch et alia: J. Amer. Chem. Soc. 1958, 80, (3), 527.
5) W Latimer: Oxidation states of the elements and their potentials in aqueous solutions: Russian translation, IL 1954.
6) Chemists' Reference Book Vol. 3, Khimiya 1964.
7) V P Kazakov et alia: Oxidation-reduction potential of thiorea complex of gold (I): Zh. Neorgan. Khim. 1964, 9, (5), 1299.
8) V M Kuz'minykh et alia: Izv VUZ Tsvetnaya Metallurgiya 1968, (4).

UDC 621.357.2

Cathodic reduction of silver from silver-saturated hydrochloric acid electrolytes

S S Sverdlov, N G Tyurin and K A Karasev (Urals Polytechnical Institute - Department of the Metallurgy of Noble Metals).

The cathodic reduction of silver from its poorly soluble chloride in contact with a metallic cathode in hydrochloric acid electrolytes takes place through a stage involving dissolution of silver chloride. The kinetics of the process are determined by the reduction of silver from the silver-saturated chloride electrolytes.

The electrolyte represents a complex equilibrium system, consisting of the H^+, Cl^-, Ag^+, Ag_2Cl^+, $AgCl_2^-$, $AgCl_3^{2-}$, and $AgCl_4^{3-}$ ions and $AgCl_{soln.}$. In view of the fact that the concentration of Ag^+ and Ag_2Cl^+ ions in the electrolyte is extremely small it is necessary to assume the discharge of a difference sort of silver-containing ions at the cathode

CHOOSING AN EFFECTIVE SORBENT FOR REMOVAL OF HEAVY METALS FROM AMMONIUM MOLYBDATE SOLUTIONS

UDC 669.28:661.183.1

A. G. Kholmogorov, S. N. Il'ichev, and I. A. Yanson

ANKB-1, the ampholyte suggested for removal of heavy metals from ammonium molybdate solutions,[1,2] partly absorbs molybdenum, which must be washed out with ammonia before copper desorption (see footnote 2). The present investigation was carried out to find a sorbent for removing heavy metals (particularly copper) from ammonium molybdate solutions which was more effective than ANKB-1.

Process solutions after ammonia leaching of the product from roasting molybdenite concentrates containing up to 0.5% Cu were used to assess the sorptive capacity of ion-exchange resins for copper ions. A weighed portion of 2 g and the prescribed volume of ion-exchanger (20 ml) was used in the experiments. The ion-exchangers were prepared by K.M. Ol'shanova's method[3] and had the folowing characteristics.

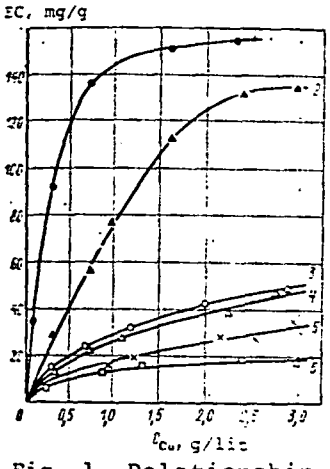

Fig. 1. Relationship of ion-exchanger saturation with copper to copper concentration in solution: 1) AMF-2 × 7P; 2) KB-2 × 7P; 3) AMF-op. 180; 4) AMF-op. 50[b]; 5) AMF-3 × 4P; 6) AMF-5 × 4 (para). Solution concentration, g/liter: 18-20 NH_3; 80-82 Mo; 22 SO_4^{2-}; Na, K, and Fe cations present.

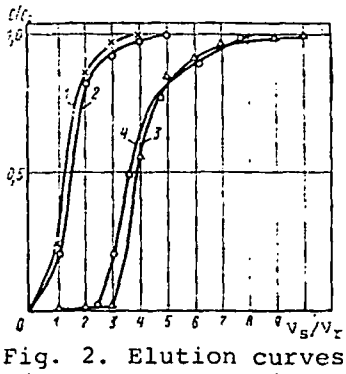

Fig. 2. Elution curves for copper sorption by ion-exchangers from ammonium molybdate solutions: C/C_0) ratio of copper concentration in sample to initial concentration (3.62 g/liter Cu); V_S/V_r) ratio of volume of solution passing through to volume of resin in column. Ion-exchangers: 1) KB-2 × 7P; 2) AMF-op. 180; 3) AMF-2 × 74; 4) ANKB-1.

1. Ampholyte-op. 50[b], based upon chloromethylmated copolymer, contained aminophosphorus groups (4.7% P, 3% N); average exchange capacity (AEC) in terms of chlorine ion 2.3 mg-eq/g.

2. Ampholyte-op. 180 was synthesized on the basis of porous chloromethylated styrene and divinylbenzene (DVB) copolymer with phosphorus and sulfur present (up to 7.5% S); AEC for sodium ion from 0.1N NaOH solution 3.7 mg-eq/g.

3. Ampholyte-2 × 7P, based upon a macroporous methacrylate and DVB copolymer, was synthesized by ammonolysis with ethylenediamine and carboxylation with chloroacetic acid; AEC for chlorine ion 5.37 mg-eq/g, swelling volumm 2.07 ml/g.

4. Ampholyte-5 × 4 (para) is based upon porous chloromethylated copolymer and para-aminophenol; AEC for chlorine ion 2.1 mg-eq/g, for sodium ion 1.5 mg-eq/g.

5. Ampholyte-3 × 4P is a bifunctional ion-exchanger based upon chloromethylated copolymer and m-aminobenzoic acid; AEC for chlorine ion 3.0 mg-eq/g, swelling volume 2.2 ml/g.

Polymerization-type ANKB-1 ampholyte and KB-2 × 7P cation-exchanger of macroporous structure, which is similar in chemical structure (active groups) to ampholyte-2 × 7P and ANKB-1, were taken for comparison.

The results of copper sorption given in Fig. 1 show that AMF-2 × 7P has good sorption properties relative to copper ammoniate. Its exchange capacity is not less than that of ANKB-1 ampholyte (see Table).

[1] A. N. Zelikman, Molybdenum, Moscow, Metallurgizdat, 1970, 440 pages, illustrated.

[2] A. G. Kholmogorov, L. M. Kuchinskaya, M. K. Makarov, et al., Scientific Works of the Siberian Non-Ferrous Metallurgy Research and Design Institute, Issue VI, Krasnoyarsk, 1973, 55-64.

[3] K. M. Ol'shanova, Guide to Ion-Exchange, Precipitation, and Partition Chromatography, Moscow, Khimiya, 1964, 134 pages, illustrated.

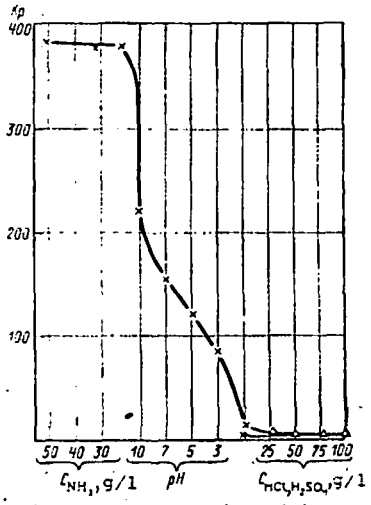

Fig. 3. Relationship of copper sorption on AMF-2 × 7P to pH: K_d is the distribution ratio.

Exchange Capacity of Ion-Exchangers in Terms of Copper (C_{Cu}^{init} = 2.05 g/liter)

Ion-exchanger	Exchange capacity			
	mg Cu/ml ion-exchanger	mg Cu/g ion-exchanger	%	to breakthrough
AMF-2X7P	6,60	154,0	15.4	8,32
ANKB-1	4,16	146,0	14.6	7,05
KB-2X7P	0,88	129,1	12,9	0,0
AMF-Op. 180	7,12	48,4	4.84	0,0

Although KB-2 × 7P cation-exchanger has an exchange capacity for copper of 12.9% it cannot be recommended for use in molybdenum technology, because it is relatively ineffective in practice in column-type apparatus (due to its low exchange capacity to breakthrough).

AMF-2 × 7P is superior to ANKB-1, both in volumetric exchange capacity for copper and in the magnitude of exchange capacity to breakthrough (Fig. 2). Consequently AMF-2 × 7P is potentially useful in molybdenum technology because of its sorption capacity for copper.

Copper sorption on AMF-2 × 7P alters little according to the free ammonia concentration in the ammonium molybdate solution; this is a valuable feature (Fig. 3). The exchange capacity of most ion-exchangers for copper falls substantially when the NH_3 content of the solution rises (see footnote 2).

There is practically no sorption of copper by AMF-2 × 7P from hydrochloric and sulfuric acid solutions; this permits complete desorption of copper with solutions of these acids. Experiments have shown that copper is completely eluted as chloride from AMF-2 × 7P with 2-3 volumes of 2N HCl. Traces of molybdenum can be detected in the eluates (chloride solutions) produced.

Consequently AMF-2 × 7P can be recommended for the removal of heavy metals (copper, nickel, and other elements) from ammonium molybdate solutions.

IN SITU
OIL·COAL·SHALE·MINERALS

IN SITU, 1(2), 125-146 (1977)

ims and Scope. This journal is devoted to the technology of in situ processing of minerals and ssil fuels, particularly emphasizing the emerging applications to oil, shale, coal, tar sands, anium, salt, copper, and other minerals and related technologies. *In Situ* is devoted to the change of common technology in the above areas, and is interdisciplinary in nature. Original ntributions of both applied and fundamental nature are encouraged.

ubscription Information. *In Situ* is published in four issues per volume by Marcel Dekker, Inc., 70 Madison Avenue, New York, New York 10016. The subscription rate for Volume 1 (1977), ntaining four issues, is $40.00 per volume (prepaid). Add $5.00 per volume for postage utside the United States.

ailing Address. *Please mail payment with order to:* Marcel Dekker Journals, P. O. Box 11305, hurch Street Station, New York, N. Y. 10249.

ontributions to this journal are published free of charge.

CODEN: ISOMDJ 1(2) 125-208 (1977)
ISSN: 0146-2520

CHEMICAL FACTORS IN IN-SITU URANIUM LEACH MINING

Philippe Galichon
Department of Chemical Engineering

Robert S. Schechter
Department of Petroleum Engineering

Alan Cowley and Mike Breland
Department of Chemistry

The University of Texas at Austin
Austin, TX 78712

ABSTRACT

The effect of varying flow rate, oxidant type and concentration, and techniques of pretreatment on the efficiency of in-situ uranium extraction has been studied. These tests, conducted in a packed tubular reactor, revealed that within the range of flow rates studied, the uranium extracted as a function of volume injected did not vary. This was interpreted to imply that the dissolution rates were mass transfer limited.

Hydrogen peroxide was found to be a more effective oxidant than sodium perchlorate, but peroxide rapidly decomposed to form oxygen and water. Thus oxygen saturated leachant should be as effective.

IN-SITU SOLUTION MINING OF SANDSTONE URANIUM ORES: AN OVERVIEW

The sandstone uranium deposits of South Texas represent a possible major energy source. Stretching along an approximately 300 mile wide band, these deposits consist mainly of widely scattered roll fronts of uranium (IV) minerals in loosely packed sands with some

uranium (VI) deposits in the outcroppings. It is thought that these deposits were formed by the down-dip migration of ground water carrying uranium (VI) species leached from the host rock, Catahoula Tuff. When the uranium-bearing waters reached a reducing zone, the uranium was precipitated, forming mainly the mineral uraninite, UO_2.[1] Much of the uranium ore in the area is low grade (< .05% U_3O_8) and is at depths of 100-400 feet.

Since 1960, various companies have been mining some of the higher grade deposits to depths of up to 200 feet using conventional strip mining techniques. The concomitant surface disruption is, of course, quite extensive, and the costs of mining and transporting large amounts of material to a mill prohibit the extensive utilization of low grade ores.

A mining technique that may overcome these difficulties to some extent and thus make more of the South Texas uranium deposits amenable to recovery is in-situ solution mining. This technique consists of pumping a chemical solution through the ore body that will dissolve the uranium minerals so that they may be drawn from the ore and then recovered from the solution. For this process to be economically feasible, a low cost solution must be available that will dissolve a large portion of the uranium present, the uranium must be easily recoverable from the leach solution, the physical attributes of the ore body must be such that the leach solution can be pumped through the ore without great loss to the surroundings, and environmental hazards must be avoided.

Uranium occurs commonly in two oxidation states, U(VI) and U(IV). In the higher +6 oxidation state, uranium forms many soluble ions, among which are the uranyl cation UO_2^{++}, the uranyl dicarbonate ion $(UO_2(CO_3)_2)^{2-}$, the uranyl tricarbonate ion $(UO_2(CO_3)_3)^{4-}$, and the uranyl sulfate anion $(UO_2(SO_4)_2)^{4-}$. Hostetler and Garrels[2] have investigated the equilibria of uranium minerals with natural solutions and found that under oxidizing conditions, stable soluble ions exist over a wide range of pH. These results suggest that in order to dissolve uranium minerals, one must provide an oxidizing agent to oxidize

U(IV) to U(VI) and a complexing agent that will form stable complex ions with U^{6+}. This can be accomplished with either an acid or an alkaline leach.

Acid leaching, the process used to recover uranium in many mill operations, consists of contacting the ore with concentrated H_2SO_4 solutions while mixing air or some other oxidant into the solution. The uranium enters into solution as a uranyl sulfate and is recovered by means of ion exchange or liquid-liquid extraction. This process recovers a high percentage of the uranium present, but could have some detrimental effects if used in-situ. If a high percentage of calcium carbonate were present (as is often the case in sandstone) much acid would be expended dissolving the $CaCO_3$. Furthermore, the Ca^{2+} present would precipitate as $CaSO_4$ thereby plugging the formation. Another possible side effect could be the destruction of some of the clays present[3] and this could also cause some plugging of the formation.

In alkaline leaching, a solution of ammonium bicarbonate, NH_4HCO_3, and ammonium carbonate, $(NH_4)_2CO_3$, along with an oxidizing agent is used to dissolve the uranium minerals. As in acid leaching, the uranium is oxidized first to the +6 state. However, the soluble complex ion, in this case, is the uranyl tricarbonate, $(UO_2(CO_3)_3)^{4-}$ anion. Oxidizing agents that have been used or suggested include: air, pure oxygen, hydrogen peroxide, H_2O_2, and sodium chlorate, $NaClO_3$. Hydrogen peroxide is being used in most operations; however, evidence to be presented here indicates that it decomposes rapidly.

One of the important goals of the present research program is to establish laboratory tests which are meaningful with regard to the design and operation of the full scale field operation. The accomplishment of this goal requires a kinetic model which can be integrated into a material balance applied to a fluid flowing within a porous medium. The results presented here demonstrate one approach to the development of a kinetic model and point to some of the profound difficulties which must be overcome before satisfactory results can be achieved.

KINETIC FACTORS

The rate of uranium dissolution must in some way be related to the accessible or leachable uranium remaining attached to the substrate. The simplest expression of this concept is:

$$\frac{\partial W}{\partial t} = -k_r(W - W_1) \qquad (1)$$

where W is the mass of uranium per mass of substrate and W_1 represents that which is not accessible. The rate constant, k_r, must depend on a number of factors including the oxidizing potential of the leachant[4] and the rate of mass transfer. Clearly, k_r must vanish as the concentration of oxidant vanishes.

If C represents the concentration of uranium in the solution, then for linear flow in a porous medium:

$$\phi \frac{\partial C}{\partial t} + u \frac{\partial C}{\partial X} = -\frac{\partial W}{\partial t} (1 - \phi) \rho_{ore} \qquad (2)$$

Here ϕ is the porosity, u is the flux of fluid in the X direction, and ρ_{ore} is the density of the ore. For the special case of linear flow through an ore bed which is short enough that the oxidant concentration remains essentially constant, k_r is constant and the effluent concentration from a bed of length, L, is given by:

$$C = 0 \quad \text{for} \quad V_p \leq 1 \qquad (3a)$$

and, (W_0 is the initial grams of uranium/gram of ore in the packed bed);

$$C = \frac{\rho_{ore} k_r (1 - \phi)(W_0 - W_1)L}{u} \exp - \left\{\frac{k_r L \phi}{u}(V_p - 1)\right\} \qquad (3b)$$

where V_p is the number of leachant pore volumes injected. This expression is derived neglecting axial dispersion which may, in fact, be a significant factor in both the field and bench scale test.

LEACH TESTS

General

The following factors were considered in designing the leach tests:

(a) insuring that the ore samples were representative of the ore body;

(b) insuring that the laboratory tests utilized field temperatures and pressures;

(c) avoiding mechanical and chemical degradation during sample preparation (e.g. breakage of sand grains and oxidation); and

(d) insuring that the fluids were uniformly distributed to avoid channeling within the ore bed.

The actual ore samples used in the present work originated in the Catahoula formation, Texas. The authors are indebted to the Westinghouse Corporation for providing these samples.

Experimental Apparatus

For each experiment, 100 grams of dry ore were carefully packed in a brass reaction vessel which was 11 centimeters long and 2.7 centimeters in diameter. The reaction end caps were designed so that when tightened, they pressed firmly against the ore column. This procedure prevented particle movement during leaching and maintained a uniform distribution of fluids throughout the bed. Before each run the packed reactor was evacuated and filled with brine. The leachant flow was maintained constant by means of a Fluid Meter, Inc. volumetric pump.

Experimental Procedure

Seven kilograms of ore were disaggregated and thoroughly mixed. Fifteen random samples were analyzed for uranium content. In this way, it was established that the mixture was essentially uniform. Th average uranium content was found to be 0.22 wt%.

The ore was tamped periodically as it was added to the reactor to obtain a firm packing. Glass wool was placed at both the top and the bottom of the ore column to prevent particles from entering the attached piping.

Two criteria were considered in selecting an appropriate range of flow rates. One possibility is to leach at rates which give residence times comparable to those expected in the field. This is difficult to do since the average residence time associated with a given field operation depends on the arrangement of wells as well as the permeability distribution and formation thickness. These latter factors are not generally well-defined, thereby making the estimation of realistic residence times difficult. Furthermore, the residence times are normally long, prolonging the time required for a single leach test. As an example consider a "typical" situation for which the well spacing is 30 feet. For a permeability of one darcy, fluxes of 5×10^{-3} cm/sec may be realistic and the residence times will range from 40 hours upward.

The test velocities may also be selected to match the field velocities. In general, bench scale tests conducted at field velocities yield quite different results than those which model field residence times. Since the laboratory reactor is usually much shorter than the distance between injection and production wells, those laboratory velocities scaled to give equal residence times will be much smaller than the actual field velocities. Laboratory tests which match the field residence times may be controlled by chemical reaction, whereas those conducted at field rates may be diffusion controlled. The results reported here were obtained using rates of flow comparable to those expected in the field.

Analytical Procedure

A fluorometric method was used for uranium analysis. Uranyl ions were extracted from aqueous solutions, added to sodium fluoride-lithium fluoride pellets and the pellets fused.[5, 6, 7] At the 0.1 ppm level this method is reported to have a relative error of about 10%; however, great care must be exercised to achieve this potential.

The ore was assayed by first digesting in a perchloric-nitric-hydrofluoric acid mixture and subsequently evaporating to dryness. The dried residue was then dissolved in nitric acid and the resulting solution analyzed using the fluorometric technique.

EXPERIMENTAL RESULTS AND THEIR INTERPRETATION

The Effect of Flow Rate

A series of tests were conducted using an aqueous leach solution having the following constant composition:

H_2O_2	0.2 wt%
NH_4HCO_3	1.0 wt%
$(NH_4)_2CO_3$	5.0 wt%

The flow rate was varied and the attendant uranium recovery measured. The results are shown in Table 1. The uranium recovery efficiency is defined as that fraction of the uranium originally present in the ore which is produced in the first 120 ml (approximately five pore volumes) of leachant.

TABLE 1

Leachant Flux	4.8×10^{-3} cm/sec	2.4×10^{-3} cm/sec	0.58×10^{-3} cm/sec
Uranium Recovery Efficiency	Run 1 46.5%	Run 1 48.9%	Run 1 52.3%
Uranium Recovery Efficiency	Run 2 57.3%	Run 2 41.7%	Run 2 53.0%
Average Recovery Efficiency	51.9%	45.3%	52.6%

The Effect of Flow Rate on Recovery Efficiency

There is considerable variability between duplicate runs and the large differences in the uranium recovery efficiencies are attributed to variations in ore samples. Each experiment utilized 100 grams of sample drawn from the large batch of ore prepared as previously described. The variation shown in Table 1 suggests that 100 gram samples are not large enough to be representative of the average. It is recommended that future tests employ larger samples.

Comparing the recovery efficiencies at differing leachant fluxes, it is evident that there is very little effect of flow rate within the range studied. It is, therefore, suggested that reaction rate is not the controlling factor. Furthermore, the effluent concentration of uranium, when represented as a function of pore volumes of leachant injected, appears to be independent of flow rate. This can be seen by examining Figures 1, 2, and 3. Examination of Equation (3b) indicates that the dimensionless grouping of terms

$$N_R = \frac{k_r L \phi}{u} \qquad (4)$$

is independent of u. In the range of laminar flows studied, the mass transfer coefficient in a packed bed[8] is proportional to the flux and the ratio k_r/u is a constant. Thus, in the range of flow rates and oxidant concentrations studied, the dissolution process is controlled by mass transfer and not by uranium reaction rate.

The theoretical curves shown in Figures 1, 2, and 3 were obtained by adjusting $k_r L/u$ so that the maximum uranium concentration is 3,600 ppm. This maximum value is roughly the average observed for all runs conducted using a peroxide concentration of 0.2 wt%.

Effect of Peroxide Concentration

A number of experiments were carried out to measure the effect of peroxide concentration on the recovery of uranium keeping all the other parameters constant. The leachant flux was adjusted to 4.8×10^{-3} cm/sec (this corresponds to a volumetric rate of 1.67 cm^3/sec or a residence time of approximately 38 minutes). The initial concentrations of ammonium bicarbonate and carbonate were maintained at 1% NH_4HCO_3 and 5% $(NH_4)_2CO_3$.

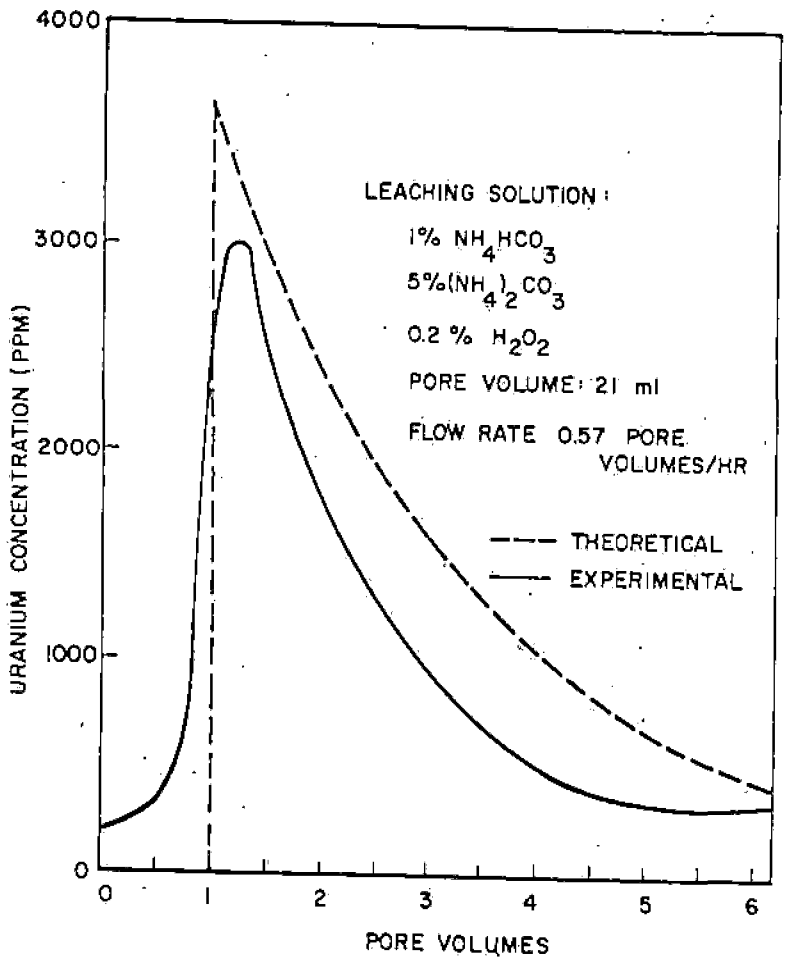

FIG. 1: Uranium Concentration of Effluent as a Function of Pore Volumes Injected. Injection Rate: 0.57 Pore Volumes/Hr.

The peroxide used was not stabilized in any way and above 0.3 wt% it decomposed rapidly in the feed vessel. Peroxide concentrations greater than 0.3 wt% were not studied since larger concentrations would not normally be used in the field. Experiments showed that the peroxide was not stable and decomposed rapidly to oxygen

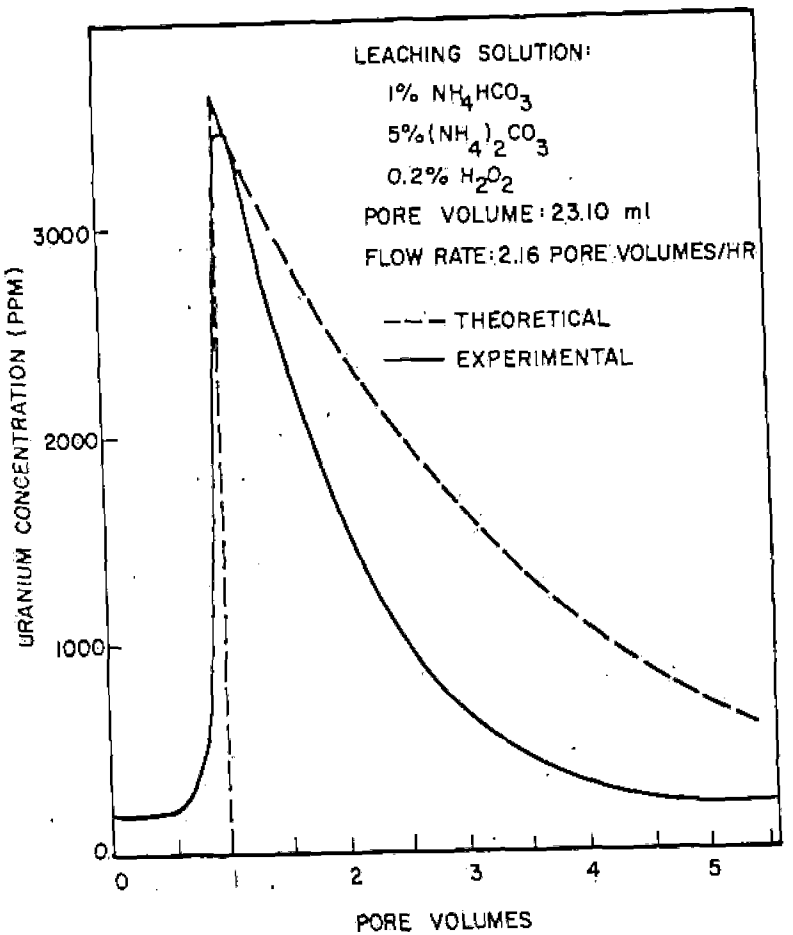

FIG. 2: Uranium Concentration of Effluent as a Function of Pore Volumes Injected. Injection Rate: 2.16 Pore Volumes/Hr.

and water. A simple calculation shows that if 0.3 wt% peroxide decomposes, the mole fraction of oxygen in the resulting solution is 0.79×10^{-3}. Using solubilty data, this mole fraction is seen to be equivalent to an oxygen pressure of roughly 468 psi. In a 200 foot deep deposit, the fluid pressure is approximately 100 psi. Thus, a separate oxygen-rich phase will form. This has at least two important consequences.

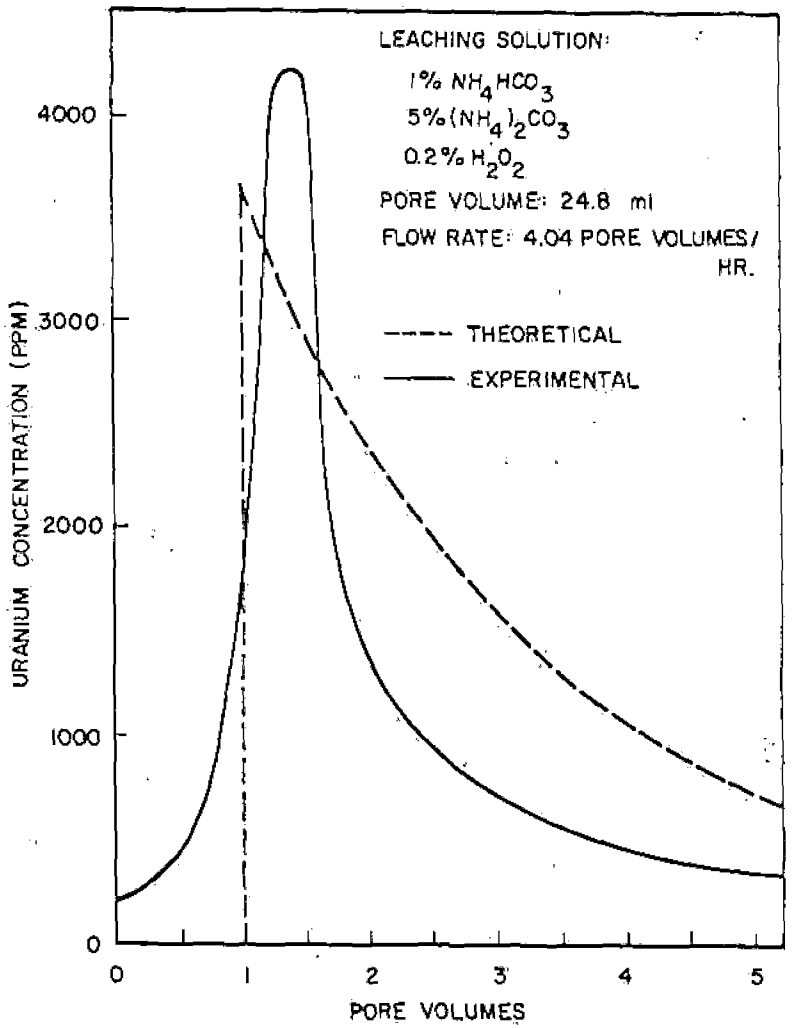

FIG. 3: Uranium Concentration of Effluent as a Function of Pore Volumes Injected. Injection Rate: 4.04 Pore Volumes/Hr.

The presence of a gas phase near the wellbore will substantially and progressively decrease injectivity. This will happen because of the mutual interference to flow resulting from the presence of two fluids commingled in the pore spaces. The relative permeability to liquid is greatly reduced by the presence of a nonwetting gas phase.

Thus, a permeability reduction should be observed upon injecting leachants containing peroxide concentrations large enough to create a second oxygen-rich phase following the decomposition of peroxide.

The presence of the gas phase may also effect the dissolution rate and the total recovery. It is not difficult to imagine a part of the formation surface being prevented from contacting the flowing leachant by the presence of oxygen bubbles.

If a leach solution containing no peroxide is injected, substantial amounts of uranium are produced (Figure 4). In other words, a significant fraction of the uranium present in the ore was UO_3. This oxidation presumably took place during storage. To simulate the response of a given ore body to a particular leach solution, it is clearly not desirable for a portion of the ore to be chemically changed by prolonged contact with air. Steps should be taken to preserve the samples and possibly the ore should be reduced before testing. This was not done in the work reported here, and the feasibility has not been verified

The U(VI) species are expected to dissolve faster than the U(IV) species which must first be oxidized. Thus, the conclusions with regard to the effect of flow rate may not apply to a fully reduced ore. This point needs to be investigated further.

The maximum uranium concentration as a function of peroxide concentration is shown in Figure 5. In general, it is seen that the maximum effluent uranium concentration depends on the oxidant concentration, although the data are scattered.

The total amount of uranium extracted as a function of leachant pore volume for various peroxide concentrations is shown in Figure 4. It should be noted that these experiments were terminated after the injection of approximately 10 pore volumes. However, at this point the uranium concentration in the effluent is small (~ 100-200 ppm), but is not zero. Thus, the curves shown in Figure 4 still have a small, but positive, slope after 10 pore volumes.

One experiment was carried out in which more than 35 pore volumes of leachant were injected. The results are shown in Figure 6.

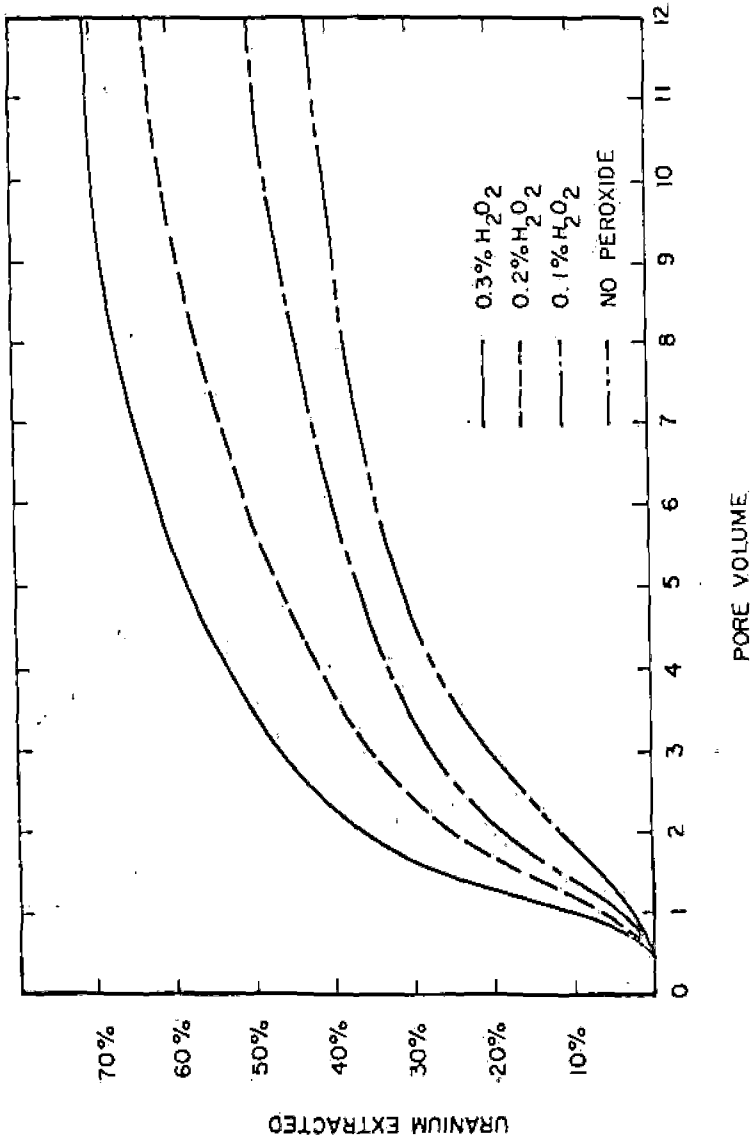

FIG. 4: Uranium Production as a Function of Pore Volumes Injected. Results for Various Peroxide Concentrations are Shown.

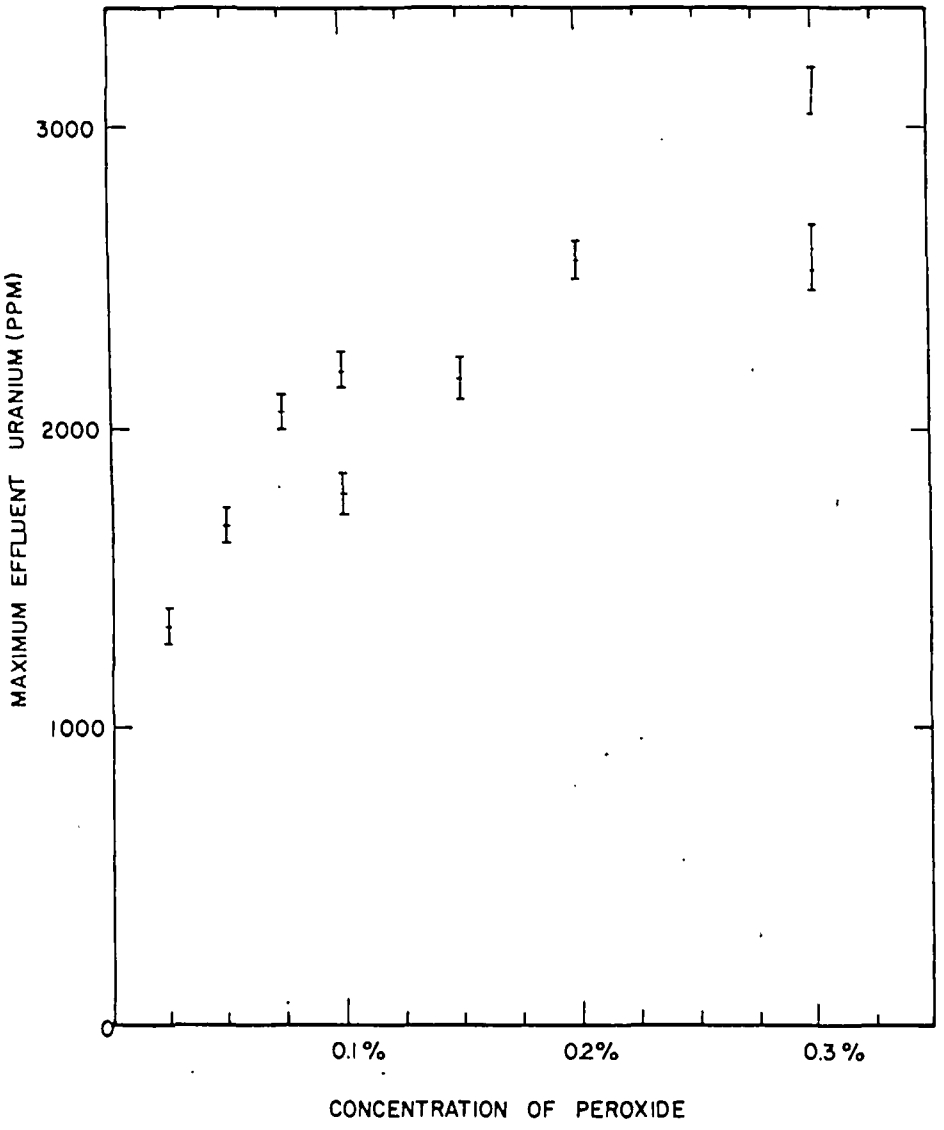

FIG. 5: The Maximum Uranium Concentration as a Function of the Inlet Hydrogen Peroxide Concentration.

The percentage of uranium recovery increased very slowly following the first 18 pore volumes and after 35 pore volumes, 75% of the uranium initially present had been recovered.

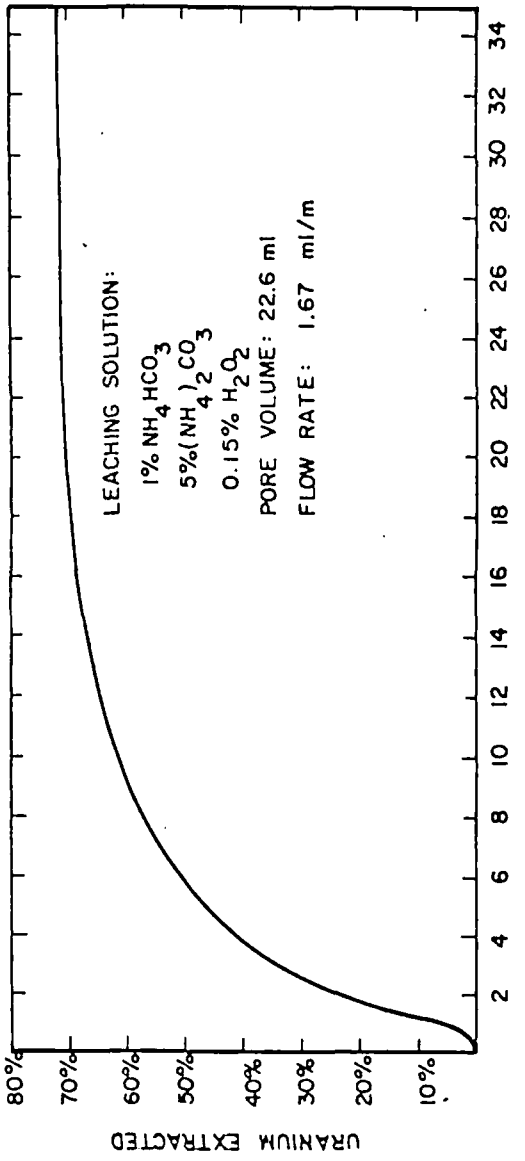

FIG. 6: Long Term Experiment Showing the Uranium Production as a Function of Pore Volumes Injected.

Several samples of leached ore were mixed to produce a composite sample and then this sample was powdered further by grinding manually. The powdered ore was then leached using 3 pore volumes of 0.3 wt% H_2O_2, 1 wt% NH_4HCO_3, and 5 wt% $(NH_4)_2\ CO_3$ solution. The residual uranium was reduced from 25 wt% to 15 wt% of the initial amount by this second stage of leaching. This implied that the recovery limit was due to the inaccessibility of the uranium.

Several attempts were made to measure the concentration of peroxide in the leachant effluent. However, in no case was any H_2O_2 detected. Thus, the peroxide was either reduced by any one of a number of reactions in the upper portion of the reactor or was decomposed. If the peroxide was reduced in the upper part of the bed, then the oxidation potential of the leach solution would have varied as the solution moved through the bed. To test this hypothesis, measurements were conducted to determine if different amounts of uranium were removed as a function of height in the packed reactor bed. The packed column was divided in four parts by means of filter paper separators. Following leaching, the residual ore in each part was analyzed. There was no significant difference in the uranium content of the different parts. This is interpreted to mean that the peroxide is very rapidly decomposed and the oxidation at almost every point is due to O_2 not H_2O_2. This raises a number of questions, some of which are related to injectivity as previously discussed. One point is, however, quite clear. There is no advantage to be gained by using peroxide as compared to solutions saturated with oxygen at reservoir pressure.

Other Oxidants

A number of other oxidants were tested and their performance compared to that obtained using peroxide.

Potassium Permanganate. Two experiments were carried out. It was found that potassium permanganate is reduced to manganese dioxide, which blocked the pores of the ore. The obvious conclusion is, therefore, that the oxidant must be selected so that its reduction product is soluble in the leachant.

$NaClO_3$. To test $NaClO_3$ as an oxidant, the other variables were maintained at their previous levels for comparison purposes. The flow rate was $4.8\ 10^{-3}$ cm/sec, 100 grams of ore were used, and the concentrations were maintained at 1% NH_4HCO_3 and 5% $(NH_4)_2CO_3$. It was found that after passing 8 pore volumes of leachant, only 36% of uranium was extracted. As shown in Figure 4, 38% of the uranium can be extracted by the same amount of leachant even if no oxidant is used. This means that at the concentration used, $NaClO_3$ did not increase the uranium recovery. Apparently, the U(VI) was recovered, but none of the U(IV) was oxidized to U(VI). Thus, $NaClO_3$ is not a useful oxidant.

Multistage Processes

Several experiments were carried out in an attempt to improve the ultimate recovery of uranium. These experiments consisted of several stages as shown in Table 2. Thus, Run 1 consisted of four stages as indicated. The first eight pore volumes of leachant contained 0.3 wt% H_2O_2 and the following 2.64 pore volumes used $NaClO_3$. The third stage involved oxidizing the ore in a hot oxygen stream at 200°C. for 16 hours and then leaching with an oxidant-free carbonate solution. Finally, an acid leach was used. Other multistage runs are indicated in Table 2.

The curves depicting the percentage of recovery as a function of the number of pore volumes of leachant are shown in Figure 7. The first stages of Runs 1 and 2 employed the same leach solution containing H_2O_2 (0.3 wt%). In both cases about 70% of the initial uranium was extracted after 10 pore volumes of leach solution. The second and third stages of these two experiments were different. The second stage of Run 1 involved passing 2.64 pore volumes of leachant containing $NaClO_3$ (0.5 wt%) and carbonate-bicarbonate solutions. No additional uranium was recovered during the second stage. Two possibilities need to be considered: (i) all of the accessible uranium was oxidized during the first stage; or (ii) some uranium still exists at U(IV), but $NaClO_3$ is not a strong enough oxidant. For the third

TABLE 2

	Run 1	Run 2	Run 3	Run 4
Stage 1	NH_4HCO_3 1% $(NH_4)_2CO_3$ 5% H_2O_2 0.3% Until 8 PV	NH_4HCO_3 1% $(NH_4)_2CO_3$ 5% H_2O_2 0.3% Until 10 PV	NH_4HCO_3 1% $(NH_4)_2CO_3$ 5% $NaClO_3$ 0.5% Until 9.2 PV	NH_4HCO_3 1% $(NH_4)_2CO_3$ 5% $NaClO_3$ 0.5% Until 9.56 PV
Stage 2	NH_4HCO_3 1% $(NH_4)_2CO_3$ 5% $NaClO_3$ 0.5% Until 10.62 PV	HNO_3 2.4N $NaClO_3$ 0.5% Until 14.4 PV	HNO_3 5N $NaClO_3$ 0.5% Until 17 PV	NH_4HCO_3 1% $(NH_4)_2CO_3$ 5% H_2O_2 0.3% Until 15.4 PV
Stage 3	O_2 at 200°C During 16 hrs. then NH_4HCO_3 1% $(NH_4)_2CO_3$ 5% Until 17.13 PV	NH_4HCO_3 1% $(NH_4)_2CO_3$ 5% H_2O_2 0.3% Until 20 PV	NH_4HCO_3 1% $(NH_4)_2CO_3$ 5% $NaClO_3$ 0.5% Until 22.5 PV	HNO_3 5N $NaClO_3$ 0.5% Until 20.40 PV
Stage 4	HNO_3 5N $NaClO_3$ 5% Until 21.1 PV		$NaClO_3$ 0.5% H_2O_2 0.3% $(NH_4)_2CO_3$ 5% Until 28.9 PV	

Description of the Multistage Tests

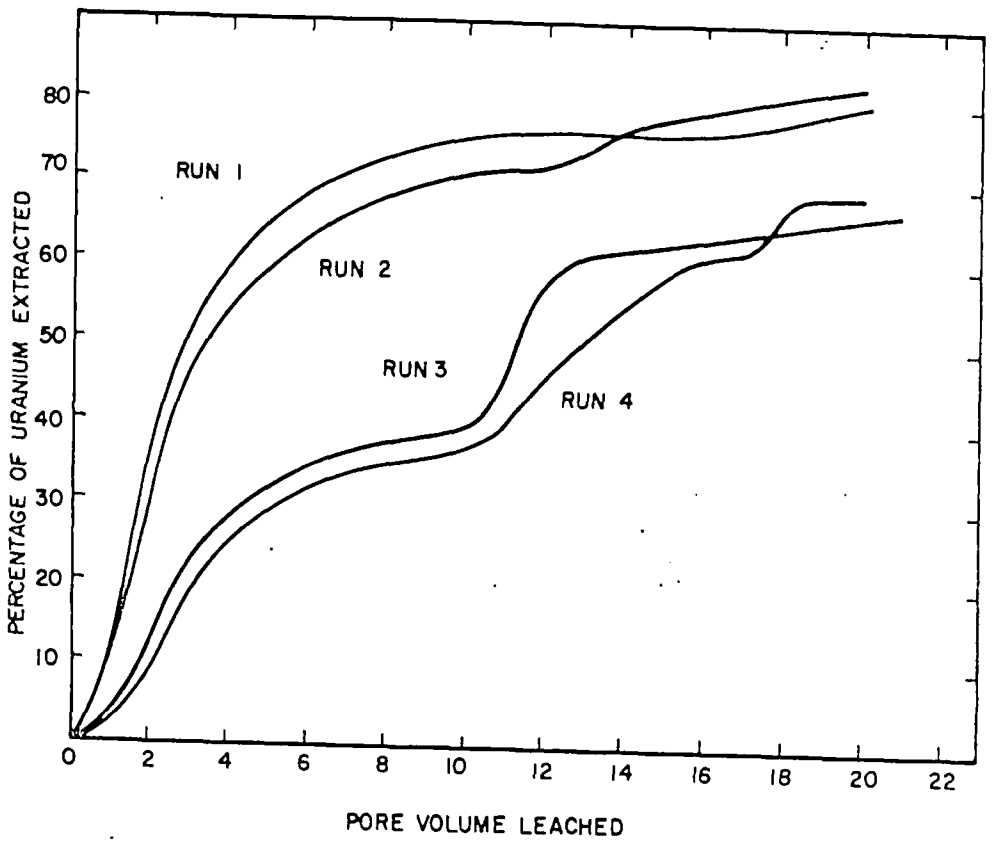

FIG. 7: Uranium Recovered Using Multistage Processes. The Run Numbers Refer to the Processes Defined in Table 2.

stage treatment, oxygen at 200°C. was used in an attempt to further oxidize the ore. This stage was followed by a carbonate leach. However, no more uranium was extracted. This means that all of the accessible uranium had been oxidized and the unrecovered uranium was inaccessible. The last stage consisted of a mixture of HNO_3 (5N) and $NaClO_3$ (0.5 wt%). An additional 5 wt% of the initial uranium was recovered.

Although HNO_3 dissolved much of the $CaCO_3$, it did not expose much more uranium to the leach solution. This suggests that much of the inaccessible uranium is embedded in clays.

The second stage of Run 2 consisted of leaching with HNO_3 (5N) and $NaClO_3$ (0.5 wt%). In this stage, 7% of the initial uranium was extracted. This was then followed by a third stage in which the leachant was H_2O_2 (0.3 wt%) and the carbonate-bicarbonate mixture. Only 4% of the initial uranium was extracted, again indicating that the treatment with nitric acid does not expose much new uranium to the leach solution.

Two other multistage experiments were carried out (Runs 3 and 4 in Table 2). The first stages of Runs 3 and 4 are the same. The leach solution contained $NaClO_3$ (0.5 wt%), carbonate and bicarbonate solutions. The recovery efficiency was 38% after passing 10 pore volumes of leach solution. It has been shown previously that the U(VI) initially present in the ore was probably recovered by this treatment, but the U(IV) apparently was not oxidized by $NaClO_3$ and is therefore not recovered.

The second stages were different. For Run 3, the ore was treated with HNO_3 (5N) and $NaClO_3$ (0.5 wt%). During this stage, 21% of uranium was extracted using 3 pore volumes of leachant. The oxidation and the dissolution steps are rapid. On the other hand, during the second stage of Run 4, the ore was treated by H_2O_2 (0.3 wt%) and a carbonate-bicarbonate solution. The increase in the percentage of uranium recovery is proportional to the number of pore volumes injected. This implies that the oxidation step is not as fast as it is in the presence of nitric acid and that the oxidation of U(IV) could be rate controlling in carbonate solutions. Additional tests are required to confirm this point since the flow rate studies would appear to contradict this conclusion.

In a final attempt to recover more uranium, the third and fourth stages of Run 3 consisted of successive treatments with $NaClO_3$ (0.5 wt%) and H_2O_2 (0.3 wt%) in carbonate solutions. During these two stages, which are not shown in Figure 7, an additional 10% of the initial uranium was extracted. The total amount of uranium recovered amounted to 73% of the initial uranium. During the third and final step of Run 4, the ore was treated with HNO_3 (5N) and $NaClO_3$ (0.5 wt%). About 5%

of the initial uranium was recovered in the first 2 pore volumes of this leach solution. This proves that the oxidation rate of U(IV) is rapid in acid solution and that the HNO_3 solution does not expose much more uranium.

The total amount of uranium extracted in a several stage process using peroxide as an oxidant during the first stage shows a recovery efficiency greater than those using $NaClO_3$ in carbonate solutions. This difference may be due to differences between ore samples. On the other hand, a first stage process using $NaClO_3$ may have in some way altered the surface, resulting in smaller quantities of uranium being leached. Thus, using perchlorate as an oxidant may actually be detremental and reduce the ultimate yield.

The conclusions which can be inferred from the multistage tests are as follows:

(a) There is a definite fraction of the uranium present which is not readily accessible to the leach solution.

(b) Most of the inaccessible uranium is not shielded from the leach solution by carbonates. It is, therefore, most likely to be embedded in the clays.

(c) The use of sodium chlorate as an oxidant may actually reduce the ultimate amount of uranium which can be extracted.

(d) The oxidation of U(IV) to U(VI) seems to be more rapid in acidic than in basic solution.

CONCLUSIONS

The following conclusions have been reached.

(a) Hydrogen peroxide, which was not stabilized, decomposes rapidly to form oxygen. Thus, there is no advantage to be gained in using peroxide as compared to oxygen saturated leachant solutions. Sodium perchlorate is not an effective oxidant and may in fact "damage" the surface, decreasing the ultimate yield.

(b) Extensive tests were performed using hydrogen peroxide as the oxidant. It was found that at field rates and high oxidant concentrations, the dissolution of uranium is mass transfer controlled. For the ore tested, the uranium yield of uranium was less than 75%.

(c) Several multistage processes were tested in an attempt to improve the recovery efficiency. The result of these tests was to show that the uranium recovery is not limited by the oxidizing potential of the leachant solutions, but that the unrecoverable uranium is not accessible to leachant. Dissolving the carbonates with acid did not improve the accessibility. The inaccessible uranium is, therefore, believed to be associated with the clays.

REFERENCES

1. Eargle, D. Hoyle, K. A. Dickinson, and B. O. Davis, "South Texas Uranium Deposits," The American Association of Petroleum Geology, 59, 766 (1975).

2. Hostetler, P. B. and R. M. Garrels, "Transportation and Precipitation of Uranium and Vanadium at Low Temperatures with Special References to Sandstone-Type Uranium Deposits," Economic Geology, 57, 138 (1962).

3. Osthaus, B. B., "Chemical Determination of Tetrahedral Ions in Nontionic and Montmorillonite," Clays and Clay Minerals, National Research Council Publication 327, A. Swinford and N. Plumma, eds., Washington, D. C. (1954).

4. Pearson, R. L. and M. E. Wadsworth, "A Kinetic Study of the Dissolution of UO_2 in Carbonate Solution," Transactions of the Metallurgical Society of AIME, 21, 294 (1958).

5. Price, G. R. R. J. Ferretti, and S. Schwartz, "Fluormetric Determination of Uranium," Analytical Chemistry, 25, 331, (1953).

6. Centanni, F. A., A. M. Ross, and M. A. Resesa, "Fluorometric Determination of Uranium," Analytical Chemistry, 28, 1651 (1956).

7. Latimer, J. N., W. E. Bush, L. J. Higgins, and R. S. Shay, Handbook of Analytical Procedures, Western Uranium Project, USAEC Contract No. AT-(05-1)-912, United States Atomic Energy Commission, Grand Junction, Colorado, 138 (1970).

8. McCune, L. K. and R. H. Wilhem, "Mass and Momentum Transfer in Solid-Liquid Systems," Industrial and Engineering Chemistry, 41, 1124 (1949).

9. Lange, N. A., ed., Handbook of Chemistry, Handbook Publishers, Inc., Sandusky, Ohio, 1092 (1956).

IN SITU, 1(2), 147-169 (1977)

HYDRAULIC FRACTURE MAPPING USING ELECTRICAL POTENTIAL MEASUREMENTS

R. J. Greenfield
Associate Professor
Geosciences Department
Pennsylvania State University
University Park, PA 16802

L. Z. Shuck
Professor & Associate Director
Engineering Experiment Station
West Virginia University
Morgantown, WV 26506

T. W. Keech
Electronic Engineer
Morgantown Energy Research Center
ERDA
Morgantown, WV 26505

ABSTRACT

A theoretical and experimental investigation of the electrical resistivity method for mapping hydraulically induced fractures in a petroleum reservoir is described. An electrical array was designed and used to measure millivolt order changes in surface potentials prior to, during and post hydraulic fracturing of a 25 ft. thick zone nominally 1950 feet deep. A 4 percent saline solution fracturing fluid was injected to provide a contrasting conductivity path in the previously water flooded reservoir. The field experiment was conducted near Bradford, PA on Minard Run Oil Company property by the Morgantown Energy Research Center, ERDA.

Changes in potentials attributed to the fracturing process were observed, but without sufficient directional characteristics to determine if single fractures propagated in a given direction. Theoretical models and various interpretations of the results are discussed.

CALCULATIONS FOR A UNIFLOW ALUMINATE SINTER LEACHING PROCESS

UDC 669.712.1

V. Ya. Abramov and E. D. Reifman

The mathematical models previously obtained for processes of sodium-aluminate extraction and insoluble alumo-compound formation can be used for the synthesis of a complete mathematical model of the aluminate sinter leaching process [1, 2].

Due to the fact that the amounts of alumina and alkali lost in the leaching process are not the same, the complete mathematical model for the process was synthesized separately for each of these constituents. The structure of these models and the synthesis methods are identical.

Calculations given in this paper relate only to the mathematical model for Al_2O_3 extraction. Equations describing the Na_2O leaching process from sinters can be obtained from the Al_2O_3 model equations by introducing the stoichiometric coefficients.

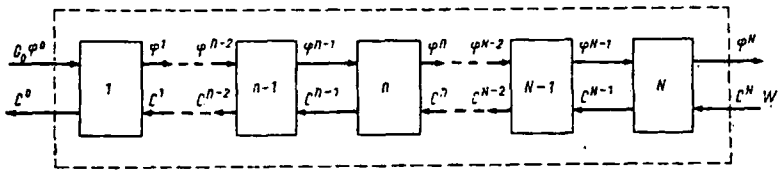

Fig. 1. Schematic diagram of multizone uniflow leacher:
G_0 - flow of constituents to be extracted coming in with the sinter, kg/hr; W - flow rate of extractant entering the leaching process, m^3/hr; n - apparatus zone serial number, n = 1, 2, ...N; N - number of zones in apparatus; c° - concentration of aluminate solution at exit from apparatus; x° $\varphi^0 = 1$ is the ratio of the radius of the unleached sinter particle region to the outer radius of the sinter particle entering the apparatus.

Mathematical models of the individual processes occurring during sinter leaching have been obtained with the proviso that the dimensions of the sinter particles being leached and the temperature and concentration of the extractant liquid are constant. The following method was therefore developed for using the results obtained in practical calculations.

The process was divided in time into a series of intervals (a series of zones applicable to specific apparatus), within which the extractant concentration and the temperature were assumed to be constant (Fig. 1). Calculations were made within each interval for sinter of multifractional composition, separately for each fairly narrow fraction. In this case, the Al_2O_3 leaching process in each interval (zone) was described by a system of equations.

1. Material balance equations:

$$\left.\begin{aligned} C_n = C_{n-1} - \frac{\sigma\eta}{(W+\Delta W\delta^n)}\sum_{i=1}^{m} G_i\left(\varphi^3_{n-1,i}-\varphi^3_{n,i}\right) + \frac{\sum_{i=1}^{m}\left(\Delta X^{hs}_{i,n}+\Delta X^{hg}_{i,n}\right)}{(W+\Delta W\delta^n)} + \frac{\Delta W}{W}C_g\left(\delta^{n+1}-\delta^n\right);\\ \varphi_{n-1,i}=\frac{r_{n-1,i}}{R_i};\quad \varphi_{n,i}=\frac{r_{n,i}}{R_i};\\ \delta^n=\begin{cases}0 & n=n'+1,\ n'+2,\ \ldots,\ N\\ 1 & n=n',\ n'-1,\ \ldots,\ 1\end{cases}, \end{aligned}\right\} \quad (1)$$

where R_i is the average radius of i-th fraction particle; $r_{n-1,i}$ and $r_{n,i}$ - is the radius of the unleached region of the sinter particle at the entry to and the exit from zone n; N - is the number of intervals (zones); G_i is the amount of the i-th fraction sinter entering the apparatus in a unit of time; W - is the extractant consumption; ΔW - the flow of alkaline solution into one of the intermediate (n') zones of the apparatus; $\Delta X^{hs}_{i,n}$ and $\Delta X^{hg}_{i,n}$ are the losses of the i-th fraction in zone n with sodium aluminum hydrosilicate and hydrogarnet; C_n, C_{n-1}, and C_g - the concentration of constituent to be extracted in the solution leaving the zone, in the solution entering the zone, and in the alkaline solution; σ and η is the total content of the constituent to be extracted and its content in the form of a soluble phase.

2. Extraction kinetics equation:

$$\frac{D_n\Delta t_n}{R_i^2} = (A_{n,i}\eta - 1)\left[\frac{1}{2}\left(\varphi^2_{n-1,i}-\varphi^2_{n,i}\right)-\frac{1}{3}\left(\varphi^3_{n-1,i}-\varphi^3_{n,i}\right)\right]+\frac{1}{6}\left[\ln\frac{\varphi_{n-1,i}}{\varphi_{n,i}}-(\varphi_{n-1,i}-\varphi_{n,i})-\left(\varphi^2_{n-1,i}-\varphi^2_{n,i}\right)\right]; \quad (2)$$

$$A_{n,i}=\frac{(1-\varepsilon')\gamma'\sigma_i}{(C-C_n)(\varepsilon'+\varepsilon'')};\quad \Delta t_n = t_n - t_{n-1}.$$

where t_{n-1} and t_n is the total time spent by the sinter in the apparatus before entering zone n and after passing through it; D_n - is the diffusion coefficient; ε' and ε" - the porosity of the sinter and the mud; γ' - the density.

3. Kinetic equations for Al_2O_3 losses with hydrogarnet:

where $\varphi_{n,i} > 0,4$:

$$\Delta X_{n,i}^{hg} = \frac{1,13d}{(1-0,66m)\,A_{n,i}}\left[\frac{D_{Si,n}}{D_n}(A_{n,i}-1)\left(\varphi_{n-1,i}^3-\varphi_{n,i}^3\right)+\left(\varphi_{n-1,i}^3-\varphi_{n,i}^3\right)-\frac{\varphi_{n-1,i}^3-\varphi_{n,i}^3}{1-\varphi_{n,i}}+\frac{3}{2}\,\frac{\frac{\varphi_{n,i}}{\varphi_{n-1,i}^2}-\varphi_{n,i}^2}{1-\varphi_{n,i}}\right]; \quad (3)$$

where $\varphi_{n,i} \leqslant 0,4$:

$$\Delta X_{n,i}^{hg} = \frac{3,39\,(\varepsilon'+\varepsilon'')\,D_{Si,n}\left(\alpha C_n - C_n^{Si}\right)(t_n - t_{n-1})\sqrt{\nu_{n,i}}}{(1-0,66m)\,R_i^2\,(1-\varepsilon')\,\gamma'\sigma};$$

$$\nu_{n,i} = \frac{K_{C_2S,n}(1-\varepsilon')\,\gamma' f R_i^2}{(\varepsilon'+\varepsilon'')\,D_{Si,n}},$$

where D_{Si} is the diffusion coefficient for silicon-bearing ions; f - the (internal) specific surface of the sinter; K_{C_2S} - the decomposition constant for β = 2CaO·SiO₂; m - the degree of hydrogarnet saturation with alumina.

4. Kinetics equations for Al_2O_3 losses with sodium aluminum hydrosilicate:

$$\Delta X_{n,i}^{hs} = K_{hs,n}\,\frac{f_i R_i^2}{\sigma D_n}\left[(A_{n,i}\eta - 1)\left(C_{Si\ av\,n} - C_{Si\ p,n}\right)\right] Z_{n,i};$$

$$Z_{n,i} = \frac{1}{2}\left(\varphi_{n-1,i}^2-\varphi_{n,i}^2\right)-\frac{1}{3}\left(\varphi_{n-1,i}^3-\varphi_{n,i}^3\right)-\frac{1}{5}\left(\varphi_{n-1,i}^5-\varphi_{n,i}^5\right)+\frac{1}{6}\left(\varphi_{n-1,i}^6-\varphi_{n,i}^6\right); \quad (4)$$

$$C_{Si\,av,n} = \alpha C_{S,n} - \alpha\left(C_{S,n}-C_n\right)\frac{1-\frac{\varphi_{n,i}}{2}-\frac{\varphi_{n,i}^2}{2}}{1-\varphi_{n,i}^3},$$

where C_S, n is the saturation coefficient and C_{Si} p,n - is the sodium aluminum hydrosilicate solubility concentration in aluminate solutions.

The total amount of alumina extracted in a specific period of leaching one fraction is calculated on the basis of the material balance equations for the appropriate zones:

$$G_{n,i} = \eta\sigma G_i\left(1-\varphi_{n-1,i}^3\right) - \sum_n X_n^{hg} - \sum_n X_n^{hs}. \quad (5)$$

The degree of Al_2O_3 extraction from the i th sinter fraction, after passing through all the zones up to n inclusive is:

$$Y_{n,i} = \frac{G_{n,i}}{\eta\sigma G_i}. \quad (6)$$

Similar equations for the entire mass of sinter being processed are readily obtained from Equations (5) and (6):

$$G_n = \eta\sigma\sum_{i=1}^{m} G_i\left(1-\varphi_{n-1,i}^3\right) - \sum_n\sum_{i=1}^{m} X_{n,i}^{hs} - \sum_n\sum_{i=1}^{m} X_{n,i}^{hg}; \quad (7)$$

$$Y_{n,i} = \frac{G_3}{\eta\sigma G}. \quad (8)$$

The following algorithm, based upon the model equations given, has been compiled for computer calculations for a leaching process in counterflow apparatus. The following were adopted as the initial values (input parameters) for calculation: the capacity of the apparatus in terms of sinter (so establishing the time spent by the material in each process zone), the particle-size composition of the sinter entering the leaching process, the physical and chemical properties of the sinter (standard extraction and content of constituents to be extracted, porosity, and inside specific surface), the process temperature in each zone, as well as the solution concentration at the exit from the apparatus.

The following were defined in the calculation algorithm:

- the values of the principal process constants for all intervals (zones) (D_n, $C_{s,n}$, $K_{0\,2}S,n$, $K_{hs,n}$, and $D_{Si,n}$) according to empirical formulas based upon processing experimental data in [1-3];
- the magnitude of φn,i for the i-th fraction of sinter at the exit from the leading zone (the magnitude of φ_{n-1},i at the entry to this zone is 1). A simplified extraction kinetics equation can be used for approximate calculations:

$$\frac{\varphi_{n-1,i}^2-\varphi_{n,i}^2}{2}-\frac{\varphi_{n-1,i}^3-\varphi_{n,i}^3}{3} = \frac{(C_{S,n}-C_n)\,D_n\Delta(t_n)}{[\gamma'-(1-\alpha)C_{S,n}]R_i^2}; \quad (9)$$

- the amount of the constituent to be extracted passing into the next zone with the

i-th fraction sinter according to the equation:

$$(G_{n.i} = \sigma_n G_i (\varphi^3_{n-1,i} - \varphi^3_{n,i});$$

- the amount of the constituent to be extracted which is lost as a result of incidental chemical reactions in the zone during leaching of the i-th fraction according to equations (3, 4);

- the degree of extraction from the i-th fraction according to Equations (5) and (6).

This concluded the calculations for the process of leaching from the i-th fraction in the first zone; they were repeated for all m fractions of sinter.

Thus, m values of $_{n,i}$, $G_{n,i}$, $X^{hg}_{n,i}$, $X^{hs}_{n,i}$, and $Y_{n,i}$ for the first zone were computed.

By adding $X^{hg}_{n,i}$, $X^{hs}_{n,i}$, and $G_{n,i}$ we obtain the total amount of the constituent to be extracted which passes to the second zone with the sinter and the total losses of this constituent under consideration. Equation (8) was then used to calculate the total extraction Y_n in the first zone and the material balance Equation (1) was used to define the solution concentration at the entry to the first zone C_{n-1}.

Calculations for the next zone along the course of the material were made in the same order. The values obtained in calculations for the previous zone were adopted as the initial data: the constituent to be extracted remaining in the sinter and the losses of that constituent for each of the fractions considered, as well as the totals of these and the magnitude of C_{n-1} (output parameters).

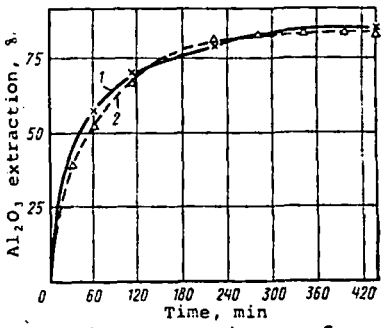

Fig. 2. Comparison of experimental (1) and calculated Al_2O_3 extraction kinetics curves when leaching bauxite sinter in a percolation unit with a 65 tons/hr capacity.

Results of Sinter Leaching

Apparatus capacity, tons/hr	Al_2O_3 content in sinter, %	Sinter fractional composition	Temperature by zones, °C: leading	middle	tail end	Absolute deviation in Al_2O_3 extraction	Standard deviation
Laboratory battery diffuser							
0,024	30,0	100% cl.—10+7 mm	95	95	95	3,1	9,7
0,031	28,2	30% cl.—10+7 mm	90	90	90	0,1	7,25
Percolation apparatus							
59,8	29,8	8,5% cl.—8+6 mm 76,5% cl.—6+3 mm	72—89	66—73	77—87	0,6	7,15
65,0	31,2	12,5% cl.—8+6 mm 60% cl.—6+3 mm	83—84	66—68	92	1,9	4,53
75,0	29,8	9% cl.—8+6 mm 91% cl.—6+3 mm	72—78	63—65	73—80	0,8	5,47

The algorithm was used as the basis for compiling a program for sinter leaching process calculations using a Minsk-22 computer.

The adequ cy of the synthesized mathematical model for the process was ascertained by comparing the output parameters of the leaching process in uniflow-type apparatus (the degree of Al_2O_3 extraction and changes in extractant concentration along the apparatus length) with the same parameters calculated using the mathematical model according to the algorithm.

Operation of a percolation unit was used as an example for comparison. The capacity, the physical and chemical characteristics of the sinter, the concentrations and the temperatures along the apparatus length, and the degree of extraction and the duration of leaching in each zone were recorded for this purpose.

In addition, data obtained by various workers on various apparatus with different routines were used to check the model. The routines differed in respect of capacity, the particle-size and phsycial and chemical composition of the sinter, and the temperature distribution along the apparatus length.

Apparatus input parameters were introduced into the model as initial data; following this, calculations according to the model were made on the Minsk-22 computer. The process output parameter values calculated in this way were compared with the corresponding parameters for the actual process.

Calculated and experimental Al_2O_3 extraction kinetics curves are given in Fig. 2 by way of example.

The adequacy of the model to the subject was assessed by reference to the standard deviation of the calculated curve from the experimental curve, by comparing the degrees of extraction of the required constituent at the exit from the apparatus obtained by experiment and by calculation.

It is apparent from the tabulated data that the standard deviation did not exceed

10% and averaged 6.9%. Comparison of the Al_2O_3 extraction values at the exit from the apparatus obtained by calculation and by experiment shows that on average the figure did not exceed ~ 1.3%.

That kind of deviation in the calculated results is permissible, having regard to the fact that the range of variation in the initial parameters within which the comparison was made was fairly wide in terms of capacity (24-75 tons/hr), temperature (62-96°C), and sinter physical and chemical characteristics (the sinter Al_2O_3 content varied from 28 to 32% and its porosity from 15 to 23%).

The obtained results indicate that the synthesized mathematical model has a sufficiently high degree of adequacy for actual leaching processes. This gives grounds for recommending the model and the method of calculation which has been developed for practical use.

REFERENCES

1. G. A. Aksel'rud, V. Ya. Abramov, E. D. Reifman, et al, Alumina Production, Collection No. 70, Leningrad, VAMI, 1970, 96-103 and 91-96.
2. G. A. Aksel'rud, V. Ya. Abramov, E. D. Reifman, and E. M. Semenishin, Tsvetnye Metally, 1971, No. 2, 31-34.
3. G. A. Aksel'rud, V. Ya. Abramov, E. D. Reifman, et al, in: Theory and Practice of Aluminate Solution Desiliconizing, Moscow, Tsvetmetinformatsiya, 1971, 39-42.

A COUPLED GAS PRESSURIZATION EXPLICIT FRACTURE MODEL FOR OIL SHALE FRAGMENTATION

B.C. Trent, C. Young, T.G. B

Science Applications, Incorp

Proceedings of the 22nd U.S. Symposium on Rock Mechanics: Rock Mechanics from Research to Application held at Mass. Inst. of Tech., June 28-July 2, 1981 compiled by H.H. Einstein

INTRODUCTION

A problem common to all in situ oil shale combustion processes for production of oil is to provide an adequate void volume distribution within the rock so that gas may pass through during the retorting process. One method to achieve this goal is to heave the earth's surface by detonating an explosive charge within a relatively shallow oil-shale thickness. This technique has been tested in the field by Geokinetics, Inc. in Uintah County, Utah, (Lekas, 1979). The void space distributions resulting from the Geokinetics blasting tests have been evaluated empirically, usually by burning the retorts.

This paper presents a general explosive fragmentation model incorporating oil shale properties specific to the Geokinetics site. Modeling their blasting program using mechanical properties of the oil shale deposit as primary input can provide an inexpensive tool for optimizing blast results. Although an actual field experiment may involve the timed detonation of hundreds of explosive boreholes, understanding the mechanics and implications of a single shot hole is important as much of the phenomenology of single-hole breakage is involved in multihole fragmentation. Also, the overall environmental impact and program cost may be significantly reduced due to more efficient rubblization.

CALCULATIONAL TECHNIQUE

The modeling efforts to study single-hole fragmentation employed an explicit finite-difference computer code called STEALTH**. STEALTH (Hofmann, 1976) solves the equations for conservation of momentum, mass, and energy and is particularly well suited to modeling dynamic phenomena such as explosive effects in rock. The constitutive equations which relate induced stresses to observed ground motions may be as complicated as the data base will allow. Previous models of explosive oil shale fragmentation have been performed (Trent, et al, 1980) and an extensive program for the study of explosive stimulation of gas shales is presently under investigation (Barbour and Young, 1980).

Rock Fracture Model

The STEALTH sub-model which provides the details of the fracturing process is called CAVS (Crack And Void Strain). The model is general and has various applications (Maxwell and Reaugh, 1980), (Barbour, et al, 1980). The unique aspect of the CAVS model is that the crack aperture (void strain) changes are coupled precisely to the three dimensional stress tensor adjustments during crack opening and closing. Due to the extensive bookkeeping system within CAVS, it is capable of determining the extent of cracking next to an explosive borehole. It has been proposed that cracks immediately adjacent to the shot hole will become filled with hot explosive reaction products and subsequently open and propagate more readily than if these gases were not present. This phenomenon has been observed and studied quantitatively in the calculations. While the concept of crack communication with the borehole (and explosive gasses) is relatively straightforward, in practice the logic could be quite sophisticated since the ultimate pathway of gas travel cannot be determined a priori.

Fracture Internal Pressurization Model

Several one-dimensional borehole calculations have been carried out which have allowed the crack internal pressurization logic to be tested. The fluid flow and pressurization model when used in conjunction with the CAVS tensile fracture model essentially works as follows:

1) Explosive detonation with the borehole initiates a compressive wave which is followed by a tensile rarefaction which initiates or propagates fractures in the rock.

2) As fractures open up adjacent to the explosive borehole, hot reactant products are free to enter the fractures at a velocity which is dependent upon the crack's width and length, zone-to-zone pressure gradients throughout the borehole/fracture system and the viscosity of the flowing fluid. The viscosity can be defined as temperature dependent to incorporate the effect of quenching as the reactants cool as they contact the rock fracture faces.

3) Fractures developed in calculational zones which "communicate" with the high pressure fluids in the borehole are free to accept fluid.

4) The effect of fluid in a fracture is analogous to pore pressure effects in effective stress analysis in that the normal stress is reduced, i.e. appears less compressive or more tensile, thereby enhancing the fracturing process.

5) As gas penetrates into the fracture system the pressure in the borehole is reduced until equilibrium is achieved, i.e. the excess volume of gas products is exhausted. Mass balance is maintained between the time dependent fluid available from the borehole and the fluid penetrating the fracture system.

** "Solids and Thermal hydraulics codes for EPRI Adapted from Lagrange TOODY and HEMP," developed for Electric Power Research Institute by Science Applications, Incorporated under Contract RP307.

The term "void strain" refers to the actual opening of a crack within a calculational zone: A value of -.01 in each of the three principal directions yields a volumetric void strain of three percent, indicating that the calculational zone has expanded by 3% due to crack opening (elastic or plastic volume charges are not reflected in this value). The most complicated aspect of CAVS is in the void closure logic since a crack must not be allowed to over-close and should display self propping. Closure times for cracks in the three directions are generally different and closure of one crack affects crack void strains in the other directions. Sub-cycling and re-arranging of closing sequences solves this problem. The addition of gas pressure to the model is trivial since the crack opening/closing logic is unchanged and only the effective stress is modified. After a crack has opened, perfect closure is not possible due to asperity mismatch. A jumbling or propping logic has been included to incorporate this effect.

The effect of gas pressurization is dramatically illustrated in Figure 1 which shows how a radial crack has opened up substantially due to the gas pressure. In addition, more cracks are actually generated due to the presence of gas pressure as illustrated in Figure 2. It is interesting to note that immediately adjacent to the borehole wall the effects of gas pressure appear to suppress cracking, however, at distances greater than 4m the extent of cracking is significantly enhanced due to the influence of gas pressure. There is an intermediate zone where both calculations yield similar crack patterns. These results are based upon material properties of gas shales.

EXPERIMENTAL DATA ON OIL SHALE

Extensive mechanical testing of oil shale has taken place over the past several years. As a result, sufficient information is available to formulate constitutive models for computer codes. Of particular interest in this analysis was the influence of the relatively weak oil shale bedding plane partings and the influence of the explosive gas pressurization on initiating and propagating fractures along the weak bedding planes.

Oil Yield - Density - Organic Volume Relationships

The Modified Fischer Retort Method was used in determing oil shale assays on core taken at the Geokinetics site (Trudell, 1979). The samples represented approximately 0.3m sections each and varied from 5 to 65 gallons of shale oil per ton of rock. The amount of organic matter in oil shale has been related to various mechanical properties, as indicated below.

Since oil yields in the Geokinetics blast section varied from approximately 10 gpt to over 60 gpt, significant impedance differences existed from layer-to-layer. These impedance mismatches are especially important to stress wave interaction from layer-to-layer. The densities of different oil-shale grades may be readily estimated from oil yield-organic volume relationships. Rock density has been found to vary with oil yield of Green River Formation oil shale according to the following relationship (Smith, 1976).

$$OY = 31.563\ (D_T)^2 - 205.998\ D_T + 326.624$$

where

OY is the oil yield in gallons per ton

D_T is the rock density in gm/cc.

Once this expression is solved for density, the percent organic volume may be found by

$$V_o = 164.85 - 60.61\ D_T \qquad \text{(Smith, 1976)}$$

where

V_o is the organic volume in percent

D_T is the rock density in gm/cc.

Tensile Strength

Tensile strengths parallel to the bedding planes of Green River Formation oil shales similar to the Geokinetics materials have been related to organic volume. Consequently, tensile strengths at this orientation can be evaluated through the blast section. However, oil shale is significantly weaker in the direction normal to the bedding planes. To incorporate this characteristic into the model, direct-pull tensile strength tests were performed on core taken from the Geokinetics site. Direct measurements of tensile strength has the advantage over indirect methods in that the weakest link in the section tested is always measured. Indirect methods determine strengths at selected depths and therefore do not necessarily test the weakest plane. Tests were performed by pulling apart .0381m samples which were .102m in length (Young and Patti, 1980). Each sample was tested once. Approximately 14m of oil shale were tested. The results are illustrated in Figure 3.

The tensile strength parallel to the bedding planes was provided by an empirical formula based on Brazilian split cylinder tests. Strengths for three types of Green River oil shales are given by the following (Smith, 1980):

Colorado: $\sigma_t = 14.78 - .0928\ V_o$

Utah: $\sigma_t = 13.64 - .1211\ V_o$

Wyoming: $\sigma_t = 23.16 - .3516\ V_o$

where

σ_t is the tensile strength in MPa

V_o is organic content in percent

For this study, the representation given for the Utah oil shale was used.

Elastic Constants

Elastic constants from stress/strain measurements on Green River Formation oil shales have been shown to vary with organic matter in the rock. The following prediction equations developed from mechanical tests permit evaluation of elastic constants with depth, (Chong, et al, 1979).

$$E_x = 10.45 - .1735\ V_o + .3841\ S$$
$$-.00519\ V_o \cdot S - 1.883 \times 10^{-7}\ S^4$$

$$E_z = 12.34 - .2196\ V_o + .07461\ S$$
$$- 6.82 \times 10^{-5}\ V_o \cdot S - 9.869 \times 10^{-8}\ S^4$$

$$\nu_{zx} = -0.04419 + .00385\ V_o + .00645\ S$$

$$\nu_{xy} = -0.03307 + .00333\ V_o + .00480\ S$$

where

z is the direction perpendicular to bedding

x,y are directions parallel to bedding

E is elastic moduli in GPa

ν is Poisson's ratio

V_o is organic volume in percent

S is stress level (actual stress/ultimate stress x 100%)

Under compressive loading the behavior of these oil shales is nearly isotropic, in spite of their laminar structure. Consequently, the elastic constants can be averaged and applied to three dimensions. The equations contain a stress level function as a percent of ultimate load. This concept may be useful for uniaxial loading, but there is some ambiquity when the stress field is fully three dimensional. In addition, since within the model the material was allowed to yield under sufficient deviatoric stress, it was assumed that the stress level was 40%, yielding mid-range values for the elastic constants.

Plasticity Model

The elastic/plastic yield surface is strongly dependent upon the density (oil yield) of the oil shale. The yield surfaces are similar up to grades of 25 gpt but drop dramatically until approximately 45 gpt at which point yielding is essentially governed by the strength of kerogen which is independent of mean stress. The following formula for yielding has been developed, (Johnson, 1979):

$$Y = Y_o + \Delta Y(1-e^{-ap})$$

where

Y is the yield stress

Y_o, ΔY and a are parameters which depend on density

p is the mean stress.

A different yield surface was incorporated into the code for each different density.

Input to the Code

The two-dimensional axisymmetric calculational grid utilized is shown in Figure 4. The top boundary condition is a free surface and all other boundaries are wall interaction (roller). The oil shale is located 9.14m below the surface and is 6.10m thick. The explosive borehole was originally .1524m in diameter and the explosive was ANFO, which had an equation-of-state described by a JWL formulation (Lee, et al, 1973).

The vertical zoning within the oil shale blast section is spaced .3048m. A careful correlation was performed and it was determined that all twenty horizons had oil yields that fit into eight groups, within $\pm 5\%$. Figure 5 illustrates the grouping of the various layers. The following table indicates the base material properties of those layers.

Material	Oil Yield(gpt)	Density (gm/cc)	Organic Volume (percent)
1	9.36	2.49	13.92
2	13.18	2.42	18.44
3	16.75	2.35	22.34
4	22.64	2.25	28.23
5	34.21	2.09	38.39
6	41.20	2.00	43.88
7	50.48	1.88	50.62
8	62.06	1.76	58.33

Above and below the blast section, the rock was assumed to have the parameters of the leanest oil shale, layer 1.

The tensile strengths shown in Figure 3 were used for the direction normal to the bedding planes. The weakest strength within a given layer indicated the stress level to initiate the first crack in a calculational zone. The next higher strength had to be exceeded for the second crack, and so on. Strengths above the third crack value increase arbitrarily by 1.05 times the last crack strength. Tensile strengths in the other two directions were determined from the organic volume relationship presented earlier.

The averaged elastic properties and the computed base tensile strength parallel to bedding are plotted in Figure 6 based upon the equations already presented. From the elastic/plastic yield data of Johnson (1979) mentioned earlier, coefficients were established for the eight materials. The yield surfaces are plotted in Figure 7. Note that since materials 7 and 8 are so rich, their yielding is not taken from the equation but rather is a constant of .1 GPa based on yield strengths of polymeric materials similar to kerogen (Johnson and Simonson, 1977).

CALCULATIONAL RESULTS

The baseline calculation was performed utilizing the stratigraphic layering and tensile strength criteria presented earlier. The explosive, ANFO, has a relatively long rise time and maintains its peak pressure for longer times than other high explosives. Approximately 44 moles of reactant products per kg of charge are produced (Edl, 1980).

A second calculation was run in which there was a uniform material model i.e., no stratigraphic variations in material properties. For this calculation all properties were defined by the formulas for material 4 (22.6 gpt).

For both calculations, initial overburden stresses were used as the initial condition and the 6.096m long explosive borehole was top detonated. The gas pressure in a zone adjacent to the borehole as a function of time is shown in Figure 8. Gas pressures further from the borehole are significantly reduced because of narrower crack widths.

Figure 9 is a contour plot of gas pressure for the baseline case after five milliseconds. This is a sub-grid of the entire mesh as noted in Figure 4. Certain horizons have little or no gas pressure while others show a tendency to channel due to the non-uniform void strain distribution. Also the borehole boundary is uneven due to the material layering. The uniform material calculation gave gas contours after five milliseconds as shown in Figure 10. Notice the relatively constant gas profile with depth and the uniform expansion of the borehole wall.

The in-plane crack patterns for the baseline and uniform cases are shown in Figures 11 and 12, respectively. The influence of the weak bedding planes is obvious. Although relatively little tensile fracturing takes place near the borehole, shear-induced cataclysmic failure is typically present in this area, providing finely fragmated rock. The out of plane (radial) cracks for the baseline case are shown for 3 layers in Figure 13. Very little stratigraphic variation in radial cracking was noted in the uniform case.

Quasi-Static Analysis

In order to investigate the influence of gas pressure at later times and to keep the computational costs to a reasonable limit, a time-step scaling technique was used. It is similar to density scaling which is an artificial increase in density resulting in a lower sound speed and a larger time step. The momentum effects are assumed to be trivial. Instead of increasing the density, a pseudo time-step was defined which was used in the equations of motion which allows a more efficient variation in the effective scale factor (Maxwell, et al, 1978).

The baseline calculation was run in a fully dynamic mode for five milliseconds until virtually all shock effects had dissipated from the region of interest. Then the pseudo time-step technique was applied and the calculation proceeded to one second. A time history of gas pressure in an oil shale zone is shown in Figure 14 (compare to Figure 8). The in-plane fracture pattern is shown in Figure 15. Contours of gas pressure after one second are shown in Figure 16. While the bedding plane fracturing is enhanced, very little increase in the radial cracking was observed.

CONCLUSIONS

Incorporation of stratigraphically varying mechanical properties such as density, elastic constants, yielding and tensile strengths can significantly affect the modeling for the explosive fracture of oil shale. The bedding planes are significantly weaker and this aspect must be incorporated into the code.

The explosive reactant products have been shown to alter the crack pattern by decreasing the amount of cracking near the shothole and increasing the amount and extent of cracking further away. No gas enters the fractured rock until about 1.0 milliseconds since the stress field is still highly compressive until this point. The effect of gas pressure at later times appears to enhance the fracturing process for bedding plane partings, however, the influence on extending radial cracks seems to be minor. Gas pressure effects at greater depths could be significantly different.

ACKNOWLEDGEMENTS

This research was supported by the Laramie Energy Technology Center, Office of Resource Characterization, Laramie, Wyoming. We would like to credit Donald E. Maxwell of Science Applications, Inc., San Leandro, California, for the initial development of the CAVS failure model. Krishan K. Wahi of Science Applications, Inc., Albuquerque, New Mexico is also acknowledged for his contributions to the fracture internal pressurization logic and implementation of the time-step scaling technique.

REFERENCES

1. Barbour, T.G., C. Young, "Numerical Analysis of Multiple Fracturing in a Wellbore", Presented at the 21st U.S. Symposium on Rock Mechanics, Rolla, Missouri, 1980.

2. Barbour, T.G., K.K. Wahi, D.E. Maxwell, "Prediction of Fragmentation Using CAVS", Society of Experimental Stress Analysis, Fall Meeting, Fort Lauderdale, Florida, 1980.

3. Chong, K.P., K. Uenishi, J.W. Smith, "Complete Elastic Constants and Stiffness Coefficients for Oil Shale," Report of Investigations, DOE/LETC/RI-79/8, Laramie Energy Technology Center, 1979.

4. Edl, J., Explosive products of ANFO, private communication, 1980.

5. Hofmann, R., "STEALTH, A Lagrange Explicit Finite-Difference Code for Solids, Structural, and Thermohydraulic Analysis", EPRI NP-260 Vol. I, User's Manual, prepared by Science Applications, Inc. for Electric Power Research Institute, Palo Alto, California, August, 1976.

6. Johnson, J.N., "Calculation of Explosive Rock Breakage: Oil Shale", Presented at 20th U.S. Symposium on Rock Mechanics, Austin, Texas, 1979.

7. Johnson, J.N., E.R. Simonson, "Analytic Failure Surfaces for Oil Shales of Varying Kerogen Content", University of California, Los Alamos Scientific Laboratory, Report LA-UR-77-1005, Los Alamos, New Mexico, 1977.

8. Lee, E.L., M. Finger, W. Collins, "JWL Equation of State Coefficients for High Explosives", Lawrence Livermore Laboratory Report UCID 16190, 1973.

9. Lekas, M.A., "Progress Report on the Geokinetics Horizontal In-Situ Retorting Process", Presented at 12th Oil Shale Symposium, Golden, Colorado, 1979

10. Maxwell, D.E., R. Hofmann, K.K. Wahi, "An Optimization Study of the Explicit Finite-Difference Method for Quasi-Static Thermo-Mechanical Simulations"; SAI-FR-821-3 prepared for Union Carbide Corporation, Contract W-7405-ENG-26, 1978.

11. Maxwell, D.E., J.E. Reaugh, "A Continuum Fracture Model called CAVS", Paper presented at Symposium on Conventional Methods in Nonlinear Structural and Solid Mechanics, Sponsored by George Washington University and NASA-Langley Research Center, Washington, D.C., October, 1980.

12. Smith, J.W., "Relationship Between Rock Density and Volume of Organic Matter in Oil Shales", Report of Investigation LERC/RI-76/6, Laramie Energy Technology Center, 1976.

13. Smith, J.W., Tensile Strength vs. Organic Content for Oil Shales from Colorado, Utah and Wyoming, private communication, October, 1980.

14. Trent, B.C., C. Young, J.W. Smith, "Stratigraphically Dependent Fracture Modeling of Oil Shale", Presented at the Third Oil Shale Conversion Symposium, Denver, Colorado, January, 1980.

15. Trudell, L., Lithologic Description of Samples Submitted for Assay, Illustration No. SBR-5029P, Laramie Energy Technology Center, Laramie, WY, April 16, 1979. Oil-Shale Assays by Modified Fischer Retort Method - Geokinetics, Inc. Corehole W-14, Illustration No. SBR-5016P, LETC, Laramie, WY, April 16, 1979.

16. Young, C., N.C. Patti, Direct-Pull Strengths for Oil Shale from the Geokinetics site; performed for LETC under P.O. #PL90977, 1979.

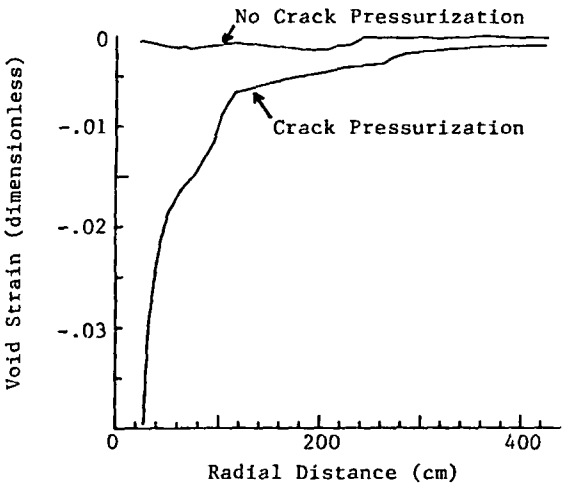

Figure 1. Effect of Gas Pressurization on Void Strain

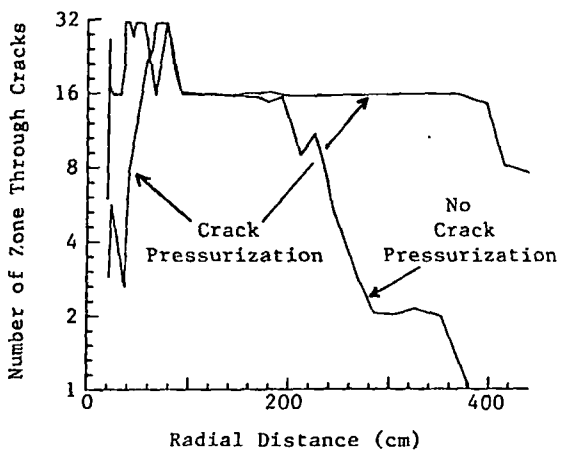

Figure 2. Effect of Gas Pressurization on Radial Cracking

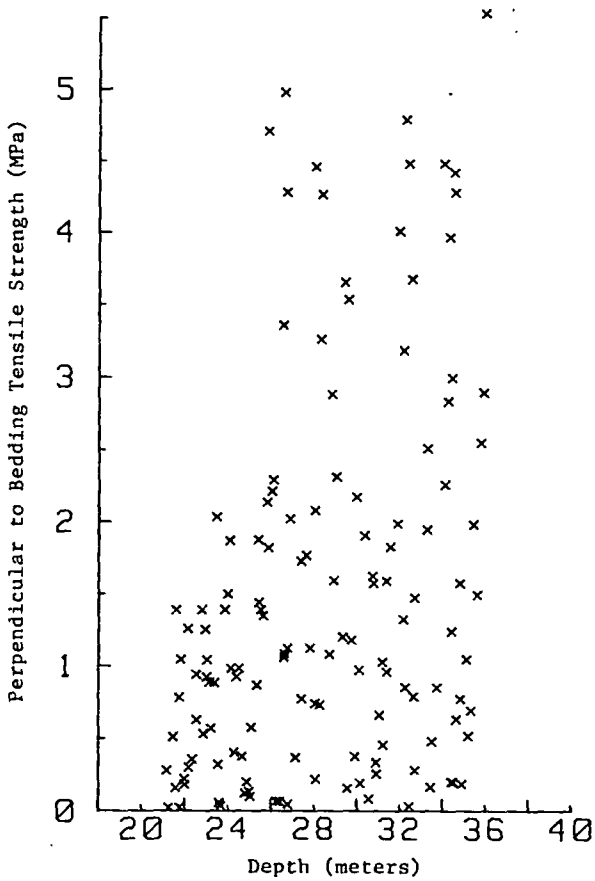

Figure 3. Direct Pull Tensile Strength - Geokinetics Site (Young and Patti, 1979)

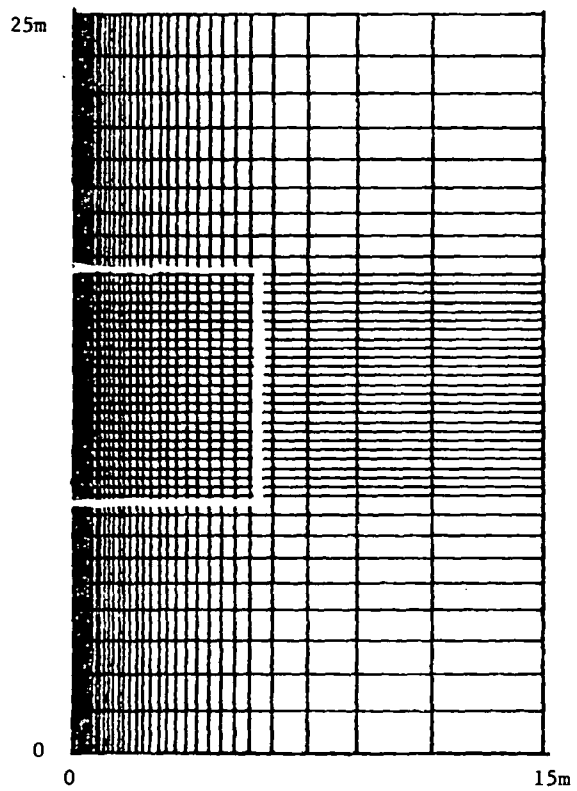

Figure 4. Calculational Grid (Note subgrid used for contour and crack plots)

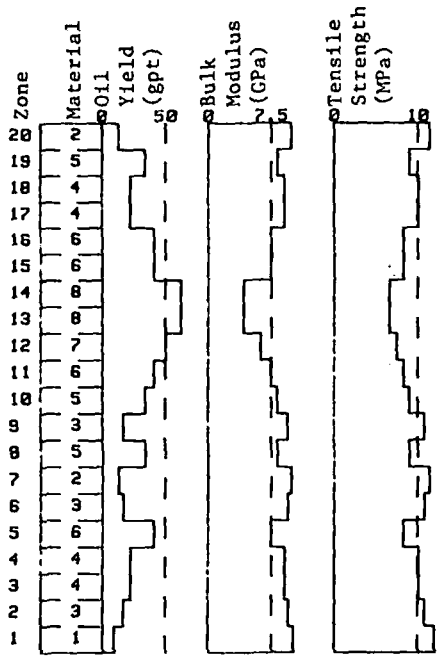

Figure 5. Oil Shale Zoning

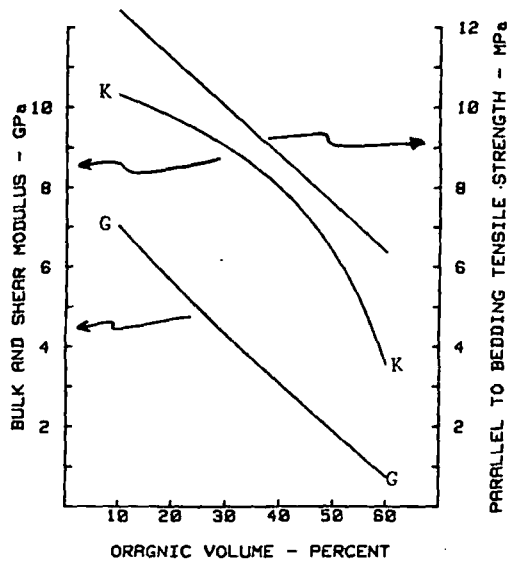

Figure 6. Organic Volume Relationships

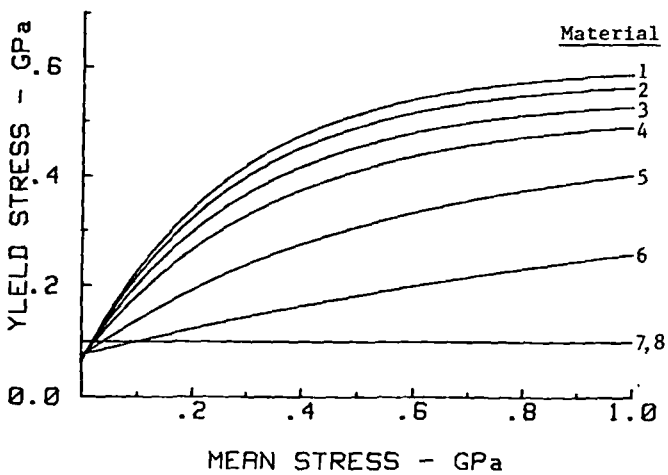

Figure 7. Oil Shale Yield Strengths

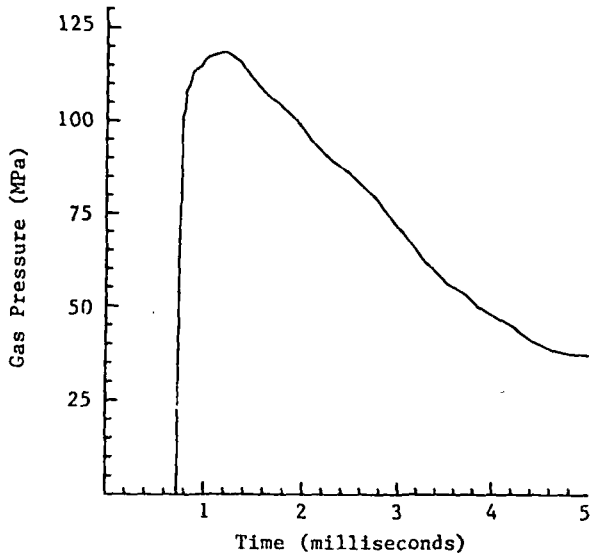

Figure 8. Gas Pressure in Oil Shale Zone

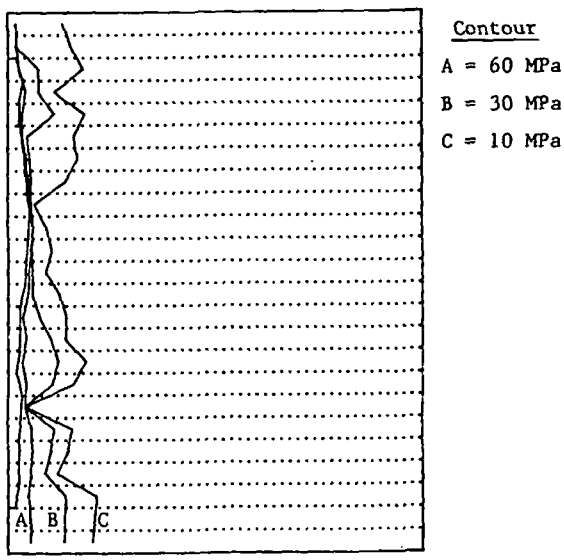

Figure 9. Gas Contours at 5mSec Baseline Case

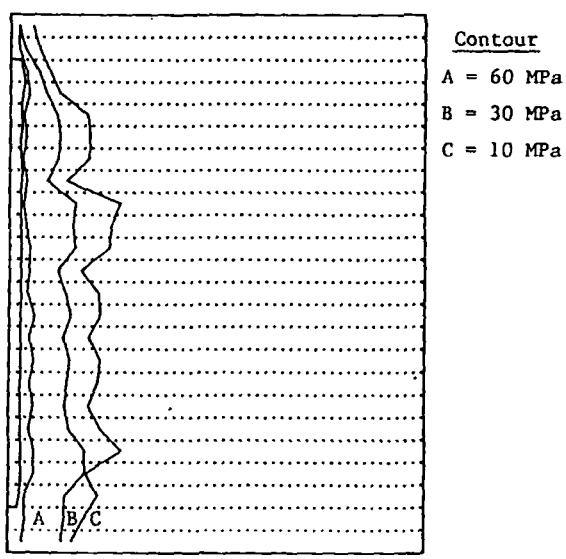

Figure 10. Gas Contours at 5mSec Uniform Material Case

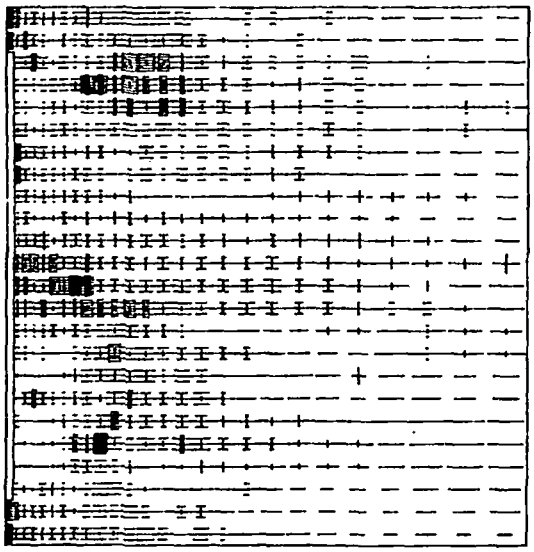

Figure 11. In-Plane Cracks at 5mSec Baseline Case

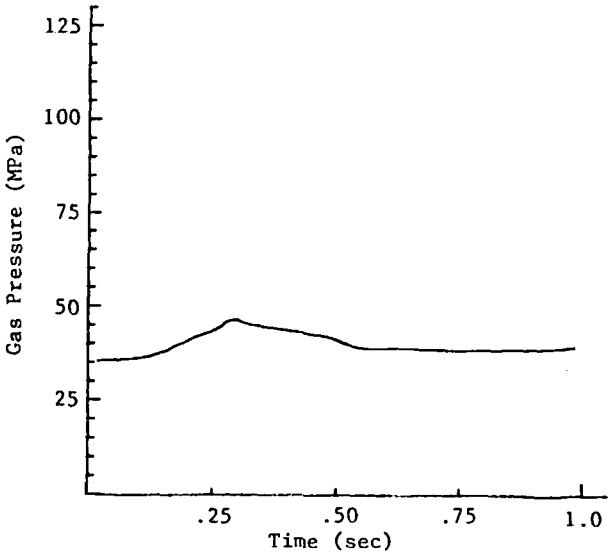

Figure 14. Gas Pressure in Oil Shale Zone

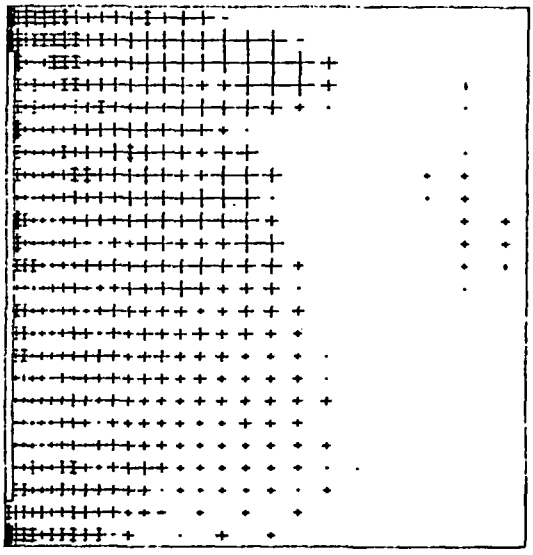

Figure 12. In-Plane Cracks Uniform Material Case

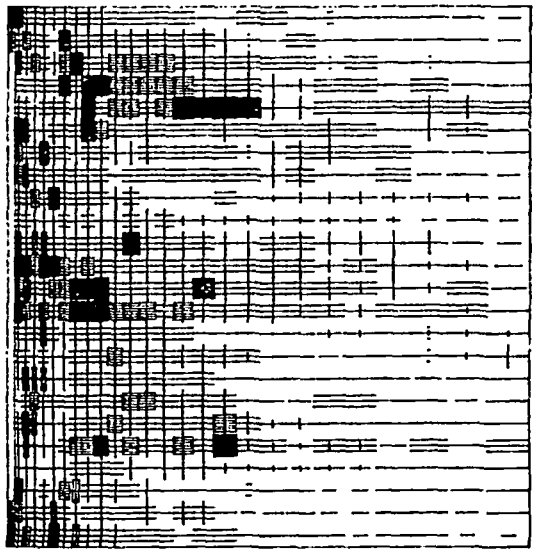

Figure 15. In-Plane Cracks at 1 sec Baseline Case

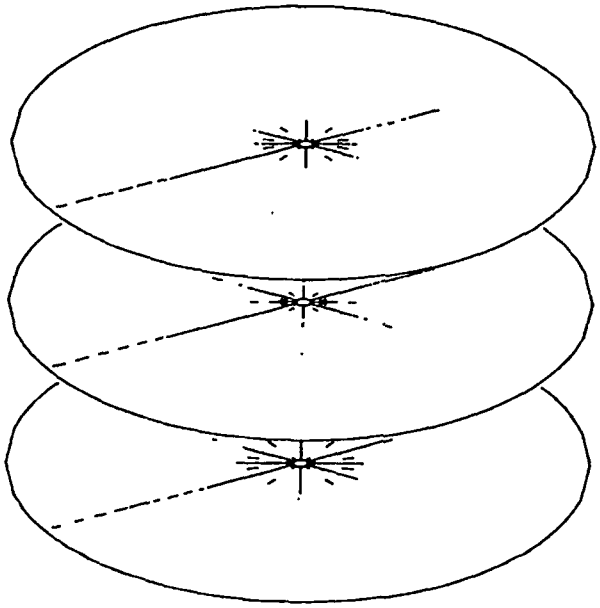

Figure 13. Typical Radial Crack Pattern
(outer radius is 3 meters)

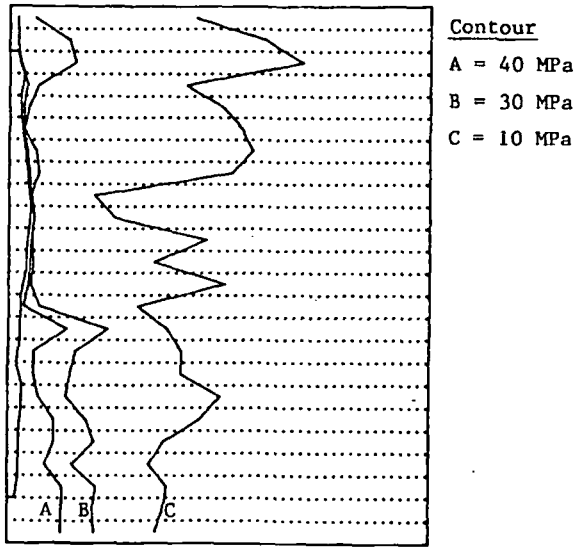

Figure 16. Gas Contours at 1 Sec. Baseline Case

Economic Geology
Vol. 74, 1979, pp. 469-474

Classification and Genesis of Biogenic Sulfur Deposits

J. C. RUCKMICK, B. H. WIMBERLY, AND A. F. EDWARDS

Abstract

Elemental sulfur occurs widely distributed in two geologic environments: basins containing hydrocarbons and zones of Cenozoic volcanism. A classification is suggested for these deposits. Essentially all economically important elemental sulfur deposits being mined today are bioepigenetic replacements of anhydrite or gypsum. These occur in two geologic styles: in cap rocks over salt diapirs and in stratabound deposits. However, all of these deposits appear to share remarkably similar origins and characteristics. They are formed in evaporite basins where petroleum-bearing beds underlie anhydrite or gypsum and occur where joints or faults permit water, hydrocarbons, and bacteria to rise into the evaporites. The bacteria oxidize hydrocarbons to CO_2, reduce sulfate ions to H_2S, and alter gypsum to calcite. Data indicate that H_2S is converted to polysulfides and these are oxidized to elemental sulfur by CO_2 in anaerobic environments. From two to four barrels of oil must be consumed per ton of sulfur, thus enormous amounts of hydrocarbons are required to form large deposits. These quantities are obtained by long-sustained artesian flushing by ground waters of areally extensive petroleum-bearing strata. A combination of unique structures form the plumbing systems required to concentrate artesian flow in the evaporites and thus localize the sulfur deposits.

Introduction

HUMAN sustenance and material progress demand a great deal of sulfur. At present the world consumes 50 million tons annually. Most of this, about 32 million tons, is produced as elemental sulfur; the remainder is supplied as sulfuric acid. Of the present annual production of elemental sulfur, a little more than 16 million tons, or about half, is mined by the Frasch process from deposits in anhydrite or gypsum. Most of the balance is recovered from sour gas and petroleum.

Although elemental sulfur deposits are widespread, very few are large enough to be of commercial importance. Until the development of the Frasch mining process in 1903, most of the world's sulfur was mined from deposits described here as volcanic and oxidative. Today essentially all elemental sulfur mined comes from bioepigenetic replacement deposits in gypsum or anhydrite. These occur in two geologic styles: in cap rocks over salt diapirs and as stratabound deposits in bedded evaporites. Examples of cap rock deposits occur in the Gulf Coast basins of Texas, Louisiana, and southern Mexico. Examples of stratabound deposits occur in the Fergana and Amudarya depressions of Central Asia, the Mesopotamian basin in Iraq, the Cis-Carpathian trough in Poland and Russia, and the Permian Basin in Texas.

Bioepigenetic sulfur is developed in anhydrite or gypsum by the activity of sulfate-reducing bacteria, most probably the species *Desulfrovibrio desulfuricans*. This anaerobe obtains energy through oxidation of hydrocarbons by the breakdown of SO_4^{-2} ions, releasing CO_2 and H_2S as waste products. Elemental sulfur is deposited where H_2S is oxidized by oxygen present as excess SO_4^{-2} and CO_2 in anaerobic systems or by O_2 in aerobic environments. In the bacterial breakdown of anhydrite and gypsum, Ca^{+2} ions combine with CO_2 to form secondary calcite as replacement or "biogenic alteration" of the evaporites.

Economic bioepigenetic sulfur deposits range in size from approximately 500 thousand tons of sulfur in the smaller cap rock deposits to more than 200 million tons of sulfur in the Mishraq stratabound deposits in Iraq (Barker et al., 1979). Table 1 lists the worldwide sources and amounts of elemental sulfur mined during 1977. Bioepigenetic deposits account for more than 98 percent of the world production. A little more than one-third of this comes from cap rock deposits, almost two-thirds come from stratabound deposits.

Classification

Elemental sulfur deposits are widely distributed throughout the world in two geological environments: basins containing hydrocarbons and zones of Cenozoic vulcanism. During our studies of, and exploration for, these deposits, the following general classification was evolved (and suggestions for its further modification are welcomed):

I. Biogenic deposits
   A. Bioepigenetic
      1. Cap rock
      2. Stratabound
   B. Biosyngenetic
II. Volcanic deposits

III. Oxidative deposits
IV. Thermogenic accumulations

Bioepigenetic deposits occur as replacements of anhydrite and gypsum by biogenic sulfur and calcite, as defined above and described in the next portion of the text. Biosyngenetic deposits are sedimentary and result from bacterial reduction of SO_4^{-2} to H_2S and oxidation of H_2S to native sulfur by oxygenated surface waters in lagoonal or otherwise restricted evaporative or euxinic marine and lacustrine environments. Examples are Lake Eyre, Southern Australia, and Chekur-Koyash and Krasnovadsk in southeast Asia (Ivanof, 1964). Some authors have attributed a biosyngenetic origin to the Sicilian sulfur deposits and to the Cis-Carpathian deposits of Russia. However, we believe that the evidence indicates that these deposits are bioepigenetic.

Many examples of volcanic extrusive, exhalative, and replacement elemental sulfur deposits occur in the Mediterranean, and around the margins of the Pacific Ocean in Japan, Central and South America, Mexico, and the western United States. Most of these deposits are relatively small, but several volcanic deposits in Japan were large enough to supply its entire domestic demand in past years. Considerable attention can be paid to classification of volcanic deposits. However, this category does not have important bearing on this discussion and will not be developed here.

The term oxidative deposits, as employed in this classification, requires special definition because almost all sulfur deposits are oxidative in that they occur by oxidation of H_2S gas. However, a separate category is required to include a broad class of hot springs and other oxidative deposits derived from either volcanic or biogenic sources. These deposits are widespread and generally small. They occur at the surface or at depth wherever volcanic or bacterially generated H_2S is oxidized by O_2, SO_4^{-2}, or CO_2. These significant characteristics of this class of deposits are: (1) they are deposited in fractures and open spaces in many different rock types, and (2) there is no evidence of biogenic replacement associated with them. Both of these characteristics are in marked contrast to the bioepigenetic deposits, a distinction critical to sulfur exploration efforts. The oxidative deposits in the Kara Kum sandstones of Turkmenia, southwest Asia, may be relatively large, but little is known of them (Ivanof, 1962). Examples of small oxidative deposits occur near Cody and Thermopolis, Wyoming; near Sulphurdale, Utah; and throughout the Permian Basin of West Texas and New Mexico.

A thermogenic classification is required to include the remarkable Lone Star Bertha Rogers No. 1 deep well in the Anadarko Basin of Oklahoma (Sec. 27, T 10 N., R. 19 W., Washita County) (Kincheloe and Scott, 1974; Rowland, 1974). This well was lost at a depth of 31,441 ft by a surge of liquid sulfur into the hole, probably generated by oxidation of H_2S derived from direct reactions between hydrocarbons and anhydrites of the Arbuckle Formation at high temperature and pressure.

TABLE 1. Annual World Production from Elemental Sulfur Deposits

For 1977, in thousands of long tons.

	Bioepigenetic		Volcanic and oxidative	Totals
	Strata-bound	Cap rock		
USA	1,890	4,280	10	6,180
Poland	5,000			5,000
USSR	2,570		30	2,600
Mexico		1,690		1,690
Iraq	550			550
China	200		50	250
South America			90	90
Italy	30		20	50
Turkey	10			10
Other	10		10	20
Totals	10,260	5,970	210	16,440
Percentages	62.4%	36.3%	1.3%	100%
	98.7%			

Geology and Genesis of Bioepigenetic Deposits

All bioepigenetic sulfur deposits share remarkably similar origins and characteristics. They are formed by anaerobic bacterial reduction of gypsum or anhydrite and oxidation of hydrocarbons in basins where evaporite beds are underlain by petroleum. Figure 1 illustrates a generalized cross section of a cap rock sulfur deposit overlying a salt dome. Figures 2, 3, and 4 are cross sections of three types of stratabound sulfur deposits. In terms of sulfur genesis, the only significant difference between the cap rock and stratabound deposits is that the position of the anhydrites above the petroleum in the cap rocks is caused by diapiric rather than by sedimentary processes. In the salt domes, the residual anhydrite of the cap rocks is accumulated by solution and removal of halite from rock salt by artesian ground waters.

Bioepigenetic sulfur deposits occur where joints and faults permit water, hydrocarbons, and bacteria to rise into evaporites or cap rocks. In this environment, bacterial oxidation of hydrocarbons to CO_2, reduction of gypsum (SO_4^{-2}) to H_2S, and alteration of gypsum (Ca^{+2} plus CO_2) to secondary calcite is well documented in the literature (Davis and Kirkland, 1973; Feely and Kulp, 1957; Ivanof, 1968; and others). However, there has been speculation over the manner of oxidation of the H_2S to elemental

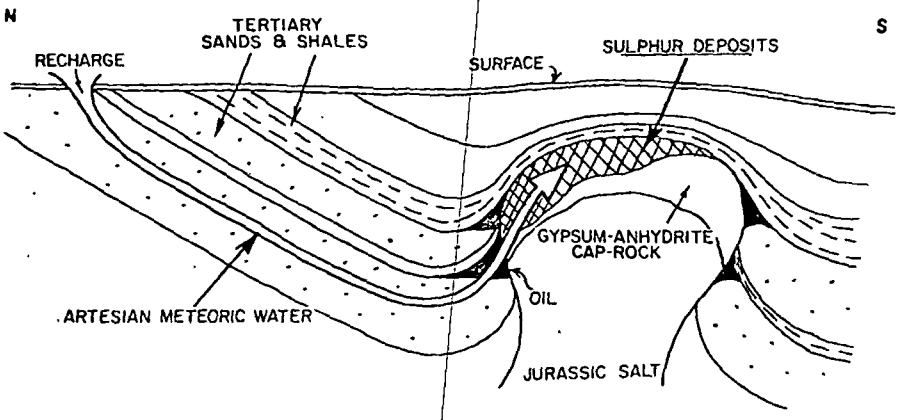

FIG. 1. Gulf Coast salt dome sulfur deposit.

sulfur. Some authors appeal to oxidation of H_2S by oxygenated ground waters. However, this does not seem to be supported by field evidence. Our sampling and analyses of the Boling dome cap rock deposits in Wharton County, Texas, and the Comanche Creek stratabound deposits in Pecos County, Texas, indicate anaerobic environments with a high concentration of H_2S and polysulfides in the contained waters. Another feature of these deposits is the abundant evidence of two distinct generations of both sulfur and calcite: (1) a colloidal or microcrystalline intergrowth of sulfur and dense gray calcite overgrown by (2) medium to large euhedral crystals of sulfur and white calcite.

These observations are best explained by the following sequence of events: (1) solution and dispersion of hydrocarbons in artesian meteoric waters containing anaerobic sulfate-reducing bacteria, most probably *Desulfovibrio desulfuricans*, (2) movement of these waters upward through anhydrite via faults and joints; (3) hydration of anhydrite to gypsum and solution of $CaSO_4$; (4) bacterial oxidation of the hydrocarbons, especially the paraffinic fractions, to CO_2 and reduction of the SO_4^{-2} to H_2S; (5) initial oxidation of H_2S to colloidal sulfur by excess SO_4^{-2} and concomittant alteration of gypsum in situ (Ca^{+2} plus CO_2) to dense calcite ($CaCO_3$); (6) development of porosity and permeability in the altered gypsum by (3), (4), and (5); (7) combination of H_2S, Ca^{+2}, and SO_4^{-2} to form calcium polysulfides in the waters in the system; (8) concentration in these waters of CO_2 (from 4); and (9) reaction between this CO_2 and calcium polysulfides causing simultaneous precipitation of sulfur and calcite crystals.

These reactions can be generalized by the following series of equations:

$$CaSO_4 + CH_4\ (+\ \text{bacteria}) \rightarrow H_2S + CaCO_3 + H_2O \quad (1)$$

$$3H_2S + SO_4^{-2} \rightarrow 4S\ (\text{colloidal}) + 2H_2O + 2OH^- \quad (2)$$

$$2H_2S + 2Ca^{+2} + 2H_2O \rightarrow Ca(OH)_2 + Ca(HS)_2 + 4H^+ \quad (3)$$

$$Ca(HS)_2 + 4S\ (\text{collodial}) \rightarrow CaS_5\ (\text{polysulfide}) + H_2S \quad (4)$$

$$CaS_5 + CO_2 + H_2O \rightarrow 4S\ (\text{crystalline}) + CaCO_3 + H_2S \quad (5)$$

The above are presented as a suggestion of the general sequence of events, not the final word. The reader will recognize the many possible variations in these systems and their probable chemical complexity. The equations representing formation of polysulfides and subsequent precipitation of sulfur and calcite crystals were presented by Davis and Kirkland (1973, p. 115) in their description of the Pokorny deposit in the Delaware Basin, Culberson County, Texas.

The key to an understanding of bioepigenetic sulfur deposits lies in artesian circulation of meteoric ground waters. The diagrammatic cross sections (Figs. 1 through 4) show such waters entering the updip beveled edges of tilted basins, circulating down permeable beds in and under petroleum-bearing strata, and flushing hydrocarbons and bacteria up through joints and faults into overlying cap rocks and evaporites. Metabolic activity of sulfate-reducing bacteria is low or nil in relatively high concentrations of hydrocarbons. Therefore, by dissolution and dispersion of both hydrocarbons and sulfate ions, circulating artesian meteoric waters in contact with both hydrocarbons and gypsum provide ideal environments for high levels of bacterial activity.

Formation of bioepigenetic deposits of economic size, however, requires at least one other parameter. The large amounts of H_2S produced by high levels of bacterial activity must be oxidized to elemental sulfur. A requirement for this appears to be relatively impermeable beds, such as shales, capping the system and allowing H_2S long enough residence time to be oxidized by SO_4^{-2} and CO_2. Where the system functions without an adequate seal, large volumes of

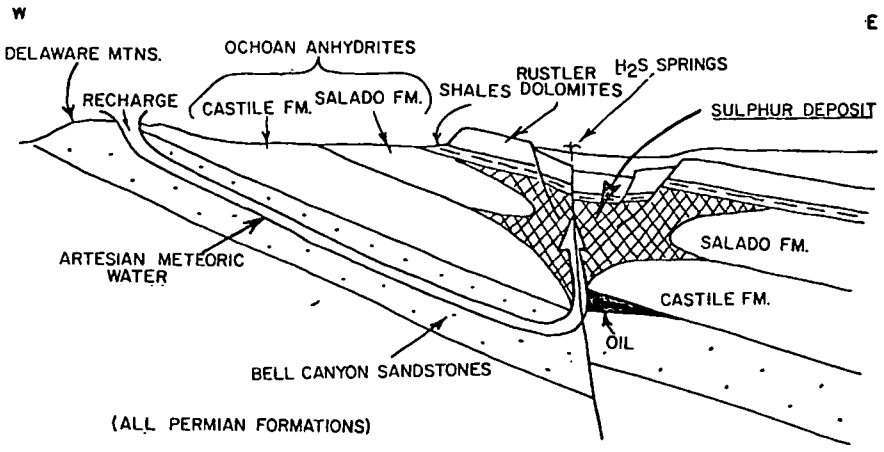

FIG. 2. Delaware Basin stratabound sulfur deposit.

gypsum can be altered to calcite containing only minor amounts of sulfur. The relatively barren calcite buttes or "castiles" in the Castile Formation of the western Delaware Basin in West Texas afford good examples of uncapped bioepigenetic systems (Bodenlos, 1973, p. 611–612).

Therefore, formation of economic bioepigenetic sulfur deposits requires unique combinations of structural and stratigraphic controls that localize hydrocarbons, artesian circulation, and the resultant sulfur deposits. For the cap rock deposits it is apparent that the structural controls are formed by the salt diapirs themselves, especially patterns of faults in the cap rocks and around the peripheries of the domes. Salt domes that are not extensively mineralized must lack one or more of the following: a supply of hydrocarbons, an adequate accumulation of anhydrite artesian flushing, or overlying impermeable beds to seal the system.

Structural controls of the stratabound bioepigenetic deposits involve either faults and joints or flexures, or both, and can be used to subdivide the larger stratabound deposits into several types. Four general variations of the larger deposits are: (1) the Rustler Hills, or Delaware Basin model probably involving only faults of modest displacement; (2) the

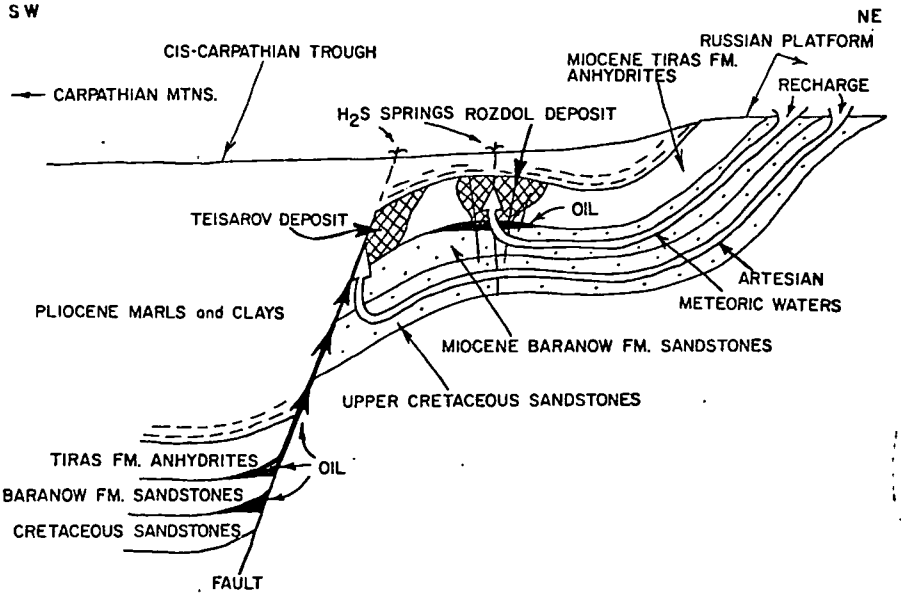

FIG. 3. Teisarov-Rozdol stratabound deposits, U.S.S.R.

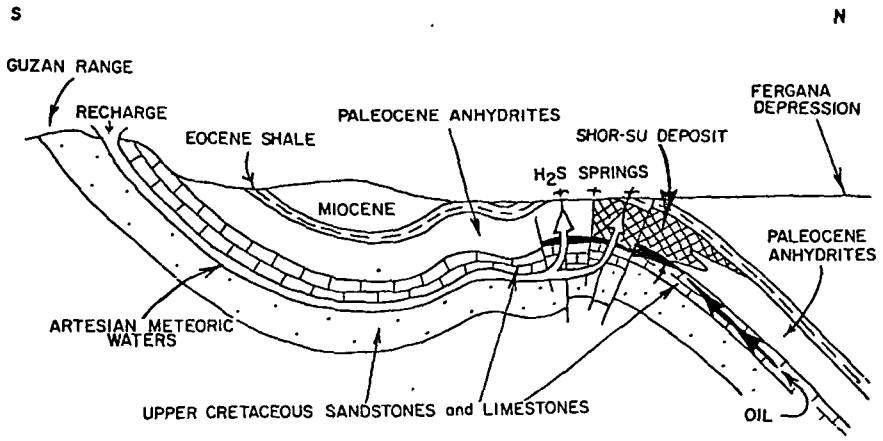

FIG. 4. Shor-Su stratabound deposit, Uzhbekistan, U.S.S.R.

Teisarov-Rozdol model controlled by normal faults of large displacement and, at the Rozdol deposit, by associated flexures along the Cis-Carpathian trough (in the U.S.S.R.) (Sakseev, 1973); (3) the Polish model where sulfur mineralization is formed in structural highs created by horst blocks in the Cis-Carpathian trough (Pawlowski et al., 1978); and (4) the Shor-Su (Fergana depression, U.S.S.R.) or Heiner (Permian Basin) models, principally controlled by anticlinal structures or by a flexure over a carbonate bank as in the Heiner deposits. Mishraq, the very large deposit in Iraq, also occurs in a prominent anticline and thus belongs in this later category (Barker et al., 1979; Lein, 1974; World Survey of Sulphur Resources, 1974).

The Delaware Basin style of deposit, highly generalized, is illustrated in Figure 2. One fault of modest displacement is shown controlling the system in the cross section, as in the case of the smaller deposits in this district. However, the large size of the Rustler Hills deposit, containing more than 50 million tons of sulfur, indicates a relatively unique concentration of artesian plumbing and hydrocarbons, such as an area of brecciation where two faults intersect. Here the artesian system has dissolved and replaced large volumes of gypsum causing karstlike collapse of the evaporites and overlying Rustler dolomite beds.

A cross section of the Teisarov-Rozdol deposits is generalized in Figure 3. The hydrocarbon and artesian water supplies in the Teisarov deposit appear to be localized by a normal fault of relatively large displacement that parallels the northeast margin of the Cis-Carpathian trough (as described by Sakseev et al., 1973). In the Rozdol deposit these features are controlled by a flexure related to the same fault (Ivanof, 1968, p. 177–251). The Shor-Su deposit is illustrated in Figure 4 (and described by Ivanof, 1968, p. 33–67). The Shor-Su, Mishraq, Heiner, and all other anticlinal deposits appear to be similar in that the artesian plumbing and subsequent sulfur mineralization are localized near the crests of the structures by axial joints and fractures.

Calculations of material balances in the reactions listed above indicate that a little more than two barrels of petroleum are consumed by the bacteria to form one ton of sulfur. Because there is good evidence that sulfate-reducing bacteria generally utilize only the paraffinic fractions, it is probable that about four barrels of oil would be required per ton of sulfur produced. Therefore, it can be calculated that something on the order of 200 million barrels of oil, or 3.6 trillion cubic feet of methane, were required to generate the Rustler Hills deposit in the Delaware Basin.

At first these amounts appear incredible, especially when coupled with the need to move hydrocarbons through the sites of sulfur mineralization in relatively diffuse form. However, such magnitudes confirm the essential role of the artesian meteoric water systems in explaining the genesis of bioepigenetic sulfur deposits. The concept of artesian flushing of relatively large areas of petroliferous strata over spans of time on the order of 20,000 years or more appears to provide the only feasible geologic explanation of the process.

Acknowledgments

Gratitude is expressed to A. J. Bodenlos of the U. S. Geological Survey for helpful suggestions and careful review of this manuscript. The concepts and data presented here were assembled and developed during the authors' employment with Texasgulf Inc. We gratefully acknowledge Texasgulf's support in making what we hope is a contribution to the geologic knowledge of our natural resources.

MINERALS EXPLORATION DIVISION
TEXASGULF, INCORPORATED
GOLDEN, COLORADO 80401
October 6, 1978

REFERENCES

Barker, J. M., Cochran, D. E., and Semrad, R., 1979, Economic geology of the Mishraq native sulfur deposit, northern Iraq: Econ. Geol., v. 74, p. 484–495.

Bodenlos, A. J., 1973, Sulfur, *in* United States mineral resources: U. S. Geol. Survey Prof. Paper 820, p. 605–618.

Davis, J. B., and Kirkland, D. W., 1973, Native sulfur deposition in the Castile Formation, Culberson County, Texas: Econ. Geol., v. 65, p. 107–121.

Feely, H. W., and Kulp, J. L., 1957, Origin of Gulf Coast salt dome sulfur: Am. Assoc. Petroleum Geologists Bull., v. 41, p. 1802–1853.

Ivanof, M. V., 1968, Microbiological processes in the formation of sulfur deposits: Israel Program for Scientific Translation, Cat. No. 1850, U. S. Dept. Commerce, 298 p. (English translation from Russian)

Kincheloe, R. L., and Scott, J., 1974, What Lone Star found at 31,441 feet: The Petroleum Engineer, July, p. 29–32.

Lein, A. W., 1974, Origin of native sulfur in the Mishraq deposit: Internat. Geology Rev., v. 17, p. 881–885.

Pawlowski, S., Pawlowska, K., and Bolesaw, K., 1978, The geology and origin of the Polish sulfur deposits: AIME Preprint No. 78-H-77,, Denver Mtg., Feb. 1978.

Rowland, T. L., 1974, Lone Star 1 Rogers unit captures world depth record: Oklahoma Geology Notes, v. 34, p. 185–189.

Sakseev, G. T., 1973, Geologic structure and genesis of the Teisarov sulfur deposit: Lithology Mineral Resources, v. 8, p. 606–612.

World Survey of Sulphur Resources, 1974, Second Ed.: London, British Sulphur Corporation Ltd., 183 p.

5748 January, 1968 SM 1

Journal of the
SOIL MECHANICS AND FOUNDATIONS DIVISION
Proceedings of the American Society of Civil Engineers

CHEMICAL GROUTING TECHNOLOGY[a]

By Reuben H. Karol,[1] M. ASCE

INTRODUCTION

Historical records of construction projects indicate that the art of grouting was recognized and accepted in the 19th century. These early grouting projects undoubtedly used suspended solids for a grouting material.

The first chemical grout was introduced in the early 1900's. This was sodium silicate, used in the Joosten process, and still used in construction projects today (1967). Only in the last decade, however, with the advent of many new and exotic materials, has chemical grouting come into its own. As equipment and procedures become more sophisticated, the beginning steps are being taken in the development of a chemical grouting technology.

The techniques used in the field to apply chemical grouts differ significantly from, and often are diametrically opposed to, those which are generally used with suspended-solids grouts. Thus, it became necessary for the manufacturers of chemical grouts to develop a technology for use with their products. One such research program (which is still continuing) was begun in 1956 by American Cyanamid Company (ACC).

Many of the basic aspects of chemical grouting technology have proven to be applicable to most of the commercial chemical grouting materials currently available. Some of these fundamentals are detailed herein.

GROUND WATER FLOW

Most applications of chemical grouts are made into saturated or partially saturated formations. There are instances in which dry, granular, or frac-

Note.—Discussion open until June 1, 1968. To extend the closing date one month, a written request must be filed with the Executive Secretary, ASCE. This paper is part of the copyrighted Journal of the Soil Mechanics and Foundations Division, Proceedings of the American Society of Civil Engineers, Vol. 94, No. SM1, January, 1968. Manuscript was submitted for review for possible publication on June 20, 1967.

[a] Presented at the May 8-12, 1967, ASCE National Meeting on Structural Engineering, held at Seattle, Wash., where it was available as Preprint No. 479.

[1] Director, Engrg. Chemicals Research Center, American Cyanamid Co., Princeton, N. J.

tured formations are grouted. All such cases, however, are those for which the purpose of treatment is to increase the strength of the formation. The majority of chemical grouting applications are related to water shut-off rather than strength increase.

The upper surface of subterranean water (the water table) generally is a subdued replica of the terrain. The elevation of the water table varies locally with surface precipitation and weather conditions. The mass of ground water itself also flows in a horizontal direction toward the exposed and subsurface drainage channels.

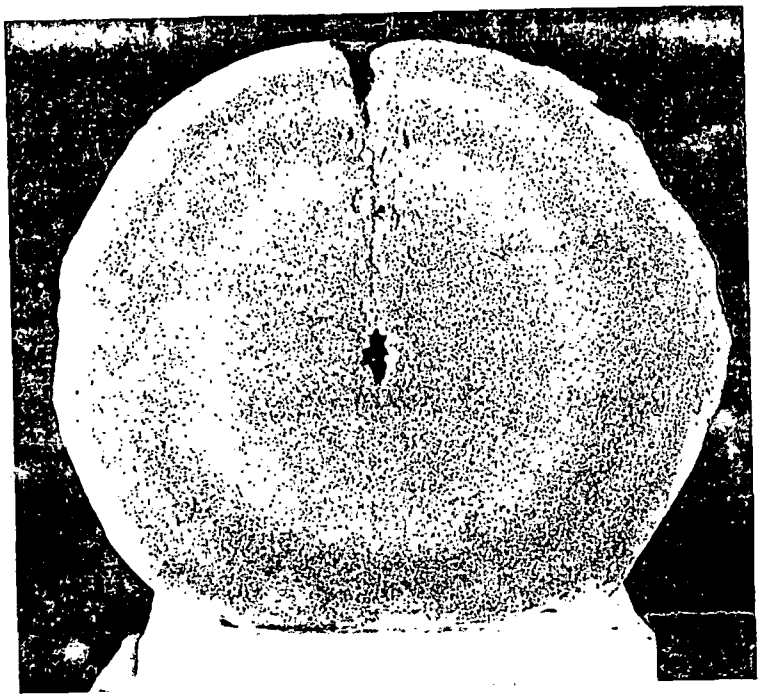

FIG. 1.—CONCENTRIC RINGS SHOW UNIFORM RADIAL SPREAD OF GROUT IN SATURATED ISOTROPIC SAND UNDER STATIC GROUND WATER

Under large expanses of level terrain, the rate of ground-water flow is relatively slow, and generally of inconsequential magnitude insofar as chemical grouting operations are concerned. In rolling or mountainous country, however, ground-water flow may be rapid enough to affect a grouting operation unfavorably. This is particularly true if the major portion of the flow occurs through a limited number of flow channels, or in formations which do not have over-all porosity. Ground-water flow is generally rapid enough to cause problems in the vicinity of an excavation which enters the water table. Even in areas where ground-water flow is normally insignificant, local conditions of high flow rates may be caused by the initial injections of a grouting program. Thus, the movement of ground water must always be considered when planning a grouting job.

Under absolutely uniform conditions (such as can be obtained in a laboratory but hardly ever in the field), it is possible to obtain accurate verification of the theory of fluid flow in a uniform, saturated, isotropic sand. Injection of grout from a point within such a sand mass would be expected to give uniform radial flow. Thus, the shape of a stabilized mass resulting from the injection of grout under these conditions would theoretically be a sphere. This is substantially true if the grout-injection pressure is significantly greater than the static head, and if the stabilized volume is small enough that hydrostatic pressures at top and bottom of the mass are not significantly different. Excellent verification has been obtained many times in experiments on a laboratory scale and also in experiments on a field scale.

Fig. 1 shows a vertical section through a grouted mass made in the laboratory under ideal conditions. Dyes were used to trace the flow of grout. A total of 6,000 cu cm of grout were injected without interruption at a rate of 500 cu cm per min into saturated, dense medium sand. The gel time was 20 min and each successive 1,000 cu cm was dyed a different color. The photograph clearly shows the concentric rings and these are seen to be close to true circles, verifying the theoretical three-dimensional uniform radial flow.

The effects of flowing water are illustrated by the cross section of a stabilized mass shown in Fig. 2. This injection was made in the same fashion as in Fig. 1, except that ground water was flowing slowly. Note that the inner concentric rings are not much affected by the ground-water flow. This will always be true as long as the rate of injection of grout is substantially greater than the volume of ground water moving past the injection plane. If the volume of liquid grout stays in a place for a considerable length of time prior to gelation, even a slow rate of ground-water flow can cause grout displacement and the attendant dilution along the grout ground-water interface. The loss of grout from the outer concentric rings is clearly visible in Fig. 2. It is also clear that the stabilized mass itself, while still roughly spherical in shape, is displaced in the direction of the ground-water flow.

When ground water is flowing at a relatively rapid rate, in addition to displacement of the grouted mass in the direction of flow, the shape of the stabilized volume will be modified to conform with the flow net caused by the introduction of a point of high potential at the end of the injection pipe. (This same effect is also caused in slowly moving ground water when time lapse between grouting and setting of the grout is very long). Fig. 3 is an illustration of a laboratory-scale injection showing conformation of a grouted mass to the flow lines. In this case, approximately 3,000 cu cm of grout were injected during 6 min. Ground-water flow was about 4 cm per min. Even though the gel time was 9 min, (only 3 min longer than the total pumping time), the grouted mass is displaced almost 7 in. (about 3/4 of its vertical dimension) from the location of the grout pipe. It is interesting to note that displacement is about half the ground-water flow distance during the grout induction period.

When injections are made into stratified deposits, the degree of displacement is related to the formation permeability and the grouted mass can take odd shapes such as illustrated in Fig. 4.

It is apparent then, that the major effect of flowing ground water is to displace the grouted mass from the location from where it enters the formation, and a minor effect is to modify the first shape of the grouted mass. The de-

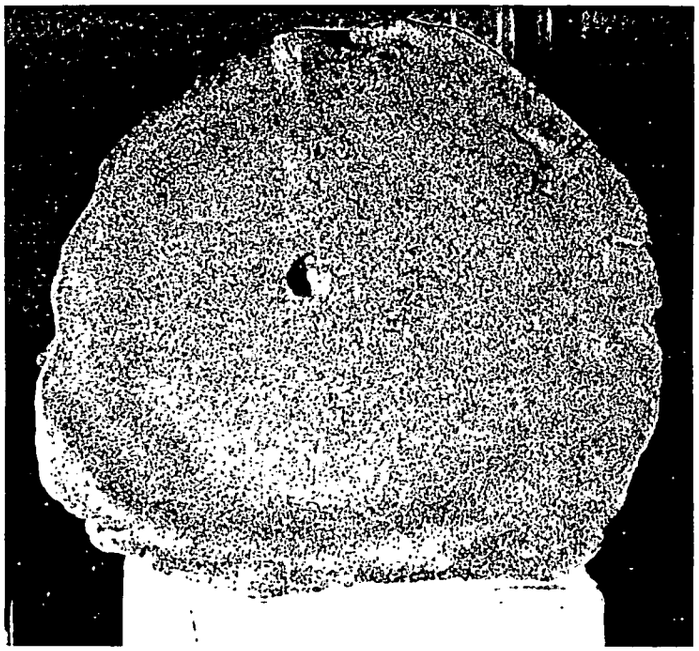

FIG. 2.—DISPLACEMENT OF GROUTED MASS AND LOSS OF GROUT CAUSED BY FLOWING GROUND WATER

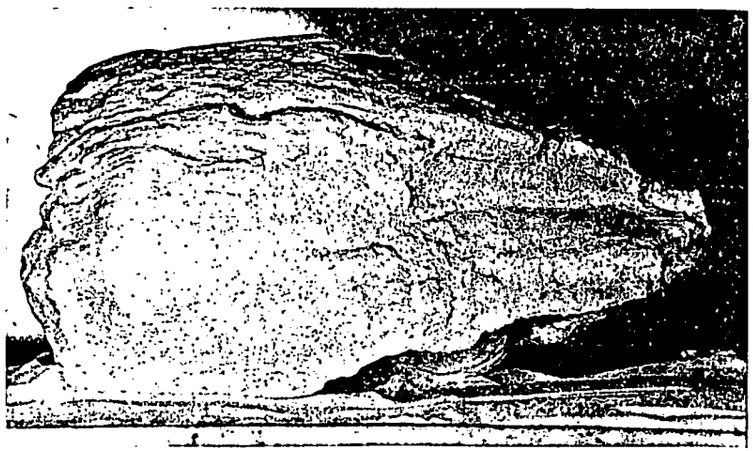

FIG. 3.—DISPLACEMENT AND DISTORTION OF THE NORMAL SHAPE OF A GROUTED MASS DUE TO GROUND-WATER FLOW AND LONG GEL TIMES

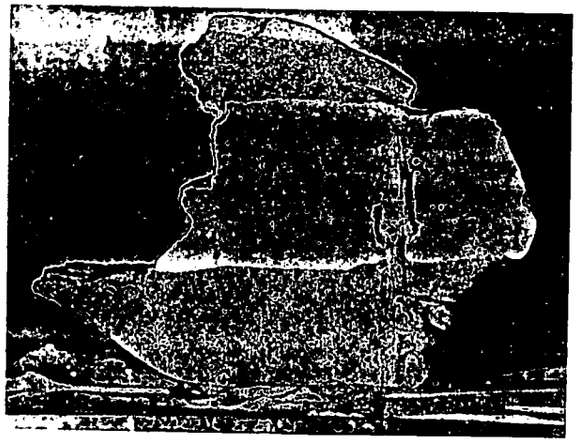

FIG. 4.—DIFFERENT DEGREES OF GROUT DISPLACEMENT OCCUR IN STRATIFIED DEPOSITS

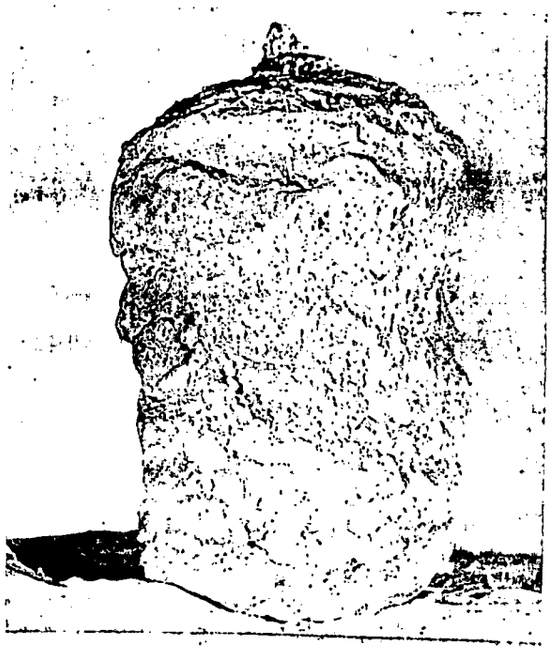

FIG. 5.—UNIFORM HORIZONTAL PENETRATION ACHIEVED BY PROPER CONTROL OF MECHANICAL PARAMETERS

gree of displacement and the shape modification are functions of the relationship between the rate of ground-water flow, the rate at which grout is placed, and the length of time for the grout to set.

UNIFORM PENETRATION

In the field, it is seldom that a pipe is driven to one depth and the entire grout volume injected at that one area. In virtually all grouting operations,

FIG. 6.—RESULTS OBTAINED WHEN PIPE IS PULLED TOO FAR BETWEEN SUCCESSIVE INJECTIONS

grout is injected at several locations along the length of the grout hole. Generally, this procedure is intended to result in a relatively uniform cylinder of stabilized material. Such results can be accomplished, as illustrated in Fig. 5. Nonuniform penetration can result in the shape shown in Fig. 6. Here, the individual spheres resulting at the different pipe elevations are tangent. Under worse conditions, they could be completely isolated. The difference between these two grouted masses is merely one of field technique. It has been found by experience that if the distance the pipe is moved between successive injections of grout is less than the radial spread of grout from any one location, the stabilized mass tends to be uniform rather than consisting of tangent or isolated masses.

The masses shown in Figs. 5 and 6 were made in uniform sands. Even when the proper relationship between volumes and pulling distance is observed, nonuniform penetration can still occur in natural deposits, when these are stratified. Resulting shapes can be as shown in Fig. 7. Under extreme conditions, degrees of permeation can vary as much as natural permeability differences as shown in Fig. 8. Such nonuniformity has obvious adverse affects on the ability to carry out a field grouting operation in accordance with the engineering design.

It would be of major value to be able to obtain uniform penetration regardless of permeability differences in the soil profile. In assessing the cause for penetration differences, it becomes apparent that the grout which is injected first will seek the easiest flow paths (through the most pervious materials) and will flow preferentially through those paths. To modify this condition, other factors must be introduced. The only factor which can be introduced by the grouter is control of setting time. Thus, if the grout were made to set prior to the completion of the grouting operation, it would set in the more open channels where it had gone first, and force the remaining grout to flow into the finer ones. Accurate control of gel time thus becomes an important factor in obtaining more uniform penetration in stratified deposits.

For field conditions where ground water may be flowing, and where permeability differences exist between the vertical and horizontal directions due to either placement or stratification, better control of grout placement can be obtained when the grout is made to set up at the instant when the desired volume has been placed. Early laboratory experiments were based on determining what happened when the attempt to control these times accurately were unsuccessful. For gel times longer than the pumping times, results have already been described. For gel times shorter than the total pumping time, it had been thought that the grouting operation would be halted by excessive pressures at the instant of gelation. Surprisingly, however, it was found that with AM-9 chemical grout (a low-viscosity polymer grout produced by Cyanamid) pumping a grout into a formation could continue for periods of time substantially longer than the gel time.

Stabilized shapes resulting from such a procedure are illustrated by the grouted mass shown in Fig. 9. The lumpy surface is typical of grouted masses in which the gel time is a small fraction of the total pumping time. The mechanism at work during this process is not obvious from a study of the results and much laboratory and field experimentation has been performed to explain the process. One of the most lucid illustrations of the principles

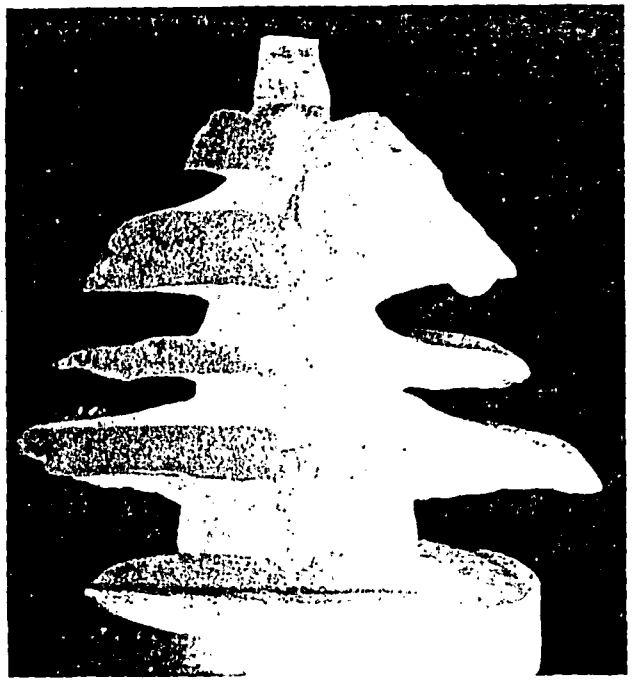

FIG. 7.—NONUNIFORM PENETRATION DUE TO STRATIFICATION

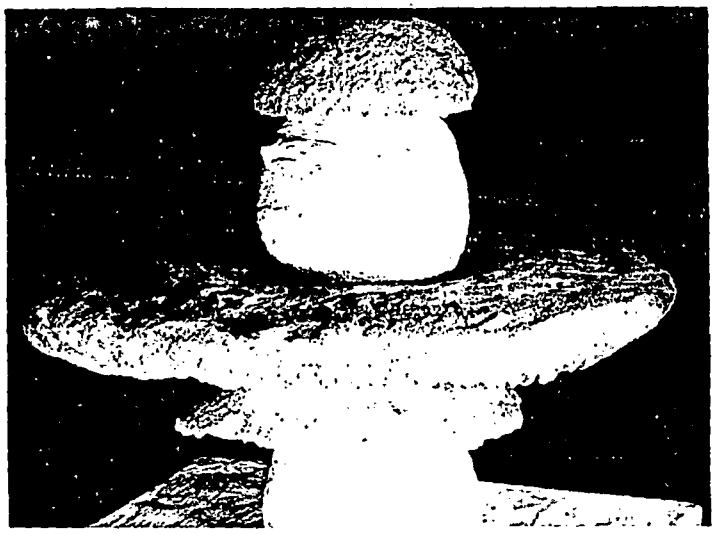

FIG. 8.—INEFFICIENT USE OF GROUT DUE TO CHANNELLING THROUGH A ZONE OF HIGH PERMEABILITY

FIG. 9.—TYPICAL LUMPY SURFACE AND ROUGH SPHERICAL SHAPE ASSOCIATED WITH THE USE OF GEL TIMES SHORTER THAN THE PUMPING TIME

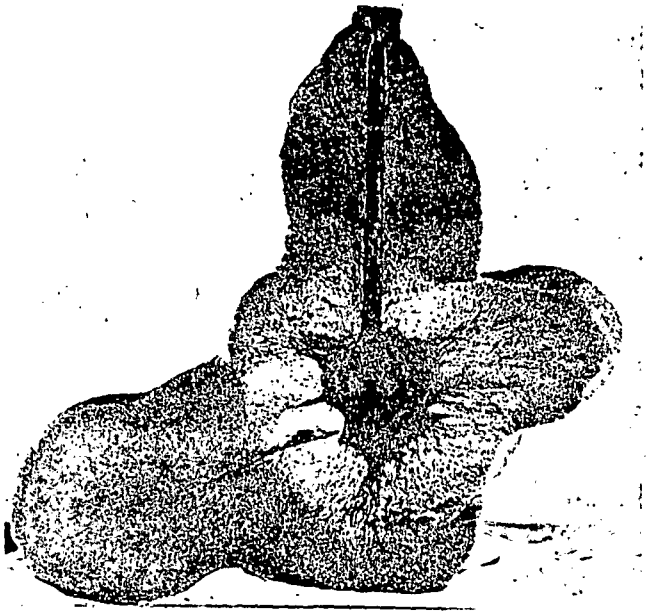

FIG. 10.—CROSS SECTION THROUGH A STABILIZED SAND MASS MADE WITH A GEL TIME MUCH LESS THAN THE TOTAL PUMPING TIME

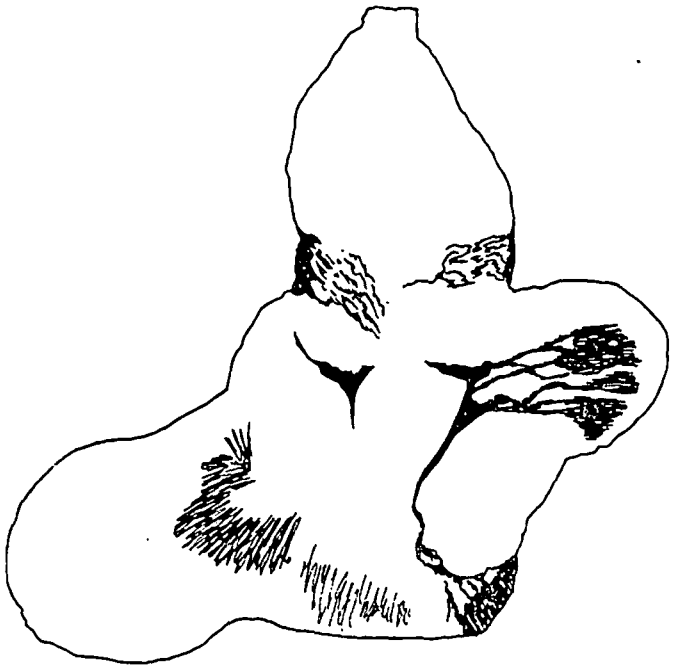

FIG. 11.—FINAL LOCATION IN THE GROUTED MASS OF FIG. 10 OF 1/6 OF THE GROUT VOLUME PLACED THIRD IN SEQUENCE

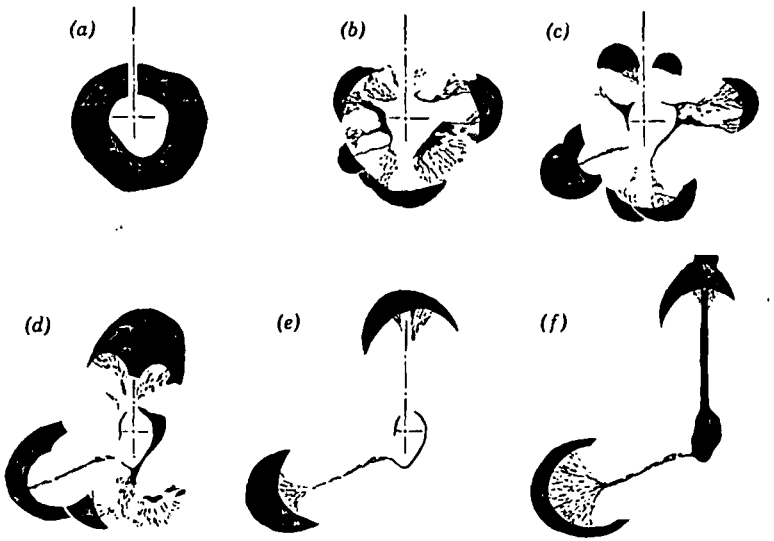

FIG. 12.—LOCATION OF GROUT VOLUME

involved resulted from a group of experiments in which dye was used to detect the sequential location of the various portions of the total grout volume.

THEORY OF SHORT GEL TIMES

Fig. 10 shows a cross section of a stabilized sand mass resulting from the injection of 6,000 cu cm of 10% AM-9 chemical grout into a dense, medium sand. This injection was made through an open-ended pipe under static groundwater conditions, at a rate of 500 cu cm per min. Six different-colored grout

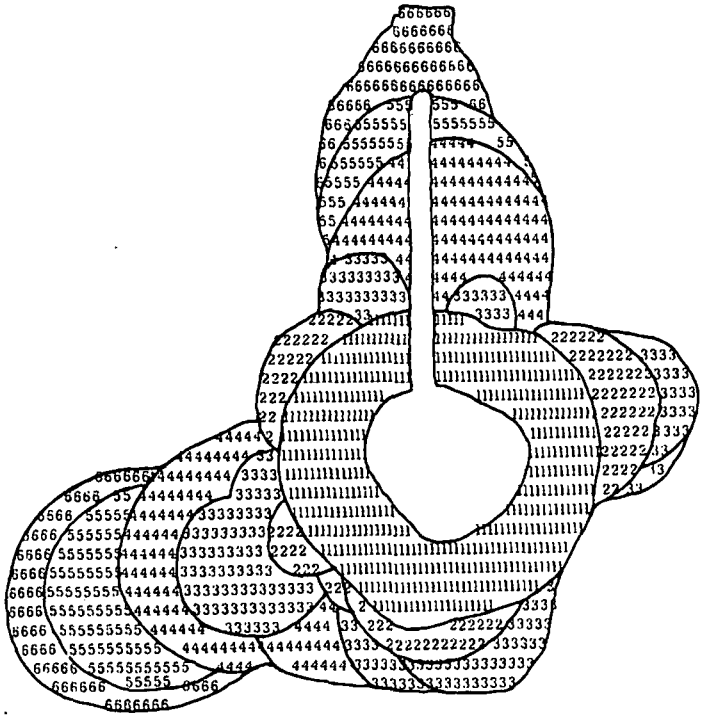

FIG. 13.—DRAWING OF FIG. 10, ILLUSTRATING BY NUMBERS THE SEQUENTIAL LOCATION OF PORTIONS OF THE TOTAL GROUT VOLUME

solutions were used, so that flow sequence could be traced. An equal-volume system was used to place the grout, with catalyst concentrations adjusted to give a gel time of 30 sec.

This experiment verifies that until gelation first occurs, the flow of fluid through the soil mass is entirely in keeping with theoretical concepts. As pumping begins, the grout is displaced radially in three dimensions from the opening in the pipe. The leading surface of the grout mass forms a sphere. The rate of motion of this leading edge is decreasing if the pumping rate remains constant. When gelation occurs, it starts at an infinitely thin shell which

is the boundary between the grout and the ground water. As pumping continues, a finite number of channels are ruptured in this thin, incipient gel; through these channels, grout continues to flow as pumping continues. It is interesting to note that the procedure described cannot take place with a batch system, since it depends upon infinitely small volumes of grout reaching the gel stage in time succession.

Much of the grout trapped without the initial thin shell also gels to form a fairly thick shell containing a finite number of open channels. The location of this shell is clearly shown in Fig. 10. The remainder of the fluid grout within the shell is forced out through the open channels as pumping continues. At the point where each of these channels comes out of the initial shell into unstabilized soil, three-dimensional radial flow again begins. In this fashion, hemispheres begin to grow on the surface of the initial sphere. Eventually, the leading surface of these new partial shells of grout will gel, and the entire process will be repeated.

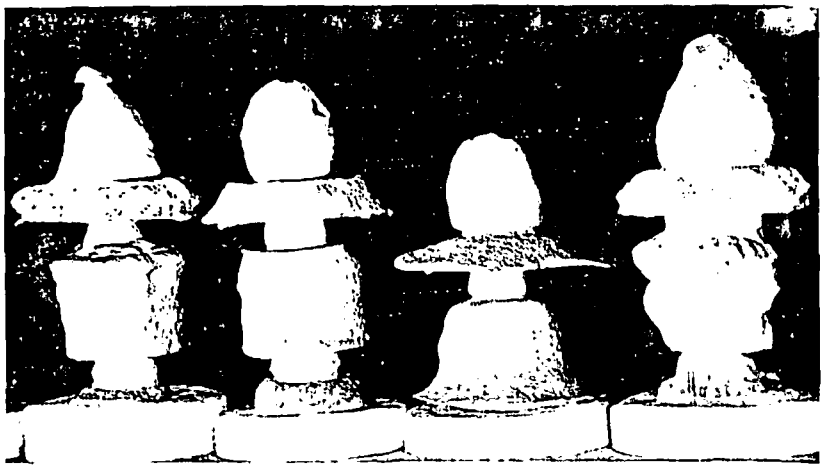

FIG. 14.—STABILIZED SAND MASSES, SHOWING THE EFFECTS OF GEL TIME ON UNIFORMITY OF PENETRATION

Since the colors show on a photograph only as shades of gray, it is not possible, from a black and white reproduction, to trace the sequence of injections. Even from color photographs, if the final location in the grout mass of one color is plotted, the results are difficult to interpret. This is illustrated in Fig. 11, which shows the final location on the cross section of the third color. The difficulty in interpretation is because the location plotted also shows the channels used by the succeeding volumes of grout. However, if each color were plotted in sequence, cancelling out the channels through that color, the results become meaningful and informative. Figs. 12(*a*) through 12(*f*) show the location in sequence of the various portions of grout. As they are inspected, in sequence, it can be seen that each succeeding volume of grout gels on the outside of a mass already solid, so that each succeeding grout mass is farther and farther from the point where the pipe is located. This data is summarized in Fig. 13. The location of each color, in sequence, is shown through the use of typed numbers.

The basic conclusion is that when the gel times are appreciably shorter than the pumping times, the grout mass forms around the pipe and grows larger, as pumping continues, into a roughly spherical shape with the material placed last being farthest from the pipe location.

Making the grout gel around the pipe is one of the major factors that has opened up a new technology in grouting. If the location of the grout pipe is known accurately and if the grout gel is made at that location, the location of the grouted mass is known. Such knowledge is, of course, necessary in order to design and carry out a grouting operation with precision and confidence.

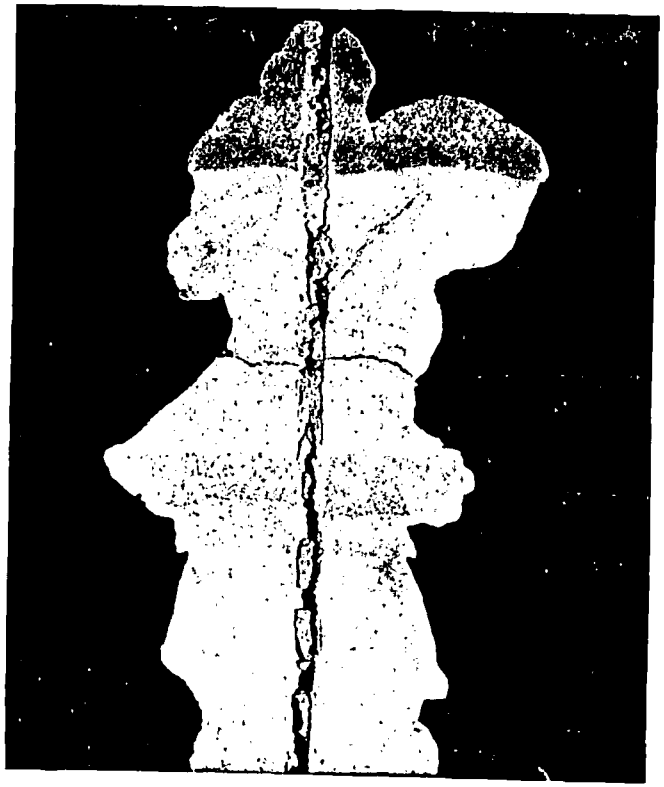

FIG. 15.—STABILIZED SAND COLUMN, SHOWING GOOD UNIFORMITY OF PENETRATION THROUGH THE USE OF SHORT GEL TIMES IN STRATIFIED DEPOSITS

USE OF SHORT GEL TIMES

A graphic illustration of the benefits of short gel time in regard to uniformity of stabilization is shown by the four stabilized masses in Fig. 14.

FIG. 17.—DECREASE IN UNIFORMITY OF PENETRATION IN THE DEPOSITS OF FIG. 16 AS THE GEL TIME IS INCREASED

FIG. 16.—REASONABLY UNIFORM PENETRATION IN STRATIFIED DEPOSITS WHEN SHORT GEL TIMES ARE USED

These masses also illustrate the empirical procedures which result in the greatest degree of improvement under filed conditions. They were made at the same time in an artificially created stratified deposit, using exactly the same injection procedures except for gel times. In each case, grout was injected at a rate of 400 cu cm per min and the grout pipe was pulled 1 in. every 15 sec.

For the mass second from the right, the gel time was 10 min. Since the entire grout volume was in the stratified formation for a considerable time before any of it gelled, most of the penetration occurred in the coarse stratum, and very little grout entered the silt strata underneath the coarse sand, even though the earliest part of the injection was at that location.

The mass second from the left used a gel time of 30 sec. The shape of this mass indicates considerably better uniformity of penetration over that obtained with a 10-min gel time.

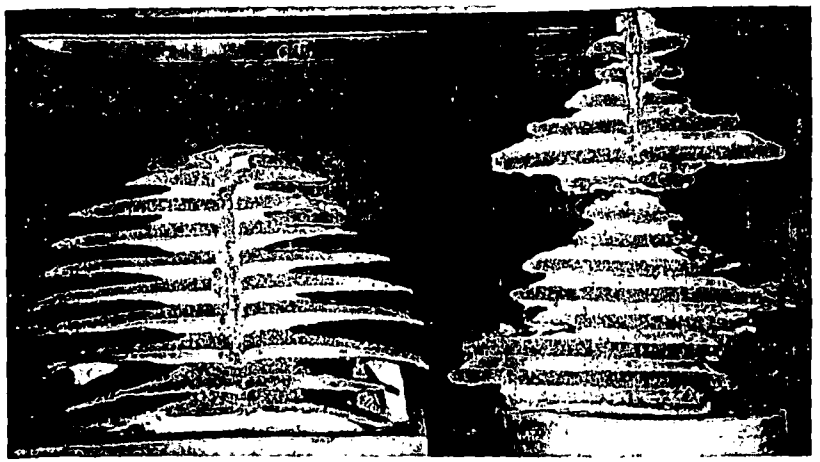

FIG. 18.—USE OF SHORT GEL TIMES RESULTS IN MORE UNIFORM PENETRATION IN ADJACENT STRATA OF VARVED DEPOSITS

The mass on the left used a 15-sec gel time. For this particular case, the gel time and pulling time were equal. The grout pipe was lifted to a higher elevation at about the instant when the grout that had been pumped began setting up at its former elevation. Although the shape of this mass is not an exact duplicate of the previous one, it would be difficult to say that either one shows significant improvement over the other in regard to uniformity of penetration.

The mass on the far right had a 6-sec gel time. For this particular grouted mass, the grout was gelling at each elevation before half of the total grout volume to be placed at that elevation had been pumped. Significantly, this mass shows a greater degree of penetration into the finer materials. Experience, both in the laboratory and in the field, has verified that the greatest degree of uniformity of penetration in stratified deposits occurs when the gel time is less than half of the pumping time at each vertical stage. The use of this empirical law is graphically illustrated by Fig. 15. For this injection, the grout was pumped at 500 cu cm per min and the grout pipe pulled 1 in. every

30 sec for 12 pulls. The gel time was 11 sec. The degree of penetration is reasonably uniform even though differences in actual horizontal permeabilities between the various strata exceed 1,000.

Figs. 16 and 17 compare two injections made under similar conditions to illustrate the degrees of improvement that can be obtained through the use of short gel times. Obviously, such degrees of improvement would be very bene-

FIG. 19.—DECREASE IN DISPLACEMENT, DISTORTION, AND LOSS OF GROUT, DUE TO THE USE OF SHORT GEL TIMES IN STRATIFIED DEPOSITS THROUGH WHICH GROUND WATER IS FLOWING

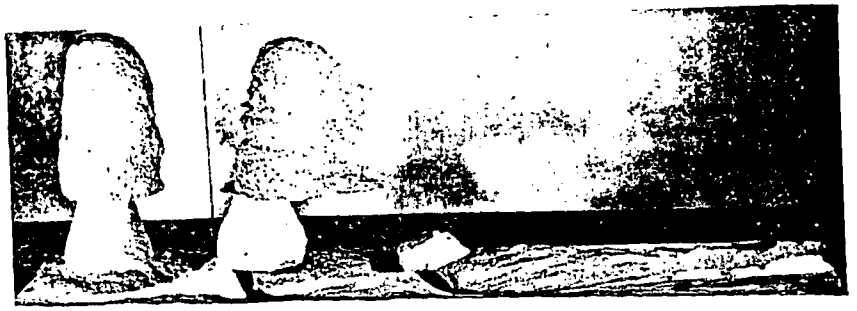

FIG. 20.—USE OF LONG GEL TIMES IN FLOWING GROUND WATER RESULTS IN COMPLETE LOSS AND WASTE OF GROUT

ficial in getting complete joining between adjacent injections in a grout pattern.

Fig. 18 illustrates that improvement in the degree of penetration can be obtained in virtually any type of deposit including varved deposits. The mass on the right was made by adhering to the empirical law previously stated. Even though penetration is far from uniform, the use of this law resulted in virtually the same amount of penetration for adjacent varves. In this case, the degree of improvement is considered significant.

The empirical law in regard to gel times is also operative under conditions of flowing ground water. Under such conditions, there are two benefits that accrue from the use of very short gel times: (1) An increase in the uniformity of penetration and (2) a decrease in displacement and dilution of the grout.

Fig. 19 is an illustration of the beneficial effects of short gel times when used in stratified deposits under conditions of ground-water flow. It shows the results of four injections made under exactly the same conditions except for gel times. In these cross sections, only the one on the far left was made under the optimum conditions previously described (gel time less than half the pipe pulling time). Actual gel times were, from left to right, 15 sec, 1 min, 4 min, and 10 min. Ground-water flow effects show up in terms of displacement in the coarser strata for gel times of 1 min and longer. For the 4 and 10 min gel times, displacement was great enough so as to lose the grout in the coarse strata entirely. Similar data has been observed in the laboratory and field many times.

Fig. 20 is another typical illustration of the fact that in flowing ground water the use of short gel times tends to minimize or eliminated displacements. In these three masses, gel times were 15 sec, 1 min, and 10 min. For the 15-sec gel time, it is not possible to detect the effects of flowing ground water. For the 1 min gel time, the effects of displacement are clearly seen at the coarse strata. For the 10-min gel time, while much of the grout gelled, its position was such as to render it useless for the purpose of establishing a cut-off wall.

GROUT CURTAINS

Many field grouting operations have an ultimate purpose of placing a relatively impermeable barrier of considerable horizontal extent (and sometimes also a considerable depth) in a predetermined location. Such barriers are generally called grout curtains or cutoff walls. They consist of one or more interlocking rows of grouted soil or rock cylinders. Each of the individual cylinders is formed by the injection of grout through a pipe or drilled hole which has been placed in the formation. Ideally, these cylinders will have relatively uniform cross sections throughout their depth.

To obtain as great a degree of uniformity as possible, it is desirable to grout short sections or stages of any individual hole so as to minimize the opportunity for grout to flow preferentially throughout the hole depth. The actual depth or stage is related to the grout take and to the pumping capacity. If take is low per unit length of hole, each stage may have to be of considerable depth in order to be able to operate the grout-pumping equipment at low capacity. When takes are high, stages can be short, usually of the order of 1 ft to 5 ft. In such cases, stage length is often determined by economics since the cost of grouting is directly related to the number of stages per hole.

When grouting in open formations, the empirical relationships previously discussed for obtaining optimum uniformity of penetration should be used. In determining actual gel times it will be found that these are directly related to pumping rates and to stage depth, and in most occasions, all of these variables cannot be predetermined with great accuracy. The initial injections of the actual grout curtain are generally used to arrive at values or ranges of values for stage length, pumping pressure, and gel time. These values, too, are

subject to modification during the actual grouting operation, since the placement of grout in a portion of the curtain often affects the acceptance of grout in other parts of the curtain.

When grouting in fine formations, whether these are soil or rock, gel times are often selected so as to coincide with the pumping time for each stage, rather than follow the empirical relationships previously established. This is primarily due to the fact that in such formations, pumping-pressure relationships are generally severe and the selection of longer gel times often alleviates problems which may otherwise result due to high pumping pressures.

Fig. 21 shows the results of a laboratory experiment performed to evaluate the results of two-row versus three-row grouting. Experience in the field, verified by laboratory work, indicates clearly that in linear patterns a minimum of three rows of holes is necessary in order to approach complete cut-off. In Fig. 21, the right-hand portion of the pattern was made using two rows of holes. In the stratum of fine sand and silt, average penetration was not

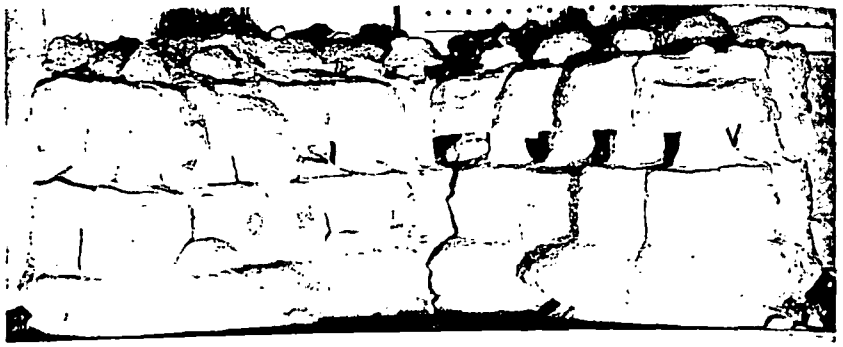

FIG. 21.—CLOSURE OF A GROUT CURTAIN BY PROPER DESIGN OF PATTERN, AND SEQUENCE OF INJECTIONS WITHIN THE PATTERN

sufficient to cause overlapping of the gel masses, resulting in fairly large open passages in this stratum. The left-hand portion of this curtain was grouted in the same fashion as the right, except for the addition of a third (central) row of holes. The photograph shows clearly that the injections in the third row, having no place else to go, were forced into the opening previously left in the least pervious stratum.

Even under the most ideal conditions that could be established in the laboratory, actual uniformity of penetration in stratified deposits may still leave something to be desired. Fig. 22 shows an attempt to make a grout curtain with a single row of holes. All of the empirical relationships previously developed for optimum uniformity were employed for these injections. In one strata, however, average penetration is quite small. In this one zone, considerable flow could still occur. Even though uniformity of penetration in all of the other strata is quite satisfactory, this curtain as a whole does not approach complete cut-off. This particular experiment clearly indicates the necessity for multiple rows of holes in curtain grouting.

Fig. 23 shows another grout curtain made under laboratory conditions. This

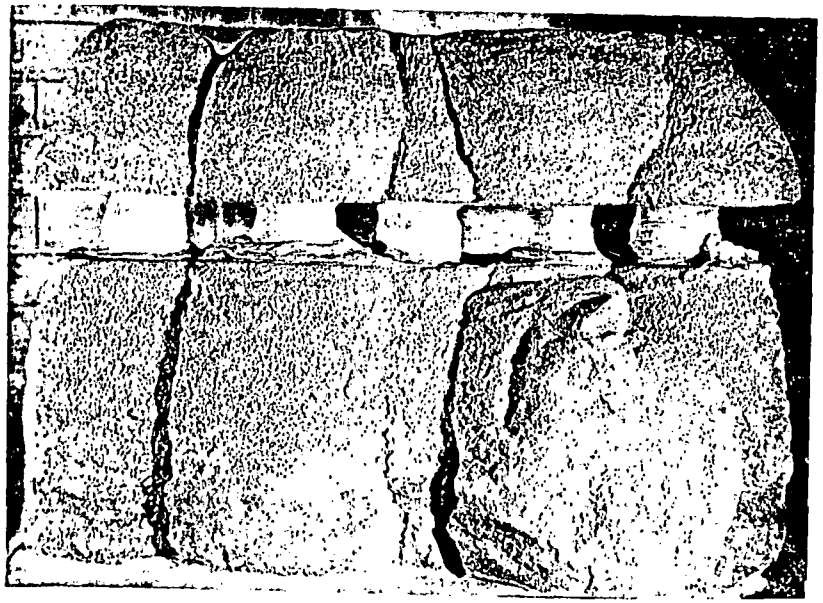

FIG. 22.—OPEN CURTAIN FORMED BY SINGLE-ROW GROUTING

FIG. 23.—GROUT CURTAIN IN FLOWING WATER FORMED BY THREE-ROW PATTERN

view is the downstream face of a three-row curtain, erected in stratified deposits under conditions of flowing ground water. Uniformity of penetration in the various strata can be seen to be good. The photograph shows two areas in which overlapping did not quite occur. Records of this particular grouting

FIG. 24.—UPPER SURFACE OF THREE-ROW PATTERN SHOWING INTERLOCKING OF SEQUENTIAL INJECTIONS

FIG. 25.—ELEVATION OF THREE-ROW PATTERN SHOWING INTERLOCKING OF SEQUENTIAL INJECTIONS

operation indicated that the pertinent holes in the center row failed to take an adequate amount of grout. In addition to verifying the utility of a three-row pattern, this particular experiment also pointed out that the keeping of complete accurate records can often enable the predication of areas in which a grout curtain did not close.

A graphic illustration of the necessity for a three-row pattern in linear grouting is shown by the photograph in Figs. 24 and 25. These are pictures of the results of grouting in heterogenous stratification, with the use of short gel times. Different colored dyes were used so that the final location of each hole could be traced. Fig. 24 is a view of the upper surface clearly showing the interlocking of the various injections. It can be seen that injections from the center row resulted in the placement of grout on the outside of the curtain, verifying the necessity for the third row of holes. In Fig. 25, though penetration is exceedingly nonuniform, the use of three rows of holes none the less resulted in a fairly tight curtain.

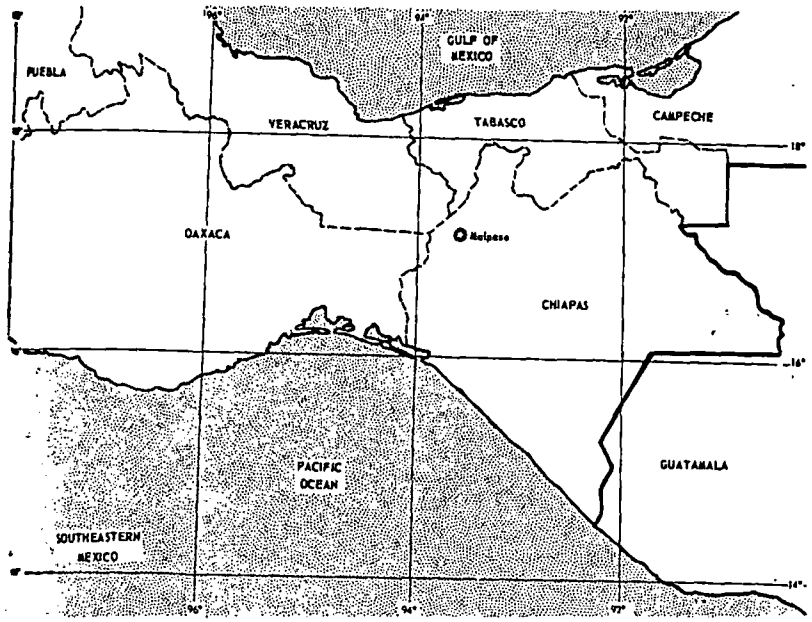

FIG. 26.—LOCATION MAP FOR FIELD GROUTING APPLICATION

Field and laboratory experience has indicated that the spacing between the outer rows of holes, and spacing between holes should be selected to form a pattern of squares. Grouting sequence is from one outer row to the other by diagonals. Thus two passes complete the outer rows. The center (third) row of holes is placed in the center of each previously formed square. Economics usually limit the spacing between holes to 5 ft or less.

In closed patterns such as a circle or square, the geometry of the pattern has the effect of providing confinement. Adequate results can generally be obtained with two rows of holes. For these cases the outer circle of holes is grouted first, working alternate holes, then filling in the spaces. The inner circle of holes is offset from the outer row by approximately half the hole

spacing, and holes in the inner row are placed between hole locations in the outer row. Sequence of grouting is to stagger holes, then fill in the gaps.

APPLICATIONS OF CHEMICAL GROUTING TECHNOLOGY

The use of the empirical procedures previously discussed is illustrated by a well documented field grouting operation.

The job was at Malpaso, Chiapas, about 500 miles SSE of Mexico City (see Fig. 26). At this location, a dam was under construction across the Grijalva River. Diversion tunnels had been built to expose the river bed in the construction area.

Although flow in the river channel was diverted, seepage was still occurring through the river bed sands. When the core area was excavated to bedrock, this seepage quickly formed a standing pool, as shown in Fig. 27. Pumps could not keep the area dry enough for construction purposes.

FIG. 27.—PHOTOGRAPH OF DAM SITE PRIOR TO GROUTING

A second excavation was made upstream in the hope that the upstream pool could contain the seepage. This left a small wall or dam between the pools. This dam, 7 m to 8 m long by about 3 m wide, was capped with concrete about 2 m thick. Seepage, however, took place through the dam, negating its purpose. Fig. 27 shows the dam, and the two pools resulting (the distant pool in which the dozer is working is the core wall area).

Grouting the dam to form a cutoff wall was attempted, with cement. However, the limited volume of the sand mass, combined with the particle size (medium to fine sand), prevented penetration. It was then decided to use chemical grout, and AM-9 was selected. Since the geometry of the curtain could not provide confining effects, a three-row pattern was dictated.

Data from which to compute an in-place void ratio was not available. Using average values for void ratios of sands, it was estimated that 25 gal per vertical ft of hole would give radial flows of 20 in. to 25 in. Accordingly, a spacing of 1 m was selected for drill holes in each row, and for the spacing between

outer rows. The third row of holes would be located in the center of the squares previously formed.

One row of holes had already been placed at about a meter apart, during the attempt at cement grouting. This row of holes became the upstream row of the chemical grout pattern. Spacing of holes in the latter two rows was more closely controlled than in the upstream row. A plan view of the location of holes in completed pattern is shown in Fig. 28.

The numbers near the drill holes in Fig. 28 represent the sequence in which the holes were grouted. It was the original intention to stagger holes in the outer rows, then fill in the outer rows, then do the center row on a stagger system. Deviations from the ideal sequence were made in the interest of expediency, to avoid long delays in completing the pattern. In the center row, holes were grouted several times; the numbers indicate the sequence of the first treatment.

Gel times during grouting were controlled by mechanical proportioning of the catalyst. Pipes were placed by jetting through previously drilled holes.

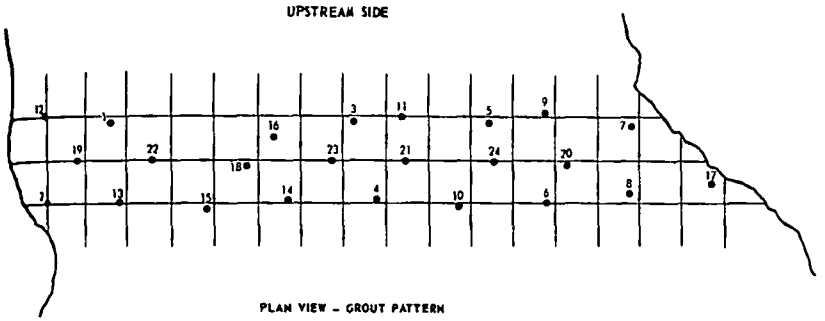

FIG. 28.—PLAN OF GROUT PATTERN FOR GROUT CURTAIN

Dye was used in all mixes for quick identification of leakages. Whenever leakage occurred, gel times were immediately shortened.

Records of significant factors were kept for each hole. A summary of these records are shown in Table 1. Of interest is that the total working time to complete the job was 51 hr, of which only 5-1/2 hr were actually spent pumping grout. It should also be noted that the average gel time is considerably shorter than the pumping time for each hole (pumping times can be found by dividing the total volume pumped by the pump rate). This relationship was deliberately maintained to improve uniformity of penetration, and keep grout travel to a minimum.

Most significant, of course, in reviewing the grouting results is the fact that the job was completely successful. During the grouting operation it became possible to pump out the core wall area. After grouting was finished, it became possible to dry the area completely.

From the complete and accurate records of the field operation, it became possible to plot the most probable location of the grouted mass resulting from each injection. By doing this, the complete grout curtain was reconstructed. In plotting the shape of the grouted mass for each injection, use was made of the following data: (1) Depth of the injection pipe; (2) number of lifts; (3)

volume pumped at each lift; (4) average radial spread of grout in sand; (5) proximity and shape of previously grouted masses; and (6) physical effects such as external seepage started or stopped, extrusion of material from other grout holes, deviations from average pressure and volume, etc.

The use of short gel times helps to insure that the grout remains near the spot where it entered the formation. The shape of stabilized masses resulting from a sequence of lifts during grouting has been established by laboratory tests under many different conditions. Some of these have been discussed in the earlier portion of this paper. It is felt that there is justifiable evidence for

TABLE 1

Hole Number	Depth Treated, in		Total Volume, in gallons	Number of Lifts	Maximum Pressure, in		Average Gel Time, in minutes	Average Pump Rate, in		Minimum Gel Time, in minutes
	meters	feet			kilograms per square centimeter	pounds per square inch		liters per minute	gallons per minute	
1	0.80	2.6	75	3	1.9	25	1.5	—	—	0.7
2	0.45	1.5	100	2	1.9	25	1.5	—	—	0.7
3	1.25	4.1	100	4	7.7	100	1.0	25	6	—
4	1.08	3.5	100	4	3.9	50	1.0	25	6	—
5	0.50	1.6	100	2	3.9	50	1.0	25	6	—
6	0.50	1.6	100	2	3.9	50	1.25	23	5.5	—
7	0.00	0.0	100	0	7.7	100	1.25	42	10	—
8	0.00	0.0	100	0	—	—	1.5	44	10.5	—
9	0.00	0.0	25	0	—	—	1.5	—	—	—
10	0.40	1.3	100	2	2.7	35	1.6	32	7.7	0.7
11	1.00	3.3	150	4	—	—	1.5	25	6	—
12	1.15	3.8	150	4	—	—	0.7	29	7	0.1
13	0.25	0.8	100	1	5.8	75	0.7	37	9	—
14	0.53	1.7	75	1	5.8	75	0.7	39	9.3	—
15	0.90	2.9	100	4	3.9	50	—	27	6.6	0.1
16	1.50	4.9	125	4	7.7	100	1.5	23	5.5	—
17	0.95	3.1	75	3	—	—	1.6	35	8.3	0.1
18	0.37	1.2	75	0	—	—	2.0	21	5.0	—
19	0.95	3.1	110	3	2.7	35	1.3	21	5.1	0.5
18	1.17	3.8	40	0	—	—	1.5	42	10	—
18	1.17	3.8	25	0	—	—	—	—	—	—
19	1.40	4.6	75	0	4.6	60	0.7	35	8.3	—
20	0.00	0.0	5	0	4.6	60	—	—	—	—
21	0.00	0.0	100	0	2.3	30	0.8	29	6.9	0.5
20	0.62	2.0	25	0	13.5	175	—	15	3.6	0.2
22	0.00	0.0	55	0	7.7	100	0.8	12	3	0.5
23	0.00	0.0	100	0	3.9	50	0.75	27	6.6	—
24	0.00	0.0	30	0	7.7	100	0.6	15	3.6	—

the shape of the stabilized masses which are constructed in Figs. 29(*a*), 29(*b*), and 29(*c*).

Figs. 29(*a*), 29(*b*), and 29(*c*) represent sections taken vertically through the grout holes in the three rows of the pattern. The sections show the concrete cap, the two large boulders which were left in place when the cap was poured, the sand through which seepage is occurring, and rock walls and bottom of the river bed. Dimensions for plotting were recorded during the drilling and grouting operation. Numbers above the cap represent the sequence in which holes were grouted. The vertical lines show the deepest penetration of the grout pipe at each hole location. The shaded area represents the grouted

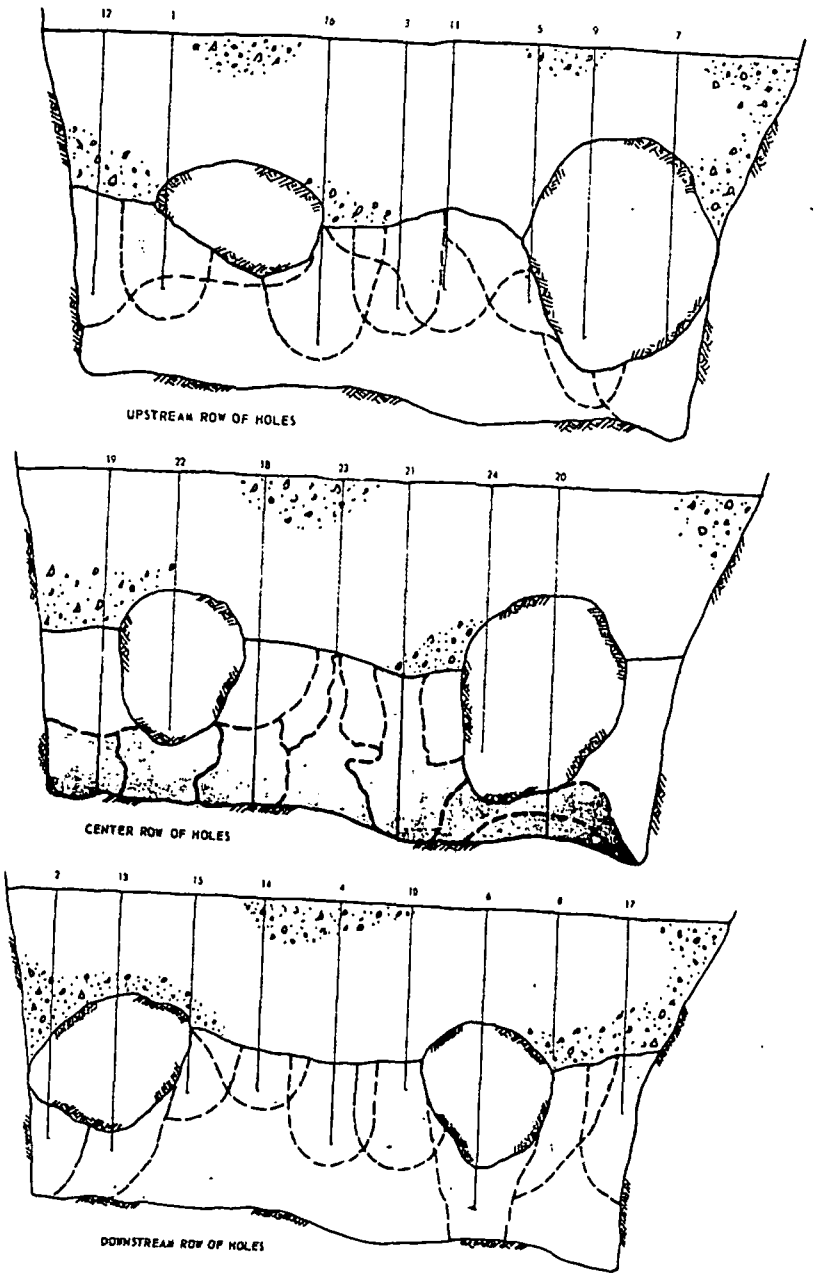

FIG. 29.—PROBABLE LOCATION OF GROUT PLACED IN UPSTREAM, DOWNSTREAM, AND CENTER ROW OF HOLES

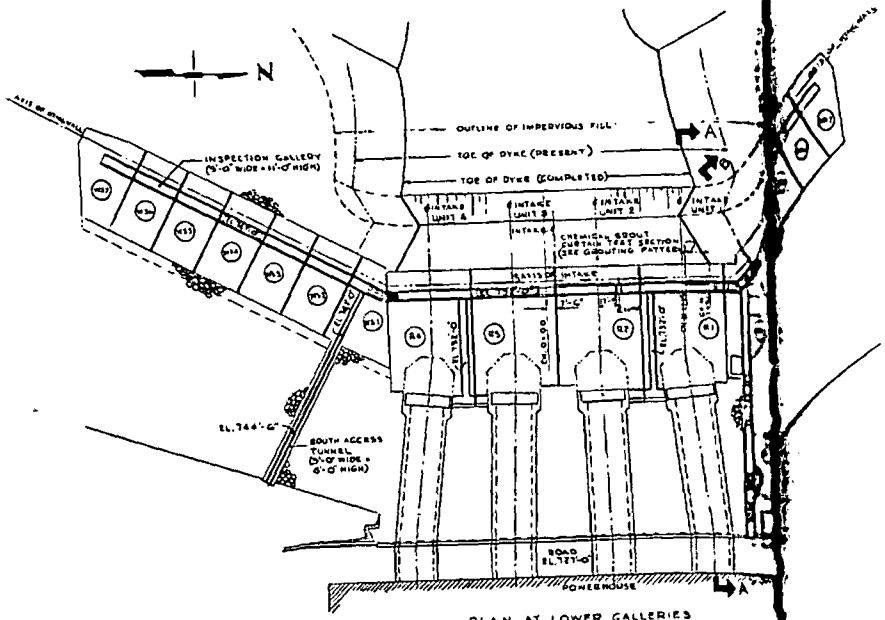

PLAN AT LOWER GALLERIES
SCALE 1" = 50'-0"

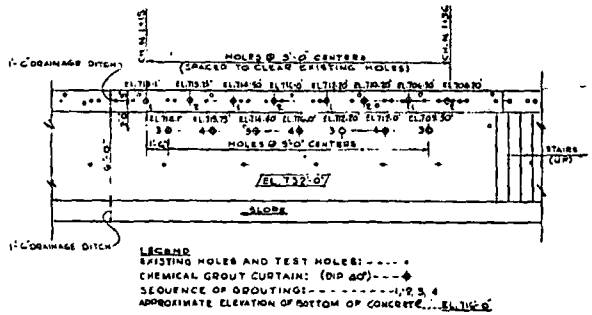

LEGEND
EXISTING HOLES AND TEST HOLES
CHEMICAL GROUT CURTAIN: (DIP 60°)
SEQUENCE OF GROUTING: 1, 2, 3, 4
APPROXIMATE ELEVATION OF BOTTOM OF CONCRETE EL. 710'-0"

GROUTING PATTERN
SCALE: 1/4" = 1'-0"

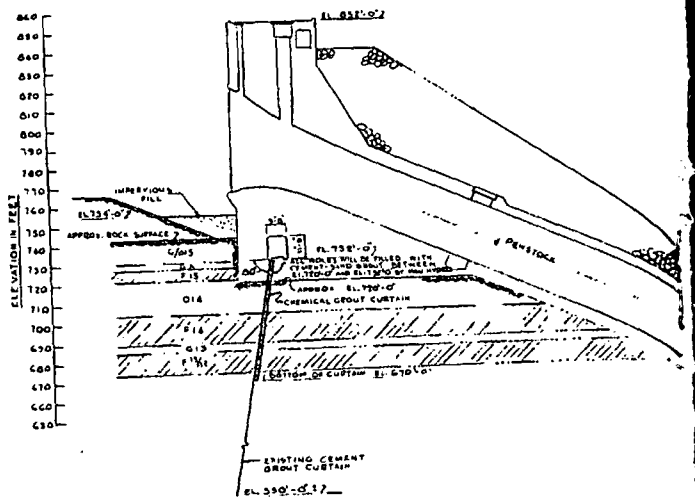

SECTION A-A
SCALE: 1" = 50'-0"

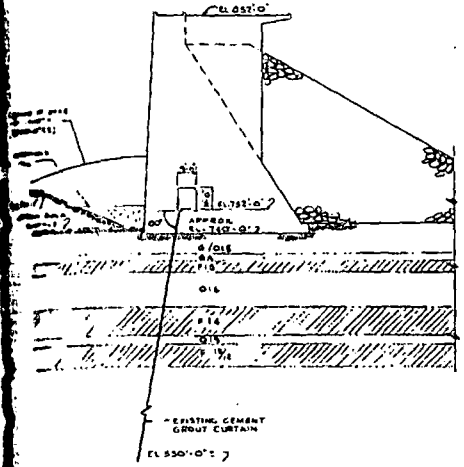

SECTION B-B
SCALE 1" = 50'-0"

NOTE:
THE FOLLOWING WILL BE DETERMINED IN THE FIELD BY THE ENGINEER:
1- EXACT LOCATION OF GROUT HOLES AND TEST HOLES
2- SEQUENCE OF DRILLING AND GROUTING

FOR SPECIFICATION PURPOSES ONLY

FIG. 30.—LOCATION AND EXTENT OF FIELD GROUT TEST PROGRAM

area. The dashed outlines around and within the shaded area represent for each hole the most probable grouted shape. These outlines were reconstructed in numerical sequence of grouting, usually the criteria previously cited.

Sections of the outer rows indicate clearly that a considerable portion of the vertical profile in the sand remained ungrouted. This, of course, was also indicated during the field operation by the records of pipe penetration. For this reason, it was imperative that holes in the center row reach bedrock. Care was taken to insure that half of them did. In several cases, specifically holes 18 and 19, it was necessary to treat the hole several times, from the top down, in order to be able to place a grout pipe to bedrock. This accounts for the extra stabilized shapes shown for those holes.

The open area shown within the sand mass in the center row represents a soil volume which the grouting records indicate as most probably stabilized by previous injections in the outer rows.

The cross section of the center row has been drawn to indicate complete stabilization down to bedrock. This is, of course, the most desirable condition. Its attainment is inferred primarily from the records of pumping pressure and volume, coupled with location of the grout pipes in this row and in the outer rows.

TABLE 2

Hole Number	Elevation, in feet		Water Test, in		Grout Volume, in gallons	Pump Time, in minutes	Pump Rate, in gallons per minute	Grout Take, in gallons per foot	Gel Time, in minutes	Pumping Pressure, in pounds per square inch
			gallons per minute	pounds per square inch						
24	12.0	28:5	3.24	90	37.8	14	2.70	2.29	16	90
24	28.5	44.5	7.08	90	182.5	44	4.15	11.40	46/22/13	90
29	12.0	40.0	6.11	90	90.5	22	4.11	3.23	11	100
30	12.0	40.0	3.89	90	47.4	23.5	2.02	1.69	9	100
31	12.0	40.0	2.49	90	41.1	22	1.87	1.47	9	100
32	9.5	28.5	0.00	90	(Test Hole)					
32	28.0	39.0	0.06	90						

Another example of the field use of the principles of chemical grouting technology is taken from an ACC intercompany communication. This report deals with two grouting tests conducted for Manitoba Hydro at the site of their Grand Rapids Generating Station dam in Hybord, Manitoba. The purpose was to establish procedures for chemical grouting in the event that seepage should occur during or after filling of the reservoir.

Both tests were conducted in the intake gallery, in February and March, 1964. The first, consisting of a three-row, 23-hole pattern, was done in a sinkhole area which had previously been heavily grouted with cement. Lack of data on void percentages, coupled with low pumping pressure limitations, resulted in placement of insufficient grout quantities for the hole spacing, and, therefore, only partial cutoff. Details of the location and extent of the first test grouting program are shown in Fig. 30.

Procedures for the second test were modified and unified on the basis of experience with the first test. This work resulted in a virtual total cutoff, and verified completely the effectiveness of AM-9 for curtain wall grouting under existing ground water conditions. Of interest is the use of the second test grouting program for the purpose of determining in-place void ratio.

Following the completion of the first grout program, five additional holes were drilled and grouted at 25-ft intervals along the intake gallery to the southern site of the sump. The purpose of these holes was to compare grout acceptance in the F-14 stratum in a relatively undisturbed area remote from the heavily cemented sinkhole area where the first test was conducted. Holes 24 through 28 were drilled and grouted to a final depth of 44-1/2 ft in two stages covering the O-14 and F-14 strata, respectively. Grout acceptance in these holes was more than the average acceptance in the first grout program. For this reason and since results from the first grout program were somewhat inconclusive, further testing was carried out in the vicinity of hole 24. The new grout pattern would also use three rows of holes. Spacing between the holes and outer rows, however, would be reduced to 2 ft. Maximum extent of the program would be eight holes, three in each of the outer rows and two in the center. Grouting results were to be assessed after grouting the first two holes in each of the outer rows. This would be done by testing the center row hole within the four grout holes. If satisfactory results

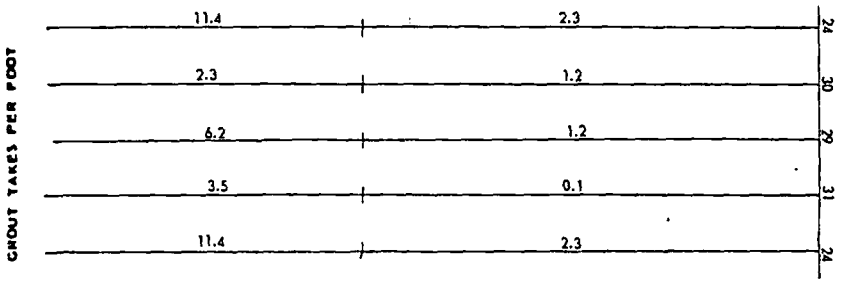

FIG. 31.—RECORD OF GROUT TAKE PER VERTICAL FOOT OF HOLE

were obtained, the second grouting program would be considered complete at this point. Details of grouting pressures and takes are shown in Table 2 for holes 24, 29, 30, 31 and test hole 32.

The grout placed in the second pattern is shown in Fig. 31, in terms of volume placed per vertical ft of hole. The average volume per ft of hole is 5/6 gal, more than twice the value of 3/8 gal in the first pattern. There were, however, very large differences in take between the O-14 and the F-14 strata.

In all respects, grouting in this second program was carried out under uniform conditions of pressure testing, depth of stage, grout pressures and gel times. For this reason, it was possible to relate a significant decrease in take per hole with the sequence of grouting. This is shown clearly by Figs. 32 and 33, which represent horizontal sections through the O-14 and F-14 strata, respectively. The sections show the most probable spread of grout, based on the recorded takes, and an assumed void ratio. The most probable value of in-place ratio was found by trial and error plotting, as the maximum value which would result in substantial pattern closure. The criterion of pattern closure is valid since water testing in hole 32 had verified that takes were reduced several orders of magnitude. The void percentages

obtained by trial and error plotting were 5% for stratum O-14 and 20% for stratum F-14. Actual void percentages would be equal to or less than those obtained by this method. (These values are representative of an area relatively free from disturbance due to washing and cement grouting).

Hole 32 was drilled in the center of the grouted area and water tested at 90 psi. Take in the O-14 stratum was 0.00 gpm and 0.062 gpm in the F-14 stratum. This latter figure corresponds to 0.0054 gpm per vertical ft of hole, and a formation permeability of 1.2×10^{-6} cm per sec. (Pregrouting formation permeabilities in the test section were as high as $1/6 \times 10^{-4}$ cm per sec.)

Since hole 32 was for practical purposes ungroutable, and therefore, redundant in the pattern, it follows that the spacing between holes and rows could probably be increased without loss of efficiency. However, the effectiveness of the cutoff is related to ground-water conditions existing during the test period. These conditions will change as the reservoir is filled.

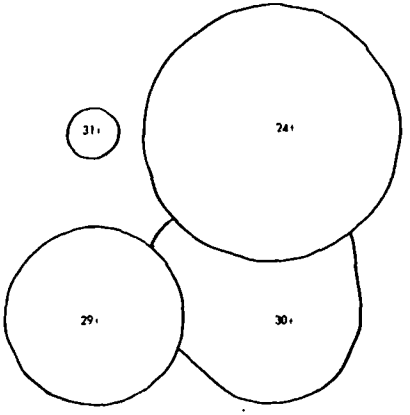

FIG. 32.—TRIAL DRAWINGS BASED ON GROUT TAKE ESTABLISH EXISTING FORMATION VOIDS IN UPPER STRATUM

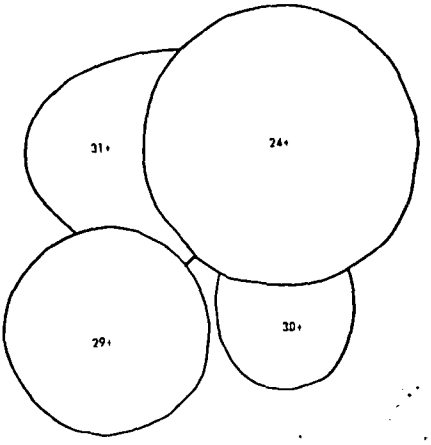

FIG. 33.—TRIAL DRAWINGS BASED ON GROUT TAKE ESTABLISH EXISTING FORMATION VOIDS IN LOWER STRATUM

CONCLUSIONS

The high cost of chemicals, as compared with clays and cements, requires a different engineering approach to their use in the field as grouting materials. The result is the development of techniques designed to obtain the utmost benefit from a limited volume of grout. This can be accomplished only if the physical location of the grout in the formation is known with reasonable certainty. The procedures necessary for proper application of chemical grouts are often diametrically opposed to those which are used with suspended-solids grouts. These procedures have, in the past decade, been assimilated into a rapidly growing core of knowledge, which is forming the basis for a new chemical grouting technology.

COPPER HYDROMETALLURGY

A Review and Outlook

By Franklin D. Cooper

information circular 8394

UNITED STATES DEPARTMENT OF THE INTERIOR

BUREAU OF MINES

This publication has been cataloged as follows:

Cooper, Franklin D

Copper hydrometallurgy: a review and outlook. [Washington] U. S. Dept. of the Interior, Bureau of Mines [1968]

18 p. (U. S. Bureau of Mines. Information circular 8394)

Includes bibliography.

1. Copper. I. Title. (Series)

TN23.U71 no. 8394 622.06173

U. S. Dept. of the Int. Library

CONTENTS

COPPER HYDROMETALLURGY

A Review and Outlook

by

Franklin D. Cooper[1]

ABSTRACT

This Bureau of Mines study reviews current and proposed methods of ...ecting copper from sub-mill-grade ore by leaching. The amount of copper ...ced by hydrometallurgy has increased dramatically in recent years and ...robably be about 200,000 tons per year by 1970.

INTRODUCTION

...opper hydrometallurgy--the leaching of siliceous low-grade copper-bearing ...nd waste rock that cannot be processed economically by milling and con-...ating--is an important low-cost process for recovering copper. In the ...orld, the United States is the principal user of this process, and in ...early 10 percent of the U.S. production of primary copper came from dump ...-situ leaching of sub-mill-grade material. In the free world, including ...ited States, such leaching accounted for 150,000 tons annually, or 3 ...of the 5-million-ton total for primary copper produced in the mid-... The production of primary copper by leaching is expected to increase ...d by 1975.

...the United States, the production of primary copper by dump and in-situ ...of sub-mill-grade material increased 359 percent from 28,531 short ...1946 to 131,000 tons in 1965. All other primary-copper production ...some heap and vat leaching, but principally milling and concentrating ... increased 122 percent from 608,737 short tons in 1946 to 1,351,734 ...1965. This report reviews the methods currently in use or under study ...ited States for the recovery of copper by hydrometallurgy.

CHEMISTRY OF LEACHING

...rous sulfate and sulfuric acid slowly form when water containing dis-...air contacts broken rock containing pyrite. In the presence of addi-...ygen and sulfuric acid, ferrous sulfate is slowly oxidized to ferric ... Several strains of oxidizing bacteria not only thrive in high-acid

...al scientist, Division of Mineral Economics, Bureau of Mines, ...gton, D.C.

copper solutions but accelerate the oxidation of sulfide minerals to form a and soluble copper and iron sulfate. Thiobacillus thiooxidans bacteria o:i- izes the oxidation of the sulfur to form sulfides as their energy source, and Thiobacillus ferrooxidans oxidizes ferrous iron to ferric iron. These bacte- rial strains complement each other in that the former produces acid which keeps the ferric iron produced by the latter in solution. This forms acidi fied ferric sulfate, a powerful lixiviant for copper minerals.

Leach solutions containing acid only can dissolve most of the oxide- copper minerals. When such minerals are leached in the absence of pyrite, sulfuric acid must be added to the leach solution in amounts ranging up to five times the weight of copper dissolved.

In the presence of dilute sulfuric acid and ferric sulfate, all copper minerals are dissolved although some minerals are dissolved slowly, often at a rate of only 1 percent per month.

Recent studies by the Bureau of Mines on chalcopyrite, the principal copper mineral in most porphyry-copper mine waste dumps, show that the dissolution rate increases twentyfold if chlorine or sodium hypochlorite is added to conventional sulfiric acid leaching solutions.

FACTORS FOR SUCCESSFUL LEACHING

The factors necessary for successful leaching follow:

1. The materials to be leached should have a low content of acid-consuming gangue and basic minerals.

2. The copper-bearing minerals must be in thorough contact with the leach solution.

3. The copper in the solution filling the interstitial space must be maintained at a low concentration to speed the diffusion of the high-copper-content solution from the voids of the rock particles.

4. The surfaces of the particles should be sequentially wetted and dried to increase contact with oxygen and to bring the pregnant solution from the voids of the rock particles by capillary action.

5. The acid concentration in the leach solution should be adjusted to attain a minimum dissolution of iron while obtaining a maximum copper loading.

UNDERGROUND LEACHING

Conventional

Underground in-situ leaching is used in areas surrounded by tight and impermeable rock to dissolve copper from fractured rock and the gob remaining after the termination of mining by block-caving or other methods.

Worked-out stopes in deep mines are either flooded with barren leach tion or are permitted to fill with indigenous acidic mine waters. Sub- capping remaining above worked-out block-caving sites is supplied with ching solution distributed by gravity from ponds and drill holes.

The pregnant solutions produced by underground leaching during a 5- to nth-contact period are usually collected in abandoned adits and pumped to rage ponds on the surface adjacent to the copper-precipitation equipment. retention of pregnant solutions in these ponds partially removes slimes clay originating in the gob left after mining and from the mill tailings for the backfilling of stopes.

The Anaconda Co. uses a flocculent and either inclined or vertical thick- to remove solids and colloidal matter from waters pumped from the Moun- Con and Steward underground mines before applying the clarified mine ers plus added acid to the Berkeley leaching dumps.

Project Sloop

In October 1967, the Kennecott Copper Corp. disclosed details of a pro- made to the U.S. Atomic Energy Commission for a joint experiment called ject Sloop in which a low-grade copper ore deposit near Safford, Ariz., d be fractured by a contained underground nuclear explosion prior to itu leaching.

The total cost of the three phases of the experiment is estimated at 9,175,000. Phase 3, a 3-year study costing $6,675,000, would use 2,600 gal- of leach solution each minute following underground reentry and rehabili- ion activities. In phase 3, industrial radiological safety problems would ive major attention while concurrent investigations would include the ination of solvent extraction methods, the electrolysis of solutions of t copper in sulfuric acid, and conventional smelting and electrorefining ods.

The experiment, if approved, could result in a new mining technology in the surface is left undisturbed and the expense and large amounts of involved in the conventional mining of waste material and ore are inated.

If Project Sloop proves feasible, the estimated 75 million short tons of r contained in U.S. ores averaging 0.86 percent copper could be supple- d by another 58 million short tons of copper in minus 0.47 percent rial.

Estimated Costs for Nuclear Fracturing and In-Situ Leaching

Preliminary calculations indicate that the direct average total cost for lear fracturing alone would be 12.8 cents per ton of ore fractured using a kiloton device, and 55.2 cents per ton using a 10-kiloton device. It may conomical to use nuclear fracturing and recovery by in-situ leaching for osits containing as little as 4 pounds of recoverable copper per ton of

material. Copper production could begin in less than one-half the time required by conventional mining methods.

The estimated capital expenditure for copper precipitating facilities alone ranges from $1,000,000 for a 10-million-pound annual capacity to $200,000 for a 1-million-pound annual capacity.

The estimated cost of copper production during a 10-year leaching operation following nuclear fracturing ranges from 17.0 cents per pound of copper produced by a 10-million-pound annual operation to 24.4 cents by a 1-million-pound annual operation. To these costs must be added the cost of the nuclear fracturing of the deposit, which may range from 0.8 to 13.8 cents per pound of recoverable copper depending on the copper content in each ton of ore and the yield of the nuclear device used.

A report issued in 1959 by the Colorado School of Mines Research Foundation included the following estimated costs related to a hypothetical situation for nuclear fracturing and in-situ leaching of a 450-foot-thick, 50-million-ton ore body:[2]

Atomic device in place	$3,500,000
50,300 feet of leach solution input holes	1,800,000
Rubber-lined pumps and pipes	285,000
Installation cost	220,000
Development of one shaft and 45,000 feet of lateral work	2,327,000

No estimated costs were shown for the cementation equipment and its ancillary facilities.

The complete evaluation and economics of a nuclear-fracturing and leaching operation await the completion of a full-scale test to determine the percolation rate of solution, the copper-recovery rate, the cost of radiation safety measures, and the time for radioactivity decay to reach a level permitting safe leaching and copper processing.

DUMP LEACHING

Sub-mill-grade waste rocks overlying some copper ore deposits have been depleted of copper by the action of bacteria, owing to gradual oxidation of the sulfide-copper minerals and leaching. Much of this soluble copper has been carried by water downwards hundreds of feet to enrich sulfide-copper ore deposits.

The sulfide-copper content in the waste ranges from cutoff grade to [illegible] at any particular mine; however, the oxide-copper content of some waste may be greater.

More than 60 percent of the solids produced in U.S. copper mines are discarded either because their copper content is below milling grade or they [illegible]

[2]Mining World. Atomic Blasting for Mining. V. 21, July 1959, pp. 31-33.

amenable to flotation treatment. Most of this waste is generated at surface mines where in 1966 over 0.37 billion short tons were added to an existing accumulation of 5 to 10 billion short tons.

The leaching of some waste dumps is hindered by the slow dissolution rate of some iron-copper sulfide minerals and by the cementing and coating of the waste surface by iron precipitates and clay.

A process developed at the Kennecott Research Center has won U.S. Patent 3,330,650.[3] The process will be used to purify a portion of the solution from the precipitation plant by removing aluminum and regenerating sulfuric acid. Iron is removed from the other portion of the solution by a change in pH. The two purified solutions are recombined to form the optimum composition for extracting copper from the mine waste.

Pregnant solutions are pumped to storage ponds located near the copper precipitation equipment. In several situations, bentonite or plastic film has been used to line the bottom and sides of storage ponds to prevent seepage.

Copper recovery by dump leaching in any one year is not proportional to the copper content of the leachable sub-mill-grade rock placed on leaching dumps in the same year. This is because time is required for some of the copper and iron minerals to oxidize enough to produce a condition favorable to leaching. Leaching continues for many years after the last of the leachable rock has been mined from an open pit.

In 1964, 125,000 short tons of copper were recovered by dump leaching. This recovery required the processing of about 42,000 U.S. gallons per minute (60 million U.S. gallons per day) of solutions averaging about 1.5 grams copper per liter (12.5 pounds copper per 1,000 U.S. gallons).

In 1965, 14 large copper-leaching operations produced pregnant solutions containing 1 to 12 ppm U_3O_8 (4 ppm average). Six of the mines, producing half of the total leach solution, had an average grade of 10 ppm U_3O_8, which is equal to 1,600 pounds of U_3O_8 per day. With the completion of expanded copper-leaching operations in the next few years, as much as 6,000 pounds of U_3O_8 a day may be available from these sources.

CEMENTATION EQUIPMENT

As recently as 1965 most of the conventional cementation (copper-precipitating) equipment comprised either gravity, rotating drum, or activated launders, most of which had substantial labor requirements. The colloidal-copper particles precipitated in rotary drum launders added to the operational problems and costs.

---

[3] Merley, S. R., E. E. Malouf, J. D. Prater, and A. K. Schellinger (assigned to Kennecott Copper Corp.). pH Adjusted Controlled-Iron-Content, Cyclic Leaching Processes for Copper-Bearing Rock Materials. U.S. Pat. 3,330,650, July 11, 1967.

The Kennecott Copper Corp. recently eliminated these disadvantages in its operations by the development of a new cementation system. Operating experience with this system demonstrated that the application of kinetic principles results in an easily filtered, 90- to 95-percent-copper product, using less scrap iron for each pound of copper precipitated than in the conventional equipment. This high-capacity system features automatic control and mechanized material handling. By use of the new continuous and self-cleaning system, 99 percent of the copper is precipitated from solutions containing 0.4 to 4.0 grams copper per liter.

The Phelps-Dodge Corp. recently developed a V-trough precipitator for use at Bisbee, Ariz., which uses sponge iron to precipitate the major portion of the copper in solutions produced by dump leaching. Scrap iron precipitates the remaining soluble copper and filters fine-grained cement copper from the partially decopperized solution.

The V-trough precipitator minimizes the former caking and blinding problems encountered when using sponge iron in static launder-type precipitators.

CONSUMPTION OF IRON AND SULFURIC ACID

The consumption of iron and sulfuric acid is a major factor affecting the cost of leaching, followed by precipitation of soluble copper by scrap iron or sponge iron.

A high acid content in pregnant solutions increases the consumption of iron in the precipitation equipment, while a high acid content in the leaching solutions applied on the dumps increases the consumption of acid by gangue or basic minerals.

Generally, during the leaching of sulfide-copper minerals in waste dumps, 16 to 17 pounds of iron equivalent is precipitated on the broken solids from each 1,000 U.S. gallons of leach solution applied. Collectively, this iron equivalent is derived from the iron used for cementation and the iron dissolved by passage of solution through the waste solids. The precipitated iron, a slimy mixture of basic ferric sulfates and ferric hydroxide, often contains clay, elemental sulfur, and bacteria. At some dumps, where the leach solution is supplied from a covering pond, it is necessary to periodically rake and remove the settled slimes on the bottom of the pond to maintain uniform percolation.

Acid

Several large leaching operations use sulfuric acid produced nearby from waste smelter gases, whereas a few smaller leaching operations use acid made from elemental sulfur or pyrite concentrate. Small amounts of suspended iron sulfates and other impurities in the acid used for leaching are not objectionable.

Sponge Iron

Sponge iron is used in one cementation system as the principal precipitant, supplemented by detinned cans as the final precipitant. However, the static beds of sponge iron become cemented and caked, and the surface of the iron quickly becomes coated with copper. This prevents further contact of the iron with the solution. The Phelps-Dodge Corp. eliminated this problem by the development of a V-shaped precipitation vessel so designed that the input solution levitates and abrades the sponge iron particles.

Based on the consumption of iron, the V-trough precipitator using sponge iron is as efficient as conventional precipitation equipment using detinned cans.

Sponge iron is used advantageously by another copper producer for the leach-precipitation-flotation (LPF) processing of an ore containing about equal amounts of oxide- and sulfide-copper. The resultant cement copper and the nonreacted portion of sponge iron comprise a portion of the solids processed in the sulfide-copper flotation recovery circuit.

Sponge iron is usually produced by the consumer, using pyrite concentrate recovered from mill tailings as the feed material that is roasted to produce a calcine. Reduction of the calcine yields a product containing up to 75 percent total iron, including 35 to 50 percent metallic iron. The cost of producing sponge iron in a 100-ton-per-day plant in 1958 was about $13.60 per short ton ($34 per short ton of contained metallic iron).

In 1963, the Phelps-Dodge Corp. developed a process for producing sponge iron from high-iron-content converter slag. The molten slag is granulated in a water bath and, after drying, is reduced by a countercurrent stream of reformed natural gas to yield sponge iron. This product contains 55 to 60 percent metallic iron and up to 5 percent copper that is recoverable in the cementation process.

Kennecott's Western Mining Division prevents the reoxidation of the hot reduced sponge iron by the presence of incandescent coke during its discharge from the reduction vessel and during the cooling cycle.

Scrap Iron

Scrap iron, having a low carbide content and a large surface-to-weight ratio, is almost universally used for precipitating copper from solutions even though it is expensive and is in short supply in some localities. Scrap cans must be burnt to remove coatings before shredding. One Utah copper producer now uses the product from a nearby plant that shreds 350 tons of steel scrap in 8 hours.

Theoretically, 1.00 pound of iron will replace 1.37 pounds of copper in acid solution. In actual operations, 1.3 to 4.0 pounds of metallic iron are consumed for each pound of copper precipitated from solution because of the formation of ferrous sulfate by the dissolution of scrap iron by both acid and ferric sulfate.

Scrap iron does not reduce the copper content in 1 liter of solution to less than 60 milligrams unless the reactants are agitated.

COST DATA FOR CONVENTIONAL PRACTICES

General

The total cost for producing copper by in-situ leaching, cementation, and subsequent conventional smelting and electrorefining is generally 5 to 15 cents a pound lower than for copper produced by the conventional open-pit mining, milling and concentrating, and smelting and electrorefining route.

The cost of labor directly related to the leaching and cementation operation is about one-tenth the value of the copper recovered by this method.

One gallon of cupriferous solution flowing continuously for 1 year and yielding 1.0 gram of copper from each liter of solution (8.3 pounds from each 1,000 U.S. gallons) will supply 4,380 pounds of copper having an annual value of $1,664, based on copper at 38.0 cents per pound. The total direct cost of leaching and precipitating copper from solution is less than 10 cents per pound.

Peruvian Mine Waters

Based on a Peruvian operation in the early 1960's, the operating cost for cementation only was 3.0 + 1.25/q cents per pound of copper precipitated, where q = copper content in grams per liter of pregnant solution. This low cost is attributed to small expenditures for labor, power, and equipment, and a low ratio of dissolved iron to copper.

In-Situ Leaching in Arizona

At one U.S. operation 9,000 short tons of copper equivalent is currently produced annually by the in-situ leaching of waste rock and ore remaining after the termination of block-caving mining. The copper is precipitated from solution, in the form of cement copper containing 70 to 80 percent copper, by scrap iron.

The approximate costs of inputs in cents per pound of contained copper recovered follow:

Labor	0.93
Acid	3.25
Iron	3.36
Pumps and piping	.08
Electricity	.28
Total	7.90

Additional expenditures to cover amortization, freight, maintenance, overhead and general expense, insurance, and taxes increase the total cost of leaching and cementation to about 10 cents per pound of recovered copper.

Cost of Marketable Copper From U.S. Dump Leaching

In several operations of varied capacity the total production cost of refined copper, originating from the dump leaching of waste rock principally containing sulfide-copper minerals or of selected waste rock and sub-mill-grade ore principally containing oxide-copper minerals, ranges from 13 to 2 + 1.25/q cents per pound, where q = copper content of the pregnant solution in grams per liter.

These total production costs include amortization, freight, operation and maintenance expenses, refining and marketing, general company expense, fringe benefits, insurance, taxes, and safety.

The production cost is near the high side of the range for one Arizona operation where oxide-copper minerals mixed with calcite are leached by solutions containing up to 5 pounds of added sulfuric acid, made from Gulf States elemental sulfur, for each pound of copper recovered. The consumption of shredded cans for precipitation in such an operation is often as much as 3 to 4 pounds per pound of copper recovered because of the greater dissolution of iron-bearing minerals during dump leaching.

SOLVENT EXTRACTION OF LEACH SOLUTIONS

Ideology

In recent years, much attention has been given to the production (in marketable condition) of the copper extracted during the leaching of waste copper minerals without recourse to cementation followed by conventional smelting and refining.

The ideal process would include solvent extraction of the copper from low-content pregnant solutions followed by stripping of the copper from the solvent by a sulfate-sulfuric acid solution. This would produce an acceptable low-iron-content feed solution for electrolytic cells, preferably containing a minimum of 10 to 25 grams copper per liter of solution.

The solvent should be selective for copper--but not for iron--at the natural low pH of the pregnant solution. The solvent should have low water solubility and should be nontoxic to those bacteria beneficial to the leaching process. The solvent should be stable at 0° to 80° C but not detrimental to the electrolytic process. The active reagent in the solvent mixture should be compatible with a cheap diluent, such as kerosine.

The solvent extraction of pregnant solutions containing insoluble material is not feasible even though low pH significantly decreases emulsion formation.

A low solvent loss is important in making any product selling for less than $1 per pound since only a few cents per pound of metal recovered can be allowed for lost solvent. Where aqueous solutions are very dilute, this cost rules out solvent extraction entirely because even a trace loss of solvent is unfavorable.

The problem of organic losses is further clouded by the lack of a simple analytical method to determine how much of the costly reagent is lost by entrainment and solution in the raffinate. Other questions bearing on the subject involve the change of copper-loading capacity, the degradation of the active compounds during long use, and the destruction of bacteria, beneficial in the oxidation of copper-sulfide minerals in the waste dumps, by organics contained in the recycled raffinate.

Carboxylic Acids and Naphthenic Acid

Carboxylic acids and naphthenic acid are cheap solvents for extracting copper from low-iron-content solutions with pH above 4.0 and 6.0, respectively. A modified carboxylic acid, α bromo lauric acid, can extract copper at 3.3 pH because of its more acidic character.

All carboxylic acids have the disadvantage that the hydrogen ions produced in amount stoichiometrically equivalent to the metal recovered during extraction must be neutralized. Even when using limestone, as it seems possible to do with α bromo lauric acid, the cost of alkali would be unacceptable when recovering copper from leach solutions containing free acid. In one investigation using naphthenic acid as a solvent, the cost of the naphthenic acid was 0.14 cent while the cost of the alkali (as caustic soda) was 5.6 cents per pound of copper recovered.

LIX-63 Reagent

A few years ago, General Mills, Inc., developed LIX-63 reagent,[4] an α hydroxime specifically useful for extracting copper from solutions produced by the conventional ammoniacal leaching of oxide-copper ores (in closed vessels). This reagent has a low solubility in water and a high specificity for copper but, because it cannot extract copper below 3.0 pH, it is not applicable for extracting solutions resulting from waste dump leaching.

LIX-64 Reagent

More recently, General Mills, Inc., developed another reagent, a mixture of 2-hydroxbenzophenoximes, known as LIX-64. The $2.50-per-pound reagent diluted with nine volumes of kerosine, in countercurrent, four-stage contact with a typical dump leach liquor, attained a loading of 2.42 grams copper per liter of solvent mixture. The raffinate contained 0.03 gram copper per liter. Copper extraction exceeded 96 percent despite the decreased extraction efficiency caused by a decrease of pH during extraction.

The extractive power of this solvent mixture ranges from very strong for Cu^{+2}, slight for Fe^{+3}, very slight for Mo^{+6} and V^{+4}, to nil for other metallic ions.

In early 1967, pilot plants using 6 to 7 volume-percent LIX-64 in kerosine as solvent were operating near the Bagdad, Esperanza, and Inspiration

[4]Reference to specific brands is made for identification only and does not imply endorsement by the Bureau of Mines.

mines. Based on 1,000 U.S. gallons of pregnant leach solution processed, the organic-solvent loss at Bagdad in a system operating at 50° C was 0.139 gallon and was valued at 1.7 cents per pound of copper recovered; at Esperanza the loss was 0.10 gallon.

Bagdad Copper, in a joint venture with the Chemetals Corp., plans to make copper powder by hydrogenating the copper-acid solution produced by stripping the loaded solvent. In March 1967, Esperanza made its first 40-ton shipment of cathode copper from a four-cell electrolysis installation in which only 10 percent of the copper was plated out of electrolyte containing 50 grams copper per liter.

Cost Estimates Using LIX-64 Reagent

Recently published cost estimates were based on laboratory and pilot plant studies using a solvent mixture of LIX-64 reagent diluted with nine volumes of kerosine to extract leach solutions containing 1.0 to 2.0 grams of copper per liter (8.3 to 16.7 pounds per 1,000 U.S. gallons). The loaded solvent was then stripped to produce solutions suitable for electrowinning.

One estimate shows the cost of solvent extraction facilities alone as $420,000 for a plant capable of recovering 10 tons of copper per day from about 2 million gallons of solution. Depreciation charges would range from 1.56 to 0.70 cent per pound of copper recovered. A full-sized extraction plant for handling 3,300 gallons per minute of leach solution at Bagdad was estimated at $1,980,000.

Estimated operational costs, in cents per pound of copper contained in the feed electrolyte supplied to the electrowinning section, follow:

Solvent loss[1]	1.0-2.5
Stripping acid	.1
Scrubbing	.0- .2
Power, 1 kwhr	1.0
Total[2]	2.1-3.8

[1] 0.05 to 0.12 U.S. gallon per 1,000 U.S. gallons of solution extracted.

[2] The total cost at the high end of this range is about equal to the cost for the scrap iron used to precipitate 1 pound of copper in conventional practice where the consumption of scrap iron is about 1.5 pounds and the delivered cost of scrap iron is $50 per short ton.

The cost for producing cathode copper from the copper-acid electrolyte is estimated as equal to or less than the processing cost of cement copper in a typical operation.

Once the economics of the solvent extraction of copper have been stabilized it is probable that commercial plants will be designed using processes similar to those used in modern uranium solvent extraction plants.

Smaller copper producers are more interested in the prospects of LIX-64 than are the major firms. The high cost of conventional smelting and electrorefining seems to be the major incentive toward attaining an economical solvent extraction process.

In October 1967, Ranchers Exploration and Development Corp. announced plans for a commercial installation comprising solvent extraction and electrowinning facilities. The 5,400-ton-per-year-capacity electrolytic section of this plant was to be installed near Miami, Ariz., at a cost of $3.5 million. The copper-acid feed solution to be processed by this facility originates from the solvent extraction of pregnant solutions produced by leaching ore loosened by ripping and placed on leaching sites.

ION-EXCHANGE RESINS FOR COPPER RECOVERY

Cationic carboxylic-type resins are the most promising with regard to selectivity and absorption capacity for stripping solutions partly decopperized by cementation. However, these resins have the disadvantages of being degraded mechanically and of being fouled by iron and aluminum ions.

MISCELLANEOUS RECOVERY PROCESSES

Demand for Nonmassive Copper

Sales of copper powder in the United States in 1965 totaled 31,200 short tons, including 1,870 tons of flake copper alloy and 936 tons of flake copper used as pigments and antifouling agents. Copper powders, selling for about 15 cents per pound more than the massive material, are generally made by atomization of molten metal, by the hydrogen reduction of copper oxide, and by precipitation from either acid or ammoniacal solutions. Two novel leaching processes described below were devised to supply some of the increasing demands for copper powder and copper oxide.

Banner's Oxide Process

One new test facility was being constructed in mid-1966 by the Banner Mining Co. in Arizona at a cost of $500,000. This venture will provide operational data useful in the construction of commercial mills using Banner's oxide process to recover copper from limestone-bearing copper ores. Ore, ground only to 10 mesh to prevent sliming, will be processed in a 60-foot counterflow drum using sodium hydroxide as one of several alkaline reagents. The amphoteric nature of copper allows it to react as either an electropositive or electronegative ion. As developed, Banner's oxide process can produce refined copper either by direct chemical processing or by electrorefining.

Hydrogenation Process

Another new process employs the hydrogen reduction of a copper solution to produce copper powder or copper oxide. Since June 1966, Arizona Chemcopper Corp. has operated a $3,350,000 plant capable of producing 8,250 tons of contained copper annually in the form of copper oxide and of copper powders and briquets.

Copper for this plant originates in the heap leaching of oxide-copper ock. Cement copper, produced by the precipitation of copper from pregnant olutions by scrap iron, is leached in an oxygen-enriched, buffered, ammonium ulfate solution. The iron content in the leach solution is allowed to build p to 15 to 20 grams per liter to accelerate the leaching rate at 2.0 pH and 0° to 200° F. The resulting pregnant solution is filtered and then auto-laved at 425 psig and 250° to 280° F in the presence of hydrogen produced rom reformed natural gas. Sulfuric acid is regenerated and copper powder is ormed during the reduction step. Polyacrylic acid is added during autoclav-ng to minimize the plating of the copper powder.

Estimates indicate the following input per pound of copper equivalent roduced in a 25-ton-per-day plant:

Electricity	kwhr..	0.3
Heat energy	Btu..	10,000
Water	gallon..	1.0
H_2SO_4	pound..	0.15
Polyacrylic acid	do...	0.01
Filter aid	do...	0.005
$(NH_4)_2\ SO_4$	do...	0.05

The estimated total cost of these seven components is 1.6 to 1.9 cents.

L-P-F Process and Dual Process

The L-P-F process converts copper in highly oxidized ores to metallic opper, by leaching and precipitation. The metallic copper responds to recov-y by flotation in the form of cement copper.

The Dual process uses in-plant leaching followed by conventional flota-ion to recover copper from ores containing about equal weights of oxide opper and sulfide copper.

Crude ore, after crushing to minus 3/4 inch, is ground to minus 3 mesh efore separating into sands and slimes. The sands are leached with sulfuric id to recover most of the oxide copper and a portion of the sulfide copper. he washed residual sands together with added lime are then ground to minus 0 mesh, after which more sulfide copper is recovered by conventional flota-ion. The tailings produced during the flotation of slimes for sulfide-copper ecovery are leached in acid solution for additional oxide-copper recovery. ix to ten pounds of burned lime is added to each ton of leach sands processed n the alkaline sulfide circuit.

Oxide copper contained in the solutions from the separate leaching of nd and slimes is precipitated by sponge iron. This sponge iron is produced rom a pyrite concentrate and recovered by flotation of tailings leaving the kaline flotation circuit.

The precipitated copper and the sulfide-copper concentrates from the otation circuit are mixed prior to smelting.

Bureau of Mines Process for Copper-Zinc Ores

Copper and zinc occurring together in an ore can now be separated using a solvent extraction process developed by the Bureau of Mines. The process eliminates costly smelter operations and provides an economic treatment of complex ores which now go unused.

Ore concentrate containing copper and zinc sulfide minerals is first calcined to remove sulfides. The oxidized material is leached with sulfuric acid to dissolve the metals. The resulting solution, after partial neutralization, is added to an organic solvent comprising 75 percent kerosine, 20 percent active di-2-ethylhexyl phosphoric acid, and 5 percent isodecyl alcohol modifier. During countercurrent extraction, the zinc is preferentially absorbed by the solvent while copper builds up in the aqueous phase. The metals are then recovered by conventional electrolysis.

Ion-Exchange Column

A process jointly developed by the Bureau of Mines and the Kennecott Copper Corp. uses a new type of ion exchange column to extract copper and uranium from pregnant solutions produced by waste dump leaching. Uranium concentrates produced by this process meet Government purity standards.

OTHER PROCESSES FOR PRECIPITATING COPPER

General

Copper can be precipitated from solution as a sulfide, cyanide, thiocyanate, or hydroxide. However, these copper compounds are difficult to settle and filter and also must be redissolved before the copper can be reprecipitated by iron.

Cyanide

Five U.S. patents[5] using cyanide-leaching techniques promise a breakthrough for producing a high-grade precipitated product from low-grade ores, copper-bearing materials, and solutions. The inventors of these patents claim low operating costs, small capital requirements, economical reagent recovery, and a method for treating refractory ores and waste.

---

[5]Hockings, W. A., D. H. Rose, and A. M. Gaudin (assigned to Copper Range Co.). Alkaline Cyanide Leaching of Refractory Copper Ore. U.S. Pat. 3,224,873, Dec. 21, 1965.

Keller, C. H. (assigned to Dow Chemical Co.). A Cyanide System For Oxide or Mixed Oxide-Sulfide Ores. U.S. Pat. 2,390,450, Dec. 11, 1945.

Lower, George William (assigned to American Cyanimid Co.). Cyanide Solution To Remove Copper Films From Gangue. U.S. Pat. 3,189,435, June 15, 1965.

Roberts, E. S. (assigned to the Treadwell Corp.). Cyanide Treatment of 0.3 to 0.8 Percent Copper Ore. U.S. Pat. 3,303,021, Feb. 7, 1967.

Roberts, E. S. (assigned to the Treadwell Corp.). Winning Copper From Solutions With HCN and SO_2. U.S. Pat. 3,321,303, May 23, 1967.

Ammonia

Little copper is now produced by the ammoniacal leaching of native copper ore or tailings. Generally, after the removal of native copper by flotation, the remaining sand is leached in closed tanks by a solution containing free ammonia and cupric ammonium carbonate. The copper is recovered by distilling off the free ammonia from the pregnant solution, thereby decomposing the cupric ammonium carbonate to precipitate copper oxides and liberate carbon dioxide and ammonia. The carbon dioxide and ammonia are recovered in water to produce a leaching solution for reuse.

Electrowinning

The electrowinning of copper-acid solutions produces marketable copper while regenerating sulfuric acid. Electrowinning equipment requires a high capital investment and is economically feasible only for solutions containing more than 10 to 25 grams copper per liter. At a lower copper concentration the presence of a significant amount of iron adversely affects the current efficiency owing to oxidation-reduction reactions. Electrowinning requires 5 to 10 times more power than does electrorefining, but the additional cost for power is nearly offset by lower labor costs. The electrowinning process requires a minimum of anode handling and scrap remelting because the insoluble antimonial-lead anodes often have a 10-year service life.

Commercial Installations

Ranchers Exploration and Development Corp. completed solvent extraction and electrowinning facilities at its Bluebird mine near Miami, Ariz., in 1967. This plant is the first of its kind to utilize the solvent extraction of copper from leach solutions followed by back extraction of the solvent by a sulfuric acid solution to produce an electrolyte from which marketable copper is precipitated by electrowinning.

For many years at Inspiration, Ariz., the copper concentration in the electrolyte processed by electrowinning has been maintained at the required level by adding a stronger solution made by the dissolution of cement copper in sulfuric acid.

CCS Electrolytic Cell

Pilot tests using the CCS cell, developed by the Continental Copper and Steel Industries, Inc., indicate that copper leach solutions from the field can be processed with a maximum current density of 30 to 35 amperes per square foot of cathode surface. This is a marked improvement over the 11- to 15-ampere current density employed in conventional copper electrowinning cells where a minimum copper concentration of 25 grams per liter is maintained in the electrolyte.

The CCS cell produces good copper deposition even though a large "bite" of the copper is removed from the electrolyte in each pass.

To date, figures suggest that the CCS cell will produce copper for about the same cost as the cementation route. Because of the continuing upswing in scrap-iron costs and the gradual downtrend in the cost of electricity, which may be even lower when more nuclear-generated electricity becomes available, the electrowinning process is expected to gain increased acceptance.

OUTLOOK FOR PRIMARY COPPER FROM LEACHING

Copper minerals in sub-mill-grade rock produced during current and future open-pit-mining activities will probably contribute most of the copper produced by out-of-plant leaching in the United States in the next 15 years, despite the optimism shown for the proposed in-situ leaching of an ore deposit fractured by a nuclear device. This statement is based on the substantial investments made since 1964 in additional dump-leaching facilities and cementation equipment utilizing the latest technology, and on a conservative prediction that dump leaching will produce 200,000 short tons per year of primary copper by 1970.

The recovery of copper from leach solutions using solvent extraction will attain diversified commercial importance for the in-plant leaching of complex ores where the volume of leach solution produced will be small compared with the volume produced during in-situ and dump leaching.

Dump-leaching practices expected to be commonly used in the future include--

1. The use of mixtures of bitumens plus mill tailings to provide impervious bottoms under dumps.

2. The improved fragmentation of materials placed on dumps to attain a greater copper recovery in a shorter time.

3. The steady input of air during leaching through ducts placed in position while building the dump.

4. The use of heated leach solutions.

5. The treatment of barren solution, after copper precipitation, to remove most of the aluminum and part of the iron content before reuse of the solution for additional leaching.

Scrap iron will continue to be the principal precipitant for removing copper from leach solutions.

From a water-pollution standpoint, the deliberate leaching of copper-bearing sub-mill-grade materials and the recovery of copper from mine-drainage waters are fine examples of the effective removal of a metal that upsets the ecology of water courses. The Anaconda Co., at a cost exceeding $12 million in a 10-year period, has minimized the contamination of the Clark Fork River in Montana. Waters from the mining and smelting operations are processed to produce an effluent of neutral pH and containing only a trace of iron. The success of Anaconda's pollution abatement plan is shown by the fact that fish are caught only a few miles downstream from the water treatment plant.

BIBLIOGRAPHY

1. McArthur, J. A., and B. J. Ledebour. Electrowinning Deposition. Ch. in Extractive Metallurgy of Copper, Nickel, and Cobalt. Interscience Publishers, New York, 1961, pp. 451-457.

2. Knobler, Richard R., and Werner Joseph. Copper Extraction and Refining at Mantos Blancos. J. Metals, v. 14, No. 1, January 1962, pp. 51-56.

3. Malouf, E. E., and J. D. Prater. New Technology of Leaching Waste Dumps. Min. Cong. J., v. 40, No. 11, November 1962, pp. 32-35.

4. Sutton, Joseph A., and John D. Corrick. Microbial Leaching of Copper Minerals. Min. Eng., v. 15, No. 6, June 1963, pp. 37-40.

5. Jacobi, J. S. The Recovery of Copper From Dilute Process Streams. Min. Eng., v. 15, No. 9, September 1963, pp. 56-62.

6. South African Mining and Engineering Journal (Johannesburg). Nchang's New Low-Grade Copper Leaching Plant. V. 74, pt. Z, No. 3684, Sept. 13, 1963, pp. 801-802, 804, 814.

7. Argall, George O., Jr. Leaching Dumps To Recover More Copper at Lower Cost. Min. World, v. 25, No. 11, October 1963, pp. 22-25, 27.

8. _____. How Leaching Recovers Copper From Waste and Leach Dumps in the Southwest. Min. World, v. 25, No. 12, November 1963, pp. 20-24.

9. McMahon A. D. Copper--A Materials Survey. BuMines Inf. Circ. 8225, 1965, 340 pp.

10. Chemical and Engineering News. New Ion Exchange Resin for Solvent Extraction Increases Copper Recovery. V. 43, No. 42, Oct. 18, 1965, pp. 48-49.

11. Agers, D. W., J. E. House, R. R. Swanson, and J. L. Drobnick. A New Reagent for Liquid Ion Exchange Recovery of Copper. Min. Eng., v. 17, No. 12, December 1965, pp. 76-80.

12. Spodden, J. R., E. E. Malouf, and J. D. Prater. Cone-Type Precipitators for Improved Copper Recovery. Min. Eng., v. 18, No. 4, April 1966, pp. 57-62.

13. Mining Engineering. Precipitation of Copper From Dilute Solutions. V. 18, No. 6, June 1966, pp. 70-74.

14. Yurko, W. J. Refining Copper by Acid Leaching and Hydrometallurgy. Chem. Eng., v. 73, No. 18, Aug. 29, 1966, pp. 64-66.

15. Engineering and Mining Journal. First Commercial-Scale H_2 Reduction Plant for Cu on Stream. V. 168, No. 1, January 1967, pp. 97-100.

16. Hogue, W. G. Use of Sponge Iron in the V-Trough Precipitator. Min. Cong. J., v. 53, No. 1, January 1967, pp. 17-20.

17. Cahalan, M. J. Solvent Extraction for Copper Recovery--Some General Considerations. Chemistry and Industry (London), No. 15, Apr. 15, 1967, pp. 610-612.

18. Chemical and Engineering News. Ion Exchange Recovery of Copper Promising. V. 85, No. 17, Apr. 17, 1967, pp. 62-64.

19. Rose, D. H., V. Lassela, and D. J. Buckwalter. White Pine Experiments With Cyanide Leaching of Copper Tailings. Min. Eng., v. 19, No. 8, August 1967, pp. 60-63.

20. Sock, Helen R. New Servo-Systems Bolster Kennecott Output. Eng. Min. J., v. 168, No. 8, August 1967, pp. 77-81.

21. Engineering and Mining Journal. Copper Leaching With Cyanide--A Review of Five Inventions. V. 168, No. 9, September 1967, pp. 123-127.

22. _____. Kennecott Sets Sights on Nuclear Test for In-Situ Recovery of Copper. V. 168, No. 11, November 1967, pp. 116-122.

23. Hardwick, William R. Fracturing a Deposit With Nuclear Explosives and Recovering Copper by the In-Situ Leaching Method. BuMines Rept. of Inv. 6996, 1967, 48 pp.

24. Mining Engineering. Kennecott Proposes Nuclear Mining Experiments at Safford Deposit. V. 19, No. 11, November 1967, pp. 66-67.

INT.-BU.OF MINES,PGH.,PA.

CONFIRMATION OF HYDROFRACTURING RESULTS THROUGH COMPARISONS WITH OTHER STRESS MEASUREMENTS

SUBJ
MNG
CHRT

Bezalel C. Haimson
Rock Mechanics and Mineral Engineering
University of Wisconsin
1509 University Avenue
Madison, Wisconsin 53706

Proceedings of the 22nd U.S. Symposium on Rock Mechanics: Rock Mechanics from Research to Application held at Mass. Inst. of Tech., June 28-July 2, 1981 compiled by H.H. Einstein

INTRODUCTION

Hydrofracturing as a method of estimating the stress regime in rock has been treated theoretically (e.g., Hubbert and Willis, 1957; Fairhurst, 1964; Haimson and Fairhurst, 1967; Zoback and Pollard, 1978) and tested in the laboratory (e.g., Haimson, 1968; Haimson and Avasthi, 1975; Zoback et al, 1977). Moreover, in most published cases of field hydrofracturing measurements the results appear plausible (Haimson, 1977a, 1978; McGarr, 1980; Zoback and Zoback, 1980). The problem is, however, that there is no direct way to verify field results. The far-field boundary conditions are typically unknown, and no theory or model can predict the state of stress at a point in rock. We can obtain some indication of the reliability of results from the consistency of different measurements in the same hole, or the agreement between tests in adjacent holes; in addition, nearby geologic structures such as faults, dikes or folds can provide a qualitative check to measured stresses. These and other devices cannot, however, unequivocally determine whether the measured stresses represent the existing stresses. One method for confirming the validity of results is to compare the stresses derived by one method with those independently determined by another. If the agreement is close and not coincidental it can be used as evidence that both methods appear to measure real and not imaginary stresses.

The hydrofracturing technique, which has rapidly developed in this country as the primary method for measuring stresses at great depths, has been directly compared with other methods in only a few cases. These comparisons, we believe, serve to reinforce the general reliability of hydrofracturing, while pointing out that it is not a precision instrument. The present paper is a report on those sites where two or more sets of in situ stress measurements were conducted and includes a discussion on the quality of the comparisons. The hydrofracturing technique used in all cases has been described elsewhere (Haimson, 1978; 1980).

THE NEVADA TEST SITE (NTS)

Chronologically, the Nevada Test Site hydrofracturing stress measurements provided the first direct comparison between results obtained by different methods. A total of 12 hydrofracturing tests were conducted in the tuff of the Rainier Mesa in the vicinity of tunnel complex U12n (Haimson et al, 1974); one test in each of the two horizontal and three vertical holes drilled from the tunnel to a depth of some 25m, and seven additional tests in a 250m vertical hole drilled from the surface in the same general area.

Figure 1 summarizes the hydrofracturing stress results. We note a steady increase with depth (taken from the top of the Mesa) of both the least (σ_{Hmin}) and the largest principal stresses (σ_{Hmax}). The measurements in the vicinity of the tunnel which were conducted in different boreholes (depths of 380

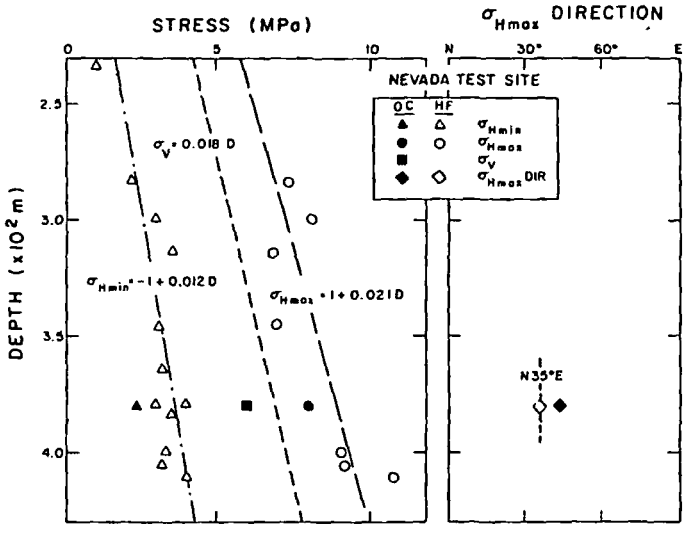

FIGURE 1. Variation of hydrofracture direction and stress magnitudes with depth at the Nevada Test Site, and overcoring results at 380m depth (D is depth in meters).

and 410m in Figure 1) yielded similar stress values which also coincided with those determined in the deep vertical hole. This consistency of results from tests run in separate holes provided strong confidence in the values obtained. Based on linear regression analysis the variation of the measured stresses with depth is given by:

$$\sigma_{Hmin} = -1 + 0.012\ D; \quad \sigma_{Hmax} = 1 + 0.021\ D \qquad (1)$$

where stresses are in megapascals and D is depth in meters. The vertical stress (σ_V) based on the measured density of the tuff is estimated at σ_V = 0.018 D. Impression packer tests indicated vertical fractures oriented at N35°E, suggesting that the latter is also the direction of σ_{Hmax}.

Several years earlier the Bureau of Mines had conducted a series of overcoring borehole-deformation-gage measurements from the same tunnel (U12n) using short holes drilled in different directions (Hooker et al, 1971). They obtained a complete stress tensor for the vicinity of the tunnel at a depth of 380m below the Mesa top. Table 1 and Figure 1 provide a direct comparison between the hydrofracturing and overcoring results. Overcoring suggests that the principal stresses act in planes that are somewhat inclined to the horizontal and vertical (up to 20°). Hydrofracturing is insensitive to such inclination. It is difficult to assess the reliability of the principal stress axes inclinations based on a few overcoring tests conducted in several holes that violate the assumption of all stress components being measured at one point. However, the overcoring horizontal and vertical secondary principal stresses match surprisingly well, both in magnitude and direction, the hydrofracturing results. Table 1 shows that the

difference in stress magnitudes measured by the two methods is only 1 MPa. This close agreement is exceptional in field tests in general, and in comparing results of two entirely different methods in particular. Moreover, the horizontal principal stress directions are practically identical (10° difference).

Table 1. Nevada Test Site-Stress Comparison at Tunnel Level (380m depth)

Stress	Hydrofrac(HF) MPa	Overcoring*(OC) MPa	HF-OC MPa/
σ_{Hmax}	9 at N35°E	8 at N45°E (8.5 at N47°E/110°)	1/10°
σ_{Hmin}	3.5 at N55°W	2.5 at N45°W (2.5 at N44°W/91°)	1/10°
σ_V	7	6 (5.7 at N42°E/20°)	1

*Given in terms of secondary principal stresses in the horizontal and vertical planes with principal stress values shown in paranthesis together with their bearing and inclination from the downward vertical.

Further support of our hydrofracturing results has come from two other sources. First, most fault plane solutions of earthquakes occurring in the general area of the Nevada Test Site strongly indicate strike-slip faulting with a subhorizontal pressure axis at N45°E (Lindh et al, 1973), in accordance with our results (Figure 1 clearly indicates a $\sigma_{Hmax} > \sigma_V > \sigma_{Hmin}$ condition). Second, subsequent hydrofracturing tests conducted by a different group near other tunnels at the Nevada Test Site yielded stress values in the same order of magnitude as ours. The direction of σ_{Hmax} was again found to be close to N45°E (Tyler and Vollendorf, 1975).

THE HELMS PUMPED STORAGE PROJECT

The Helms Project of the Pacific Gas and Electric Company, located in the central Sierra Nevada Mountains, is a 1050 megawatt hydroelectric pumped storage facility. As part of the pre-excavation site investigation and design nine successful hydrofracturing stress measurements were conducted in granite in two drillholes, seven in a vertical NX size hole between the depths of 119 and 326m, and two in an inclined hole at depths 239, and 271m (Haimson, 1977b). The inclined hole was 30° off the vertical in the N27°E direction which parallels the general direction of the hydrofractures in the vertical hole (N25°E). Hence, vertical axial hydrofractures in the inclined hole would confirm the results obtained in the vertical hole. The fractures induced were indeed nearly axial, with subvertical dips (80°SE). The tests in the inclined hole increased our confidence in the results obtained in the vertical hole and reinforced the assertion that the principal stresses were approximately vertical and horizontal, with the maximum horizontal stress (σ_{Hmax}) oriented at N25°E. Figure 2 gives the measurements as a function of depth. The steady increase with depth of all the stresses can be approximated by linear regression:

$$\sigma_{Hmin} = 3.5 + 0.006\ D;\quad \sigma_{Hmax} = -0.65 + 0.035\ D \qquad (2)$$

The vertical stress based on measured rock density is $\sigma_V = 0.027\ D$. The uniqueness of these measurements was that for the first time an inclined hole

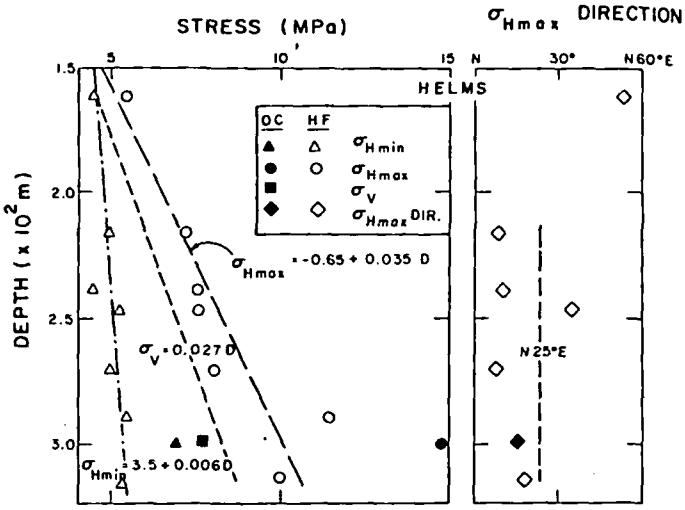

FIGURE 2. Variation of hydrofracture direction and stress magnitudes with depth at Helms, and overcoring results at 300m depth (D is depth in meters).

was used for hydrofracturing tests in order to verify the orientation of the principal stresses. As shown in Figure 2 the inclined hole results cannot be distinguished from those obtained in the vertical hole.

The results of these pre-excavation stress measurements were checked some years later against a series of overcoring borehole-deformation-gage tests conducted from a drift just off the site of the hydrofracturing test holes at the future powerhouse level (Sweeney et al, 1980). Table 2 and Figure 2 juxtapose the overcoring horizontal and vertical secondary principal stresses versus the hydrofracturing results at 300m depth.

Table 2. Helms Project-Stress Comparison at Powerhouse Level (300m depth)

Stress	Hydrofrac(HF) MPa	Overcoring*(OC) MPa	HF-OC MPa/
σ_{Hmax}	10 at N25°E	15 at N17°E (15.5 at N01°W/65°)	-5/8°
σ_{Hmin}	5.5 at N65°W	7 at N73°W (6.7 at N74°W/104°)	-1.5/8°
σ_V	8	7.7 (7.5 at N43°E/29°)	0.3

*Given in terms of secondary principal stresses in the horizontal and vertical planes, with principal stress values shown in paranthesis together with their bearing and inclination from the downward vertical.

The overcoring principal stresses are inclined up to 30° from the vertical. This is plausible in view of the mountainous terrain and considering that the hydrofractures were also inclined up to about 10°. The overcoring secondary principal stresses (Table 2) are reasonably close to the hydrofracturing results with the largest discrepancy in the σ_{Hmax} value (5 MPa). The directions of the horizontal stresses agree within 10°.

THE BAD CREEK PUMPED STORAGE PROJECT

The 1000 megawatt Bad Creek Pumped Storage Project of Duke Power Company is located along the south-eastern edge of the Blue Ridge Escarpment in the northwest corner of South Carolina. A 275m vertical NQ hole was drilled in the Toxaway gneiss from the surface to the level of the future underground powerhouse. As part of the pre-excavation site investigation seven successful hydrofracturing stress measurements were conducted at different depths in the hole between 120m and 270m (Haimson, 1977b). The results indicated a state of rather high horizontal stresses, and a steady increase in stress with depth with consistent least horizontal principal stresses, and a rather wide scatter in the magnitudes of the largest horizontal principal stress (Figure 3). The linear approximation of stress versus depth for the range of 100-300m is given by:

$$\sigma_{Hmin} = -3 + 0.08\ D; \quad \sigma_{Hmax} = -8 + 0.14\ D$$
$$\sigma_V = 0.026\ D \qquad (3)$$

Unlike the previous two cases, the least horizontal compressive stress is not the smallest overall principal stress but rather the intermediate component. The negative (tensile) values that the two horizontal stresses appear to attain at shallow depths may or may not be real. In general, extrapolations beyond the range of depths within which tests have been carried out is not recommended. The vertical stress in equation (3) is based both on rock density and on hydrofracturing results which yielded both vertical and horizontal fractures and respective shut-in pressures (Haimson, 1977b). The direction of σ_{Hmax} in the 180-270m zone was approximately N60°E (Figure 3).

The stress results were used as the basis for laying out a pilot tunnel into the powerhouse area. After the pilot tunnel was completed, the in situ stresses were determined again in the general area of the planned powerhouse using the borehole-deformation-gage method (H. G. McKay and R. E. Steffens, personal communication, 1978). Again, the results are in good agreement with the hydrofracturing horizontal stresses (Table 3, Figure 3). The least principal stress is the subvertical component, with the other principal stresses acting at about 15° from the horizontal and in directions practically identical to those determined by hydrofracturing. The magnitudes of both horizontal secondary principal stresses are within 2.5 and 4.5 MPa respectively from the hydrofrac results, but because of the high stress magnitudes those discrepancies are relatively small. Only the vertical stress is substantially different; however, we note that this is nearly the minimum principal stress which is the least accurately determined in overcoring.

Table 3. Bad Creek Project - Stress Comparison at Powerhouse Level (230m depth)

Stress	Hydrofrac(HF) MPa	Overcoring*(OC) MPa	HF-OC MPa/
σ_{Hmax}	24 at N60°E	28.5 at N56°E (29 at N57°E/110°)	-4.5/4°
σ_{Hmin}	15.5 at N30°W	17.5 at N34°W (18.5 at N32°W/112°)	-2.5/4°
σ_V	6	11.5 (10 at N S72°E/15°)	-5.5

*Given in terms of secondary principal stresses in the horizontal and vertical planes with principal stress values shown in paranthesis togehter with their bearing and inclination from the downward vertical.

THE NEAR-SURFACE TEST FACILITY - HANFORD SITE, WASHINGTON

Two sets of in situ stress measurements were conducted in conjunction with the excavation of the Near-Surface Test Facility (NSTF) in the basalt of Gable Mountain, Hanford Reservation. Hydrofracturing was carried out in a 120m, NQ size vertical hole near the western end of Gable Mountain. The six tests conducted in this hole were part of the pre-excavation design stage of the underground test facility (Haimson, 1979). The borehole-deformation-gage technique was used after the completion of the NSTF (Kim, 1980). Both methods of stress measurements were adversely affected by the fractured nature of the basalt (averaging 15 fractures per meter).

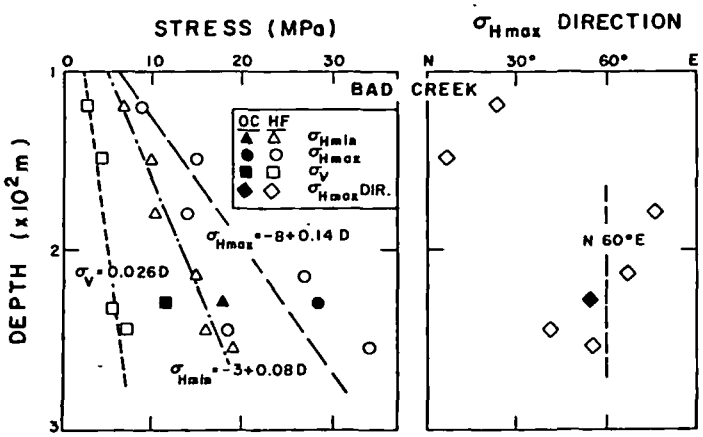

FIGURE 3. Variation of hydrofracture direction and stress magnitudes with depth at Bad Creek, and overcoring results at 230m depth (D is depth in meters).

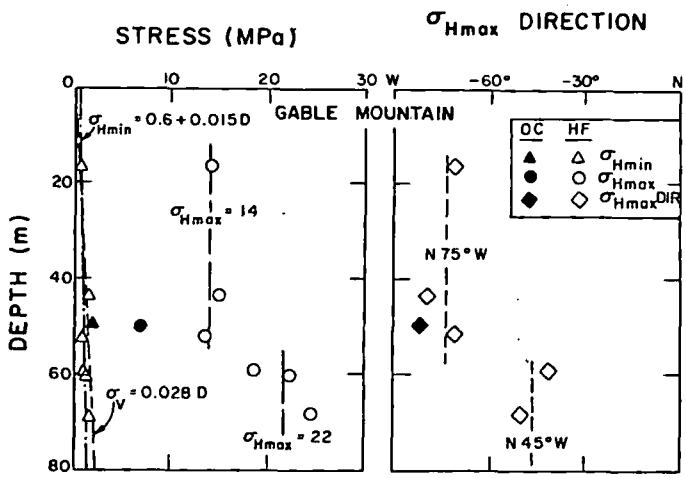

FIGURE 4. Variation of hydrofracture direction and stress magnitudes with depth at Gable Mountain, and overcoring results at 50m depth (D is depth in meters).

The hydrofracturing results and the juxtaposed overcoring measurements at the NSTF level (approximately 50m below the collar of the test hole) are shown in Figure 4. While the σ_{Hmin} values appear to increase steadily with depth σ_{Hmax} is constant in the top 55m but increases substantially below that. Hence no attempt was made to fit a curve to its variation with depth. The stresses are approximated by:

$$\sigma_{Hmin} = 0.6 + 0.015\ D; \quad \sigma_{Hmax} = 14\ (0\text{-}55m) = 22\ (55\text{-}70m) \qquad (4)$$

The vertical stress was calculated based on the basalt density: $\sigma_V = 0.028\ D$. It should be noted that because of the large magnitude of σ_{Hmax} it could not be calculated by using the field value of the tensile strength. The latter can be estimated from the pressure-time records (Haimson, 1980) only if $\sigma_{Hmax} < 3\ \sigma_{Hmin}$ (in absence of pore pressure, which was the case at the NSTF). At Gable Mountain σ_{Hmax} is considerably greater than $3\ \sigma_{Hmin}$ so only the laboratory determined hydrofracturing-tensile strength of extracted core could be used (equal to 17 MPa in the 0-55m interval, and 25.5 MPa in the 55-70m range). Typically, field obtained tensile strengths are considerably lower than laboratory ones by a factor which appears to vary from site to site. Hence, at NSTF we can only assert with some certainty that the hydrofracturing determined σ_{Hmax} is probably an upper limit of the value. It is interesting to note that some change probably does occur at around 55m depth which is reflected by the large increase in the tensile strength, and the subsequent value of σ_{Hmax}, as well as a sharp change in the σ_{Hmax} direction from an average of N75°W in the 0-55m range to N45°W in the 55-70m range. A comparison between the results of the two stress methods is given in Table 4.

Table 4. Gable Mountain, Hanford - Stress Comparison at NSTF Level (50m depth)

Stress	Hydrofrac(HF) MPa	Overcoring*(OC) MPa	HF-OC MPa/
σ_{Hmax}	14 at N75°W	7 at N81°W/101°	7/6°
σ_{Hmin}	1.5 at N15°E	2 at N8°E/95°	-0.5/7°
σ_V	1.5	2 at N65°E/167°	-0.5

*Given in terms of the principal stresses which because of their small inclination are approximately equal to the secondary values in the horizontal and vertical planes. The inclination is given with respect to the downward vertical direction.

Figure 4 and Table 4 show a good agreement between the two methods with respect to σ_{Hmin} magnitude, and a major discrepancy (2:1 ratio) for values of σ_{Hmax}. In view of the discussion above regarding the tensile strength such a discrepancy could be expected. The overcoring σ_{Hmax} result is probably more reasonable, but additional tests may be needed to settle the difference. The agreement as far as the directions of the horizontal stresses is again remarkable. We note that σ_{Hmax} direction (N75°W-N80°W) is also roughly parallel to the Gable Mountain axis, which should be expected in view of the limited width of the mountain and the proximity of the test hole (250m) to the very steep south-southwestern slope.

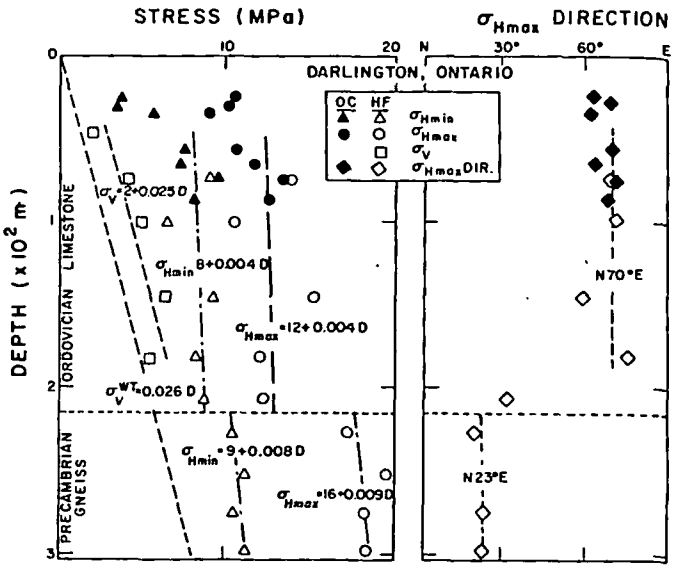

FIGURE 5. Variation of stress magnitudes and σ_{Hmax} direction with depth at Darlington, based on hydrofracturing and overcoring measurements (D is depth in meters).

DARLINGTON, ONTARIO

The existence of high horizontal stresses in many of the Silurian, Ordovician and Precambrian rocks of Ontario has been well documented and recognized in recent years (e.g. Coates, 1964; Franklin and Hungr, 1978). It was with this background information in mind that Ontario Hydro decided to incorporate in situ stress measurements into the conceptual design and evaluation of an underground nuclear power station. While no specific sites have been considered for an underground nuclear power plant, a 303m deep NQ size test hole was drilled for generic study purposes on the construction site of the Darlington Generating Station near Bowmanville, Ontario, 65 km east of Toronto, on the north shore of Lake Ontario. The test hole penetrated through 26m of overburden, 193m of Ordovician limestone and siltstone, and 84m of Precambrian granitic gneiss. An unprecedented follow-up to the hydrofracturing tests consisted of their verification by near-surface to shallow-depth overcoring measurements and by borehole TV camera scanning of the hydraulically induced fractures.

As shown in Figure 5 a total of ten hydrofracturing tests were conducted, six of them in the limestone between 46m and 208m, and four in the gneiss (228-300m). The top five tests yielded both vertical and horizontal hydrofractures as well as two respective shut-in pressures. This enabled, like in the case of the Bad Creek tests, the estimation of the vertical stress directly from the hydrofracturing results (Haimson and Lee, 1979, 1980). The results revealed two apparently different or decoupled stress fields, one in the limestone and another in the gneiss. In the range of 46-208m (limestone) linear approximations of stress-depth behavior are:

$$\sigma_{Hmin} = 8 + 0.004\ D; \quad \sigma_{Hmax} = 12 + 0.004\ D$$
$$\sigma_V = 2 + 0.025\ D \qquad (5)$$

The vertical stress calculated based on rock density

is σ_V = 0.026 D so that the hydrofracturing σ_V values are consistently larger by about 2 MPa in the depth range considered. The variation with depth of both horizontal stresses is very small in the Paleozoic zone (~0.6 MPa) and for all practical purposes can be considered negligible. The direction of σ_{Hmax} is quite consistent at N70°E (Figure 5).

In the Precambrian gneiss (228-300m) a rather sharp increase in stress magnitudes is observed (Figure 5):

$$\sigma_{Hmin} = 9 + 0.008\ D; \quad \sigma_{Hmax} = 16 + 0.009\ D \qquad (6)$$

accompanied by a change in direction, with σ_{Hmax} acting consistently in a N23°E direction. The transition in direction is evidenced by the lowest test in the limestone (207m depth) which yields a σ_{Hmax} direction of N32°E. The decoupling of the stress regime along the Precambrian-Paleozoic contact is probably due to the existence of residual stresses in the Precambrian rocks prior to the deposition and formation of the Ordovician sediments.

The magnitudes of the Precambrian stresses have not been checked by an independent method, but the orientation of the hydrofractures were verified by a borehole TV camera which confirmed their inclinations (vertical) and strikes within an average of 5° from the ones determined by the hydrofracturing impression packer-magnetic orienting tool.

Using a borehole-deformation-gage Ontario Hydro also independently conducted a series of overcoring stress measurements at shallow depths at a site about 1.6 km from the hydrofracturing test hole. The original tests and results which were published by Haimson and Lee (1979, 1980) were considered by Ontario Hydro as not sufficiently reliable, and a new set of overcoring tests in two separate vertical holes were conducted in 1980 at depths from 26 to 88m (C. Lee, personal communication, 1981). The results are plotted in Figure 5. These tests could only yield the horizontal principal stresses. It is evident from the top three overcoring tests, at depths of 26-30m, that the stresses just under the overburden are relieved, not unlike the behavior observed for example at Waterloo, Wisconsin (Haimson, 1980). On the other hand, in the 58-88m zone the four overcoring tests yield results that cannot be distinguished from the hydrofracturing stresses. This holds true for both magnitudes and directions as shown in Table 5.

Table 5. Darlington, Ontario - Stress Comparison at 70m Depth

Stress	Hydrofrac(HF) MPa	Overcoring(OC) MPa	HF-OC MPa
σ_{Hmax}	12 at N70°E	12 at N70°E	0
σ_{Hmin}	8 at N20°W	8 at N20°W	0

Clearly this comparison is the best of all those listed in this paper and no better one can be expected anywhere.

STRIPA, SWEDEN

This case history is described in detail in a separate paper in these Proceedings (Doe et al, 1981) and only the aspects directly related to the present paper will be repeated here. A 380m vertical NX test

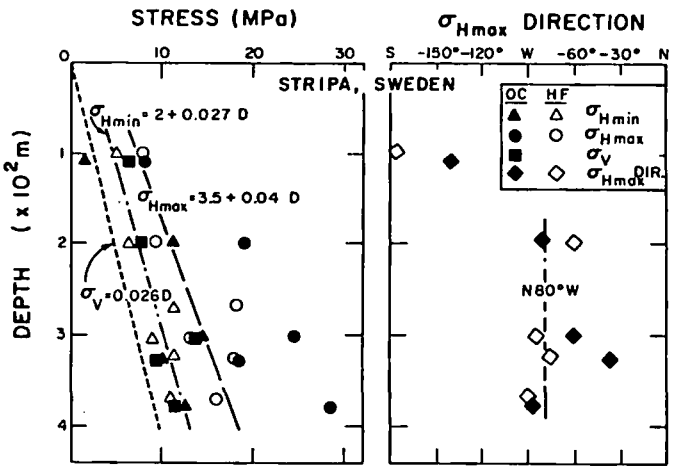

FIGURE 6. Variation and stress magnitudes and σ_{Hmax} direction with depth at Stripa, based on hydrofracturing and overcoring measurements (D is depth in meters). After Doe et al, (1981).

hole was drilled from the surface into granite just outside the perimeter of the underground Stripa Mine which has been used for generic nuclear waste disposal research. This is probably the first case in which the same test hole has been used for exhaustive stress testing both by hydrofracturing and by overcoring (in this case the Leeman triaxial cell technique modified by the Swedish State Power Board for deep measurements, Hiltscher et al, 1979). The averages of 16 hydrofracturing and 17 overcoring tests have been clustered in Figure 6 around five depths. The hydrofracturing results show a consistent increase with depth:

$$\sigma_{Hmin} = 2 + 0.027\ D; \quad \sigma_{Hmax} = 3.5 + 0.04\ D \qquad (7)$$

The value of σ_V based on rock density is σ_V = 0.026 D. The mean σ_{Hmax} direction is N80°W. The overcoring stresses which generally increase with depth, are less consistent and display a larger scatter than the respective hydrofracturing stresses. A quick comparison between the two sets of results (Figure 6) show that the overcoring vertical and maximum horizontal stresses are considerably higher than the density based σ_V and the hydrofracturing σ_{Hmax}. There is, however, good agreement with respect to σ_{Hmin} magnitude, as well as the directions of the horizontal stresses.

Table 6 is a comparison of results at 320m depth which is the depth of interest in the mine. Owing to the availability both of direct measurements in the immediate vicinity of this depth and of the general trend of stress vs. depth as shown in Figure 6, two sets of comparisons have been made (Table 6) based on data from Doe et al, (1981). The agreement between interpolated stresses (case a in Table 6) is good for σ_{Hmin}, fair for σ_{Hmax}, poor for σ_V and excellent for σ_{Hmax} direction. However, the agreement between direct measurements at about 320m (case b) is considerably better, with each of the horizontal stresses differing by only 1 MPa, but with a somewhat larger discrepancy in stress directions (within 40°).

Table 6. Stripa, Sweden - Stress Comparison at 320m Depth

Stress		Hydrofrac(HF) MPa	Overcoring*(OC) MPa	HF-OC MPa
σ_{Hmax}	(a)	16.5 at N80°W	23.5 at N67°W	-7/13°
	(b)	18 at N76°W	18.5 at N36°W (20 at incl 130°)	-0.5/40°
σ_{Hmin}	(a)	10.5 at N10°E	12.5 at N23°E	-2/13°
	(b)	11.5 at N14°E	10.5 at N54°E (11 at incl 116°)	+1/40°
σ_V	(a)	8.5	13	-4.5
	(b)	8.5	10 (8 at incl 34°)	-1.5

*Overcoring results are given in terms of secondary principal stresses in the horizontal and vertical planes, with the principal stresses, and their inclination shown in paranthesis.
(a) based on linear approximation of stress-depth variation
(b) based on actual test results at 326m for overcoring and at 138, 326 and 329m for hydrofracturing.

DISCUSSION AND CONCLUSIONS

It has been said that hydrofracturing is well developed but poorly understood. It is perhaps difficult to challenge this statement except for pointing out that the same may be said about almost any other rock field test now in use. This paper certainly does not add much to the understanding of the method; rather it is an attempt to verify whether it works. The inescapable answer, based on the six comparisons with overcoring is an unequivocal yes, provided we keep in mind that hydrofracturing is not a precision measurement device but a method of estimating the magnitudes and directions of the horizontal principal stresses in deep vertical drill holes.

Analyzing the comparisons in Tables 1-6 we first notice that the stresses determined by hydrofracturing and overcoring are basically in the same "ball park". This approximate coincidence of results supports the assertion that both methods, using radically different approaches, estimate the same field parameter, namely the stress regime. Two major conclusions can be drawn directly from these tables:

1. Both methods yield the same stress condition ($\sigma_V > \sigma_{Hmax} > \sigma_{Hmin}$ or $\sigma_{Hmax} > \sigma_V > \sigma_{Hmax}$ or $\sigma_{Hmax} > \sigma_{Hmin} > \sigma_V$).
2. The inclinations of the overcoring principal axes are usually within 30° from the hydrofrac principal axes (vertical and horizontal).

Additional conclusions can be drawn either from Tables 1-6 or from the summary given in Table 7:

3. The directions of the horizontal principal stresses as determined by the two methods are typically within ±10°.
4. The magnitudes of σ_{Hmin} as determined by the two methods are within ±2 MPa. This is equivalent to a discrepancy of up to 30% of the hydrofrac σ_{Hmin}.

Table 7. Summary of Stress Comparisons

Site	$\Delta\sigma$ σ_{Hmin} MPa	$\Delta\sigma$ σ_{Hmax} MPa	$\Delta\sigma/\sigma_{HF}$ x100% σ_{Hmin}	$\Delta\sigma/\sigma_{HF}$ x100% σ_{Hmax}	$\Delta\sigma_{Hmax}$ Dir.
NTS	1	1	29	11	-10°
Helms	-1.5	-5	-27	-50	8°
Bad Creek	-2	-4.5	-13	-19	4°
Gable Mt.	-0.5	7	-33	100	-6°
Darlington	0	0	0	0	0
Stripa	-2/1*-	7/-0.5*	-19/10*-	42/3*	13°/40°*

$\Delta\sigma$ = Hydrofrac stress - overcoring stress
σ_{HF} = Hydrofrac stress
$\Delta\sigma_{Hmax}$ Dir = The difference in σ_{Hmax} direction between hydrofrac and overcoring results.
* case a/case b (see Table 6).

5. The magnitudes of σ_{Hmax} as determined by the two methods are typically within ±5 MPa. At Gable Mountain and Stripa (case a) the differences are slightly higher, but they are not typical as explained above. In terms of percentage of the hydrofrac σ_{Hmax} value the discrepancy can reach 50%.

The above conclusions, we believe, provide strong support for the reliability of hydrofracturing. The almost identical results with respect to stress directions and the magnitudes of σ_{Hmin} are remarkable. The larger discrepancy in the estimation of σ_{Hmax} magnitude is expected owing to the rather illusive 'tensile strength' parameter which enters the calculation in the hydrofracturing method. One must also be aware that the discrepancy may in part be due to a tendency to exaggerate stress magnitudes in overcoring by using a rock modulus based on core testing which is often higher than the equivalent field value. Still the discrepancy is tolerable in most cases and more importantly, in most uses.

Hydrofracturing has been used so far in four major areas: in preexcavation site investigation and design of large underground openings, in design of in situ mining projects (such as oil and hot-dry-rock geothermal energy extraction), in waste disposal studies, and in tectonophysics and earthquake research. In all these endeavors the information provided by deep-hole hydrofracturing stress measurements is, despite possible discrepancies in principal axes inclinations and σ_{Hmax} magnitude, extremely valuable and sufficiently accurate for most utilizations.

ACKNOWLEDGEMENT

I thank Tom Doe for allowing me to use the Stripa Mine stress data which are being published for the first time in this volume (Doe et al, 1981).

REFERENCES

Coates, D.F., 1964, Some cases of residual stress effects in engineering works, in State of Stress in Earth's Crust, American Elsevier, pp 679-688.
Doe, T., K. Lugevald, L. Strindell, B. Haimson and H. Carlsson, 1981, Hydraulic fracturing and overcoring stress measurements in a deep borehole at the Stripa Test Mine, Sweden, Proceedings of the

22nd U.S. Rock Mechanics Symposium, this volume.
Fairhurst, C., 1964, Measurement of in situ rock stresses with particular reference to hydraulic fracturing, Rock Mechanics and Engineering Geology, Vol. 2, 129-147.
Franklin, J.A., and Hungr, O., 1978, Rock stresses in Canada, Proceedings of the 25th Geomechanical Colloquy, Salzburg, Austria.
Haimson, B.C., 1968, Hydraulic fracturing in porous and nonporous rock and its potential for determining in-situ stresses at great depth, Ph.D. thesis, Univ. of Minnesota, Minneapolis.
Haimson, B.C., 1977a, Crustal stress in the continental U.S. as derived from hydrofacturing tests, in The Earth's Crust (Geophysical Monograph 20), (ed.) J.C. Heacock, American Geophysical Union, pp. 576-592.
Haimson, B.C., 1977b, Design of underground powerhouses and the importance of preexcavation stress measurements, in Design Methods in Rock Mechanics (Proceedings of the 16th Symposium on Rock Mechancis), (Ed.) C. Fairhurst and S.L. Crouch, Am. Soc. of Civil Engineers, New York, pp. 197-204.
Haimson, B.C., 1978, The hydrofracturing stress measuring method and recent field results, Int. J. Rock Mech. Min. Sci. & Geomech. Abstr., Vol. 15, 167-178.
Haimson, B.C., 1979, Hydraulic fracturing results at Gable Mountain, Report LBL-7061, Lawrence Berkeley Laboratory, Berkeley, California.
Haimson, B.C., 1980, Near-surface and deep hydrofracturing stress measurements in the Waterloo quartzite, Int. J. Rock Mech. Min. Sci. & Geomech. Abstr., Vol. 17, 81-88.
Haimson, B.C., and J.M. Avasthi, 1975, Stress measurements in anisotropic rock by hydraulic fracturing, in Applications of Rock Mechanics, (ed.) E.R. Hoskins, Jr., American Society of Civil Engineers, pp 135-156.
Haimson, B. and C. Fairhurst, 1967, Initiation and extension of hydraulic fractures in rock, Soc. Petrol. Engrg. J., Vol. 7, 310-318.
Haimson, B.C., J. Lacomb, A.H. Jones, and S.J. Grenn, 1976, Deep stress measurements in tuff at the Nevada test site, in Advances in Rock Mechanics, Vol. IIa, Nat. Acad. of Sci., Washington, D.C., pp 557-561.
Haimson, B.C. and C.F. Lee, 1979, Stress measurements in underground nuclear plant design, Proceedings 1979 Rapid Excavation and Tunneling Conference, (eds.) A.C. Maejis and W.A. Hustrulid, Society of Mining Engineers of AIME, Vol. 1, pp 122-135.
Haimson, B.C. and C.F. Lee, 1980, Hydrofracturing stress determination at Darlington, Ontario, in Underground Rock Engineering (Proceedings of the 13th Canadian Symposium on Rock Mechanics, Canadian Institute of Mining and Metallurgy, special volume, pp 42-50.
Hiltscher, J., F. Martna and L. Strindell, 1979, The measurement of triaxial rock stresses in deep boreholes in the design and construction of underground openings, Proceedings 4th Congress Int. Soc. Rock Mech., Vol. 1, pp 227-234.
Hooker, V.E., T.R. Aggson, and D.C. Bickel, 1971, In-Situ determination of stresses in Rainier Mesa, Nevada Test Site, Report, U.S. Bur. of Mines.
Hubbert, M.K. and D.G. Willis, 1957, Mechanics of hydraulic fracturing, Trans. AIME, Vol. 210, 153-160.
Kim, K., 1980, Rock mechanics field test results to date, in Document RHO-BWI-80-100 Rockwell Hanford Operations, Richland, Washington, pp V26-V34.
Lindh, A.G., F.G. Fisher and A.M. Pitt, 1973, Nevada forcal mechanisms and regional stress fields (abstract), Eos Trans. Am. Geophys. Union, Vol. 54, p 1133.
McGarr, A., 1980, Some constraints on levels of shear stress in the crust from observations and theory, J. Geophys. Res., Vol. 85, 6231-6238.
Sweeney, N.F., J. A. Davis and A.G. Strassburger, 1980, A practical/economic rock mechanic program, Proceedings of the 21st U.S. Rock Mechanics Symposium, Rolla, Missouri, pp 729-743.
Tyler, L.D. and W.C. Vollendorf, 1975, Physical observations and mapping of cracks resulting from hydraulic fracturing in situ stress measurements, paper presented at the Annual Meeting of the Society of Petroleum Engineers of AIME, Dallas, Texas.
Zobock, M.D. and D.D. Pollard, 1978, Hydraulic Fracture propagation and the interpretation of pressure-time records for in situ stress determination, Proceedings 19th U.S. Symposium on Rock Mechanics, University of Nevada-Reno, pp 14-22.
Zoback, M.D., F. Rummel, R. Jung, H.J. Alheid, and C.B. Raleigh, 1977, Rate controlled hydraulic fracturing experiments in intact and pre-fractured rock, Int. J. Rock Mech. Mining Soc. and Geomech. Abstr., Vol. 14, 49-58.
Zoback M.L. and M. Zoback, 1980, State of stress in the continental United States, J. Geophys. Res. Vol. 85, 6113-6156.

U.S. BUREAU OF MINES
IN SITU MINING BIBLIOGRAPHY

UPDATED ON 7/24/81

KEYWORD: COPPER

4 New
Marked with
blue slash
"

FOR MORE INFORMATION, CONTACT:

WILLIAM C. LARSON
(612) 725-3464

U.S. DEPT. OF INTERIOR
BUREAU OF MINES
TWIN CITIES RESEARCH CENTER
5629 MINNEHAHA AVE. S.
MINNEAPOLIS, MN 55417

1. Anderson, A. E., and F. K. Cameron. Recovery of Copper by Leaching, Ohio Copper Co. of Utah. Trans. AIME, V. 73, 1926, pp. 31-57.

2. Anderson, M. L. Improved Productivity from in Situ Leaching. Proc. on Productivity in Mining, Univ. Missouri--Rolla, Rolla, Mo., May 13-15, 1974, ed. by J. J. Scott, pp. 82-83.

3. Anderson, M. L. (assigned to Mobil Oil Corporation, a corp. of New York). Methods of Selectively Improving the Fluid Communication of Earth Formations. U.S. Pat. 3,565,173, Feb. 23, 1971.

4. Arnold, W. D., and D. J. Crouse. Radioactive Contamination of Copper Recovered from Ore Fractured with Nuclear Explosions. Oak Ridge National Laboratory, Rept. ORNL-4677, September 1971, 55 pp.

5. Austin, W. L. Process of Extracting Copper from Ore. U.S. Pat. 975,106, Nov. 8, 1910.

6. Axen, S., D. Baughman, and R. V. Huff. In Situ Mining - A New Engineering Opportunity. SME Preprint 79-323, 11 pp.

7. Ballard, J. K. Solution Mining. Min. Eng., V. 23, No. 2, February 1971, p. 109.

8. Bartlett, R. W. A Combined Pore Diffusion and Chalcopyrite Dissolution Kinetics Model for In Situ Leaching of a Fragmented Copper Porphyry. Proc. Second Internat. Symp. on Hydrometallurgy, ed. by D. J. I. Evans, and R. S. Shoemaker. V. 1, Ch. 14, 1973, pp. 331-374.

9. Bhappu, R. B. Economic Evaluation of In Place Leaching and Solution Mining Situations. Pres. at a Short Course in In-Place Leaching and Solution Mining, the Mackay School of Mines, Univ. Nevada--Reno, Reno, Nev., Nov. 10-14, 1975, 22 pp.

10. Bhappu, R. B. In Situ Extraction and Leaching Technology. Pres. at Inter-Regional Seminar on the Economics of Mineral Engineering, Ankara, Turkey, Apr. 5-16, 1976, 39 pp.

11. Bhappu, R. B. In Situ Mining Technology - Practical and Economic Aspects. Pres. at the Turkish Mining Institute, Ankara, Turkey, Apr. 5-16, 1976, 29 pp.

12. Bhappu, R. B., and F. M. Lewis. Economic Evaluation of Available Processes for Treating Oxide Copper Ores. Pres. at Fall Meeting, Soc. of Min. Eng., AIME, Acapulco, Mexico, Sept. 22-25, 1974, Preprint No. 74-AS-334, 20 pp.

48. Eisenbarth, W. A. Reconcilation: Environmental Issues in In-Situ Mining vs Regulatory Constraints. Pres. at Uranium Resource Tech. Seminar II. Colorado School of Mines, Golden, Colorado, Mar. 12-14, 1979, 7 pp.

49. Engineering and Mining Journal. AEC and KCC Will Jointly Study Potential of Nuclear Blasting to Mine Copper Ore. V. 174, No. 4, April 1973, pp. 26-30.

50. Engineering and Mining Journal. Asarco and Dow Chemical to Leach Deep Copper Orebody In Situ in Arizona. V. 173, No. 6, June 1972, p. 19.

51. Engineering and Mining Journal. Copper Leaching with Cyanide - A Review of Five Inventions. V. 168, No. 9, September 1967, pp. 123-127.

52. Engineering and Mining Journal. Economics Provide Motive for Growth of Bacteria Leaching. V. 167, No. 6, June 1966, 543 pp.

53. Engineering and Mining Journal. The Estimated Cost of a Nuclear Leaching Experiment on Copper Ore. V. 169, No. 6, June 1968, p. 186.

54. Engineering and Mining Journal. India Studies Possibility of Copper Mining by Nuclear Blasts. V. 171, No. 7, July 1970, 33 pp.

55. Engineering and Mining Journal. Kennecott Investigates Solution Mining Potential of Deep Cu Deposit. V. 176, No. 9, September 1975, pp. 37, 41.

56. Engineering and Mining Journal. Kennecott Sets Sights on Nuclear Test for In Situ Recovery of Copper. V. 168, No. 11, November 1967, pp. 116-122.

57. Engineering and Mining Journal. The Oxymin Project at Miami, Arizona. A Summary of A Presentation Made to Miami, Arizona Town Council, Sept. 12, 1977, 9 pp.

58. Engineering and Mining Journal. Ranchers Big Blast Shatters Copper Orebody for In-Situ Leaching. V. 173, No. 4, April 1972, pp. 98-100.

59. Engineering and Mining Journal. Solution Mining Opening New Reserves. V. 175, No. 7, July 1974, pp. 62-71.

60. Fehlner, F. P. Electrochemical Method of Mining. U.S. Pat. 3,819,231, June 25, 1974.

61. Finlay, W. L. Molecular Mining of Keweenaw Copper, A Prime Candidate for the Enlargement of Non-Renewable Mineral Reserves through Technology. Panel Discussion at the Joint NAS-NAE Meeting on National Policy, Washington D.C., Oct. 25, 1973, 15 pp.

76. Hardwick, W. R. Fracturing a Deposit with Nuclear Explosives and Recovering Copper by the In-Situ Leaching Method. BuMines RI 6996, 1967, 48 pp.

77. Heinen, H. J., T. G. Carnahan, and J. A. Eisele (assigned to the United States of America, as represented by the Secretary of the Interior, Washington, D.C.). Chemical Mining of Copper Porphyry Ores. U.S. Pat. 3,890,007, June 17, 1975.

78. Hockings, W. A., and W. L. Freyberger. Laboratory Studies of In Situ Ammonia Leaching of Michigan Copper Ores. Proc. Internat. Symp. on Copper Extraction and Refining, Met. Soc., AIME, Las Vegas, Nev., Feb. 22-26, 1976 (pub. as Extractive Metallurgy of Copper--Hydrometallurgy and Electrowinning, ed. by J. C. Yannopoulos and J. C. Agarwal). Port City Press, Baltimore, Md., V. II, 1976, pp. 873-906.

79. Hockings, W. A., and W. L. Freyberger. A Plan for Determining the Feasibility of In Situ Leaching of Native Copper Ores. Institute of Mineral Research, Michigan Technological University, Houghton, Michigan. Prepared for Homestake Copper Co., Calumet, Michigan, June 14, 1974, 36 pp.

80. Hogan, D. K. In-Situ Copper Leaching at the Old Reliable Mine. Min. Mag., V. 24, No. 5, May 1974, pp. 353-359.

81. Holderreed, F. L. Copper Extraction by the Acid Leaching of Broken Ore. Pincock, Allen and Holt, Inc. Report, 1975, 19 pp.

82. Hougen, L. R., and H. Zachariasen. Recovery of Nickel, Copper and Precious Metal Concentrate from High Grade Precious Metal Mattes. J. Metals, V. 27, No. 5, May 1975, pp. 6-9.

83. Hsueh, L., R. A. Hard, D. H. Davidson, and R. V. Huff (assigned to Kennecott Copper Corp.). In-Situ Mining Method and Apparatus. U.S. Pat. 4,116,488, Sept. 26, 1978.

84. Hsuen, L., R. A. Hurd, D. H. Davidson, and R. V. Huff (assigned to Kennecott Copper Corp.). In-Situ Mining of Copper and Nickel. U.S. Pat. 4,045,084, August 30, 1977.

85. Huff, R. V., and D. H. Davidson (assinged to Kennecott Copper Corporation). Method for In Situ Minefields. U.S. Pat. 4,125,289, Nov. 14, 1978.

86. Huff, R. V., and H. Davidson. In-Situ Leaching Materials Considerations. Pres. at 54th Ann. Fall Tech. Conf. and Exhibition, Soc. Petrol. Eng., AIME, Las Vegas, Nev., Sept. 23-26, 1979, SPE Preprint 8320, 6 pp.

87. Huff, R. V., and P. A. Huska (assigned to Kennecott Copper Corp.). Wellbore Oxidation of Lixivants. U.S. Pat. 3,894,770, July 15, 1975.

100. Lampard, W. J. (assigned to Kennecott Copper Corporation, New York, N.Y.). Controlled In Situ Leaching of Ore Deposits Utilizing Pre-split Blasting. U.S. Pat. 3,863,987, Feb. 4, 1975.

101. Larson, D. R. A Report Comparing Open Pit Mining and Heap Leaching with an In Situ Leaching System for a Hypothetical Oxide Copper Deposit Based on the Characteristics of the Cactus Deposit, Miami, Arizona. M.S. Thesis, Univ. Minnesota, Dept. of Mineral and Metallurgical Eng., June 1973, 254 pp.

102. Laswell, G. W. Considerations Applicable to Utilization of Rotary Drilling for In-Place Recovery of Minerals and Hydrocarbons. Servco Div. of Smith Internat., Inc. Report, February 1975, 8 pp.

103. Laswell, G. W. Wanted: Rotary Drilling Technology for In Situ Mining Systems. Min. Eng., V. 27, No. 1, January 1976, pp. 22-26.

104. Leach, D. L., and R. L. Braun. Leaching of Primary Sulfide Ores in Sulfuric Acid Solutions at Elevated Temperatures and Pressures. Pres. at Ann. Meeting, Soc. Min. Eng., AIME, New York, Feb. 16-20, 1975, Preprint 75B68, 20 pp.

105. Lewis, A. E. Chemical Mining of Primary Copper Ores by Use of Nuclear Technology. Proc. Symp. of Engineering with Nuclear Explosives, Las Vegas, Nev., Jan. 14-16, 1970, Conf. 700101, V. 21, pp. 907-917.

106. Lewis, A. E. In Situ Pressure Leaching Method. U.S. Pat. 3,640,579, Feb, 8, 1972.

107. Lewis, A. E. (assigned to the United States of America as Represented by the U.S. Atomic Energy Commission, Washington, D.C.). Situ Leaching Solvent Extraction-Process. U.S. Pat. 3,823,981, July 16, 1974.

108. Lewis, A. E., and R. L. Braun. Nuclear Chemical Mining of Primary Copper Sulfides. Pres. at the AIME Meeting, San Francisco, Calif., Jan. 27, 1972, 30 pp.

109. Lewis, A. E., R. L. Braun, C. J. Sisemore, and R. G. Mallon. Nuclear Solution Mining-breaking and Leaching Considerations. Proc. Solution Mining Symp., AIME Ann. Meeting, Dallas, Texas, Feb. 25-27, 1974, pp. 56-75.

110. Lewis, F. M., and R. B. Bhappu. Evaluating Mining Ventures Via Feasibility Studies. Min. Eng., V. 27, No. 10, October 1975, pp. 48-54.

125. Mining Engineering. Ranchers Development Sets Off Blast, Will Leach at Big Mike. V. 25, No. 8, August 1973, p. 10.

126. Mining Magazine. Winning of Useful Elements from Minerals by Leaching Underground. V. 118, No. 2, February 1968, pp. 129-134.

127. Mining Record (Denver, Colorado). Ranchers Blasts Old Reliable to Test New Mining Technique. V. 83, No. 12, Mar. 22, 1972, P. 1.

128. Murphy, J. New Returns from Old Reliable. Source Unknown, pp. 20-23; Copy Available for Consultation at Bureau of Mines, Twin Cities Research Center, Minneapolis, Minnesota.

129. Myers, D. L. Mining Copper In Situ. The Mines Mag., V. 31, No. 6, June 1941, pp. 255-263.

130. Occidental Minerals Corp. The Oxymin Project at Miami, Arizona. A Summary of a Presentation Made to Miami, Arizona Town Council, Sept. 12, 1977, 5 PP.; for Further Information, Contact Bob Zache, Occidental Minerals Corp., 918 Live Oak St., Miami, Arizona 85539.

131. O'Rourke, J. E., R. J. Essex, and B. K. Ranson. Field Permeability Test Methods with Applications to Solution Mining. Woodward-Clyde Consultants (San Diego, Calif.), Contract No. J0265045. BuMines Open File Rept. 136-77, July 1977, 180 PP.; Available from National Technical Information Service, Springfield, Va., PB 272 452/AS.

132. Ortloff, G. D., C. E. Cooke, Jr., and D. K. Atwood (assigned to Esso Production Research Company). Mineral Recovery. U.S. Pat. 3,574,599, Apr. 13, 1971.

133. Pay Dirt, Arizona Edition (Bisbee, Arizona). Companies Sue Town of Miami, Charging it Prevents Copper Mine Development. No. 502, April 1981, pp. 6-10.

134. Pay Dirt, Arizona Edition (Bisbee, Arizona). Oxymin Plans Final In Situ Copper Leaching Tests at Miami. No. 486, December 1979, pp. 1, 4.

135. Petrovic, L. J., R. A. Hard, and I. V. Klumpar. Economic Considerations for Recovering Copper from Deep Sulfide Deposits by Nuclear Rubblization. In Situ, V. 1, No. 3, 1977, pp. 235-248.

136. Pings, W. B. Bacterial Leaching. Miner. Ind. Bull., V. 2, No. 3, May 1968, 19 pp.

137. Pojar, M. In-Place Leaching of a Copper Sulfide Deposit. Pres. at Duluth Meeting, Soc. of Min. Eng., AIME, Duluth, Minn., Jan. 16-18, 1974, 9 pp.

153. Rouse, J. V. Environmental Aspects of In Situ Mining and Dump Leaching. Proc. Solution Mining Symp., AIME Ann. Meeting, Dallas, Texas, Feb. 25-27, 1974, pp. 3-14.

154. Rudershausen, C. G. Copper Solution Mining at Old Reliable. Pres. at National Meeting of American Inst. of Chemical Eng., Salt Lake City, Nev., Aug. 18-21, 1974, 11 pp.

155. St. Peter, A. L. In Situ Leaching of Orebodies Design and Management. Pincock, Allen and Holt, Inc. Report, 1975, 20 pp.

156. St. Peter, A. L. In Situ Mining -- A Design for Positive Results. Pres. at 105th Ann. Meeting, AIME, Las Vegas, Nev., Feb. 22-26, 1976, Preprint 76-AS-36, 43 pp.

157. Sareen, S. S., L. Girard, III, and R. A. Hard. Stimulation of Recovery from Underground Deposits. U.S. Pat. 3,865,435, Feb. 11, 1975.

158. Schlitt, W. J., B. P. Ream, L. J. Haug, and W. D. Southard. Precipitating and Drying Cement Copper at Kennecotts Bingham Canyon Facility. Min. Eng., V. 31, No. 6, June 1979, pp. 671-678.

159. Scott, W. G. (assigned to Inspiration Consolidated Copper Company, a Corporation of Maine). Leaching Copper Ores. U.S. Pat. 2,563,623, Aug. 7, 1951.

160. Selim, A. A. A Decision Analysis Approach to In Situ Extraction of Copper. Ph.d. Thesis, Univ. Minnesota, Minneapolis, Minn., March 1976, 659 pp.

161. Selim, A. A., and D. H. Yardley. The Design and Cost of a Fragmentation System for In Situ Extraction of Copper. Pres. at 14th Internat. Symp. on the Application of Computer Methods in the Mineral Industry, the Pennsylvania State University, University Park, Pa., Oct. 14-16, 1976.

162. Selim, A. A., and D. H. Yardley. In Situ Leaching of Copper -- an Economic Simulation Approach. Pres. at 107th Ann. Meeting, AIME, Atlanta, Ga., March 1977, Preprint 77-AS-68, 24 pp.

163. Sheffer, H. W., and L. G. Evans. Copper Leaching Practices in the Western United States. BuMines IC 8341, 1968, 57 pp.

164. Shock, D. A. Developments in Solution Mining Portend Greater Use for In Situ Leaching. Min. Eng., V. 22, No. 2, February 1970, p. 73.

165. Shock, D. A., and J. G. Davis, II. (assigned to Continental Oil Company, Ponca City, Okla., a corporation of Delaware). Fracturing Method in Solution Mining. U.S. Pat. 3,387,888, June 11, 1968.

13. Braithwaite, J. W., and M. E. Wadsworth. Oxidation of Chalcopyrite under Simulated Conditions of Deep Solution Mining. Proc. Internat. Symp. on Copper Extraction and Refining, Met. Soc., AIME, Las Vegas, Nev., Feb. 22-26, 1976 (pub. as Extractive Metallurgy of Copper--Hydrometallurgy and Electrowinning, ed. by J. C. Yannopoulos and J. C. Agarwal). Port City Press, Baltimore, Md., V. II, 1976, pp. 752-775.

14. Braun, R. L., and A. E. Lewis. Nuclear Solution Mining: Part VIII - Oxygen Distribution. Lawrence Radiation Laboratory, Rept. UCID-16008, March 1972, 31 pp.

15. Braun, R. L., A. E. Lewis, and M. E. Wadsworth. In Place Leaching of Primary Sulfide Ores: Laboratory Leaching Data and Kinetics Model. Proc. Solution Mining Symp., AIME Ann. Meeting, Dallas, Tex., Feb. 25-27, 1974, pp. 295-323; Met. Trans., V. 5, No. 8, August 1974, pp. 1717-1726.

16. Braun, R. L., and R. G. Mallon. Combined Leach-Circulation Calculation for Predicting In-Situ Copper Leaching of Primary Sulfide Ore. Trans. Soc. of Min. Eng., AIME, V. 258, No. 2, June 1975, pp. 103-110.

17. Brierley, C. L. Column Leaching of Low-Grade Chalcopyrite Ore Using Thermophilic Bacteria. New Mexico Bureau of Mines and Mineral Resources (Socorro, New Mexico), BuMines Grant No. G0177100, June 1978, 44 pp.

18. Brierley, C. L. Leaching: Use of a High-Temperature Microbe. Ch. 31 in Solution Mining Symposium, ed. by F. F. Alpan, W. K. McKinney, and A. D. Pernichele. The American Institute of Mining, Metallurgical, and Petroleum Engineers, Inc., New York, 1974, pp. 461-469.

19. Brinckerhoff, C. M. Assessment of Research and Development Needs and Priorities for In Situ Leaching of Copper. Consultants Final Report, BuMines Contract J0166036, July 26, 1976, 5 pp.

20. Bruynesteyn, A., and D. W. Duncan. Effect of Particle Size on the Microbiological Leaching of Chalcopyrite Bearing Ore. Proc. Solution Mining Symp., AIME Ann. Meeting, Dallas, Texas, Feb. 25-27, 1974, pp. 324-337.

21. Cannon, K. J. Solvent Extraction - Electrowinning Technology for Copper. Australian Mining, March 1977, pp. 47-51.

22. Carnahan, T. G., and H. J. Heinen (assigned to the United States of America as Represented by the Secretary of the Interior, Washington, D.C.). Chemical Mining of Copper Porphyry Ores. U.S. Pat. 3,912,330, Oct. 14, 1975.

23. Carnahan, T. G., and H. J. Heinen. Simulated In Situ Leaching of Copper from a Porphyry Ore. BuMines TPR 69, May 1973, 11 pp.

180. Trussell, P. C., D. W. Duncan, and C. C. Walden. Biological Mining. Can. Min. J., V. 85, No. 3, March 1964, pp. 46-49.

181. U.S. Bureau of Mines. Project Proposal: Porphyry Copper - In Situ Recovery by Leaching Following Non-Nuclear Fracturing. Interdisciplinary Research Task Force, Comp. by L. W. Gibbs, Nov. 23, 1971, (rev. Dec. 6, 1971), 20 pp. Available for Consultation at Bureau of Mines, Twin Cities Mining Research Center, Minneapolis, Minnesota.

182. U.S. Energy Research and Development Administration. In Situ Leaching of a Nuclear Rubblized Copper Ore Body (in Two Volumes). V. 1, Results of Feasibility Study U.S. ERDA Report NVO-155, June 1975, 30 PP.; V. 2, Detailed Design, Calculations, and Procedures, Report NVO-155, June 1975, 318 pp.

183. Van Poolen, H. K., and R. V. Huff (assigned to Kennecott Copper Corp.). Oxidation of Sulfide Deposits Containing Copper Values. U.S. Pat. 3,881,774, May 6, 1975.

184. Vortman, L. J. Airblast from Sequential Detonation of Groups of Charges in Vertical Drilled Holes. Unlimited Release Sand 75-0194, U.S. Energy Research and Development Admin. Contract AT(29-1)-789, September 1975, 48 PP.; Available from National Technical Information Service, 5285 Port Royal Road, Springfield, Virginia 22151, Sand75-0194.

185. Ward, M. H. Engineering for In Situ Leaching. Min. Cong. J., V. 59, No. 1, January 1973, pp. 21-27.

186. Ward, M. H. Surface Blasting Followed by In Situ Leaching the Big Mike Mine. Proc. Solution Mining Symp., AIME Ann. Meeting, Dallas, Texas, Feb. 25-27, 1974, pp. 243-251.

187. Watson, J. D., Sr., W. A. Mod, and F. N. Teumac (assigned to Dow Chemical Co.). Extraction of Copper, Nickel, Cobalt or Chromium Values from Sulfide, Oxide or Silicate Ores Thereof. U.S. Pat. 3,475,163, Oct. 28, 1969.

188. Weed, R. C. Cananeas Program for Leaching In Place. Min. Eng., V. 8, No. 7, July 1, 1956, pp. 721-723.

189. Wormser, F. E. Leaching a Copper Mine. Eng. and Min. J., V. 116, No. 16, October 1923, pp. 665-670.

190. Zimmer, P. F., and M. A. Lekas. (comp. and ed. by). Project Sloop (Nuclear Explosives-Peaceful Applications). U.S. Atomic Energy Commission Report No. PNE 1300, June 1, 1967, 44 pp.

36. D'Andrea, D. V., and S. M. Runke. In Situ Copper Leaching Research at the Emerald Isle Mine. Proc. Joint Meeting of the Mining and Metallurgical Institute of Japan and the American Institute of Mining, Metallurgical, and Petroleum Engineers, Denver, Colo., Sept. 1-3, 1976 (pub. as World Mining and Metals Technology, ed. by A. Weiss), V. 1, 1976, pp. 409-419.

37. Davidson, D. H. In-Situ Leaching of Non-Ferrous Metals. Science Applications, Inc. Internal Report 1979, 16 PP.; Available from Science Applications, Inc., 1200 Prospect Street, La Jolla, California.

38. Davidson, D. H. In-Situ Leaching of Nonferrous Metals. Min. Cong. J., V. 66, No. 7, July 1980, pp. 52-54, 57.

39. Davidson, D. H. Optimization of In-Situ Leaching Strategies. Science Applications, Inc. Internal Report 1979, 17 PP.; Available from Science Applications, Inc., 1200 Prospect Street, La Jolla, California.

40. Davidson, D. H., and R. V. Huff (assigned to Kennecott Copper Corp.). Well Stimulation for Solution Mining. U.S. Pat. 3,917,345, Nov. 4, 1975.

41. Davidson, D. H., R. V. Huff, and W. E. Sonstelie. Measurement and Control in Solution Mining of Deep-Lying Deposits of Copper or Uranium. Pres. at Instrument Soc. of America Min. and Met. Ind. Div. Symp., Denver, Colo., Nov. 1-3, 1978, 7 pp.

42. Davis, L. L. Bureau of Mines Research to Improve Underground Metal/Nonmetal Mining Technology. Pres. at AIME Ann. Meeting, New Orleans, La., Feb. 18-22, 1979, Preprint 79-46, 14 pp.

43. Dick, R. A. In Situ Fragmentation for Solution Mining - A Research Need. Pres. at the Second Internat. Symp. on Drilling and Blasting, Phoenix, Arizona, Feb. 12-16, 1973; Available for Consultation at Bureau of Mines, Twin Cities Research Center, Minneapolis, Minnesota.

44. Dravo Corporation. Solution Mining. Section 6.6.2 in Analysis of Large Scale Non-Coal Underground Mining Methods, BuMines Contract Report S0122059, January 1974, pp. 455-464.

45. Dudas, L., H. Maass, and R. B. Bhappu. Role of Mineralogy in Heap and In Situ Leaching of Copper Ores. Proc. Solution Mining Symp., AIME Ann. Meeting, Dallas, Texas, Feb. 25-27, 1974, pp. 193-209.

46. Duncan, D. W., and C. J. Teather (assigned to British Columbia Research Council). Method for the Microbiological Leaching of Copper, Nickel, Zinc, Molybdenum. U.S. Pat. 3,266,889, Aug. 16, 1966.

47. Duncan, D. W., C. C. Walden, and P. C. Trussell. Biological Leaching of Mill Products. Can. Min. and Met. Bull., V. 59, No. 653, September 1966, pp. 1075-1079.

1. ANDERSON, A. E., AND F. K. CAMERON. RECOVERY OF COPPER BY LEACHING, OHIO COPPER CO. OF UTAH. TRANS. AIME, V. 73, 1926, PP. 31-57.

2. ANDERSON, M. L. IMPROVED PRODUCTIVITY FROM IN SITU LEACHING. PROC. ON PRODUCTIVITY IN MINING, UNIV. MISSOURI--ROLLA, ROLLA, MO., MAY 13-15, 1974, ED. BY J. J. SCOTT, PP. 82-83.

3. ANDERSON, M. L. (ASSIGNED TO MOBIL OIL CORPORATION, A CORP. OF NEW YORK). METHODS OF SELECTIVELY IMPROVING THE FLUID COMMUNICATION OF EARTH FORMATIONS. U.S. PAT. 3,565,173, FEB. 23, 1971.

4. ARNOLD, W. D., AND D. J. CROUSE. RADIOACTIVE CONTAMINATION OF COPPER RECOVERED FROM ORE FRACTURED WITH NUCLEAR EXPLOSIONS. OAK RIDGE NATIONAL LABORATORY, REPT. ORNL-4677, SEPTEMBER 1971. 55 PP.

5. AUSTIN, W. L. PROCESS OF EXTRACTING COPPER FROM ORE. U.S. PAT. 975,106, NOV. 8, 1910.

6. BALLARD, J. K. SOLUTION MINING. MIN. ENG., V. 23, NO. 2, FEBRUARY 1971, P. 109.

7. BARTLETT, R. W. A COMBINED PORE DIFFUSION AND CHALCOPYRITE DISSOLUTION KINETICS MODEL FOR IN SITU LEACHING OF A FRAGMENTED COPPER PORPHYRY. PROC. SECOND INTERNAT. SYMP. ON HYDROMETALLURGY, ED. BY D. J. I. EVANS, AND R. S. SHOEMAKER. V. 1, CH. 14, 1973, PP. 331-374.

8. BHAPPU, R. B. ECONOMIC EVALUATION OF IN PLACE LEACHING AND SOLUTION MINING SITUATIONS. PRES. AT A SHORT COURSE IN IN-PLACE LEACHING AND SOLUTION MINING, THE MACKAY SCHOOL OF MINES, UNIV. NEVADA--RENO, RENO, NEV., NOV. 10-14, 1975, 22 PP.

9. BHAPPU, R. B. IN SITU EXTRACTION AND LEACHING TECHNOLOGY. PRES. AT INTER-REGIONAL SEMINAR ON THE ECONOMICS OF MINERAL ENGINEERING, ANKARA, TURKEY, APR. 5-16, 1976, 39 PP.

10. BHAPPU, R. B. IN SITU MINING TECHNOLOGY - PRACTICAL AND ECONOMIC ASPECTS. PRES. AT THE TURKISH MINING INSTITUTE, ANKARA, TURKEY, APR. 5-16, 1976, 29 PP.

11. BHAPPU, R. B., AND F. M. LEWIS. ECONOMIC EVALUATION OF AVAILABLE PROCESSES FOR TREATING OXIDE COPPER ORES. PRES. AT FALL MEETING, SOC. OF MIN. ENG., AIME, ACAPULCO, MEXICO, SEPT. 22-25, 1974, PREPRINT NO. 74-AS-334, 20 PP.

12. BRAITHWAITE, J. W., AND M. E. WADSWORTH. OXIDATION OF CHALCOPYRITE UNDER SIMULATED CONDITIONS OF DEEP SOLUTION MINING. PROC. INTERNAT. SYMP. ON COPPER EXTRACTION AND REFINING, MET. SOC., AIME, LAS VEGAS, NEV., FEB. 22-26, 1976 (PUB. AS EXTRACTIVE METALLURGY OF COPPER--HYDROMETALLURGY AND ELECTROWINNING, ED. BY J. C. YANNOPOULOS AND J. C. AGARWAL). PORT CITY PRESS, BALTIMORE, MD., V. II, 1976, PP. 752-775.

13. BRAUN, R. L., AND A. E. LEWIS. NUCLEAR SOLUTION MINING: PART VIII - OXYGEN DISTRIBUTION. LAWRENCE RADIATION LABORATORY. REPT. UCID-16008, MARCH 1972. 31 PP.

14. BRAUN, R. L., AND R. G. MALLON. COMBINED LEACH-CIRCULATION CALCULATION FOR PREDICTING IN-SITU COPPER LEACHING OF PRIMARY SULFIDE ORE. TRANS. SOC. OF MIN. ENG., AIME, V. 258, NO. 2, JUNE 1975. PP. 103-110.

15. BRIERLEY, C. L. COLUMN LEACHING OF LOW-GRADE CHALCOPYRITE ORE USING THERMOPHILIC BACTERIA. NEW MEXICO BUREAU OF MINES AND MINERAL RESOURCES (SOCORRO, NEW MEXICO). BUMINES GRANT NO. G0177100, JUNE 1978. 44 PP.

16. BRIERLEY, C. L. LEACHING: USE OF A HIGH-TEMPERATURE MICROBE. CH. 31 IN SOLUTION MINING SYMPOSIUM, ED. BY F. F. ALPAN, W. K. MCKINNEY, AND A. D. PERNICHELE. THE AMERICAN INSTITUTE OF MINING, METALLURGICAL, AND PETROLEUM ENGINEERS, INC., NEW YORK, 1974. PP. 461-469.

17. BRINCKERHOFF, C. M. ASSESSMENT OF RESEARCH AND DEVELOPMENT NEEDS AND PRIORITIES FOR IN SITU LEACHING OF COPPER. CONSULTANTS FINAL REPORT, BUMINES CONTRACT J0166036, JULY 26, 1976. 5 PP.

18. BRUYNESTEYN, A., AND D. W. DUNCAN. EFFECT OF PARTICLE SIZE ON THE MICROBIOLOGICAL LEACHING OF CHALCOPYRITE BEARING ORE. PROC. SOLUTION MINING SYMP., AIME ANN. MEETING, DALLAS, TEXAS, FEB. 25-27, 1974. PP. 324-337.

19. CANNON, K. J. SOLVENT EXTRACTION - ELECTROWINNING TECHNOLOGY FOR COPPER. AUSTRALIAN MINING, MARCH 1977. PP. 47-51.

20. CARNAHAN, T. G., AND H. J. HEINEN (ASSIGNED TO THE UNITED STATES OF AMERICA AS REPRESENTED BY THE SECRETARY OF THE INTERIOR, WASHINGTON, D.C.). CHEMICAL MINING OF COPPER PORPHYRY ORES. U.S. PAT. 3,912,330, OCT. 14, 1975.

21. CARNAHAN, T. G., AND H. J. HEINEN. SIMULATED IN SITU LEACHING OF COPPER FROM A PORPHYRY ORE. BUMINES TPR 69, MAY 1973. 11 PP.

22. CARPENTER, R. H., AND R. R. RHAPPU. HYDROMETALLURGY AND LOW GRADE ORE POTENTIAL. PRES. AT 107TH ANN. MEETING, AIME, ATLANTA, GA., MAR. 6-10, 1977.

23. CATANACH, C. B. DEVELOPMENT AND IN PLACE LEACHING OF MOUNTAIN CITY CHALCOCITE ORE BODY. PROC. INTERNAT. SYMP. ON COPPER EXTRACTION AND REFINING, MET. SOC., AIME, LAS VEGAS, NEV., FEB. 22-26, 1976 (PUB. AS EXTRACTIVE METALLURGY OF COPPER--HYDROMETALLURGY AND ELECTROWINNING, ED. BY J. C. YANNOPOULOS AND J. C. AGARWAL). PORT CITY PRESS, BALTIMORE, MD., V. II, 1976. PP. 849-872.

24. CATANACH, C. B., E. F. MORAN, D. D. PORTER, C. G. RUDERSHAUSEN, AND R. W. SOMMERS. COPPER LEACHING FROM AN OREBODY BLASTED IN PLACE. IN SITU, V. 1, NO. 4, 1977. PP. 283-303.

25. CHAMBERLAIN, C., J. NEWTON, AND D. CLIFTON. HOW CYANIDATION CAN TREAT COPPER ORES. ENG. AND MIN. J., V. 170, NO. 10, OCTOBER 1969, PP. 90-91.

26. CHAMBERLAIN, P. G. IN-PLACE LEACHING RESEARCH AT THE SENECA MINE, MOHAWK, MICH. PRES. AT ANN. SPRING TECHNICAL MEETING OF UPPER PENINSULA SECTION, AIME, MICHIGAN TECHNOLOGICAL UNIV., HOUGHTON, MICH., APR. 21, 1977, 14 PP.; AVAILABLE FROM PETER G. CHAMBERLAIN, U.S. BUREAU OF MINES, P.O. BOX 1660, TWIN CITIES, MINNESOTA 55111.

27. CHILSON, R. E. CONTINUOUSLY LEACHING AN ORE COLUMN. U.S. PAT. 4,071,611, JAN. 31, 1978.

28. COOPER, F. D. COPPER HYDROMETALLURGY: A REVIEW AND OUTLOOK. BUMINES IC 8394, 1968, 18 PP.

29. D'ANDREA, D. V., P. G. CHAMBERLAIN, AND J. K. AHLNESS. A TEST BLAST FOR IN SITU COPPER LEACHING. PRES. AT 1978 AIME ANN. MEETING, DENVER, COLO., FEB. 26 - MAR. 2, 1978, PREPRINT 78-AS-112, 13 PP.

30. D'ANDREA, D. V., P. G. CHAMBERLAIN, AND L. R. FLETCHER. GROUND CHARACTERIZATION FOR IN SITU COPPER LEACHING. PRES. AT 109TH ANNUAL MEETING, SOC. MIN. ENG., AIME, LAS VEGAS, NEVADA, FEB. 24-28, 1980.

31. D'ANDREA, D. V., R. A. DICK, R. C. STECKLEY, AND W. C. LARSON. A FRAGMENTATION EXPERIMENT FOR IN SITU EXTRACTION. PROC. SOLUTION MINING SYMP., AIME ANN. MEETING, DALLAS, TEX., FEB. 25-27, 1974, PP. 148-161.

32. D'ANDREA, D. V., W. C. LARSON, P. G. CHAMBERLAIN, AND J. J. OLSON. SOME CONSIDERATIONS IN THE DESIGN OF BLASTS FOR IN SITU COPPER LEACHING. PRES. AT 17TH U.S. SYMP. ON ROCK MECH., SNOWBIRD, UTAH, AUG. 25-27, 1976, 15 PP.

33. D'ANDREA, D. V., W. C. LARSON, L. R. FLETCHER, P. G. CHAMBERLAIN, AND W. H. ENGELMANN. IN SITU LEACHING RESEARCH IN A COPPER DEPOSIT AT THE EMERALD ISLE MINE. BUMINES RI 8236, 1977, 43 PP.

34. D'ANDREA, D. V., AND S. M. RUNKE. IN SITU COPPER LEACHING RESEARCH AT THE EMERALD ISLE MINE. PROC. JOINT MEETING OF THE MINING AND METALLURGICAL INSTITUTE OF JAPAN AND THE AMERICAN INSTITUTE OF MINING, METALLURGICAL, AND PETROLEUM ENGINEERS, DENVER, COLO., SEPT. 1-3, 1976 (PUB. AS WORLD MINING AND METALS TECHNOLOGY, ED. BY A. WEISS), V. 1, 1976, PP. 409-419.

35. DAVIDSON, D. H. IN-SITU LEACHING OF NON-FERROUS METALS. SCIENCE APPLICATIONS, INC. INTERNAL REPORT 1979, 16 PP.; AVAILABLE FROM SCIENCE APPLICATIONS, INC., 1200 PROSPECT STREET, LA JOLLA, CALIFORNIA.

36. DAVIDSON, D. H. OPTIMIZATION OF IN-SITU LEACHING STRATEGIES. SCIENCE APPLICATIONS, INC. INTERNAL REPORT 1979, 17 PP.; AVAILABLE FROM SCIENCE APPLICATIONS, INC., 1200 PROSPECT STREET, LA JOLLA, CALIFORNIA.

37. DAVIDSON, D. H. IN-SITU LEACHING OF NONFERROUS METALS. MIN. CONG. J., V. 66, NO. 7, JULY 1980, PP. 52-54, 57.

38. DAVIDSON, D. H., AND R. V. HUFF (ASSIGNED TO KENNECOTT COPPER CORP.). WELL STIMULATION FOR SOLUTION MINING. U.S. PAT. 3,917,345, NOV. 4, 1975.

39. DAVIDSON, D. H., R. V. HUFF, AND W. E. SONSTELIE. MEASUREMENT AND CONTROL IN SOLUTION MINING OF DEEP-LYING DEPOSITS OF COPPER OR URANIUM. PRES. AT INSTRUMENT SOC. OF AMERICA MIN. AND MET. IND. DIV. SYMP., DENVER, COLO., NOV. 1-3, 1978, 7 PP.

40. DICK, R. A. IN SITU FRAGMENTATION FOR SOLUTION MINING - A RESEARCH NEED. PRES. AT THE SECOND INTERNAT. SYMP. ON DRILLING AND BLASTING, PHOENIX, ARIZONA, FEB. 12-16, 1973; AVAILABLE FOR CONSULTATION AT BUREAU OF MINES, TWIN CITIES MINING RESEARCH CENTER, MINNEAPOLIS, MINNESOTA.

41. DRAVO CORPORATION. SOLUTION MINING. SECTION 6.6.2 IN ANALYSIS OF LARGE SCALE NON-COAL UNDERGROUND MINING METHODS, BUMINES CONTRACT REPORT S0122059, JANUARY 1974, PP. 455-464.

42. DUDAS, L., H. MAASS, AND P. B. BHAPPU. ROLE OF MINERALOGY IN HEAP AND IN SITU LEACHING OF COPPER ORES. PROC. SOLUTION MINING SYMP., AIME ANN. MEETING, DALLAS, TEXAS, FEB. 25-27, 1974, PP. 193-209.

43. DUNCAN, D. W., AND C. J. TEATHER (ASSIGNED TO BRITISH COLUMBIA RESEARCH COUNCIL). METHOD FOR THE MICROBIOLOGICAL LEACHING OF COPPER, NICKEL, ZINC, MOLYBDENUM. U.S. PAT. 3,266,889, AUG. 16, 1966.

44. DUNCAN, D. W., C. C. WALDEN, AND P. C. TRUSSELL. BIOLOGICAL LEACHING OF MILL PRODUCTS. CAN. MIN. AND MET. BULL., V. 59, NO. 653, SEPTEMBER 1966, PP. 1075-1079.

45. FISENBARTH, W. A. RECONCILATION: ENVIRONMENTAL ISSUES IN IN-SITU MINING VS REGULATORY CONSTRAINTS. PRES. AT URANIUM RESOURCE TECH. SEMINAR II, COLORADO SCHOOL OF MINES, GOLDEN, COLORADO, MAR. 12-14, 1979, 7 PP.

46. ENGINEERING AND MINING JOURNAL. AEC AND KCC WILL JOINTLY STUDY POTENTIAL OF NUCLEAR BLASTING TO MINE COPPER ORE. V. 174, NO. 4, APRIL 1973, PP. 26-30.

47. ENGINEERING AND MINING JOURNAL. ASARCO AND DOW CHEMICAL TO LEACH DEEP COPPER OREBODY IN SITU IN ARIZONA. V. 173, NO. 6, JUNE 1972, P. 19.

48. ENGINEERING AND MINING JOURNAL. COPPER LEACHING WITH CYANIDE - A REVIEW OF FIVE INVENTIONS. V. 169, NO. 9, SEPTEMBER 1967, PP. 123-127.

49. ENGINEERING AND MINING JOURNAL. ECONOMICS PROVIDE MOTIVE FOR GROWTH OF BACTERIA LEACHING. V. 167, NO. 6, JUNE 1966, 543 PP.

50. ENGINEERING AND MINING JOURNAL. THE ESTIMATED COST OF A NUCLEAR LEACHING EXPERIMENT ON COPPER ORE. V. 169, NO. 6, JUNE 1968. P. 186.

51. ENGINEERING AND MINING JOURNAL. INDIA STUDIES POSSIBILITY OF COPPER MINING BY NUCLEAR BLASTS. V. 171, NO. 7, JULY 1970, 33 PP.

52. ENGINEERING AND MINING JOURNAL. KENNECOTT INVESTIGATES SOLUTION MINING POTENTIAL OF DEEP CU DEPOSIT. V. 176, NO. 9, SEPTEMBER 1975. PP. 37, 41.

53. ENGINEERING AND MINING JOURNAL. KENNECOTT SETS SIGHTS ON NUCLEAR TEST FOR IN SITU RECOVERY OF COPPER. V. 168, NO. 11, NOVEMBER 1967, PP. 116-122.

54. ENGINEERING AND MINING JOURNAL. THE OXYMIN PROJECT AT MIAMI, ARIZONA. A SUMMARY OF A PRESENTATION MADE TO MIAMI, ARIZONA TOWN COUNCIL, SEPT. 12, 1977, 9 PP.

55. ENGINEERING AND MINING JOURNAL. RANCHERS BIG BLAST SHATTERS COPPER OREBODY FOR IN-SITU LEACHING. V. 173, NO. 4, APRIL 1972. PP. 98-100.

56. ENGINEERING AND MINING JOURNAL. SOLUTION MINING OPENING NEW RESERVES. V. 175, NO. 7, JULY 1974, PP. 62-71.

57. FEHLNER, F. P. ELECTROCHEMICAL METHOD OF MINING. U.S. PAT. 3,819,231, JUNE 25, 1974.

58. FINLAY, W. L. MOLECULAR MINING OF KEWEENAW COPPER, A PRIME CANDIDATE FOR THE ENLARGEMENT OF NON-RENEWABLE MINERAL RESERVES THROUGH TECHNOLOGY. PANEL DISCUSSION AT THE JOINT NAS-NAE MEETING ON NATIONAL POLICY, WASHINGTON D.C., OCT. 25, 1973, 15 PP.

59. FITCH, J. L., AND B. G. HURD (ASSIGNED TO MOBIL OIL CORPORATION, A CORPORATION OF NEW YORK). IN SITU LEACHING METHOD. U.S. PAT. 3,278,232, OCT. 11, 1966.

60. FLETCHER, D. A. (ASSIGNED TO TALLEY-FRAC CORPORATION, PRYOR, OKLA., A CORP. OF DEL.). WELL FRACTURING METHOD USING EXPLOSIVE SLURRY. U.S. PAT. 3,561,532, FEB. 9, 1971.

61. FLETCHER, J. B. IN PLACE LEACHING. SKILLINGS MINING REVIEW, V. 63, NO. 17, APR. 27, 1974, PP. 7-10.

62. FLETCHER, J. B. IN PLACE LEACHING AT MIAMI MINE, MIAMI, ARIZONA. PRES. AT AIME CENTENNIAL ANN. MEETING, SOC. OF MIN. ENG., AIME, NEW YORK, N.Y., MARCH 1971, AIME PREPRINT 71-AS-40: TRANS. SOC. OF MIN. ENG., AIME, V. 250, NO. 4, DECEMBER 1971. PP. 310-314.

63. FLETCHER, J. B. IN PLACE LEACHING MIAMI MINE. PRES. AT ARIZONA SECTION MEETING, MILLING DIV., AIME, APR. 6, 1962, 9 PP.

64. GERLACH, J. K., AND F. F. PAWLEK. ON THE KINETICS OF PRESSURE LEACHING OF METAL SULFIDES AND ORES. PRES. AT THE TMS-AIME ANN. MEETING, FEB. 25-29, 1968, NEW YORK, 1968, TMS PAPER A68-4, 15 PP.

65. GIRARD, L., AND R. A. HARD. (ASSIGNED TO KENNECOTT COPPER CORPORATION, NEW YORK, N.Y.). STIMULATION OF PRODUCTION WELL FOR IN SITU METAL MINING. U.S. PAT. 3,841,705, OCT. 15, 1974.

66. GRANT, R. F., F. B. RICHARDS, AND H. F. WETHERBEE. LEACHING PROCESS. U.S. PAT. 1,690,446, NOV. 6, 1928.

67. GREENWOOD, C. C. UNDERGROUND LEACHING AT CANANEA. ENG. AND MIN. J., V. 121, NO. 13, MARCH 1926, PP. 518-521.

68. GRISWOLD, G. B. ROCK FRACTURING TECHNIQUES FOR IN PLACE LEACHING. PRES. ANN. MEETING OF THE SOC. OF MIN. ENG., AIME, WASHINGTON D.C., FEB. 16-20, 1969, AIME PREPRINT 69-AS-74, 4 PP.

69. GROVES, R. D., T. H. JEFFERS, AND G. M. POTTER. LEACHING COARSE NATIVE COPPER ORE WITH DILUTE AMMONIUM CARBONATE SOLUTION. PROC. SOLUTION MINING SYMP., AIME ANN. MEETING, DALLAS, TEXAS, FEB. 25-27, 1974, PP. 381-389.

70. HANSEN, S. M. NUCLEAR BLASTING FOR MINING AND LEACHING. WORLD MINING, V. 1, NO. 1, SEPTEMBER 1965, PP. 20-27.

71. HANSEN, S. M., AND A. R. JAGER. HOW TO MAKE ORE FROM MARGINAL DEPOSITS. ENG. AND MIN. J., V. 169, NO. 12, DECEMBER 1968, PP. 75-81.

72. HARD, R. A. (ASSIGNED TO KENNECOTT COPPER CORPORATION, NEW YORK, N.Y.). PROCESS FOR IN-SITU MINING. U.S. PAT. 3,910,636, OCT. 7, 1975.

73. HARDWICK, W. R. FRACTURING A DEPOSIT WITH NUCLEAR EXPLOSIVES AND RECOVERING COPPER BY THE IN-SITU LEACHING METHOD. BUMINES RI 6996, 1967, 48 PP.

74. HEINEN, H. J., T. G. CARNAHAN, AND J. A. FISELE (ASSIGNED TO THE UNITED STATES OF AMERICA, AS REPRESENTED BY THE SECRETARY OF THE INTERIOR, WASHINGTON, D.C.). CHEMICAL MINING OF COPPER PORPHYRY ORES. U.S. PAT. 3,890,007, JUNE 17, 1975.

75. HOCKINGS, W. A., AND W. L. FREYBERGER. LABORATORY STUDIES OF IN SITU AMMONIA LEACHING OF MICHIGAN COPPER ORES. PROC. INTERNAT. SYMP. ON COPPER EXTRACTION AND REFINING, MET. SOC., AIME, LAS VEGAS, NEV., FEB. 22-26, 1976 (PUB. AS EXTRACTIVE METALLURGY OF COPPER--HYDROMETALLURGY AND ELECTROWINNING. ED. BY J. C. YANNOPOULOS AND J. C. AGARWAL). PORT CITY PRESS, BALTIMORE, MD., V. II, 1976, PP. 873-906.

76. HOCKINGS, W. A., AND W. L. FREYBERGER. A PLAN FOR DETERMINING THE FEASIBILITY OF IN SITU LEACHING OF NATIVE COPPER ORES. INSTITUTE OF MINERAL RESEARCH, MICHIGAN TECHNOLOGICAL UNIVERSITY, HOUGHTON, MICHIGAN. PREPARED FOR HOMESTAKE COPPER CO., CALUMET, MICHIGAN. JUNE 14, 1974. 36 PP.

77. HOGAN, D. K. IN-SITU COPPER LEACHING AT THE OLD RELIABLE MINE. MIN. MAG., V. 24, NO. 5, MAY 1974. PP. 353-359.

78. HOLDERREED, F. L. COPPER EXTRACTION BY THE ACID LEACHING OF BROKEN ORE. PINCOCK, ALLEN AND HOLT, INC. REPORT, 1975, 19 PP.

79. HOUGEN, L. R., AND H. ZACHARIASEN. RECOVERY OF NICKEL, COPPER AND PRECIOUS METAL CONCENTRATE FROM HIGH GRADE PRECIOUS METAL MATTES. J. METALS, V. 27, NO. 5, MAY 1975, PP. 6-9.

80. HSUEH, L., R. A. HARD, D. H. DAVIDSON, AND R. V. HUFF (ASSIGNED TO KENNECOTT COPPER CORP.). IN-SITU MINING METHOD AND APPARATUS. U.S. PAT. 4,116,488, SEPT. 26, 1978.

81. HSUEH, L., P. A. HURD, D. H. DAVIDSON, AND R. V. HUFF (ASSIGNED TO KENNECOTT COPPER CORP.). IN-SITU MINING OF COPPER AND NICKEL. U.S. PAT. 4,045,084, AUGUST 30, 1977.

82. HUFF, R. V., AND H. DAVIDSON. IN-SITU LEACHING MATERIALS CONSIDERATIONS. PRES. AT 54TH ANN. FALL TECHNICAL CONFERENCE AND EXHIBITION, SOC. PETROL. ENG., AIME, LAS VEGAS, NEVADA, SEPT. 23-26, 1979, SPE PREPRINT 8320, 6 PP.

83. HUFF, R. V., AND P. A. HUSKA (ASSIGNED TO KENNECOTT COPPER CORP.). WELLBORE OXIDATION OF LIXIVANTS. U.S. PAT. 3,894,770, JULY 15, 1975.

84. HUFF, R. V., AND D. J. MOYNIHAN (ASSIGNED TO KENNECOTT COPPER CORP.). LIXIVIANT RECIRCULATOR FOR IN SITU MINING. U.S. PAT. 4,079,998, MAR. 21, 1978.

85. HUNKIN, G. G. A REVIEW OF IN SITU LEACHING. PRES. AT AIME ANN. MEETING, SOC. OF MIN. ENG., AIME, NEW YORK, N.Y., FEB. 26 - MAR. 4, 1971, AIME PREPRINT 71-AS-88, 23 PP.

86. HURD, B. G., AND J. L. FITCH (ASSIGNED TO MOBIL OIL CORPORATION, A CORPORATION OF NEW YORK). IN SITU LEACHING OF SUBTERRANEAN DEPOSITS. U.S. PAT. 3,278,233, OCT. 11, 1966.

87. ITO, I. PRESENT STATUS OF PRACTICE AND RESEARCH WORKS ON IN-PLACE LEACHING IN JAPAN. PROC. JOINT MEETING OF THE MINING AND METALLURGICAL INSTITUTE OF JAPAN AND THE AMERICAN INSTITUTE OF MINING, METALLURGICAL, AND PETROLEUM ENGINEERS, DENVER, COLO., SEPT. 1-3, 1976 (PUB. AS WORLD MINING AND METALS TECHNOLOGY, ED. BY A. WEISS), V. 1, 1976, PP. 349-364.

88. JACOBY, C. H. (ASSIGNED TO AKZONA INC., ASHEVILLE, N.C.). IN SITU EXTRACTION OF MINERAL VALUES FROM ORE DEPOSITS. U.S. PAT. 3,822,916, JULY 9, 1974.

89. JOHNSON, P. H. (ASSIGNED TO HOWARD E. JOHNSON AND ASSOCIATES). HYDRO-METALLURGICAL METHOD AND APPARATUS. U.S. PAT. 3,264,099. AUG. 2, 1966.

90. JOHNSON, P. H., AND R. R. BHAPPU. CHEMICAL MINING - A STUDY OF LEACHING AGENTS. NEW MEXICO BUREAU OF MINES AND MINERAL RESOURCES, CIRC. 99, 1969. 7 PP.

91. JOHNSON, P. H., AND R. R. BHAPPU. CHEMICAL MINING - THEORETICAL AND PRACTICAL ASPECTS. PRES. AT SME FALL MEETING - ROCKY MOUNTAIN MINERALS CONF., LAS VEGAS, NEVADA, SEPT. 6-8, 1967. 20 PP.

92. KACZYNSKI, D. A., G. W. LOWER, AND W. A. HOCKINGS. KINETICS OF LEACHING METALLIC COPPER IN AQUEOUS CUPRIC AMMONIUM NITRATE SOLUTIONS. PROC. SOLUTION MINING SYMP., AIME ANN. MEETING, DALLAS, TEXAS, FEB. 25-27, 1974, PP. 390-400.

93. KALABIN, A. I. WINNING OF USEFUL ELEMENTS FROM MINERALS BY LEACHING UNDERGROUND. MIN. MAG. (LONDON), V. 118, NO. 2, FEBRUARY 1968, PP. 129-134.

94. KELSEAUX, R. M. (ASSIGNED TO CITIES SERVICE OIL COMPANY, TULSA, OKLA.). STIMULATION OF RECOVERY FROM UNDERGROUND DEPOSITS. U.S. PAT. 3,593,793, JULY 20, 1971.

95. KEYES, H. F. DISCUSSION OF IN PLACE LEACHING AT MIAMI MINE, MIAMI, ARIZONA, BY J. B. FLETCHER, IN TRANS. SOC. OF MIN. ENG., V. 250, NO. 4, DECEMBER 1971. PP. 310-314. TRANS. SOC. OF MIN. ENG., V. 252, NO. 2, JUNE 1972, PP. 186-187.

96. LAMPARD, W. J. (ASSIGNED TO KENNECOTT COPPER CORPORATION, NEW YORK, N.Y.). CONTROLLED IN SITU LEACHING OF ORE DEPOSITS UTILIZING PRE-SPLIT BLASTING. U.S. PAT. 3,863,987, FEB. 4, 1975.

97. LARSON, D. R. A REPORT COMPARING OPEN PIT MINING AND HEAP LEACHING WITH AN IN SITU LEACHING SYSTEM FOR A HYPOTHETICAL OXIDE COPPER DEPOSIT BASED ON THE CHARACTERISTICS OF THE CACTUS DEPOSIT, MIAMI, ARIZONA. M.S. THESIS, UNIV. MINNESOTA, DEPT. OF MINERAL AND METALLURGICAL ENG., JUNE 1973, 254 PP.

98. LASWELL, G. W. CONSIDERATIONS APPLICABLE TO UTILIZATION OF ROTARY DRILLING FOR IN-PLACE RECOVERY OF MINERALS AND HYDROCARBONS. SERVCO DIV. OF SMITH INTERNAT., INC. REPORT. FEBRUARY 1975. 8 PP.

99. LASWELL, G. W. WANTED: ROTARY DRILLING TECHNOLOGY FOR IN SITU MINING SYSTEMS. MIN. ENG., V. 27, NO. 1, JANUARY 1976, PP. 22-26.

100. LEACH, D. L., AND R. L. BRAUN. LEACHING OF PRIMARY SULFIDE ORES IN SULFURIC ACID SOLUTIONS AT ELEVATED TEMPERATURES AND PRESSURES. PRES. AT ANN. MEETING, SOC. MIN. ENG., AIME, NEW YORK, FEB. 16-20, 1975, PREPRINT 75B6A, 20 PP.

101. LEWIS, A. E. CHEMICAL MINING OF PRIMARY COPPER ORES BY USE OF NUCLEAR TECHNOLOGY. PROC. SYMP. OF ENGINEERING WITH NUCLEAR EXPLOSIVES, LAS VEGAS, NEV., JAN. 14-16, 1970, CONF. 700101, V. 21, PP. 907-917.

102. LEWIS, A. E. IN SITU PRESSURE LEACHING METHOD. U.S. PAT. 3,640,579, FEB. 8, 1972.

103. LEWIS, A. E. (ASSIGNED TO THE UNITED STATES OF AMERICA AS REPRESENTED BY THE U.S. ATOMIC ENERGY COMMISSION, WASHINGTON, D.C.). SITU LEACHING SOLVENT EXTRACTION-PROCESS. U.S. PAT. 3,823,981, JULY 16, 1974.

104. LEWIS, A. E., AND R. L. BRAUN. NUCLEAR CHEMICAL MINING OF PRIMARY COPPER SULFIDES. PRES. AT THE AIME MEETING, SAN FRANCISCO, CALIF., JAN. 27, 1972, 30 PP.

105. LEWIS, A. E., R. L. BRAUN, C. J. SISEMORE, AND R. G. MALLON. NUCLEAR SOLUTION MINING-BREAKING AND LEACHING CONSIDERATIONS. PROC. SOLUTION MINING SYMP., AIME ANN. MEETING, DALLAS, TEXAS, FEB. 25-27, 1974, PP. 56-75.

106. LEWIS, F. M., AND R. R. BHAPPU. EVALUATING MINING VENTURES VIA FEASIBILITY STUDIES. MIN. ENG., V. 27, NO. 10, OCTOBER 1975, PP. 48-54.

107. LEWIS, F. M., C. K. CHASE, AND R. R. BHAPPU. ECONOMIC EVALUATION OF IN SITU EXTRACTION FOR COPPER, GOLD, AND URANIUM. PROC. JOINT MEETING OF THE MINING AND METALLURGICAL INSTITUTE OF JAPAN AND THE AMERICAN INSTITUTE OF MINING, METALLURGICAL, AND PETROLEUM ENGINEERS, DENVER, COLO., SEPT. 1-3, 1976 (PUB. AS WORLD MINING AND METALS TECHNOLOGY, ED. BY A. WEISS). V. 1, 1976, PP. 333-348.

108. LONGWELL, R. L. IN PLACE LEACHING OF A MIXED COPPER ORE BODY. PROC. SOLUTION MINING SYMP., AIME ANN. MEETING, DALLAS, TEXAS, FEB. 25-27, 1974, PP. 233-242.

109. MALOUF, E. E. COPPER LEACHING PRACTICES. PRES. AT ANN. MEETING, SOC. OF MIN. ENG., AIME, SAN FRANCISCO, CALIF., FEB. 20-24, 1972, AIME PREPRINT 72-AS-84, 7 PP.

110. MALOUF, E. E. INTRODUCTION TO DUMP LEACHING PRACTICE. PART I OF SECOND TUTORIAL SYMP. ON EXTRACTIVE METALLURGY, UNIV. UTAH, DEC. 14-16, 1972, 26 PP.

111. MALOUF, E. E. LEACHING AS A MINING TOOL. INTERNAT. SYMP. ON HYDROMETALLURGY, CHICAGO, ILL., FEB. 25-MAR. 1, 1973, CH. 23, PP. 615-626.

112. MALOUF, E. E. THE ROLE OF MICROORGANISMS IN CHEMICAL MINING. MIN. ENG., V. 23, NO. 11, NOVEMBER 1971, PP. 43-46.

113. MAYLING, A. A. METHOD FOR EXTRACTING COPPER, ZINC, LEAD, NICKEL, COBALT, MOLYBDENUM OR OTHER METAL VALUES FROM LOW-GRADE SULFIDE ORE BODIES. CAN. PAT. 825,473, OCT. 21, 1969.

114. MCKINNEY, W. A. SOLUTION MINING. MIN. ENG., V. 25, NO. 2, FEBRUARY 1973, PP. 56-57.

115. MICHIGAN TECHNOLOGICAL UNIVERSITY. A PLAN FOR DETERMINING THE FEASIBILITY OF AN IN SITU LEACHING OF NATIVE COPPER ORES. PREPARED FOR HOMESTAKE COPPER COMPANY, CALUMET, MICHIGAN, JUNE 14, 1974, 35 PP.

116. MILLER, J. D. PROCESSING OF LEACH LIQUORS PRODUCED BY NUCLEAR SOLUTION MINING. LAWRENCE LIVERMORE LABORATORY, REPT. UCRL-51350, FEB. 15, 1973, 18 PP.

117. MINING CONGRESS JOURNAL. AN EXPERIMENTAL IN-PLACE LEACHING TEST. V. 59, NO. 5, MAY 1973, P. 10.

118. MINING ENGINEERING. KENNECOTT PROPOSES NUCLEAR MINING EXPERIMENTS AT SAFFORD DEPOSIT. V. 19, NO. 11, NOVEMBER 1967, PP. 66-67.

119. MINING ENGINEERING. OXYMIN DETAILS PLANS FOR IN SITU LEACH PROJECT IN ARIZONA. V. 29, NO. 11, NOVEMBER 1977, PP. 13, 16.

120. MINING ENGINEERING. RANCHERS DEVELOPMENT SETS OFF BLAST, WILL LEACH AT BIG MIKE. V. 25, NO. 8, AUGUST 1973, P. 10.

121. MINING MAGAZINE. WINNING OF USEFUL ELEMENTS FROM MINERALS BY LEACHING UNDERGROUND. V. 118, NO. 2, FEBRUARY 1968, PP. 129-134.

122. MINING RECORD (DENVER, COLORADO). RANCHERS BLASTS OLD RELIABLE TO TEST NEW MINING TECHNIQUE. V. 83, NO. 12, MAR. 22, 1972. P. 1.

123. MURPHY, J. NEW RETURNS FROM OLD RELIABLE. SOURCE UNKNOWN, PP. 20-23; COPY AVAILABLE FOR CONSULTATION AT BUREAU OF MINES, TWIN CITIES MINING RESEARCH CENTER, MINNEAPOLIS, MINNESOTA.

124. MYERS, O. L. MINING COPPER IN SITU. THE MINES MAG., V. 31, NO. 6, JUNE 1941, PP. 255-263.

125. OCCIDENTAL MINERALS CORP. THE OXYMIN PROJECT AT MIAMI, ARIZONA. A SUMMARY OF A PRESENTATION MADE TO MIAMI, ARIZONA TOWN COUNCIL, SEPT. 12, 1977, 5 PP.: FOR FURTHER INFORMATION, CONTACT BOB ZACHE, OCCIDENTAL MINERALS CORP., 918 LIVE OAK ST., MIAMI, ARIZONA 85539.

126. OROURKE, J. E., R. J. ESSEX, AND R. K. RANSON. FIELD PERMEABILITY TEST METHODS WITH APPLICATIONS TO SOLUTION MINING. WOODWARD-CLYDE CONSULTANTS (SAN DIEGO, CALIF.), CONTRACT NO. J0265045. BUMINES OPEN FILE REPT. 136-77, JULY 1977, 180 PP.: AVAILABLE FROM NATIONAL TECHNICAL INFORMATION SERVICE, SPRINGFIELD, VA., PB 272 452/AS.

127. ORTLOFF, G. D., C. E. COOKE, JR., AND D. K. ATWOOD (ASSIGNED TO ESSO PRODUCTION RESEARCH COMPANY). MINERAL RECOVERY. U.S. PAT. 3,574,599, APR. 13, 1971.

128. PAY DIRT, ARIZONA EDITION (BISBEE, ARIZONA). OXYMIN PLANS FINAL IN SITU COPPER LEACHING TESTS AT MIAMI, DECEMBER 1979, NO. 486, PP. 1, 4.

129. PETROVIC, L. J., R. A. HARD, AND I. V. KLUMPAR. ECONOMIC CONSIDERATIONS FOR RECOVERING COPPER FROM DEEP SULFIDE DEPOSITS BY NUCLEAR RUBBLIZATION. IN SITU, V. 1, NO. 3, 1977, PP. 235-248.

130. PINGS, W. R. BACTERIAL LEACHING. MINER. IND. BULL., V. 2, NO. 3, MAY 1968, 19 PP.

131. POJAR, M. IN-PLACE LEACHING OF A COPPER SULFIDE DEPOSIT. PRES. AT DULUTH MEETING, SOC. OF MIN. ENG., AIME, DULUTH, MINN., JAN. 16-18, 1974, 9 PP.

132. PORTER, D. D. BLAST DESIGN FOR IN SITU LEACHING. PRES. AT SOUTHWEST MINERAL INDUSTRY CONF., PHOENIX, ARIZ., APR. 27, 1973, 7 PP.; AVAILABLE FROM E. I. DU PONT DE NEMOURS AND CO., INC., WILMINGTON, DEL. 19898.

133. PORTER, D. D., AND H. G. CARLEVATO. IN SITU LEACHING: A NEW BLASTING CHALLENGE. PROC. SOLUTION MINING SYMP., AIME ANN. MEETING, DALLAS, TEXAS, FEB. 25-27, 1974, PP. 33-43.

134. POTTER, G. M. SOLUTION MINING. MIN. ENG., V. 21, NO. 1, FEBRUARY 1969, PP. 68-69.

135. PRESCOTT NEWSPAPER (PRESCOTT, ARIZONA). KIRKLAND BLAST WILL OPEN NEW BODY OF COPPER. APR. 18, 1973, P. 1.

136. RABB, D. D. LEACHING OF COPPER ORES AND THE USE OF BACTERIA. LAWRENCE RADIATION LABORATORY, REPT. UCID-4958, JAN. 22, 1965, 25 PP.

137. RABB, D. D. PENETRATION OF LEACH SOLUTION INTO ROCKS FRACTURED BY A NUCLEAR EXPLOSION. PRES. AT ANN. MEETING OF SOC. OF MIN. ENG., AIME, WASHINGTON, D.C., FEB. 16-20, 1969, V. 1:A, AIME PREPRINT 69-AS-4, 14 PP.

138. RABB, D. D. SOLUTION MINING. MIN. ENG., V. 24, NO. 2, FEBRUARY 1972, PP. 62-64.

139. RAGHAVAN, S. AMMONIACAL LEACHING OF A CHRYSOCOLLA BEARING COPPER ORE. TO BE PRES. AT AIME ANN. MEETING, NEW ORLEANS, LA., FEB. 18-22, 1979.

140. RANCHERS EXPLORATION AND DEVELOPMENT CORP. THE OLD RELIABLE PROJECT - A TEST OF NEW TECHNOLOGY. COMPANY REPORT, 1972, 4 PP.

141. RICKARD, R. S. CHEMICAL CONSTRAINTS ON IN-SITU LEACHING AND METAL RECOVERY. PROC. SOLUTION MINING SYMP., AIME ANN. MEETING, DALLAS, TEXAS, FEB. 25-27, 1974, PP. 185-192.

142. ROMAN, R. J. THE LIMITATIONS OF LABORATORY TESTING AND EVALUATION OF DUMP AND IN SITU LEACHING. IN SITU, V. 1, NO. 4, 1977, PP. 305-324.

143. ROMAN, R. J. SOLUTION MINING. MIN. ENG., V. 26, NO. 2, FEBRUARY 1974, PP. 43-44.

144. ROOT, T. E. LEGAL ASPECTS OF MINING BY THE IN-SITU LEACHING METHOD. PRES. AT 22ND ANN. ROCKY MOUNTAIN MINERAL LAW INST., SUN VALLEY, IDAHO, JULY 22-24, 1976. 18 PP.

145. ROSENBAUM, J. B., AND W. A. MCKINNEY. IN SITU RECOVERY OF COPPER FROM SULFIDE ORE BODIES FOLLOWING NUCLEAR FRACTURING. PROC. SYMP. OF ENGINEERING WITH NUCLEAR EXPLOSIVES, LAS VEGAS, NEV., JAN. 14-16, 1970, CONF. 700101, V. 2, PP. 877-887.

146. ROSENZWEIG, M. D. NEW COPPER TECHNOLOGY IS WINNING THE ORE. CHEM. ENG., V. 74, NO. 25, DEC. 4, 1967. PP. 88-90, 92.

147. ROUSE, J. V. ENVIRONMENTAL ASPECTS OF IN SITU MINING AND DUMP LEACHING. PROC. SOLUTION MINING SYMP., AIME ANN. MEETING, DALLAS, TEXAS, FEB. 25-27, 1974, PP. 3-14.

148. RUDERSHAUSEN, C. G. COPPER SOLUTION MINING AT OLD RELIABLE. PRES. AT NATIONAL MEETING OF AMERICAN INST. OF CHEMICAL ENG., SALT LAKE CITY, NEV., AUG. 18-21, 1974, 11 PP.

149. ST. PETER, A. L. IN SITU LEACHING OF OREBODIES DESIGN AND MANAGEMENT. PINCOCK, ALLEN AND HOLT, INC. REPORT, 1975, 20 PP.

150. ST. PETER, A. L. IN SITU MINING -- A DESIGN FOR POSITIVE RESULTS. PRES. AT 105TH ANN. MEETING, AIME, LAS VEGAS, NEV., FEB. 22-26, 1976, PREPRINT 76-AS-36, 43 PP.

151. SAREEN, S. S., L. GIRARD, III, AND R. A. HARD. STIMULATION OF RECOVERY FROM UNDERGROUND DEPOSITS. U.S. PAT. 3,865,435, FEB. 11, 1975.

152. SCHLITT, W. J., R. P. REAM, L. J. HAUG, AND W. D. SOUTHARD. PRECIPITATING AND DRYING CEMENT COPPER AT KENNECOTTS BINGHAM CANYON FACILITY. MIN. ENG., V. 31, NO. 6, JUNE 1979, PP. 671-678.

153. SCOTT, W. G. (ASSIGNED TO INSPIRATION CONSOLIDATED COPPER COMPANY, A CORPORATION OF MAINE). LEACHING COPPER ORES. U.S. PAT. 2,563,623, AUG. 7, 1951.

154. SELIM, A. A. A DECISION ANALYSIS APPROACH TO IN SITU EXTRACTION OF COPPER. PH.D. THESIS, UNIV. MINNESOTA, MINNEAPOLIS, MINN., MARCH 1976, 659 PP.

155. SELIM, A. A., AND D. H. YARDLEY. THE DESIGN AND COST OF A FRAGMENTATION SYSTEM FOR IN SITU EXTRACTION OF COPPER. PRES. AT 14TH INTERNAT. SYMP. ON THE APPLICATION OF COMPUTER METHODS IN THE MINERAL INDUSTRY, THE PENNSYLVANIA STATE UNIVERSITY, UNIVERSITY PARK, PA., OCT. 14-16, 1976.

156. SELIM, A. A., AND D. H. YARDLEY. IN SITU LEACHING OF COPPER -- AN ECONOMIC SIMULATION APPROACH. PRES. AT 107TH ANN. MEETING, AIME, ATLANTA, GA., MARCH 1977, PREPRINT 77-AS-68, 24 PP.

157. SHEFFER, H. W., AND L. G. EVANS. COPPER LEACHING PRACTICES IN THE WESTERN UNITED STATES. BUMINES IC 8341, 1968, 57 PP.

158. SHOCK, D. A. DEVELOPMENTS IN SOLUTION MINING PORTEND GREATER USE FOR IN SITU LEACHING. MIN. ENG., V. 22, NO. 2, FEBRUARY 1970, P. 73.

159. SHOCK, D. A., AND J. G. DAVIS, II. (ASSIGNED TO CONTINENTAL OIL COMPANY, PONCA CITY, OKLA., A CORP. OF DELAWARE). FRACTURING METHOD IN SOLUTION MINING. U.S. PAT. 3,387,888. JUNE 11, 1968.

160. SHOEMAKER, R. S. AMMONIA REVIVAL FOR THE KEWEENAW. MIN. ENG., V. 24, NO. 5, MAY 1972, PP. 45-47.

161. SKILLINGS MINING REVIEW. EL PASO STUDYING IN SITU LEACHING AT EMERALD ISLE. V. 63, NO. 52. DEC. 28, 1974, P. 8.

162. SKILLINGS MINING REVIEW. OXYMINS IN-SITU COPPER LEACHING PROJECT AT MIAMI, ARIZ. V. 66, NO. 52, DEC. 24, 1977, PP. 1, 10-12.

163. SKILLINGS MINING REVIEW. RANCHERS DETONATES LARGE BLAST AT BIG MIKE MINE IN NEVADA. V. 62, NO. 29. JULY 21, 1973, P. 5.

164. SMITH, P. R., JR., D. W. BAILEY, AND R. E. DOANE. TRENDS IN CHEMICAL PROCESSING AND HYDROMETALLURGY. ENG. AND MIN. J., V. 173, NO. 6, JUNE 1972, PP. 173-177.

165. SPEDDEN, H. R., AND E. E. MALOUF (ASSIGNED TO KENNECOTT COPPER CORPORATION, NEW YORK, N.Y.). CONTROLLED IN-SITU LEACHING OF MINERAL VALUES. U.S. PAT. 3,815,957. JUNE 11, 1974.

166. SPEDDEN, H. R., AND E. E. MALOUF (ASSIGNED TO KENNECOTT COPPER CORPORATION, NEW YORK, N.Y.). IN-SITU GENERATION OF ACID FOR IN-SITU LEACHING OF COPPER. U.S. PAT. 3,834,760. SEPT. 10, 1974.

167. SPEDDEN, H. R., E. E. MALOUF, AND J. D. DAVIS. IN SITU LEACHING OF COPPER--PILOT PLANT TEST. PRES. AT ANN. MEETING, AIME, NEW YORK, FEBRUARY 1971, 21 PP.

168. SPENCE, A. P. (ASSIGNED TO ATLANTIC RICHFIELD CO., NM URANIUM INC., AND U.S. STEEL CORP.). METHOD FOR THE RECOVERY OF A MINERAL. U.S. PAT. 4,082,359, APR. 4, 1978.

169. STAUTER, J. C., AND A. G. FONSECA. LEACHING OF OXIDE COPPER ORE WITH AMMONIUM HYDROGEN SULPHATE: BENCH-SCALE TESTING. CAN. MIN. AND MET. BULL., V. 67, NO. 742, FEBRUARY 1974, PP. 135-136.

170. STECKLEY, R. C., W. C. LARSON, AND D. V. DANDREA. BLASTING TESTS IN A PORPHYRY COPPER DEPOSIT IN PREPARATION FOR IN SITU EXTRACTION. BUMINES RI 8070, 1975, 47 PP.

171. STEWART, R. M., AND K. E. NIERMEYER. NUCLEAR TECHNOLOGY AND MINERAL RECOVERY. PROC. SYMP. ON ENGINEERING WITH NUCLEAR EXPLOSIVES, LAS VEGAS, NEV., JAN. 14-16, 1970. CONF. 700101, V. 2, PP. 864-876.

172. TEWES, H. A., H. B. LEVY, AND L. L. SCHWARTZ. NUCLEAR CHEMICAL COPPER MINING AND REFINING: RADIOLOGICAL CONSIDERATIONS. LAWRENCE LIVERMORE LABORATORY, REPT. UCRL-51345, REV. 1, JUNE 3, 1974, 34 PP.

173. THOMAS, R. W. LEACHING COPPER FROM WORKED-OUT AREAS OF THE RAY MINES, ARIZONA. MIN. AND MET., V. 19, NOVEMBER 1938, PP. 481-485.

174. TRUSSELL, P. C., D. W. DUNCAN, AND C. C. WALDEN. BIOLOGICAL MINING. CAN. MIN. J., V. 85, NO. 3, MARCH 1964, PP. 46-49.

175. U.S. BUREAU OF MINES. PROJECT PROPOSAL: PORPHYRY COPPER - IN SITU RECOVERY BY LEACHING FOLLOWING NON-NUCLEAR FRACTURING. INTERDISCIPLINARY RESEARCH TASK FORCE, COMP. BY L. W. GIBBS, NOV. 23, 1971, (REV. DEC. 6, 1971), 20 PP. AVAILABLE FOR CONSULTATION AT BUREAU OF MINES, TWIN CITIES MINING RESEARCH CENTER, MINNEAPOLIS, MINNESOTA.

176. U.S. ENERGY RESEARCH AND DEVELOPMENT ADMINISTRATION. IN SITU LEACHING OF A NUCLEAR RUBBLIZED COPPER ORE BODY (IN TWO VOLUMES). V. 1, RESULTS OF FEASIBILITY STUDY. U.S. ERDA REPORT NVO-155, JUNE 1975, 30 PP.; V. 2, DETAILED DESIGN, CALCULATIONS, AND PROCEDURES. REPORT NVO-155, JUNE 1975, 318 PP.

177. VAN POOLEN, H. K., AND R. V. HUFF (ASSIGNED TO KENNECOTT COPPER CORP.). OXIDATION OF SULFIDE DEPOSITS CONTAINING COPPER VALUES. U.S. PAT. 3,881,774, MAY 6, 1975.

178. VORTMAN, L. J. AIRBLAST FROM SEQUENTIAL DETONATION OF GROUPS OF CHARGES IN VERTICAL DRILLED HOLES. UNLIMITED RELEASE SAND 75-0194, U.S. ENERGY RESEARCH AND DEVELOPMENT ADMIN. CONTRACT AT(29-1)-789, SEPTEMBER 1975, 48 PP.; AVAILABLE FROM NATIONAL TECHNICAL INFORMATION SERVICE, 5285 PORT ROYAL ROAD, SPRINGFIELD, VIRGINIA 22151, SAND75-0194.

179. WARD, M. H. ENGINEERING FOR IN SITU LEACHING. MIN. CONG. J., V. 59, NO. 1, JANUARY 1973, PP. 21-27.

180. WARD, M. H. SURFACE BLASTING FOLLOWED BY IN SITU LEACHING THE BIG MIKE MINE. PROC. SOLUTION MINING SYMP., AIME ANN. MEETING, DALLAS, TEXAS, FEB. 25-27, 1974, PP. 243-251.

181. WATSON, J. D., SR., W. A. MOD, AND F. N. TEUMAC (ASSIGNED TO DOW CHEMICAL CO.). EXTRACTION OF COPPER, NICKEL, COBALT OR CHROMIUM VALUES FROM SULFIDE, OXIDE OR SILICATE ORES THEREOF. U.S. PAT. 3,475,163, OCT. 28, 1969.

182. WEED, R. C. CANANEAS PROGRAM FOR LEACHING IN PLACE. MIN. ENG., V. 8, NO. 7, JULY 1, 1956, PP. 721-723.

183. WORMSER, F. E. LEACHING A COPPER MINE. ENG. AND MIN. J., V. 116, NO. 16, OCTOBER 1923, PP. 665-670.

184. ZIMMER, P. F., AND M. A. LEKAS. (COMP. AND ED. BY). PROJECT SLOOP (NUCLEAR EXPLOSIVES-PEACEFUL APPLICATIONS). U.S. ATOMIC ENERGY COMMISSION REPORT NO. PNE 1300, JUNE 1, 1967, 44 PP.

a series of experiments were carried out with careful control of the weight of the metal and of the crucible with the charge before and after treatment in the furnace.

The increase in the weight of the metal on account of reaction (5) (ΔP_{Me}) is related to the amount of oxidised silicon (P_{Si}) by the equation:

$$P_{Si} = \Delta P_{Me} - \frac{A_{Si}}{2A_{Fe} - A_{Si}} \quad (8)$$

Similarly we find that:

$$P_C = \Delta P_{tot} \frac{A_C}{M_{CO}}; \quad \Delta P_{Me} = \Delta P_{Me}^{obs} - \frac{P_{tot}(A_{Fe} - A_C)}{M_{CO}} \quad (9)$$

where:

P_C = the amount of carbon oxidised by reaction (7);

ΔP_{tot} and ΔP_{Me}^{obs} = the experimentally observed changes in the weight of the crucible with the charge and of the metal.

From the P_{Si} and P_C values it is possible to obtain the oxidation rates of Si and C by means of equations similar to equation (6). In these experiments three identical crucibles containing slag (38g) were placed in the furnace at the same time, and after fusion ingots of ferro-nickel were added (S = 2.5cm²). They were then removed in turn, cooled and weighed. The results from the experiments, given in fig. 2, show good agreement in the results obtained by the gravimetric and chemical-analytical methods. The v_C values ($0.04\text{-}0.35 \cdot 10^{-6}$ g-atom C/cm² · sec) were an order of magnitude lower than v_{Si} and the values obtained with the absence of silicon in the metal[7,8]). This shows that the oxidation of carbon is retarded in the presence of silicon.

The oxidation rate of the silicon increases with its concentration in the metal for Si < 1.5% and is almost independent of it at higher content (fig. 2). On the other hand, with the addition of ferrous oxide (Si = 1.5-3%) v_{Si} increases proportionately (fig. 2, curve 11). This relation is less clearly defined only with Si < 1%. With increase in the intensity of agitation the oxidation rate increases, and this indicates the presence of diffusion limitations. An analogous conclusion was reached in[9]) for 25-45% Si in the metal. This makes it possible to explain the unique concentration dependence of v_{Si} by the fact that in the region of low silicon concentrations the process is limited by its diffusion in the metal and at high silicon concentrations it is limited by diffusion of FeO in the slag. Accordingly, the order of the reaction in Si varies from first to zero, while the opposite holds for FeO. Kinetic analysis of reaction (5)[10]) leads to the following expression for the critical concentrations of FeO and Si, corresponding to exchange of the limiting stages:

$$[Si]_{cr} = \left(\frac{D_{FeO}}{D_{Si}}\right)^{0.5} \frac{d_{sl}}{d_{Me}} \frac{A_{Si}}{2M_{FeO}} \approx \frac{(FeO)_{cr}}{20} \quad (10)$$

Here it is assumed that D_{FeO}/D_{Si} is 0.1[10]), $d_{sl} \approx 3$, and $d_{Me} \approx 7 g/cm^3$[2]). For 12% FeO, $[Si]_{cr} \approx 0.6\%$, which is appreciably lower than the experimental value of ~1.5%. This is probably due to kinetic complications which become appreciable when Si < 1%[10]).

Conclusions

The results from the investigation demonstrate the considerable reserves for reducing the concentration of silicon in ferro-nickel as a result of measures reducing its degree of reduction and intensifying the oxidation of silicon by the slag. The latter can be realised with improvement in the conditions for contact between the metal and slag and for intense convection in the phases (emulsification, joint release, agitation of the products with gas etc).

References

1) P V Gel'd et alia: High-temperature reduction processes (in Russian), Sverdlovsk Metallurigzdat 1957.
2) N I Gran' et alia: Electrosmelting of oxidised nickel ores (in Russian): Moscow, Metallurgiya 1971.
3) Ya S Shchedrovitskii: Complex silicon ferro-alloys (in Russian): Metallurgiya 1968.
4) G R Pevzner et alia: Byul. Tsvetnaya Metallurgiya 1969, (23), 16.
5) G V Il'ichev et alia: Tsvetmetinformatsiya, Moscow 1969, p. 300.
6) V P Schastlivyi et alia: Byul. Tsvetnaya Metallurgiya 1970, (10), 35.
7) L N Sheludyakov et alia: Tr. Inst. Khim. Nauk Akad. Nauk KazSSR, Vol. 18, Alma-Ata 1967, p. 110.
8) V M Dorovskikh et alia: Izv VUZ Tsvetnaya Metallurgiya 1975, (2).
9) Yu P Nikitin et alia: Izv VUZ Chernaya Metallurgiya 1972, (8), 14.
10) V N Boronenkov: Collection: Physicochemical investigations of metallurgical processes (in Russian): Vol. 1, Sverdlovsk, Izd. UPI 1973, p. 18.

UDC 541.49

Complex ions of trivalent iron in alkaline aluminate solutions

M M Gol'dman, L P Ni, L V Bunchuk and S P Pivovarov (Institute of Metallurgy and Concentration, Academy of Sciences of the Kazakh SSR)

A large amount of experimental material has recently accumulated on the composition, properties, and structure of the iron-containing products from alumina production[1]). In this connection the need has arisen to determine the reasons for the selective formation of one or the other iron-containing phases and the complex ions which take part in the formation of the solid products. Polarography, electronic spectroscopy, and nuclear and electron paramagnetic resonance were used to solve these problems.

In the present article the interaction in the Na_2O-Al_2O_3-Fe_2O_3-SiO_2-H_2O system at 100°C is examined. According to modern ideas, the structure of solutions of sodium hydroxide is determined by their concentration and temperature. Measurements of the concentration dependence of the spin-lattice relaxation time for the protons of water in alkaline solutions makes it possible to observe how their structure gradually changes with increase in the NaOH concentration in the solutions (removal of water from the coordination pairs). From these positions the complex formation with trivalent iron in alkaline solutions must be associated with hydration phenomena, which are determined by the concentration of the solution in respect of NaOH.

Two regions, interaction in which leads to the formation of complex ions with various compositions, were distinguished on the basis of the electronic spectra and polarograms of solutions in the Na_2O-Fe_2O_3-H_2O system (figs. 1 and 2). In alkaline solutions with low concentrations (20-200 g/l Na_2O) aquahydroxoferrite ions of the $[Fe(OH)_n(H_2O)_{6-n}]^{3-n}$ type, to which a positive sign was attributed on the basis of electrophoretic investigations, can exist. A coordination number of 6 is characteristic of Fe(III) ions, and it is therefore correct to suppose that iron ions in this region of solutions exist in an octahedral environ-

ment. Consequently, the maximum at $\lambda = 365$ nm in the electronic spectra of solutions in the low-concentration region must be assigned to the absorption of the aquahydroxo complex, in which the iron has sixfold coordination. The shift of the maximum towards the short-wave region in the spectrum of the solution containing 300 g/l Na_2O (fig.2, curve 6) may signify that as a result of substitution of water molecules by OH^- groups the former are situated somewhat further from the central atom than in the octahedra. The absence of this maximum in the spectrum of a solution with 350 g/l Na_2O (fig.2, curve 7) is due to a decrease in the content of the aqua complexes inthe solution, i.e., with increase in the NaOH concentration the equilibrium is shifted towards the formation of the hydroxo complexes.

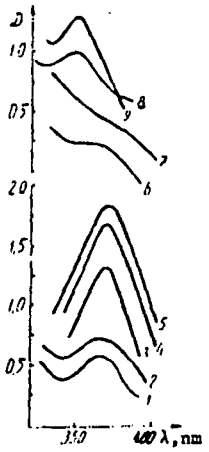

Fig.1. The electronic spectra of solutions in the Na_2O-Fe_2O_3-H_2O system with various Na_2O concentrations (g/l): 1 - 20; 2 - 50; 3 - 100; 4 - 150; 5 - 200; 6 - 300; 7 - 350; 8 - 400; 9 - 500.

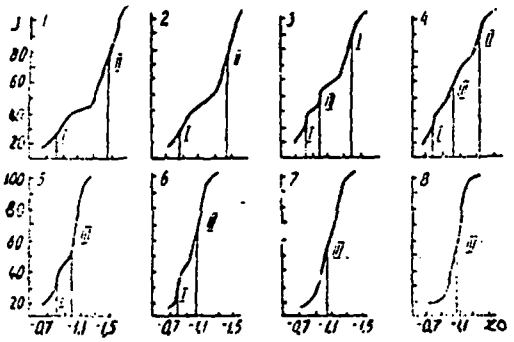

Fig.2 Polarograms of solutions in the Na_2O-Fe_2O_3-H_2O system. Na_2O concentration g/l 1 - 50; 2 - 100; 3 - 150; 4 - 200; 5 - 300; 6 - 350; 7 - 400; 8 - 500.

A maximum at $\lambda = 340$ nm is recorded in the spectra of concentrated alkaline solutions (400, 500 g/l Na_2O, fig.1, curves 8 and 9). This absorption is due to the appearance of a new complex ion of iron, for which a coordination number of 4 is obtained for Fe(III) by the polarographic method [2].

Thus, a redistribution of the relative amounts of iron ions in the tetrahedral and octahedral coordinations is observed with variation inthe concentration of the alkaline solution with the preferential formation of $Fe(OH)_4^-$ in concentrated solutions. The composition and structure of the iron-containing solid phases formed in the Na_2O-Fe_2O_3-H_2O system are consistent with this. In the low-alkali region hydrohaematite $Fe_2O_3 \cdot nH_2O$ crystallises, and in the high-alkali region sodium hydroferrite $Na_2O \cdot Fe_2O_3 \cdot (1\text{-}2)H_2O$ crystallises [3]. The FeO_6 groups are characteristic of the hydrohaematite structure, and mainly FeO_4 groups are characteristic of sodium hydroferrite.

With the addition of silica to the solution the relationships established during investigation of the complex formation of Fe(III) in alkaline solutions are retained. According to data from investigations of solutions of sodium silicate, silicic acid is considerably polymerised in solutions with low NaOH concentrations (50-200 g/l Na_2O) and can be represented by various ions [4]: $[Si_2O_5]_n^{2n-}$, $[SiO_3]^{2-}$, $[Si_3O_9]^{6-}$, ... , $[Si_mO_n]$.

In the reaction of such ions with the iron ion which exists under these conditions a stable iron-silicon complex is formed, and this can be represented diagrammatically as $[Fe(OH)_n \cdot (H_2O)_{6-n} \cdot Si_mO_n]^{-q}$. In concentrated alkaline solutions, where the complex anion $Fe(OH)_4^-$ is present and silicic acid is hardly polymerised at all and is present in the form of the monomeric ion $[SiO_4]^{4-}$, the reaction takes place within the limits of one structural group, which we represent arbitrarily as $[(Fe, Si)(OH)_4]$ [5]. With substitutions of such a type the electronic spectra do not undergo any substantial change. Nevertheless, the observed increase in the maximum is evidently due to the formation of a new complex, in which the Fe-O-Si bond which forms is considerably shorter than the Fe-O-H bond, and the electronic transitions in the ion therefore become more frequent, and as a result the intensity of the absorption increases.

For the solid products in the Na_2O-Fe_2O_3-SiO_2H_2O system a clear relation was also detected between the phase composition and the alkalinity of the medium. Thus, in spite of the fact that all the components required for the formation of the mineral aegirite ($Na_2O \cdot Fe_2O_3 \cdot 4SiO_2$) are present in the concentrated solutions, it only crystallises when the alkalinity of the solution is low [6]. Clearly, the appearance of aegirite is determined by the presence of the necessary iron cations in the solution and by the possibility of the formation of polymeric ions $[SiO_3]_n^{2n-}$. It is known that aegirite is a chain-type silicate, while the iron in it is present in an octahedral environment [7].

Sodium hydrosilicoferrite $Na_2O \cdot Fe_2O_3 \cdot nSiO_2 \cdot mH_2O$ with variable composition in silica crystallises from solutions with high alkalinity [8]. It is an orthosilicate, i.e., its structure is based on the $[SiO_4]$ group, while the iron is represented mainly by FeO_4 groups.

It is possible with sufficient justification to speak of the formation of a stable aluminium-iron complex $[(Fe, Al)(OH)_4]^-$ in the low-caustic solutions of the Na_2O-Al_2O_3-H_2O system [9]. During analysis of the electronic spectra of solutions with $\alpha_c = 1.75$ and 3.75 the possibility was established of the reaction of iron ions with aluminium ions in concentrated alkaline solutions, where $Fe(OH)_4^-$ ions are present. Unlike alkaline solutions containing iron ions, in the spectra of low-caustic aluminate solutions at the corresponding concentrations (fig.3) there is a new maximum at $\lambda = 325$ nm, which in our opinion corresponds to the absorption of the aluminium-iron ion. Indicative in this respect are aluminate solutions with concentrations of 200 g/l Na_2O (fig.3, curve 3). In their spectra there are two maxima at 325 and 365 nm, indicating the simultaneous presence of various ions in the solution. The first corresponds to the absorption of the aluminium-iron complex, and the second corresponds to the absorption of the aquahydroxo complex, which (as seen from the spectrum) does not undergo any changes in aluminate solutions. Consequently, the presence of $Fe(OH)_4^-$ ions in the solution is necessary for the formation of the aluminium-iron ion.

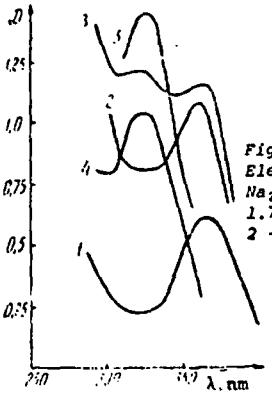

Fig.3 Electronic spectra of solutions in the Na_2O-Al_2O_3-Fe_2O_3-H_2O system with α_c = 1.75. Na_2O concentration g/l: 1 - 100; 2 - 150; 3 - 200; 4 - 300; 5 - 400.

The results from spectroscopic investigation agree with the data from nuclear and electron magnetic resonance. In the ESR spectra of the low-caustic aluminate solutions (fig.4) and also of the solid phases crystallising from them there are two well resolved lines with g factors of 4 and 2. These can be assigned[10]) to the tetrahedral and octahedral environment of the Fe(III), and with increase in the concentration of the solution in NaOH a large part of the iron is present in a tetrahedral oxygen environment. The observed shift of the g factor in the spectra of low-caustic aluminate solutions can be explained by an increase in the energies of the exchange interactions between the iron and aluminium ions with a continuous transition from paramagnetism to supermagnetism and then to ferromagnetism, which is characteristic of iron in purely alkaline solutions.

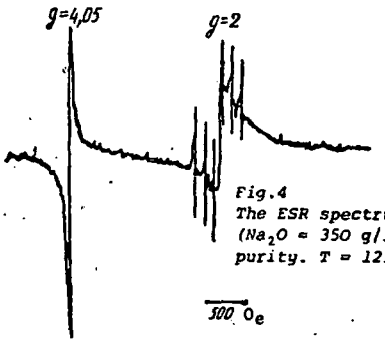

Fig.4 The ESR spectrum of an aluminate solution (Na_2O = 350 g/l α_c = 3.7) with iron impurity. T = 123°K.

Thus, physicochemical methods record the existence of an aluminium-iron complex ion in concentrated low-caustic solutions. Aluminium-iron hydrogarnets, in the structure of which part of the iron in the tetrahedral groups is substituted by aluminium, have been detected in the products from alumina production[11]). The reaction of Fe(III) with high-caustic aluminate solutions is of the same type as the reaction with alkaline solutions.

In solutions of the complex Na_2O-Al_2O_3-Fe_2O_3-SiO_2-H_2O system the aluminium-silicon-iron complex was not detected. Ions with various compositions - either $[(Fe, Al)(OH)_4]^-$ or $[Fe(OH)_n(H_2O)_{6-n} \cdot (Si_mO_n)]^{-q}$ - are formed, depending on the concentration of the solutions in respect of NaOH and the caustic ratio. For this reason there are no compounds with complex composition in the solid products of this system, and sodium hydroaluminosilicate, hydrohaematite, and aegirite crystallise from solutions with low concentrations in NaOH; sodium hydroaluminosilicate and sodium hydrosilicoferrite, consisting of the same structural groups as those present in the solution, crystallise from concentrated solutions.

Conclusions

1. By electronic spectroscopy, polarography, and ESR spectra it was established that trivalent iron reacts with alkaline-aluminate solutions to form complex ions with various compositions.
2. It was demonstrated that there is a relation between the state of the ions in the alkaline-aluminate solutions and the structure of the solid products which crystallise.

References

1) L P Ni et alia: Oxides of iron in alumina production. Nauka, Alma-Ata 1971.
2) L V Bunchuk et alia: Tr. Inst. MiO, Akad. Nauk KazSSR, Alma-Ata, 1970, 37, p.37.
3) T V Solenko et alia: Zh. Neorgan. Khim., 1968, 13, (2), p.334.
4) N G Stretenskaya: Experimental investigations of mineral formation processes. Nauka, Moscow 1970.
5) L V Buchuk et alia: Tr. Inst. MiO Akad. Nauk KazSSR. Alma-Ata 1973, 49, p.24.
6) M M Gol'dman et alia: Zap. Vses Mineralog. O-va, Vtoraya seriya 1968, 97, 497.
7) U A Dir et alia: Rock-forming minerals (Russian Translation), Moscow, Mir, 1965, 2.
8) T V Solenko et alia: Tr. Inst. MiO, Akad, Nauk KazSSR, Alma-Ata 1967, 23, p.3.
9) L V Bunchuk et alia: Tr. Inst. MiO KazSSR, Alma-Ata 1973, 49, p.27.
10) G O Karapet'yan et alia: FTT, 1963, 5, (2), p.627.
11) L P Ni et alia: Zh. Neorgan. Khim., 1968, 13, (11), 3075.

UDC 66.074.248

Investigation of the electrokinetic potential and hydrophilicity of slime from wet gas purification in Al-Si alloy production

V S Mal'ts, T V Yarygina, A I Ivanov and S I Kuznetsov (Urals Polytechnical Institute. Dneprovsk Aluminium Plant)

In the smelting of Al-Si alloys a considerable amount of dusty gases is released from the electric furnaces. They are cleaned from dust and sulphur compounds in high-speed turbulent washers, irrigated with technological solutions containing 50-80 g/l Na_2SO_4, 0.28 - 1.5 g/l Na_2CO_3, and 0.45 - 5.0 $NaHCO_3$. Sodium carbonates are added to the irrigating solutions to neutralise the sulphur compounds contained in the gases. During the gas purification process the sodium sulphate concentration in the irrigated solutions increases by 1 - 3 g/l in each cycle. The sodium carbonate and bicarbonate content of the solutions decreases accordingly.

The recycled water supply system from the gas purification plant contains single-stage thickeners, in which the gas-purification slime is separated and washed from the irrigated solution. The slime settling process is not very effective and requires further investigation in order to improve it. The gas-purification slime contains useful components such as aluminium and silicon oxides and is a valuable raw material for further production of Al-Si alloys. The present article gives the results from an investigation into the electrokinetic potential and hydrophilicity of the gas-purification slime for irrigating solutions with various compositions. A knowledge of these properties, which are associated with the existence of an electric double layer at the interface, is important for understanding the processes occurring in dispersed systems, e.g., the susceptibility of the slimes to aggregation[1]). The stability or instability of colloidal systems depends on the value of the ζ potential and the presence of solvate shells in the particles of the disperse phase[2]).

The gas-purification slime is largely represented by a material in a state of fine aggregation and consisting of slightly dehydrated kaolinite and aluminium oxide. Consequently, the properties of the slime (the electrokinetic potential and hydrophilicity) are determined by the characteristics of the main components.

The electrokinetic potentials of many clay minerals and also of aluminium oxide in water and in various solutions have been studied in a series of researches. It has been established, for example, that particles of clay in water acquire a negative charge on account of the selective adsorption of OH^- ions[3]). We know of no information on this subject as far as the ζ potential of clay minerals and aluminium oxide and hydroxide in soda, alkaline, and sulphate solutions is concerned.

[1]The charging of the slime particles can be assessed from their electrokinetic mobility, for the observation of which electrophoresis and electroosmosis are used. The electro-

Table 1. Boundary Layer Coefficients

Material	α'	β'	Cleavage or Fracture
Quartz	1.022	4.008	Conchoidal fracture
Galena	1.038	3.01	Perfect cubic
Sylvite	1.038	3.01	Perfect cubic
Kallodoc	0.942	3.03	Spheres made from methyl methacrylate polymer
Sphalerite	1.05	5.90	Perfect dodecahedral (011)
Mica	2.43	5.70	Calculated, thickness = 0.1 × diam
Mica	7.69	12.29	Calculated, thickness = 0.01 × diam
Anthracite	1.41	3.96	Not given
Epidote	1.09	5.10	Perfect on (001), imperfect on (100)
Magnetite	1.00	6.32	Octahedral parting
Pyrrhotite	1.07	8.01	Irregular fracture
Chalcocite			Flat and scaly (conchoidal)
Arsenopyrite			Irregular fracture

modified to
of α' and β'
literature fo

lified
ted
f minerals.

Although the values for mica were calculated, they were close enough to allow accurate design of hydraulic sizing equipment by the author.

Table 1 is a correction and expansion of Table 3 in the original paper. The listing is sufficiently complete in commonly encountered shapes that the author has been able to successfully predict the settling rate of other minerals by selecting the α' and β' values of a similarly shaped mineral in the list.

The modified free settling equation presented in this note, in combination with the expanded list of boundary layer coefficients, provides a powerful tool which has proven its worth in designing and trouble-shooting hydraulic classifiers and thickeners.

References

1 Swanson, V.F., "The Development of Formula for Direct Determination of Free-Settling Velocity of Any Size Particle," *Trans. SME/AIME*, Vol. 238, 1967, pp. 160-166.
2 Schlighting, H., *Boundary Layer Theory*, (trans. by J. Kestin), 4th Ed., McGraw-Hill, New York, 1960.

Combined Leach-Circulation Calculation for Predicting In-Situ Copper Leaching of Primary Sulfide Ore

by R. L. Braun and R. G. Mallon

Primary copper-sulfide ore deposits that are well below the water table can be chemically mined by in-situ high-pressure leaching. The leaching is accomplished by pumping oxygen gas into the bottom of a large underground flooded column of rubblized ore. Part of the injected oxygen dissolves under the high hydrostatic pressure in the column. With a high enough injection rate, the excess oxygen gas induces a convective circulation of oxygenated solution within the rubble column, which transports dissolved oxygen throughout the system. At elevated temperatures, this results in a relatively rapid dissolution of the copper minerals. A method of calculating the leaching rates is presented. The calculation is done by means of a finite-difference computer code that couples all of the processes relating to copper leaching, convective circulation, and the injection, dissolution, and consumption of oxygen. Results of the calculation for a typical case show that over 70% of the copper can be extracted in less than six years with good efficiency in oxygen utilization.

A method for in-situ chemical mining of primary sulfide ores, which promises to have a major impact on the technology and economics of copper recovery, has been under investigation.[1-6] The proposed method is depicted in Fig. 1. A column of rubblized ore well below the water table is first prepared using either a nuclear explosive or more conventional mining methods. The rubble column, or chimney, is then filled with water, either artificially or by natural inflow, until the original water level is restored. This results in a high hydrostatic pressure within the chimney. Oxygen gas is then introduced into the bottom of the chimney at pressures slightly above the hydrostatic pressure. As the gas bubbles rise through the chimney, part of the oxygen dissolves. The rising undissolved oxygen provides a lifting force that induces an internal circulation, transporting dissolved oxygen to all parts of the chimney. The dissolved oxygen oxidizes the primary sulfide minerals to produce sulfuric acid and heat, which lowers the pH and raises the temperature. The net result is a rapid dissolution of the copper minerals under conditions of elevated temperature and relatively high concentrations of dissolved oxygen.

Our previous models for predicting in-situ copper-leaching rates have treated the processes of leaching and circulation separately. First, the leaching rates were calculated for an average oxygen concentration, which was assumed to remain constant during the entire leaching time.[4] Then, in a separate calculation, the oxygen-injection rate to supply the oxygen consumed in the chemical reactions and needed to induce internal circulation of the chimney solution to achieve the stipulated average oxygen concentration was estimated.[6]

In the present paper, we will couple the leach and circulation calculations so that: (1) the leaching rate at

R. L. BRAUN, Member SME, and R. G. MALLON are Research Scientists, Lawrence Livermore Laboratory, University of California, Livermore, Cal. TP 74AS237. Manuscript, Dec. 13, 1974. Discussion of this paper, submitted in duplicate prior to Sep. 15, 1975, will appear in SME Transactions, December 1975, and in AIME Transactions, 1975, Vol. 258.

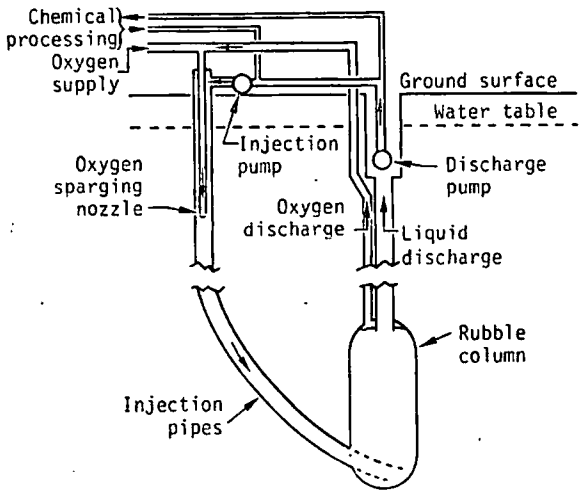

Fig. 1—Schematic of rubble column flow.

any given time will be determined by the oxygen concentration, and (2) the oxygen concentration, in turn, will be determined by the rates of chemical consumption of oxygen, of oxygen injection, and of solution circulation. Furthermore, instead of considering the entire chimney as having a uniform oxygen concentration, we will recognize two distinct regions: one region in which the source of dissolved oxygen is primarily the dissolution of oxygen bubbles, and a second region of lower average concentration in which the source of dissolved oxygen is only the transport of oxygenated solution circulating from the first region.

Calculation of Copper Leaching and Oxygen Distribution

Review of Laboratory Leaching Experiments and Leaching Model: Experimental studies of laboratory leaching of primary copper sulfide ore in sulfuric acid systems pressurized with oxygen have provided information on leaching chemistry and kinetics. This information has served as a basis for developing a leaching model.[3] The essential conclusions of these studies will now be reviewed.

The net chemical reactions of the sulfide minerals in laboratory leaching of an ore containing a pyrite/chalcopyrite mole ratio (Py/Cp) of 2 is

$$CuFeS_2 + 2FeS_2 + \frac{45}{4}O_2 + \frac{43}{6}H_2O = Cu^{+2} + Fe_3(SO_4)_2(OH)_5 \cdot 2H_2O + \frac{1}{3}S^\circ + \frac{11}{3}SO_4^{-2} + \frac{16}{3}H^+. \quad (1)$$

The hydrogen ions produced in this reaction are mostly consumed either by reaction with calcite to produce calcium sulfate or by reaction with other gangue minerals to release equivalent amounts of other cations, principally Mg^{+2} and Al^{+3}. The system is observed to be buffered at a quenched pH of about 2, representing a steady-state balance of H^+-dependent reactions. This buffering effect is an important feature of the leaching system, since a quenched pH of 2 is low enough to prevent Cu^{+2} from precipitating as basic copper sulfate and high enough to minimize decrepitation of the ore. Moreover, if small quantities of acid are added (as in the raffinate returning from the solvent-extraction plant), the buffering capacity of the system is great enough to prevent a pH excursion.

For ores with Py/Cp = 1, the net chemical reaction of the sulfide minerals is

$$CuFeS_2 + FeS_2 + \frac{15}{2}O_2 + \frac{13}{3}H_2O = Cu^{+2} + \frac{2}{3}Fe_3(SO_4)_2(OH)_5 \cdot 2H_2O + \frac{1}{3}S^\circ + \frac{7}{3}SO_4^{-2} + \frac{8}{3}H^+. \quad (2)$$

In this reaction, both oxygen consumption and acid production are lower than in Eq. 1. However, the acid production is still sufficient to provide enough H^+ for reaction with the normally encountered quantities of calcite and other reactive gangue minerals. For certain ores, a small amount of acid may have to be added.

The preceding net reactions yield the needed stoichiometry factor between chemical consumption of oxygen and production of copper. If the ore contains appreciable amounts of Fe^{+3}, as in biotite-rich ores, then the stoichiometry factor will be somewhat greater. However, the additional oxygen requirement is low, since only 0.25 mol oxygen per mole Fe^{+2} is consumed in the oxidation of Fe^{+2}.

Examination of partially leached ore fragments has shown that the sulfide reaction can be generally depicted as occurring in a narrow zone separating an unreacted core from a reacted shell. A leaching model to describe mathematically the moving reaction zone has been derived and tested with the laboratory leaching experiments.[3] The model is based on a mixed-kinetics mechanism involving first, the chemical reaction between dissolved oxygen and sulfide minerals in a moving reaction zone, and second, the diffusion of dissolved oxygen through the solution-filled pores of the reacted shell of the ore fragment.

The model also treats two other important phenomena (1) the enhanced initial leaching rate that comes from the natural enrichment of sulfide mineralization near the ore fragments' external surfaces and (2) the increase in interfacial reaction-zone area due to preferential penetration of the reaction zone along preexisting fractures or along fissures generated during the leaching process. The enlarged reaction area also gives enhanced leaching rates, particularly in the long-term leaching of large ore fragments. Also included in the leaching model is the explicit dependence of the copper leaching rate on the oxygen concentration, the oxygen-copper stoichiometry factor, the ore grade, and the ore particle size.

The leaching model has been found to be applicable to a wide range of ore particle sizes. It adequately describes both initial leaching rates and long-term leaching characteristics, even after partial decrepitation of the ore particles.

Extension of Leaching Model to In-Situ Conditions: To apply the laboratory leaching model to the calculation of copper extraction in a flooded chimney of rubblized ore, we must specify the particle-size distribution and know the time variation of temperature and oxygen concentration.

The particle-size distribution will, in general, be grossly dependent on rock type, preexisting fracture pattern, and method of fracturing. Three different particle-size distributions, shown in Fig. 2, are used in this paper: (1) the measured distribution of sizes in the Pile-driver chimney[4] created by a 61-kiloton nuclear explosive in a granitic medium, (2) the measured distribution of sizes in monzonite-type open-pit mine waste,[7] and (3) the intermediate distribution of sizes used as

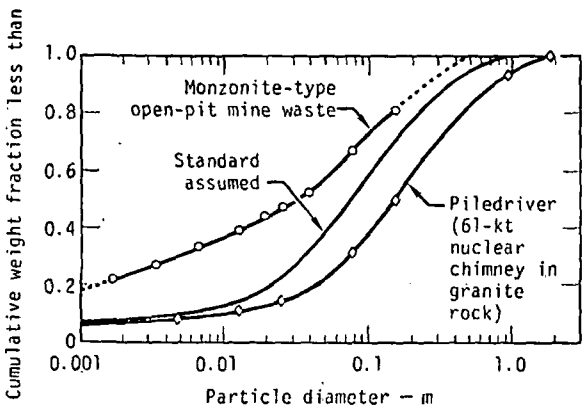

Fig. 2—Particle-size distributions.

the standard particle-size distribution for a rubble column in a copper-ore deposit.

Temperature data is important since the leaching model includes such temperature-dependent parameters as the chemical-reaction-rate constant, the oxygen-diffusion-rate coefficient, and the oxygen solubility. The temperature is assumed to be uniform throughout the entire leaching system, but is allowed to vary with time. A reasonable initial temperature of 333 K is assumed, although higher temperatures could readily be obtained by injecting high-pressure steam. The temperature change during the leaching process is determined by the rate of heat generation within the chimney and the rate of heat loss from the chimney. The generated heat derives primarily from the oxidation of pyrite and chalcopyrite. The net amount, calculated from standard heats of formation, is 2.93 megajoule per mol Cu for Eq. 2. For other Py/Cp mole ratios, the calculated exothermic heat is 4.39 megajoule per mol Cu for Py/Cp = 2 and 2.20 megajoule per mol Cu for Py/Cp = 0.5. Heat will be lost from the chimney to the surrounding rock by thermal conductivity, and the rate of heat loss is calculated by the standard equation for one-dimensional heat flow.

During the leaching calculation, the temperature is allowed to increase in accordance with the heat balance within the chimney until 363 K is reached, Thereafter, the temperature is not allowed to exceed 363 K. This temperature restriction is made for two reasons: (1) it facilitates handling of the pregnant liquor above ground, and (2) it lessens deleterious side reactions involving depletion of copper from solution within the chimney.

Finally, knowledge of the oxygen concentration is needed because the dissolution rate of the sulfide minerals is proportional to the oxygen concentration. In a laboratory leaching experiment with adequate stirring, the oxygen concentration is determined primarily by the solubility limit at the operating temperature and oxygen partial pressure, with secondary limitations imposed by the ionic strength of the solution. In a very large underground rubble column, however, the oxygen concentration will be effectivly limited by other processes, namely, the rate of oxygen injection, the geometric dispersion of the injected oxygen gas, the dissolution rate of oxygen, the rate of chemical consumption of oxygen, and the rate of internal circulation of the oxygenated solution. These factors will be discussed in the next section.

Oxygen Concentration in Leach Solution: A key technical issue in the successful application of this mining method is that a relatively high content of dissolved oxygen must be achieved in as much of the chimney solution as possible. This is important because regions of the chimney having a low content of dissolved oxygen not only will have a low rate of dissolution of the copper sulfide minerals, but also may have undesirable accompanying side effects, such as depletion of the copper already in solution to form secondary sulfides. The various processes that control the oxygen concentration will be discussed here only in general terms. The mathematical treatment is given in the Appendices.

The problem of bringing dissolved oxygen into contact with most of the broken ore would be solved if it were feasible to achieve a widespread dispersion of rising oxygen bubbles throughout the entire chimney. The feasibility of doing this depends upon the complexity of the gas inlet system and upon the extent of geometric dispersion that results from the flow of gas through a flooded bed of broken rock. We will now examine this feasibility.

The gas-injection system consists of one or more semihorizontal pipes extending across the bottom of the chimney. Each is perforated along part of its length within the chimney to provide one or more line sources of injected solution containing oxygen bubbles. As the oxygen bubbles rise through the chimney solution, they partially dissolve, and as they move around the ore fragments, they undergo lateral displacements. A random-walk model (Appendix A) can be used to estimate the effective coverage of the chimney with dispersed oxygen bubbles as a function of the particle-size distribution of the packed bed, the cross-sectional area of the chimney, and the vertical traverse of the injected gas from the gas-injection line to the top of the chimney. The resulting gas-bubble coverage calculated at mid-height in the chimney is depicted in Fig. 3 for three injection pipes.

In our reference case, the chimney is assumed to have the standard particle-size distribution, a cross-sectional area of 5140 sq m, and a height of 346 m. The shaded region will hereafter be referred to as the bubble region and the unshaded region as the nonbubble region. The injection lines are spaced so that there is an equal width of nonbubble region on either side of each line. Shifting the peripheral lines toward the center of the chimney would maximize the bubble region, but at the same time would maximize the distance of part of the nonbubble region from the nearest dispersed gas. More complete results of the dispersion calculation for a range of chimney geometries and injection lines are given in Table 1.

Rather than attempt to disperse oxygen gas bubbles throughout the entire chimney volume, a preferable approach is to accept a limited coverage and rely on internal circulation of the oxygenated solution to transport dissolved oxygen from the bubble region, in which oxygen is dissolving, to the nonbubble region. The transport mechanism is the difference in fluid densities between the bubble and nonbubble regions. The resulting

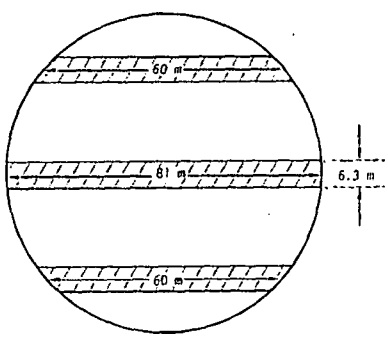

Fig. 3—Gas-bubble dispersion; shaded region is the average coverage of the chimney with dispersed oxygen bubbles (24.6% for the reference case).

Table 1. Dispersion of Injected Oxygen Gas Bubbles

Chimney Size Radius, m	Chimney Size Height,* m	Particle-Size Distribution†	Volume Fraction of Chimney in Bubble Region for Indicated Number of Oxygen-Injection Pipes 1	2	3	4	5
40.45	346	Standard	0.099	0.172	0.246	0.324	0.399
40.45	346	Piledriver	0.130	0.226	0.325	0.426	0.526
40.45	346	Mine Waste	0.066	0.114	0.164	0.216	0.266
48.30	491	Standard	0.099	0.171	0.245	0.323	0.398
25.96	145	Standard	0.100	0.174	0.249	0.327	0.404

* Vertical distance from gas-injection pipe to top of chimney.
† See Fig. 2.

buoyancy force overcomes the frictional pressure drop associated with the flow of the solution through a packed bed, inducing a convective circulation of upward-flowing solution in the bubble region and downward-flowing solution in the nonbubble region. The solution velocities in each region, as calculated from buoyancy and frictional pressure-drop equations, are a function of the quantity of undissolved oxygen in the bubble region and the physical properties of the packed bed. The concentration of dissolved oxygen at a given location in the chimney can then be calculated from the local rates for oxygen dissolution, flow of oxygenated solution, and oxygen consumption in the leaching reactions.

Combined Leach-Circulation Calculation: By coupling all of the preceding physical and chemical processes in a finite-difference computer code, we can solve the leaching and circulation equations in a self-consistent manner. The details of the computation are given in Appendix B.

The computation is performed using two nested, iterative loops at each time step. The inner-loop iteration matches the buoyancy and frictional pressure-drop terms. Quantities that are allowed to change during the iteration are the fluid-flow velocities and the concentrations of dissolved and undissolved oxygen in the bubble region.

The outer-loop iteration matches the oxygen concentration and leaching rate in both bubble and nonbubble regions. Quantities that are allowed to change in this iteration are the leaching rates in both regions and the concentration of dissolved oxygen at the bottom of the nonbubble region.

When satisfactory convergence have been obtained in the outer loop, all of the required conditions have been satisfied for one time step. As a result of this procedure the fraction of copper leached is obtained as separate functions of time for the bubble and nonbubble regions. In addition, at each time step the distribution of both dissolved and undissolved oxygen within the chimney is obtained. From this, the required rate of oxygen supply from the producing plant is obtained as a function of time.

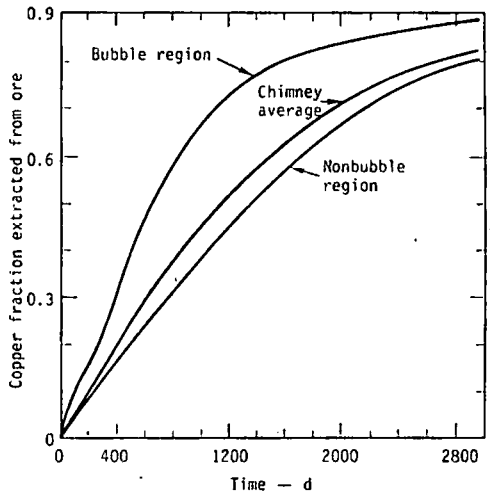

Fig. 4—Copper extraction calculation (for reference case).

Results and Discussion

Results of the leach-circulation calculations are summarized in Table 2, and the chimney properties assumed in those calculations are listed in Table 3. For Case 001, the reference case, a liquid-injection flow rate of 0.088 cu m per sec (1400 gpm) yields an extraction of 0.708 of the copper during a leaching time of 2000 days. The injection flow rate is the volumetric flow rate of solution pumped out of the top of the chimney, into which the required quantity of oxygen gas is dispersed before reinjection into the bottom of the chimney. The detailed leaching calculations for the reference case are shown in Fig. 4. The leaching rate is significantly greater in the bubble than in the nonbubble region as a result of the greater concentration of oxygen that can be maintained in the former with the specified injection flow rate.

The rate of oxygen demand for the reference case is shown in Fig. 5. Oxygen demand is the rate at which oxygen must be supplied to the chimney by the oxygen plant. This rate is equal to the rate at which oxygen is being consumed in the leaching reactions plus the rate

Table 2. Summary of Leach-Circulation Calculations

Case No.	Grade Wt % Cu	Py/Cp Mole Ratio	Particle-Size Distribution	Chimney Radius,* m	Injection Flow Rate, cu m per sec	No. of Injection Pipes	Fraction of Chimney in Bubble Region	Fraction of Cu Extracted at 2000 days	Fraction of Cu Extracted at 2740 days
001†	0.5	1.0	Standard	40.45	0.088	3	0.246	0.708	0.803
002	0.5	1.0	Piledriver	40.45	0.088	3	0.325	0.637	0.699
003	0.5	1.0	Mine Waste	40.45	0.088	3	0.164	0.539	0.676
012	0.5	1.0	Piledriver	40.45	0.189	5	0.526	0.673	0.723
013	0.5	1.0	Mine Waste	40.45	0.135	4	0.216	0.708	0.824
004	0.5	0.5	Standard	40.45	0.057	3	0.246	0.708	0.813
011	0.5	2.0	Standard	40.45	0.148	4	0.324	0.708	0.788
006	0.5	1.0	Standard	48.30	0.173	5	0.398	0.708	0.802
007	0.5	1.0	Standard	25.96	0.0083	1	0.100	0.708	0.803
008	1.0	1.0	Standard	40.45	0.088	3	0.246	0.498	0.611
015	1.0	1.0	Standard	40.45	0.221‡	3.	0.246	0.575	0.675

* For chimney properties, see Table 3.
† Case 001 is the reference case.
‡ For Case 015, the injection flow rate was 0.221 cu m per sec for the first 1310 days and then lowered to 0.126 cu m per sec for the remaining time.

Table 3. Chimney Properties

Radius, m	Height,* m	Area,† sq m	Fluid Volume, cu m	Bulking Porosity	Oxygen Partial Pressure at Top of Chimney, Pascal	Mass Ore, kg
25.98	145	2120	7.33×10^4	0.23	3.62×10^6	6.5×10^8
40.45	345	5140	2.77×10^5	0.15	3.62×10^6	4.1×10^9
48.30	491	7330	4.72×10^5	0.13	3.62×10^6	8.4×10^9

* Vertical distance from gas-injection pipe to top of chimney.
† Cross-sectional area of chimney.

at which oxygen is being lost by evolution from leach liquor leaving the chimney.

Results for other ore particle-size distributions are given in Cases 002, 012, 003, and 013 in Table 2. In Case 002 only 0.637 of the copper is extracted in 2000 days because of the lower leaching rates of the coarser Piledriver-ore size distribution. In Case 003, again for the same injection flow rate, only 0.539 of the copper is extracted in 2000 days. This lower extraction compared with the reference case is due primarily to the higher frictional pressure drop associated with the flow of solution through the finer mine-waste size distribution. In Cases 012 and 013, the effects of increased injection flow rates for the Piledriver and mine-waste size distributions are shown.

The required injection flow rate is also sensitive to the pyrite content of the ore, as shown in Cases 004 and 011 of Table 2. To achieve a copper extraction of 0.708 in 2000 days, an injection flow rate of 64% of that in the reference case is needed for ore having a Py/Cp mole ratio of 0.5; an injection flow rate of 168% of that in the reference case is needed for ore having a Py/Cp mole ratio of 2.0.

Finally, the injection flow rates and leaching results for variations in chimney size (Cases 006 and 007) and for variations in ore grade (Cases 008 and 015) are also shown in Table 2. For an ore grade of 1 wt % Cu, it was found desirable to have a high injection rate for the first 1310 days of leaching, during which the rate of chemical consumption of oxygen in the bubble region is high, and to decrease the injection rate thereafter.

Appendix A

Random-Walk Model for Dispersion of Oxygen Gas Bubbles: The gas distribution can be calculated by a random-walk model in which each rising gas bubble undergoes a lateral step for each vertical step of rise. The magnitude of the lateral step cannot be rigorously derived because of the uncertainty in the gas bubble's exact point of contact with the bottom surface of the particle. If we assume that all particles have diameter D_p, the lateral step will range from zero (for contact between two particles) to $\pm 1/2\ D_p$ (for contact at the center of the particle). The magnitude of the vertical step cannot be rigorously derived either, because of its intricate dependence on the packing arrangement of the particles. If we postulate an average lateral step of $\pm 1/4\ D_p$ for each vertical step of D_p, then the gas distribution curve at any desired height in the chimney can be calculated by:

$$R_f = \frac{\left[\left(\frac{d_1}{2D_p}\right)!\right]^2}{\left(\frac{d_1}{2D_p} - \frac{2d_2}{D_p}\right)!\left(\frac{d_1}{2D_p} + \frac{2d_2}{D_p}\right)!} \qquad (3)$$

where R_f is the relative gas-bubble flow rate at a point located at a distance d_1 above the gas-injection line and a distance d_2 in a direction perpendicular to the gas-injection line measured from the vertical axis of gas flow. Eq. 3 is normalized to $R_f = 1$ for $d_2 = 0$. In calculating the factorials, $d_1/2D_p$ and $2d_2/D_p$ are rounded to the nearest integer.

In a more generalized calculation, the size distribution of the broken rock must also be taken into account. At a given point in the chimney, the probability of a gas bubble contacting a rock of diameter d_i is proportional to the weight fraction X_i having that diameter. In contacting an arbitrary rock fragment, therefore, the gas bubble will have an induced lateral displacement of $1/4\ X_i d_i$, owing to the probability X_i that the rock has a diameter d_i. Summed over all particle sizes, the average induced lateral displacement per contact is equal to $\Sigma\ 1/4\ X_i d_i$. Thus, the rock-size distribution can be effectively taken into account by using the following weighted-average rock diameter:

$$D_p = \Sigma\ X_i d_i. \qquad (4)$$

For the three particle-size distributions shown in Fig. 1, the average diameters calculated by Eq. 4 are 0.36 m for Piledriver, 0.09 m for mine waste, and 0.18 m for the intermediate (standard) particle-size distribution.

For a specified average particle diameter, we can thus calculate the gas distribution curve at any desired height above the injection pipe. As a measure of the average coverage of a given chimney with dispersed oxygen bubbles, we will use the width of the gas distribution curve at 8% of its peak height calculated for midheight in the chimney. This width is 8.3, 6.3, and 4.2 m for the Piledriver, standard, and mine-waste size distributions, respectively.

To determine the applicability of the random-walk gas-bubble dispersion model, the process was simulated in a laboratory apparatus. The apparatus, which was in effect a two-dimensional chimney (1.2 m high, 40 cm wide, and 3 cm thick) filled with water and 0.9-cm-diam glass marbles and equipped with a point gas-injection source, simulated an actual three-dimensional chimney having a horizontal line-injection source. The gas distribution was measured at a height of 0.96 m above the gas inlet by collecting the effluent gas in a centrally positioned row of inverted, water-filled test tubes of 0.8-cm ID. The excellent agreement between the measured and calculated distributions indicated that the proposed calculational model adequately describes the dispersion process.

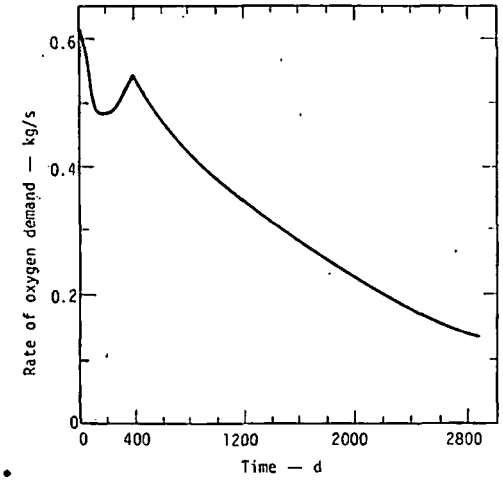

Fig. 5—Rate of oxygen demand from oxygen-producing plant (for reference case).

Appendix B

Computation Procedure for a Combined Leach-Circulation Calculation: This Appendix describes the sequence of calculations performed in a finite-difference computer code to achieve a self-consistent solution of the physical and chemical processes involved in leaching a flooded column of rubblized ore.

Before beginning the calculation, we must choose values for the fixed quantities. These include the dimensions of the chimney, the size distribution of the broken rock, the number of injection lines, the liquid-injection rate, and the copper-ore characteristics. These quantities are shown in Tables 2 and 3 for the particular case being analyzed.

In the following calculations, we will need to refer to the saturation concentration of dissolved oxygen at a given point in the chimney. This is most conveniently obtained by defining a datum plane near the Earth's surface such that at a distance h below this plane, the pressure is

$$P = k_2 h \qquad (5)$$

where $k_2 = 9807$ Pascal per m. Then, the saturation concentration of oxygen (kg/per cu m) is

$$C_s = k_1 h \qquad (6)$$

where $k_1 = 40.13 \times 10^{-3} - 20.51 \times 10^{-5} T + 2.781 \times 10^{-7} T^2$. Eq. 6, giving the temperature and pressure dependence of oxygen solubility in water, was derived from solubility measurements of Zoss, et al.[8] For a given case being analyzed, the values of h at the top (h_t) and bottom (h_b) of the chimney are determined from the specified oxygen partial pressure at the top of the chimney and from the height of the chimney.

The first calculation is to determine the mass rate of oxygen injection. For reasons of flow stability[9] the volume fraction of oxygen just downstream of the oxygen sparging nozzle is regulated at 20%. Then the mass rate of oxygen injection is

$$R_i = \frac{M_o P_N V_I}{4RT} \qquad (7)$$

where M_o is the molecular weight of oxygen (0.032 kg per mol), P_N is the nozzle pressure (3.55×10^6 Pascal), V_I is the specified volume rate of liquid injection, and R is the gas constant (8.3143 joule per mol per K). We assume that the liquid entering the bottom of the chimney is saturated with dissolved oxygen. Then the mass rate of upward flow of undissolved oxygen at the bottom of the bubble region is

$$r_b = R_i - V_I k_1 h_b. \qquad (8)$$

Next, the rate of leaching in the bubble region is calculated. For the first time step, this rate is calculated from an assumed initial average oxygen concentration. In subsequent time steps, the leaching rate is calculated from the average oxygen concentration in the bubble region obtained from the previous time step. The mass rate of oxygen consumption in the bubble region, R_B, is then obtained from the copper-leaching rate and from the known stoichiometric relationship between copper production and oxygen consumption.

At this point, the computation sequence enters two nested, iterative loops. The first step in the iteration is to obtain an estimated value for the superficial liquid velocity in the nonbubble region, U_{SN}. The volume rate of liquid flow in the bubble region is the sum of the volume rate of liquid flow in the nonbubble region and the volume rate of liquid injection. That is,

$$U_{SB} A F_B = U_{SN} A (1 - F_B) + V_I \qquad (9)$$

where U_{SB} is the superficial liquid velocity in the bubble region, A is the cross-sectional area of the chimney, and F_B is the fraction of chimney volume occupied by the bubble region. From Eq. 9, U_{SN} can be calculated using some value of U_{SB}. For the first traverse of the inner loop during the first time step, an assumed value of U_{SB} is used. During any given time step, corrected values of U_{SB} are obtained from the iterative procedure described below. For the first traverse of the inner loop during all but the first time step, the value of U_{SB} is that which gave satisfactory convergence during the previous time step.

The concentration of dissolved oxygen at the bottom of the bubble region, C_{bB}, is then calculated from the following equation based on conservation of dissolved oxygen in the merging liquid streams from the injection pipes and nonbubble region:

$$U_{SB} A F_B C_{bB} = V_I k_1 h_b + U_{SN} A (1 - F_B) C_{bN} \qquad (10)$$

where C_{bN} is the concentration of dissolved oxygen at the bottom of the nonbubble region. Initially, C_{bN} is assumed to be zero. Later steps in the iteration provide updated values of C_{bN} to be used in Eq. 10.

Next we calculate the vertical distribution of dissolved and undissolved oxygen in the bubble region. Applying conservation of oxygen between h_b and h,

$$r_b \left(\frac{a}{a_i}\right)^3 \left(\frac{h}{h_t}\right) + U_{SB} A F_B C + \left(\frac{h_b - h}{h_b - h_t}\right) R_B = r_b + U_{SB} A F_B C_{bB} \qquad (11)$$

where C is the concentration of dissolved oxygen at h, a_i is the initial radius of an individual oxygen bubble at h_b, and a is the radius at h. The third term on the left side of Eq. 11 represents the oxygen consumed by the ore between h_b and h in the bubble region. The quantity a/a_i must now be derived as a function of h by considering the kinetics of oxygen dissolution.

The dissolution rate of a sparingly soluble gas, such as oxygen in water, is controlled by the removal of the dissolving material from the surface of the gas bubble into the body of the liquid, i.e., by convective diffusion. For the bubble sizes apparently encountered in this bubbling process (i.e., $0.001 < a < 0.01$ m), the convective mass transfer can be expressed as[10]

$$\frac{dm}{dt} = -4\pi a^2 [k_d (C_s - C) a^{1/4}] \qquad (12)$$

where k_d is the mass-transfer coefficient. It has been shown[5] that the mass-transfer coefficient for dissolution of oxygen in a large-scale laboratory leaching experiment can be expressed as

$$k_d = k_3 a_i^{3/4} \qquad (13)$$

where $k_3 = 0.083$ sec^{-1}. We may further write that the mass of an individual oxygen bubble at height h is

$$m = \frac{4}{3}\pi a^3 \left(\frac{M_o k_2 h}{RT}\right) \qquad (14)$$

and the total derivative of m is

$$\frac{dm}{dt} = 4\pi \left(\frac{M_o k_2}{RT}\right) \left(a^2 h \frac{da}{dt} + \frac{a^3}{3}\frac{dh}{dt}\right). \qquad (15)$$

Combining Eqs. 12, 13, and 15 and substituting $dh/dt = -U_g$ (the gas-bubble velocity) and $da/dt = -U_g\, da/dh$ gives the desired expression

$$\frac{d\left(\frac{a}{a_i}\right)}{dh} = \frac{1}{h}\left[\frac{k_3 RT(C_s - C)}{M_o k_v U_g}\left(\frac{a}{a_i}\right)^{1/3} - \frac{1}{3}\left(\frac{a}{a_i}\right)\right] . \quad (16)$$

The vertical distribution of dissolved and undissolved oxygen is then obtained by stepwise integration of Eqs. 11 and 16, beginning at the bottom of the bubble region. The calculated concentration of dissolved oxygen in the bubble region as a function of chimney height is shown as the upper curve in Fig. 6.

The numerical value of U_g used in the above calculations is based on the following considerations. If we assume that only bubbles of radius greater than 0.001 m are encountered in the bubbling process, the velocity of rise for an individual bubble is independent of the exact bubble dimension.[10] Although bubbles of this size rising in water have a mean velocity of 0.3 m per sec, observations of bubble flow in a packed bed indicate a mean velocity of approximately 0.15 m per sec. The latter value is therefore used in this calculation. Furthermore, Gal-Or and Walatka[11] have shown that the velocity of rise for a swarm of bubbles is very close to the velocity of an individual bubble for the low (<0.01) volumetric gas-phase fraction that is of interest in this application.

The next step in the iterative calculation is to calculate the buoyancy and fluid-flow pressure drops. The buoyancy pressure drop is

$$\Delta P_1 = g\Delta\rho \quad (17)$$

where g is the gravitational acceleration (9.807 m per sec^2) and $\Delta\rho$ is the difference in fluid densities between the bubble and nonbubble regions. At a given height in the chimney, the latter quantity is given by

$$\Delta\rho = m_g\left(\frac{RT\rho}{M_o P} - 1\right)\left(\frac{H}{V F_h}\right) \quad (18)$$

where m_g is the mass of undissolved oxygen per unit chimney height, P is pressure, H is total chimney height, V is total chimney fluid volume, and ρ is liquid density (assumed 1000 kg per cu m). The quantity m_g is given by

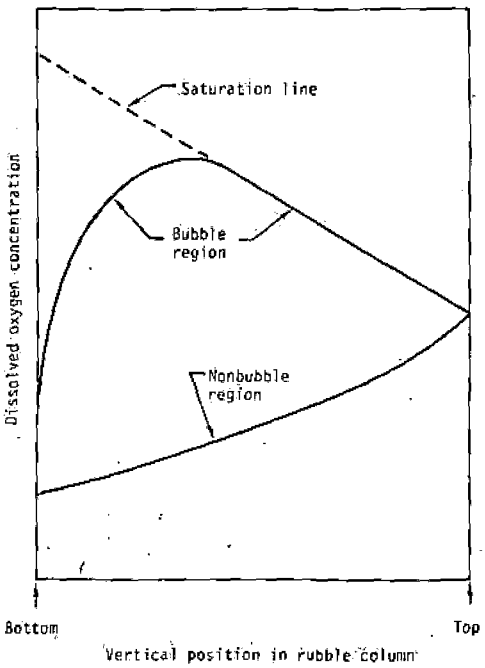

Fig. 6—Distribution of dissolved oxygen.

$$m_g = \frac{r}{U_g} \quad (19)$$

where r is the mass rate at which undissolved oxygen is rising past a horizontal plane at the given chimney height.

Combining Eqs. 17 through 19 gives

$$\Delta P_1 = \left(\frac{RT\rho}{M_o} - P\right)\left(\frac{gH}{VF_h U_g}\right)\left(\frac{r}{P}\right) . \quad (20)$$

Then the average buoyancy pressure drop per unit chimney height is

$$\overline{\Delta P_1} = -\left(\frac{RT\rho}{M_o} - \overline{P}\right)\left(\frac{g}{VF_h U_g}\right)\int_{h_b}^{h_t}\frac{r}{P}\,dh . \quad (21)$$

In Eq. 21, $RT\rho/M_o >> P$; therefore, in the first factor, P has been replaced by the average pressure $\overline{P}$ for simplification. The integrand, r/P, is obtained from the previously calculated undissolved-gas distribution using the relationship

$$\frac{r}{P} = \left(\frac{a}{a_i}\right)^{n'}\left(\frac{r_b}{k_2 h_b}\right) . \quad (22)$$

We must now consider the balancing pressure drop per unit chimney height due to the frictional flow of solution through a packed bed of solid particles. An expression for this has been given by Leva:[12]

$$\Delta P_2 = \frac{2fU_s^2\rho}{D_p\epsilon^3}\left(\frac{1-\epsilon}{\phi}\right)^{3-n} \quad (23)$$

where f is the friction factor, n is the state of flow factor, ϵ is the bulking porosity of the packed bed, ϕ is the particle-shape factor (assumed value 0.65), D_p is the particle's weighted average diameter,[13,14] and U_s is the superficial fluid velocity.

Eq. 23 is applicable to either liquid or gas flowing alone. In the bubble region of the chimney, both liquid and gas phases are present. When two phases move together through a pipe or packed column, the resulting pressure drop can be significantly greater than that predicted by equations for single-phase flow.[15] For the cases analyzed, the gas velocity is more than 100 times greater than the liquid velocity, so the two phases are not moving together. Accordingly, the motion of the gas bubbles will be unaffected by the liquid flow. Furthermore, since gas occupies only a very small fraction of the chimney void, the liquid flow will be essentially unaffected by presence of the gas.

The total frictional pressure drop per unit chimney height is then

$$\Delta P_2 = \frac{2fU_{sn}^2\rho}{D_p\epsilon^3}\left(\frac{1-\epsilon}{\phi}\right)^{3-n} + \frac{2f'U_{sN}^2\rho}{D_p\epsilon^3}\left(\frac{1-\epsilon}{\phi}\right)^{3-n'} \quad (24)$$

where f and n refer to the bubble region and f' and n' refer to the nonbubble region. The values used for these friction and state-of-flow factors are those given by Leva.[12]

The calculated values of $\overline{\Delta P_1}$ and ΔP_2 are compared. If they are not in satisfactory agreement, a corrected value of U_{sn} is calculated from the difference between the ΔP values, and the computation returns to the calculation of U_{sN} by Eq. 9. If they are in satisfactory agreement, the computation exits the inner loop.

Next, the rate of oxygen consumption in the leaching reactions in the nonbubble region is calculated. This is obtained as the difference between the rate of oxygen entering and leaving the nonbubble region:

$$R_N = U_{BN} A (1 - F_B) (C_{tN} - C_{bN}) \quad (25)$$

where C_{tN} and C_{bN} are the concentrations of dissolved oxygen at the top and bottom of the nonbubble region, respectively. The quantity C_{tN} was obtained in solving Eqs. 11 and 16, since the oxygen concentration at the top of the nonbubble region is equal to that at the top of the bubble region. Using this value of R_N, we perform a leaching calculation to determine the average concentration of dissolved oxygen in the nonbubble region, $\overline{C}_N$.

Finally, a corrected value for C_{bN} can be obtained. The distribution of dissolved oxygen in the nonbubble region is derived assuming a uniform chemical reactivity of the copper ore. This is exactly true only at the beginning of leaching, but is believed to be a good approximation during most of the leaching operation. Using this assumption, the rate at which dissolved oxygen is removed from the leaching solution is directly proportional to the concentration of dissolved oxygen. This, in turn, results in a distribution of dissolved oxygen that is a decreasing exponential function of distance below the top of the rubble column, as shown in Fig. 6.

It is then readily shown that

$$\overline{C}_N = \frac{C_{bN} - C_{tN}}{\ln\left(\frac{C_{bN}}{C_{tN}}\right)}. \quad (26)$$

Eq. 26 is numerically solved for C_{bN} and the result is compared with the value of C_{bN} used when the iterative loops were entered. If the two values are not in satisfactory agreement, the computation returns to the beginning of the inner loop and Eq. 10 is again solved using the corrected value of C_{bN}. If the two values of C_{bN} are in satisfactory agreement, the computation exits the outer loop.

The required conditions for consistency between the leaching and circulation equations have now been satisfied for one time step. The new chimney temperature is then calculated from the heat generated in the leaching reactions and from the heat lost through the chimney walls, with the constraint that the temperature not exceed 363 K. Calculations for the next time step are then begun at Eq. 7.

Acknowledgment

This work was performed under the auspices of the U.S. Atomic Energy Commission.

References

[1] Lewis, A.E., "Chemical Mining of Primary Copper Ores by Use of Nuclear Technology," *Proceedings, Symposium on Engineering with Nuclear Explosives*, American Nuclear Society, Vol. 2, CONF-700101, 1970.

[2] Lewis, A.E., and Braun, R.L., "Nuclear Chemical Mining of Primary Copper Sulfides," *Trans. SME-AIME*, Vol. 254, 1973, p. 217.

[3] Braun, R.L., Lewis, A.E., and Wadsworth, M.E., "In-Place Leaching of Primary Sulfide Ores: Laboratory Leaching Data and Kinetics Model," *Trans. TMS-AIME/ASM*, Vol. 5, 1974, p. 1717.

[4] Lewis, A.E., et al., "Nuclear Solution Mining—Breaking and Leaching Considerations," *Solution Mining Symposium*, F.F. Aplan, W.A. McKinney, and A.D. Pernichele, eds., AIME, New York, 1974, pp. 56-75.

[5] Braun, R.L., Mallon, R.G., and Lewis, A.E., "Distribution of Injected Oxygen in a Large Underground Flooded Region of Broken Ore," Report No. UCRL-75290, 1974, Lawrence Livermore Laboratory.

[6] Rabb, D.D., "Particle Size Distribution Study: Piledriver Event," Report No. UCRL-72078, 1969, Lawrence Livermore Laboratory.

[7] Potter, G.M., U.S. Bureau of Mines, Salt Lake City, Utah, private communication, Oct. 6, 1971.

[8] Zoss, L.M., Suciu, S.N., and Sibbitt, W.L., "The Solubility of Oxygen in Water," *Transactions, American Society of Mechanical Engineers*, Vol. 76, 1954, p. 69.

[9] Martin, C.S., "Transition from Bubbly to Slug Flow of a Vertically Downward Air-Water Mixture," *Flow Studies in Air and Water Pollution*, Applied Mechanics-Fluids Engineering Symposium, American Society of Mechanical Engineers, Atlanta, Ga., 1973.

[10] Levich, V.G., *Physicochemical Hydrodynamics*, Prentice-Hall, Englewood Cliffs, N.J., 1962, pp. 467-468.

[11] Gal-Or, B. and Walatka, V., "A Theoretical Analysis of Some Interrelationships and Mechanisms of Heat and Mass Transfer in Dispersion," *Journal*, American Institute of Chemical Engineers, Vol. 13, 1967, p. 650.

[12] Leva, M., "Fluid Flow Through Packed Beds," *Chemical Engineering*, Vol. 56, 1949, p. 115.

[13] Leva, M., "Pressure Drop Through Packed Tubes," *Chemical Engineering Progress*, Vol. 43, 1947, p. 549.

[14] Leva, M., and Grummer, M., "Heat Transfer to Gases Through Packed Tubes—Effect of Particle Characteristics," *Industrial and Engineering Chemistry*, Vol. 40, 1948, p. 415.

[15] Lockhart, R.W., and Martinelli, R.C., "Proposed Correlation of Data for Isothermal Two-Phase, Two-Component Flow in Pipes," *Chemical Engineering Progress*, Vol. 45, 1949, p. 39.

PREPRINT NUMBER
79-358

COMPARISON OF LEACHING-SOLVENT EXTRACTION ELECTROWINNING WITH LEACHING-CEMENTATION FOR PROCESSING LOW-GRADE COPPER SULFIDE ORES

Brent W. Madsen
Metallurgist

Rees D. Groves
Metallurgist

Salt Lake City Research Center
Bureau of Mines
U.S. Department of the Interior
Salt Lake City, Utah

For presentation at the SME-AIME Fall Meeting and Exhibit
Tucson, Arizona - October 17-19, 1979

Abstract. To assist in fulfilling the Bureau of Mines goals of maintaining adequate mineral supplies to meet national economic and strategic needs, and to minimize the environmental impacts associated with mineral-processing operations, a leaching-solvent extraction-electrowinning technique was compared with a leaching-cementation technique for processing low-grade copper ores. Large-scale laboratory column leaching tests (6 to 7 tonnes) were conducted on minus 37-cm chalcocitic ore using ferric sulfate leach solutions at 25° C. Two columns contained 11 percent minus 1.27-cm fines, and two columns contained 32 percent minus 1.27-cm fines. After 416 days of leaching ore samples containing 11 percent minus 1.27-cm fines, copper extraction was 48 and 51 percent for the leach-cementation and leach-solvent extraction-electrowinning procedures, respectively. When leaching ore samples containing 32 percent minus 1.27-cm fines, the leaching-solvent extraction-electrowinning technique extracted 60 percent of the copper after 568 days, whereas the leaching-cementation technique extracted only 48 percent of the copper. In the latter test, leach solution ponded on the ore, which reflected a decrease in ore column permeability. The decreased permeability was attributed to the generation of excessive amounts of iron salts during cementation; the salts precipitated on the fine ore particles and in the interstices, thus plugging the column. This decrease also lowered the available oxygen, resulting in poor aerobic bacterial activity which slowed the oxidation rate of ferrous ions to ferric ions. Sulfuric acid required to maintain a leachant pH of 2 was nearly halved when copper was recovered by solvent extraction and electrowinning rather than by cementation.

Introduction

In the commercial dump leaching of copper, two methods have been generally accepted as a means for recovering copper from pregnant leach liquors. The oldest and most widely used technique is cementation with scrap iron. The newer technique involves solvent extraction and electrowinning. As part of a program to assure adequate domestic supplies of essential metals, the Bureau of Mines, U.S. Department of the Interior, conducted comparative tests of leaching-cementation and leaching-solvent extraction-electrowinning. The objective of this research is to supply information for improving copper recoveries from copper leach dumps, thus extending and conserving copper reserves.

One of the major problems encountered in dump leaching is the precipitation of iron salts that render the ore impermeable to leaching solutions. This condition decreases the copper extraction rate and may eventually produce a dormant dump that may leave much undissolved copper within the ore bed (1). In addition to iron dissolved from the ore during leaching, iron derived from the cementation step may significantly contribute to the plugging of a leach dump. The newer solvent extraction-electrowinning method recovers copper from leach solutions without adding iron to the leach system.

Although economic comparisons between cementation and solvent extraction-electrowinning techniques have been reported (2), the results of studies that compare effects of the two recovery techniques on leaching have not been reported. The Bureau of Mines, aware of the problems associated with maintaining leach dump permeability, has reported the beneficial effects of removing ore fines prior to leaching (3) and the enhancement of the copper leaching rate by injecting gaseous oxygen into a nearly dormant leaching system (4). To supply further information concerning copper dump leaching, this report describes the results of leach-cementation and leach-solvent extraction-electrowinning procedures, using 6- to 7-tonne ore samples.

Materials and Methods

Ore Sample Description

Low-grade Montana open pit mine waste containing about 0.25 percent copper was used in the leach testing. The host rock was an altered quartz monzonite containing about 5 weight-percent pyrite. The copper content was distributed among several minerals with chalcocite predominating. The distribution in weight-percent was 66 chalcocite-digenite, 17 chalcopyrite, 11 covellite, and 6 enargite.

One objective of the investigation was to determine the effect of the amount of minus 1.27-cm fines on bed permeability using the alternate copper recovery techniques. Two comparative tests were made with samples that contained 11 percent minus 1.27-cm fines, and another comparison was made with samples that contained 32 percent minus 1.27-cm fines. The samples were prepared by combining various size fractions of the ore sample to yield the particle size distributions shown in Figure 1. The top size of each sample was 37 cm. Each sample containing 11 percent minus 1.27-cm fines whereas the samples containing a higher proportion of fines assayed 0.26 percent copper.

Leaching Procedure

The ore samples were leached in glass-fiber-reinforced polyester columns 1.37 m in diameter by 3.05 m high. For the comparison with ore containing 11 percent fines (minus 1.27 cm) 6800-kg samples were used; for the comparison with ore containing 32 percent fines, 6410-kg samples were used. Leach solution with a pH of 2.0 was pumped to the top of the ore at an initial rate of 3000 l/m^2 d and uniformly distributed over the ore. The solution percolated downward through the ore, was collected in a surge tank, and recirculated back to the top of the ore until the copper content was 1 to 2 g/l. The pumping was then stopped and the soluble copper recovered by the appropriate method. The barren solution was acidulated to a pH of 2.0 with sulfuric acid and used to leach additional copper.

Copper Recovery Procedures

Copper recovery by cementation was accomplished in a glass column 15 cm in diameter by 2.3 m high containing shredded detinned iron scrap. Pregnant solution was pumped upward through the iron. Sulfuric acid was added to the solution prior to passage through column to maintain an effluent pH of 2.0 to prevent precipitation of

iron salts.

The solvent extraction recovery system was comprised of a four-stage countercurrent mixer-settler unit for extraction followed by a four-stage countercurrent stripping unit and an electrowinning cell. The organic extractant consisted of 10 volume-percent LIX-64N[1/] in kerosine. The solvent extraction system was operated with an organic flow rate of 0.7 *l*/min and an aqueous flow of 0.9 *l*/min. The aqueous feed to the solvent extraction section contained 1 to 2 g/*l* of Cu and raffinate containing less than 0.1 g/*l* of Cu was returned to the leaching circuit. The solvent was loaded to nearly 1.5 g/*l* of Cu; stripping reduced the copper concentration to 0.1 g/*l* of Cu. The stripping and electrowinning units were operated to maintain a balanced copper extraction unit. The electrolyte used in the stripping unit was circulated at 0.15 *l*/min and contained 20 to 30 g/*l* of Cu and 150 g/*l* of H_2SO_4. The electrowinning cell was operated at a current density of 172 A/m^2.

Experimental Results

Leaching the Coarse Ore

The two coarse ore samples (11 percent minus 1.27 cm) were leached for 416 days. Copper was recovered from solution 32 times in each leach test. Copper extractions, based on leach solution and ore residue assays, are shown in Figure 2. After 416 days, copper extraction was 48 percent for the leach-cementation test and 51 percent for the leach-solvent extraction-electrowinning test.

Acid addition to maintain the leach solution at pH 2.0 for the leach-cementation test was 7.5 kg H_2SO_4/t of ore; whereas, the leach-solvent extraction-electrowinning test required only 4.6 kg H_2SO_4/t of ore.

The iron concentration increased in the leach solutions of both tests, but the rate of increase was more rapid in the test using cementation. After 131 days of leaching, the iron concentrations were 31 g/*l* in the leach-cementation test solution and 14 g/*l* in the leach-solvent extraction-electrowinning test solution. Beyond 131 days, the iron concentrations were maintained at 10 g/*l* by bleeding solution from each system and replacing it with water. This procedure simulates large-scale leaching practice in which dissolved iron is controlled by oxidation and settling in ponds.

In the leach-cementation test, the amount of iron added to the system during the cementation operations was 6.15 kg/t of ore and 3 kg of iron per tonne of ore was bled from the system. At the completion of the test, only 0.35 kg of iron per tonne of ore remained in solution. Based on these amounts, 2.8 kg of iron per tonne of ore accumulated in the ore. However, the accumulated iron in form of precipitated salts was not in sufficient quantity to cause ponding of the ore in either test, and a solution flow rate of 3000 *l*/m^2 d was maintained throughout the test.

The presence of both iron- and sulfur-oxidizing bacteria in both leach solutions was verified by semiquantitative bacteriological tests. Good bacterial activity was evidenced in both tests by the low ferrous iron levels (less than 0.1 g/*l*) throughout the test period.

Leaching the Fine Ore

The two fine ore samples (32 percent minus 1.27 cm) were leached for 568 days during which time copper was recovered from solution 25 times. Copper extractions for the two tests are shown in Figure 3. At the completion of the tests, copper extraction was 60 percent for the leach-solvent extraction-electrowinning test and 48 percent for the leach-cementation test. Although similar extractions were achieved during the first 200 days, a noticeable difference in copper extraction was apparent after 300 days.

Acid addition to maintain the leach solution at pH 2 was 7.0 kg H_2SO_4/t of ore for the leach-cementation process and 2.9 kg H_2SO_4/t of ore for the leach-solvent extraction-electrowinning process.

Maximum total iron concentrations in leach liquors reached during 568 days of leaching were 20 g/*l* using cementation and only 10 g/*l* using solvent extraction. Leach liquor ferrous iron concentration remained at 0.1 g/*l* or less when solvent extraction was used. Using cementation, however, the ferrous iron content held at 0.1 g/*l* during most of the first 151 days of leaching and then increased to a level of 70 percent to 100 percent of the total iron content during the remainder of the test.

A leach solution percolation rate of 3000 *l*/m^2 d was maintained when solvent extraction was used; however, the percolation rate decreased to only 77 *l*/m^2 d after 162 days when cementation was used. Precipitation of iron compounds from the high-iron leach liquor in the leach-cementation test impeded the percolation rate through the fine-ore bed and the cyclic nature of the percolation rate is shown in Figure 4.

Copper extraction became retarded when the ore contained 32 percent minus 1.27-cm fines and copper was removed by cementation. Decreased copper extraction was attributed to two related factors. Leach solution percolation rate was greatly decreased by blinding of the bed with precipitated iron compounds, and the concentration of ferric iron, a solvent for the copper sulfide minerals, decreased. The oxidation of ferrous to ferric iron largely was due to the action of aerobic bacteria within the bed and poor bed permeability caused oxygen starvation that dimished bacterial action. This conclusion was reached when gas samples from a perforated tube embedded in the ore were taken on the 150th day of leaching. Gas analyses showed oxygen contents of 20 and 4.2 percent for the leach-solvent extraction and leach-cementation tests, respectively. Thus, copper removal by solvent extraction enabled better copper leaching when the ore contained a large proportion of fines.

Consumption of sulfuric acid was least when solvent extraction was used because acid consumption was related to the relatively large amount of iron dissolved during cementation. Sulfuric acid was used by the reaction of iron and acid, equation 1, and by the oxidation of ferrous iron, equation 2.

$$H_2SO_4 + Fe \rightarrow FeSO_4 + H_2 \qquad (1)$$

1/ Reference to specific trade names or manufacturers does not imply endorsement by the Bureau of Mines.

$$2FeSO_4 + H_2SO_4 + 1/2\ O_2 \rightarrow Fe_2(SO_4)_3 + H_2O \quad (2)$$

Less acid was used when leaching the fine ore, and this was believed to result from leaching the fines that contained a higher proportion of friable iron sulfide minerals than the harder, coarse material. The dissolution of pyrite, for example, is shown by equation 3; this reaction plus the oxidation reaction 2 gives the net reaction 4.

$$FeS_2 + 7Fe_2(SO_4)_3 + 8H_2O \rightarrow 15FeSO_4 + 8H_2SO_4 \quad (3)$$

$$2FeS_2 + 7\text{-}1/2\ O_2 + H_2O \rightarrow Fe_2(SO_4)_3 + H_2SO_4 \quad (4)$$

Conclusions

Comparative leaching tests were made to determine copper extractions from low-grade chalcocitic ore using either cementation or solvent extraction-electrowinning methods to recover copper from the acidic leach liquors. Two minus 37-cm ore samples that had different particle size distributions were tested; one sample contained 11 percent minus 1.27-cm fines, and the other had 32 percent minus 1.27-cm fines.

The copper recovery system had little, if any, effect on copper extraction using the relatively coarse ore sample that contained 11 percent minus 1.27-cm fines. After 416 days of leaching, copper extractions were 48 percent for the leach-cementation test and 51 percent for the leach-solvent extraction-electrowinning test.

In comparative tests using the ore sample that contained 32 percent minus 1.27-cm material, the solvent extraction-electrowinning copper recovery system yielded the highest copper extraction. After 568 days of leaching, copper extractions were 48 percent for the leach-cementation test and 60 percent for the leach-solvent extraction-electrowinning test. Cementation of the copper, unlike solvent extraction-electrowinning, contributed additional iron to the leach column, which resulted in the precipitation of iron compounds that decreased ore permeability. The eventual plugging of the ore bed resulted in low oxygen content within the column, poor bacterial activity, and low ferric iron concentrations. These factors led to a slow copper leaching rate.

Consumption of sulfuric acid, necessary to maintain a pH of 2, was minimized by using solvent extraction-electrowinning for copper recovery. The leach-cementation test required more acid because acid was consumed by the dissolution of metallic iron during cementation and by the oxidation of the resulting ferrous iron.

References

1. Sheffer, H. W., and Evans, L. G., "Copper Leaching Practices in the Western United States," Bureau of Mines IC 8341, 1968, 57 pp.
2. Palley, J. N., and Paige, P. M., "Can Electrowinning Replace Cement Copper?" Engineering and Mining Journal, Vol. 173, No. 7, July 1972, pp. 94-96.
3. Madsen, B. W., Groves, R. D., Evans, L. G., and Potter, G. M., "Prompt Copper Recovery from Mine Strip Waste," Bureau of Mines RI 8012, 1975, 19 pp.
4. Madsen, B. W., and Groves, R. D., "Using Oxygen to Reactivate a Nearly Dormant Copper Sulfide Leach," Bureau of Mines RI 8056, 1975, 9 pp.

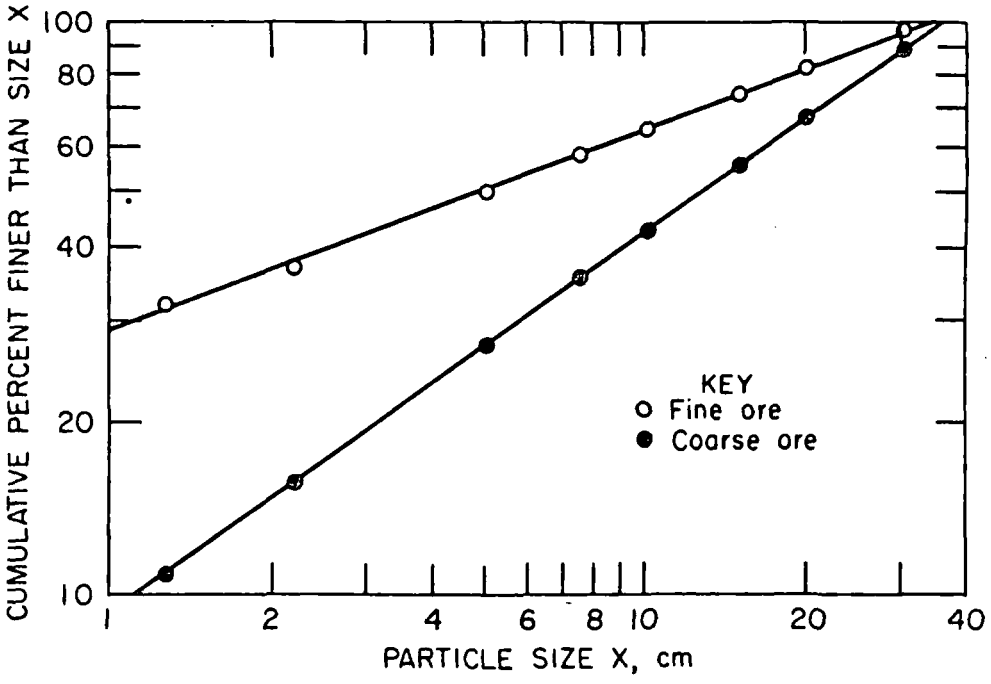

FIGURE 1.-Schuhmann plot of the size distribution of ore samples used in the leach testing.

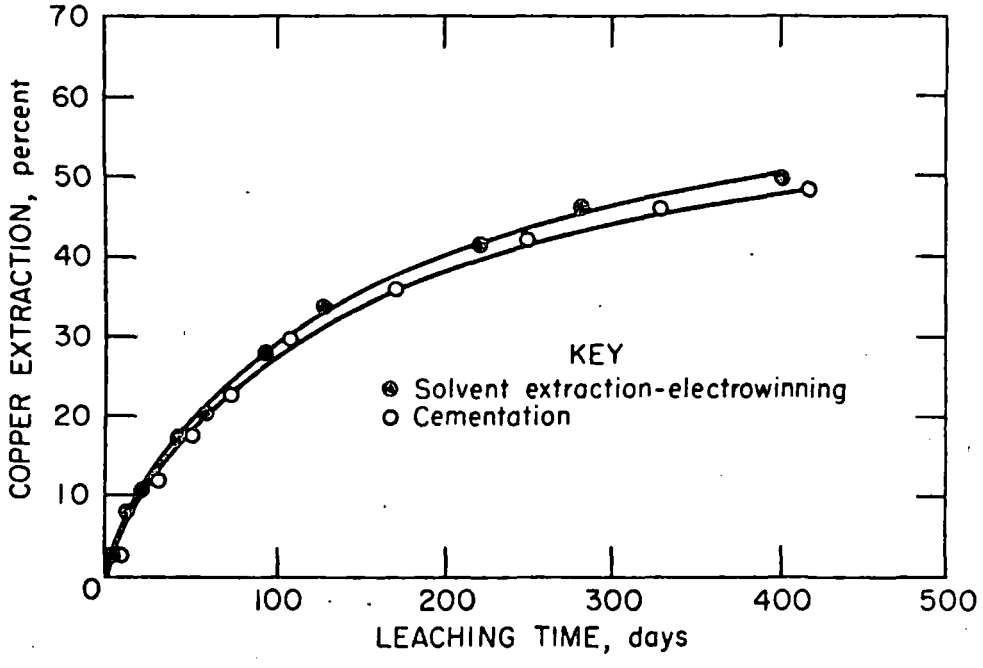

FIGURE 2.-Copper extraction from coarse ore sample using two different copper recovery methods.

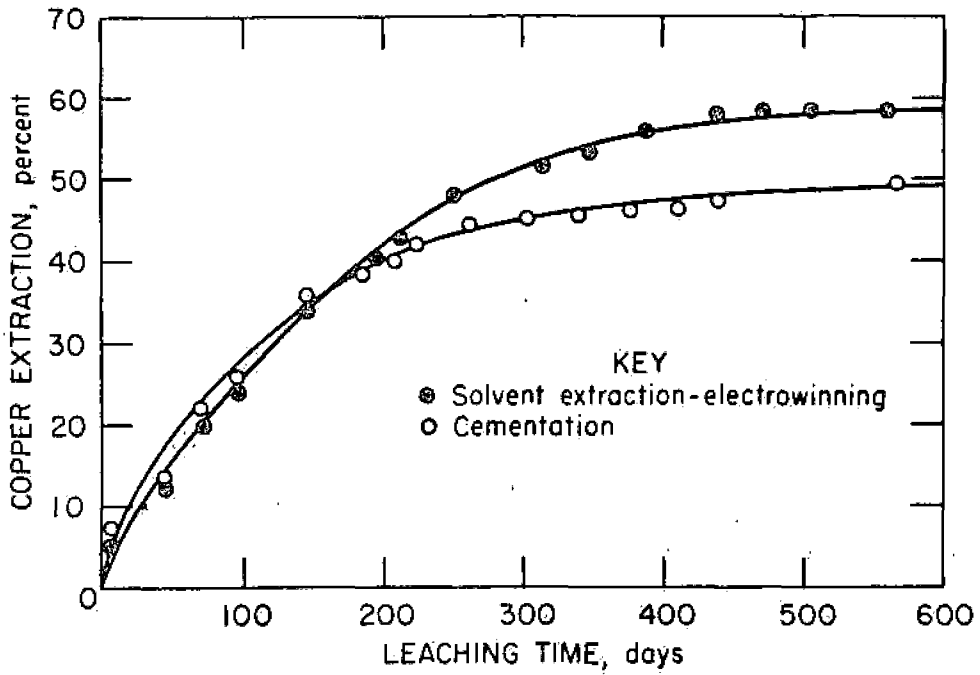

FIGURE 3.-Copper extraction from fine ore sample using two different copper recovery methods.

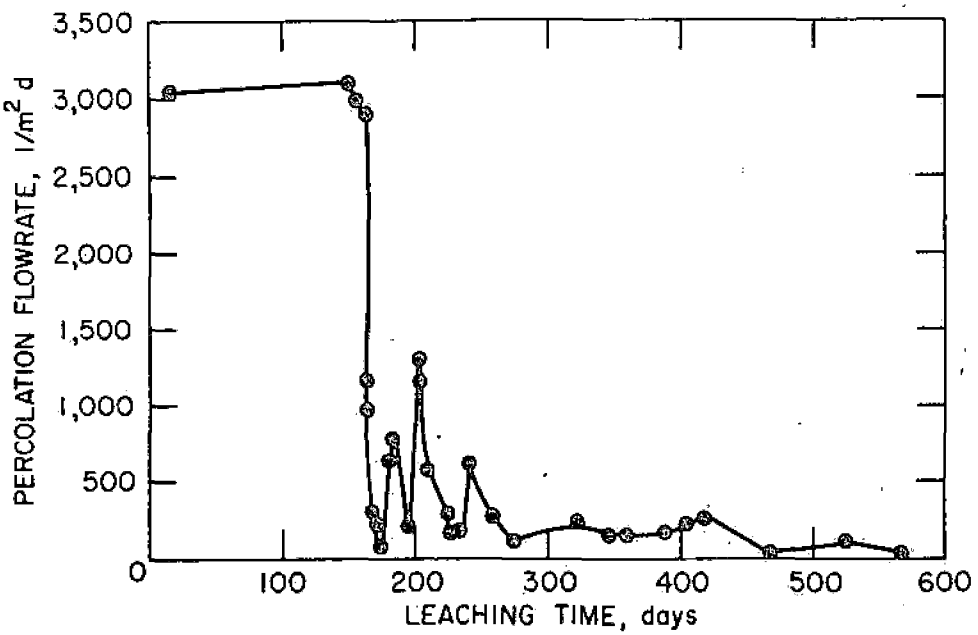

FIGURE 4.-Leach liquor percolation rate through the fine ore sample when copper was recovered by cementation.

COPPER LEACHING PRACTICES IN THE WESTERN UNITED STATES

By Herman W. Sheffer and LaMar G. Evans

* * * * * * * * * * * * information circular 8341

UNITED STATES DEPARTMENT OF THE INTERIOR
Stewart L. Udall, Secretary

BUREAU OF MINES
Walter R. Hibbard, Jr., Director

This publication has been cataloged as follows:

Sheffer, Herman W

Copper leaching practices in the western United States, by Herman W. Sheffer and LaMar G. Evans. [Washington] U.S. Dept. of the Interior, Bureau of Mines [1968]

57 p. illus., table. (U.S. Bureau of Mines. Information circular 8341)

1. Copper ores. 2. Leaching. I. Evans, LaMar G., jt. auth. II. Title. (Series)

TN23.U71 no. 8341 622.06173

U.S. Dept. of the Int. Library

For sale by the Superintendent of Documents, U.S. Government Printing Office
Washington, D.C. 20402 – Price 75 cents

CONTENTS

CONTENTS--Continued

ILLUSTRATIONS

Fig.

ILLUSTRATIONS--Continued

TABLE

COPPER LEACHING PRACTICES IN THE WESTERN UNITED STATES

by

Herman W. Sheffer[1] and LaMar G. Evans[2]

ABSTRACT

This report describes and discusses present-day leaching technology employed to recover copper from low-grade mine and dump materials derived from the exploitation of copper ore deposits in the Western United States. Illustrations of the integral parts of the leaching, precipitation, and recovery operations at several copper-producing companies are presented. Schematic drawings are included to present typical flowsheets of leaching and precipitation operations. Operational problems common to most copper leaching and precipitation plants are discussed. Areas of present and future research to improve leaching techniques are cited.

INTRODUCTION

The first large-scale leaching and precipitation of copper was probably at Rio Tinto in Spain about 1752. The method employed comprised open-air water leaching of weathered piles of copper-bearing ore followed by precipitation of the copper by iron. A description of leaching and precipitation of copper at Rio Tinto in the 20th century is given by Taylor and Whelan (81).[3] This method is essentially the same as that practiced at present by most of the copper-leaching companies in the Western United States. Nearly 12 percent of the total copper production in the Western States in 1965 was obtained from the precipitation of copper from leach liquors by metallic scrap iron. Almost all of the cement copper produced was shipped to smelters and used as feed in reverberatory furnaces.

The purpose of this report is to describe and discuss the different leaching and recovery methods currently employed in the production of copper from low-grade ores in the Western States. The data included in this report were obtained from a literature search and from visits to most of the larger

---

[1] Mining engineer, Area V Mineral Resource Office, Salt Lake City Field Office, Bureau of Mines, Salt Lake City, Utah.

[2] Supervisory metallurgist, Salt Lake City Metallurgy Research Center, Bureau of Mines, Salt Lake City, Utah.

[3] Underlined numbers in parentheses refer to items in the list of references at the end of this report.

leaching operations in the West. Topics discussed include the physical and mineralogical types of material being leached, the physical nature of dumps and heaps, the emplacement of dumps, methods of introduction of leach solutions, the nature of the leach solutions and the copper-bearing liquors, and methods of recovery of copper from solution.

MINERALOGY OF RAW MATERIALS

Copper in the Western United States is produced from low-grade ore bodies found predominately in igneous host rocks, chiefly quartz monzonite, quartz porphyry, monzonite porphyry, granite porphyry, and quartz diorite. Less important deposits are found in dacite porphyry, rhyolitic flows, conglomerate, diabase, limestone, sandstone, and schist. Most of the open-pit deposits encompass facies of different mineral composition and alteration.

The principal copper sulfide minerals in the host rocks are chalcopyrite and chalcocite. Minor amounts of bornite, covellite, and enargite are present. The principal copper oxide minerals are azurite, chrysocolla, and malachite. Varying amounts of cuprite, native copper, and tenorite also are present.

CHEMICAL REACTIONS

Oxidized copper ores, mixed oxide-sulfide ores, and those sulfide ores too low in grade to concentrate by froth flotation are treated by various leaching methods. The principal copper oxide minerals dissolved by leaching are azurite, chrysocolla, and malachite, although varying amounts of cuprite, tenorite, and native copper also are known to be contained in some ores and are simultaneously dissolved. The copper sulfide minerals prevalent in many sulfide ores and dissolved during leaching are chalcocite, chalcopyrite, and covellite. Pyrite is an important mineral found in many sulfide ores and is oxidized during leaching to form ferrous sulfate and sulfuric acid.

Reactions by which specific copper minerals are dissolved in leaching, either with sulfuric acid or sulfuric acid plus ferric iron were given by Van Arsdale (83, pp. 11-16):

Azurite

$$Cu_3(OH)_2 \cdot (CO_3)_2 + 3H_2SO_4 \rightleftharpoons 3CuSO_4 + 2CO_2 + 4H_2O$$

Malachite

$$Cu_2(OH)_2 \cdot CO_3 + 2H_2SO_4 \rightleftharpoons 2CuSO_4 + CO_2 + 3H_2O$$

Chrysocolla

$$CuSiO_3 \cdot 2H_2O + H_2SO_4 \rightleftharpoons CuSO_4 + SiO_2 + 3H_2O$$

Cuprite

$$Cu_2O + H_2SO_4 \rightleftharpoons CuSO_4 + Cu + H_2O$$

$$Cu_2O + H_2SO_4 + Fe_2(SO_4)_3 \rightleftharpoons 2CuSO_4 + H_2O + 2FeSO_4$$

Native Copper

$$Cu + Fe_2(SO_4)_3 \rightleftharpoons CuSO_4 + 2FeSO_4$$

Tenorite

$$CuO + H_2SO_4 \rightleftharpoons CuSO_4 + H_2O$$

$$3CuO + Fe_2(SO_4)_3 + 3H_2O \rightleftharpoons 3CuSO_4 + 2Fe(OH)_3$$

$$4CuO + 4FeSO_4 + 6H_2O + O_2 \rightleftharpoons 4CuSO_4 + 4Fe(OH)_3$$

Chalcocite

$$Cu_2S + Fe_2(SO_4)_3 \rightleftharpoons CuS + CuSO_4 + 2FeSO_4$$

$$Cu_2S + 2Fe_2(SO_4)_3 \rightleftharpoons 2CuSO_4 + 4FeSO_4 + S$$

Covellite

$$CuS + Fe_2(SO_4)_3 \rightleftharpoons CuSO_4 + 2FeSO_4 + S$$

Chalcopyrite will slowly dissolve in acid ferric sulfate solutions and also will oxidize according to the following reactions:

$$CuFeS_2 + 2O_2 \rightleftharpoons CuS + FeSO_4;$$

$$CuS + 2O_2 \rightleftharpoons CuSO_4.$$

Pyrite, a prevalent mineral found in many ore deposits, oxidizes according to the following reaction:

$$2FeS_2 + 2H_2O + 7O_2 \rightleftharpoons 2FeSO_4 + 2H_2SO_4.$$

The preceding are only a few of the many and complex chemical reactions that take place within leach dumps.

Studies relative to leaching various copper minerals have been made (13, 46, 54-55, 63, 69-79, 85-86). Patents concerned with the recovery of copper and other metals from ores by chemical means have been issued (12, 18, 21-23, 37-39, 45, 48, 53, 66, 87). Results of these investigations show that several copper sulfide minerals are soluble to some extent in sulfuric acid solutions containing ferric sulfate and that many copper oxide minerals are soluble in ammoniacal solutions. This information has served as the basis for the current leaching technology.

Other metallic minerals and many products of alteration of the host rock are found associated with the copper minerals. Noncarbonate gangue is usually unaffected by leach solutions but metals other than copper; for example, aluminum, uranium, and zinc are found in the pregnant liquors from leaching. Their presence is the result of the partial or complete dissolution of the other metallic minerals and the alteration products. The present study is concerned principally with leaching and recovery of copper; however, the occurrence of these additional metallic elements in the pregnant liquors indicates that appreciable quantities of these metals also might be recovered.

METHODS OF LEACHING

The principal methods of leaching used at present are dump, heap, inplace, and vat. These methods are interrelated, and many items considered necessary for effective leaching by one method are also applicable to the other methods.

Choice of leaching method depends upon the chemical and physical characteristics of the specific material to be treated. The grade of the ore, the solubility of the copper minerals, the amount of acid-consuming associated gangue material, the size of the operation, and the mode of occurrence of the copper-bearing minerals are some of the important factors to be considered.

Dump leaching is used to extract copper from waste material produced during the large-scale open-pit mining of copper ore deposits. Almost all of the copper oxide and sulfide minerals encountered in such deposits are leachable by this method, since the leach cycle is measured in years.

Heap leaching is used primarily to extract copper from uncrushed porous oxidized copper ore which has been piled on prepared drainage pads. The copper oxide minerals in the ore material are readily soluble in sulfuric acid solutions, and the leach cycle for this method is measured in months.

Inplace leaching involves the leaching of broken ore in the ground as it occurs. Current inplace leaching employs the dissolution of copper minerals contained in underground mines that previously utilized block-caving mining methods. Copper minerals leachable by inplace leaching are the same as those leachable by dump leaching, again since the leaching cycle is measured in years.

Vat leaching principally employs the dissolution of copper oxide minerals by sulfuric acid from crushed, nonporous ore material that has been placed in confined tanks. This method is used when rapid extraction of copper is desired, since the leach cycle is measured in days.

Brief descriptions and illustrations of dump, heap, inplace, and vat leaching operations are given in the following sections.

Dump Leaching

Dump leaching is used for low-grade and waste material stripped from open-pit operations. Run-of-mine ore materials containing copper in amounts less

the cutoff grade (usually 0.4 percent copper) deemed necessary for the profitable recovery by the usual mining and concentrating methods are leached by this method. A description of the technology of leaching waste dumps has been given by Malouf and Prater (52). Figure 1 presents a generalized flowsheet for dump leaching and iron precipitation.

Emplacement of Dumps

Ground Preparation

Most leach dumps are deposited upon the existing topography. The locations of the dumps are selected to assure impermeable surfaces and to utilize the natural slope of ridges and valleys for the recovery and collection of the pregnant liquors (fig. 2). Examples of this method of dump emplacement are found at numerous leaching operations in Arizona, Nevada, New Mexico, and Utah (figs. 3, 4, 7).

In several instances leach dumps have been deposited on specially prepared areas. Ground preparation for dump emplacement is represented by the following specific examples.

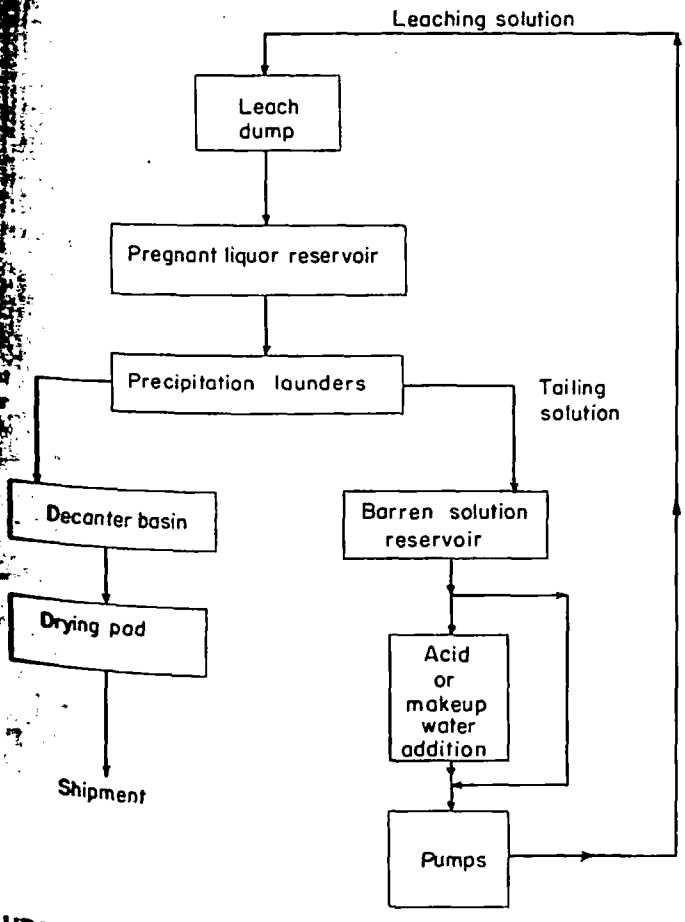

FIGURE 1. - Generalized Flowsheet for Dump Leaching and Iron Precipitation.

The original surface in the dump area of The Anaconda Company, Butte, Mont., is composed of 5 to 80 feet of alluvium which has been deposited on quartz monzonite. Because solution loss through the alluvial material would have been substantial, an impervious pad (fig. 6) to prevent solution loss was constructed in steps as follows: (1) The vegetation was removed by bulldozers; (2) the scraped surface was graded and then compacted using sheepsfoot and vibratory rollers; (3) a 4-inch layer of minus 1-1/2-inch slag was placed on the surface and compacted with a vibratory roller; (4) a coating of asphalt primer was placed above the slag; (5) a compacted 3-1/4-inch layer of asphalt (blacktop) was placed on top of the primed surface of the slag; (6) a 1/8-inch layer of asphaltic sealant then was blown onto

FIGURE 2. - Pregnant Liquor Reservoir, Leaching Operation at the Esperanza Mine, Duval Corp. Note diagnostic blue color of copper-bearing pregnant liquor.

FIGURE 3. - Leach Dump at Mineral Park Operation, Duval Corp. Brown-red areas are country rock, light-gray areas are leach material, and brown iron precipitate is apparent on surface of leach dump.

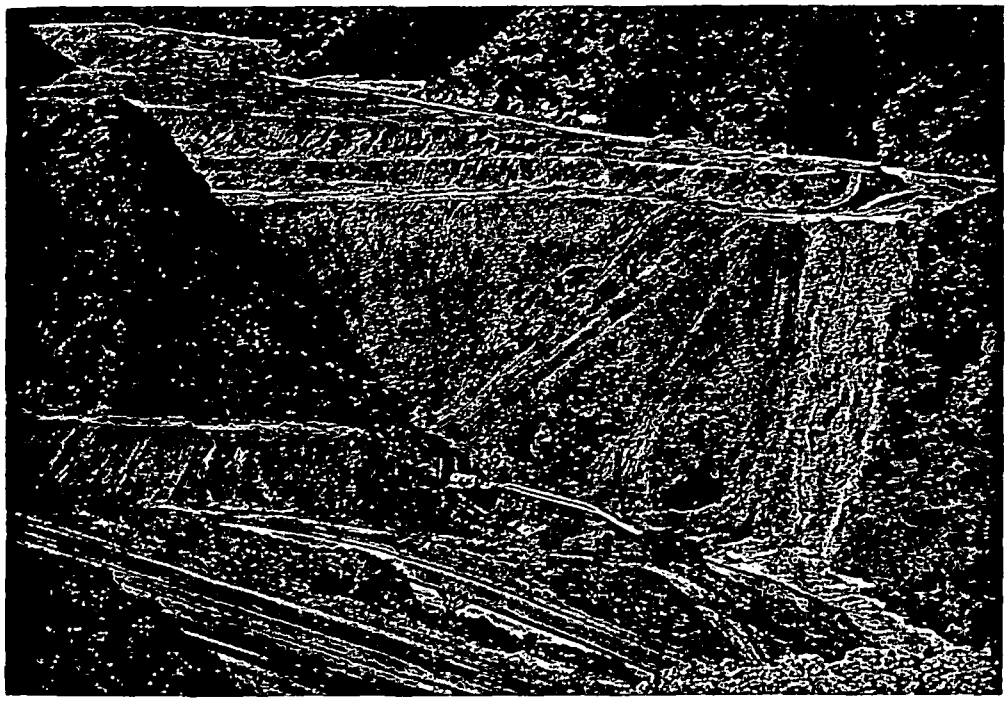

FIGURE 4. - Leach Dump, Bagdad Copper Corp. Note how the dark-brown slopes of the ridges and valleys provide natural boundaries and pathways for the recovery and collection of pregnant liquors after percolation through the specially prepared light-tan dumps.

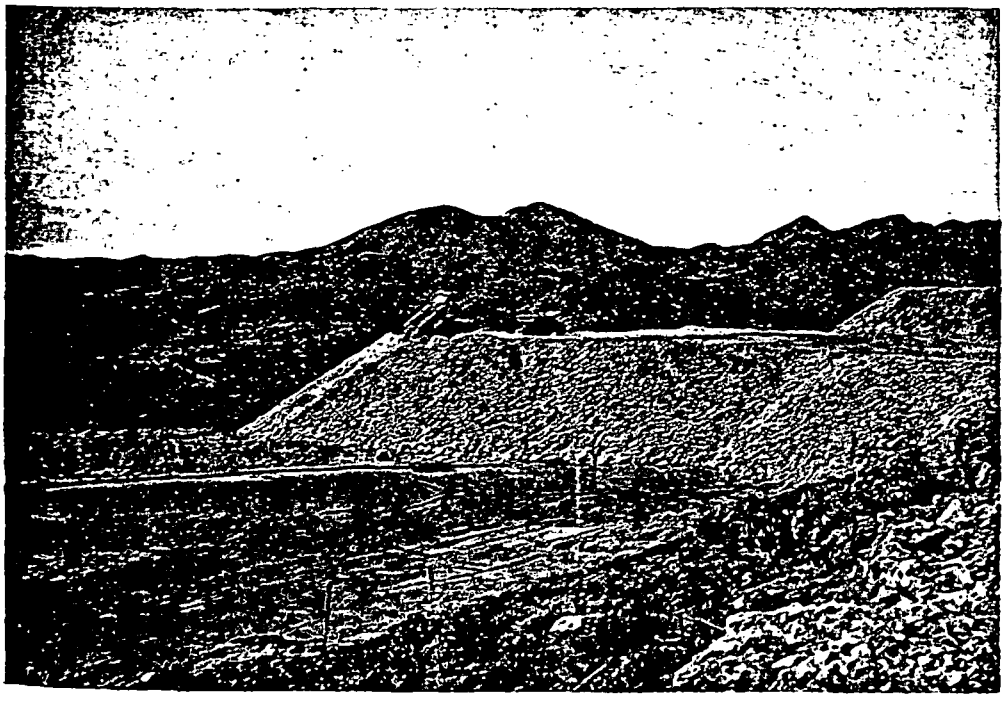

FIGURE 5. - New 50-Foot Lift Being Placed on Surface of Old Dump at Esperanza Mine, Duval Corp. Note light-colored area at left of 50-foot slope where new material is being placed.

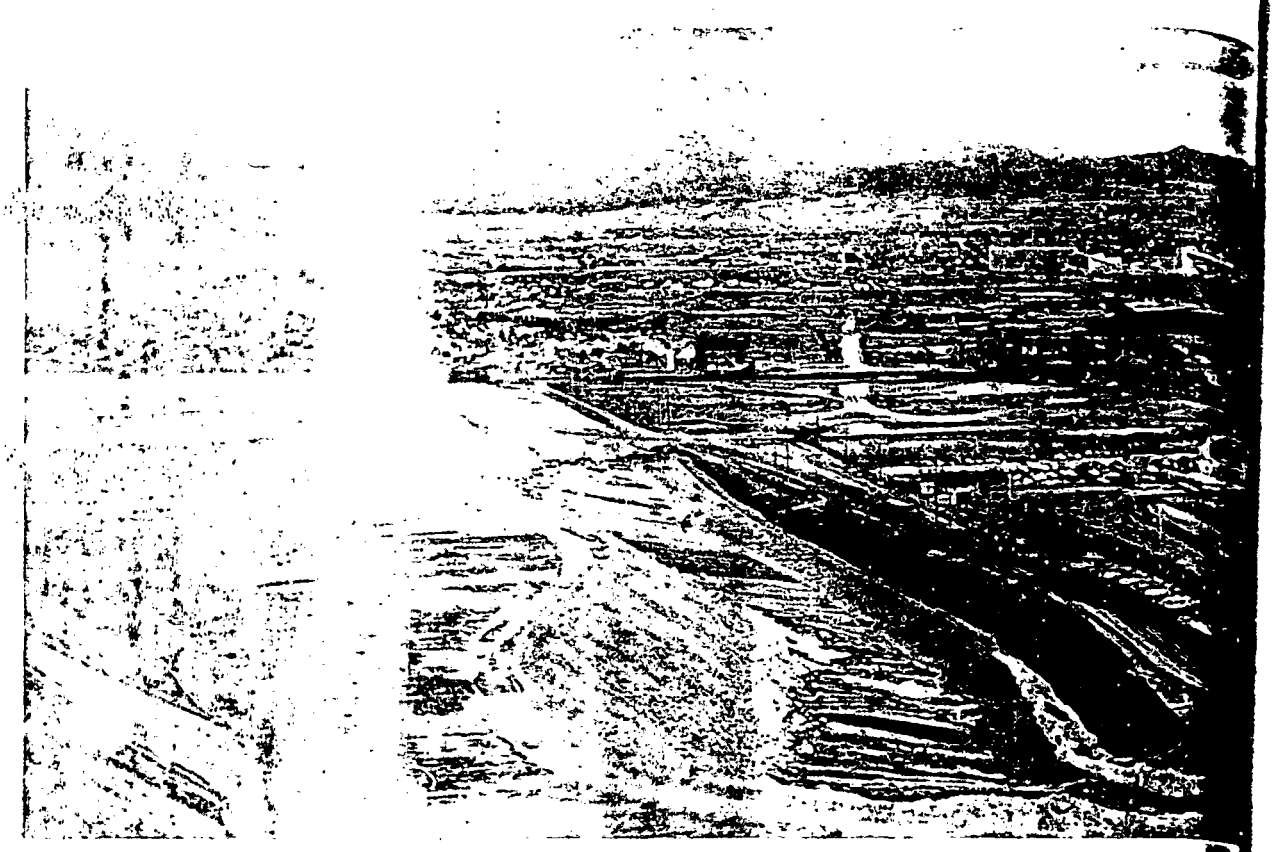

FIGURE 6. - Dump Emplacement on Impervious Pad at Butte Leaching Operation, The Anaconda Company. Note the dark strip in lower right-hand corner of photo.

the surface of the blacktop; (7) a 12-inch minimum thickness of fine pit-run material was placed on the asphalt mat to protect the surface from rupture by heavy truck travel, and (8) a 5- to 6-foot thickness of coarse pit-run material was placed on the fine material to provide protection against damage to the pad by boulders cascading down the slope of the high dump. Recovery of leaching solutions from the dumps constructed on this impervious pad has been very high.

The leach dumps at the Weed Heights, Nev., operation of The Anaconda Company were placed on a dry lakebed after the lakebed had been leveled by bulldozer and compacted by sheepsfoot rollers.

Method of Dump Emplacement

Leach material, in most operations, is hauled from the open-pit mines to the dumps by truck trains. Bulldozers are used to level the surfaces and slopes of the dumps. Large dumps usually are raised in lifts of 50 to 100 feet (fig. 5), [illegible] to keep haulage minimal with respect to both grade of ascent and distance of haul and to form a porous dump favorable for percolation of leaching solutions.

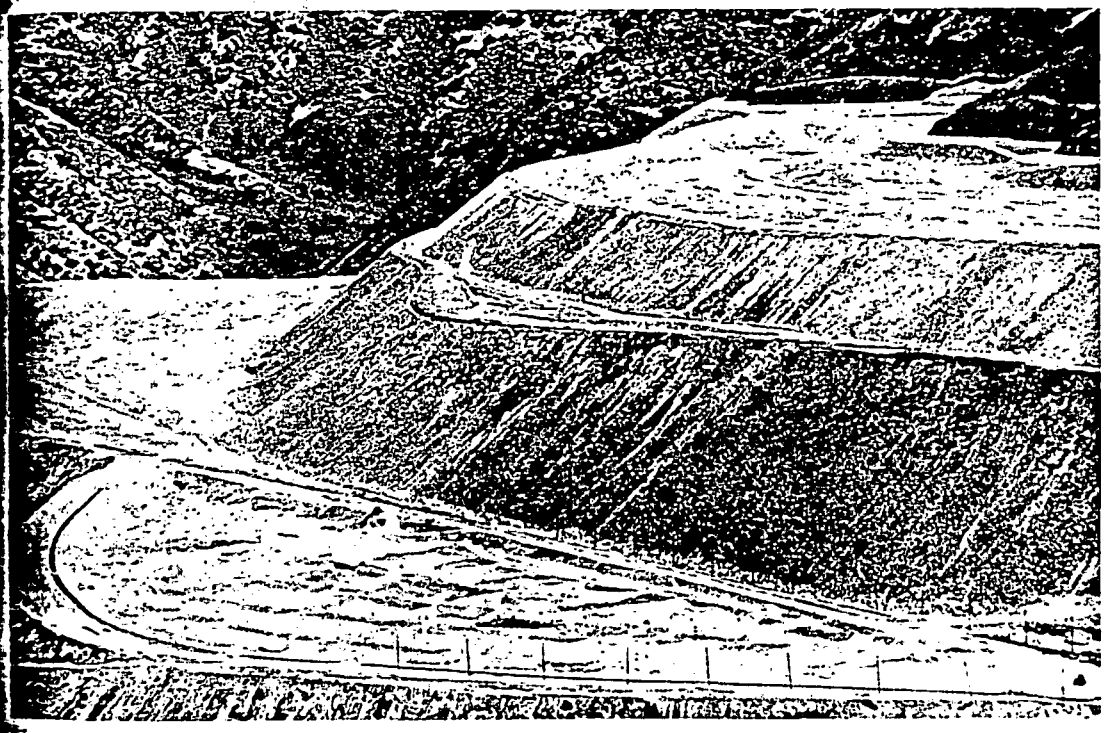

FIGURE 7. - Leach Dump at Bingham Canyon Mine, Kennecott Copper Corp.
(Courtesy, Don Green, Photographer, Kennecott Research Center, Salt Lake City, Utah.)

Physical Nature of Dumps

Size of Leach Material

The majority of the material currently placed on leach dumps is run-of-mine material that has been loaded by power shovels as part of the normal mining operation. The leach material therefore includes boulders as large as several feet in diameter and weighing many tons; however, most of the material is less than 2 feet in diameter and includes many fine particle sizes. Leach material being placed on dumps at present generally is smaller in size than that placed on dumps in the past. The reduction in size is chiefly the result of improved blasting techniques which provide better rock fragmentation.

Geometry and Volume of Dumps

The shape of most leach dumps is that of a truncated cone. This configuration is developed by the method of dump emplacement used in most operations. The leach material forms a slope having an angle of repose peculiar to the type and size of material.

The tonnage of the major leach dumps in the Western States varies approximately from 5.5 million tons at the Mineral Park, Ariz., operation of the Duval Corp., to 4 billion tons at the Bingham Canyon, Utah, operation of Kennecott Copper Corp. More complete figures on the tonnage and geometry of leach dumps together with other pertinent data concerning leaching and precipitation are given in table 1.

Company	Source materials: Host rock	Source materials: Principal copper minerals	Source materials: Minor copper minerals	Type of leaching	Quantity 1,000 tons (est.)	Geometry: Area, 1,000 sq ft	Geometry: Maximum height, ft
American Smelting and Refining Co., Silver Bell unit, Silver Bell, Ariz.	Alaskite, dacite porphyry, monzonite.	Chalcocite and chrysocolla.	Chalcopyrite, azurite, malachite, cuprite.	Dump.....	[1]30,000	5,650	200
The Anaconda Company:							
Butte, Mont.....	Quartz monzonite.....	Chalcocite.....	Chalcopyrite, bornite, azurite, malachite.		10,000	390	195
				....do....	[5]23,000	{860 400	175 50
Yerington mine, Weed Heights, Nev.	.....do.....	Chrysocolla.....	Tenorite, malachite, cuprite, azurite.	Dump and vat.[10]	30,000	20	165
Bagdad Copper Corp., Bagdad, Ariz.	Monzonite porphyry....	Chrysocolla, malachite, azurite.	Tenorite and cuprite....	Dump.....	[1]40,000	2,390	240
Duval Corp.:							
Esperanza mine, Sahuarita, Ariz.	Quartz monzonite, rhyolite flows, quartz diorite.	Chalcocite, some chalcopyrite.	Cuprite, malachite, azurite, tenorite.	....do....	19,000	830	220
Mineral Park, Ariz.....	Quartz porphyry and quartz monzonite.	Chalcocite.....	Chalcopyrite, covellite, turquoise.	....do....	[1]5,500	340	250
Inspiration Consolidated Copper Co., Inspiration, Ariz.	Schist and granite porphyry.	Chrysocolla, azurite, malachite.	Chalcocite and chalcopyrite.	Dump, inplace, vat.[10]	30,000	750	200
Kennecott Copper Corp.:							
Utah Copper Division, Bingham Canyon, Utah.	Quartz monzonite.....	Chalcopyrite.....	Chalcocite, covellite, bornite; oxide copper minerals 0.05-0.07 pct.	Dump.....	[16]4,000,000	31,000	1,200
Chino Mines Division, Santa Rita, N. Mex.	Granodiorite porphyry.	Chalcocite.....	Chalcopyrite and nonsulfide copper minerals.	....do....	425,000	28,000	300
Ray Mines Division, Ray, Ariz.	Schist and diabase....	.....do.....	Cuprite, native copper, chalcopyrite, chrysocolla, azurite, malachite.		94,000	12,000	125
				Dump and inplace.	31,000	2,000	80
					44,000	6,000	85
					[24]17,500	NA	NA
Miami Copper Co., Miami, Ariz.:							
Castle Dome unit.....	Quartz monzonite and granite porphyry.	Chalcopyrite and chalcocite.	Covellite, cuprite, azurite, malachite, chalcanthite, turquoise.	Dump.....	48,000	NA	NA
Copper Cities unit.....	Quartz monzonite.....	.....do.....	Covellite, turquoise, malachite, azurite.	....do....	NA	NA	150
Miami unit.....	Schist and granite porphyry.	Chalcocite.....	Chalcopyrite, bornite, covellite, malachite, azurite, chrysocolla, cuprite, native copper.	Inplace...	NA	([20])	NA
Phelps Dodge Corp.:							
Bisbee, Ariz.....	Quartz monzonite and conglomerate.	Chalcocite, some azurite and malachite.	Some bornite and turquoise.	Dump.....	47,000	3,850	170
Morenci, Ariz.....	Quartz monzonite porphyry.	Chalcocite.....	Chalcopyrite, covellite, oxide minerals.	....do....	NA	NA	NA
Ranchers Exploration and Development Corp., Bluebird mine, Miami, Ariz.	Granite porphyry.....	Malachite and azurite	None.....	Heap.....	500	100	80
J. H. Trigg Co., Tyrone, N. Mex.:							
Property No. 1.....	Quartz monzonite.....	Chrysocolla and azurite.	Malachite and tenorite.	....do....	150	20	75
Property No. 2.....	.....do.....	Malachite.....	Chrysocolla and azurite.				
Zontelli Western Mining Co., Page, Ariz.	Sandstone.....	Malachite, azurite, chrysocolla.	Some chalcocite.....	....do....	100	30	40
				....do....	500	300	40

NA--Not available.
[1]In 2 dumps.
[2]Sloping.
[3]Launder tailing solution.
[4]Barren solution sent to dumps.
[5]Main dump is divided into high and low dump sections.
[6]July and August.
[7]January and February.
[8]March.
[9]6 parallel rows of launders, 5 cells per row.
[10]Data presented in table do not a
[11]Double cells.
[12]Approximately 2.5 pounds of acid
[13]Maximum.
[14]December 1963.
[15]4-compartment cells; cell dimen
[16]Chiefly in East Dump.
[17]Present.
[18]Future.

TABLE 1. - Data from copper leaching and precipita operations in the Western United States

ty ons)	Leach material: Geometry: Area, 1,000 sq ft	Geometry: Maximum height, ft	Ground preparation	Method of emplacement	Leach solutions: Method of introduction of leach solutions	H_2SO_4 addition, gpl	Flow rate to dumps, gpm	Influent: pH	Influent: Copper content, gpl	Influent: Temperature, °F	
000	5,650	200	Leach material is deposited on the existing topography.	Leach material is hauled and dumped by trucks. Edges and surfaces of dumps are leveled by bulldozer.	Ponding and trenching	None	1,000	3.4	<0.01	NA	
000	390	195	The main dump is underlain by an impervious pad. See complete description in body of report under ground preparation for dump emplacement.	....do....	Solutions introduced through perforated plastic pipes spaced 100 ft apart on grid.	0.1	5,000	1.9	.11	85	2
000	{860 {400	175 50									
000	20	165	The leach dumps have been deposited on a dry lake bed which was leveled by bulldozer and compacted by sheepsfoot rollers.	....do....	Spraying.....	7.0-8.0	4,000	1.2-1.3	.08	60	
000	2,390	240	Leach material is deposited on the existing topography.	....do....	.....do.....	([12])	3,300	1.4-1.6	.02	70	2
000	830	220	.....do.....	.....do.....	.....do.....	.4	[13]1,600	2.5	<.01	[14]46	2.
500	340	250	.....do.....	.....do.....	.....do.....	None	750	3.5	<.01	NA	
000	750	200	.....do.....	.....do.....	Spraying, ponding, and trenching.	2.0	1,700	2.6-3.0	.10	NA	>
000	31,000	1,200	.....do.....	Leach material is hauled and dumped by trucks and train. Edges and surfaces of dumps are leveled by bulldozer.	Solutions introduced into strips or channels.	.1	{[17]8,000-10,000 [18]35,000	2.8-3.0	.12-.18	92-94	
00	28,000	300	.....do.....	.....do.....	Ponding and trenching	Varies	13,000-15,000	3.5	.08-.36	70-78	
00	12,000	125		Leach material is hauled and dumped by trucks. Edges and surfaces of dumps are leveled by bulldozer.	Ponding.....	Small amounts.	7,000	2.5-3.8	<.06	73-85	2.
00	2,000	80	.....do.....								
00	6,000	85									
00	NA	NA									
00	NA	NA	.....do.....	.....do.....	Spraying and ponding.	None	NA	2.7	.04-.32	NA	2
	NA	150	.....do.....	.....do.....	Spraying.....	.4	1,800	2.6	.01	73-74	2
	([26])	NA	Surface topography on which solutions are introduced is a depression resulting from block-caving operations beneath.	Copper minerals remain in block-caved stopes, pillars, and capping.	Spraying of surface above block-caved areas	4.0	2,000	1.4	.02	NA	2
0	3,850	170	Leach material is deposited on the existing topography.	Leach material is hauled and dumped by trucks. Edges and surfaces of dumps are leveled by bulldozer.	Ponding.....	None	2,300	2.8-3.1	.03-.07	[27]90-95	2.0
	NA	NA	Strip material is sometimes deposited on preexisting dumps that were deposited on the existing topography.	Leach material is hauled and dumped by side-dump railroad cars.	.....do.....	None	{[17]300 [18]5,000	3.8-4.2	.01-.02	NA	2.8-
	100	80	Ground is dressed, soil is cemented and covered with diluted tar for curing and sealing purposes.	Leach material is hauled by bottom-dump scrapers to the heaps. Motor grader levels the heap area.	Percolated through plastic pipes spaced 8 ft apart on surface of the heaps.	{[28]50.0 {[29]20.0	([30])	2.5	{[31].00 {[32]3.00	[33]50	1.4-
	20	75	Leach material is deposited on the existing topography.	Blasted material is loaded by scoopers into dumpsters. The dumpsters unload the material on a pile. Bulldozer levels the dump material.	Ponding.....	1.7-1.8	1,000	2.2	.18	40-60	3.0-
	30	40	.....do.....	.....do.....							
	300	40	A special pad is prepared. See complete description in body of report under ground preparation for dump emplacement.	Leach material is hauled and dumped by trucks. The surfaces of the heaps are leveled by bulldozer.	NA Ponding.....	NA ([35])	NA NA	NA NA	NA .10	NA [7]38	NA NA

ented in table do not apply to vat leaching. See descriptions of vat leaching in text.
lls.
tely 2.5 pounds of acid per pound of copper precipitated.

1963.
ment cells; cell dimensions are for each compartment.
n East Dump.

[12]4 parallel rows of launders, 12 cells per row.
[30]Cone precipitators. Dimensions, 14 ft diam by 24 ft deep.
[31]April through September.
[32]October through March.
[33]Cone precipitators. Dimensions, 18 ft diam by 34 ft deep.
[34]Total for other 3 dumps.
[35]6 units of 4 to 6 pairs of cells.
[36]Block-caved stopes, pillars, and capping.
[37]Summer.

n United States

H_2SO_4 addition, gpl	Flow rate to dumps, gpm	Leach solutions: Influent pH	Influent Copper content, gpl	Influent Temperature, ° F	Effluent pH	Effluent Copper content, gpl	Effluent Temperature, ° F	Area seasonal temperature, ° F: Summer	Area seasonal temperature, ° F: Winter	Type of precipitant used	Can factor, lb Fe/lb Cu	Precipitation operation: Precipitation units: Number of cells	Cell dimensions, ft: Length	Width	Depth	Influe: Cu	Fe++	Fe+++
None	1,000	3.4	<0.01	NA	2.4-2.8	1.09	NA	85-95	50-60	Burned, shredded tin cans.	1.6-2.0	10	12	8	[2]6-1/2-11-1/2	1.09	0.01	0.5
0.1	5,000	1.9	.11	85	2.2-2.3	.80-1.00	67	[6]80-90	[7]20 [8]20-45	Burned, compacted tin cans.	1.5	[9]30	100	8-1/2	2-1/2	.87	.09	.4
7.0-8.0	4,000	1.2-1.3	.08	60	1.9	1.20	55	80	53	Burned, shredded tin cans and discarded clippings from can manufacture.	1.3	[11]20	60	20	4	1.20-1.30	.00	1.0
([12])	3,300	1.4-1.6	.02	70	2.1-2.4	1.18	70	95	35	Mine scrap and burned, shredded tin cans.	1.8	22	10	10	6	1.00-1.25	.09	2.0
.4	[13]1,600	2.5	<.01	[14]46	2.3-3.3	1.32-1.56	[14]63	70-85	45-55	Burned, shredded tin cans.	1.4	[15]12	12	4	[2]5-10	1.60	<.10	.2
None	750	3.5	<.01	NA	2.4	1.24	NA	75	40	.....do.....	1.4	[16]12	12	5	10	1.24	.01	.4
2.0	1,700	2.6-3.0	.10	NA	>2.0	1.10	NA	100-102	50-60	.....do.....	1.2-1.3	[11]4	60	20	5	1.50	.56	.4
.1	[17]8,000-10,000 [18]35,000	2.8-3.0	.12-.18	92-94	2.5	1.80	110-125	75-85	20-25	Burned, shredded tin cans. Shredded clippings	2.5 1.5-1.8	[19]48 [20]26	80 ([20])	4 ([20])	4 ([20])	1.80 1.80	3.36 3.36	1.4 1.4
Varies	13,000-15,000	3.5	.08-.36	70-78	2.5	1.40	90-95	[21]66	[22]43	Detinned scrap (tin cans, light trimmings and punchings, some shreadded auto bodies).	1.0-1.8	[23]30 [23]4	40 ([23])	5 ([23])	4 ([23])	1.32-2.16	NA	.05 1.0
Small amounts.	7,000	2.5-3.8	<.06	73-85	2.1-3.0	.90	73-100	85-95	50-60	Clippings discarded from can production. Some burned, shredded tin cans.	1.7-1.8	[25]48-72	40	5	5	.90	<.05	.3 .6
None	NA	2.7	.04-.32	NA	2.3	.85	NA	85-95	50-60	Burned, shredded tin cans.	1.8	5	52	10	4-1/4	.85	.02	1.(
.4	1,800	2.6	.01	73-74	2.5	.75-2.25	73-80	85-95	50-60	.....do.....	1.5	24	27	4-1/2	3	.75-2.25	.02	.
4.0	2,000	1.4	.02	NA	2.4	1.75-2.00	NA	85-95	50-60	.....do.....	1.4	24	27	4-1/2	3	2.14	1.15	1.(
None	2,300	2.8-3.1	.03-.07	[27]90-95	2.0-2.2	.96-1.80	[27]100	85-95	50-60	Burned, shredded cans. Sponge iron from Douglas smelter. Heavy scrap.	2.5	24	25	8	[2]3-10	1.32	3.60	3.
None	[17]300 [18]5,000	3.8-4.2	.01-.02	NA	2.8-3.2	1.00-3.60	NA	75-85	40-50	Burned, shredded tin cans, heavy scrap, and turnings from shop.	1.3	4	20	20	3	NA	.01	.
[28]50.0 [29]20.0	([30])	2.5	[31].00 [32]3.00	50	1.4-2.8	2.00-8.00	70-85	85-95	50-60	Burned, shredded tin cans, baling wire, shredded car bodies being evaluated.	1.5-1.7	Several	30	3-1/2	8	3.00-7.00	NA	N
1.7-1.8	1,000	2.2	.18	40-60	3.0-3.5	1.80	40-60	64-95	23-54	Burned, shredded tin cans.	1.5-2.0	4	35	5	4-1/2	1.80	.60-1.80	.
NA ([33])	NA NA	NA NA	NA .10	NA [7]38	NA NA	NA 1.00	NA [7]45	NA 84-88	NA 33-37	.....do..... Scrap iron and scrap tin cans.	NA 1.3	NA 13	NA 28	NA 4	NA 8	NA 1.00	NA NA	

launders, 12 cells per row.
. Dimensions, 14 ft diam by 24 ft deep.
ember.
rch.
. Dimensions, 18 ft diam by 34 ft deep.
dumps.
pairs of cells.
, pillars, and capping.

[28] Initial.
[29] Minimum.
[30] Each needle valve, 2 ft apart along the pipes, feeds at rate of 180 cu cm/mi
[31] Fresh water.
[32] Recirculated solutions.
[33] From 6.5 to 7.0 pounds of acid per pound of copper precipitated.

	Area seasonal temperature, ° F		Type of precipitant used	Can factor, lb Fe/lb Cu	Precipitation operation: Precipitation units: Number of cells	Cell dimensions, ft: Length	Width	Depth	Analyses of solutions, gpl: Influent: Cu	Fe^{++}	Fe^{+++}	Free acid	pH	Effluent: Cu	Fe^{++}	Fe^{+++}	Free acid	pH
ra- ° F	Summer	Winter																
A	85-95	50-60	Burned, shredded tin cans.	1.6-2.0	10	12	8	[2]6-1/2-11-1/2	1.09	0.01	0.57	0.60	2.3	[30]0.01 [4].01	2.08 1.67	Trace 0.04	0.08 .06	3.6 3.3
7	[6]80-90	[7]20 [8]20-45	Burned, compacted tin cans.	1.5	[9]30	100	8-1/2	2-1/2	.87	.09	.41	NA	2.3	.02	1.50	.05	NA	2.8
5	80	53	Burned, shredded tin cans and discarded clippings from can manufacture.	1.3	[11]20	60	20	4	1.20-1.30	.00	1.00	3.90	1.9	.08	1.30-1.40	.00-.20	1.50	3.0
0	95	35	Mine scrap and burned, shredded tin cans.	1.8	22	10	10	6	1.00-1.25	.09	2.00	1.50-2.50	<2.0	.02	3.80-3.90	.10-.20	NA	2.4
3	70-85	45-55	Burned, shredded tin cans.	1.4	[15]12	12	4	[2]5-10	1.60	<.10	.20	NA	2.6	<.01	1.90	Trace	NA	3.9
A	75	40	.....do.....	1.4	[16]12	12	5	10	1.24	.01	.47	NA	2.3	<.01	2.45	.01	NA	3.7
A	100-102	50-60	.....do.....	1.2-1.3	[11]4	60	20	5	1.50	.56	.46	1.00	NA	.01	3.30	Trace	Trace	3.5
125	75-85	20-25	Burned, shredded tin cans.	2.5	[19]48	80	4	4	1.80	3.36	1.44	NA	2.5	.12-.18	8.39	.00	NA	3.5-3.8
			Shredded clippings	1.5-1.8	[20]26	([20])	([20])	([20])	1.80	3.36	1.44	NA	2.5	.02-.05	7.00	.00	NA	2.9-3.0
95	[21]66	[22]43	Detinned scrap (tin cans, light trimmings and punchings, some shredded auto bodies).	1.0-1.8	[30] [33]4	40 ([23])	5 ([23])	4 ([23])	1.32-2.16	NA	.05-1.08	.04-.84	2.5	.08-.36	NA	.06-.24	.08-.22	NA
100	85-95	50-60	Clippings discarded from can production. Some burned, shredded tin cans.	1.7-1.8	[25]48-72	40	5	5	.90	<.05	.36-.60	NA	1.5-3.0	.06	2.16	.00	NA	3.0-3.8
A	85-95	50-60	Burned, shredded tin cans.	1.8	5	52	10	4-1/4	.85	.02	1.06	.15	2.3	[3].02 [4].07	2.20 1.26	.06 .30	Trace .05	3.0 2.7
80	85-95	50-60	.....do.....	1.5	24	27	4-1/2	3	.75-2.25	.02	.32	.25	2.5	<.01	1.02	.03	Trace	3.6
NA	85-95	50-60	.....do.....	1.4	24	27	4-1/2	3	2.14	1.15	1.05	.25	2.4	.02	4.60	.10	Trace	4.2
00	85-95	50-60	Burned, shredded cans. Sponge iron from Douglas smelter. Heavy scrap.	2.5	24	25	8	[2]3-10	1.32	3.60	3.00	NA	2.0	.03	8.77	.06	NA	3.1
NA	75-85	40-50	Burned, shredded tin cans, heavy scrap, and turnings from shop.	1.3	4	20	20	3	NA	.01	.27	NA	3.0	NA	2.01	<.01	NA	4.4
-85	85-95	50-60	Burned, shredded tin cans, baling wire, shredded car bodies being evaluated.	1.5-1.7	Several	30	3-1/2	8	3.00-7.00	NA	NA	NA	1.4-2.8	NA	NA	NA	NA	NA
-60	64-95	23-54	Burned, shredded tin cans.	1.5-2.0	4	35	5	4-1/2	1.80	.60-1.80	.24-.72	.30	3.0-3.5	.12	2.40	.06	.06	NA
NA 45	NA 84-88	NA 33-37	.....do..... Scrap iron and scrap tin cans.	NA 1.3	NA 13	NA 28	NA 4	NA 8	NA 1.00	NA NA	NA NA	NA 7.50	NA NA	NA .10	NA NA	NA NA	NA 6.80	NA NA

[28] Initial.
[29] Minimum.
[30] Each needle valve, 2 ft apart along the pipes, feeds at rate of 180 cu cm/min.
[31] Fresh water.
[32] Recirculated solutions.
[33] From 6.5 to 7.0 pounds of acid per pound of copper precipitated.

Settling of Dumps

Most leach dumps settle after the leach solutions have been introduced because (1) the percolating solutions tend to transport the finer particles t the voids between larger particles and thereby compact the dump as a whole, (2) the total weight of the dump is increased by the weight of the solutions which causes a downward compression of the dump, and (3) the dissolution and disintegration of minerals in the dump causes the dump to settle.

Leaching Operation

The leaching operation comprises the introduction of a sulfuric acid sol tion containing varying amounts of ferrous and ferric sulfate onto the surfac or into the interior of the dumps for the purpose of effecting the dissolutio of copper minerals. The end product of the leaching operation is a pregnant liquor containing copper in the form of copper sulfate.

Leach Solution

Most companies recirculate the tailing solutions from their precipitati operations (fig. 8) along with makeup water and concentrated sulfuric acid to be used as the leach solution. Analyses of tailing solutions from various operations are given in table 1. Makeup water is added to replenish the wat lost by evaporation or seepage during leaching. Sulfuric acid is added to lower the pH of the leach solution generally to the range of 1.5 to 3.0. The reasons for maintaining this pH are (1) to have adequate acid for dissolution of the copper minerals, (2) to prevent the destruction of bacteria in the dumps, and (3) to minimize the hydrolyzation and precipitation of iron and other metals in pipelines and on the surfaces or in the interior of the dump

Water added to the leach solution comes from several sources, such as wells, springs, underground mines, or streams. Polluted stream waters from nearby towns are sometimes used; however, the organic material contained in sewage waters is thought to be a deterrent to bacterial activity and therefor is not used in many leach circuits.

The sulfuric acid used in most of the larger leaching operations is pro duced and supplied by the operating company. In smaller operations the acid is obtained from commercial suppliers. The development of contact sulfuric acid plants coupled with a constant supply of high-grade sulfur has simplifi the manufacture of sulfuric acid. A typical example of a contact sulfuric acid plant is the Bagdad Copper Corp. facility, Bagdad, Ariz. (fig. 9), located adjacent to the company's precipitation plant. A thorough descriptio of this semiautomatically controlled acid plant has been given by Bogart (11)

Methods of Solution Introduction

Leach solutions are introduced onto or into dumps by means of spraying, flooding, or vertical pipes. The method chosen for a given operation is base on careful consideration and knowledge of climatic conditions, dump height,

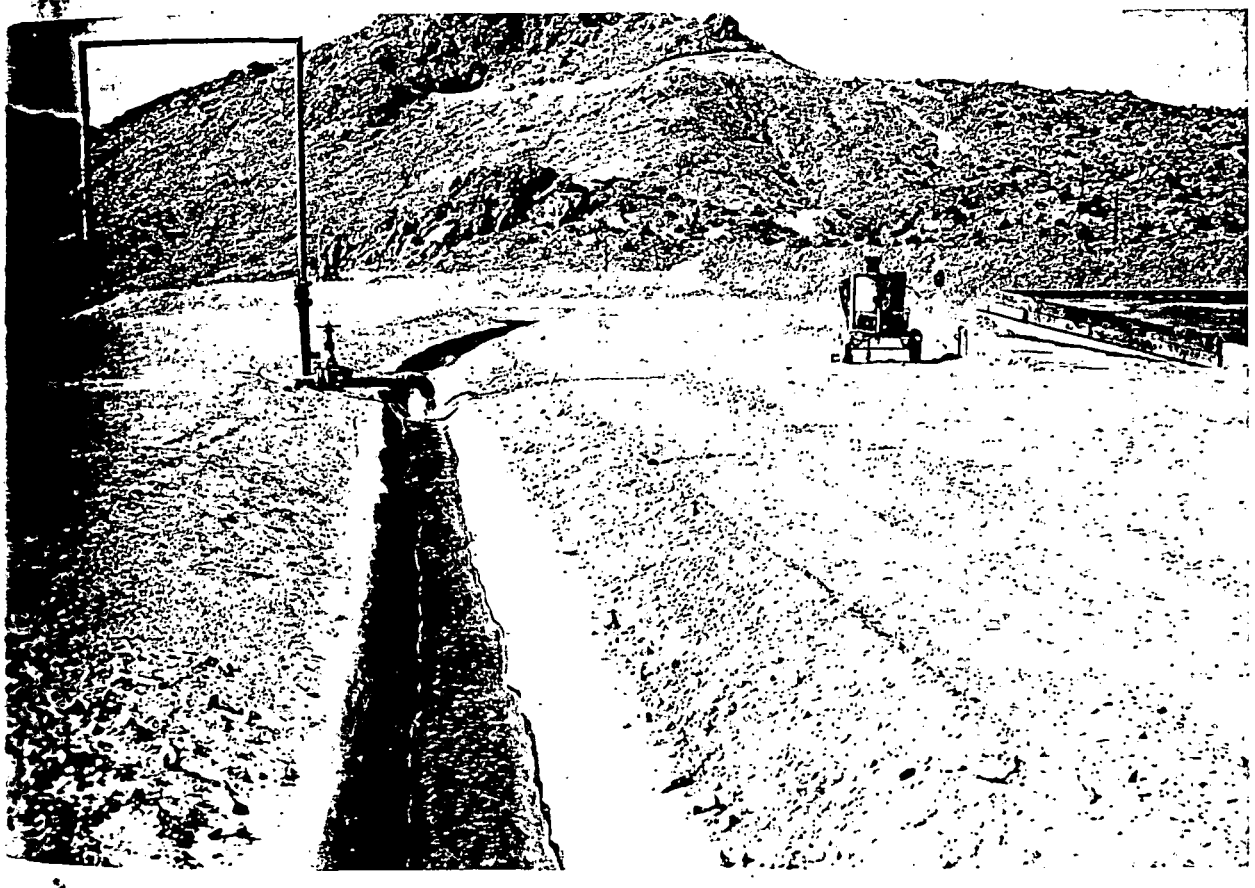

FIGURE 8. - Makeup Water Addition to Tailing Solution From Mineral Park Precipitation Plant, Duval Corp.

surface area, mineralogy, scale of operation, and size of leach material. Brief descriptions of each method, with examples, are presented in paragraphs that follow.

Spraying.--Leach solutions at the different operations are introduced into the dumps by various methods of spraying. The advantage of spraying is that it provides a uniform distribution of the leach solutions over the surface area of the dumps. The principal disadvantage of this method is the evaporation loss which in arid regions may range up to 60 percent.

The commonest spraying method involves the use of perforated plastic pipes. The Inspiration Consolidated Copper Co., Inspiration, Ariz. (fig. 10), and The Anaconda Company at Weed Heights, Nev. (fig. 11), use this method. The solutions are pumped to the surface of the dumps through 8- to 12-inch cement-asbestos, plastic-lined pipelines and are carried from the main distributing lines in 2- to 4-inch perforated plastic pipes. The pressure created in the pipelines causes the leach solutions to be discharged through the perforations in the form of a spray. Height and distance of coverage of the sprays are functions of the pipeline pressures.

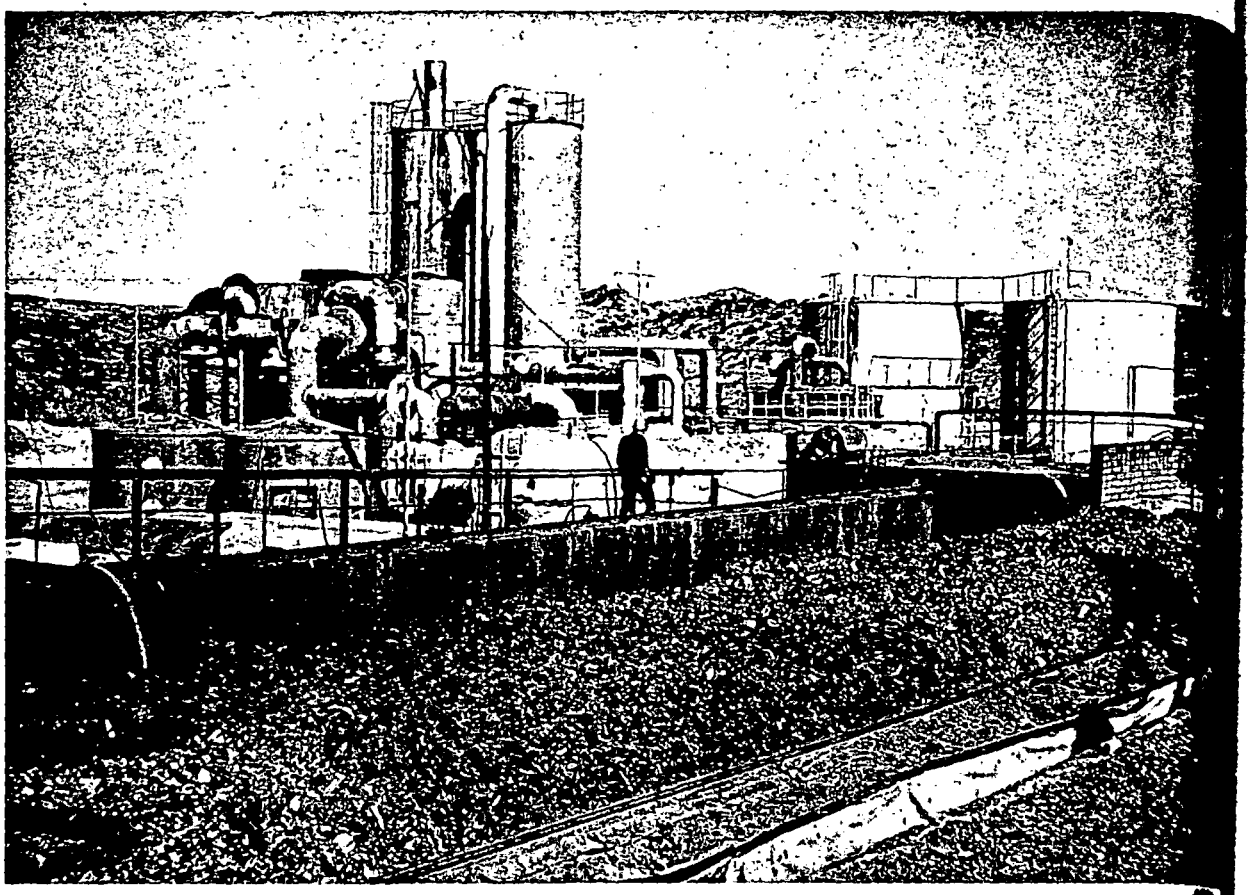

FIGURE 9. - Sulfuric Acid Plant Adjacent to Precipitation Plant, Bagdad Copper Corp.

Metal or plastic sprinkler heads available commercially are used at the Esperanza operation of Duval Corp., Sahuarita, Ariz., to distribute the leach solutions in an overlapping circular pattern (fig. 12). The size of the water droplets determines the amount of evaporation to be expected. The larger the droplets in the spray, the less the amount of evaporation.

Bagdad Copper Corp. has experimented with and is using a form of sprinkler head made of surgical tubing. The tubings are attached to reducers at the end of the plastic pipes that carry the leach solution from the main distributing lines to the surface of the dump. The tubing is very pliable and reacts vigorously to the solution flow. A nominal length (about 18 inches) is used to impart a random oscillating motion to the tubing whereby a circular pattern of spray coverage is created (fig. 13).

Spraying methods also are used to distribute leach solutions over the slope portions of dumps that are being leached by flooding methods. Lengths of small-diameter plastic pipe are placed on the slope area from the top to the base of the dumps. Proper coverage of the slope area is extremely difficult because the solutions tend to form channels down the slope and rapidly flow from the slopes without penetrating the surface. Large tonnages of material in the slope area therefore are not contacted by the leach solutions.

FIGURE 10. - Spraying of Leach Solution on Dump, Inspiration Consolidated Copper Co. The white spray rises from the dark-brown perforated plastic pipes laid on the light-tan leach dump.

Flooding.--Leach solutions are introduced onto the surfaces of dumps by flooding or ponding by forming furrows, ditches, ponds, or channels on the surfaces of the dumps by bulldozer or front-end loaders. The leach solutions are channeled into these conduits and allowed to build up to a certain depth in order to create a substantial flow of solution onto the dumps. Several companies use this method of solution introduction; for example, the Silver Bell, Ariz., operation of American Smelting and Refining Co. (fig. 14). Selected areas of the dump surface are saturated for a specified period, followed by a period with no solution addition. In actual practice, a section of a dump is flooded with leach solution until such time as the copper content of the pregnant liquor obtained from that section falls below a predetermined percentage. The flooding then is discontinued on that section and begun on another. Hudson and Van Arsdale (40) and Van Arsdale (83, pp. 77-78) state that alternating periods of wetting and drying of leach dumps produces the most efficient dissolution and removal of copper from the leach material.

Benches or furrows made by bulldozers on the slopes of the leach dumps are used in conjunction with sprays at the Castle Dome operation of Miami Copper Co., Miami, Ariz. The leach solution is ponded in the furrows and allowed to percolate through the slope area in an attempt to increase distribution throughout the slope area.

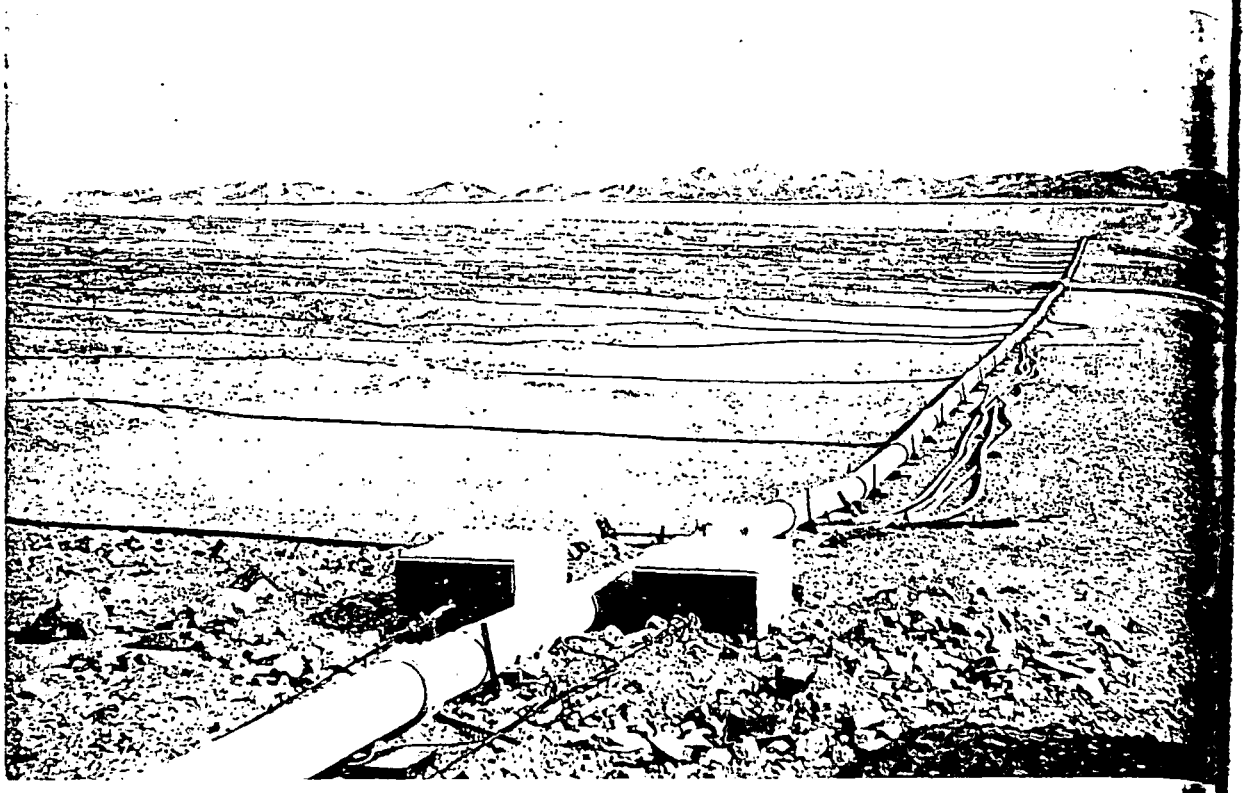

FIGURE 11. - Plastic Pipe Layout Used to Distribute Leach Solution on Dump at the Wes Heights Operation, The Anaconda Company.

Vertical Pipes.--The newest method of solution introduction is that pr ticed at the Butte, Mont., operation of The Anaconda Company. The leach so tion is introduced through perforated plastic pipes into the interior of th dumps (fig. 15). Six-inch churn-drill holes are drilled at the intersectio of a 100-foot grid pattern and cased to a depth of about two-thirds the du height. A 4-inch perforated plastic pipe is then placed inside the casing over the entire depth of each hole. The casing is then removed. The spaci of the churn-drill holes has varied from a 100-foot grid pattern to a 50- 25-foot pattern. Leach solution flows to the dump area from solution reser voirs at a higher elevation. Ditches are provided along the grid lines to permit the solution to flow into the top of the plastic pipes and down the drillholes. The method promotes a thorough distribution of the leach solu and air within the dumps.

The slope areas of the high dump at the Butte operation are also wett with leach solutions through cased churn-drill holes that have been drille side-slope roads constructed by bulldozers.

Distribution of Solutions in Dumps

One of the most important requirements in all dump leaching operatio the thorough distribution of the leach solutions throughout the dumps. To attain satisfactory recovery of the copper, the leach solutions must cont

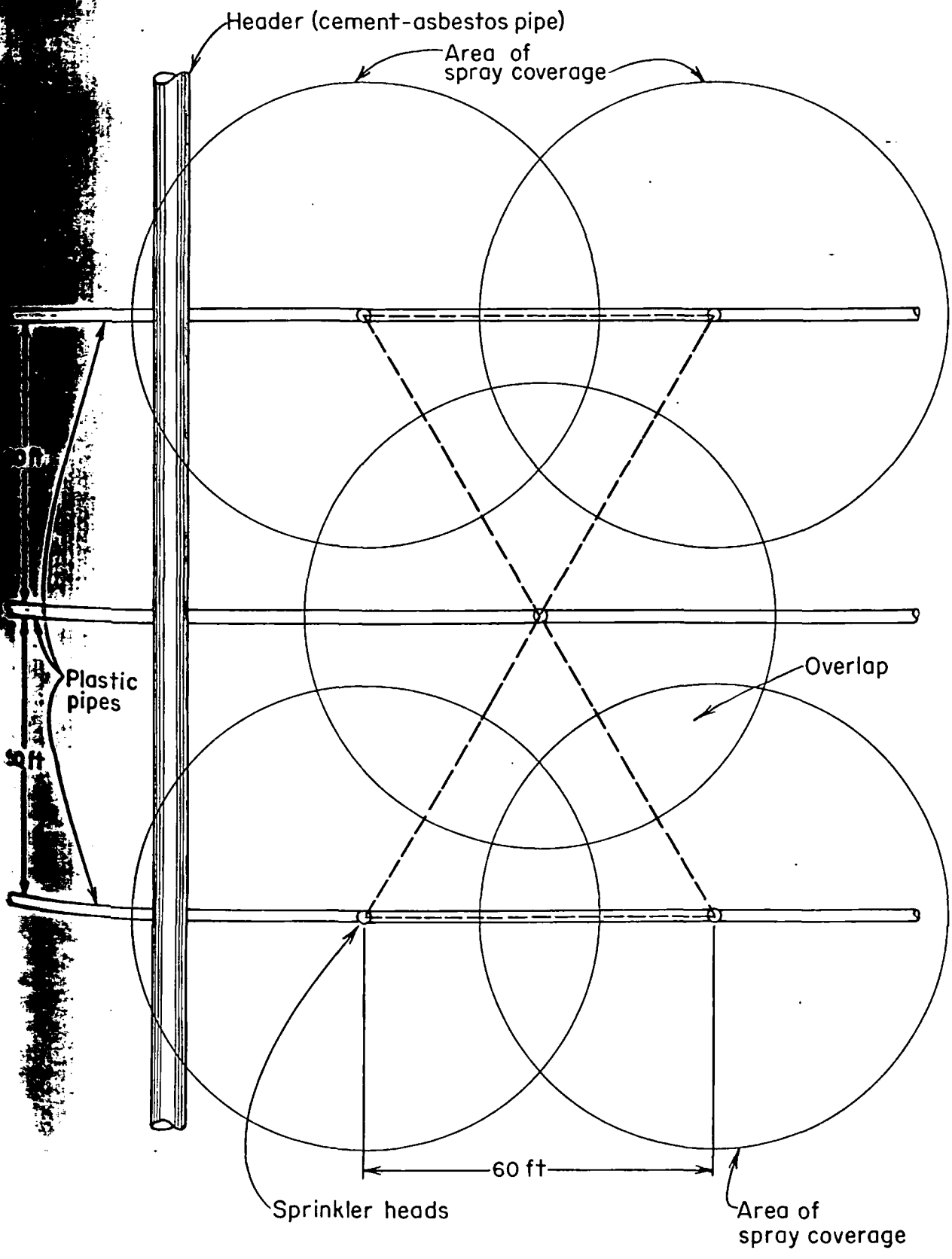

FIGURE 12. --Typical Design of Overlapping Spray System.

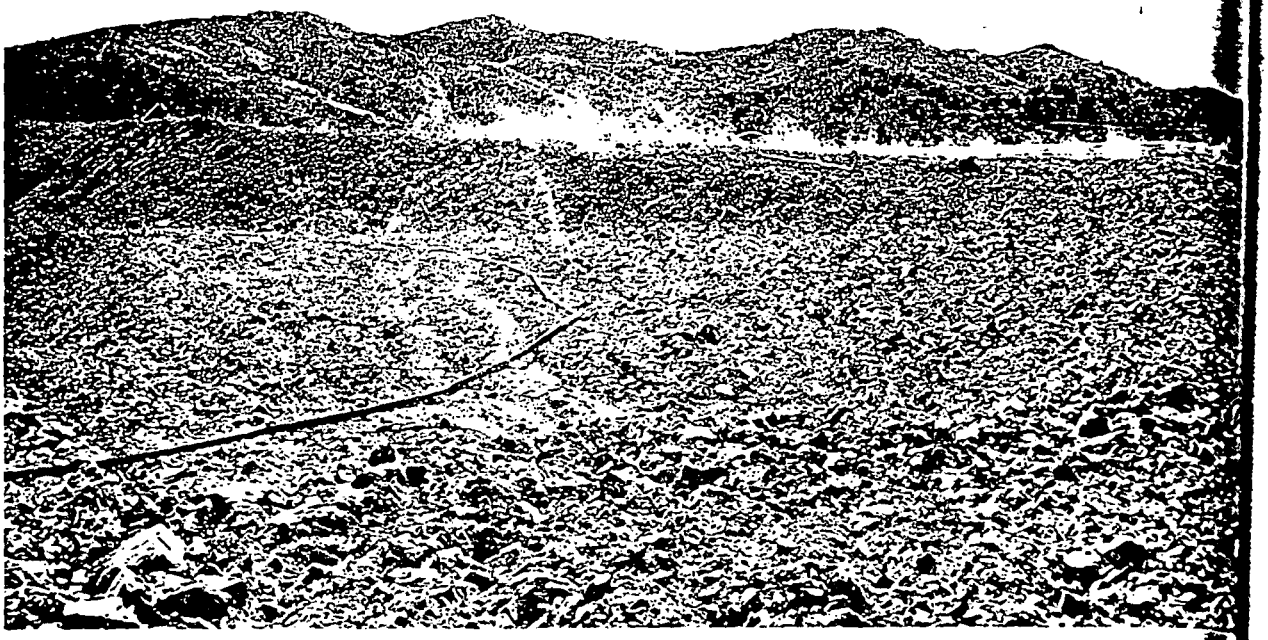

FIGURE 13. - Wiggler-Type Sprays Used by Bagdad Copper Corp.

as much of the copper-bearing material as possible. An ideal distribution will fill all existing voids within the dump. Numerous problems inherent in most leaching operations, however, prevent attaining ideal distribution.

A natural sorting of coarse and fine material is created in most dumps because many of the larger particles roll down the dump slopes as the leach material is unloaded from trucks or trains. Bulldozer leveling of many dumps creates layering while the leach dumps are constructed. The overall effect is to produce alternating layers of coarse and fine material within the dumps. The leach solutions follow courses of least resistance in penetrating the dumps. Hence, when the dumps contain layers of fine and coarse material, the solutions may travel horizontally within the dumps and discharge from the sides instead of from the base of the dumps. The problem of complete distribution of leach solutions within the dumps remains unsolved.

Temperature of Leach Solutions

The temperature of the leach solutions is an important factor that affects the rate of dissolution of copper from leach dumps. Temperatures of leach solutions introduced onto dumps varies from a low of 38° F during January and February at the Page operation of Zontelli Western Mining Co. to a high of 90° to 95° F during the summer at the Bingham Canyon operation of Kennecott Copper Corp. and the Bisbee, Ariz., operation of Phelps Dodge Corp.

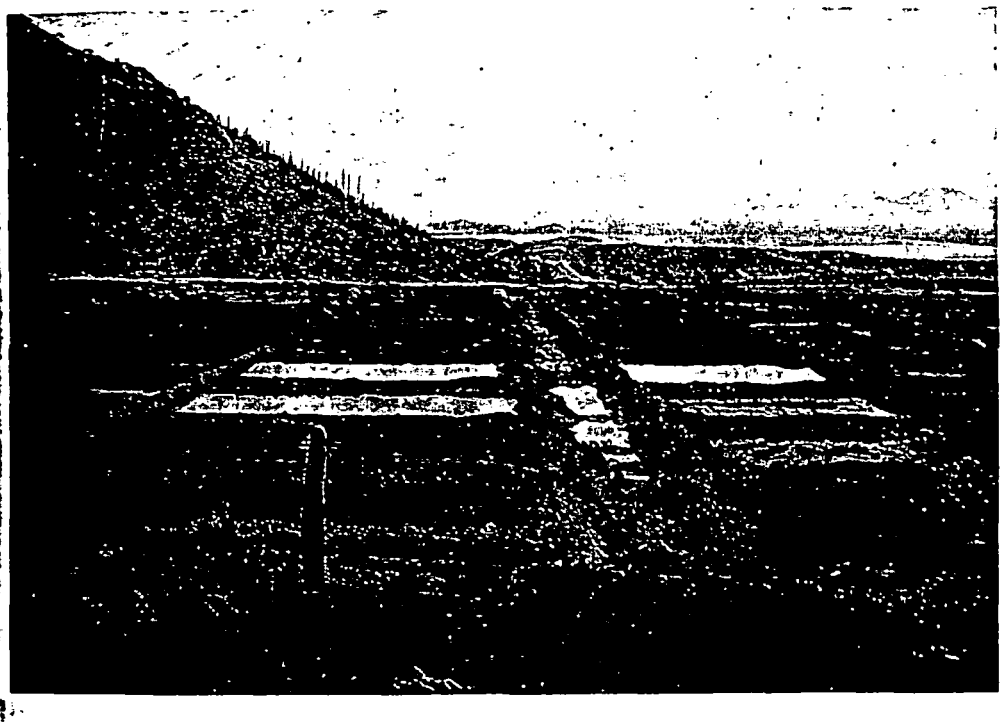

FIGURE 14. - Leach Solution Ponds on Dump at Silver Bell Operation, American Smelting and Refining Co. Light reflection from the sky masks the brown high-iron-bearing leach solutions being introduced into dump by ponding, and brown iron salt precipitate in adjacent ponds in different phases of the drying cycle is quite evident.

Temperature is one of the most important environmental factors in a microbial reaction. Corrick and Sutton (19) have shown that the optimum temperature for maximum microbial oxidation of pyrite is 35° C (95° F), and Bryner, Anderson, and Palmer (17) also have shown that 35° C is the optimum temperature for the biological oxidation of copper sulfide.

Influence of Bacteria

The role played by micro-organisms in the formation and alteration of mineral deposits is presented by Kuznetsov and coworkers (47). The importance of certain iron oxidizing bacteria during cyclic leaching processes has been described by Zimmerley and coworkers (87). The use of bacteria in leaching copper sulfide and other metallic sulfides has been investigated and described (16, 17, 19, 21, 24, 28, 43, 51, 64, 77-79). The presence of certain bacteria in the leach solutions or within the dumps promotes and accelerates oxidation of pyrite to ferric sulfate and sulfuric acid and the oxidation of copper sulfide minerals to copper sulfate. Experiments by many of the aforementioned investigators have shown that oxidation rates are accelerated by as much as 1,000 to 1. Factors mentioned by the investigators as important controls in bacterial leaching are shielding from light, thorough aeration of bacterial solutions, and high rates of solution circulation.

FIGURE 15. - Introduction of Leach Solution Through Plastic Pipes in the Dump at the Bu Leaching Operation, The Anaconda Company.

Control of Iron Salts in Solution

Probably the most troublesome problem encountered in the leaching oper tion is precipitation of iron salts in pipelines, on the surface of dumps (fig. 16), or within the dumps. These salts precipitate from solution when the pH of the solution is higher than 3.0. A pH of 2.4 is required to prev the formation of iron salts and a pH of 2.1 is required to redissolve the salts after they have been precipitated. Strict control of iron content an pH is necessary to minimize the precipitation of the iron salts.

Pipelines constricted by precipitated iron salts are cleaned with mech ical devices such as balls and chains ("pigs") or cutting tools. Precipit iron salts which have plugged the surfaces of dumps periodically are furro or scraped and pushed over the edge of the dumps. At the Silver Bell unit American Smelting and Refining Co., however, the iron precipitates (fig. 1 are not removed from the surfaces of the ponds. During the "drying-out"

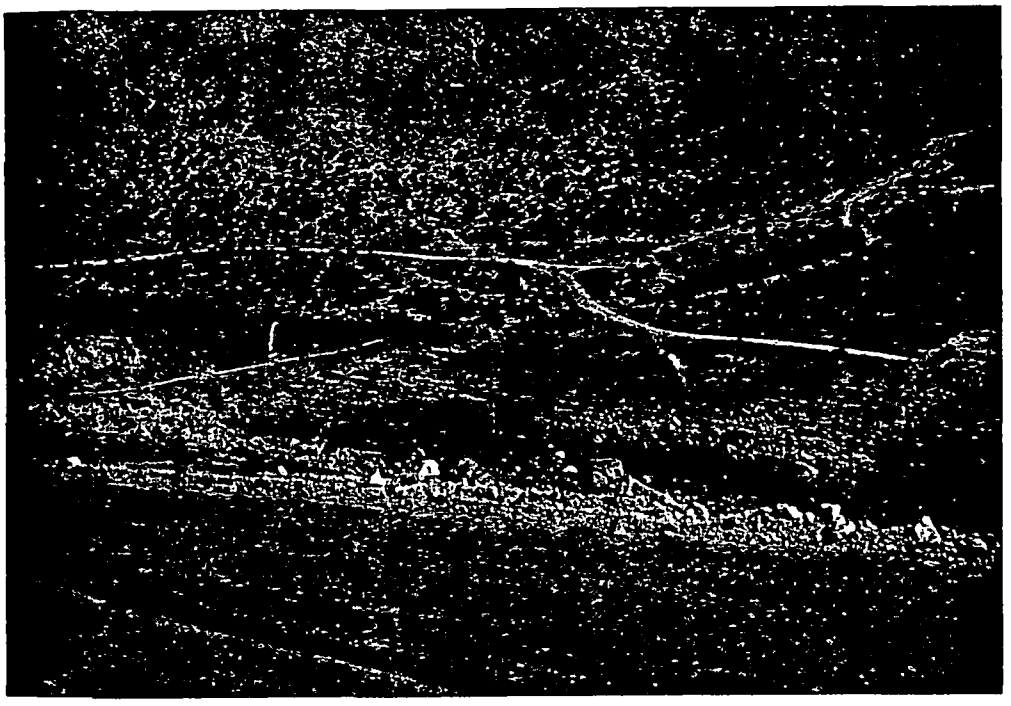

FIGURE 16. - Brown Iron Salt Formation on Surface of Leach Dump at Mineral Park Property, Duval Corp.

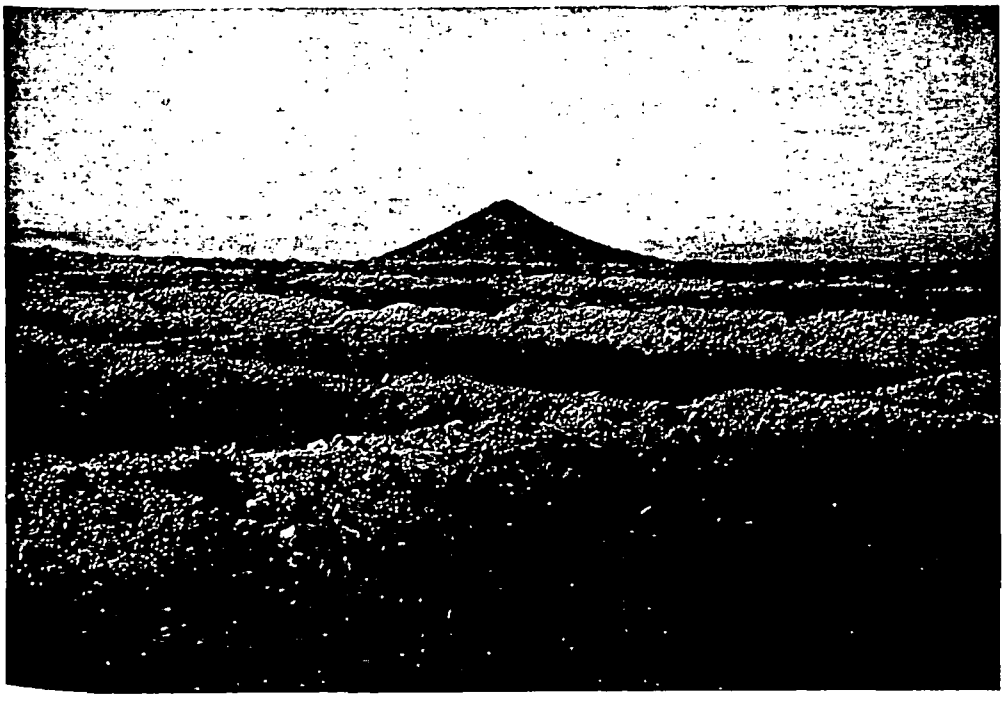

FIGURE 17. - Brown Iron Salts Precipitated on Surface of Dump, Silver Bell Operation, American Smelting and Refining Co.

period, the iron precipitates dry and crack and present only slight resistance to solution flow at the time the next flooding period is initiated.

Iron salt precipitation within the dumps is extremely difficult to overcome. The normal result of iron salt precipitation here is the formation of impervious layers which prevent movement of leach solutions within the dumps. Copper-bearing materials below the layers have no contact with leach solutions. Operating personnel of several companies (Miami Copper Co. and others) have stated that large tonnages of iron are being deposited daily within the leach dumps. The chemical reactions involved during the precipitation operation provide the major quantity of iron in the circulating solutions. Some of the iron in the pregnant liquors is derived from the dissolution of the iron-bearing minerals within the dumps.

Most operators recirculate the tailing solutions from their precipitation plants to the dumps without purification. Some companies, however, purify the solutions prior to introduction to the dump surfaces to control the iron content. At the Castle Dome operation of the Miami Copper Co., the tailing solution flows through shallow ponds and is cascaded down the banks to precipitate basic iron salts and thereby lower the iron content. The resultant solution is collected and pumped to the dumps and used as the leach solution.

Tailing solutions from the precipitation plant at the Mineral Park property of Duval Corp. and the Silver Bell operation of American Smelting and Refining Co. (fig. 18) are collected in settling ponds where some iron salts are allowed to precipitate. The brown color of the water is typical of such tailing solutions which have low copper and high iron contents. At the Silver Bell operation, the water is pumped from the pond to the leach dumps by floor-mounted pumps. A new reservoir has been constructed as part of the new leaching and precipitation plant at the Bingham Canyon operation of Kennecott Copper Corp. The reservoir will hold 500 million gallons of solution. Half of the tailing solution from the precipitation operation will be fed to this reservoir. The primary purpose of the new reservoir is to impound and provide makeup water to the leach solution distribution system. A second purpose is to allow time for oxidation of some of the iron from the ferrous state to the ferric state and thereby precipitate some of the contained iron.

Pregnant Liquor

Composition.--Chemical analyses of typical pregnant liquors from several operations (see table 1) show a wide variation in copper content, total iron, ratio of ferrous to ferric iron present, total acid, and pH. Copper content of pregnant liquors vary from 0.75 to 2.16 grams per liter. Total iron varies from 0.20 to 6.60 grams per liter. An interesting point to note when considering the iron content of the pregnant liquors is the extreme variation in the ratio of ferrous to ferric iron from one operation to another.

Temperature.--The temperature of the pregnant liquors in nearly all leaching operations is generally from 5° to 20° F higher than that of the leach solutions. A rise in temperature is to be expected because of the exothermic reactions taking place during the oxidation of sulfide minerals within the

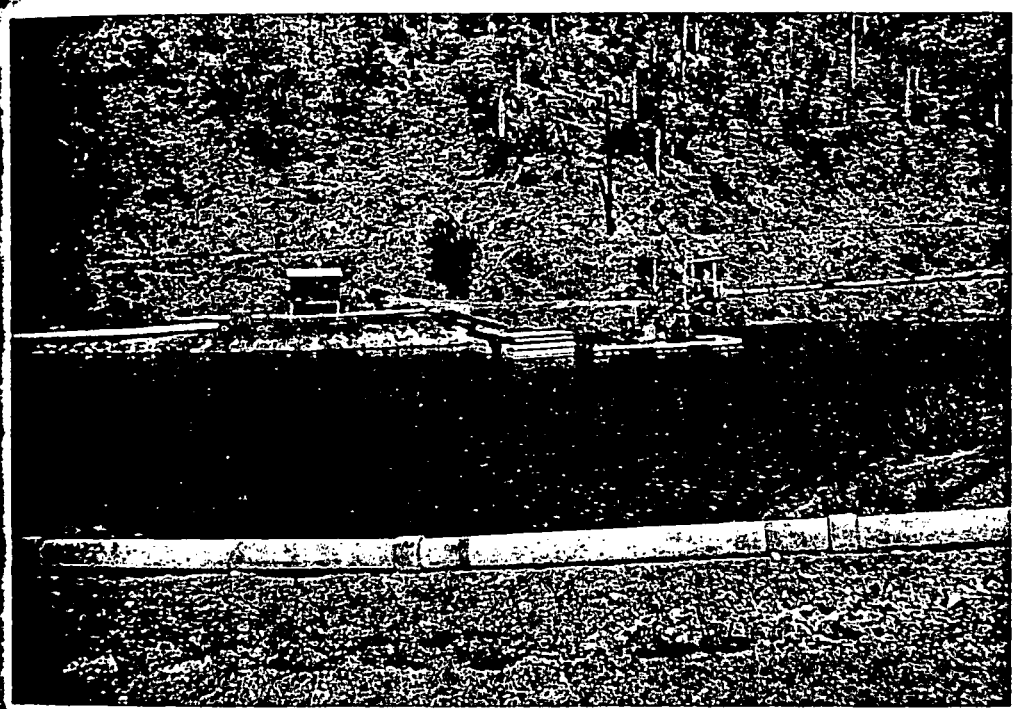

FIGURE 18. - Tailing Solution Pond With Float Pumps at Silver Bell Operation, American Smelting and Refining Co. Brown color of water is typical of tailing water that contains high iron and low copper from precipitation operations.

FIGURE 19. - Leach Solution Distribution Over Block-Caved Area, Miami Copper Co. White aluminum salts are precipitating on the red surface.

dumps. The air temperature is known to be as high as 135° F within one leach dump at the Bingham Canyon operation of Kennecott Copper Corp. High temperatures reflect accelerated oxidation rates in the dumps and presumably account for the dissolution of some of the difficultly soluble minerals, more especially chalcopyrite.

Operational Control During Leaching

Control of the pH of the leach solutions is mandatory for effective leaching. Sulfuric acid is added in many leaching operations prior to the introduction of the leach solutions onto the dumps. Numerous monitoring devices are used and acid addition is controlled automatically. Pregnant solutions are sampled periodically and choice of sections of the dumps to be leached is governed by analyses of these solutions. When the copper content of the pregnant liquor falls below a predetermined amount, leaching is discontinued in the sections of the dumps being leached and begun on new sections. Additional amounts of acid usually are added to the leach solutions when the tailing solutions from the precipitation plants have a pH of more than 3.0.

Heap Leaching

Heap leaching is employed to dissolve copper from porous oxide ore that has been placed on a prepared surface. Heap leaching contrasts with dump leaching principally in that ore material is leached instead of waste material. This method is not applicable to the dissolution of copper sulfide minerals or to ores containing large amounts of carbonate or other acid soluble gangue minerals. Companies currently employing heap leaching are Ranchers Exploration and Development Corp. at the Bluebird mine near Miami, Ariz., the J. H. Trigg Co. operation at Tyrone, N. Mex., and Zontelli Western Mining Co. operation at Page, Ariz.

Emplacement of Heaps

Ground Preparation

Leach heaps are deposited primarily on areas after the ground surface has been prepared. One exception to this procedure is at the heap leaching operation of the J. H. Trigg Co., where the leach heaps are deposited on the existing topography. Examples of prepared surfaces are given by the following.

At the Bluebird mine of the Ranchers Exploration and Development Corp. the ground was first cleared of vegetation; then the soil was cemented and covered with diluted tar for curing and sealing purposes.

The area used for emplacement of the leach heaps at the Zontelli Western Mining Co. operation was leveled by bulldozer, with a slope maintained toward the pregnant liquor sump adjacent to the precipitation vats. After the leaching operation was completed, a 10-inch layer of fine sand was spread on the surface, followed by a layer of 10-mil polyethylene plastic. A 12-inch layer of fine sand then was placed on the polyethylene plastic. Asbestos pipe perforated with 1/2-inch holes and protected by wooden cribbing then was placed on the 12-inch sand layer at 15-foot intervals across the width of the heap

drainpipes extend from the ends of the heaps and are alined to taper toward the pregnant liquor sump.

Method of Heap Emplacement

The material for heap leaching operations is blasted or ripped and then loaded by bulldozer or hauled by bottom dump scrapers and dumpsters to the heaps. The method employed at the Bluebird mine of Ranchers Exploration and Development Corp. (27) is typical of this type of operation. This method was designed to produce minimum compaction in the heaps which are built in 15- to 25-foot lifts. When starting a new heap, scrapers place the leach material in a 30-foot-wide strip along the centerline of the new heap. Subsequent loads are dumped along the outer edge of the strip and pushed over the side with a motorgrader to build the heap to its full width without compaction. In this method only the top few feet of the heap becomes compacted, and this layer is subsequently loosened by a bulldozer equipped with a ripper.

Physical Nature of Heaps

The leach material at the J. H. Trigg Co. property No. 1 is less than 6 inches in size and that at property No. 2 is less than 2 feet in size. The maximum size of heap leach material at Ranchers Exploration and Development Corp. is approximately 12 inches. The bulk of the material, however, is less than 4 inches. The leach material at Zontelli Western Mining Co. is crushed to minus 4 inches.

The volume of leach material on heaps is considerably less than that of leach dumps and varies from 100,000 tons at J. H. Trigg Co. to 500,000 tons at Zontelli Western Mining Co. and Ranchers Exploration and Development Corp.

Leaching Operation

The overall heap leaching operation is similar in many respects to that of dump leaching, with a few exceptions.

More concentrated sulfuric acid solutions are used in heap leaching because of the acid strength necessary for dissolution of the copper oxide minerals. Acid is not regenerated within the heaps because of the absence of pyrite in the oxidized ore. As much as 50 grams per liter of sulfuric acid is added to the leach solution at the Ranchers Exploration and Development Corp.'s Bluebird mine.

A different approach for removal of iron produced in the precipitation plant is conducted by Ranchers Exploration and Development Corp. In addition to high-grade material placed on heaps for leaching, material containing less than 0.3 percent copper is placed on mine waste dumps. The tailing solution from the precipitation plant is circulated through the waste dumps to allow some of the iron to precipitate. Some acid is consumed in this process, but copper also is dissolved. The solution from the waste dumps then is returned to the leach heaps to be used as the leach solution.

Because of the higher grade of the heaps, the stronger acid solution, and the ready solubility of oxidized copper minerals, the pregnant solutions produced generally are much higher in copper content than pregnant solutions obtained from dump leaching. Copper content of the pregnant liquor at Ranchers Exploration and Development Corp. varies from 3 to 7 grams per liter.

Inplace Leaching

Inplace leaching techniques are applicable to leaching oxide and sulfide ores of copper and other metals. The basic principles involved are similar to those for dump or heap leaching. The leach solutions must pass downward through the ore and contact and dissolve the copper-bearing minerals. Adequate arrangements are necessary to collect the resultant copper-bearing liquors without appreciable loss. Provision usually must be made to pump the liquors to the surface where the copper can be recovered.

Leaching inplace and precipitation of copper at the Ohio Copper Co. mine, Bingham Canyon, Utah, has been described by Anderson (5). Leach solutions were distributed upon the surface of a large rockfill overlying a portion of the caved zone of the underground mine. Slow percolation was used in the leaching because it was believed this method would promote the oxidizing conditions deemed favorable for continued and rapid dissolution of the copper sulfide minerals.

Thomas (82) has described the inplace leaching of copper from worked-out areas of the Ray mines in Arizona. Sprays that were moved from one area to another were used to uniformly distribute fresh water to the caved area. This practice promoted the oxidation of pyrite and the copper minerals and therefore their dissolution. The copper-bearing liquors were pumped to the surface and the copper was recovered by precipitation with iron.

The Miami mine of the Miami Copper Co. is the best example of a current inplace leaching operation. The company is leaching copper from the underground ore bodies which previously were mined principally by block-caving methods. Various amounts of copper remain in the capping, in the stopes below the capping, and in the crushed pillars in the mine. A description of the inplace leaching operation at the Miami mine is given by Fletcher (30). Acid is added to tailing water from the precipitation plant, and this solution is distributed by sprays onto the surface area which overlies the former block-caving operation (fig. 19). The leach solution percolates downward through 600 feet of material, the bottom 150 feet of which contains the mixture of ore and waste with the largest percentage of copper. The solution moves from the surface to the 1,000-foot level of the mine within 3 to 4 weeks. Pregnant liquor that is collected in a reservoir on the 1,000-foot level is emptied periodically into a sump from which the liquor is pumped to the precipitation plant on the surface.

Vat Leaching

Vat leaching is employed to extract copper from oxide or mixed oxide-sulfide ores containing more than 0.5 percent acid-soluble copper. This method is used in preference to heap leaching if the ore material is not friable and crushing is necessary to permit adequate contact between the leach solution and the copper minerals. Despite increased costs necessary for crushing and screening, numerous advantages are achieved by vat leaching. Higher copper recovery in shorter periods is realized; pregnant liquor losses are negligible; and copper content of the pregnant liquor is much higher, benefitting recovery of the copper by means other than precipitation by iron.

Seidel (67) has discussed numerous factors which influence vat leaching processes. Percolation flow rates are affected chiefly by the texture or permeability of the ore bed in the vats. Air or other gas bubbles present in the ore beds reduce the percolation rates of the leaching solutions. Higher temperatures of aqueous leach solutions will produce higher percolation rates. Numerous variables, such as particle size, particle porosity, temperature, reagent strength, and percolation rates, greatly affect the mass transfer operations during the dissolution of the mineral particles and the washing and recovery of the dissolved copper from the leach residue.

Ores processed by vat leaching are made suitable for placement in the vats by crushing and screening. Descriptions and illustrations of the vat leaching operations of The Anaconda Company, Weed Heights, Nev., and the Inspiration Consolidated Copper Corp., Inspiration, Ariz., are given in the following sections.

The Anaconda Company

The ore treated by vat leaching at the Weed Heights operation of The Anaconda Company (fig. 20) is predominately oxide ore containing 0.59 percent copper. Approximately 86,000 tons of ore is treated per week in eight vats, each measuring 120 feet wide, 139 feet long, and 19 feet deep. Descriptions of this operation have been given by Huttl (41) and in "Mining World" (58). The oxide ore is crushed and screened to minus 7/16 inch. Water sprays are used to increase the moisture content of the minus 7/16-inch material to 5 or 6 percent as it is layered on the conveyor belt that moves the material to the leaching vats. Because of the increased moisture content the fine particles tend to adhere to the coarser particles and also to cling together to form larger particles. Agglomerating the fines in this manner obviates the necessity for removing the fines which normally would reduce the porosity of the ore beds in the vats and therefore prevent effective leaching.

The principal copper-bearing mineral in the ore is chrysocolla. Dilute sulfuric acid solutions containing from 30 to 35 grams per liter of acid are used to leach the ore. The pregnant liquors and wash waters obtained from the vat leaching operation are pumped to a precipitation plant where the copper is recovered by use of iron scrap.

Inspiration Consolidated Copper Co.

The ore treated in the vat leaching operation of the Inspiration Consolidated Copper Co. (fig. 22) is mixed oxide-sulfide ore. Presently chrysocolla is the predominant oxide mineral and chalcopyrite is the predominant sulfide mineral. Early methods of leaching Inspiration ore have been described by Aldrich and Scott (3-4) and Van Arsdale (84). The design of the original leaching plant to treat underground ores, which consisted of approximate proportions of 60 percent oxide minerals and 40 percent chalcocite, was based on the ready solubility of chalcocite in a solvent containing sulfuric acid and ferric sulfate. The ore mined and treated contained an increasing amount of chalcopyrite as the method of mining was gradually changed from underground to open pit. Chalcopyrite is only slowly soluble in a ferric sulfate leach, and it became necessary to employ a system to recover copper separately from both the oxide and sulfide minerals.

In the present operation the ore is crushed, screened, passed through rod sets of rolls, and then rescreened. The final sand product is suitable for leaching with a maximum size of three-eighths of an inch and with a minimum amount of fine material detrimental to the flow of leach solutions. The slime fraction obtained from the rake classifiers and cyclones in the circuit contains 85 percent minus 200-mesh material and is used as a feed to a separate slime leaching operation. A generalized flowsheet of the Inspiration leaching plant is given in figure 21.

Approximately 9,600 dry tons of ore is loaded into each of 13 leaching tanks by a gantry-mounted clamshell bucket. Each tank is approximately 68 feet wide, 175 feet long, and 18-1/2 feet deep. The oxide minerals are batch leached by using the return solution from the electrolytic tankhouse as the leach solution. The leach solution is heated to about 53° C and is introduced into the ore at a rate of 2,400 gallons per minute. The leach solution and the pregnant liquor derived from the leaching operation is represented by the following typical chemical analyses with the data expressed in grams per liter:

	Cu	H_2SO_4	Fe^{++}	Fe^{+++}
Leach solution.....	24.1	18.0	3.5	4.1
Pregnant liquor....	28.7	9.0	6.8	.8

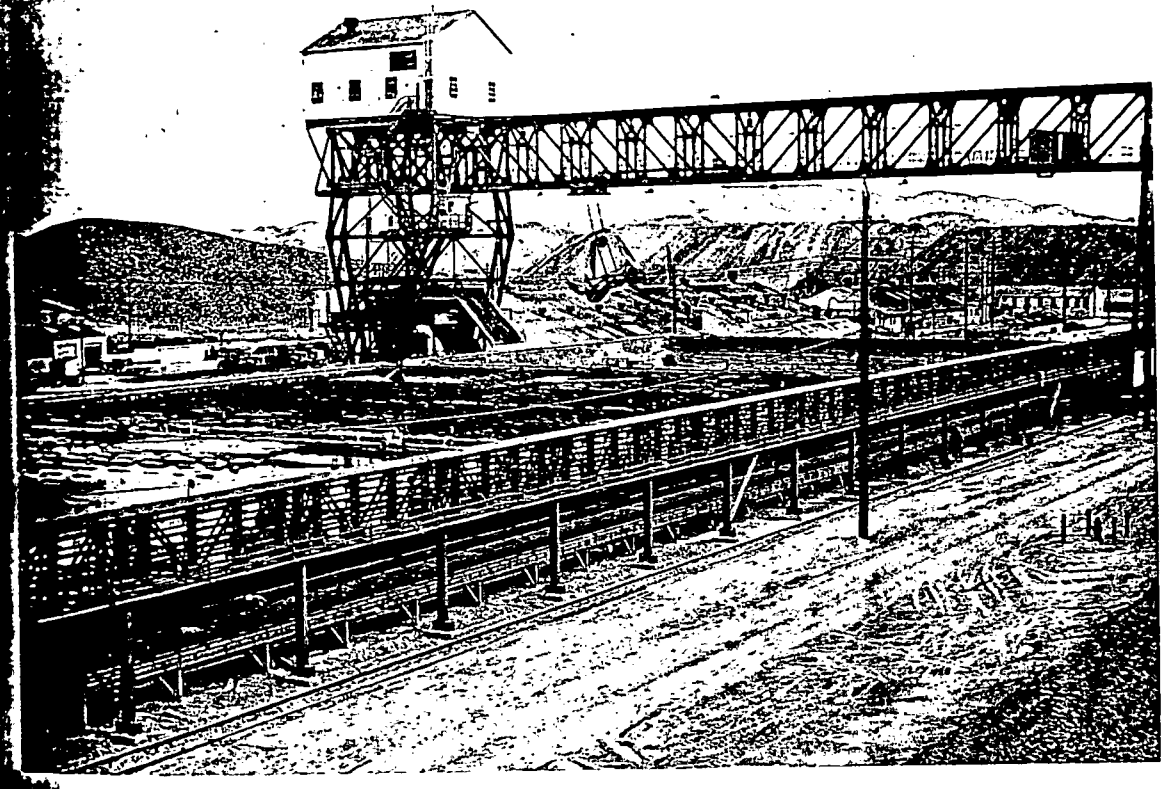

FIGURE 20. - Vat Leaching at Weed Heights Operation, The Anaconda Company.

Chalcopyrite is not readily soluble in the leach solution, but is recovered later from the vat tailing. The tailing from the vat leaching operation is excavated by clamshell and transported by train to the company's concentrating plant where the chalcopyrite is recovered with other sulfides by conventional flotation methods.

During 1965, Inspiration Consolidated Copper Co. installed the latest innovation in bulk-handling systems which consists of a bucket line reclaimer used to continuously empty the leach tanks at the rate of 1,100 tons per hour and feed a 7,400-foot overland belt conveyor system connecting the leach tanks with the concentrating plant. A description of this innovation is given in "Engineering and Mining Journal" (26).

Copper is recovered from the vat leach liquors by electrolytic deposition. Copper is recovered from the slime fraction mentioned earlier by flotation of the sulfides and by subsequent leaching of the oxides.

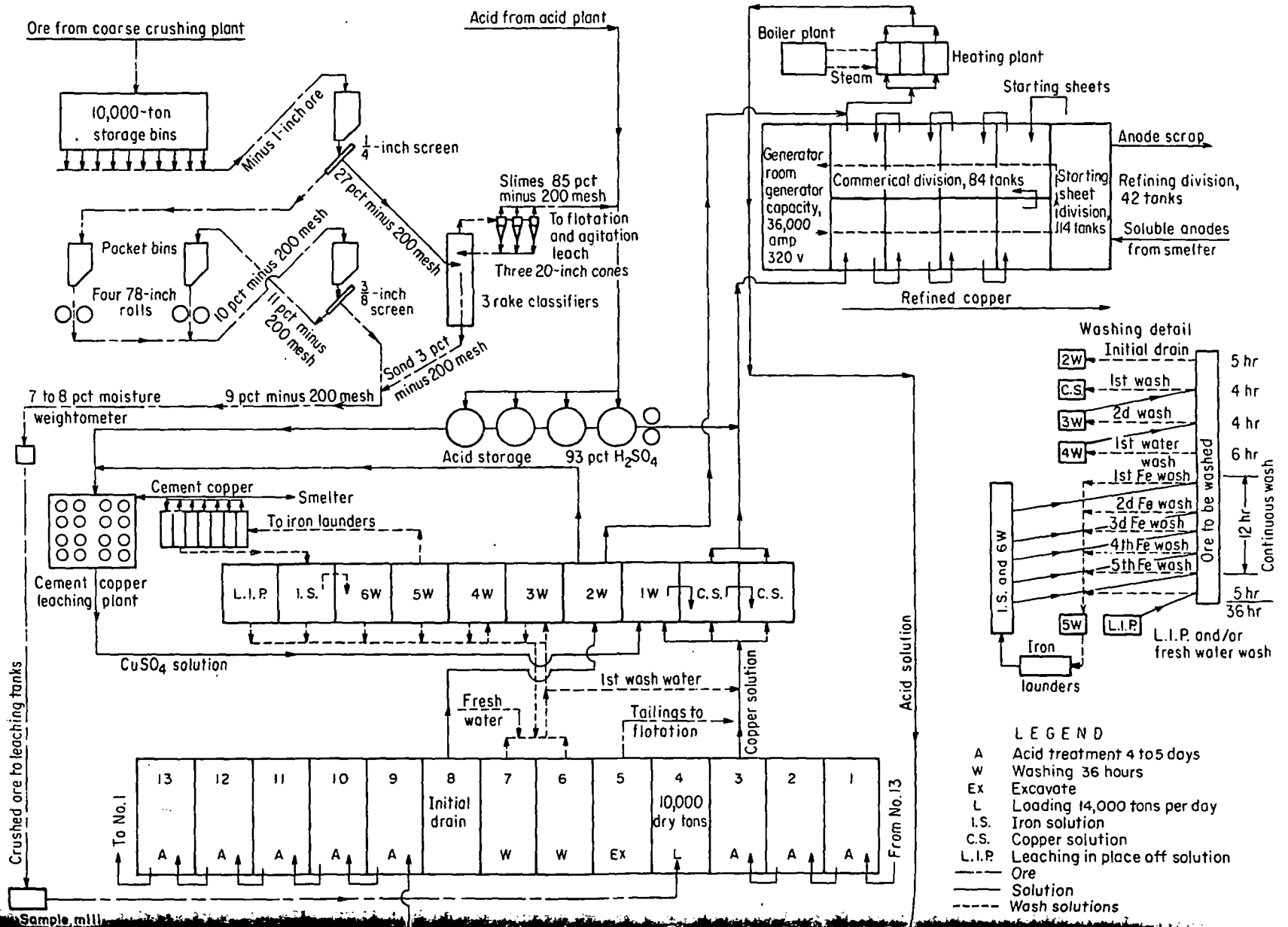
Ore from coarse crushing plant
10,000-ton storage bins
Minus 1-inch ore
1/4-inch screen
27 pct minus 200 mesh
Slimes 85 pct minus 200 mesh
To flotation and agitation leach
Three 20-inch cones
3 rake classifiers
Pocket bins
Four 78-inch rolls
10 pct minus 200 mesh
11 pct minus 200 mesh
3/8-inch screen
Sand 3 pct minus 200 mesh
7 to 8 pct moisture
weightometer
9 pct minus 200 mesh
Acid from acid plant
Acid storage
93 pct H2SO4
Cement copper
Smelter
To iron launders
Cement copper leaching plant
L.I.P.
I.S.
6W
5W
4W
3W
2W
1W
C.S.
C.S.
CuSO4 solution
1st wash water
Fresh water
Tailings to flotation
Copper solution
Acid solution
Crushed ore to leaching tanks
To No.1
13
12
11
10
9
8
Initial drain
7
6
5
4
10,000 dry tons
3
2
1
A
A
A
A
A
W
W
Ex
L
A
A
A
From No.13
Sample mill
Boiler plant
Steam
Heating plant
Starting sheets
Anode scrap
Generator room generator capacity, 36,000 amp 320 v
Commerical division, 84 tanks
Starting sheet division, 114 tanks
Refining division, 42 tanks
Soluble anodes from smelter
Refined copper
Washing detail
2W
Initial drain
5 hr
C.S.
1st wash
4 hr
3W
2d wash
4 hr
4W
1st water wash
6 hr
1st Fe wash
2d Fe wash
3d Fe wash
4th Fe wash
5th Fe wash
12 hr
Continuous wash
5 hr
36 hr
Ore to be washed
I.S. and 6W
5W
L.I.P.
L.I.P. and/or fresh water wash
Iron launders
LEGEND
A Acid treatment 4 to 5 days
W Washing 36 hours
Ex Excavate
L Loading 14,000 tons per day
I.S. Iron solution
C.S. Copper solution
L.I.P. Leaching in place off solution
Ore
Solution
Wash solutions

Other Methods of Leaching

Several minor methods of leaching presently are used to recover copper mixed oxide-sulfide ores or from the slime fraction obtained from crushoxide ores used in vat leaching. These methods are referred to as leachcipitation-flotation (LPF) and slime leaching, respectively, and are scribed in the following sections. Ammonia leaching has been used in the to recover copper from copper oxide minerals associated with carbonate gue material. Descriptions of a former ammonia leaching operation have given by Duggan (22-23) and Eddy (25). Leaching of copper minerals by ide solutions has been proposed by Lower and Booth (49-50), but as yet has been used in practice.

Leach-Precipitation-Flotation

The original LPF process, according to Bean (10), was conceived and loped by F. W. Maclennon and Harmon Keyes of the Miami Copper Co. during years 1929-34. The process was designed to supplement a conventional cation operation by adding a leach circuit to the mill.

Many of the porphyry-type copper deposits in the Western United States highly altered and contain readily acid-soluble oxidized copper minerals ociated with sulfide copper minerals. The nonsulfide minerals often occur coatings and stains on the gangue and ore minerals and not as discrete ains in the rock as a whole. To recover both the oxide and sulfide copper erals, leaching and froth flotation methods have to be employed. In some plants the sulfide minerals are recovered by froth flotation and the resultant ailing then is leached to recover the remaining copper. More common practice to acid leach the oxide minerals, precipitate the dissolved copper with and recover the resultant cement copper and the sulfide minerals in the flotation circuit. Descriptions of LPF circuits have been given by Franz (26), Huttle (42), and Milliken and Goodwin (57).

The first unit operation in the LPF process comprises crushing and grinding to liberate the sulfide minerals. The finely ground ore is classified in classifiers, drag classifiers, and cyclones to produce a uniform feed for leaching and flotation.

The ground pulp is agitation leached in tanks for about 30 minutes with a sufficient amount of sulfuric acid to maintain a solution pH between 1.5 and 2.0. From the leach tanks the pulp is introduced into a series of precipitation tanks or cells where finely divided iron is added to precipitate the dissolved copper. The pulp is then moved to acid-proof froth flotation cells to recover a concentrate containing both cement copper and copper sulfides. The pH of the flotation pulp in most plants is regulated to about pH 4 by the addition of lime, although metallic iron also has been used for this purpose. Because the flotation feed is acidic, dixanthogen is the commonly used collector. Copper recovery by the LPF process is generally about 90 percent.

The main improvement in recent years in the LPF process has been the availability of more durable equipment. Flotation cells, pumps, and tanks are lined with new types of organic and rubber materials which prevent excessive corrosion and erosion of the equipment.

Sample mill

Slime Leaching

The slime fraction in the ore obtained from the preparation of the vat leach feed at the plant of Inspiration Consolidated Copper Co. is treated first by conventional flotation methods to recover the sulfide copper minerals. The flotation tailing then is thickened to about 40 percent solids and sent to the slime leach plant for extraction of copper from the acid-soluble oxidized copper minerals. The process has been described by Power (61). The slime plant consists of three 20-foot-diameter redwood leach tanks. Each tank is equipped with a mechanical agitator having a 4-inch airlift in the shaft of the agitator for removal of the leached pulp. Separation of the resultant copper sulfate solution from the acid insoluble residue is accomplished by countercurrent washing in four 150-foot concrete traction thickeners, each equipped with three 4-inch airlifts on the spigot product and one 4-inch lead lined centrifugal pump on the overflow. The pregnant copper sulfate solution is pumped to an iron launder where the copper is precipitated by scrap iron. The sulfuric acid requirements for leaching the slimes ranges from 3.9 to 4.2 pounds of acid per pound of copper recovered. Iron consumption for precipitating the cement copper amounts to 1.6 pounds of iron per pound of copper precipitated. Copper recovery from the slime leach plant feed is about 95 percent.

COPPER RECOVERY

Copper presently is recovered from leach liquors almost entirely by means of precipitation by metallic iron. Copper in the vat leach liquors at Inspiration Consolidated Copper Co. is recovered by electrolytic deposition. Other methods of precipitation have been suggested by Baarson and Ray (6) and Croasdale (20). Numerous investigators, including Forward (31), Peters and Hahn (59), and Schaufelberger (65), have shown that at elevated temperatures and pressures, copper can be precipitated from solution by hydrogen reduction.

Bagdad Copper Corp. is constructing a plant to produce copper powders by application of hydrogen reduction principles. Other methods of recovering copper from solution, suggested by Agers and coworkers (1-2), Fletcher and Flett (29), Quarm (62), and Swanson and Agers (80), are by solvent extraction and ion exchange. At present, however, copper recovery is accomplished in practice only by the methods of precipitation by metallic iron and electrolytic deposition, and the following descriptions focus attention on these methods.

Precipitation by Iron

Metallic iron precipitates copper from solution according to the well-known reaction: $CuSO_4 + Fe \rightleftharpoons Cu + FeSO_4$. In practice copper is recovered from copper-bearing pregnant liquors almost entirely by application of the principle of this equation.

Sources of Iron

Shredded scrap cans (fig. 23) are the chief source of iron used as a precipitant in the recovery of copper from copper-bearing solutions. They

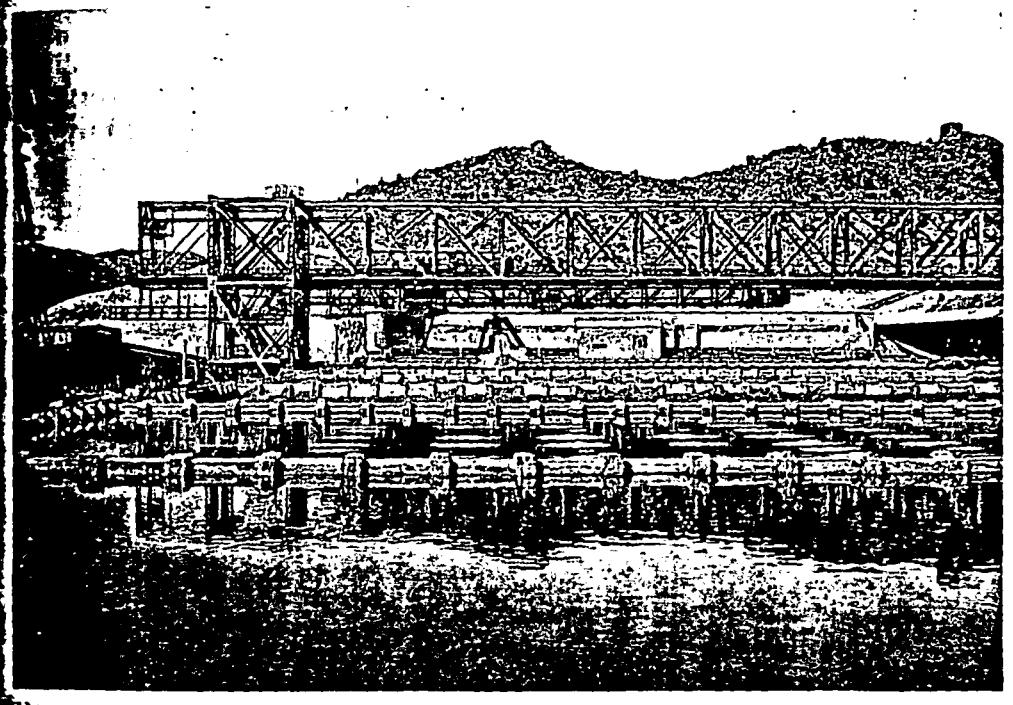

FIGURE 22. - Vat Leaching Operation, Inspiration Consolidated Copper Co. Intense blue solution contains as much as 30 grams per liter of copper.

FIGURE 23. - Stockpile of Partially Oxidized, Burned, and Shredded Cans at Mineral Park Precipitation Plant, Duval Corp. Brown color is typical of the oxidized detinned and shredded cans.

first burned to remove paper labels and organic material. The tin content of scrap cans is often removed by a caustic leach process. The principal Western suppliers of shredded, detinned cans are Proler Steel Corp., with plants at Houston and El Paso, Tex., and San Francisco, Calif., and the Los Angeles By-Products Co., with plants at Bakersfield and Los Angeles, Calif.

Scrap punchings and clippings produced during the manufacture of cans attained significant importance during recent years as a source of iron for copper precipitation. These materials are good precipitators for copper because of their relative uniformity in size and absence of deleterious impurities, such as organic materials and other solids. Proler Steel Corp. has recently erected a shredding plant near Copperton, Utah, to supply the Bingham Canyon precipitation operation of Kennecott Copper Corp. The product will be used in the newly installed cone precipitators.

Another source of iron that has been used as a precipitant is turnings from lathes and other cutting machines. This type of precipitant has proved unsatisfactory, however, because of inclusions of oil and other lubricants. An additional deterrent to the use of turnings is the slow precipitation of copper attained because of the low surface-to-weight ratio of the iron.

Heavy scrap iron has been used as a precipitant for copper in several operations. Low cost of the scrap iron obtained from the mine and milling operations has made this type of precipitant attractive. Deterrents to using heavy scrap as a precipitant, however, are the difficulty in handling the scrap during loading and cleaning of the precipitation launders and the small surface area per unit of weight available for reaction. A few operators have used heavy scrap in the head section of the launders to reduce the ferric ion content of the pregnant solution and thereby reduce the shredded can consumption in the remaining cells, since ferric sulfate and sulfuric acid are responsible for the iron consumed in the launders according to the reactions

$$Fe_2(SO_4)_3 + Fe \rightleftharpoons 3FeSO_4;$$

$$H_2SO_4 + Fe \rightleftharpoons H_2 + FeSO_4.$$

Finely divided sponge iron is an effective precipitant of copper, although at present it is not competitive in cost with available shredded scrap cans. The principal advantage in using sponge iron seems to be the relatively faster copper precipitation rate obtained with particulate iron compared to that obtained with more massive scrap iron products. According to Back (7), sponge iron is most effective as a precipitant for copper when used in conjunction with cone-type precipitators. High-grade magnetite, iron ore, and pyrite cinders are the chief sources for producing sponge iron suitable as a reactive precipitant for copper. Kennecott Copper Corp. is investigating the feasibility of producing sponge iron for copper precipitation by the reduction of the iron in copper reverberatory slag from the firm's smelter.

Types of Precipitation Plants

Copper is precipitated from solutions in a series of gravity launders or cone precipitators. Descriptions and examples of each type currently employed are given in addition to illustrations of certain aspects of operating practices.

Precipitation Launders

Current precipitation practice is typified by the use of gravity launders. Typical top, end, and side views of a series of gravity launders are shown in figure 24. Launder dimensions at numerous operations are given in table 1.

Ballard (9), Jacky (44), and Power (60) have described the precipitation launders of The Anaconda Company and the American Smelting and Refining Co. These launders are of concrete construction, with wooden planks to protect the ends of the launder walls. Plywood and/or stainless steel gratings are used to support the iron precipitant within the launders.

The launders of the precipitation plants are charged with cans by means of different mechanical devices. The launders of the Copper Cities precipitation plant of the Miami Copper Co. are loaded with cans that are discharged from a belt conveyor by a moving tripper. A crane-mounted magnet is used to charge and clean launders at the Silver Bell precipitation plant of the American Smelting and Refining Co. A gantry-mounted clamshell bucket is used to load cans into the launders at the Butte precipitation plant of The Anaconda Company. Front-end loaders are used at the Morenci precipitation plant of Phelps Dodge Corp., and at the Mineral Park plant of the Duval Corp. Part of the cells at the latter plant are loaded by a belt conveyor (fig. 25). Kennecott Copper Corp. at its Bingham Canyon original launder precipitation plant uses a forklift loader to load the launders with cans.

Copper-bearing liquors are introduced into the upper end of gravity launder plants through a solution feed launder and allowed to trickle downward through the shredded cans. Launder arrangement is such that solution flow is in series. Baffles and pumps are utilized in order that any launder may be bypassed and solutions returned to any particular launder. The copper, ferric iron, and free sulfuric acid content of the pregnant liquors and the surface area of iron available for reaction are the more important factors in determining the rate and degree of recovery of copper in each particular launder. Copper usually is washed three times a week from the first few launders, which in most plants precipitate more than 60 percent of the total copper. The copper precipitated in the remaining launders is removed usually from once a week to once a month. Tailing (barren) solutions discharge by gravity from the lower ends of the plants.

The "Yerington-type" plant differs from those described in that the pregnant solution flow is upward through the iron precipitant. The pregnant liquor is introduced into the launders under pressure through three parallel, 1-inch plastic tubes which lie in gutters in the floors of the launders. The tubes have been perforated with 5/8-inch holes spaced from 1 to 3 feet apart

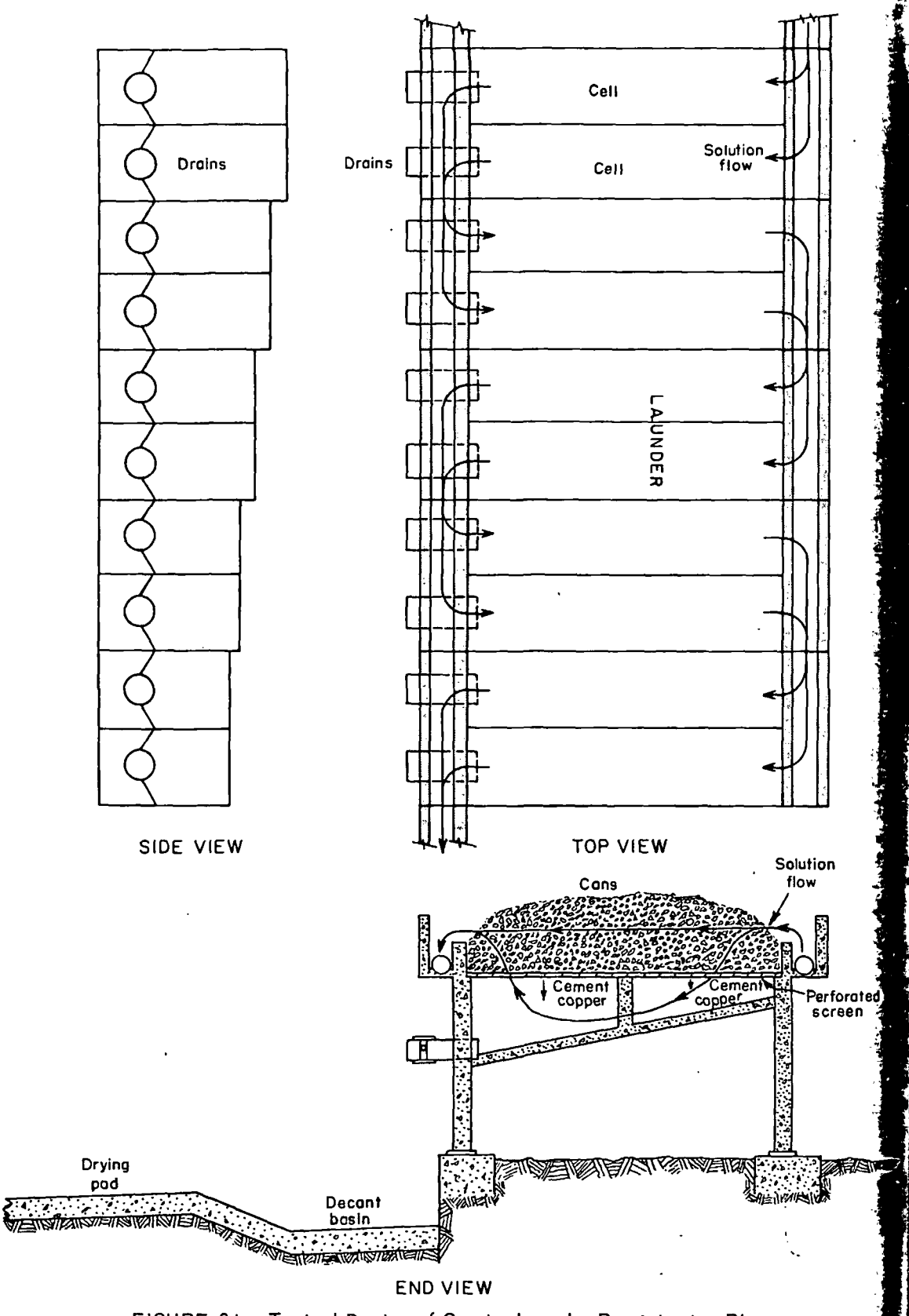

FIGURE 24. - Typical Design of Gravity Launder-Precipitation Plant.

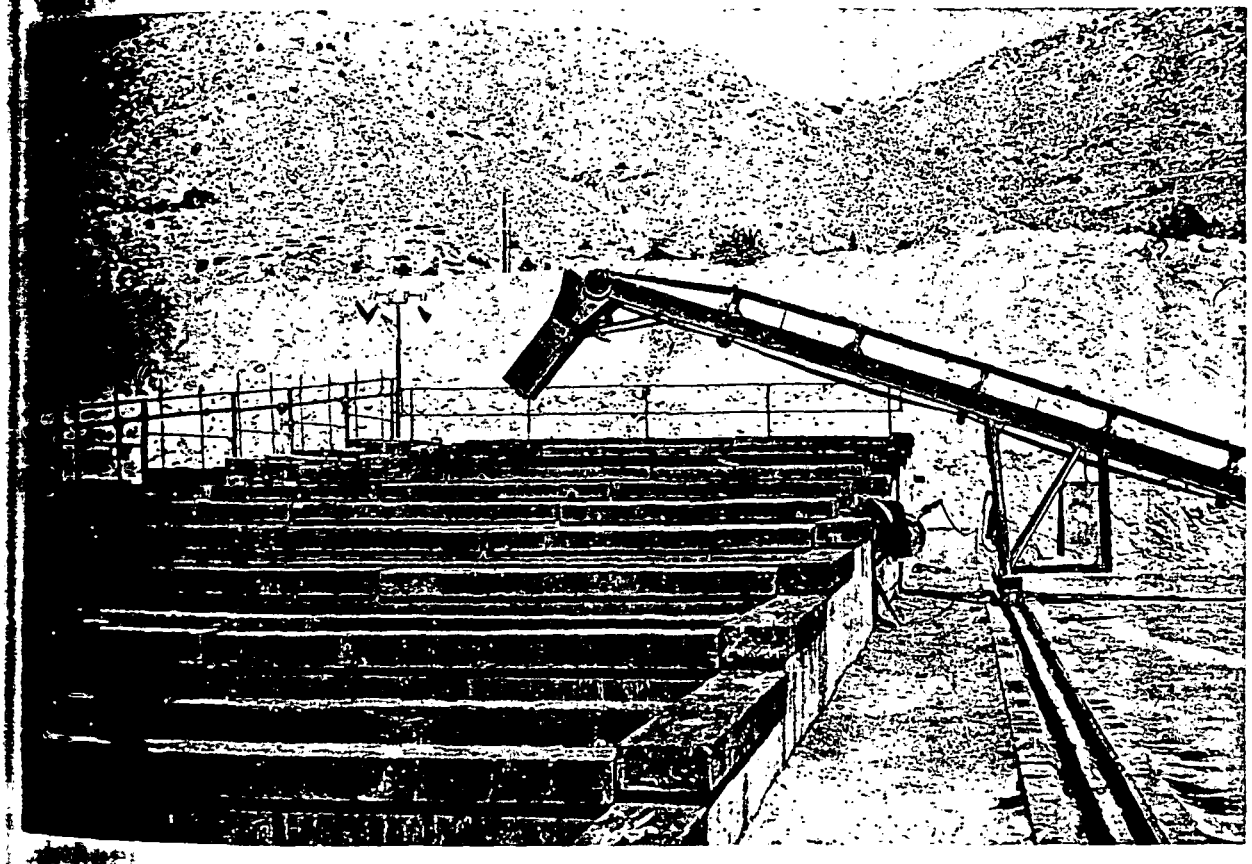

FIGURE 25. - Sliding Conveyor Used to Load Cans Into Cells of Precipitation Plant at Mineral Park Property, Duval Corp.

26). High-solution velocities are maintained in the launders and a cement copper product is formed. Higher purity and lower moisture are synonymous with this coarser product.

Pregnant liquors introduced into, and tailing (barren) solutions discharged from, precipitation plants are sampled continuously. The solutions analyzed for pH and copper, iron, and acid content by wet chemical methods, although other methods are being adopted such as X-ray, electrolytic, and absorption. Typical analyses of such solutions from numerous precipitation plants in the Western States are given in table 1. The pH of the pregnant liquors varies from 1.4 to 3.5, copper content from 0.75 to 7.0 grams per liter, ferrous iron content from 0.00 to 3.60 grams per liter, ferric iron content from 0.05 to 3.00 grams per liter, and free acid content from 0.04 to 3.30 grams per liter. The recovery of copper is high in all operations, averaging well above 90 percent. The copper content of the tailing solutions therefore is low and ranges from less than 0.01 to 0.36 gram per liter. The pH of the tailing solutions is higher, in the range of 2.4 to 4.4, as a result of the decrease in acid content. The decrease in acid and an increase in ferrous iron content (almost entirely ferrous iron) is the result of the several acid-consuming reactions that take place during precipitation.

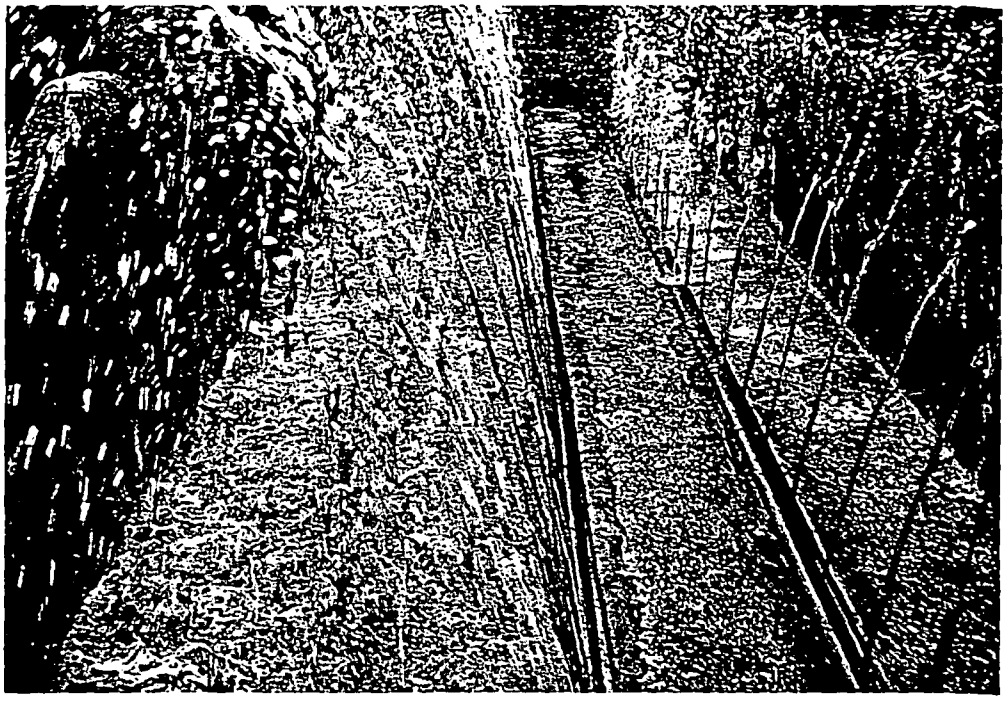

FIGURE 26. - View of Empty Launder at Weed Heights Precipitation Plant of The Anaconda Company Showing Pregnant Solution Introduction Under Pressure Through Perforated Plastic Pipes. Blue-green color of solution is indicative of copper content.

FIGURE 27. - Removing Red-Brown Cement Copper From Cells by High-Pressure Hoses at the Silver Bell Precipitation Plant, American Smelting and Refining Co.

The amount of iron consumed per pound of copper precipitated (commonly known as the "can factor") is an important concern in all plants. Iron consumption varies from operation to operation, but is always higher than the theoretical 0.88 pound of iron per pound of copper required for the iron replacement by copper reaction. The can factors range from a low of 1.2 to a high of 2.5 at the various operations. A list of can factors is given in table 1.

Precipitators

A recent innovation in the recovery of copper from copper-bearing solutions is the cone-type precipitator developed by the Kennecott Copper Corp. and described by Spedden and coworkers (68). A cutaway diagram of the precipitation cone is shown in figure 28. Copper-bearing solution is pumped through a manifold system in the bottom of the cone and is injected through nozzles into shredded, detinned iron scrap, which is semicontinuously loaded into the inner cone above a heavy-gage, stainless steel screen. The injection of the solution under pressure into the iron material has a dual effect. Copper is rapidly precipitated and quickly removed from the iron surfaces by the turbulent action, creating fresh, clean surfaces of iron for continued precipitation of the copper.

Methods of Handling Cement Copper

Various methods are used to handle the cement copper following its precipitation in the launders or in the cones. The purpose in each instance is the same, to obtain as pure a product as possible with minimum moisture content.

Removal From Precipitation Unit

The most frequently used method for removing cement copper from precipitation launders is with high-pressure streams of water. The water is pumped at about 100 pounds of pressure to wash hoses equipped with quick shutoff nozzles (fig. 27). The cement copper is washed from the unreacted iron, and the resultant slurry is emptied into decant basins through drain valves in the bottoms of the cells.

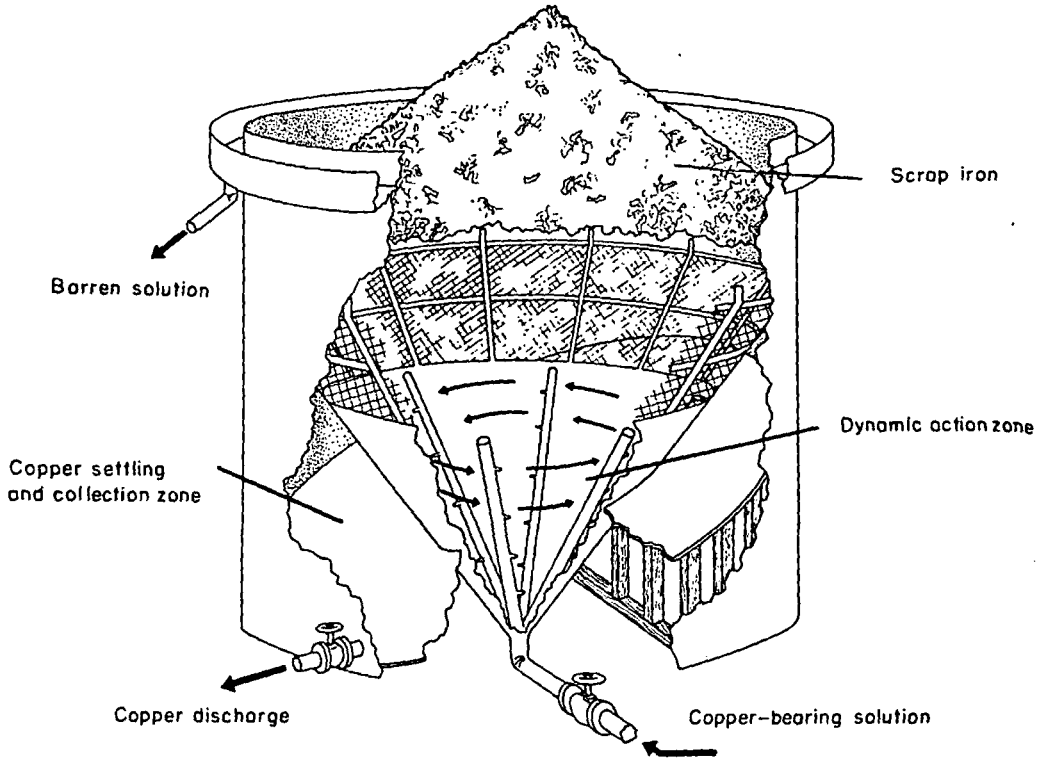

FIGURE 28. - Cutaway Diagram of Cone Precipitator Designed by Kennecott Copper Corp. (Neal Bishop, Kennecott Research Center.)

FIGURE 29. - Airlift Pumps Used for Removing Cement Copper From Precipitation Ce
Bagdad Copper Corp.

Airlift pumps (fig. 29) are used by Bagdad Copper Corp. to remove the cement copper from the bottom of the launders after the cement copper has been washed from the unreacted cans. The slurry of cement copper and water, after being discharged from the airlift pumps, flows by gravity into settling basins (fig. 30).

Hydraulic slushers (fig. 31), consisting of a trussed bridge which spans all six of the parallel launders at The Anaconda Company's Butte precipitation plant, are used to agitate the cans in the launders, remove the cement copper from the cans, and slush (sweep) the cement copper along the launders to drop tanks. After the drop tanks are nearly full, the water is decanted by pumping and the cement copper is loaded into railroad cars by an overhead clamshell bucket.

A few operations use a gantry-operated clamshell bucket to unload the cement copper and unreacted cans from the precipitation launders. The combined material then is charged into a trommel (fig. 32) fitted with stainless steel screens having small-diameter openings to separate the cement copper and unreacted cans from one another. The unreacted cans are returned to the precipitation launders and the cement copper is discharged into settling basins.

The cement copper produced in Kennecott's cone precipitators settles through the stainless steel screen, drops to the bottom of the tank, and is removed intermittently through a pneumatically operated valve. Higher grade products, analyzing 90 to 95 percent copper, are obtained by this method of precipitation. Other benefits from this method are a substantially lower consumption of iron and the elimination of the need for the usual labor involved in a launder-type plant.

Decanting

The cement copper is allowed to settle in basins. The clear water is decanted and returned by pumping to the precipitation launders to prevent the loss of any suspended fine particles of copper.

Drying

The cement copper is removed from the settling basins by various mechanical devices, such as front-end loaders and crane-mounted clamshell buckets. The cement copper removed from the settling basins is dried before shipment to smelters or other markets. Concrete drying pads are generally used, and in most instances are constructed adjacent to the settling basins. The cement copper at the Weed Heights, Nev., operation of The Anaconda Company is dried on large gas-fired hotplates (fig. 34).

Atmospheric drying of the cement copper reduces the moisture content from about 50 percent to between 25 and 30 percent. The cement copper dried by hotplates at Weed Heights contains 15 percent moisture.

Plate-and-frame filter presses are used to reduce the moisture content of the cement copper produced in the cone precipitators at the Bingham Canyon

FIGURE 30. - Decant Basin Adjacent to Precipitation Plant, Bagdad Copper Corp. Blue is copper-bearing water in decant basin; wooden trough in left foreground is delivering red-brown slurry of cement copper and water from the plant's precipitation cells to decant basin.

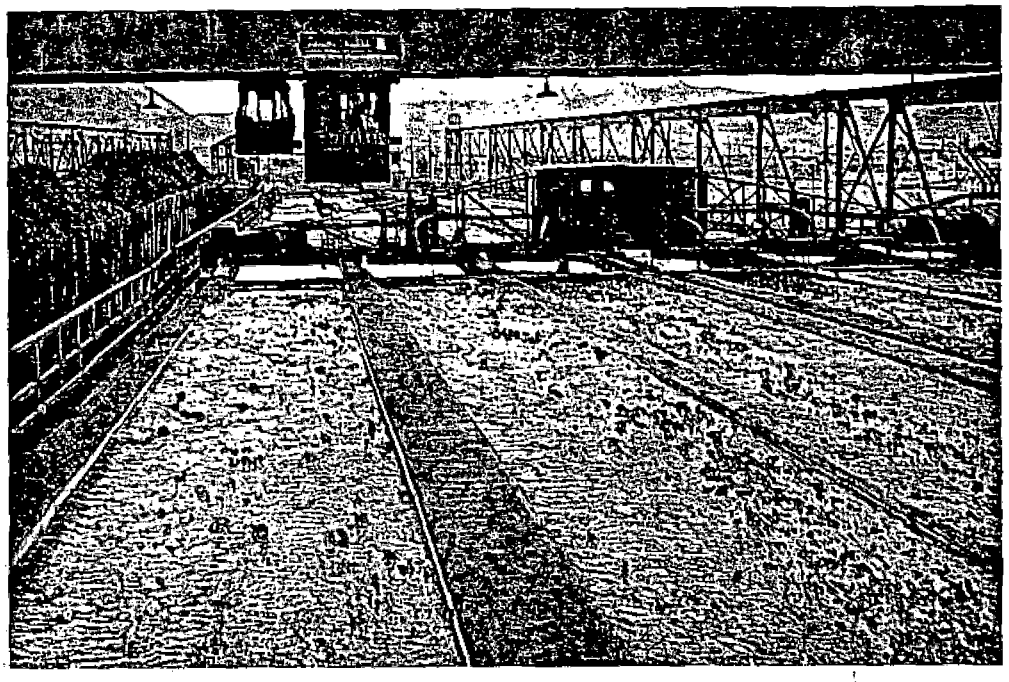

FIGURE 31. - Hydraulic Slushers Used To Remove Cement Copper From the Cells of the Butte Precipitation Plant, The Anaconda Company. The copper-red color of the cement copper in the cells can be seen as copper replaces the iron in the cans.

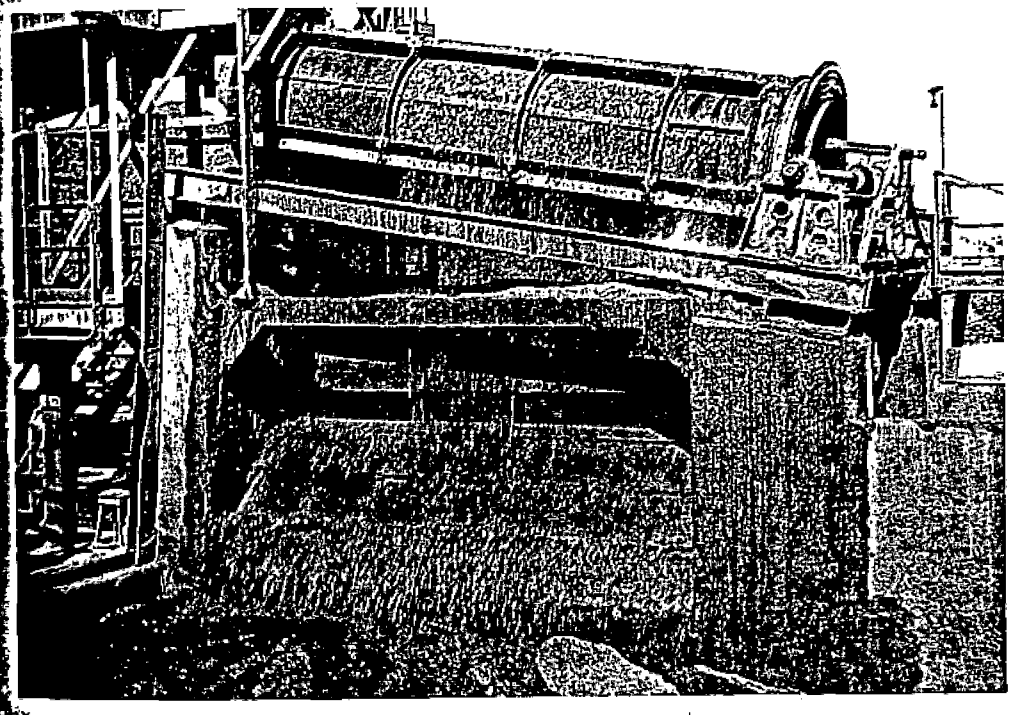

FIGURE 32. - Trommel Used for Screening Cement Copper at Weed Heights Precipitation Plant, The Anaconda Company. Red-brown cement copper is passing through the screen sections on the trommel.

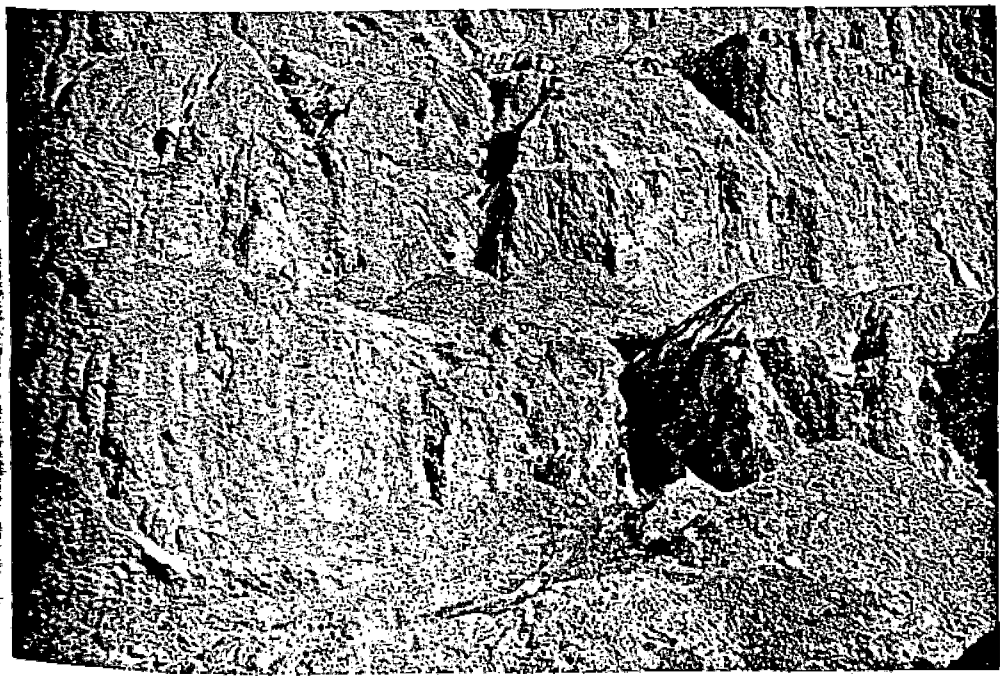

FIGURE 33. - Impervious Layers of Brown Iron Salts Above Blue-Green Copper Minerals in Leached, Block-Caved Area of Underground Mine, Inspiration Consolidated Copper Co.

operation of Kennecott Copper Corp. The final product contains from 8 to 1[0] percent moisture.

Additional Treatment

The cement copper produced in a few plants is processed further to increase the purity of the final product. The cement copper is screened through small-mesh vibrating screens by the Inspiration Consolidated Copper Co. Flotation techniques are used at the Bingham Canyon operation of Kennecott Copper Corp. to improve the quality of part of the cement copper from a launder plant for direct sale to consumers.

Electrolytic Deposition

The Inspiration Consolidated Copper Co. recovers copper from vat leach liquors by electrolytic deposition using insoluble anodes. The process is termed electrowinning. Liquors containing from 25 to 30 grams per liter of copper serve as the electrolyte for the electrowinning process. A descrip[tion] of the electrowinning process and operating data for the Inspiration plant have been given by McMahon (56).

The principal advantages of this process are that electrolytically re[covered] copper does not require additional treatment--that is, the usual smelting [and] ation required for copper production is eliminated--and sulfuric acid and [ferr]ic sulfate needed as solvents during the leaching operation are regenerat[ed].

RESEARCH

Most companies currently engaged in copper leaching are researching or are planning to research the following: (1) The solvent extraction of copp[er] from leach liquors; (2) the use of other precipitants such as sponge iron [or] aluminum; (3) bacterial leaching; (4) the nature of dumps (by drilling and analysis of drill samples); (5) chemical relationships of dump materials and solutions; (6) effectiveness of acid and other solvent additions to the le[ach]ing solution; and (7) dump emplacement techniques.

SUMMARY

A more rapid and more complete recovery of copper from leach dumps is ultimate concern of all companies engaged in copper leaching. Close atten[tion] must be given to numerous problems inherent in the leach cycle to achieve [a] satisfactory leach rate and recovery of the copper.

FIGURE

Iron
princ
in lea
vol
s. E
ently
Bingha
. Ari
the
pH by

Chanr
yed t
natir
ed mat
e met
egatic

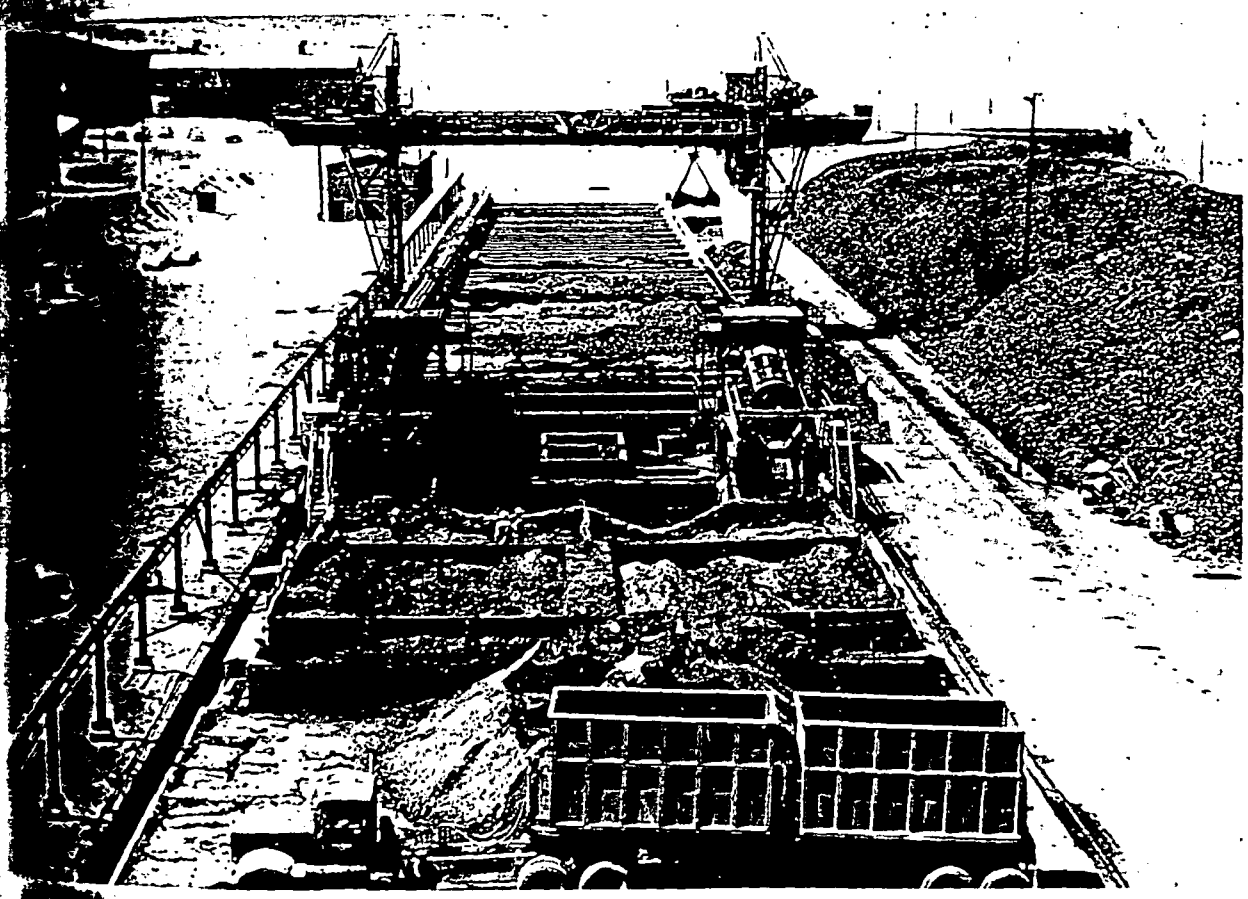

FIGURE 34. - Hotplates (in Foreground) Used for Drying Cement Copper at Weed Heights Precipitation Plant, The Anaconda Company.

Iron salt precipitation on the surface or within leach dumps is one of principal problems encountered in leaching. Impervious layers formed within leach dumps act like blankets through which leach solutions cannot pass. volumes of copper-bearing material are not contacted by the leach solu- Examples of this phenomenon can be seen in the Ohio Copper Co. mine ently exposed in the open-pit mining operation of Kennecott Copper Corp. Bingham, Utah, and at the Inspiration Consolidated Copper Corp. at Inspira- Ariz. (fig. 33). A partial solution to this problem seems to be to min- the iron salt precipitation within the dumps by maintaining a low solu- pH by acid additions to the leach solutions.

Channeling is created in many leach dumps as a result of the methods loyed to build the dumps. Solution flow often is horizontal following ternating layers of coarse and fine material; hence, large volumes of miner- ized material may not be contacted by the leach solutions. Close attention the method of constructing the leach dump is needed to minimize size gregation.

Another important problem encountered is the loss of leach and pregnant solutions. Losses of leach waters frequently are encountered in the Southwest where evaporation is abnormally high. Pregnant solution loss is high whenever the ground upon which leach dumps are deposited is permeable or contains many fractures and faults. Use of prepared pads for dump emplacement is a partial means of solving this problem. Solution loss can result from entrapment of leach solutions within iron salt-lined cavities in the dumps. Improved pH control can partially correct this situation.

The formation of iron precipitates in pipelines and pumps has caused maintenance problems. The solution to this problem is to prevent the iron salts from precipitating by controlling the acidity of the circulating solutions.

Numerous unsuccessful attempts have been made to build up the copper content of the pregnant solution by recycling. Recent investigations by Grunen (35) have shown that clay products within the dumps act as ion exchangers to absorb copper.

Conditions of equilibrium likewise influence the solubility of the many minerals, both ore and gangue, that are contained in the leach material. Copper, iron, and aluminum compounds are both formed and redissolved at different depths within the leach dumps, depending upon environmental conditions prevalent at a given time and site. The chemical and physical reactions taking place within the dumps are numerous and complex. Under a given set of conditions, it is possible that as much copper is being removed from solution as being dissolved.

The chief problem in copper precipitation is maximum extraction of copper with relatively low iron consumption. Iron consumption is high and the cement copper product is contaminated with impurities when the pregnant liquors contain excessive ferric iron and acid and low amounts of copper. A low-quality cement copper is obtained also when the precipitant is heavy metal and is unsuitable with respect to freedom from acid-insoluble impurities.

Improper plant design causes materials-handling problems. Mechanical and chemical problems, such as seal and bearing failures in pumps and acid attack on reactive surfaces, are common to nearly all operations.

Production of copper by use of the various leaching methods is increasing continually and accounts for a larger part of the total copper production in the Western United States. Many of the major copper producing companies currently are improving and expanding their leaching operations. Other companies are planning to increase their outputs by leaching in the near future.

Significant amounts of aluminum, uranium, and other metals are present in the pregnant liquors produced by leaching. Several companies and the Bureau of Mines are conducting research to find means of profitably recovering these metals as byproducts following the removal of copper from solution by precipitation.

REFERENCES[4]

Agers, D. W., J. E. House, R. R. Swanson, and J. L. Drobnick. Copper Recovery From Acid Solutions Using Liquid Ion Exchange. Pres. at ann. meeting, AIME, New York, February 1966, 28 pp.

_____. A New Reagent for Liquid Ion Exchange Recovery for Copper. Min. Eng., v. 17, No. 12, December 1965, pp. 76-80.

Aldrich, H. W., and W. G. Scott. The Inspiration Leaching Plant. Trans. AIME, v. 106, 1933, pp. 650-677.

_____. Leaching Mixed Oxide and Sulfide Copper at Inspiration. Eng. and Min. J., v. 128, 1929, pp. 612-619.

Anderson, A. E., and F. K. Cameron. Recovery of Copper by Leaching, Ohio Copper Company of Utah. Trans. AIME, v. 73, 1926, pp. 31-57.

Baarson, R. E., and C. L. Ray. Precipitate Flotation - A New Extraction and Concentration Technique. Pres. at ann. meeting, AIME, Dallas, Tex., February 1963, 31 pp.

Back, A. E. Use of Particulate Iron in the Precipitation of Copper From Dilute Solutions. Pres. at ann. meeting, AIME, New York, February 1966, 12 pp.

Back, A. E., K. E. Fisher, and J. Kocherhans. Process and Apparatus for the Precipitation of Copper From Dilute Acid Solutions. U.S. Pat. 3,154,411, Oct. 27, 1964.

Ballard, James K. Copper Precipitation at Anaconda's Butte Plant. Pres. at ann. meeting, AIME, New York, February 1966, 11 pp.

Bean, J. J. The Leach, Precipitation, Flotation, Concentration Method at Miami Copper. Colorado Sch. Mines Quart., v. 56, No. 3, 1961, pp. 263-281.

Bogart, R. C. Profits From the Waste Pit. Instrumentation, v. 15, No. 1, 1962, pp. 4-7.

Brace, E. C., and F. E. Horton. Recovery of Copper Sponge From Oxidized Copper Ores. U.S. Pat. 3,148,130, Sept. 8, 1964.

Brown, S. L., and J. D. Sullivan. Dissolution of Various Copper Minerals. BuMines Rept. of Inv. 3228, 1934, pp. 37-51.

Bryner, L. C., and R. Anderson. Microorganisms in Leaching Sulfide Minerals. Ind. and Eng. Chem., v. 49, No. 10, October 1957, pp. 1721-1724.

[4] References 1, 6-7, 9, 17, 21, 28, 30, 35, 44, 49, 51, 59-61, 68, and 80 are available at the Area V Mineral Resources Field Office, Salt Lake City, Utah.

15. Bryner, L. C., J. V. Beck, D. B. Davis, and D. G. Wilson. Microorganisms in Leaching Sulfide Minerals. Ind. and Eng. Chem., v. 46, No. 12, December 1954, pp. 2587-2592.

16. Bryner, L. C., and A. K. Jameson. Microorganisms in Leaching Sulfide Minerals. Applied Microbiology, v. 6, 1958, pp. 281-287.

17. Bryner, L. C., R. B. Walker, and R. Palmer. Some Factors Influencing Biological and Non-Biological Oxidation of Sulfide Minerals. Pres. ann. meeting, AIME, New York, February 1966, 19 pp.

18. Carlson, D. O. Process for Recovery of Copper From Cupriferous Ore. U. Pat. 2,730,493, Jan. 10, 1956.

19. Corrick, J. D., and J. A. Sutton. Copper Extraction From a Low-Grade by Ferrobacillus Ferrooxidans: Effect of Environmental and Nutriti Factors. BuMines Rept. of Inv. 6714, 1965, 21 pp.

20. Croasdale, Stuart. The Action of Iron Sulfides on Copper Solutions. and Min. J., v. 97, No. 15, 1914, pp. 745-748.

21. DeCuyper, J. A. Bacterial Leaching of Low Grade Copper and Cobalt Ore Pres. at ann. meeting, AIME, Dallas, Tex., February 1963, 21 pp.

22. Duggan, E. J. Ammonia Leaching at Kennecott. Trans. AIME, v. 106, 19 pp. 547-558.

23. _____. Flotation and Leaching at Kennecott. Eng. and Min. J., v. 12 No. 26, December 1928, pp. 1008-1015.

24. Duncan, D. W., P. C. Trussell, and C. C. Walden. Leaching of Chalcop rite With Thiobacillus Ferrooxidans: Effects of Surfactants and Sh ing. Applied Microbiology, v. 12, 1964, pp. 122-126.

25. Eddy, Lawrence. Ammonia Leaching of Copper Ores. Eng. and Min. J., v. 107, No. 26, June 1919, pp. 1162-1167.

26. Engineering and Mining Journal. Arizona Plant Raises Copper Product to 20,000 tpd. V. 166, No. 11, 1965, pp. 108-110.

27. _____. Cu Metal Formula: Rip and Leach. V. 167, No. 7, July 1966, pp. 84-85.

28. Fisher, J. R., F. C. Lendrum, and B. G. MacDermid. Laboratory and ground Studies of Bacterial Leaching of Elliot Lake Ores. Pres. meeting, AIME, New York, February 1966, 9 pp.

29. Fletcher, A. W., and D. S. Flett. Carboxylic Acids as Reagents for Solvent Extraction of Metals. Warren Spring Lab., Stevenage, Herts England, September 1965, 17 pp.

Fletcher, J. B. In Place Leaching, Miami Mine. Pres. at Arizona section meeting, Milling Div., AIME, Apr. 6, 1962, 9 pp.

Forward, F. A. Hydrometallurgical Process Yields Pure Metal Powders From Sulfides. J. Metals, v. 5, 1953, pp. 775-779.

_____. Method of Extracting Copper Values From Copper Bearing Mineral Sulfides. U.S. Pat. 2,822,263, Feb. 4, 1958.

Forward, F. A., and V. N. Mackiw. Hydrometallurgical Method of Extracting Metal Values. U.S. Pat. 2,726,934, Dec. 13, 1955.

Franz, M. W. Leach-Precipitation-Flotation Process. J. Metals, v. 11, No. 6, 1959, pp. 382-385.

Grunig, J. K. Some Factors of Ore and Solution Chemistry in the Heap Leaching of Copper Ores. Pres. at regional conf., Pacific Northwest Min. and Met., April 1966, 7 pp.

Guggenheim, M., and J. D. Sullivan. Acceleration of Extraction of Soluble Copper From Leached Ores. BuMines Tech. Paper 472, 1930, 30 pp.

Hermann, W. A. O. Method of Extracting Metal Values From Metal Bearing Material. U.S. Pat. 2,740,707, Apr. 3, 1956.

Hilliard, R. V., and C. T. Baroch. Process of Extracting and Recovering Metals by Leaching and Electrolysis. U.S. Pat. 2,655,472, Oct. 13, 1953.

Horton, F. E. Process and Apparatus for Treating Oxidized Copper Ores. U.S. Pat. 2,970,096, Jan. 31, 1961.

Hudson, A. W., and G. D. Van Arsdale. Heap Leaching at Bisbee, Arizona. Trans. AIME, v. 69, 1923, pp. 137-154.

Huttl, J. R. Anaconda Adds 5000-tpd Concentrator to Yerington Enterprise at Weed Heights. Eng. and Min. J., v. 163, No. 3, March 1962, pp. 74-81.

_____. How New Leach-Float Plant Handles Greater Butte's Ore. Eng. and Min. J., v. 154, No. 6, June 1953, pp. 90-93.

Ivanov, V. I., and F. I. Nagirnyak. Intensifying the Leaching of Copper-Sulfide Minerals With Thionine Bacteria. Tsvetn. Metal, v. 3, No. 8, 1962, pp. 33-38.

Jacky, Howard W. Copper Precipitation Methods and Concepts at Anaconda's Yerington Mine, Weed Heights, Nevada. Pres. at ann. meeting, AIME, New York, February 1966, 9 pp.

45. Kenny, H. C., and H. A. Abramson. Method of Leaching Copper Sulfide Materials With Ammoniacal Leach Solution. U.S. Pat. 2,727,818, Dec. 20, 1955.

46. Keyes, H. E. Innovations in Copper Leaching Employing Ferric Sulfate Sulfuric Acid. BuMines Bull. 321, 1930, 67 pp.

47. Kuznetsov, S. I., M. V. Ivanov, and N. N. Lyalikova. Introduction to Geological Microbiology. McGraw-Hill Book Co., Inc., New York, 1963, 252 pp.

48. Lower, G. W. Leaching of Copper From Ores With Cyanide and Recovery of Copper From Cyanide Solutions. U.S. Pat. 3,189,435, June 15, 1965.

49. Lower, G. W., and R. B. Booth. Cyanidation Studies: Recovery of Copper by Cyanidation. Pres. at ann. meeting, AIME, New York, February 1965, 26 pp.

50. _____. Recovery of Copper by Cyanidation. Min. Eng., v. 17, No. 11, November 1965, pp. 56-60.

51. Malouf, E. E., and J. D. Prater. Role of Bacteria in Alteration of Sulfide Minerals. Pres. at ann. meeting, AIME, St. Louis, Mo., February 1961, 18 pp.

52. _____. New Technology of Leaching Waste Dumps. Min. Cong. J., v. 48, No. 11, November 1962, pp. 82-85.

53. McGauley, P. J., and E. S. Roberts. Process for the Recovery of Copper From Its Ores and Minerals. U.S. Pat. 2,568,963, Sept. 25, 1951.

54. McKinney, W. A., and C. Rampacek. Acid Curing and Countercurrent Decantation Washing of an Oxidized Copper Ore From Pinal County, Ariz. BuMines Rept. of Inv. 5685, 1960, 10 pp.

55. _____. Acid Leaching of Oxidized Copper Ores by Downward Percolation. BuMines Rept. of Inv. 5629, 1960, 16 pp.

56. McMahon, A. D. Copper: A Materials Survey. BuMines Inf. Circ. 8225, 1965, pp. 105, 107.

57. Milliken, F. R., and R. Goodwin. Ohio Copper Company Tailings Retreatment Plant. Trans. AIME, v. 153, 1943, pp. 609-618.

58. Mining World. Agglomeration Proves Key to Low Cost Circulation Leach for High Recovery. V. 16, No. 8, July 1954, pp. 56-58.

59. Peters, E., and E. A. Hahn. The Precipitation of Copper From Aqueous Solutions by Hydrogen Reduction. Pres. at ann. meeting, AIME, Dallas, Tex., February 1963, 35 pp.

Power, Kenneth L. Copper Leaching at ASARCO's Silver Bell Unit, Arizona. Pres. at ann. meeting, AIME, Dallas, Tex., February 1963, 27 pp.

_____. Slimes Treatment Plants. Pres. at Arizona section meeting, Ore Dressing Div., AIME, Apr. 9, 1960, 3 pp.

Quarm, T. A. A. Recovery of Copper From Mine Drainage Water by Ion Exchange. Inst. Min. and Met. Bull. 577, 1954, pp. 109-117.

Ralston, O. C. The Ferric Sulfate-Sulfuric Acid Process. BuMines Bull. 260, 1927, 122 pp.

Razzell, W. E. Bacterial Leaching of Metallic Sulfides. Canadian Min. and Met. Bull. 55, 1962, pp. 190-191.

Schaufelberger, F. A. Precipitation of Metal From Salt Solution by Reduction With Hydrogen. Min. Eng., v. 8, 1956, pp. 539-548.

Scott, W. G. Leaching Copper Ores. U.S. Pat. 2,563,623, Aug. 7, 1951.

Seidel, D. C. Percolation Leaching. Colorado Sch. Mines Research Foundation, Inc., Golden, Colo., February 1963, 17 pp.

Spedden, H. R., E. E. Malouf, and J. D. Prater. Use of Cone-Type Copper Precipitators To Recover Copper From Copper-Bearing Solutions. Pres. at ann. meeting, AIME, New York, February 1966, 18 pp.

Sullivan, J. D. Chemical and Physical Features of Copper Leaching. Trans. AIME, v. 106, 1933, pp. 515-546.

_____. Chemistry of Leaching Bornite. BuMines Tech. Paper 486, 1931, 20 pp.

_____. Chemistry of Leaching Chalcocite. BuMines Tech. Paper 473, 1930, 24 pp.

_____. Chemistry of Leaching Covellite. BuMines Tech. Paper 487, 1930, 18 pp.

_____. Dissolution of Various Oxidized Copper Minerals. BuMines Rept. of Inv. 2934, 1929, 9 pp.

Sullivan, J. D., and K. O. Bayard. Extraction of Soluble Copper From Ores in Leaching by Percolation. BuMines Rept. of Inv. 3073, 1931, 43 pp.

Sullivan, J. D., and G. L. Oldright. Leaching Oxidized Copper Ores: Effect of Strength of Acid in Leaching Solvent. BuMines Rept. of Inv. 3106, 1931, 9 pp.

76. _____. The Dissolution of Cuprite in Sulfuric Acid and in Ferric Sulfate Solutions. BuMines Rept. of Inv. 2967, 1929, 9 pp.

77. Sutton, J. A., and J. D. Corrick. Bacteria in Mining and Metallurgy: Leaching Selected Ores and Minerals. Experiments With Thiobacillus Thiooxidans. BuMines Rept. of Inv. 5839, 1961, 16 pp.

78. _____. Microbial Leaching of Copper Minerals. Min. Eng., v. 15, No. 1963, pp. 37-40.

79. _____. Leaching Copper Sulfide Minerals With Selected Autotrophic Bacteria. BuMines Rept. of Inv. 6423, 1964, 23 pp.

80. Swanson, R. R., and D. W. Agers. A New Reagent for the Extraction of Copper. Pres. at ann. meeting, AIME, New York, February 1964, 17 pp.

81. Taylor, J. H., and P. F. Whelan. The Leaching of Cupreous Pyrites and the Precipitation of Copper at Rio Tinto, Spain. Inst. Min. and Met. Bull. 457, 1942, pp. 1-36.

82. Thomas, Robert W. Leaching Copper From Worked-Out Areas of the Ray Mi Arizona. Min. and Met., v. 19, 1938, pp. 481-485.

83. Van Arsdale, G. D. Hydrometallurgy of Base Metals. McGraw-Hill Book Inc., New York, 1953, pp. 11-16, 77-78.

84. _____. Leaching Mixed Copper Ores With Ferric Sulfate; Inspiration Copper Co. Trans. AIME, v. 73, 1926, pp. 58-83.

85. Van Barneveld, C. E., and E. S. Leaver. Leaching Nonsulfide Copper Ores With Sulfur Dioxide. BuMines Tech. Paper 312, 1923, 91 pp.

86. _____. The Sulfur Dioxide Leaching Process. BuMines Rept. of Inv. 1922, 14 pp.

87. Zimmerley, S. R., D. G. Wilson, and J. D. Prater. Cyclic Leaching Process Employing Iron Oxidizing Bacteria. U.S. Pat. 2,829,964, Apr. 1958.

BIBLIOGRAPHY

1. Aannerud, S. A. Process for Total Treatment of Copper-Containing Iron Pyrites. U.S. Pat. 2,653,905, Sept. 29, 1953.

2. Amenabar, A. Process of Treating Copper Ores. U.S. Pat. 2,357,990, Sept. 12, 1944.

3. American Cyanamid Co. Extraction of Copper. British Pat. 986,299, Mar. 17, 1965.

4. Arbiter, Nathaniel. Oxidized Copper-Part III. Eng. and Min. J., v. 158, No. 3, March 1957, pp. 80-85.

5. Argall, G. O., Jr. How Leaching Recovers Copper From Waste and Leach Dumps in Southwest. Min. World, v. 25, November 1963, pp. 20-24.

6. _____. Leaching Dumps To Recover More Southwest Copper at Lower Cost. Min. World, v. 25, October 1963, pp. 22-27.

7. Austin, W. L. Leaching Copper Products at the Steptoe Works. Trans. AIME, v. 49, 1914, pp. 668-670.

8. _____. The Treatment of Copper Ore by Leaching Methods. Trans. AIME, v. 49, 1914, pp. 659-667.

9. Beall, John V. Southwest Copper - A Position Survey. Min. Eng., v. 17, No. 10, October 1965, pp. 77-92.

10. Bell, G. A. Leaching Practice and Costs at the New Cornelia Mines of the Calumet and Arizona Mining Co., Ajo, Ariz. BuMines Inf. Circ. 6303, 1930, 29 pp.

11. Benedict, C. H. Methods and Costs of Treatment at the Calumet and Hecla Reclamation Plant. BuMines Inf. Circ. 6357, 1930, 11 pp.

12. Blasket, K. S. Sulfide Copper Ores and Their Poor Relations - the Carbonates. Chem. Eng. Min. Rev. 43, 1951, pp. 447-451.

13. Bogart, J. R. New Leach Plant Ups Bagdad's Copper Production by 67 Percent. Min. World, v. 23, August 1961, pp. 26-28.

14. Byerley, J. J., and E. Peters. The Reduction of Cupric Salts in Aqueous Solutions by Carbon Monoxide. Pres. at ann. meeting, AIME, Dallas, Tex., February 1963, 30 pp.

15. Callaway, L. A., and F. N. Koepel. The Metallurgical Plant of the Andes Copper Mining Company at Potrerillos, Chile. Trans. AIME, v. 106, 1933, pp. 678-728.

16. Campbell, T. C. A Brief Description of the Reduction Plant of the Chi... Exploration Company at Chuquicamata, Chile, S. A. Trans. AIME, v. 10... 1933, pp. 559-608.

17. Chemical Construction Corp. Leaching of Non-Ferrous Metals From Ores... Containing Metalloids. British Pat. 797,607, July 2, 1958.

18. Cloke, F. Natural Acidity and Copper Precipitation. Min. Mag., v. 76... 1947, pp. 211-212.

19. Croasdale, Stuart. Leaching Experiments on the Ajo Ores. Trans. AI... v. 49, 1914, pp. 610-658.

20. Dennis, W. H. Recovery of Copper by Leaching. Mine and Quarry Eng.... v. 36, 1947, pp. 140-146.

21. Fetscher, C. A. Extraction of a Metal From Solutions Containing Same. U.S. Pat. 3,088,798, May 7, 1963.

22. Franklin, J. W. Oxidized Copper-Part I. Eng. and Min. J., v. 157, No... July 1956, pp. 97-103.

23. _____. Oxidized Copper-Part II. Eng. and Min. J., v. 157, No. 8, Au... 1956, pp. 80-85.

24. Frick, F. F. Sponge Iron Used as a Precipitant for Copper. J. Metals... v. 5, 1953, p. 395.

25. Groves, R. D. Preparation of Copper Powder From Leach Solutions Afte... Precipitation With Iron. BuMines Rept. of Inv. 6486, 1964, 23 pp.

26. Hansen, Spenst M. Nuclear Blasting for Mining and Leaching. World Mi... v. 18, No. 10, September 1965, 9 pp.

27. Hazen, W. C. Hydrometallurgical Process. U.S. Pat. 2,954,276, Sept... 1960.

28. Heinink, C. J., G. G. Olson, and J. T. Long. Gewinnung von Kupfer a... kupferhaltigan wasarigen Losungen (Recovery of Copper From Copper C... taining Aqueous Solutions). German Pat. 1,142,443, Jan. 17, 1963.

29. Hermann E., and G. Thomas. Verfahren zur Gewinnung von Kupfer aus K... erzen (Process for the Recovery of Copper From Copper Ores). Germa... Pat. 1,020,795, Dec. 12, 1957.

30. Horton, F. E., and E. C. Brace. Method of Recovering Cuprate Anions... Their Metal Salt Solutions. U.S. Pat. 2,970,036, Jan. 31, 1961.

31. Huttl, J. R. Cement Copper Begins at Bagdad. Eng. and Min. J., v. ... No. 6, June 1961, pp. 86-88.

Jackson, K. J., and J. D. H. Strickland. The Dissolution of Sulfide Ores in Acid Chlorine Solutions: A Study of the More Common Sulfide Minerals. Trans. AIME, v. 212, 1958, pp. 373-379.

Jacobi, J. S. The Recovery of Copper From Dilute Process Streams. Pres. at ann. meeting, AIME, Dallas, Tex., February 1963, 38 pp.

Johnson, P. H. Acid-Ferric Sulfate Solutions for Chemical Mining. Min. Eng., v. 64, August 1965, pp. 64-68.

Junghanss, H., G. Henrich, and W. Hoffman. Verfahren zur Gewinnung von Kupfer aus Losungen (Process for the Recovery of Copper From Solutions). German Pat. 1,153,907, Sept. 5, 1963.

Keller, C. H. Recovery of Copper From Copper-Bearing Solutions. U.S. Pat. 2,390,540, Dec. 11, 1945.

Kenny, H. C., and H. A. Abramson. Ammoniacal Leaching Process. U.S. Pat. 2,687,953, Aug. 31, 1954.

Keyes, H. E. Can Leaching Aid the Copper Mines? J. Metals, v. 1, No. 12, 1949, pp. 29-31.

Kuzell, C. R., M. G. Fowler, J. H. Davis, L. Klein, and I. MacDougall. Method for Producing Sponge Iron. U.S. Pat. 3,125,439, Mar. 17, 1964.

Laist, F., and H. W. Aldrich. Experimental Leaching at Anaconda. Trans. AIME, v. 49, 1914, pp. 671-690.

Lichtenwalter, M. Separation of Copper. U.S. Pat. 2,440,612, Apr. 27, 1948.

Lyle, A. G. Production of Copper Sulfate From Mine Water Precipitate. Can. Min. Met. Bull. 475, 1951, pp. 715-716.

Maier, C. G. Sponge-Iron Experiments at Mococo. BuMines Bull. 396, 1937, 81 pp.

Majima, H., and E. Peters. Oxidation Rates of Sulfide Minerals by Aqueous Oxidation at Elevated Temperatures. Pres. at ann. meeting, AIME, New York, February 1966, 25 pp.

McGauley, P. J., and E. S. Roberts. Verfahren zur Gewinnung von Kupfer (Process for the Recovery of Copper). German Pat. 864,918, Dec. 11, 1952.

Mitchell, David W. Study of Precipitation of Copper on Iron From Acid Solutions. New Mexico State Bur. Mines and Min. Res., Circ. 86, 1966, 5 pp.

47. Monninger, F. M. Precipitation of Copper on Iron. Min. Cong. J., v. 4
October 1963, pp. 48-51.

48. Morse, H. W., and H. A. Tobelmann. Leaching Tests at New Cornelia.
Trans. AIME, v. 55, 1916, pp. 830-855.

49. Nadkarni, R. M., C. E. Jelden, K. C. Bowles, H. E. Flanders, and M. E.
Wadsworth. A Kinetic Study of Copper Precipitation on Iron - Part
Pres. at ann. meeting, AIME, New York, February 1966, 17 pp.

50. Oldright, G. L., H. E. Keyes, V. Miller, and W. A. Sloan. Precipitati
of Lead and Copper From Solution on Sponge Iron. BuMines Bull. 28
1928, 131 pp.

51. O'Leary, V. D. Clarification and Treatment of Mine Drainage Water Pri
To Use for Dump Leaching in Butte. Pres. at ann. meeting, AIME,
New York, February 1966, 13 pp.

52. Orkla Grube-Aktiebolag. A Process for the Treatment of Copper-Contain
Iron Pyrites. British Pat. 650,202, Feb. 14, 1951.

53. Parker, G. W. Leach Dump Operation in Butte, Montana. Pres. at regio
conf., Pacific Northwest Min. and Met., April 1966, 7 pp.

54. Ricketts, L. D. Some Problems in Copper Leaching. Trans. AIME, v. 52
1915, pp. 737-764.

55. Roberts, E. S. Precipitation of Pure Metallic Copper From Copper-Bear
Solutions. U.S. Pat. 2,647,825, Aug. 4, 1953.

56. Schlecten, A. W., and J. L. Bruce. New Acid-Leaching Section Raises
Cyprus Copper Recovery by 10%. Eng. and Min. J., v. 153, No. 12,
pp. 88-91.

57. Sherritt Gordon Mines Ltd. Improved Method of Extracting Copper Val
From Material Containing Copper. British Pat. 791,916, Mar. 12,

58. Silo, R. S. A New Process for Oxidized Ore of Copper by Leaching.
at ann. meeting, AIME, Chicago, Ill., February 1965, 20 pp.

59. Sobiev, B. M., and L. V. Khodov. Copper Obtainable by Underground L
ing: An Important Reserve. Zeitshrift fur angewandte Geologie, V
No. 6, 1964, pp. 303-304.

60. Stanczyk, M. H., and C. Rampacek. Oxidation Leaching of Copper Sulfi
in Acidic Pulps at Elevated Temperatures and Pressures. BuMines R
of Inv. 6193, 1963, 15 pp.

61. Straschil, Heinrich. Verfahren zur Gewinnung von Kupfersalzlaugen a
Kupferhaltigen Schwefelerzen (Process for the Recovery of Copper S
From Copper-Containing Sulfide Ores). Austrian Pat. 176,023, Feb.
1953.

Sullivan, J. D. Factors Involved in the Heap Leaching of Copper Ores. BuMines Inf. Circ. 6425, 1931, 12 pp.

Sullivan, J. D., W. E. Keck, and G. L. Oldright. Factors Governing the Entry of Solutions Into Ores During Leaching. BuMines Tech. Paper 441, 1929, 38 pp.

Sullivan, J. D., and E. O. Ostrea. Factors Governing the Entry of Solutions Into Ores During Leaching. BuMines Tech. Paper 498, 1931, 23 pp.

Sullivan, J. D., and A. J. Sweet. Factors Governing Removal of Soluble Copper From Leached Ores. BuMines Tech. Paper 453, 1929, 26 pp.

Sullivan, J. D., and A. P. Towne. Agglomeration and Leaching of Slimes and Other Finely Divided Ores. BuMines Bull. 329, 1930, 60 pp.

_____. Leaching Copper Ores: Advantages of Wet Charging. BuMines Rept. of Inv. 3050, 1930, 26 pp.

Thomsen, A. M. Process of Recovering Metal Values From Leach Liquors. U.S. Pat. 2,670,271, Feb. 23, 1954.

Tobelmann, H. A., and J. A. Potter. First Year of Leaching by the New Cornelia Copper Co., Trans. AIME, v. 60, 1919, pp. 22-77.

Toll, R. W. Copper Recovery From Low-Grade Waters. Min. Mag. 77, 1947, pp. 83-84.

Velichkin, A. N. On the Possibility of Processing Virgin Ore Pillars by a Subsurface Leaching Method. Tr. Inst. Gornogo Dela, Akad Nauk Kaz. SSR 12, 1963, pp. 159-163.

Walsh, C. L., and B. A. Adams. An Improved Process for the Recovery of Metal Ions From Solutions. British Pat. 641,918, Aug. 23, 1950.

Wartman, F. S., and A. H. Roberson. Precipitation of Copper From Acid Mine Water. BuMines Rept. of Inv. 3746, 1944, 16 pp.

Weed, R. C. Cananea's Program for Leaching In Place. Min. Eng., v. 8, 1956, pp. 721-723.

West, W. F. Verfahren zur Extraktion von Kupfer aus Erzen (Process for the Extraction of Copper From Ores). German Pat. 1,149,173, May 22, 1963.

Wheeler, A. E., and H. Y. Eagle. Development of the Leaching Operations of the Union Minière du Haut Katanga. Trans. AIME, v. 106, 1933, pp. 609-649.

* U.S. GOVERNMENT PRINTING OFFICE : 1968 O—275-661

Copper leaching with cyanide—

A review of five inventions

Metal recovery from low-grade copper bearing materials and solutions — which are not otherwise amenable to known processing techniques — may provide the metallurgical breakthrough for low cost extraction

FIVE PATENTED cyanide-leaching techniques raise hopes of milling men with the promise of a breakthrough for producing a high-grade copper product from low-grade ores, copper bearing materials and solutions. Other claims of these inventions include lower operating costs, smaller capital requirements, economical reagent recovery and a method for treating refractory ores which are now considered waste.

Cyanide for these processes is supplied to industry in the form of white sodium cyanide, crude calcium cyanide and hydrogen cyanide (hydrocyanic acid). Based on gram mol equivalents, white cyanide contains 50 to 53% active leaching ingredients, calcium cyanide 48 to 50%, and HCN about 96%.

Although only the following procedures are described, it is E/MJ's understanding that other cyanide leaching systems for copper with even greater potential are in the works. When these become available E/MJ will publish the related information.

1—Winning copper from solutions with HCN and SO_2

Edward S. Roberts, in U.S. Patent 3,321,303 (assigned to Treadwell Corp.), describes his novel and continuous method for recovering red metal from solutions containing copper salts with hydrocyanic acid (HCN). His principal objective is to recover substantially pure copper at a cost more economical than that for copper produced by electrowinning and cementation, and in most instances at less than that by smelting and electrorefining.

Typical solutions which may be treated following Roberts' directions could be derived from sulphuric acid leaching of oxidized copper ores or copper bearing materials; from mine waters; from leaching, roasted copper sulphide concentrates or from scrap metal containing copper.

A modification of this invention replaces HCN with crude hydrogen cyanide (HCN burner gases produced by the Andrussow process, U.S. Patent 1,934,838). Reactions by either route can be represented as:

Step 1

$$2CuSO_4 + 2HCN + SO_2 + 2H_2O \rightarrow 2CuCN + 3H_2SO_4$$

or

$$CuSO_4 + 2HCN + CU \rightarrow 2CuCn + H_2SO_4$$

Step 2

$$2CUCN + H_2 \rightarrow 2Cu + 2HCN$$

In general, the inventor carries out the first step at below 100° C, precipitates CuCN by reacting HCN with the copper salts in an acid medium (pH 0 to 4), and converts the copper present to its cuprous state with sufficient reducing material. Since CuCN is extremely insoluble in H_2SO_4 its recovery in this first step approaches the theoretical limit. Copper so produced is a finely divided precipitate which may be separated from the barren liquor by any conventional method.

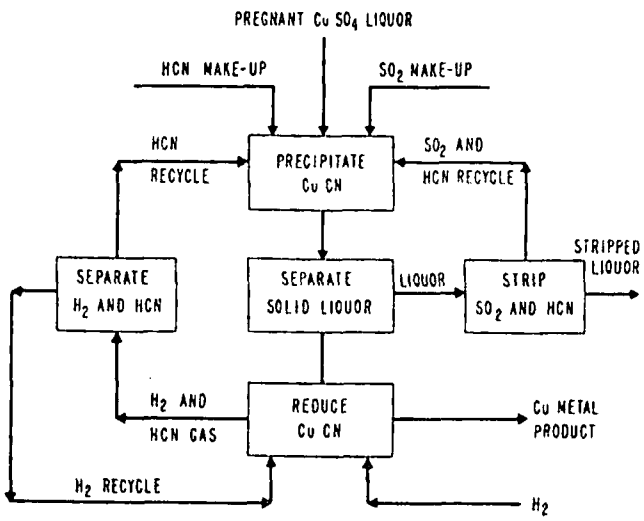

Continuous process for winning pure copper metal using HCN and SO_2. These reductants are regenerated to save on costs.

According to the inventor, to maintain a satisfactory reaction rate and limit cyanide decomposition to an acceptable minimum, metal reduction is preferably conducted between 300° to 400°C.

High quality copper (99.8%) is recovered in quantitative amounts and, at the same time, relatively pure HCN is regenerated for recycling. The production of relatively pure Cu metal and HCN by this method is unique and recovery ranges from 65 to 100% of the copper. Attempts by the researcher at reducing other metal cyanides to metal or at recovering HCN with hydrogen reaction were dismally unsuccessful, Roberts says.

Alternate reducing agents may be used but under present economic conditions only two SO_2 and recycled copper powder from the second step are attractive. When using SO_2, as an alternate reductant, facilities must be provided to dispose of or use the dilute and impure H_2SO_4 made.

Typically, leach liquors should contain from 1 to 50 g of copper per liter, which require at least 60% of the stoichiometric amount of HCN for the reaction. When using SO_2 as an alternate reagent, a convenient method of operation is to maintain a substantially saturated SO_2 solution, thereby minimizing the effect of this reagent being consumed by reducible salts other than cupric sulphate. For example, ferric sulphate would require SO_2 for the ferric to ferrous conversion according to this equation:

$$Fe_2(SO_4)_3 + SO_2 + 2H_2O \rightarrow Fe_2(SO_4)_2 + 2H_2SO_4$$

Cupric sulphate reacts in this manner:

$$2CuSO_4 + SO_2 + 2HCN + 2H_2O \rightarrow 2CuCN + 3H_2SO_4$$

Thus, this invention provides a novel process for producing a relatively pure cuprous cyanide from leach liquors.

2—Cyanide treatment of 0.2 to 0.8% copper ore

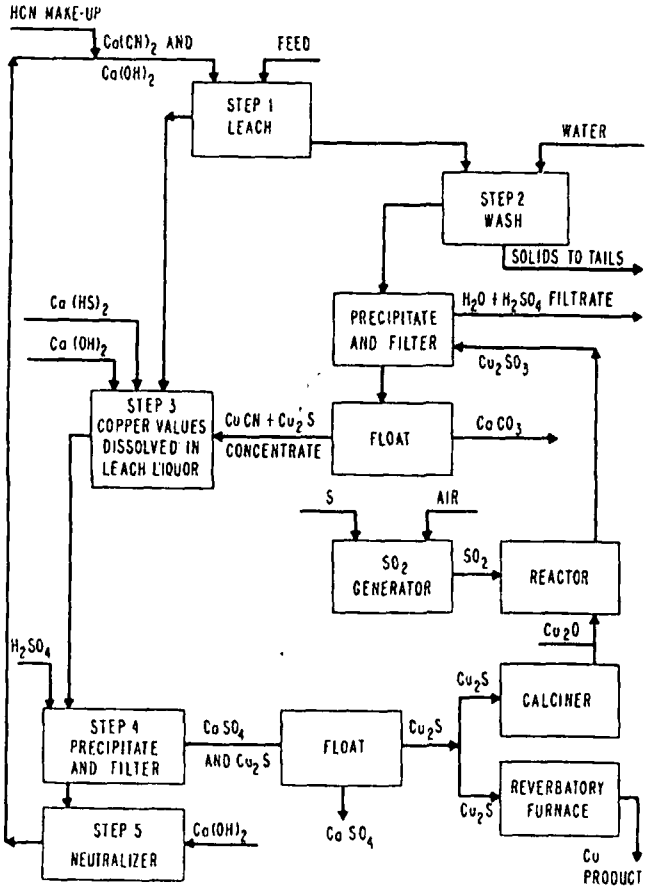

Metal of exceptionally high purity is claimed for process since solution impurities do not enter and contaminate Cu.

Tailings, overburden and other low-grade copper sulphide materials, including ores—associated with an alkaline gangue—and also having some of these characteristics: A low copper concentration (0.2 to 0.8% Cu metal content), a fine particle size, and a widely disseminated mineralization are claimed to be economically processed by the teachings of a new patent (U.S. 3,303,021).

The inventor, E. S. Roberts, Treadwell Corp., says that the specifications call for metal recovery from a copper-bearing material by an alkaline cyanide leaching step, but, for the process to be economically attractive, the copper values and the cyanide adhering to the solids must be recovered.

The initial step, leaching with an alkaline cyanide medium, produces a leach liquor of soluble calcium copper complex and calcium sulfhydrate ($Ca(HS)_2$), which is separated from the solids. These reactions occur:

$$2Cu_2S + 5Ca(OH)_2 + 16HCN \rightarrow 4CaHCu(CN)_4 + Ca(HS)_2 + 10H_2O$$
$$2Cu_2S + 5Ca(CN)_2 + 6HCN \rightarrow 4CaHCu(CN)_4 + Ca(HS)_2$$
$$2Cu_2S + 8Ca(CN)_2 + 6H_2O \rightarrow 4CaHCu(CN)_4 + Ca(HS)_2 + 3Ca(OH)_2$$
$$2HCN + Ca(OH)_2 \rightarrow Ca(CN)_2 + 2H_2O$$

Following this initial reaction, the solids produced are washed with water and sent to tails, the copper and cyanide values are recovered by reacting the wash liquor with either cuprous sulphite or sulphate and sulphur dioxide to precipitate cuprous cyanide and cuprous sulphide. These reactions occur:

$$4CaHCu(CN)_4 + Ca(HS)_2 + 8Cu_2SO_3 \rightarrow 16CuCN + 2Cu_2S + 5CaSO_4 + 3H_2SO_3$$
$$4CaHCu(CN)_4 + Ca(HS)_2 + 16CuSO_4 + 8SO_2 + 16H_2O \rightarrow 16CuCN + 2CU_2S + 5CaSO_4 + 19H_2SO_4$$

After this, the complex precipitate is separated from the wash solution and dissolved in the leach liquor with the simultaneous introduction of $Ca(OH)_2$ and $Ca(HS)_2$ to form soluble calcium copper cyanide in the following manner:

$$2CaHCu(CN)_4 + 4CuCN + Ca(OH)_2 \rightarrow 3CaCu_2(CN)_4 + 2H_2O$$

In step four, the loaded solution from step 3 is reacted with H_2SO_4 to precipitate Cu_2S and $CaSO_4$ as shown below:

$$2CaCu_2(CN)_4 + 3H_2SO_4 + Ca(HS)_2 \rightarrow 2Cu_2S + 3CaSO_4 + 8HCN$$
$$4CaHCu(CN)_4 + 6H_2SO_4 \rightarrow 2Cu_2S + 4CaSO_4 + 16HCN + 4O_2$$
$$Ca(HS)_2 + H_2SO_4 \rightarrow CaSO_4 + 2H_2S$$

The components of this precipitate are separated by flotation (using pine oil as a frother and secondary butyl xanthate as a promoter) sending the $CaSO_4$ to waste, or a separate dump, and the Cu_2S is converted to a relatively pure copper by any conventional method.

The last step involves the neutralization of the filtrate from step four with calcium hydroxide. The resulting solution is recycled as the alkaline cyanide leaching medium. These equations apply to this step:

$$2HCN + Ca(OH)_2 \rightarrow Ca(CN)_2 + 2H_2O$$
$$H_2SO_4 + Ca(OH)_2 \rightarrow CaSO_4 + 2H_2O$$

Make-up HCN is added to this alkaline cyanide leaching medium to provide the necessary strength for reaction with the copper content of the ore.

All of the steps are conducted at ambient temperatures and atmospheric pressures in either open air, or in adequately ventilated enclosures. Under these conditions, the highly toxic hydrocyanic acid (HCN) gas concentration should not present a problem.

Reagents used in the various steps are added in stoichiometric amounts. Per mol of recoverable copper in the ore, about 4 mols HCN (most of which is regenerated and recycled), about 0.5 mols of H_2SO_4 and about 2 mols of calcium hydroxide are needed.

3—Alkaline cyanide leaching of refractory copper ore

Claimed as an improved method for recovering cuprous sulphide material, a recent invention (U.S. Patent 3,224,835, assigned to Copper Range Co. by W. A. Hockings, D. H. Rose, and A. M. Gaudin), involves leaching with alkaline cyanide solutions at a pH above 7.4 to dissolve the metal content, followed by pH adjustment to below 7.4 whereby cuprous sulphide is precipitated with the addition of SO_2 or other acid. All reactions are conducted under non-oxidizing conditions, according to the inventors. End solution from the process is then treated with lime to regenerate the alkaline cyanide leach solution which is recycled.

An advantageous system for utilizing the invention involves percolation leaching of low-grade copper bearing flotation tailings. The feed are the tails remaining after removing a concentrate from an ore consisting mainly of chalcotite. This aqueous pulp typically contains 25% by weight of solids measuring 100% —325-mesh. The copper content, about 0.15% by weight of solids, is said to be too low in grade to be economically recovered by any known

commercial method now in operation.

In the first step, a sand-slime separation is made and the slimes are discarded. The thickened sands are passed to a closed leaching tank, and are subjected to a downward percolation leach under non-oxidizing conditions with the cyanide solution.

Any low strength leach solution from the reactor may be transferred to the recycle solution tank for reuse. When copper concentration in the pregnant liquor approaches the saturation level (5.5 gpl of Cu) it is collected in the rich solution storage tank. Thereafter, the leach tank charge is washed and its effluent (1.2 gpl Cu and 2.5 gpl CN) is passed to the ends solution tank. This leach step extracts up to 85% of the copper and allows the operators to discard the tails.

Leach solution percolation rates are speeded by applying a vacuum to the bottom of the leach tank. Maximum possible recovery of cyanide, gases and vapors withdrawn by the pump are collected with milk of lime in a scrubber.

End solution and rich solution is treated separately. Rich solution from storage is passed through a battery of rich precipitation vessels arranged in series. During this operation CO_2 gas is bubbled through the reactors countercurrent to the flow of pregnant liquor. Leach solution at this time decreases in pH from 10.5 to 5.7 and, at the same time, about 60% of the copper and 70% of the calcium present is precipitated as cuprous sulphide and $Ca(CO_3)_2$, respectively.

Off-gases from these reactors are vented to scrubber 2, where CO_2 and HCN are absorbed in milk of lime.

From the last reactor, the complex slurry is thickened in a hydrocyclone and dewatered further by filter 1, before being sent to the smelter for further processing.

The vortex discharge from hydrocyclone 2 is substantially free from solids and is delivered to the recycle solution tank for storage and later use.

Solution from filter 1 passes next to the cleanup precipitation equipment for further reagent recovery.

End solution is treated essentially the same as the rich solution, but liquor from its hydrocyclone dewatering step passes to cleanup precipitation for chemical regeneration. Off-gases from the precipitation reactors are also passed to scrubber 2 for the recovery of CO_2 and HCN.

CO_2 and N_2 for the process is advantageously obtained from flue gases derived from burning carbonaceous matter.

The N_2 so produced purges the leach tanks while they are being charged to maintain a non-oxidizing atmosphere.

In the reagent cleanup system the combined solution is adjusted in pH to 2.5 with H_2SO_4. Simultaneously, sodium hydrosulphide is injected to build up sulphide ion concentration and precipitate cuprous sulphide. This step is not essential, but it does eliminate recycling dilute copper and cyanide bearing solutions, and increases somewhat copper recovery.

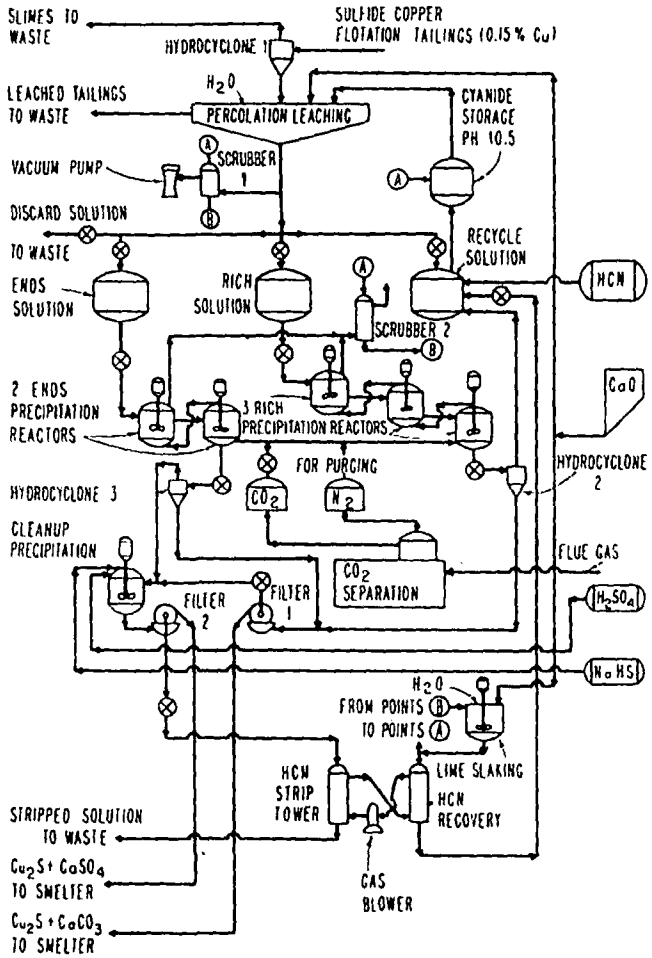

The above process is considered by the inventor to be advantageous for treating low-grade copper bearing tailing.

In the final step, HCN is stripped for reuse from filtrate discharged from filter 2.

Recent pilot plant tests indicate that an overall copper recovery of 91.7% can be obtained using this process. At the same time, consumption of reagents per pound of copper recovered would be 0.362 lb NaCN, 2.06 lb lime, 3.60 lb spent sulphuric acid, and 0.099 lb sodium bisulphide. Cost-wise this represents 9 to 10¢ per lb of copper recovered. Pilot tests also indicate that much of the previously wasted copper in flotation tails (14-million lb annually) can be recovered profitably, but capital costs for such a plant are estimated to be from 50 to 100% higher than for an equivalent sized flotation plant. For comparison, $1,300 to $1,400 per ton of material treated is required to build a cyanide plant.

4—Cyanide solutions remove copper films from gangue

A cyanide system reported on in E/MJ, August 1965, has been designed (U.S. Patent No. 3,189,435 by George William Lower, assigned to American Cyanamid Co., Stamford, Conn.) to recover copper from tailings and other low-grade sources economically. Previous methods were uneconomical because leaching time was high and reagent consumption too costly.

Key to the new process is a critically modified leaching cycle. Leaching time has been reduced from 48 hours to periods of 4 hours or less. Instead of directly acidifying the cyanide solution containing soluble copper (as in previous processes), the solution is first treated with a critical deficiency of soluble sulphide prior to acidification. By this method, 75% or more of the copper values can be recovered, and cyanide losses are low.

Cyanide losses are low because only a limited quantity of the cyanide is converted to thiocyanate, and copper is precipitated as a sulphide rather than the cyanide. This prevents cyanide decomposition and loss, and permits cyanide recovery and recycling for further use.

The following chemical equations show (1) the sequence of reactions which take place in the older, less efficient extraction processes, and (2) the reactions for the newly patented process where copper is precipitated as a sulphide, and the cyanide is available for recycling.

Copper minerals leach time — a comparison

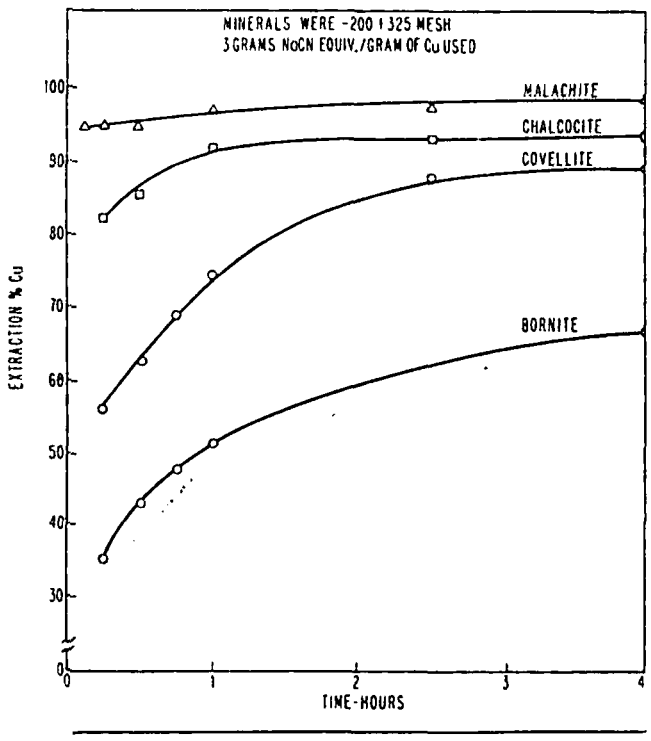

1) $$2Cu_2S + 11NaCN + 2\tfrac{1}{2}O_2 + H_2O \rightarrow 2NaCu(CN)_2 + 2Na_2Cu(CN)_3 + NaCNS + Na_2SO_4 + 2NaOH$$

2) $$Cu_2S + 6CN^- = 2Cu(CN)_3^- + S^-$$
$$2Cu(CN)_3^- + S^- + 3H_2SO_4 \rightarrow Cu_2S + 6HCN + 3SO_4^-$$

Cyanidation can be effected by inorganic cyanides such as hydrocyanic acid, sodium cyanide, potassium cyanide or calcium cyanide or mixtures of them; or organic products such as lactonitrile (considered a by-product from acrylonitrile processing). Useful ratio of cyanide reagent to copper (based in NaCN equivalent) is about 2½ to 4 moles of cyanide per mole of copper extracted. It is critical that cyanidation conditions be maintained for no longer than a few hours, and preferably for less than 90 minutes. The cyanide must be added in stages. Any soluble sulphide may be used to precipitate the copper from the cyanide solution.

The accompanying table shows batch leach tests for various tailings and mill products. Leaching time was one hour. In one 500-g test on a cleaner tailing running 1.077% Cu, 75.9% of the total copper present was recovered as a sulphide precipitate assaying 16.95% Cu. Of the total cyanide used, 94.4% was regenerated. Cyanide consumed was 0.2 lb of NaCN equivalent per pound of copper recovered. The patent claims that this method can be used on tailings which are being discarded at a rate of 4,000 tpd at one western copper mine, and that the patented method could be used to recover 60,000 lb of copper now going to waste per day.

Three cyanide extractants give good yields

Test	Type	Percent Cu	Percent total copper recovered	Pounds used per pound of copper recovered: NaCN equiv.	Pounds used per pound of copper recovered: Precipitant equity NaHS equiv.
1.	Copper ore	1.07	84.7	0.3	0.26
2.	Concentrate from slime flotation	2.14	76.2	0.2	0.25
3.	Slime fractions cycloned from rougher flotation tailings	0.58	71.1	0.25	0.21

Test 1: Sodium cyanide used as extractant; sodium sulphide used as precipitant.
Test 2: Lactonitrile used as extractant; calcium sulphide used as precipitant.
Test 3: Hydrocyanic acid with lime used as extractant; hydrogen sulphide used as precipitant.

5—A cyanide system for oxide or mixed oxide-sulphide ores

Another invention, similar to the first Roberts' patent, claims certain advantages over the more commonly used techniques of electrolytic and cementation recovery from copper bearing solutions. This invention, assigned to Dow Chemical Co., was issued as U.S. Patent 2,390,540 on Dec. 11, 1945, and was first publicized in E/M.J. June 1966.

According to C. H. Keller, the inventor, his method is more economical in reagent consumption, and requires a smaller capital outlay than other operational modes for recovery of copper present in mine and mill solutions. The process can be applied equally well to acid or neutral liquors, the reagents can be regenerated and recycled, copper can be completely extracted from solution in almost theoretical quantities, and copper of smelter grade can be produced.

His method is based on the precipitation of cupric ions from cold or warm solutions as cuprous thiocyanate. The cuprous thiocyanate precipitate is then treated with a soluble alkaline agent converting it to soluble thiocyanate and leaving an insoluble copper compound as a residue.

In practice, SO_2, sulphites, bisulphites, Zn, Fe, or any mixture of these materials acts as the reductant. The basic chemistry underlying this method is:

1) $$2CuSO_4 + H_2SO_3 + 2NH_4CNS + H_2O \rightarrow 2CuCNS + (NH_4)_2SO_4 + 2H_2SO_4$$

2) $$2CuCNS + 2NaOH \rightarrow Cu_2O + 2NaCNS + H_2O$$

3) $$2CuCNS + CA(OH)_2 \rightarrow Cu_2O + Ca(CNS)_2 + H_2O$$

Interesting developments include a system of electrometric control for regulating addition of thiocyanate to leach liquor, and a system for controlling the color of cuprous oxide for use as a paint pigment when NaOH is used for conversion. Also significant is this reaction of the Cu_2O produced in equation (1) with sulphuric acid:

$$Cu_2O + H_2SO_4 \rightarrow CuSO_4 + Cu + H_2O$$

By this reaction some of the copper can be routed for copper powder work or smelted to bars while half goes to copper sulphate for the tank house.

On mixed copper ore ground to 66% — 200-mesh tests similar to the flow scheme on the opposite page were conducted, and typical results indicated a sulphide copper recovery between 93.5 and 96.0%, an oxide copper recovery between 86.1 and 88.0%, an overall copper recovery between 91.4 and 92.6%, and thiocyanate recovery between 97.0 and 97.2%.

In the practice of this invention, the flow schemes used can vary considerably but still employ the basic principles of the thiocyanate process. Dow Chemical Co. carried out extensive laboratory work, and some of the systems it tried were sulphide flotation, followed by acid leaching; acid leaching, followed by sulphide flotation; a cycle test of sulphide flotation, followed by acid leaching; and flotation of CuCNS from ore pulps. All tests normally gave over 91.0% total copper recovery and, at the same time, allowed at least 97.0% of the thiocyanate to be regenerated for reuse.

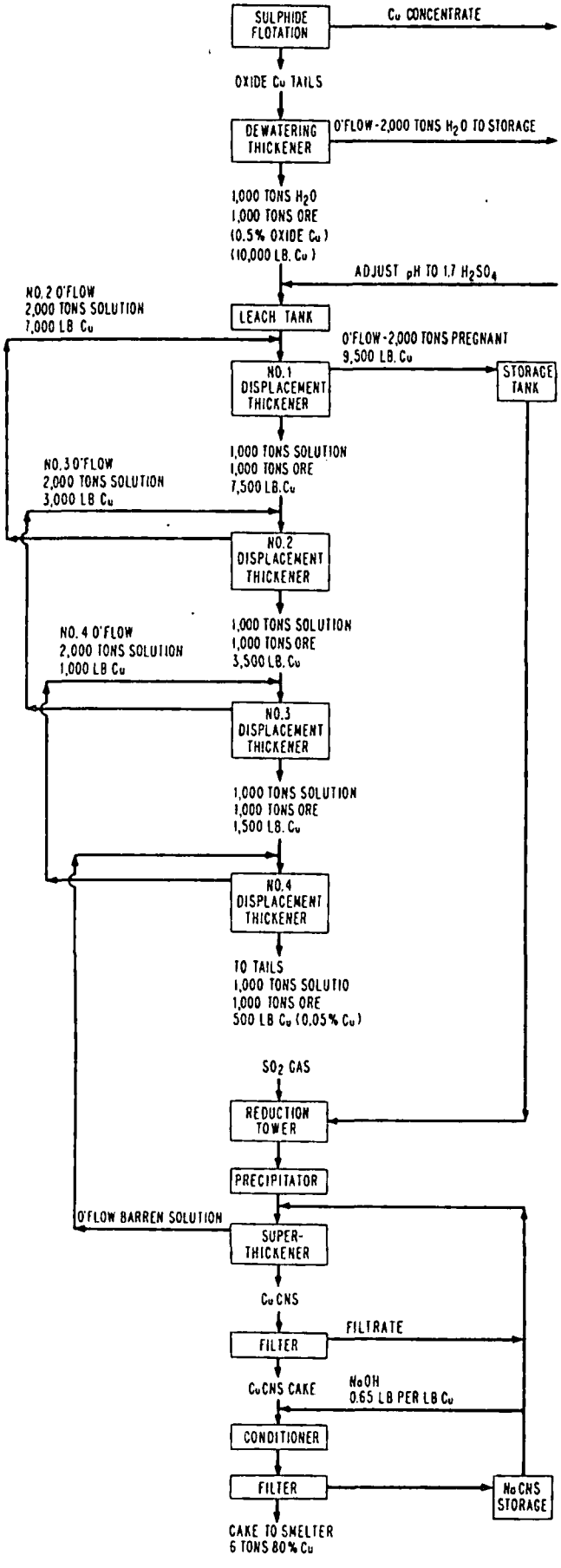

The Keller system recovers over 90% of the thiocyanate used by regeneration with lime, caustic soda or potash, or soluble alkali sulphides. Process also works on acidic copper bearing solutions.

A word of caution:

For the safe handling, storage and use of hydrocyanic acid (HCN)

Essential information for safe handling and use of hydrocyanic acid (HCN) contained in the Chemical Data Sheet SD-67 (Manufacturing Chemists Association Inc. (MCA), 1825 Connecticut Ave. N.W., Washington 9, D.C.) states that 96% strength HCN liquid is classified by the Interstate Commerce Commission (ICC) as a Class A poison. Poisoning results from inhalation, from swallowing, and from contact with mucous membranes or with skin.

Explosive over wide mixture range

HCN (also known as prussic acid and hydrogen cyanide) is flammable, it can be ignited by an open flame, hot surface, or spark, and it forms explosive mixtures in quantities between 6 and 41% by volume in air.

Threshold limit low for workers

The maximum atmospheric concentration (threshold limit) of hydrocyanic acid to which workers may be exposed for an eight-hour day without injury to health is generally accepted as 10 ppm by volume.

Solution only mildly corrosive

Stabilized HCN is only mildly corrosive but, because of its highly toxic nature, Type 316 stainless steel piping and fittings have proven more satisfactory for handling it. Teflon (tetrafluorethylene) gaskets have also performed satisfactorily in this application.

Shipping controlled by ICC regulations

Handling and storage of HCN presents some unusual restrictions too. The liquid product must be shipped in either ICC approved steel cylinders or tank cars. The tank cars must also be equipped with cork insulation at least four inches in thickness.

Storage requires refrigeration

Stored HCN should be maintained between 5° and 10° C by recirculation through an external heat exchanger. Freon refrigeration units are usually used.

For complete information on this subject, the reader is referred to Data Sheet SD-67 from the MCA.

Use OK when employing safe practices

As an extra precaution, explosion vents are a safeguard to reduce destructive damage to building and equipment in which flammable vapors may collect. The type, size and design of explosion venting facilities, and the vent ratios, are based upon the particular properties of hydrocyanic acid gas and should be determined only by competent engineers. Good ventilation prevents dangerous concentrations.

In spite of these warnings, HCN can be safely stored and used if its physical, chemical, and hazardous properties are fully understood and, in addition, the necessary precautions are taken to assure safe practices.

Copper leaching with cyanide—A review of five inventions

Metal recovery from low-grade copper bearing materials and solutions — which are not otherwise amenable to known processing techniques — may provide the metallurgical breakthrough for low cost extraction

FIVE PATENTED cyanide-leaching techniques raise hopes of milling men with the promise of a breakthrough for producing a high-grade copper product from low-grade ores, copper bearing materials and solutions. Other claims of these inventions include lower operating costs, smaller capital requirements, economical reagent recovery and a method for treating refractory ores which are now considered waste.

Cyanide for these processes is supplied to industry in the form of white sodium cyanide, crude calcium cyanide and hydrogen cyanide (hydrocyanic acid). Based on gram mol equivalents, white cyanide contains 50 to 53% active leaching ingredients, calcium cyanide 48 to 50%, and HCN about 96%.

Although only the following procedures are described, it is E/MJ's understanding that other cyanide leaching systems for copper with even greater potential are in the works. When these become available E/MJ will publish the related information.

1—Winning copper from solutions with HCN and SO_2

Edward S. Roberts, in U.S. Patent 3,321,303 (assigned to Treadwell Corp.), describes his novel and continuous method for recovering red metal from solutions containing copper salts with hydrocyanic acid (HCN). His principal objective is to recover substantially pure copper at a cost more economical than that for copper produced by electrowinning and cementation, and in most instances at less than that by smelting and electrorefining.

Typical solutions which may be treated following Roberts' directions could be derived from sulphuric acid leaching of oxidized copper ores or copper bearing materials; from mine waters; from leaching, roasted copper sulphide concentrates or from scrap metal containing copper.

A modification of this invention replaces HCN with crude hydrogen cyanide (HCN burner gases produced by the Andrussow process, U.S. Patent 1,934,838). Reactions by either route can be represented as:

Step 1

$$2CuSO_4 + 2HCN + SO_2 + 2H_2O \rightarrow 2CuCN + 3H_2SO_4$$

or

$$CuSO_4 + 2HCN + CU \rightarrow 2CuCn + H_2SO_4$$

Step 2

$$2CUCN + H_2 \rightarrow 2Cu + 2HCN$$

In general, the inventor carries out the first step at below 100° C, precipitates CuCN by reacting HCN with the copper salts in an acid medium (pH 0 to 4), and converts the copper present to its cuprous state with sufficient reducing material. Since CuCN is extremely insoluble in H_2SO_4 its recovery in this first step approaches the theoretical limit. Copper so produced is a finely divided precipitate which may be separated from the barren liquor by any conventional method.

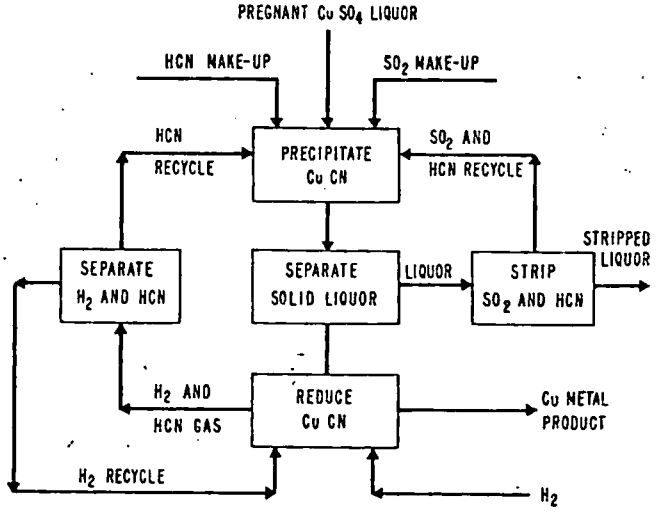

Continuous process for winning pure copper metal using HCN and SO_2. These reductants are regenerated to save on costs.

According to the inventor, to maintain a satisfactory reaction rate and limit cyanide decomposition to an acceptable minimum, metal reduction is preferably conducted between 300° to 400°C.

High quality copper (99.8%) is recovered in quantitative amounts and, at the same time, relatively pure HCN is regenerated for recycling. The production of relatively pure Cu metal and HCN by this method is unique and recovery ranges from 65 to 100% of the copper. Attempts by the researcher at reducing other metal cyanides to metal or at recovering HCN with hydrogen reaction were dismally unsuccessful, Roberts says.

Alternate reducing agents may be used but under present economic conditions only two SO_2 and recycled copper powder from the second step are attractive. When using SO_2, as an alternate reductant, facilities must be provided to dispose of or use the dilute and impure H_2SO_4 made.

Typically, leach liquors should contain from 1 to 50 g of copper per liter, which require at least 60% of the stoichiometric amount of HCN for the reaction. When using SO_2 as an alternate reagent, a convenient method of operation is to maintain a substantially saturated SO_2 solution, thereby minimizing the effect of this reagent being consumed by reducible salts other than cupric sulphate. For example, ferric sulphate would require SO_2 for the ferric to ferrous conversion according to this equation:

$$Fe(SO_4)_3 + SO_2 + 2H_2O \rightarrow Fe(SO_4)_2 + 2H_2SO_4$$

Cupric sulphate reacts in this manner:

$$2CuSO_4 + SO_2 + 2HCN + 2H_2O \rightarrow 2CuCN + 3H_2SO_4$$

Thus, this invention provides a novel process for producing a relatively pure cuprous cyanide from leach liquors.

2—Cyanide treatment of 0.2 to 0.8% copper ore

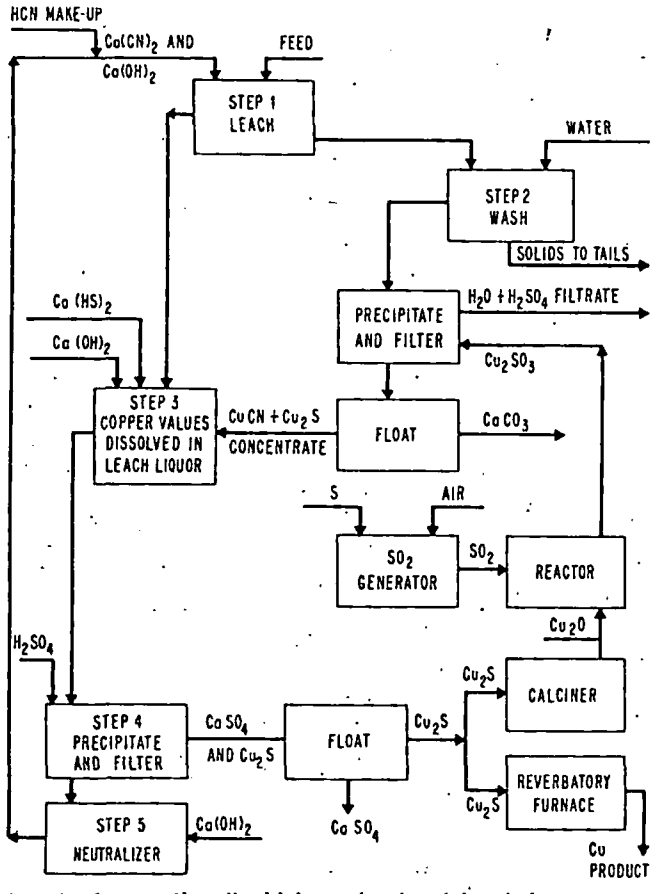

Metal of exceptionally high purity is claimed for process since solution impurities do not enter and contaminate Cu.

Tailings, overburden and other low-grade copper sulphide materials, including ores—associated with an alkaline gangue—and also having some of these characteristics: A low copper concentration (0.2 to 0.8% Cu metal content), a fine particle size, and a widely disseminated mineralization are claimed to be economically processed by the teachings of a new patent (U.S. 3,303,021).

The inventor, E. S. Roberts, Treadwell Corp., says that the specifications call for metal recovery from a copper-bearing material by an alkaline cyanide leaching step, but, for the process to be economically attractive, the copper values and the cyanide adhering to the solids must be recovered.

The initial step, leaching with an alkaline cyanide medium, produces a leach liquor of soluble calcium copper complex and calcium sulfhydrate ($Ca(HS)_2$), which is separated from the solids. These reactions occur:

$$2Cu_2S + 5Ca(OH)_2 + 16HCN \rightarrow 4CaHCu(CN)_4 + Ca(HS)_2 + 10H_2O$$
$$2Cu_2S + 5Ca(CN)_2 + 6HCN \rightarrow 4CaHCu(CN)_4 + Ca(HS)_2$$
$$2Cu_2S + 8Ca(CN)_2 + 6H_2O \rightarrow 4CaHCu(CN)_4 + Ca(HS)_2 + 3Ca(OH)_2$$
$$2HCN + Ca(OH)_2 \rightarrow Ca(CN)_2 + 2H_2O$$

Following this initial reaction, the solids produced are washed with water and sent to tails, the copper and cyanide values are recovered by reacting the wash liquor with either cuprous sulphite or sulphate and sulphur dioxide to precipitate cuprous cyanide and cuprous sulphide. These reactions occur:

$$4CaHCu(CN)_4 + Ca(HS)_2 + 8Cu_2SO_3 \rightarrow 16CuCN + 2Cu_2S + 5CaSO_4 + 3H_2SO_3$$
$$4CaHCu(CN)_4 + Ca(HS)_2 + 16CuSO_4 + 8SO_2 + 16H_2O \rightarrow 16CuCN + 2CU_2S + 5CaSO_4 + 19H_2SO_4$$

After this, the complex precipitate is separated from the wash solution and dissolved in the leach liquor with the simultaneous introduction of $Ca(OH)_2$ and $Ca(HS)_2$ to form soluble calcium copper cyanide in the following manner:

$$2CaHCu(CN)_4 + 4CuCN + Ca(OH)_2 \rightarrow 3CaCu_2(CN)_4 + 2H_2O$$

In step four, the loaded solution from step 3 is reacted with H_2SO_4 to precipitate Cu_2S and $CaSO_4$ as shown below:

$$2CaCu_2(CN)_4 + 3H_2SO_4 + Ca(HS)_2 \rightarrow 2Cu_2S + 3CaSO_4 + 8HCN$$
$$4CaHCu(CN)_4 + 6H_2SO_4 \rightarrow 2Cu_2S + 4CaSO_4 + 16HCN + 4O_2$$
$$Ca(HS)_2 + H_2SO_4 \rightarrow CaSO_4 + 2H_2S$$

The components of this precipitate are separated by flotation (using pine oil as a frother and secondary butyl xanthate as a promoter) sending the $CaSO_4$ to waste, or a separate dump, and the Cu_2S is converted to a relatively pure copper by any conventional method.

The last step involves the neutralization of the filtrate from step four with calcium hydroxide. The resulting solution is recycled as the alkaline cyanide leaching medium. These equations apply to this step:

$$2HCN + Ca(OH)_2 \rightarrow Ca(CN)_2 + 2H_2O$$
$$H_2SO_4 + Ca(OH)_2 \rightarrow CaSO_4 + 2H_2O$$

Make-up HCN is added to this alkaline cyanide leaching medium to provide the necessary strength for reaction with the copper content of the ore.

All of the steps are conducted at ambient temperatures and atmospheric pressures in either open air, or in adequately ventilated enclosures. Under these conditions, the highly toxic hydrocyanic acid (HCN) gas concentration should not present a problem.

Reagents used in the various steps are added in stoichiometric amounts. Per mol of recoverable copper in the ore, about 4 mols HCN (most of which is regenerated and recycled), about 0.5 mols of H_2SO_4 and about 2 mols of calcium hydroxide are needed.

3—Alkaline cyanide leaching of refractory copper ore

Claimed as an improved method for recovering cuprous sulphide material, a recent invention (U.S. Patent 3,224,-835, assigned to Copper Range Co. by W. A. Hockings, D. H. Rose, and A. M. Gaudin), involves leaching with alkaline cyanide solutions at a pH above 7.4 to dissolve the metal content, followed by pH adjustment to below 7.4 whereby cuprous sulphide is precipitated with the addition of SO_2 or other acid. All reactions are conducted under non-oxidizing conditions, according to the inventors. End solution from the process is then treated with lime to regenerate the alkaline cyanide leach solution which is recycled.

An advantageous system for utilizing the invention involves percolation leaching of low-grade copper bearing flotation tailings. The feed are the tails remaining after removing a concentrate from an ore consisting mainly of chalcotite. This aqueous pulp typically contains 25% by weight of solids measuring 100% —325-mesh. The copper content, about 0.15% by weight of solids, is said to be too low in grade to be economically recovered by any known

commercial method now in operation.

In the first step, a sand-slime separation is made and the slimes are discarded. The thickened sands are passed to a closed leaching tank, and are subjected to a downward percolation leach under non-oxidizing conditions with the cyanide solution.

Any low strength leach solution from the reactor may be transferred to the recycle solution tank for reuse. When copper concentration in the pregnant liquor approaches the saturation level (5.5 gpl of Cu) it is collected in the rich solution storage tank. Thereafter, the leach tank charge is washed and its effluent (1.2 gpl Cu and 2.5 gpl CN) is passed to the ends solution tank. This leach step extracts up to 85% of the copper and allows the operators to discard the tails.

Leach solution percolation rates are speeded by applying a vacuum to the bottom of the leach tank. Maximum possible recovery of cyanide, gases and vapors withdrawn by the pump are collected with milk of lime in a scrubber.

End solution and rich solution is treated separately. Rich solution from storage is passed through a battery of rich precipitation vessels arranged in series. During this operation CO_2 gas is bubbled through the reactors countercurrent to the flow of pregnant liquor. Leach solution at this time decreases in pH from 10.5 to 5.7 and, at the same time, about 60% of the copper and 70% of the calcium present is precipitated as cuprous sulphide and $Ca(CO_3)_2$, respectively.

Off-gases from these reactors are vented to scrubber 2, where CO_2 and HCN are absorbed in milk of lime.

From the last reactor, the complex slurry is thickened in a hydrocyclone and dewatered further by filter 1, before being sent to the smelter for further processing.

The vortex discharge from hydrocyclone 2 is substantially free from solids and is delivered to the recycle solution tank for storage and later use.

Solution from filter 1 passes next to the cleanup precipitation equipment for further reagent recovery.

End solution is treated essentially the same as the rich solution, but liquor from its hydrocyclone dewatering step passes to cleanup precipitation for chemical regeneration. Off-gases from the precipitation reactors are also passed to scrubber 2 for the recovery of CO_2 and HCN.

CO_2 and N_2 for the process is advantageously obtained from flue gases derived from burning carbonaceous matter.

The N_2 so produced purges the leach tanks while they are being charged to maintain a non-oxidizing atmosphere.

In the reagent cleanup system the combined solution is adjusted in pH to 2.5 with H_2SO_4. Simultaneously, sodium hydrosulphide is injected to build up sulphide ion concentration and precipitate cuprous sulphide. This step is not essential, but it does eliminate recycling dilute copper and cyanide bearing solutions, and increases somewhat copper recovery.

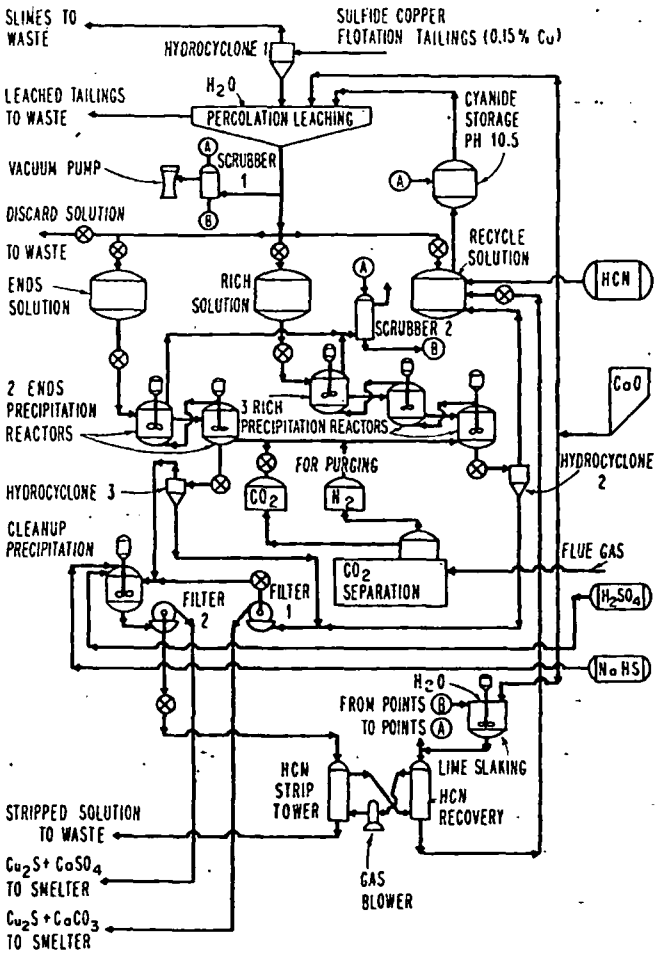

The above process is considered by the inventor to be advantageous for treating low-grade copper bearing tailing.

In the final step, HCN is stripped for reuse from filtrate discharged from filter 2.

Recent pilot plant tests indicate that an overall copper recovery of 91.7% can be obtained using this process. At the same time, consumption of reagents per pound of copper recovered would be 0.362 lb NaCN, 2.06 lb lime, 3.60 lb spent sulphuric acid, and 0.099 lb sodium bisulphide. Cost-wise this represents 9 to 10¢ per lb of copper recovered. Pilot tests also indicate that much of the previously wasted copper in flotation tails (14-million lb annually) can be recovered profitably, but capital costs for such a plant are estimated to be from 50 to 100% higher than for an equivalent sized flotation plant. For comparison, $1,300 to $1,400 per ton of material treated is required to build a cyanide plant.

4—Cyanide solutions remove copper films from gangue

A cyanide system reported on in E/MJ, August 1965, has been designed (U.S. Patent No. 3,189,435 by George William Lower, assigned to American Cyanamid Co., Stamford, Conn.) to recover copper from tailings and other low-grade sources economically. Previous methods were uneconomical because leaching time was high and reagent consumption too costly.

Key to the new process is a critically modified leaching cycle. Leaching time has been reduced from 48 hours to periods of 4 hours or less. Instead of directly acidifying the cyanide solution containing soluble copper (as in previous processes), the solution is first treated with a critical deficiency of soluble sulphide prior to acidification. By this method, 75% or more of the copper values can be recovered, and cyanide losses are low.

Cyanide losses are low because only a limited quantity of the cyanide is converted to thiocyanate, and copper is precipitated as a sulphide rather than the cyanide. This prevents cyanide decomposition and loss, and permits cyanide recovery and recycling for further use.

The following chemical equations show (1) the sequence of reactions which take place in the older, less efficient extraction processes, and (2) the reactions for the newly patented process where copper is precipitated as a sulphide, and the cyanide is available for recycling.

Copper minerals leach time — a comparison

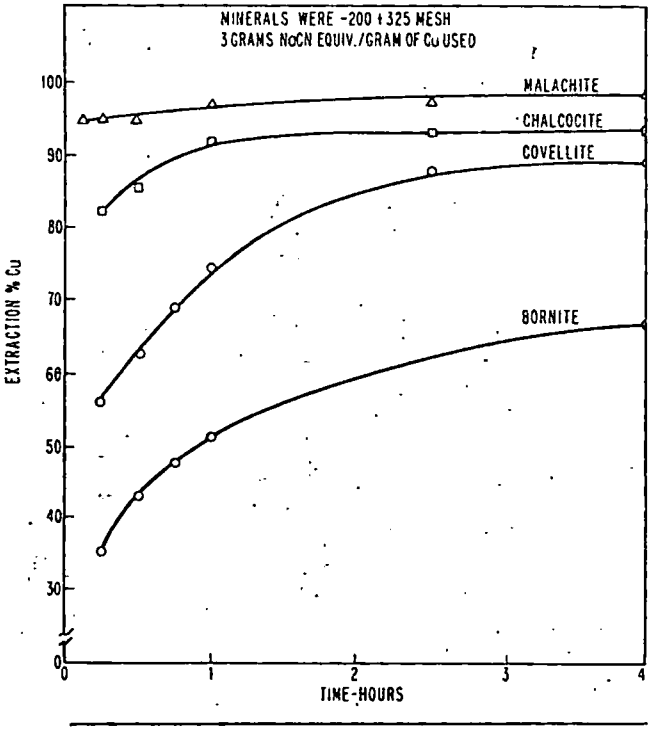

1) $$2Cu_2S + 11NaCN + 2\tfrac{1}{2}O_2 + H_2O \rightarrow 2NaCu(CN)_2 + 2Na_2Cu(CN)_3 + NaCNS + Na_2SO_4 + 2NaOH$$

2) $$Cu_2S + 6CN^- = 2Cu(CN)_3^= + S^=$$
$$2Cu(CN)_3^= + S^= + 3H_2SO_4 \rightarrow Cu_2S + 6HCN + 3SO_4^=$$

Cyanidation can be effected by inorganic cyanides such as hydrocyanic acid, sodium cyanide, potassium cyanide or calcium cyanide or mixtures of them; or organic products such as lactonitrile (considered a by-product from acrylonitrile processing). Useful ratio of cyanide reagent to copper (based in NaCN equivalent) is about 2½ to 4 moles of cyanide per mole of copper extracted. It is critical that cyanidation conditions be maintained for no longer than a few hours, and preferably for less than 90 minutes. The cyanide must be added in stages. Any soluble sulphide may be used to precipitate the copper from the cyanide solution.

The accompanying table shows batch leach tests for various tailings and mill products. Leaching time was one hour. In one 500-g test on a cleaner tailing running 1.077% Cu, 75.9% of the total copper present was recovered as a sulphide precipitate assaying 16.95% Cu. Of the total cyanide used, 94.4% was regenerated. Cyanide consumed was 0.2 lb of NaCN equivalent per pound of copper recovered. The patent claims that this method can be used on tailings which are being discarded at a rate of 4,000 tpd at one western copper mine, and that the patented method could be used to recover 60,000 lb of copper now going to waste per day.

Three cyanide extractants give good yields

Test	Type	Percent Cu	Percent total copper recovered	Pounds used per pound of copper recovered: NaCN equiv.	Pounds used per pound of copper recovered: Precipitant equity NaHS equiv.
1.	Copper ore	1.07	84.7	0.3	0.26
2.	Concentrate from slime flotation	2.14	76.2	0.2	0.25
3.	Slime fractions cycloned from rougher flotation tailings	0.58	71.1	0.25	0.21

Test 1: Sodium cyanide used as extractant; sodium sulphide used as precipitant.
Test 2: Lactonitrile used as extractant; calcium sulphide used as precipitant.
Test 3: Hydrocyanic acid with lime used as extractant; hydrogen sulphide used as precipitant.

5—A cyanide system for oxide or mixed oxide-sulphide ores

Another invention, similar to the first Roberts' patent, claims certain advantages over the more commonly used techniques of electrolytic and cementation recovery from copper bearing solutions. This invention, assigned to Dow Chemical Co., was issued as U.S. Patent 2,390,540 on Dec. 11, 1945, and was first publicized in E/MJ, June 1966.

According to C. H. Keller, the inventor, his method is more economical in reagent consumption, and requires a smaller capital outlay than other operational modes for recovery of copper present in mine and mill solutions. The process can be applied equally well to acid or neutral liquors, the reagents can be regenerated and recycled, copper can be completely extracted from solution in almost theoretical quantities, and copper of smelter grade can be produced.

His method is based on the precipitation of cupric ions from cold or warm solutions as cuprous thiocyanate. The cuprous thiocyanate precipitate is then treated with a soluble alkaline agent converting it to soluble thiocyanate and leaving an insoluble copper compound as a residue.

In practice, SO_2, sulphites, bisulphites, Zn, Fe, or any mixture of these materials acts as the reductant. The basic chemistry underlying this method is:

1) $$2CuSO_4 + H_2SO_3 + 2NH_4CNS + H_2O \rightarrow 2CuCNS + (NH_4)_2SO_4 + 2H_2SO_4$$

2) $$2CuCNS + 2NaOH \rightarrow Cu_2O + 2NaCNS + H_2O$$

3) $$2CuCNS + CA(OH)_2 \rightarrow Cu_2O + Ca(CNS)_2 + H_2O$$

Interesting developments include a system of electrometric control for regulating addition of thiocyanate to leach liquor, and a system for controlling the color of cuprous oxide for use as a paint pigment when NaOH is used for conversion. Also significant is this reaction of the Cu_2O produced in equation (1) with sulphuric acid:

$$Cu_2O + H_2SO_4 \rightarrow CuSO_4 + Cu + H_2O$$

By this reaction some of the copper can be routed for copper powder work or smelted to bars while half goes to copper sulphate for the tank house.

On mixed copper ore ground to 66% — 200-mesh tests similar to the flow scheme on the opposite page were conducted, and typical results indicated a sulphide copper recovery between 93.5 and 96.0%, an oxide copper recovery between 86.1 and 88.0%, an overall copper recovery between 91.4 and 92.6%, and thiocyanate recovery between 97.0 and 97.2%.

In the practice of this invention, the flow schemes used can vary considerably but still employ the basic principles of the thiocyanate process. Dow Chemical Co. carried out extensive laboratory work, and some of the systems it tried were sulphide flotation, followed by acid leaching; acid leaching, followed by sulphide flotation; a cycle test of sulphide flotation, followed by acid leaching; and flotation of CuCNS from ore pulps. All tests normally gave over 91.0% total copper recovery and, at the same time, allowed at least 97.0% of the thiocyanate to be regenerated for reuse.

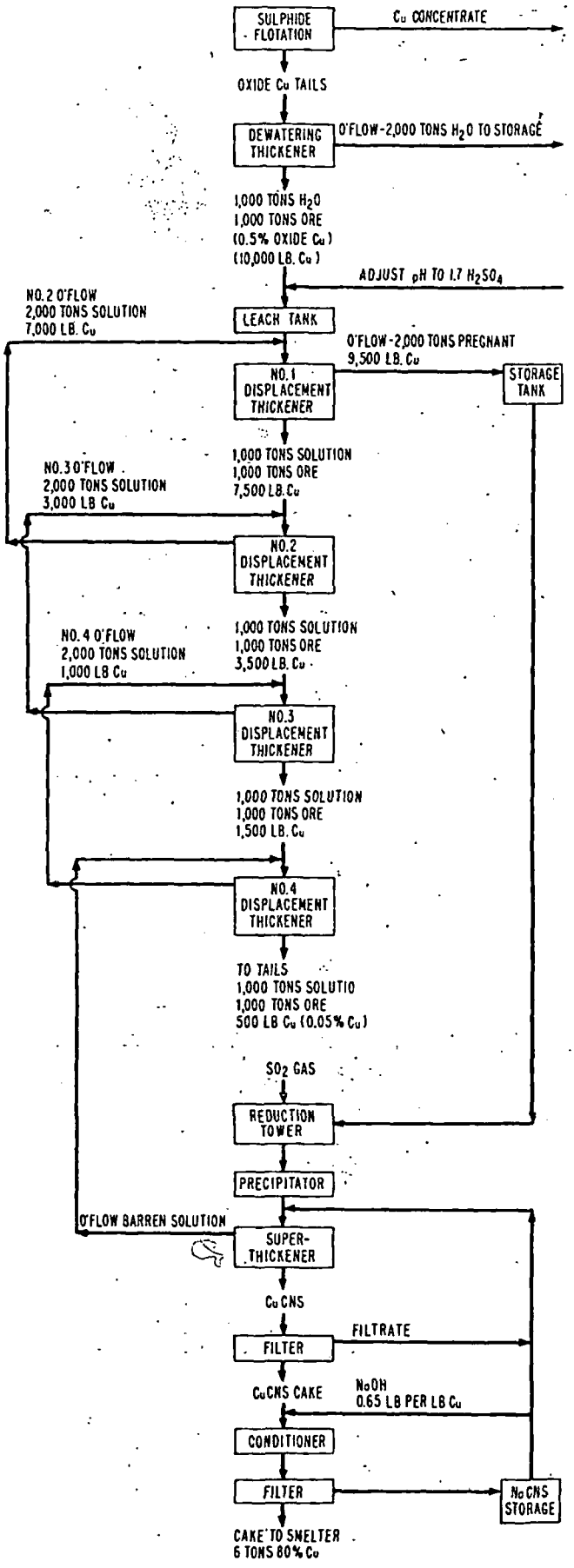

The Keller system recovers over 90% of the thiocyanate used by regeneration with lime, caustic soda or potash, or soluble alkali sulphides. Process also works on acidic copper bearing solutions.

A word of caution:

For the safe handling, storage and use of hydrocyanic acid (HCN)

Essential information for safe handling and use of hydrocyanic acid (HCN) contained in the Chemical Data Sheet SD-67 (Manufacturing Chemists Association Inc. (MCA), 1825 Connecticut Ave. N.W., Washington 9, D.C.) states that 96% strength HCN liquid is classified by the Interstate Commerce Commission (ICC) as a Class A poison. Poisoning results from inhalation, from swallowing, and from contact with mucous membranes or with skin.

Explosive over wide mixture range

HCN (also known as prussic acid and hydrogen cyanide) is flammable, it can be ignited by an open flame, hot surface, or spark, and it forms explosive mixtures in quantities between 6 and 41% by volume in air.

Threshold limit low for workers

The maximum atmospheric concentration (threshold limit) of hydrocyanic acid to which workers may be exposed for an eight-hour day without injury to health is generally accepted as 10 ppm by volume.

Solution only mildly corrosive

Stabilized HCN is only mildly corrosive but, because of its highly toxic nature, Type 316 stainless steel piping and fittings have proven more satisfactory for handling it. Teflon (tetrafluorethylene) gaskets have also performed satisfactorily in this application.

Shipping controlled by ICC regulations

Handling and storage of HCN presents some unusual restrictions too. The liquid product must be shipped in either ICC approved steel cylinders or tank cars. The tank cars must also be equipped with cork insulation at least four inches in thickness.

Storage requires refrigeration

Stored HCN should be maintained between 5° and 10° C by recirculation through an external heat exchanger. Freon refrigeration units are usually used.

For complete information on this subject, the reader is referred to Data Sheet SD-67 from the MCA.

Use OK when employing safe practices

As an extra precaution, explosion vents are a safeguard to reduce destructive damage to building and equipment in which flammable vapors may collect. The type, size and design of explosion venting facilities, and the vent ratios, are based upon the particular properties of hydrocyanic acid gas and should be determined only by competent engineers. Good ventilation prevents dangerous concentrations.

In spite of these warnings, HCN can be safely stored and used if its physical, chemical, and hazardous properties are fully understood and, in addition, the necessary precautions are taken to assure safe practices.